A Center of Excellence for Rural and Intermodal Transportation

MPC REPORT NO. 99-99B

Cyclic Lateral Loading of a Model Pile Group in Clay Soil

Joseph A. Caliendo
Loren R. Anderson
Robb Eric S. Moss

February 1999

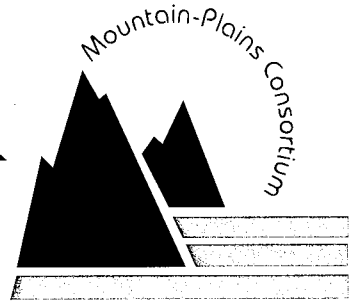

Colorado State University
Fort Collins, Colorado

North Dakota State University
Fargo, North Dakota

University of Wyoming
Laramie, Wyoming

Utah State University
Logan, Utah

CYCLIC LATERAL LOADING OF A MODEL PILE GROUP IN CLAY SOIL

PHASE 2B

Joseph A. Caliendo
Loren R. Anderson
Robb Eric S. Moss

Utah State University
Department of Civil and Environmental Engineering

February 1999

Acknowledgments

To Dr. Joe Caliendo, I would like to express my sincere gratitude for providing me the opportunity to achieve my full potential in so many different areas. Thanks for the teaching opportunities, research opportunities, guidance, looking out for me, taking care of me, letting me run with the ball when I needed to, and checking my ambition when that was in order.

Thanks to Mark Rawlings for being a great colleague and friend. Without Mark there would have been no project to join, and no one to handle the mechanical engineering side of things.

I also would like to thank Dr. Loren Anderson, Dr. Marv Halling, and Dr. Reynold Watkins for their advice on the research. This project was a team effort and everyone deserves credit for its success.

REPORT DOCUMENTATION PAGE

Form Approved
OMB No. 0704-0188

1 PB99-140584

2. REPORT DATE: February 1999

3. REPORT TYPE AND DATES COVERED: project technical

4. TITLE AND SUBTITLE

Cyclic Lateral Loading of a Model Pile Group in Clay Soil Phase 2B

5. FUNDING NUMBERS

6. AUTHOR(S)

Joseph A. Caliendo, Loren Anderson, Robb Eric S. Moss
Utah State University

7. PERFORMING ORGANIZATION NAME(S) AND ADDRESS(ES)

Mountain Plains Consortium
North Dakota State University
Fargo, ND

8. PERFORMING ORGANIZATION REPORT NUMBER

MPC 99-99B

9. SPONSORING/MONITORING AGENCY NAME(S) AND ADDRESS(ES)

University Transportation Centers Program
U.S. Department of Transportation
Washington, DC

10. SPONSORING/MONITORING AGENCY REPORT NUMBER

11. SUPPLEMENTARY NOTES

12a. DISTRIBUTION/AVAILABILITY STATEMENT

12b. DISTRIBUTION CODE

13. ABSTRACT (Maximum 200 words)

In certain regions of the world, designing deep foundations to withstand seismic loading is a reality. Seismic loading of structures and foundations reaches a critical state as a laterally applied force. The response of soils and foundations to repetitive lateral forces is highly complex, relegating most design methods to be based on empirical research. The primary objective of this research was to analyze mechanics of seismic loading of pile groups in clay soils. To achieve this a model testing facility was constructed to house a fully instrumented 1 x 5 model pile group that was subjected to cyclic lateral loading. The results from this testing include bending moment distributions per pile and cycle, load distributions, deflection curves, normalized design curves, and p-y curves. These results are presented to expand volume of empirical data on laterally-loaded pile groups and further the knowledge in seismic design of deep foundations.

14. SUBJECT TERMS

cyclic lateral loading, pile groups, soil, seismic loading

15. NUMBER OF PAGES: 360

16. PRICE CODE

17. SECURITY CLASSIFICATION OF REPORT	18. SECURITY CLASSIFICATION OF THIS PAGE	19. SECURITY CLASSIFICATION OF ABSTRACT	20. LIMITATION OF ABSTRACT
			UL

This report is part of an ongoing investigation on the responses of individual piles and pile groups to various types of lateral loadings. This research has been undertaken on behalf of the Utah Department of Transportation and the Mountain Plains Consortium. Phase 1 of the study was completed in March 1996 and involved design and construction of a model test facility. A model pile was designed, instrumented, and laterally loaded under monotonic conditions.

This report is the report for phase 2B of the project. It presents an in-depth analysis and design applications for pile groups subjected to the cyclic lateral loadings developed in the previous phase.

The report for phase 2A of the project has also been completed. This report addresses the design, construction, calibration, and preliminary test results for a pile group subjected to cyclic lateral loading.

A much briefer executive summary of the two phases will be submitted as phase 2C.

ABSTRACT

In certain regions of the world, designing deep foundations to withstand seismic loading is a reality. Seismic loading of structures and foundations reaches a critical state as a laterally applied force. The response of soils and foundations to repetitive lateral forces is highly complex, relegating most design methods to be based on empirical research. The primary objective of this research was to analyze mechanics of seismic loading of pile groups in clay soils. To achieve this a model testing facility was constructed to house a fully instrumented 1x5 model pile group that was subjected to cyclic lateral loading. The results from this testing include: bending moment distributions per pile and cycle, load distributions, deflection curves, normalized design curves, and p-y curves. These results are presented to expand volume of empirical data on laterally-loaded pile groups and further the knowledge in seismic design of deep foundations.

TABLE OF CONTENTS

LIST OF FIGURES

CHAPTER I

INTRODUCTION

Designing pile groups to withstand lateral loads is a concern where piles are subjected to seismic loads, wave action, ship impacts, and earth or water pressures. In Utah the primary concern is seismic loading. Northern Utah is subjected to effects of basin and range extension which results in North-South trending normal faults. The normal faults have a history of seismic activity of a magnitude that can be detrimental to man-made structures. The majority of Utah's population lives in close proximity to various segments of the Wasatch fault and the potential for earthquake damage to buildings, highways, and other large structures is high. Each segment of the Wasatch fault can release enough energy to register a 7.0 on the moment magnitude scale. Paleoseismic studies show that the potential for a earthquake in the near future is highly likely (eg. the Brigham City segment is approximately 300 years overdue for a release).

Research Basis

To address the concern of seismic foundation integrity, the Utah Department of Transportation (UDOT) initiated a multiphase research project. The objective was to determine pile group response under cyclic lateral loading for a typical UDOT pile group installed in local lacustrian clays. The test results could then be used to validate FLORIDA PIER (FLPIER) software for deep foundation design in Utah. This research is part of that UDOT project. The cost of testing full scale deep foundations is prohibitively expensive for repeated tests, therefore, a model testing facility was developed at Utah State University to run multiple tests. The model testing was run in conjunction with full scale testing conducted in the Salt Lake valley.

Model Testing Facility

The model testing facility is a large steel tank, 10 x 3ft (3 x 1m) in plan view and 4.5ft (1.4m) deep. The tank was lined with an impermeable geomembrane and a geofabric for consolidation drainage. It was filled with lacustrian clay (CL) in slurry form, which was then consolidated to an average undrained shear strength of 800psf (40kPa) using hydraulic rams. Shear strength profiles are shown in Figures 1 and 2, with additional soil properties in Figure 3. Excess pore pressure was dissipated through the geofabric and out exit drains. The clay was maintained in a saturated condition throughout testing to simulate UU conditions.

Two phases of model testing have been completed; cyclic lateral loading of a single pile and cyclic lateral loading of a 1 by 5 pile group. This thesis covers the later half of the 1 by 5 pile group testing, Phase 2B. For detailed information on equipment and design specifications see Phase 2A, Rawlings (1997).

The model pile group was composed of five piles arranged in a linear fashion, pinned at the top to a pile cap (Figure 4). A linear pile group allowed for focus on group and shadowing effects inherent in closely spaced groups. A pile spacing of 3d (d = outside diameter) was chosen for this test because it is the recommended minimum spacing used by UDOT and FHWA for group design. The prototype pile was a typical closed end steel pipe pile used ubiquitously in Utah by UDOT. The prototype pile had an OD of 12.75 inches (324mm) and a wall thickness of 3/8in (9.52mm). The model piles were constructed of 6061 aluminum pipe (OD = 1.315 in/33.401mm and wall thickness = 0.133 in/3.378mm) after rigorous similitude analysis. They were 60 inches (1524mm) long of which 85 percent was embedded in the clay soil: see Caliendo & Anderson (1996).

Each pile was instrumented with 14 pairs of strain gages, mounted diametrically opposed on the inner diameter of the pile. Gage locations are shown in Figure 5 with red and black denoting each gage in a pair. The pinned pile cap was instrumented with strain gages mounted on the top and bottom between

each pile. At the ends of the pile cap were master load cells that measured the group load via strain gages. Pile top displacement and slope was measured using two LVDTs. With an additional pile installed remotely for temperature compensation, the number of input channels totaled 182.

A highly specialized data acquisition system was designed and built in-house to acquire the 182 channels of information in an expedient manner (Figure 6). The four main components of the system are; a PC, A/D board, power supply, and acquisition hardware. There is a full Wheatstone bridge for each strain gage; one strain gage in a pile accompanied by three resistors located on their respective circuit boards. Fourteen circuit boards were needed to acquire all 182 channels of information. The acquisition system was controlled by LABVIEW software, which also controls the loading system in a closed loop format.

Cyclic loading of the pile group was accomplished via hydraulic rams. The hydraulic rams were mounted horizontally in plane with the pile cap. The connecting equipment is shown in plan view in Figure 7. Loading force was provided by a hydro-pneumatic tank and regulator (Figure 8). The actuation of the loading force was controlled by a solenoid switch which is in turn controlled by LABVIEW. The program written using the LABVIEW software, allowed for real time analysis of; group load, pile top deflection and slope, bending stresses in each pile, and the maximum stress in any one pile during the test.

Load, as opposed to deflection or hertz, was chosen as the control for testing. During an earthquake, a structure and its foundation will be experiencing forces at some peak level. The force level applied to the pile group was approximately 65 percent of the yield stress of the aluminum model piles. This was the peak level which was cycled through the pile group throughout the test.

A load scheme was designed after generating predictions using FLPIER and Com624P software, and trial and error testing in the lab. The pile group was laterally loaded from zero to 450lb (2000N) and back to zero in approximately one minute while the acquisition system recorded data at the rate of four samples a second. That is 182 channels recorded in 0.25 seconds, acquired continuously throughout the

loading. The group was then loaded in the same manner but in the opposite direction, thus completing one cycle. This was carried out for 50 cycles of loading. The complete test yielded 52 megabytes of data, read continuously for every cycle, encompassing loads from 0 to 450lb (2000N) for each cycle.

The loading scheme was designed to look at the mechanics of cyclic lateral loading of pile groups only, not dynamic responses such as inertial or kinematic effects. This phase of the research targeted soil degradation due to load and cycle, and a comparison of the results with predicted results from design software. The wave pattern of the loading can be seen in Figure 9. UU conditions were maintained throughout the test to simulate the soil conditions during a seismic event. During groundshaking, a clay soil has no time to dissipate excess pore pressure generated by the seismic motion. Although the loading scheme used in these model tests were of low frequency, it is assumed that maintaining UU conditions eliminates frequency as a variable when considering deflection, maximum bending moment, moment distribution, load distribution, pile shadowing, group effects, and other mechanical interactions between the pile group and the surrounding soil.

Upon completion of the cyclic load test a final calibration test was necessary to determine exact correlation between measured voltages and bending stresses. This was done using the cyclic load testing set up with the program slightly modified for calibration. A known load was applied to the piles at a known location and the measured output was compared to the theoretical bending stresses. A linear regression was done on the comparison. The result was a calibration factor for each gage which fine tuned the raw output: see Rawlings (1997).

Empirical Objectives

Many types of results were generated from the volumes of data acquired. The first group of results contain; load distribution, moment distribution per pile, moment distribution per cycle, and load vs. deflection. A comparison of the test results with the FLPIER predictions are provided showing load vs. deflection and maximum bending moment vs. deflection. The second group of results include normalized bending moment and deflection curves for use as design tools. The third group of results include p-y curves for different piles at different depths and different cycles as well as accompanying graphs for explanation. These results were generated to define more clearly the response of pile groups in clay soils and ultimately mitigate seismic hazard by increasing the confidence in deep foundation design when cyclic loads are a concern.

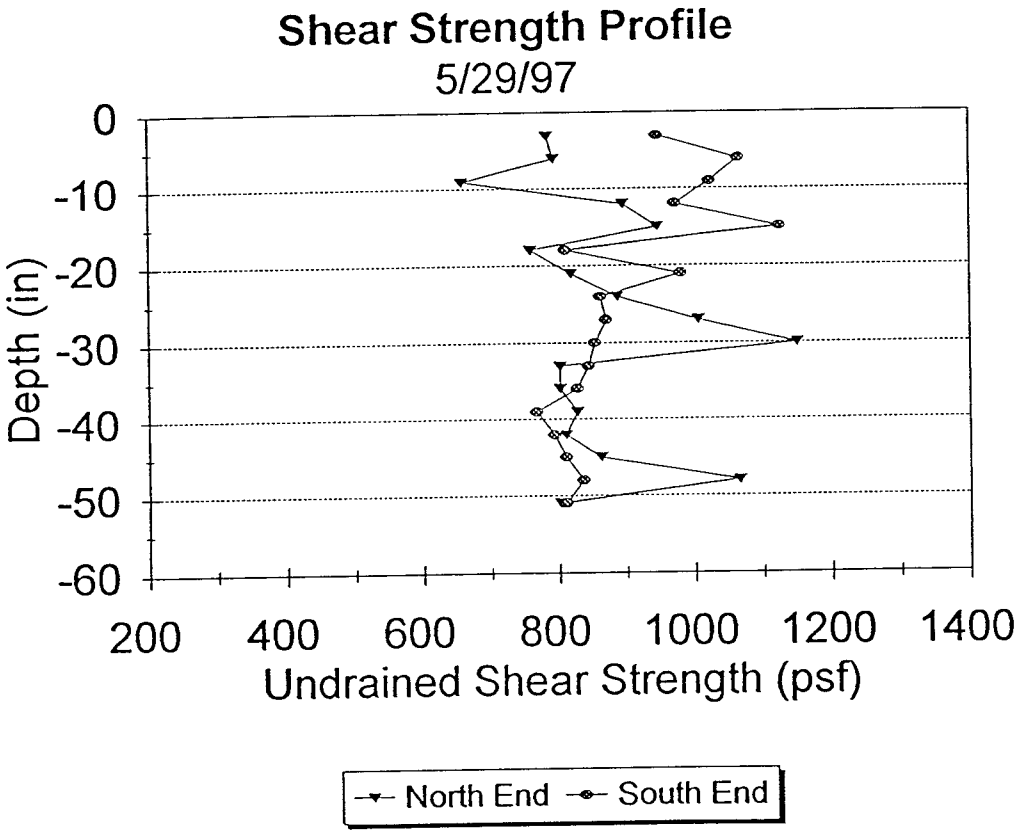

Figure 1. Shear strength profile (English units).

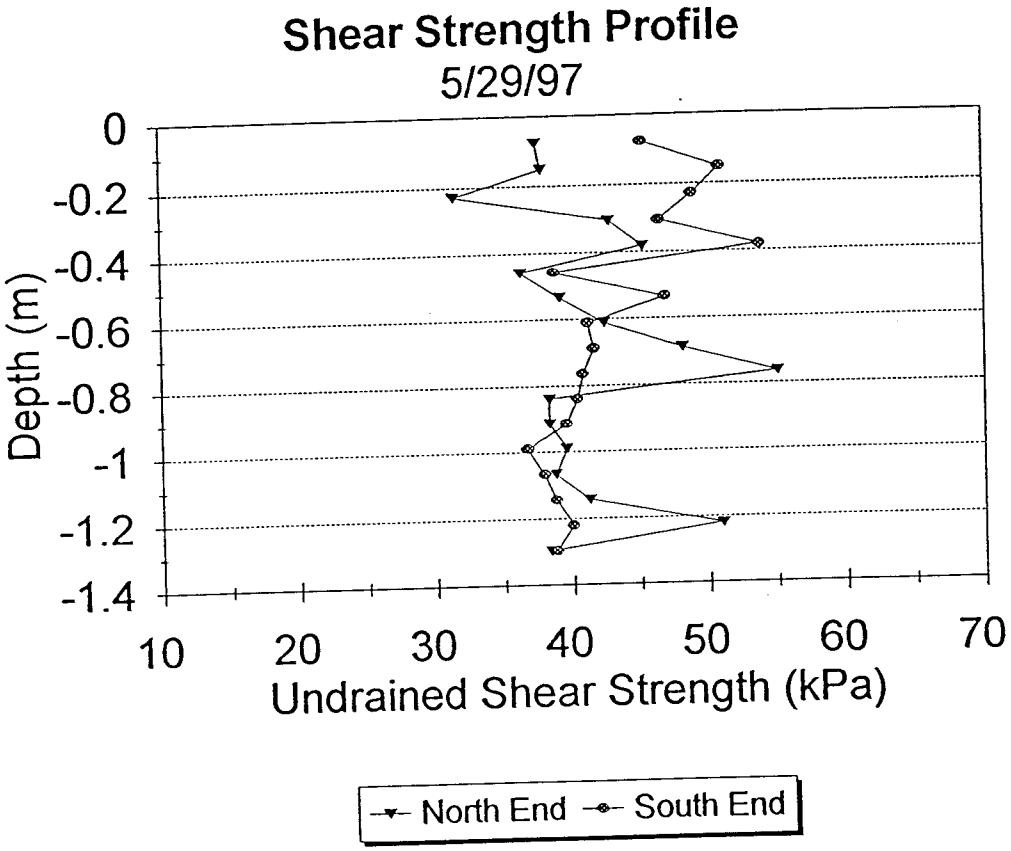

Figure 2. Shear strength profile (SI units).

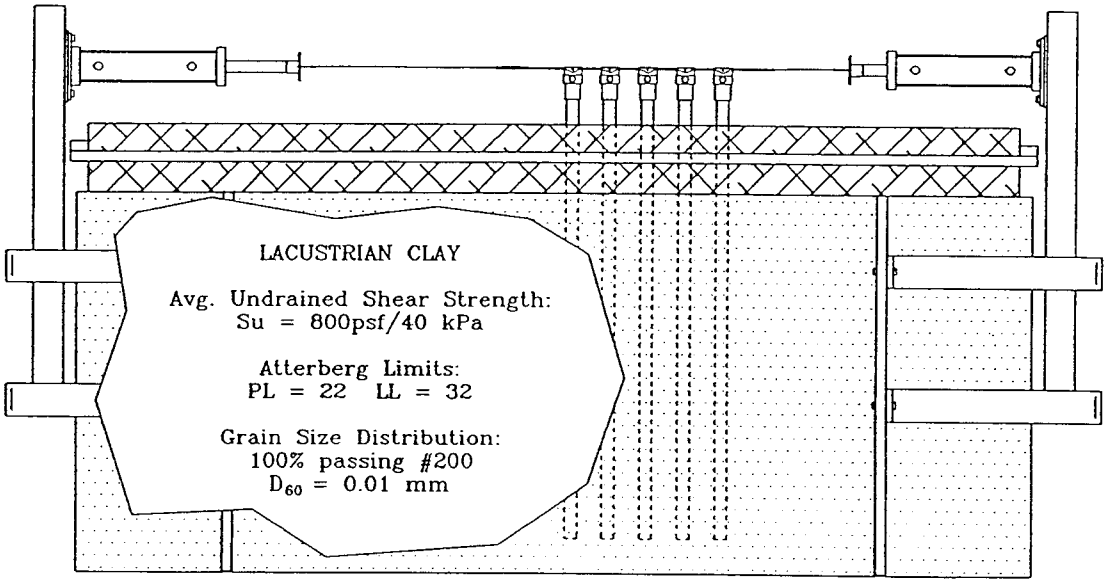

Figure 3. Testing facility with soil properties.

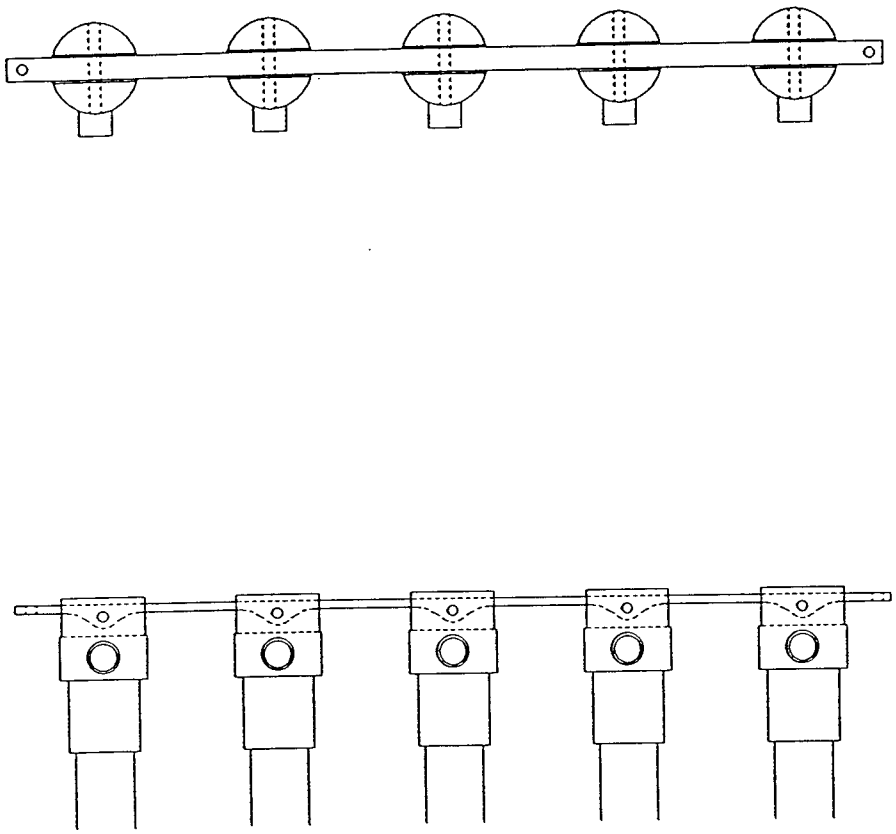

Figure 4. Load rod/pinned pile cap.

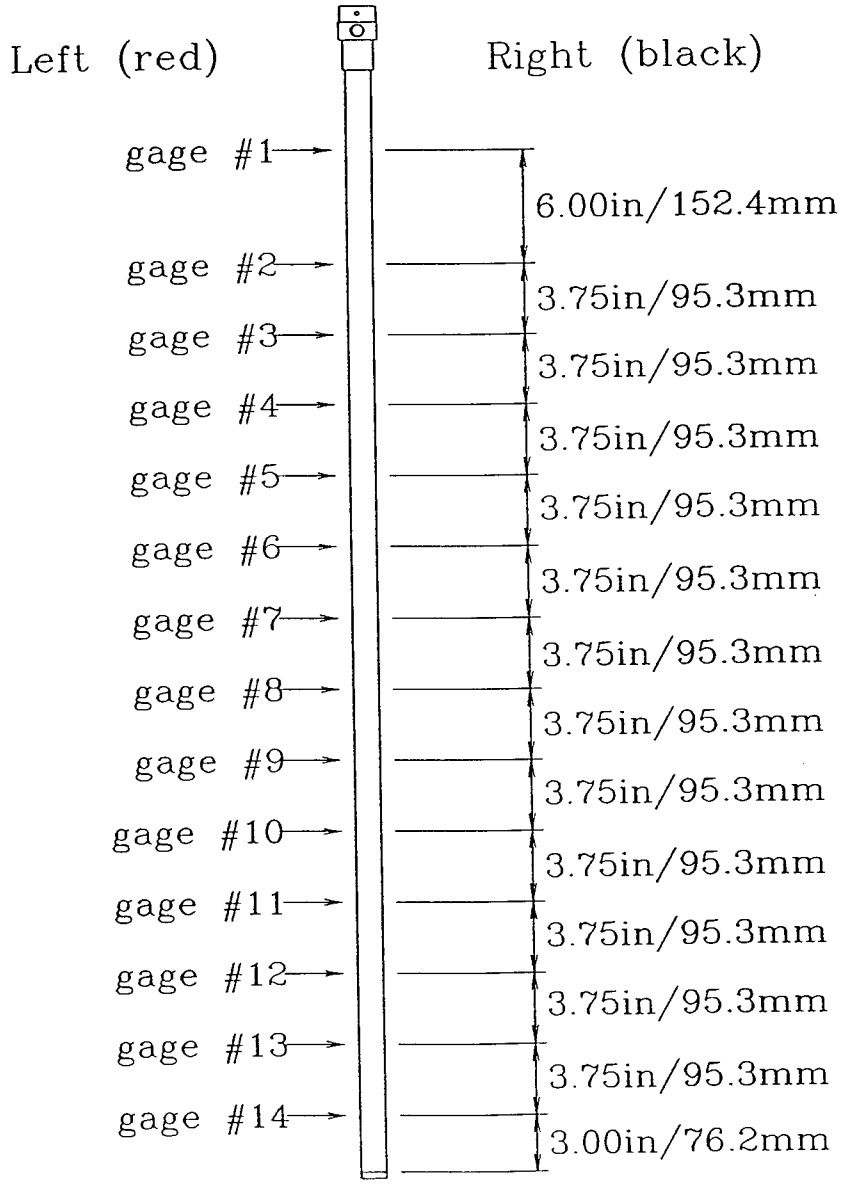

Figure 5. Strain gage locations.

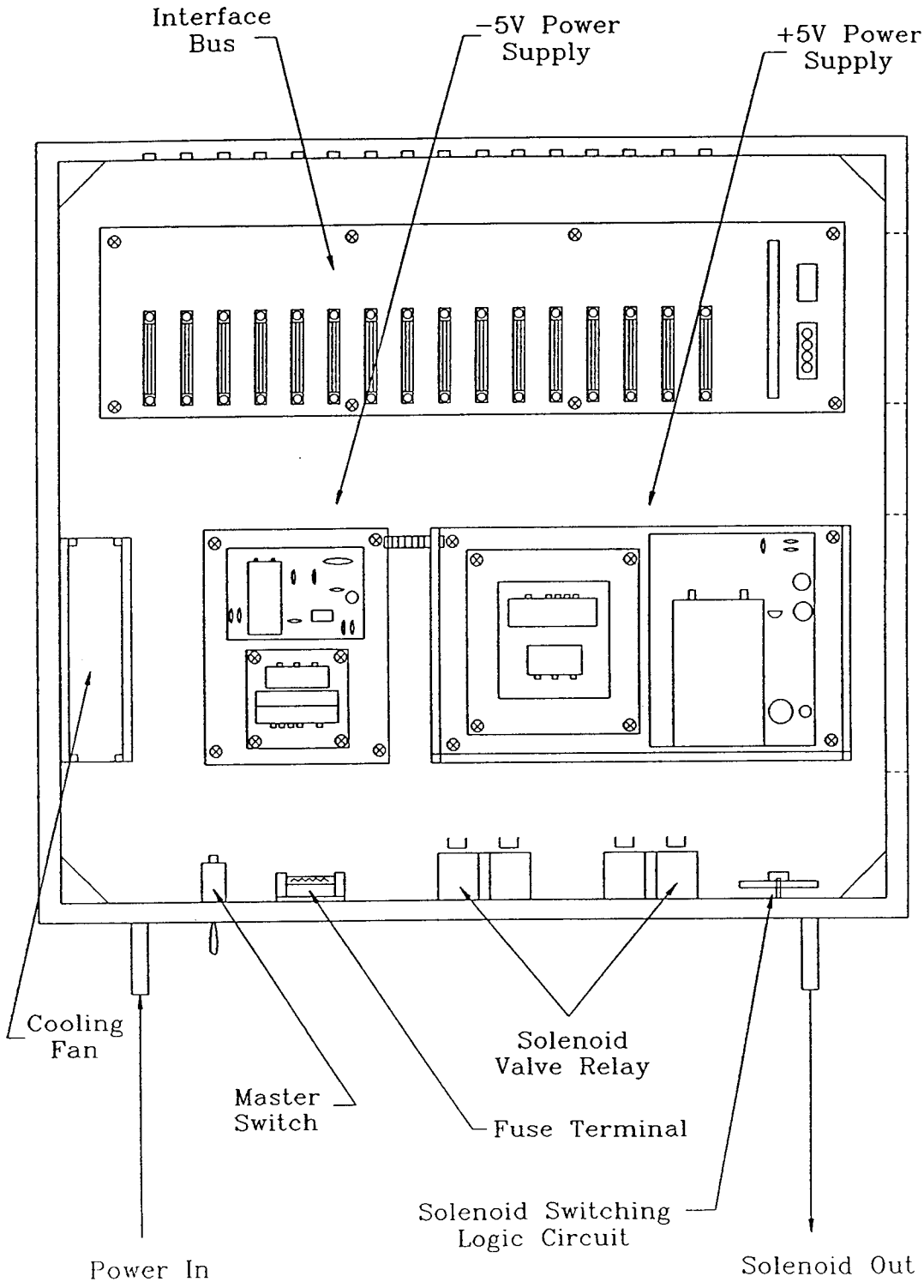

Figure 6. Data acquisition system (i.e. black box).

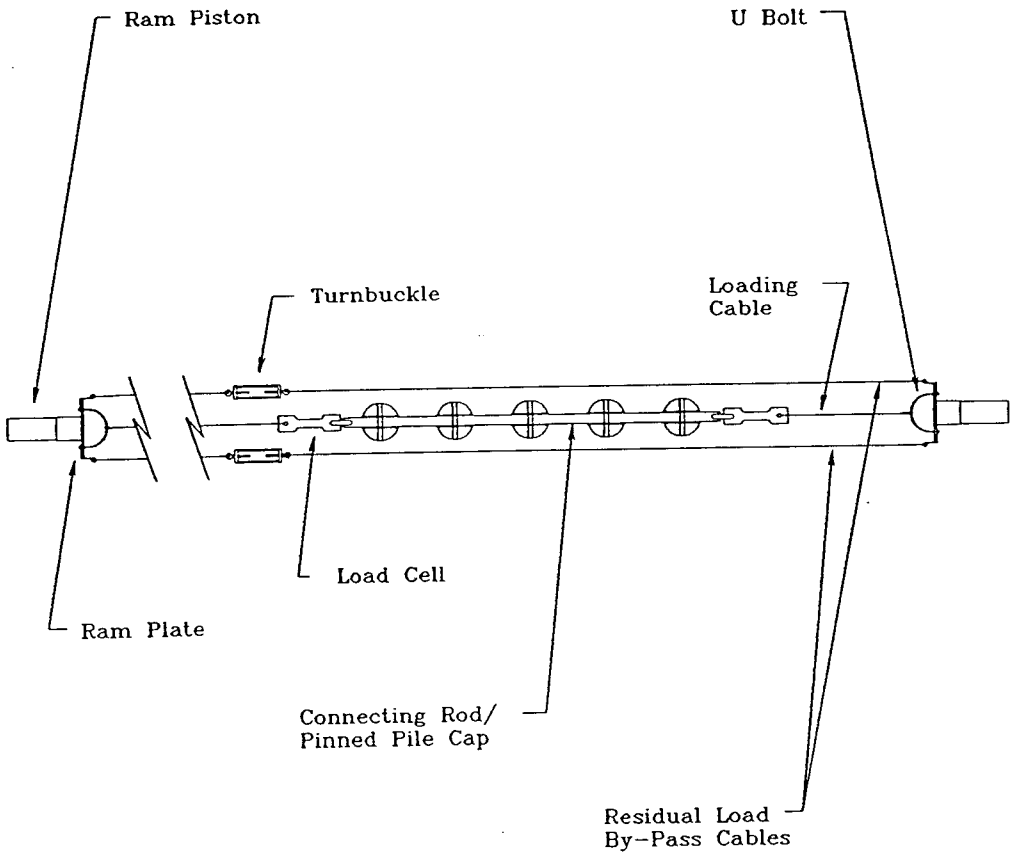

Figure 7. Pile group loading linkage.

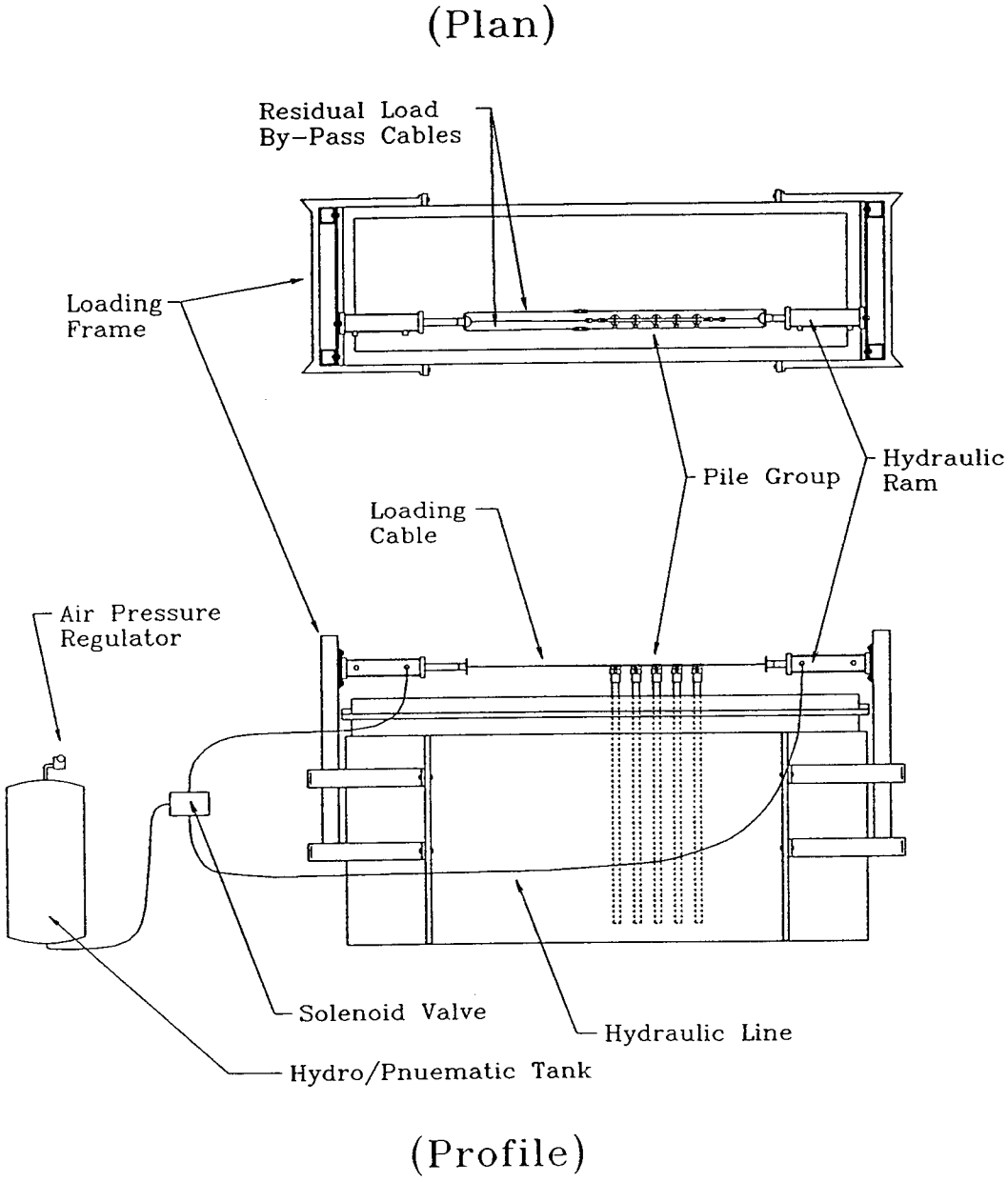

Figure 8. Loading system equipment.

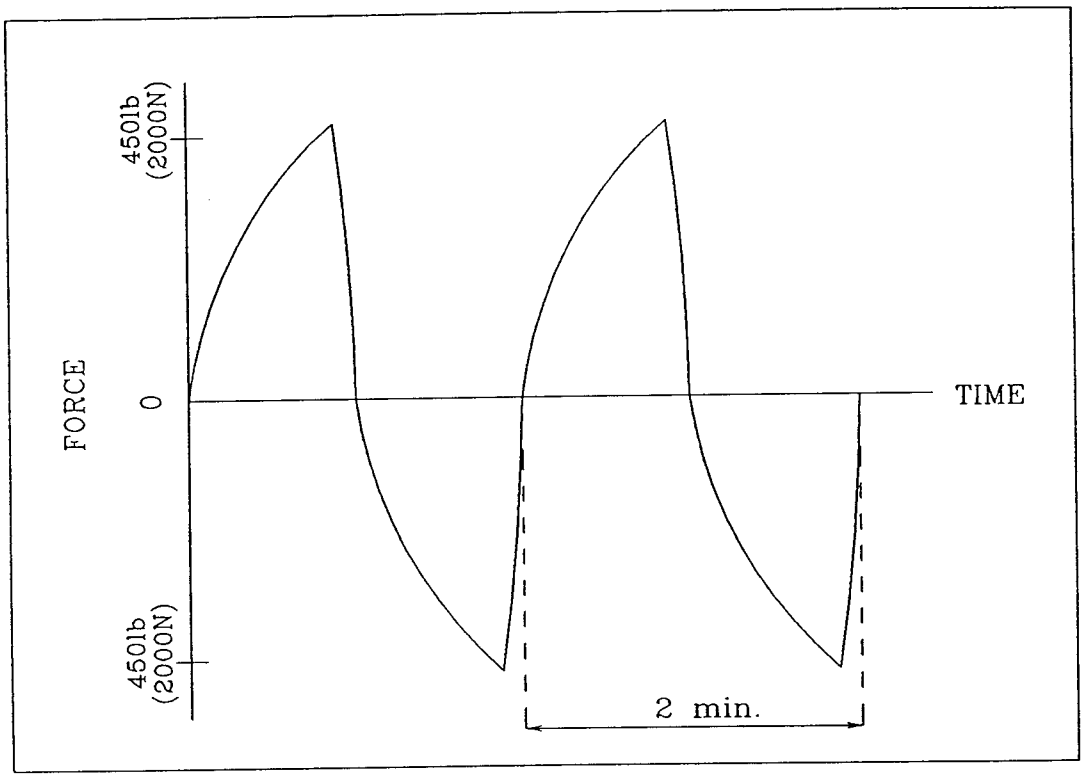

Figure 9. Load wave form.

CHAPTER II

LITERATURE REVIEW

The study of laterally-loaded piles was brought about mainly by offshore oil exploration that was being conducted in the Gulf of Mexico in the 1940's and 1950's. The platforms that supported the drilling equipment were subjected to constant wave action and, at times, lateral ship impact. Research was initiated to quantify the response and integrity of piles exposed to the lateral loads. The ground work was laid by these early studies of offshore piles and has since progressed to encompass the study of individual piles and pile groups that experience lateral loads not only due to lateral wave and ship loading but earthquake, wind, and other types of lateral loading.

Single Piles

The early studies of single piles subjected to lateral loads led to three common methods of soil-structure analysis: 1. the Winkler model or subgrade reaction model which represents the soil as discrete uncoupled nonlinear springs, Winkler (1876), 2. modelling the pile as a beam on an ideal elastic continuum, Poulos (1971), or 3. the finite element approach for modelling the soil, Desai and Appel (1976). The most common method is the Winkler model, which denotes the nonlinear springs as p-y curves.

P-Y Curves

The concept of the p-y curve was first suggested by McClelland and Focht (1958) and Matlock and Ripperger (1956). The use of the p-y approach expanded with subsequent research due to the fact that it is easy to use and easy to modify for nonlinear soil response and cyclic loading. State of the art software for pile and pile group design use a combination of p-y curves and finite element methods to

solve for pile response, with the emphasis being on the p-y curves due to the short computation time and simple solutions involved.

When representing soil as an elastic medium and a pile as an elastic beam the governing differential equation as derived by Hetenyi (1946) is shown (equation 2.1). The nonlinear springs can be calculated at each depth from the given beam equations for p and y (equations 2.2 and 2.3).

$$EI\frac{d^4y}{dz^4} + Pz\frac{d^2y}{dz^2} + p - w = 0 \quad \ldots\ldots\ldots\ldots\ldots\ldots\ldots \quad (2.1)$$

Pz = axial load in the pile

y = lateral deflection of the pile at a specific depth z

p = soil reaction per unit length

EI = pile stiffness

w = distributed load along the length of the pile

$$p = \frac{d^2M(z)}{dz^2} \quad \text{..... (2.2)}$$

$$y = \frac{1}{EI}\int\int M(z)\ dz \quad \text{..... (2.3)}$$

M = bending moment

$p = -E_s y$

E_s = secant modulus of soil reaction

The analytical basis for p-y curves began with Terzaghi's (1955) paper on the coefficient of subgrade reaction. A linear relationship between soil resistance and deflection was presented with the assumption that this relationship was valid only up to half the maximum bearing stress. Ultimate resistance models were developed by Reese (see McClelland and Focht, 1958) for undrained clays failed by laterally loaded piles. The results showed the nonlinear nature of soil resistance versus deflection at high strains.

Pile Groups

When piles are placed in a group with a close spacing there tends to arise group phenomena that cannot be accounted for by single pile analysis. Pile-soil-pile interaction comes about as a function of the pile spacing. Some of the effects of pile-soil-pile interaction are greater deflection of a group than a single pile loaded to the same intensity. Piles in trailing rows have significantly less resistance to a

lateral load than piles in lead rows, Brown, Morrison, and Reese (1988). The term "group effect" refers to the fact that a group will exhibit less lateral capacity than the sum of the lateral capacities of the individual piles (i.e. an efficiency less than one). And "pile shadowing" is exhibited when a trailing pile's lateral capacity is diminished by soil disturbance caused by the leading pile.

The complexity of group interaction is evidenced by the number of analytical models that have been outlined for dealing with the phenomena. There are five general types of models:

1. finite element
2. continuum
3. modified continuum
4. modified unit load transfer
5. hybrid

All these methods address the complex nature of pile group interaction and attempt to predict outcomes with varying degrees of success.

A qualitative and simple method that has been used to some success is the p multiplier method as suggested by Brown, Morrison, and Reese (1988), which accounts for the group effects. This concept softens the p-y curves according to the row position of the pile in question. The multipliers applied to the p-y curves are highly debatable and depend on a number of soil, pile, and group parameters. The multipliers used have been generated from full scale testing of pile groups and vary from test to test.

Seismic Response

The seismic response of a pile group is complex. Pile group response is affected by linear and nonlinear soil properties, frequency content and amplitude of the seismic disturbance, and the natural frequency and damping of the structure-foundation-soil unit. Group response is dominated by dynamic soil structure interaction or DSSI. For a group of piles in soil, DSSI is composed of two separate phenomena; inertial effects and kinematic effects; O'Reilly and Brown (1991). These effects are induced

by ground motion that originated at the seismic source. Free field motion is the ground motion one would experience at the soil surface. Near field motion is a transformation of free field motion due to properties of the structure and its foundation. Pile group response is unique to the dynamic properties of the structure-foundation-soil unit, therefore the foundation, surrounding soil, and structure must be coupled in analysis.

Kinematic effects are due to wave scatter when an incoming energy wave strikes a stiffness discontinuity. When a energy wave emanating from the seismic source reaches a pile group, the wave is diffracted and reflected in an infinite number of directions resulting in constructive and destructive wave interference; the wave cannot follow its free field pattern. This results in highly varied energy dissipation over a small area. Kinematic interaction will occur whenever stiffness of the foundation resists development of free field motion; Krammer (1996).

Inertial effects are due to mass discontinuity between the soil and the foundation. The impedance of the foundation and its inability to flex and absorb energy like the soil results in structural vibrations. The foundation moves in response to the soil movement as dictated by its natural frequency and damping. This movement is highly dependent on the frequency content and amplitude of the ground motion and its relation to the dynamic properties of the foundation; Krammer (1996).

For a complete list of reviewed literature see the extended bibliography in Appendix A.

CHAPTER III

GROUP PREDICTIONS

Predicting the group response prior to testing was necessary for designing the testing equipment. Specifically, maximum displacements were required to conFigure the LVDTs, and maximum loads were needed to design the loading system. Two software packages were used to make predictions: COM624P (v 2.0) and FLORIDA-PIER (v. 5.21). The exact dimensions, stiffness, and elastic characteristics of the model group could be entered and analyzed by both programs, eliminating any dimensional interpretation of the results. At the outset of this research, the objective was to validate FLORIDA-PIER for use in Utah in deep foundation design. On completion of this research the predictions were useful in pinpointing the deficiencies of current design methods for deep foundations in clay soil subjected to cyclic lateral loading.

COM624P

COM624P uses a finite difference method to solve differential equation 2.1. COM624P was designed to deal with single isolated piles but can be used for pile group analysis following the suggestions of Brown and Bollman (1993) as outlined in the Federal Highway Administration Manual, Volume I (1996). Using COM624P for group analysis does not account for group effects or pile shadowing but will give reasonable numbers for group deflection, bending moment, etc. Default p-y curves for soft clay below the water table were chosen. The input soil properties were measured *in-situ* at the testing facility and at the lab from soil samples. Cyclic loading was stipulated by entering the desired number of cycles and the program was run. The output p-y curves were then scaled using p-y multipliers to model each pile's respective nonlinear lateral response characteristics. P-y multipliers of 0.8 for the lead pile, 0.4 for the second pile, and 0.3 for each subsequent pile were applied as per recommendations.

The p-y curves were scaled manually using a spreadsheet and then entered back into a COM624P input file. The software was then run for each pile and the results averaged to give group predictions.

FLORIDA-PIER

FLORIDA-PIER (FLPIER) is a nonlinear finite element program that also solves differential equation 2.1. FLPIER was designed to analyze bridge pier structures and can account for group and shadowing effects. The nonlinear lateral response was modeled using p-y curves with p-y multipliers applied to each respective pile in the group according to its group location. The p-y curves used in the FLPIER predictions are the same default curves that were used in COM624P. The multipliers were the same as well.

Utility of Predictions

Predictions from FLPIER and COM624P provided a range of deflections and bending stresses that could be used as target parameters for the design of the testing equipment. Plots of the predictions are shown in Figures 10 to 13. The purchase and design of the equipment relied heavily on the deflection predictions. For instance, the LVDT range had to be known before investing in such expensive measuring devices. The predictions proved vital not only to design and set up of the testing equipment but also to the analysis and interpretation of the empirical results.

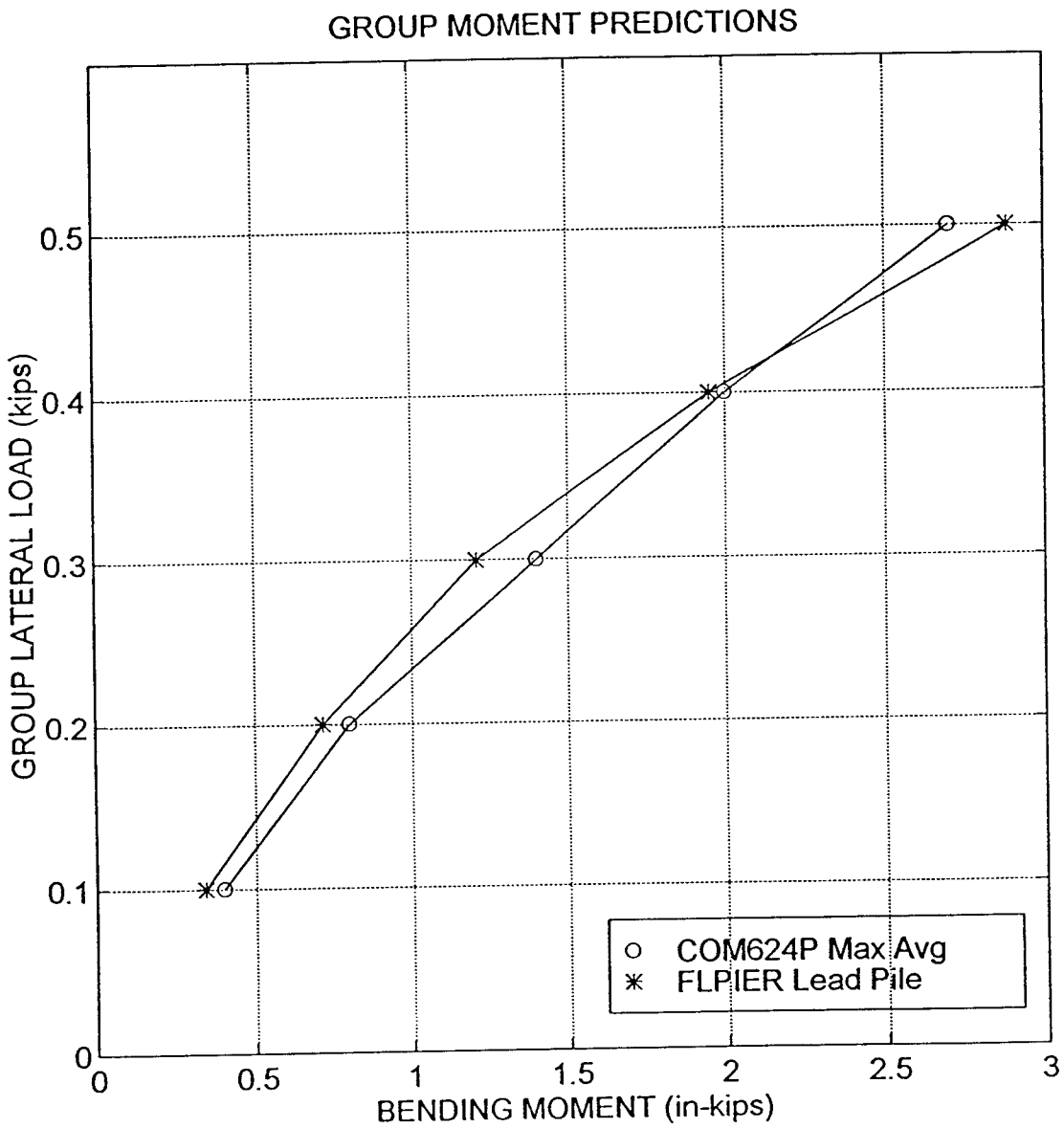

Figure 10. Software moment predictions (English units).

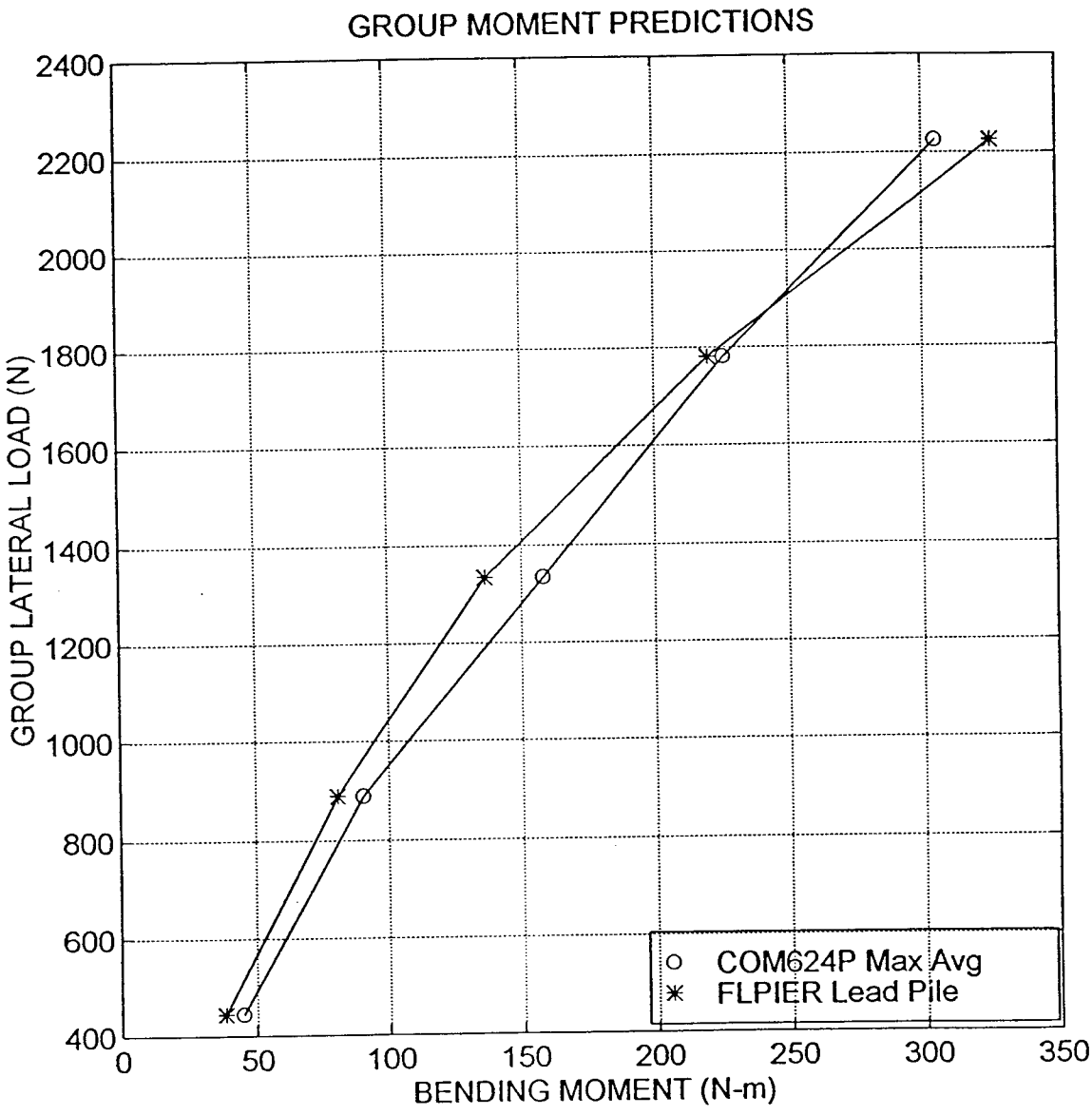

Figure 11. Software moment predictions (SI units).

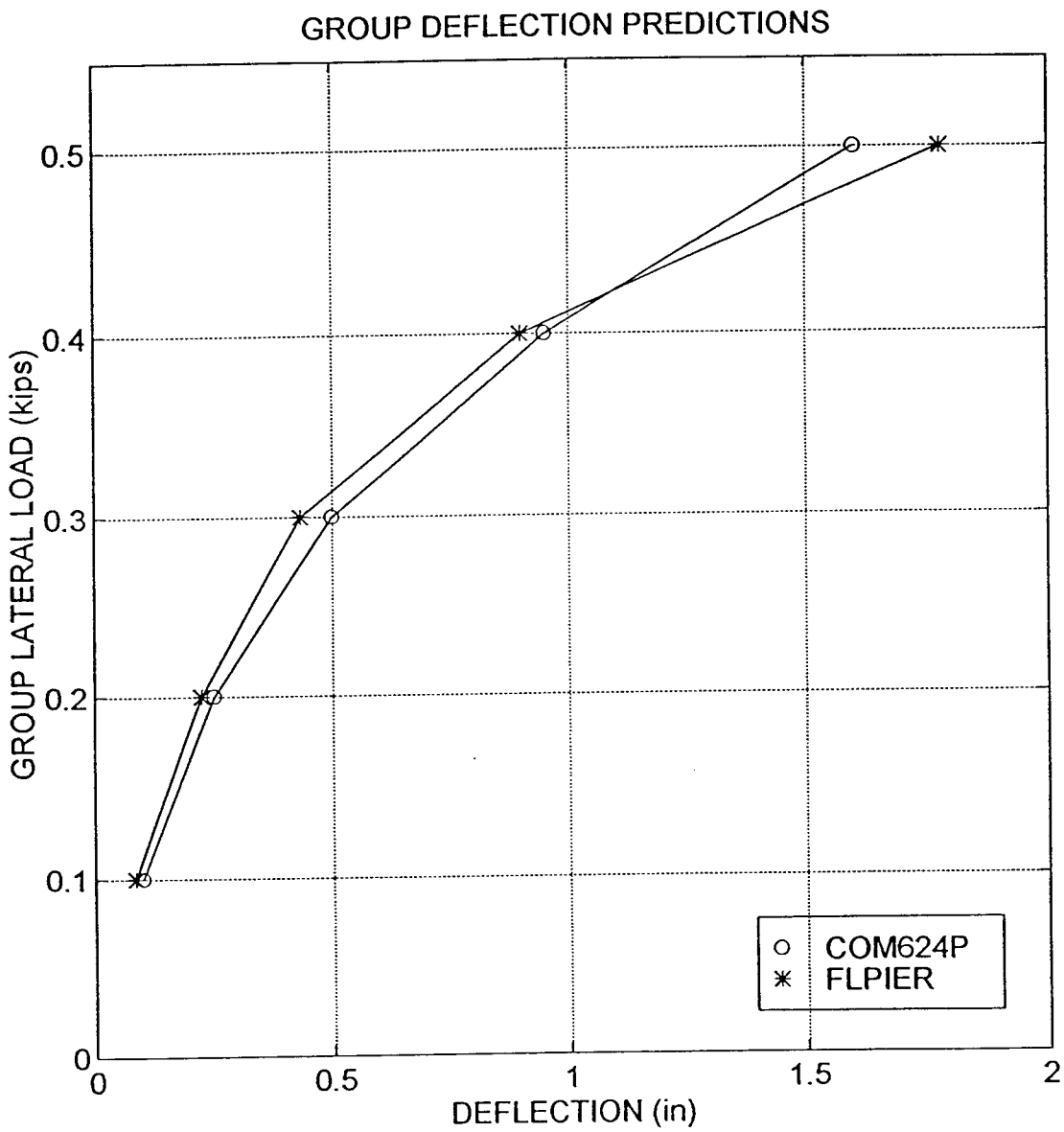

Figure 12. Software deflection predictions (English units).

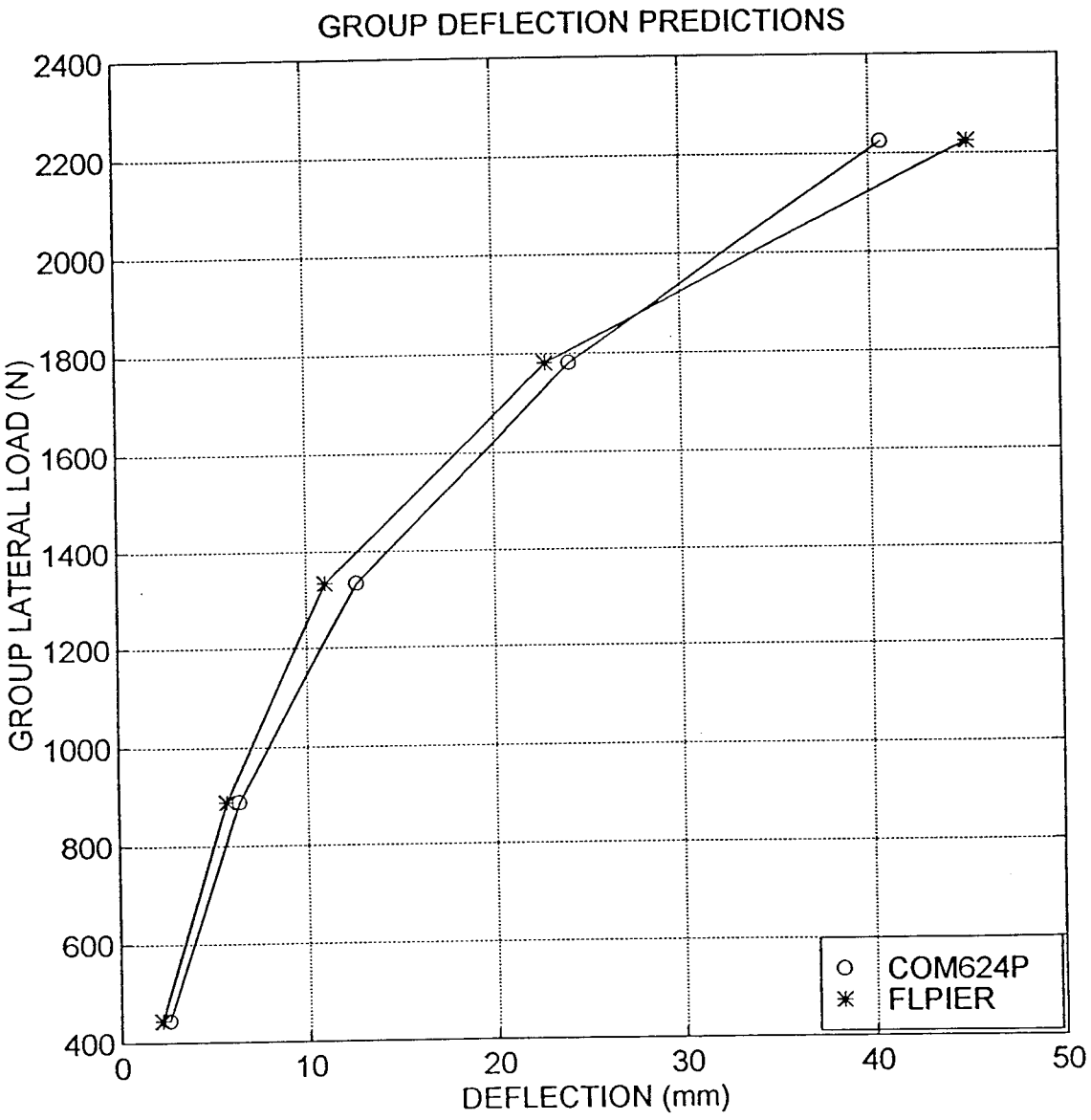

Figure 13. Software deflection predictions (SI units).

CHAPTER IV

DATA EXTRACTION AND REDUCTION

The extraction and reduction of data from the 52 megabytes of data was a major task. The data was organized into files for every half cycle (i.e. left cycle 1, right cycle 1, left cycle 2, etc...). Each file was composed of numbers of 16 by 16 matrices that constituted one sample at a specific load. With a rate of four samples per second and the half cycle loadings lasting approximately a minute, the files contained on the order of 200 to 300 matrices each. The data was arranged as shown in Figures 14 and 15. MATLAB (v. 4), a powerful tool that accepts commands in Fortran like hard code from subroutines called M files, was used in all reduction and results generation procedures for this research.

Identification

The first step in data manipulation was identifying the specific matrices of interest. We chose seven loads to work with; 150, 200, 250, 300, 350, 400, and 450lb (665, 890, 1110, 1335, 1555, 1780, and 2000N). The cycle numbers that these loads were extracted from were cycles 1, 5, 10, 25, 50. The true loads had to be calculated for each 16 by 16 matrix since the calibration factors were determined after the testing was complete. An M file was created to calculate the true loads and identify the location of these matrices in the file for the cycles and loads of interest. These matrices could then be extracted from the bulk of the data for further analysis.

left1(1729:1744,:)

108.0000	288.4727	0.4138	0.4956	0.3845	0.3857	0.1099	0.3711	0.3223	0.5249	0.3735	0.5359	0.4163	0.4492	0.3003	2.4988
108.0000	288.4727	0.3760	0.5127	0.4199	0.4724	-0.0195	0.4150	0.3430	0.5017	0.3210	0.5994	0.3833	0.3870	0.5090	2.4988
108.0000	288.4727	0.3467	0.5396	0.3748	0.4468	-0.0378	0.4285	0.2588	0.5664	0.3015	0.6006	0.4053	0.4053	0.3821	2.4988
108.0000	288.4727	0.4150	0.5103	0.4089	0.4822	0.0049	0.4272	0.3333	0.5286	0.3040	0.6018	0.3711	0.3796	0.4089	2.4988
108.0000	288.4727	0.4785	0.4883	0.3784	0.4297	0.0073	0.3992	0.2881	0.5469	0.3418	0.5603	0.4272	0.4053	0.3906	2.4988
108.0000	288.4727	0.4932	0.4272	0.4114	0.4321	0.0171	0.3796	0.3406	0.4846	0.3638	0.5457	0.3857	0.4663	0.3833	2.4988
108.0000	288.4727	0.5225	0.3857	0.4260	0.3809	0.0537	0.3406	0.3503	0.4712	0.3882	0.4956	0.4150	0.4224	0.3174	2.4988
108.0000	288.4727	0.5359	0.3967	0.4346	0.3552	0.0732	0.3552	0.3918	0.4456	0.4163	0.4822	0.4248	0.4236	0.4480	2.4988
108.0000	288.4727	0.5396	0.3857	0.4419	0.3625	0.1257	0.3308	0.4297	0.4431	0.4016	0.5115	0.4150	0.3967	0.4858	2.4988
108.0000	288.4727	0.4895	0.3821	0.4541	0.3577	0.1062	0.3735	0.4028	0.4517	0.3931	0.5286	0.4163	0.3369	0.4346	2.4988
108.0000	288.4727	0.5115	0.4126	0.4553	0.3540	0.0903	0.2820	0.3894	0.4529	0.3955	0.5237	0.4077	0.4358	0.3357	2.4988
108.0000	288.4727	0.5054	0.4175	0.4419	0.3711	0.1074	0.4626	0.3735	0.4688	0.3967	0.4602	0.4187	0.3870	0.4077	2.4988
108.0000	288.4727	0.4883	0.5200	0.4773	0.3638	0.0891	0.8276	0.3894	0.4309	0.4480	0.4529	0.3955	0.3906	2.4988	2.4988
108.0000	288.4727	0.5042	0.4395	0.4517	-2.5000	0.0220	0.3430	0.4150	0.4407	0.4236	0.4517	0.3906	0.4041	2.4988	2.4988
108.0000	288.4727	2.4988	2.4988	2.4988	2.4988	2.4988	2.4988	2.4988	2.4988	2.4988	2.4988	2.4988	2.4988	2.4988	0.1672
108.0000	288.4727	2.4988	2.4988	2.4988	2.4988	-0.5774	2.4988	2.4988	2.4988	2.4988	2.4988	2.4988	2.4988	2.4988	-0.0476

Figure 14. Data file matrix.

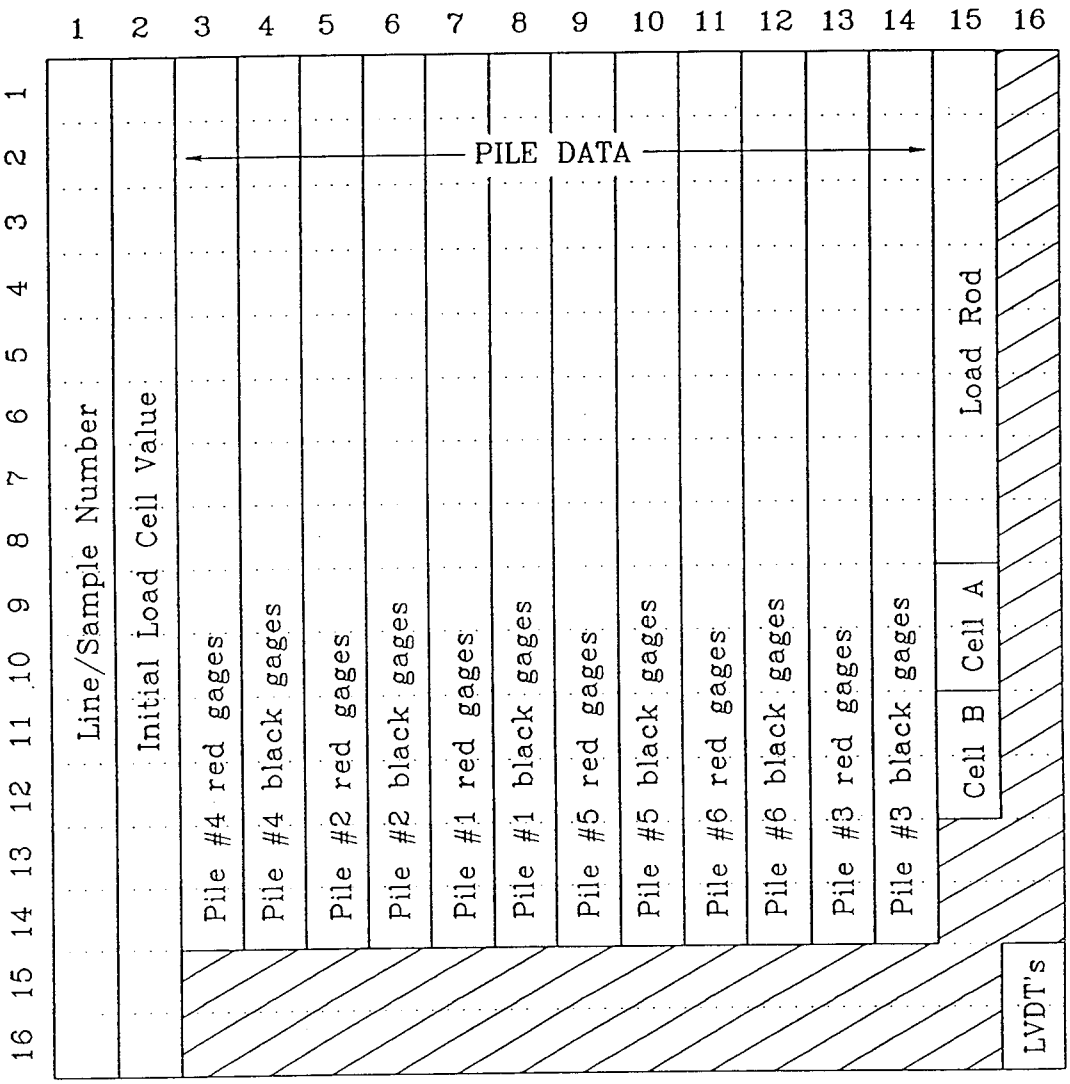

Figure 15. Schematic of raw data matrix.

Zeroing and Balancing of Defective Gages

Further steps had to be taken before data could actually represent something useable. Once the specific matrices of interest were identified they were extracted and stored under variable names that identified the half cycle direction, cycle number, and load each represented — 98 matrices in all. The zero matrix was then subtracted from each stored matrix. The zero matrix was the initial reading at the start of the test. Subtracting it removed most of the inherent electrical noise in the system and gave the actual readings for each channel. Two of the 140 strain gages instrumenting the pile group were defective (gage 11 black in pile 1 and gage 2 red in pile 2). Designing the pile instrumentation to be redundant at each depth was done to accommodate just such a problem. The two erroneous gage readings were replaced by the negative reading of its pair in each matrix of data. The raw data was now in a useable form for calculating moment distributions, load distributions, deflection curves, p-y curves, etc.

Moments, Loads, and Deflections

Generating results for moments, loads, and deflections involved different MATLAB procedures for each. Many M files often were required to process the data to generate one class of results. The steps are outlined as follows:

Moment Distributions

Moment distribution generation was a lengthy process. First, the calibration factors for each strain gage were entered and stored under their own variable according to the pile number and gage color (red or black). The factors were then multiplied by the raw data for each pile and stored as a 14 by 12 matrix. The data was now in a corrected voltage form. To calculate moment from voltage, the data had to be converted to strain (equation 4.1), then stress (equation 4.2), and finally to bending moment (equation 4.3).

$$\epsilon = \frac{V_o(R_2+R_3)^2}{V_s S R_2 R_3 \text{Amplification}} \quad \ldots\ldots\ldots\ldots\ldots\ldots\ldots\ldots \quad (4.1)$$

ϵ = strain (in/in)

V_o = voltage difference (volts)

R_2 = resistance of resistors in the bridge (160 Ohms)

R_3 = resistance of strain gage (120 Ohms)

V_s = magnitude of supply voltage (5 volts)

S = stain gage factor (2.11)

Amplification= 100

$$\sigma = E\epsilon \quad \ldots\ldots\ldots\ldots\ldots\ldots\ldots\ldots\ldots\ldots\ldots\ldots\ldots\ldots\ldots\ldots \quad (4.2)$$

σ = stress (psi)

E = modulus of elasticity (10,000,000 psi for aluminum)

ϵ = stain (in/in)

$$M = \frac{\sigma I}{c} \quad \ldots\ldots\ldots\ldots\ldots\ldots\ldots\ldots\ldots\ldots\ldots\ldots\ldots\ldots\ldots\ldots \quad (4.3)$$

M = bending moment (in*lb)

σ = stress (psi)

I = moment of inertia (0.08734 in^4)

c = distance from neutral axis to furthest most fiber (0.5245 in)

The moments were calculated for each pile with the red and black gages averaged. The calculations were accomplished with a master M file for each pile encompassing all loads and cycles for loading left and right. Separate M files were then created to generate plots for load distribution with depth per pile and cycle (35 plots) and group load distribution with depth per load and cycle (35 plots).

Load Distributions

Load distribution data was derived from the load cells mounted on the load rod and the master load cells at the ends of the rod (Figure 16). The raw data was converted from voltage to corrected voltage using calibration factors, to strain (equation 4.1), to stress (equation 4.2), and finally to load (equation 4.4).

$$P = \sigma A \quad \ldots\ldots\ldots\ldots\ldots\ldots\ldots\ldots\ldots\ldots\ldots\ldots\ldots\ldots\ldots\ldots\ldots\ldots\ldots\ldots \quad (4.4)$$

P = lateral load (lb)

σ = stress (psi)

A = cross sectional area (0.09375 in^2)

The load readings for each location were an average of the top and bottom strain gages to give a true load reading. An M file per load and cycle were used to calculate and plot the load distribution between the piles of the group (35 plots).

Deflections

Load values for the deflection curves were generated using the same procedure as the load distribution curves. Deflection measurements were acquired from the red LVDT (Figure 17). The raw data from the LVDT simply needed to be multiplied by a calibration factor to convert from voltage to length measurements. M files were written to plot load vs. deflection for each cycle and a composite of all the cycles (6 plots).

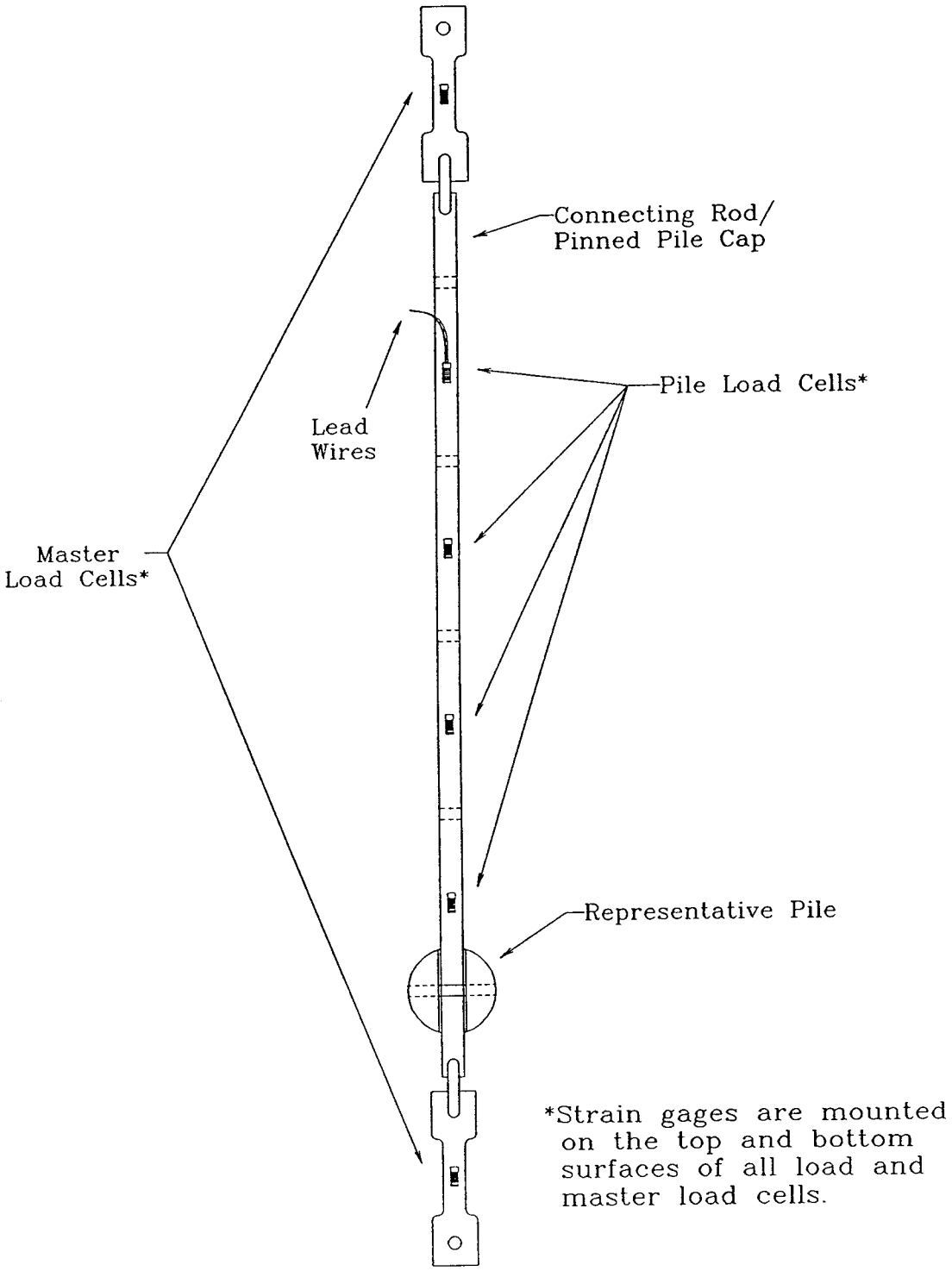

Figure 16. Load measuring equipment.

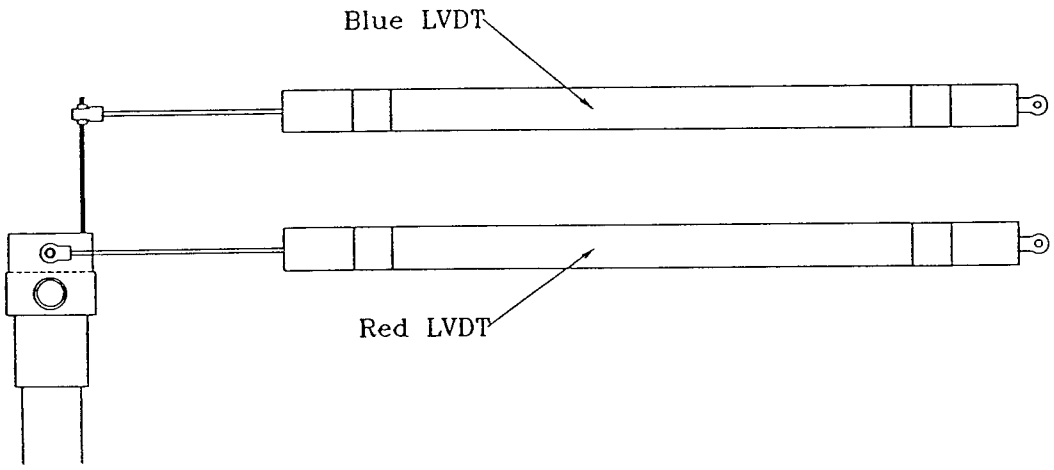

Figure 17. LVDT configuration.

P-Y Curves

When modeling the soil as nonlinear springs (i.e. Winkler model), the response to lateral loads can be expressed as a fourth order differential equation as given by Brown and Reese (1985), shown as equation 4.5.

$$EI\frac{d^4y}{dz^4} + Px\frac{d^2y}{dz^2} + E_sy - w = 0 \quad \text{..... (4.5)}$$

Using the bending moment data calculated in the first portion of the data reduction process, the soil resistance per unit length of pile, p (equation 2.2), and the deflection, y (equation 2.3), for the nonlinear springs can been determined (equations reprinted below).

$$p = \frac{d^2M(z)}{dz^2} \quad \text{..... (2.2)}$$

$$y = \frac{1}{EI}\int\int M(z)\, dz \quad \text{..... (2.3)}$$

Boundary Conditions

To solve the three constants of integration that result from integrating equation 4.1, certain boundary conditions had to be known. The three boundary conditions were; bending moment at the top of the pile, pile top slope, and pile top deflection. The pinned connection that held each pile to the connection rod was designed as a moment free connection to apply it as a boundary condition when generating the p-y curves. The pile top slope and deflection was determined from the two LVDTs placed at the pile tops. The red LVDT was located at the point of load application for the pile group and the blue LVDT was located 3in (76mm) above this. The LVDT data was multiplied by its respective calibration constants which was in volts per inch. The data was then averaged for left and right loading per cycle.

The slope was determined by taking the arctan of the difference of the two LVDTs and dividing that by the vertical distance between them. Converting this to radians renders the slope in a useable form for a boundary condition. The deflection was taken from the red LVDT in a similar manner.

Deflections

$$M = f(z) \quad \Rightarrow \quad \Theta = \int M(z) \quad \Rightarrow \quad y = \int\int M(z$$

M = moment: BC M(top) = 0

θ = slope: BC θ(top) = measured slope

y = deflection: BC y(top) = measured deflection

Soil Resistance

$$M = f(z) \quad \Rightarrow \quad V = \frac{dM(z)}{dz} \quad \Rightarrow \quad p = \frac{d^2M(z)}{dz^2}$$

M = moment: BC M(top) = 0

V = shear

p = load per unit depth

Curve Fitting

The bending moment data for loading left and right was averaged, per cycle and load. Each moment curve, consisting of seven points for the seven chosen loads, was then fit with a 4th degree polynomial after considering recommendations by Brown and Reese (1985). The boundary condition of M(top) = 0 was applied. Load per unit depth (p) was calculated by double differentiating the symbolic 4th degree polynomial and evaluating at every gage depth. A 4th degree polynomial was fit to the moment curves to achieve a function of p versus depth that was nonlinear. The 4th degree polynomial was integrated once and then evaluated at the various gage depths. The second boundary condition of

measured pile top slope was then applied and integration carried out a second time. The measured pile top deflection boundary condition was applied, and the function was evaluated at all gage depths to determine deflection (y). The results were plotted from an M file for a specific cycle and gage depth.

Cycles of Interest

According to Seed and Idriss (1982), a certain number of cycles at 65 percent the maximum shear stress for a given magnitude event can be expected. For a 7.5 magnitude event, the high end of the scale for Utah, 15 cycles is the representative number. With that in mind, p-y curves were developed for cycles 1, 2, and 15 to address this critical region of dynamic soil degradation.

CHAPTER V

USE OF NORMALIZED CURVES FOR DESIGN

The results for deflection at the pile top and maximum bending moment in the lead piles are presented in a normalized, dimensionless form for design use (Figures 18 and 19). The dimensionless factors used for plotting the deflection and bending moment results include all pertinent variables (EI = pile stiffness and D = pile diameter), except the amount of fixity at the pile cap and the free length of the piles above the soil surface (e). To use these normalized curves, one would enter into them with a design load (P) induced at the pile cap and pile properties (EI and D). The expected pile top deflection and maximum bending moment in the lead pile could then be extracted. The curves are dimensionless therefore they can be used for either SI or English units as long as the units are consistent throughout. These results are valid only for similar clay soil profiles (i.e.CL with an average undrained shear strength of 800psf/40kPa).

Fixity and Free Length

Accounting for differing fixity and free length is necessary for accurate predictions when using normalized curves. One suggestion is using normalized curves from previous research that account for differences in fixity and free length; eg. Broms' method shown in Figure 20 (Broms, 1965). The curves were derived from a single pile test, but offer a means of scaling the results from the deflection and moment curves for different fixity and free length. In other words, this allows a designer to predict bending moment and deflection of a 5x5 pile group in a CL soil with similar undrained shear strength for any fixity or free length.

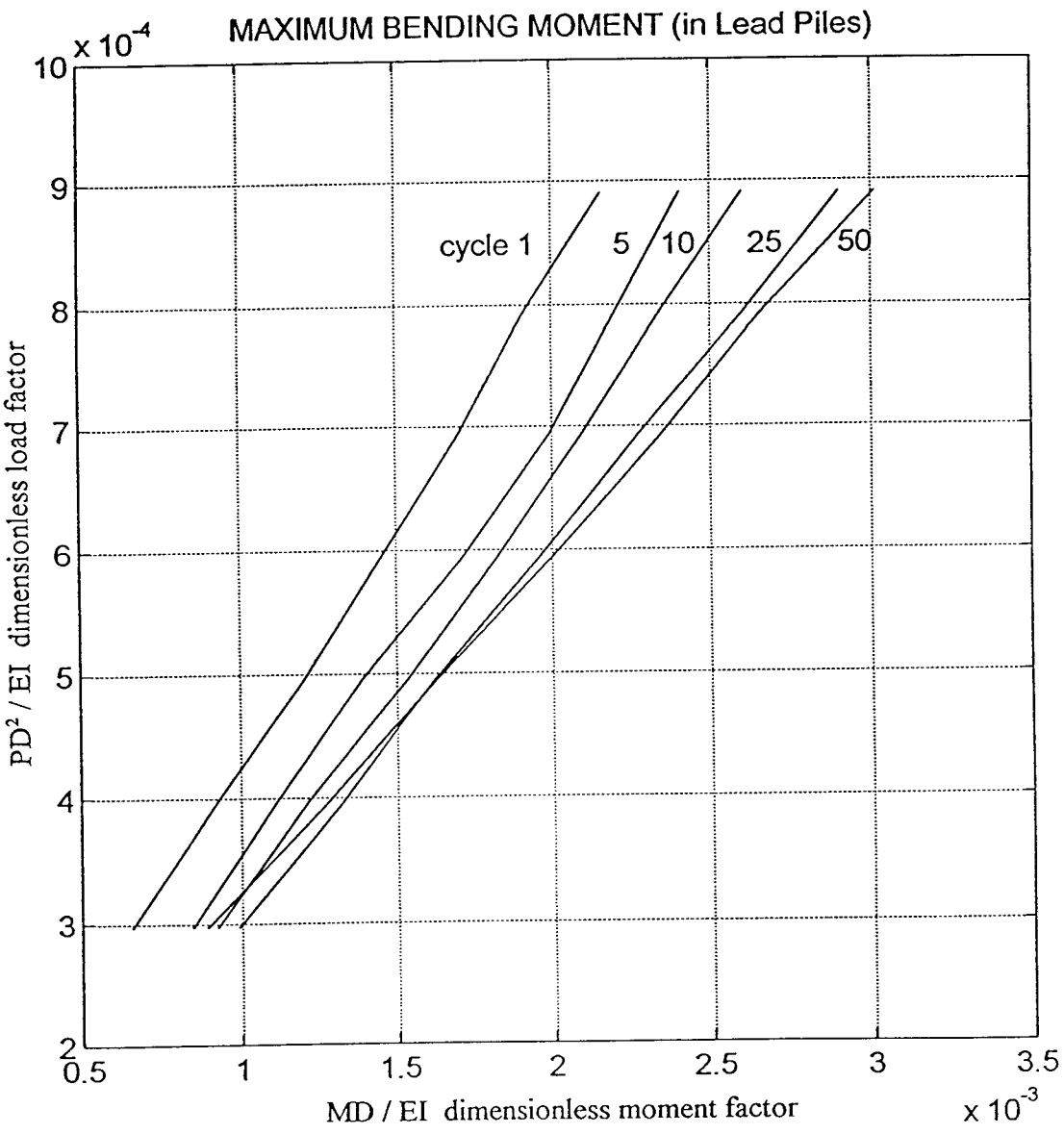

Figure 18. Normalized maximum bending moment curves.

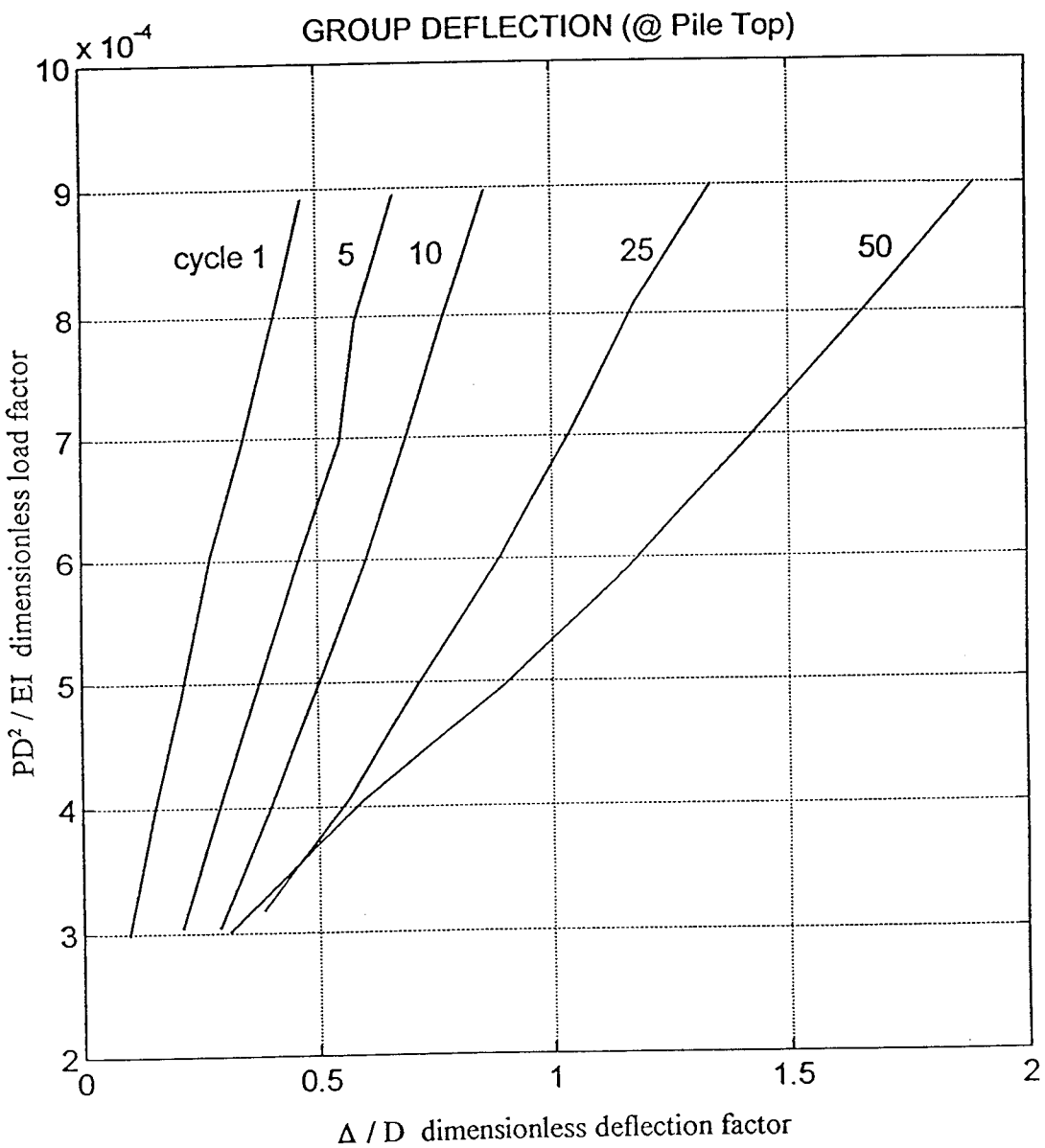

Figure 19. Normalized group deflection curves.

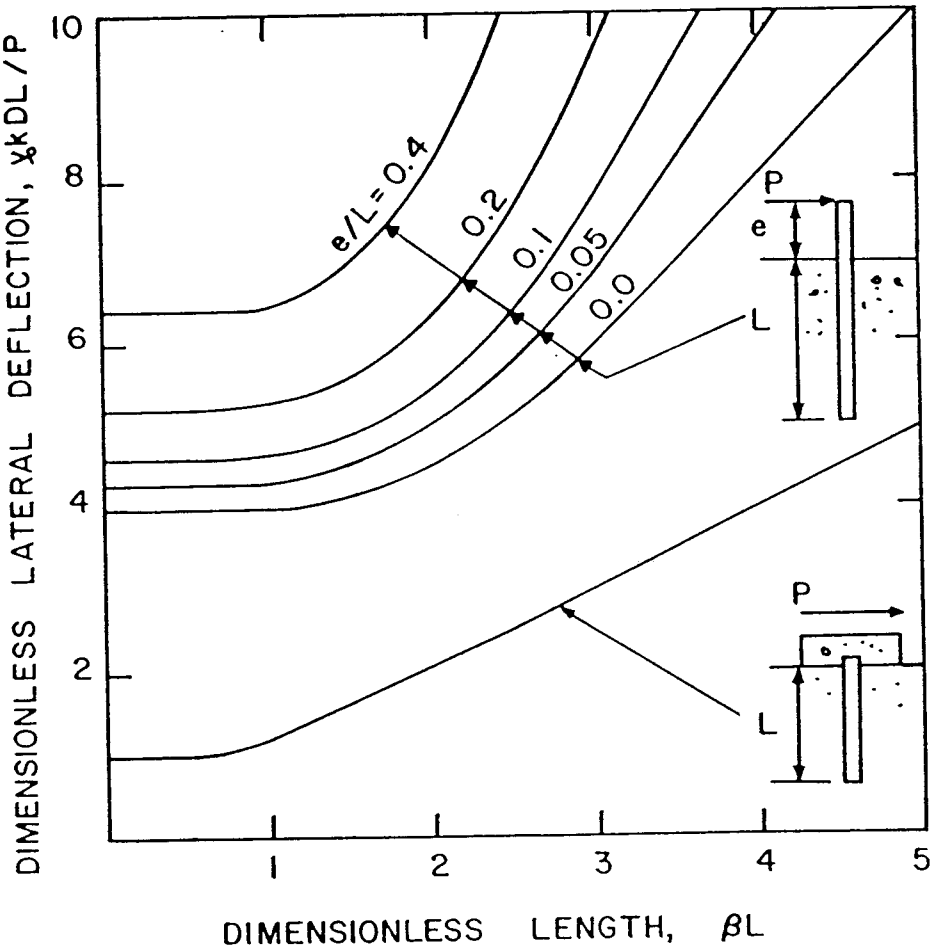

Figure 20. Fixity and free length curves from Broms (1965).

To determine a scaling factor from Brom's curves, first, calculate the dimensionless length factor βL (equation 5.1) for the design piles. Second, determine the free length to embedded length ratio, e/L, and the amount of fixity the pile group will be experiencing. The e/L ratio for the model study was 0.2. The amount of fixity is synonymous with the amount of moment that will be induced at the top of the pile group when a lateral load is applied. A free-headed pile group is free to rotate at the pile top without any induced moment, whereas a truly fixed pile group will translate with no pile top rotation at all. It is highly unlikely that a pile group can ever be truly fixed, and the fixed pile curve in Figure 20 is a theoretical lower bound. Some interpolation is required for partially fixed pile groups between the free and fixed curves. The third and last step is to calculate a scaling factor of the e/L(model) ratio to the e/L(design) ratio. Tabulated values for e/L(model) : e/L(design) ratios are presented in table 1.

$$\beta = \sqrt[4]{\frac{k_h D}{4EI}} \qquad \text{(5.1)}$$

k_h = coefficient of horizontal subgrade reaction (assumed constant in clay)

D = pile diameter

EI = pile stiffness

L = embedded length of pile

Table 1. Tabulated values of e/L(model) : e/L(design) ratios from Figure 20

Ratio			e/L (design)			
βL	0.4	0.2	0.1	0.05	0.0	fixed
0	1.23	1.00	0.89	0.83	0.76	0.19
1	1.20	1.00	0.87	0.81	0.76	0.23
2	1.30	1.00	0.86	0.79	0.73	0.33
3	-	1.00	0.81	0.73	0.63	0.31

Use of Normalized Curves

The ratio of e/L(model): e/L(design) will allow for scaling of deflections and moments for varying free length and fixity. Dimensionless deflection and moment values can be taken off Figures 18 and 19, calculated in either English or SI units for the design pile properties, and then scaled using the fixity and free length ratio. The results are deflection and moment values for a full scale 5 by 5 pile group in clay. They can be compared with predictions from known design software to provide confidence in the design parameters.

Comparison of test results to FLPIER are shown for reference (Figures 21 through 24). As the graphs show, the moment predictions compare nicely with the test results, but the deflection predictions are not that close. The discrepancy of the deflection predictions and deflection results may be explained by gapping, differing p-y shape and softness, and possibly scaling factors show up in the test results, but are unaccounted for by the FLPIER program.

Numerical Example

A geotechnical engineer was asked to design a 5-by-5 pile group in similar soil conditions. This pile group was to have no free length whatsoever; the pile cap is sitting on the soil surface but there may be some minimal rotation between the piles and the cap (a safe assumption). The group was to be

designed for a maximum lateral load of 20 tons (178kN) cycled 10 times, this based on regional seismic information and structural analysis. The piles were 60 ft (18.3m) in length and were of the closed end steel pipe variety. The coefficient of horizontal subgrade reaction was assumed to be $k_h = 500 lb/in^3$ ($3.5(10^6)$ N/m^3): see Tomlinson (1994). Given a pile stiffeness of $EI = 9(10^9) lb*in^2$ ($2.58(10^7)$ $N*m^2$) and a pile diameter of 13 in (330.2mm), the expected bending moment and deflections were determined.

Step One

First, the scaling factor is calculated:

$\beta L(design) = 1.24$

$e/L(design) = 0.0$

$e/L(model):e/L(design) = 0.75$ (from either Figure 20 or table 1)

The difference in free length and fixity was accounted for. There is a 75 percent reduction in deflections and bending moments from the model to design pile group.

Step Two

Next, the dimensionless load factor was determined:

$PD^2/EI = 7.5\ (10^{-4})$

Step Three

From the normalized deflection and moment curves (Figures 18 and 19), dimensionless deflection and moment values are taken:

$\Delta/D = 0.75$

$MD/EI = 2.25$

Step Four

The values are then brought back to dimensional form using properties of the design pile group and then scaled for the difference in free length and fixity:

$\Delta = 9.75in * 0.75 = \underline{7.3in}$ (185mm)

$M = 1.5(10^9)in*lb * 0.75 = \underline{1.13(10^9)in*lb}$ $(1.27(10^8)N*m)$

The Figures calculated are the expected response of a full scale 5-by-5 pile group, with the above soil and pile properties, subjected to 10 cycles at 20tons (178kN) lateral load.

These results are useful in determining integrity of a pile group subjected to seismic loading and in bolstering the confidence of its seismic design.

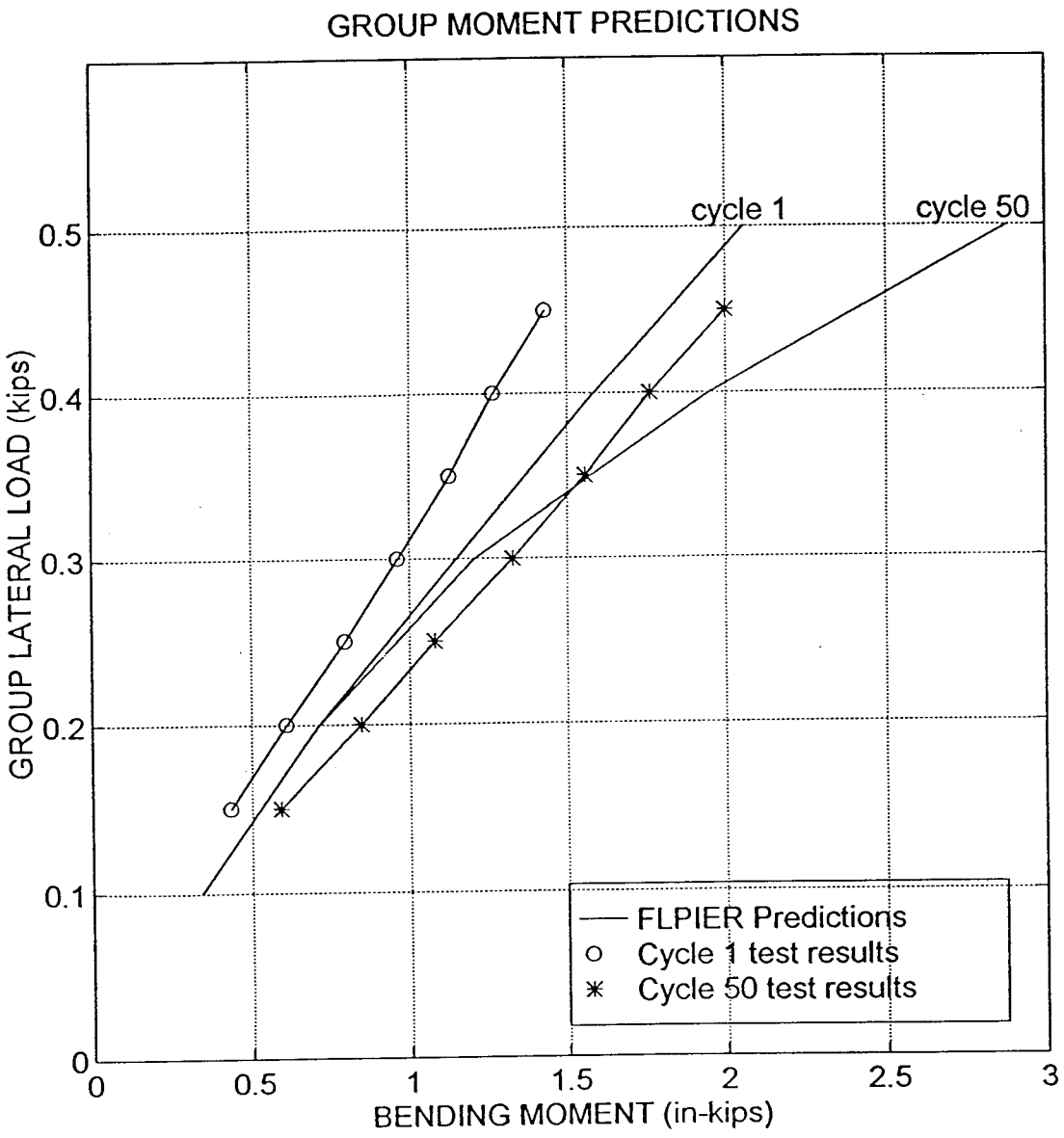

Figure 21. Comparison of maximum bending moment curves: FLPIER predictions vs. test results (English units).

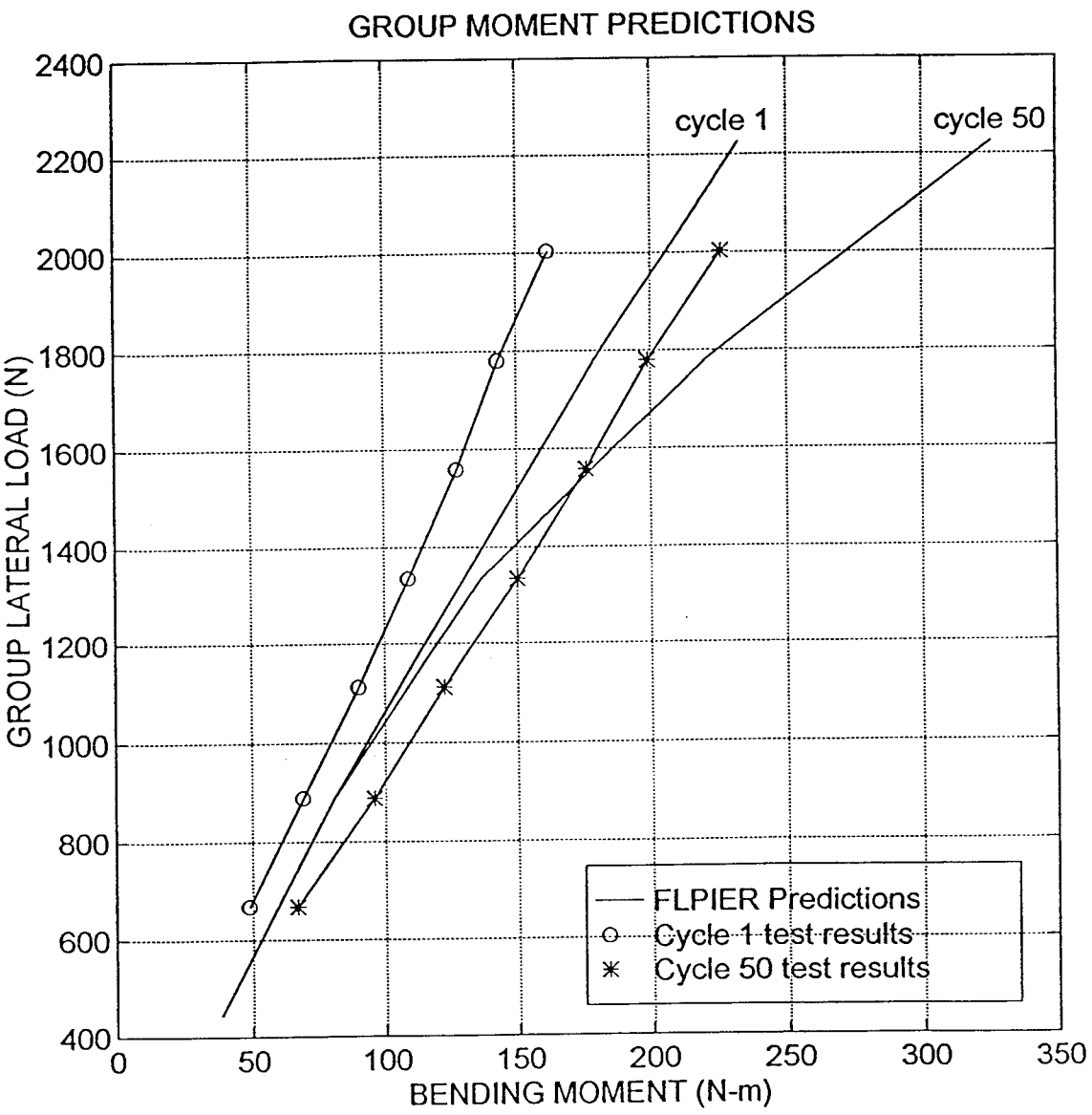

Figure 22. Comparison of maximum bending moment curves: FLPIER predictions vs. test results (SI units).

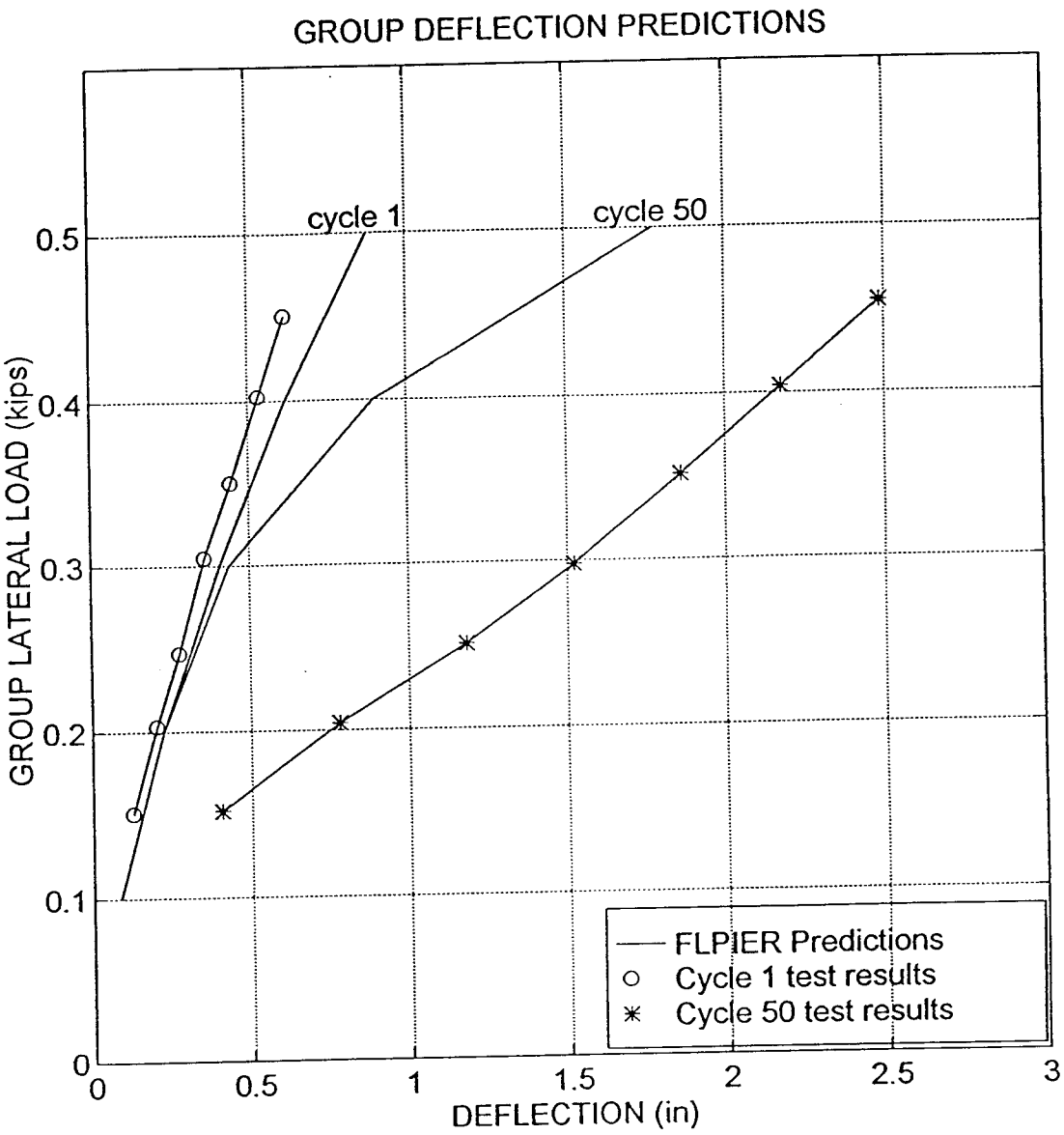

Figure 23. Comparison of group deflection curves: FLPIER predictions vs. test results (English units).

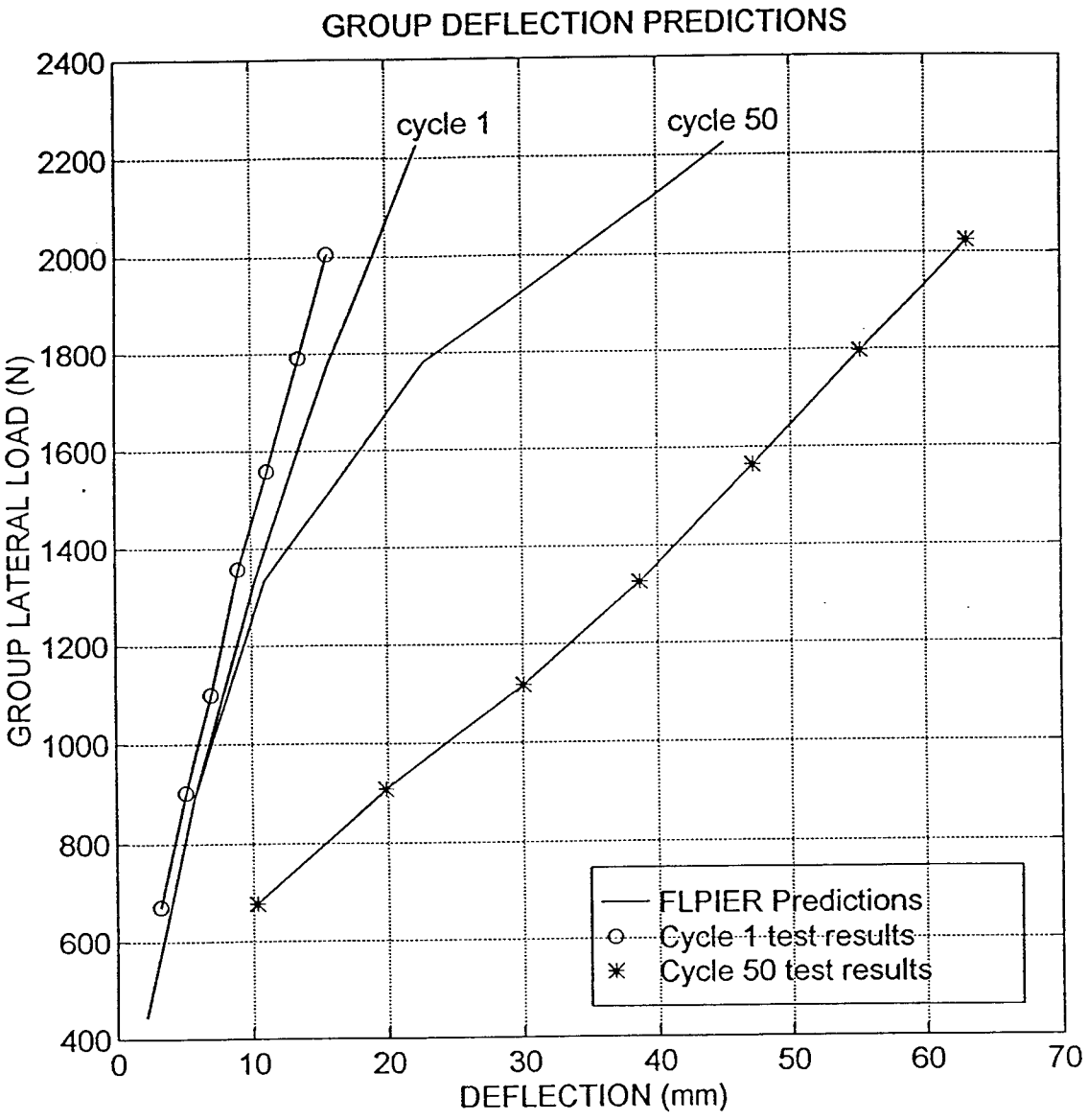

Figure 24. Comparison of group deflection curves: FLPIER predictions vs. test results (SI units).

CHAPTER VI

RESULTS

Results generated for phase 2A included bending moment with respect to load, bending moment with respect to cycle, load distribution, and load vs. deflection. A thorough discussion of this group of results can be found in Phase 2A, Rawlings (1997). The following is a short synopsis prior to delving into results for Phase 2B. The bending moment showed a gradual progression down the pile with an increase in cycles, as was to be expected. The good moment results were fortuitous since they were the basis for all p-y curve data. The load distribution data was hard to interpret conclusively which was attributed to the lack of high sensitivity in the load measuring equipment. The load vs. deflection results were the most interesting since the maximum deflections exceeded the software predicted deflections. These four classes of results can be seen in graphical form in Appendix B, Figures B1 through B16.

Deflections

The large deflections encountered were unanticipated prior to testing. As can be seen in Figures 23 or 24, the maximum expected pile top deflection was on the order of 1.7in (43mm) for 50 cycles as predicted by FLPIER. This was using input data of the exact geometry and material properties of the model pile group, the shear strength profile of the clay in the test facility, and default p-y curves for clay (eg. cyclic p-y curves for soft clay below the water table). At cycle 50 of the test, the pile top deflection of the group was on the order of 2.5in (64mm). What also can be seen from Figures 23 or 24, is that the curves for the test data show some initial offset for cycle 50 with respect to cycle 1, whereas the predicted curves originate at the same point regardless of cycle.

Interpretations of why discrepancy exists between the predicted and empirical deflection results fall into three categories, which are not mutually exclusive. The first explanation is that gapping of the soil around the pile has a significant effect on group deflection which the default p-y curves do not take

into account. A good analogy is that of cracked vs. uncracked analysis of structural beams. The default p-y curves model an uncracked analysis in which the piles are in contact with the soil at all times during cyclic loading. This is evident by the load deflection curves originating at the same point for cycles 1 through 50. The test results, however, model a cracked analysis where gapping has occurred; there is some permanent deformation. The permanent deformation is seen in the offset between cycles 1 and 50 on the load deflection curves. Load is being applied to the group but there is no soil to provide resistance due to the gap, therefore deflection is simply translation of the top of the pile group until soil resistance is encountered. Figures 25 and 26, show a hysteretic loop of the pile top deflection derived from the LVDT's. Shown is the loading and unloading of the group for cycles 1, 5, 10, 25, and 50. The unloading curves show the deflection offset due to soil gapping. Energy is absorbed by the clay as permanent deformation during lateral loading which leaves a significant and noticeable gap. The origin of each loading curve was undefined and therefore left blank, but the unloading termination point was defined well enough to show in the plots.

The second and third interpretations of the discrepancy between predicted and empirical deflection results may or may not coexist with the first interpretation. There is question as to the applicability of the default p-y curves to the Bonneville silty clay used in this experiment. A slight deviation in actual soil response from the response modeled by the default p-y curves could result in large changes in deflection. Lastly, as suggested in conversation with Dr. Mike O'Neil and Dr. Dan Brown, there could be scaling effects inherent in the model testing facility between the piles and the soil. It is the author's opinion that the large deflections can be attributed mainly to gapping with a bit of consideration given to ill fitting default p-y curves.

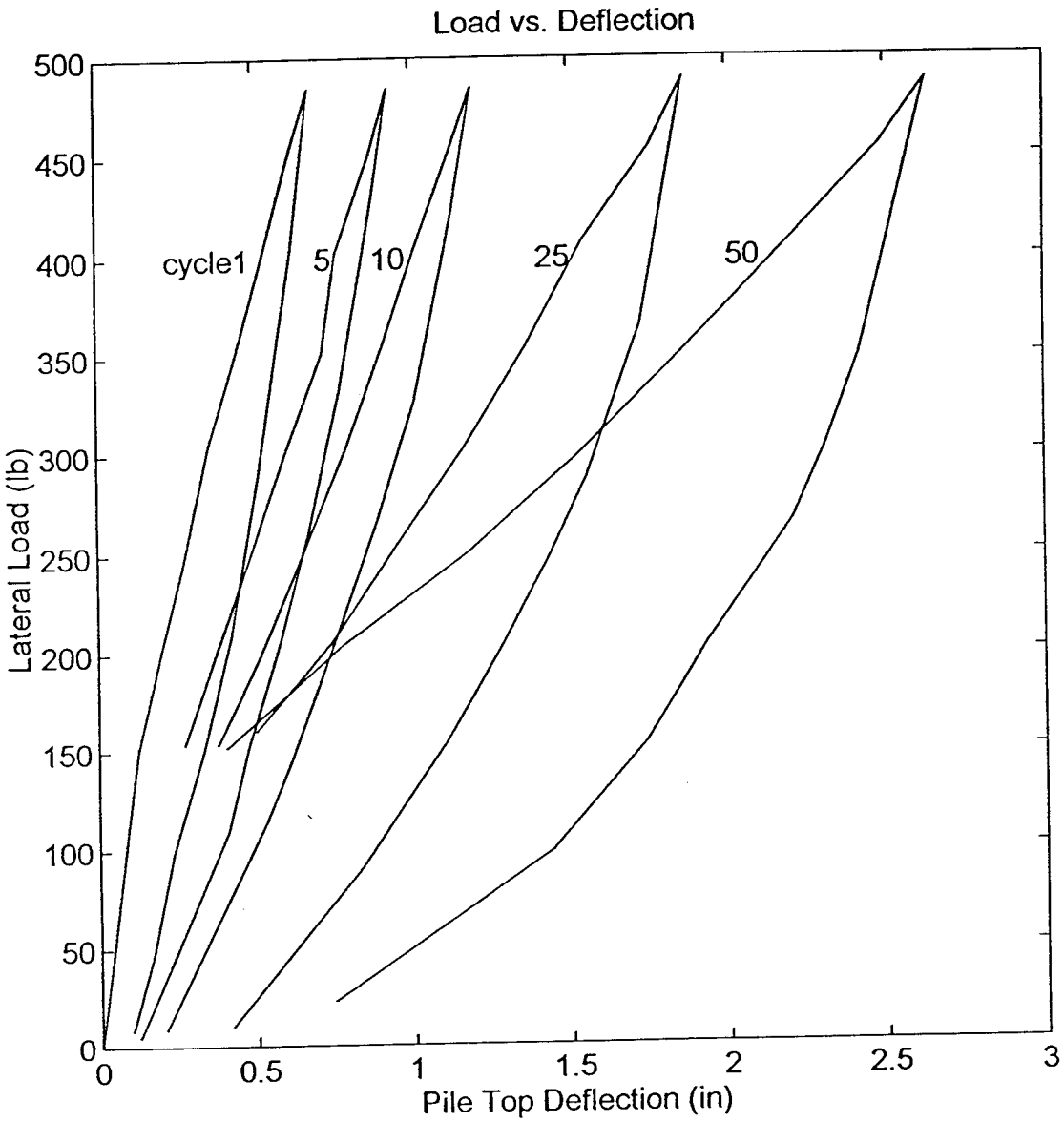

Figure 25. Hysteretic load-deflection curves (English units).

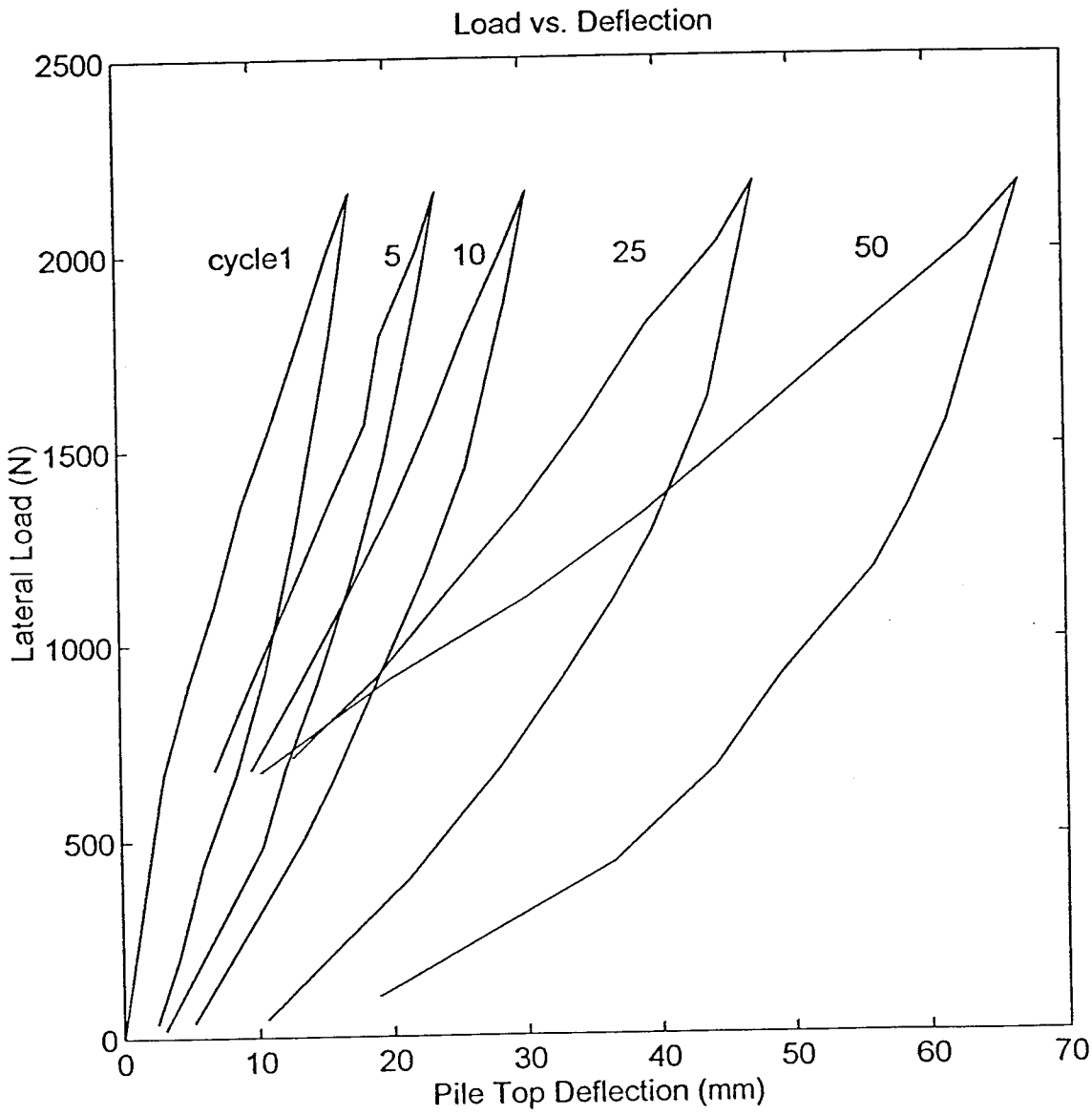

Figure 26. Hysteretic load-deflection curves (SI units).

Correlating the model pile group response to a prototype group response is accomplished using the scaling relationships determined during similitude analysis. The scaling factors are shown in equations 6.1 and 6.2, from Caliendo and Anderson (1996). A pile top deflection of 24.3 in (616mm) is expected for a prototype pile group experiencing a 22.2 ton (197.4kN) lateral load applied cyclically for 50 cycles. This large amount of deflection is reasonable when considering the free length of the model pile group, 11in (279mm), which in prototype scale is approximately 8.9 ft (2.7m). The group is in effect acting as a large cantilever, producing large deflections and bending moments. The prototype deflection was checked against a hand calculation method from Tomlinson (1994). First, the depth to the point of fixity of a single prototype pile was determined. This was added to its free length. The single pile was then modeled as a cantilever beam with a representative load applied at the end. The hand calculation gives a prototype pile top deflection of over a foot (1/3 meter), which is within the ballpark.

$$P_p = (98.6)\ P_m \quad \ldots\ldots (6.1)$$

$$\Delta_p = (9.7)\ \Delta_m \quad \ldots\ldots (6.2)$$

P = applied lateral load

Δ = deflection

p subscript = prototype pile group

m subscript = model pile group

P-Y Curves

The majority of Phase 2B consisted of generating p-y curves. The process was troublesome and highly time consuming. The p-y curves for the group were resolved only at low strain ranges due to testing and equipment limitations. The low strain ranges did not allow the curves to fully develop but do demonstrate excellent group properties and relationships. The best p-y resolution came out at depths of 1,

7, 28, and 34 in. (25, 178, 711, and 864 mm.). The best resolution occurred around the points of highest bending moment in the pile; where the most soil disturbance occurred. At regions where an inflection point occurred in the pile, the soil did not experience enough strain to push it out of the elastic region, therefore exhibiting linear response.

Plots of soil deflection (y) vs. depth, and soil resistance (p) vs. depth are shown in Figures 27 through 30. The soil resistance (p) is non-linear with depth, which was the objective when fitting moment data with a 4th order polynomial. On the soil deflection (y) plots the significant effect of large pile top deflections can be seen.

The gapping that is thought to be the culprit for excessive deflections is represented in the generated p-y curves as an offset. This offset is shown as a dashed line and was chosen by imitating the slope of the initial part of cycle 1 p-y curves. The assumption behind this being that the initial portion of cycle 1 p-y curves represents the elastic range and at low strains should be demonstrated regardless of the cycle number. The exact offset could not be determined empirically due to the unreliability of the low load range data. The p-y curves for the lead, 2nd, and 3rd piles are shown for depths 1, 7, 28, and 34 in. (25, 178, 711, and 864 mm) in Figures 31 through 54. Notice the obvious softening of the curves with an increase in cycles. The softening also is accompanied by a increase in deflection. The curves actually are pushed over as the cycles increase, a reduction in both p and y.

Curves for the lead pile at various depths are shown in Figures 55 through 60. These curves exhibit a stiffening as depth increases along the length of the pile. This behavior was typical for each pile and was the expected behavior. The offsets were taken off the previous set of p-y curves.

The p-multiplier method (see Brown, Morrison, and Reese, 1988) used to scale p-y curves for cyclic design purposes is a useful but highly generalized tool. It allows scaling of p-y curves for various group row positions from single pile p-y curves thereby eliminating the need for a full scale group test to generate p-y curves for each row position. Figures 61 through 64 were generated to address this issue. These plots show a similar trend as found by Brown, Morrison, and Reese, but demonstrate a pushing

over of the single pile curve and not simply a reduction of the soil resistance (i.e. p-multiplier). These curves are at too low of a strain range to be useful in determining a p-multiplier and there must be many more tests done to come to a statistical conclusion. From preliminary analysis at the highest strain range of this test the p-multipliers for the lead, 2nd, and 3rd rows are 0.60, 0.45, and 0.40 respectively.

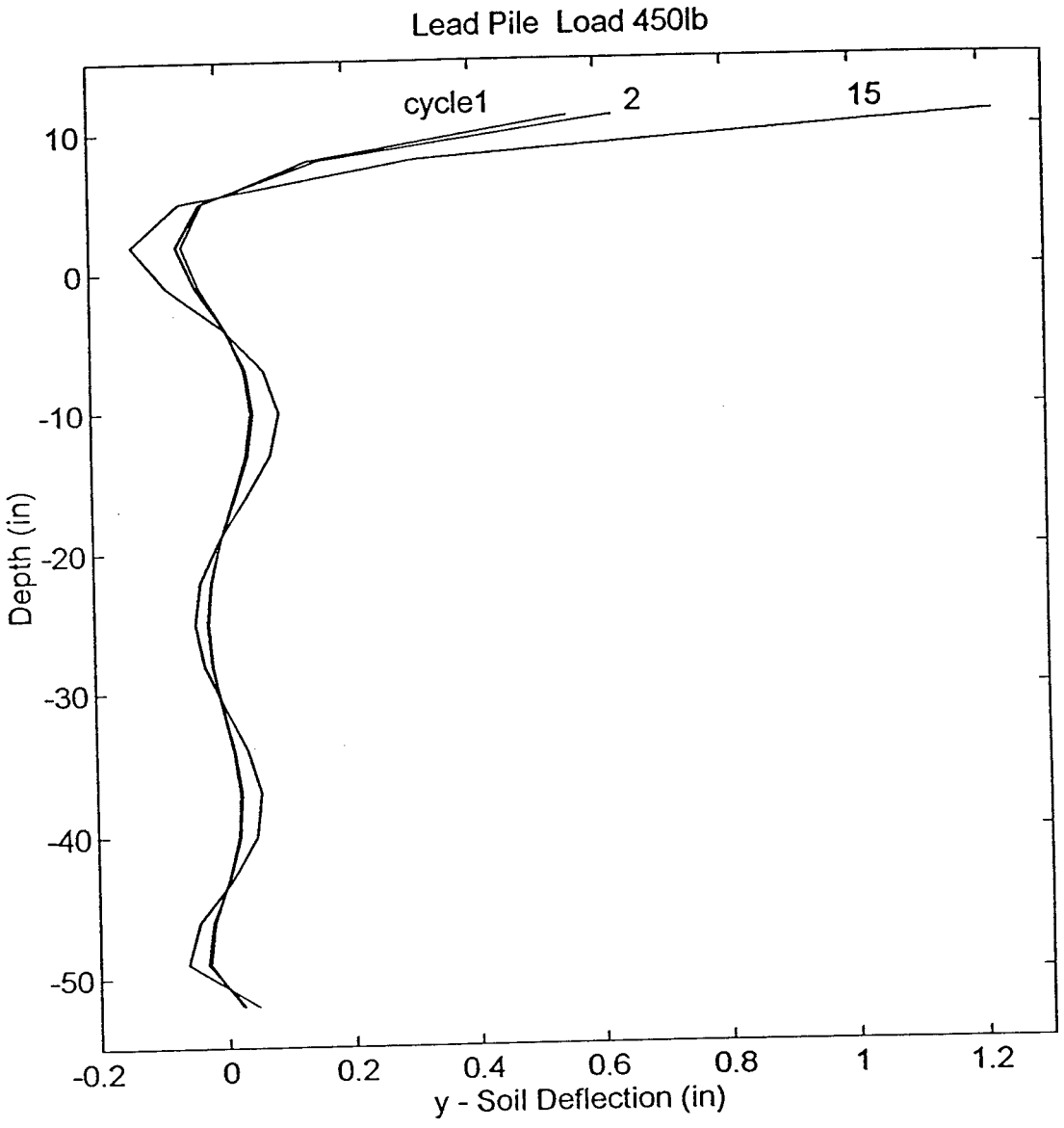

Figure 27. Soil deflection with depth (English units).

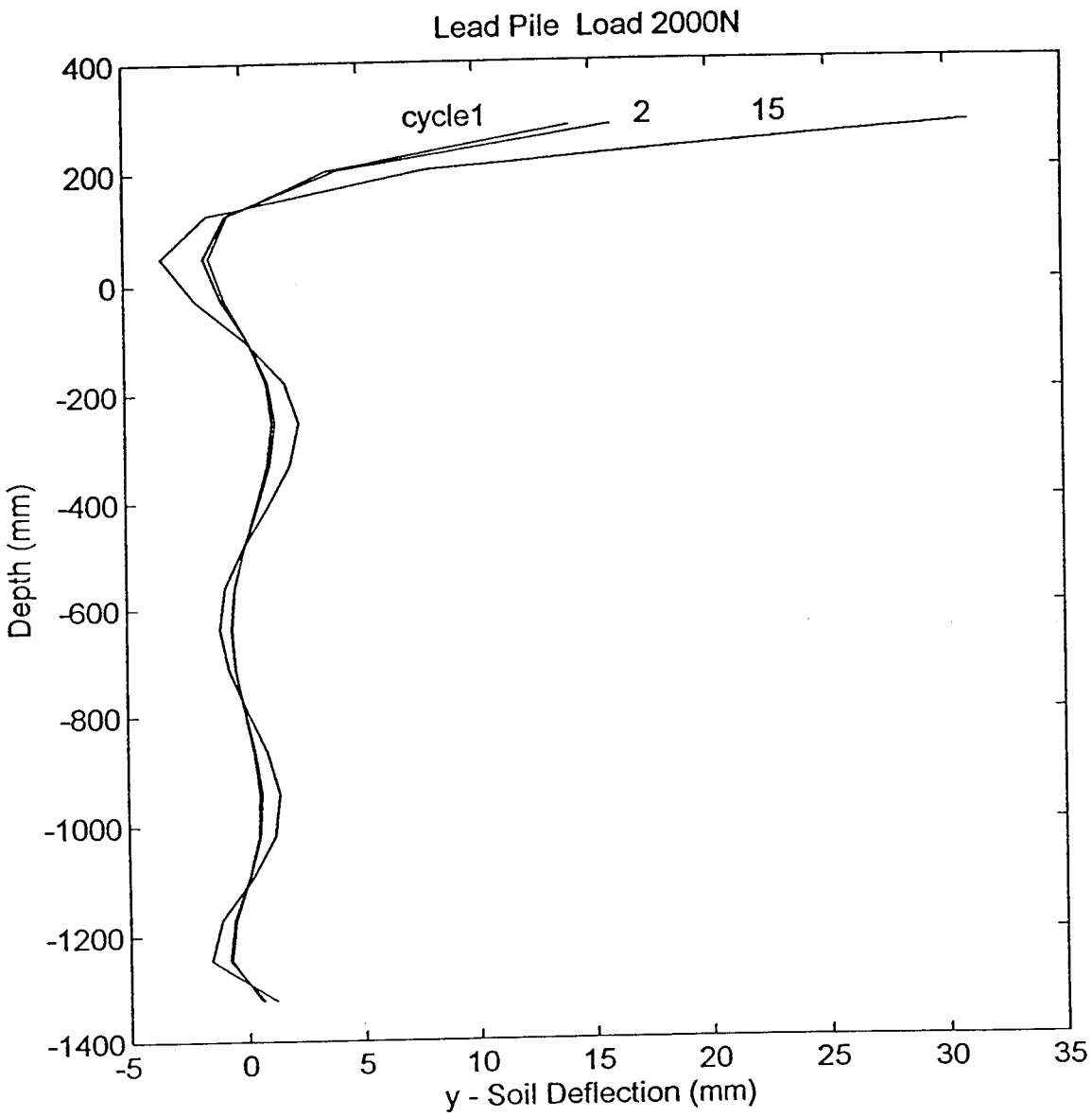

Figure 28. Soil deflection with depth (SI units).

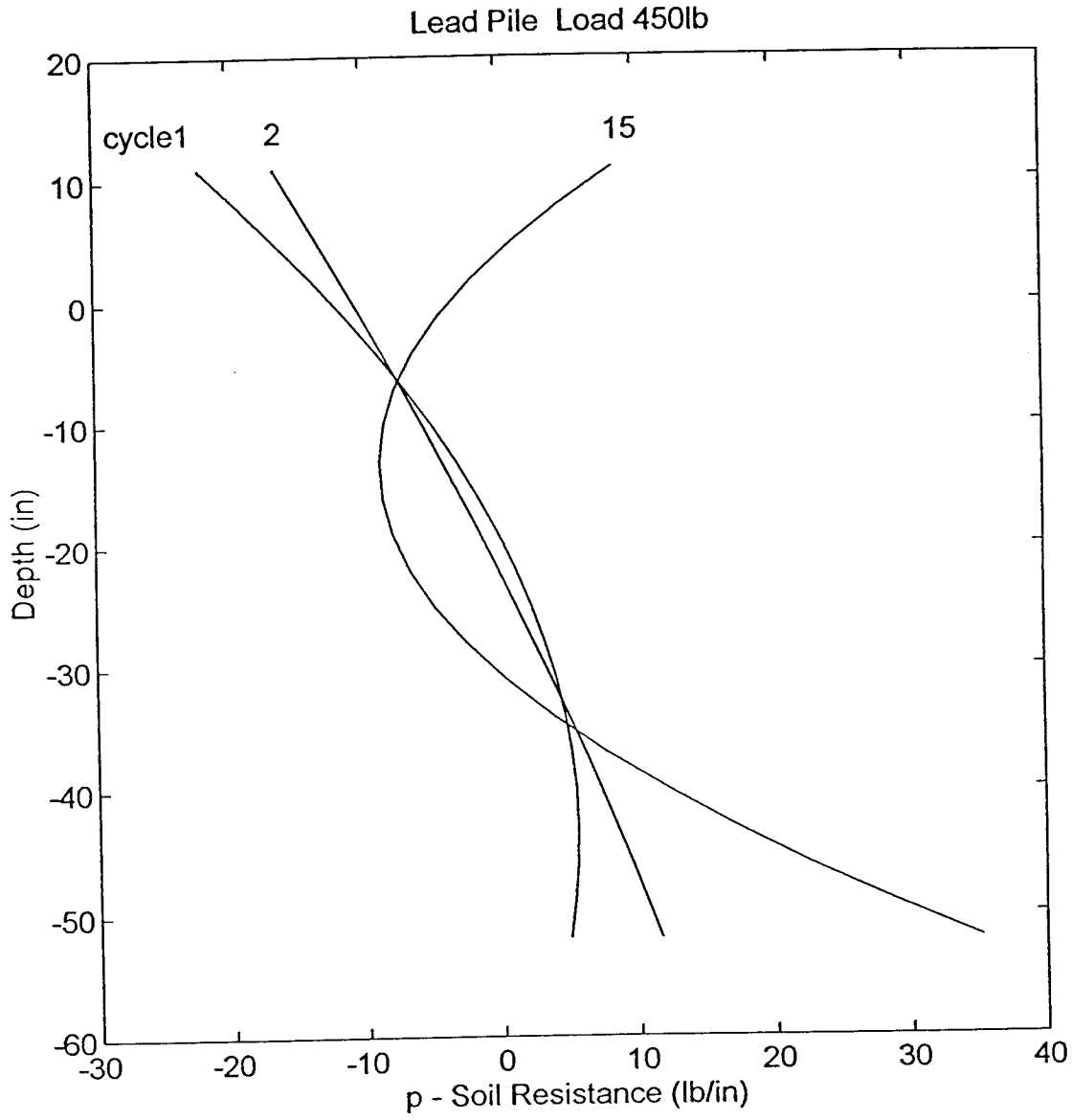

Figure 29. Soil resistance with depth (English units).

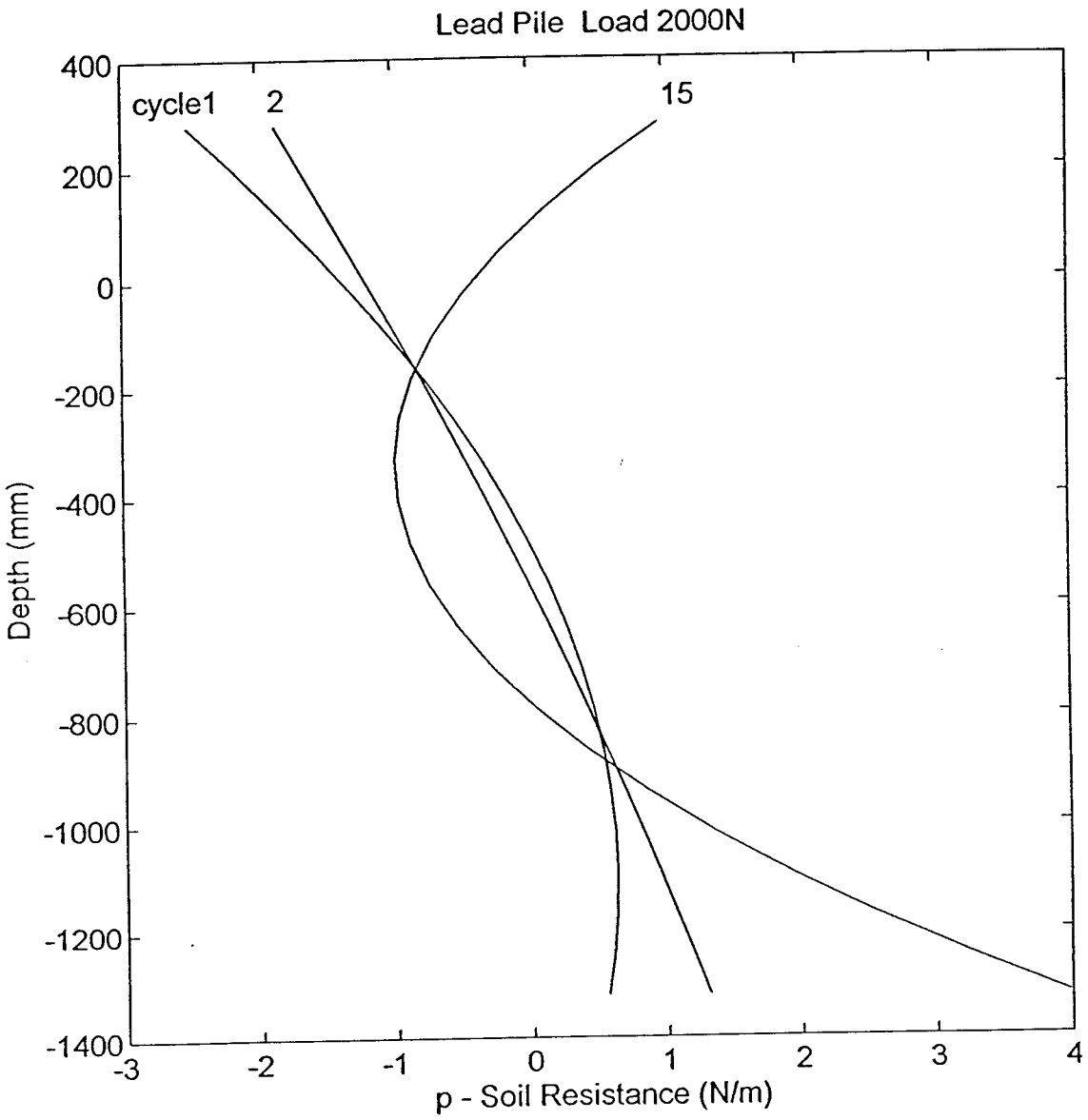

Figure 30. Soil resistance with depth (SI units).

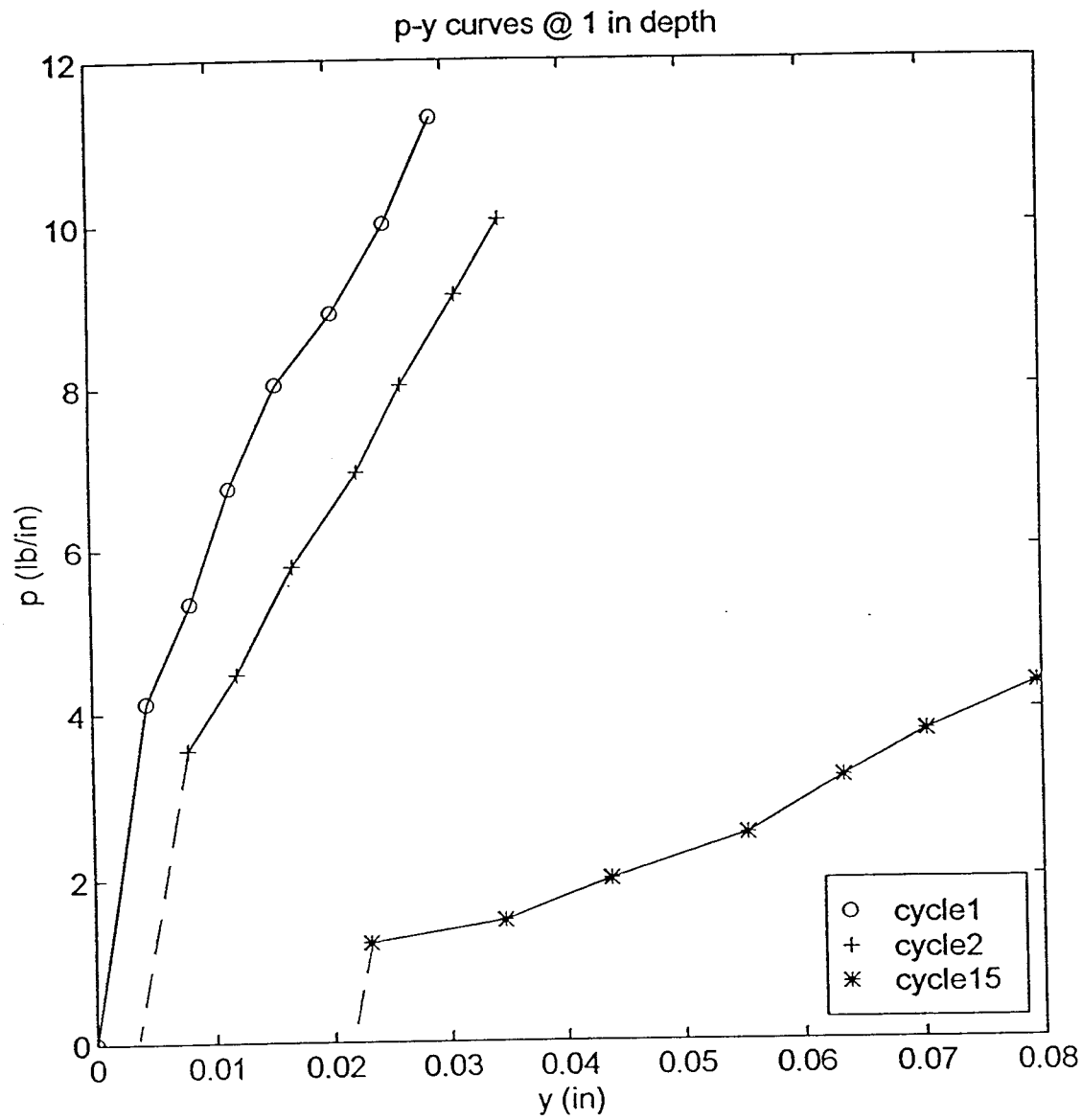

Figure 31. Lead pile p-y curves @ 1 in. depth.

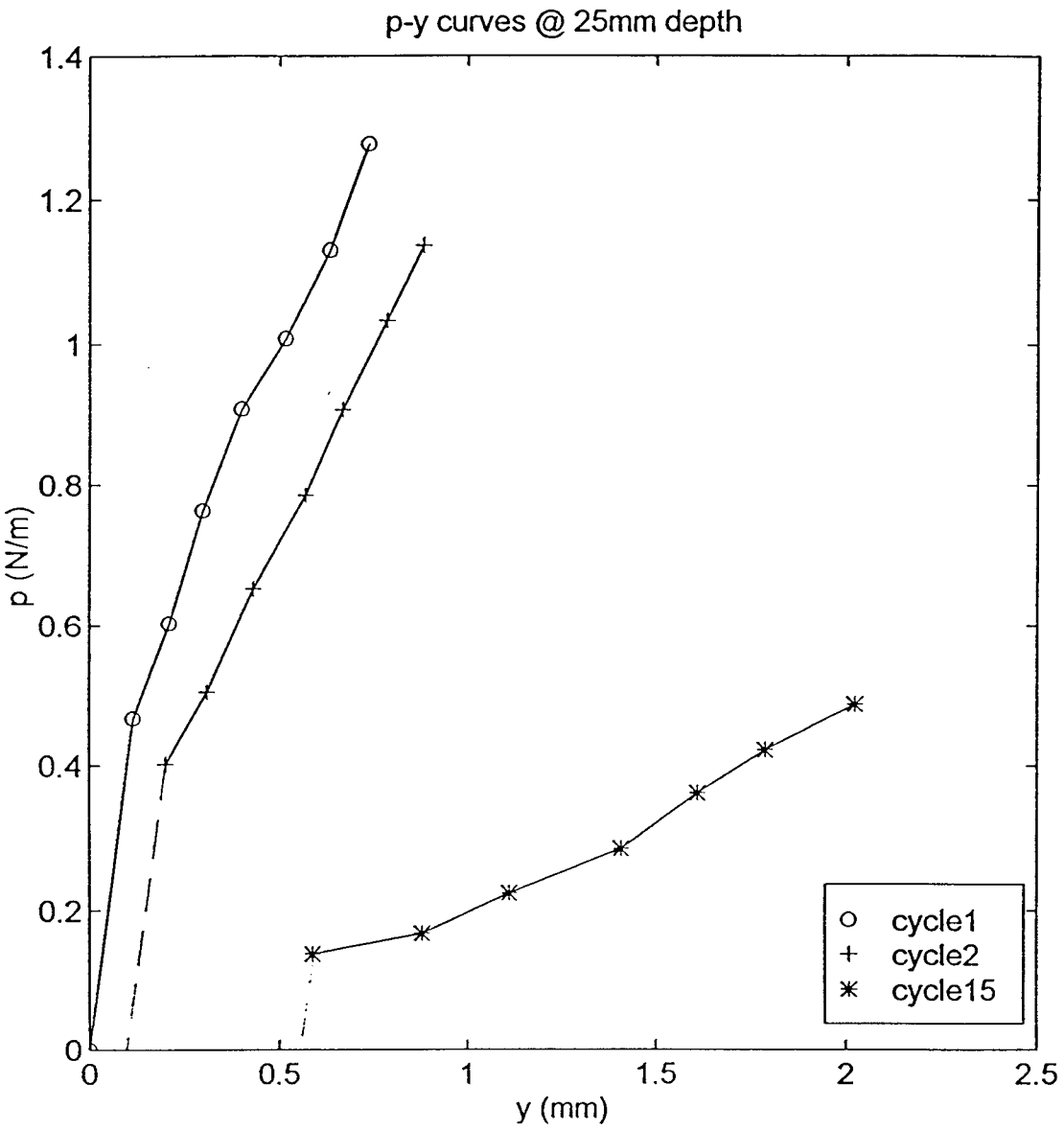

Figure 32. Lead pile p-y curves @ 25 mm depth.

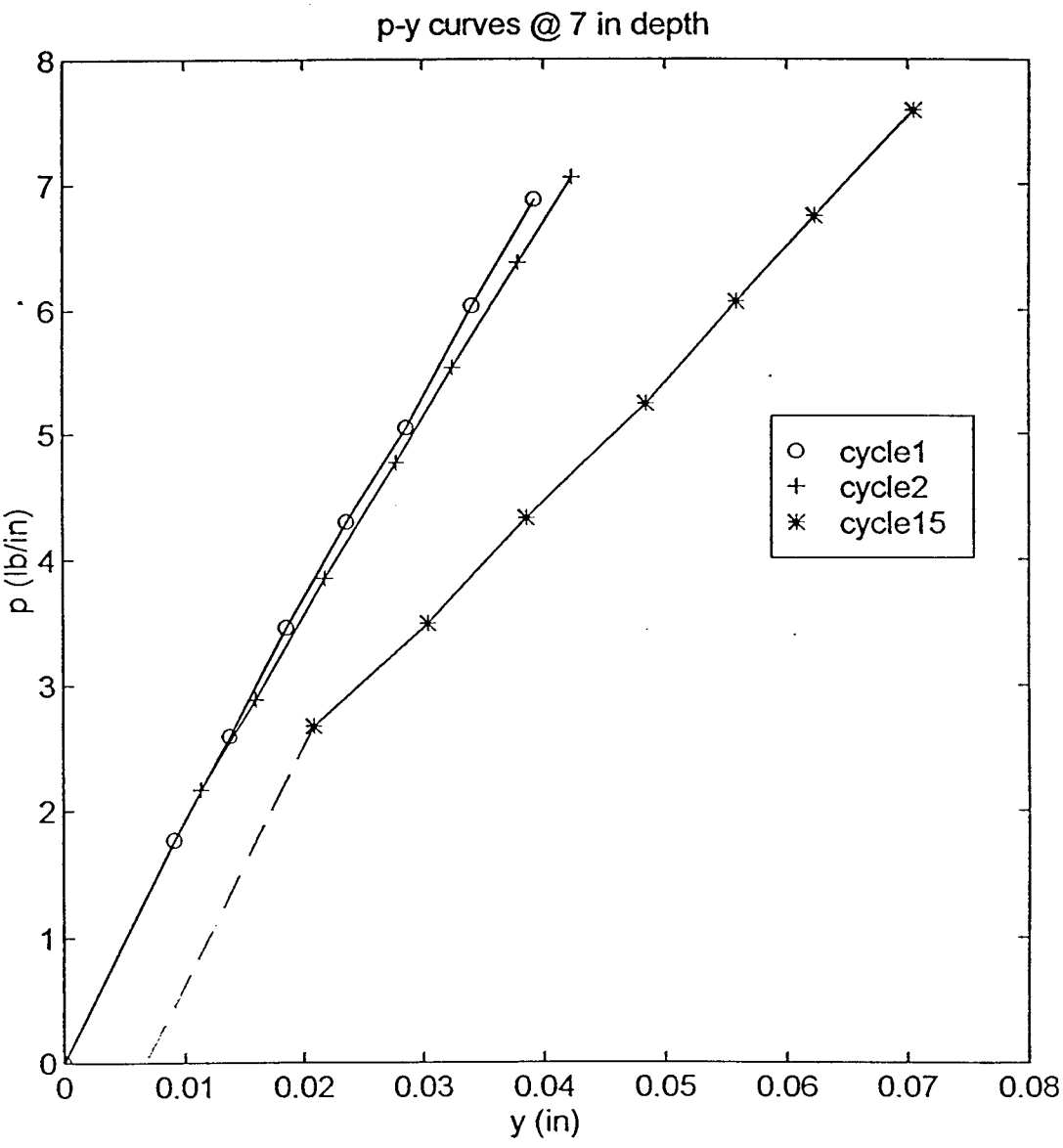

Figure 33. Lead pile p-y curves @ 7 in. depth.

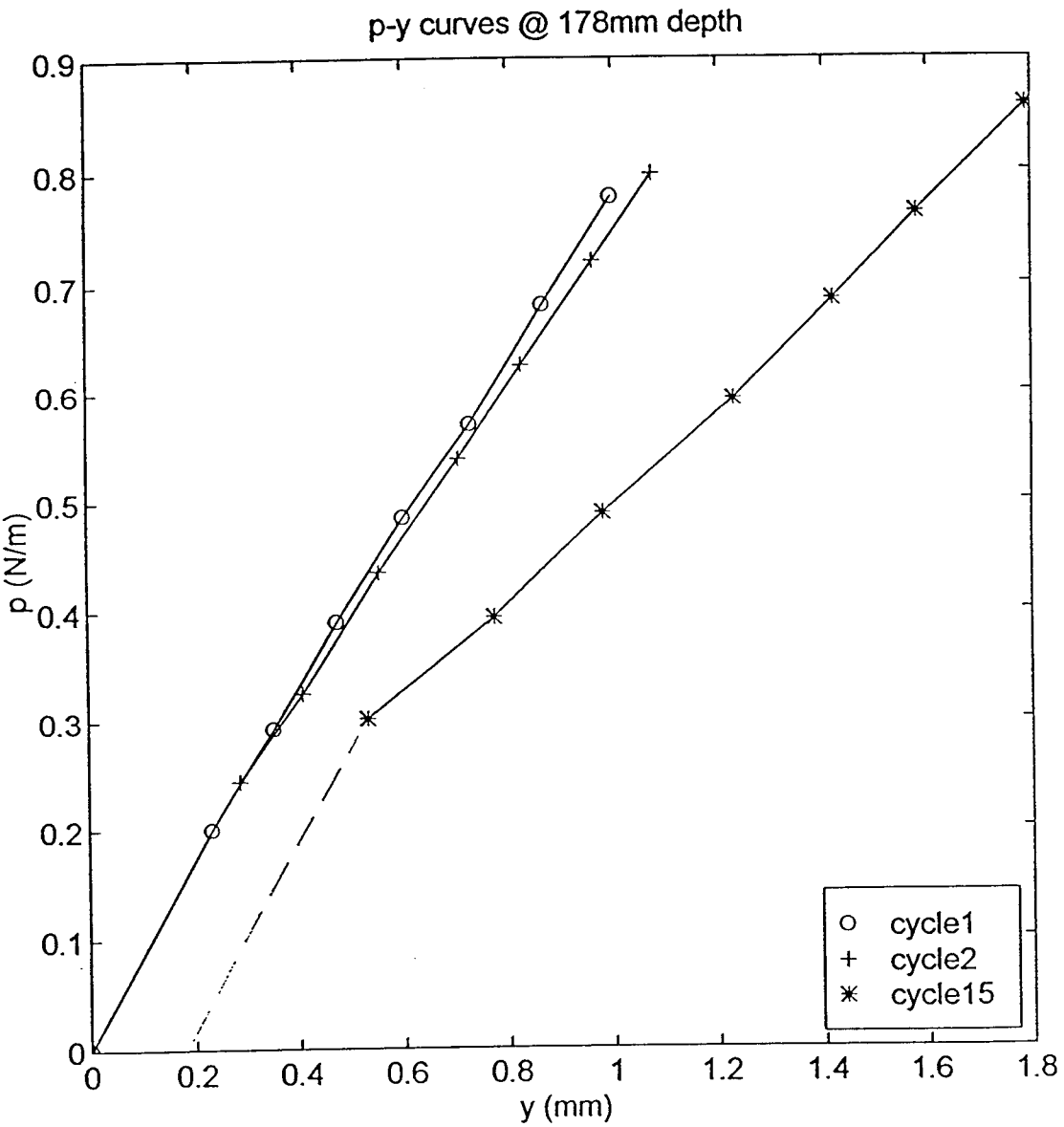

Figure 34. Lead pile p-y curves @ 178 mm depth.

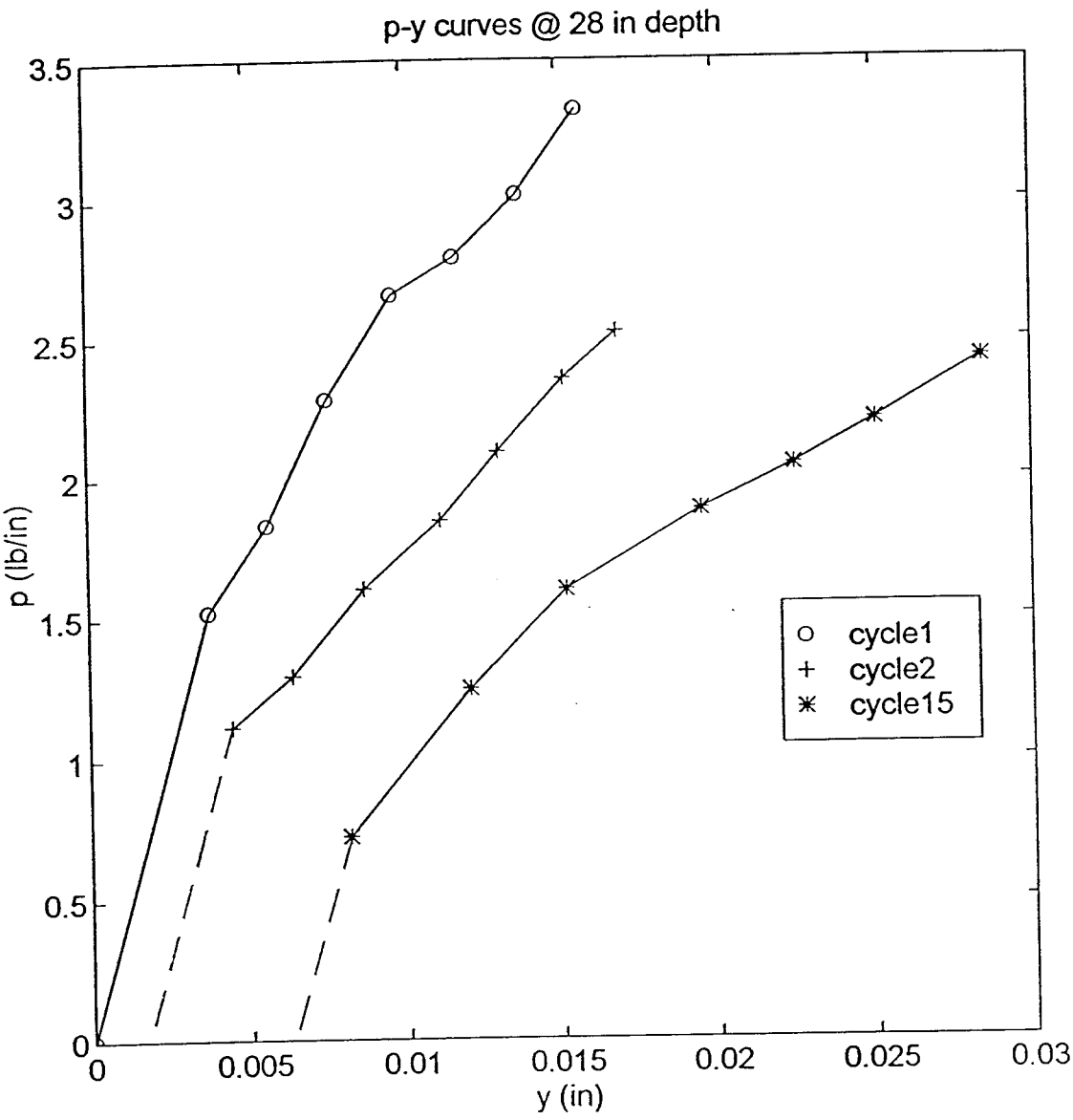

Figure 35. Lead pile p-y curves @ 28 in. depth.

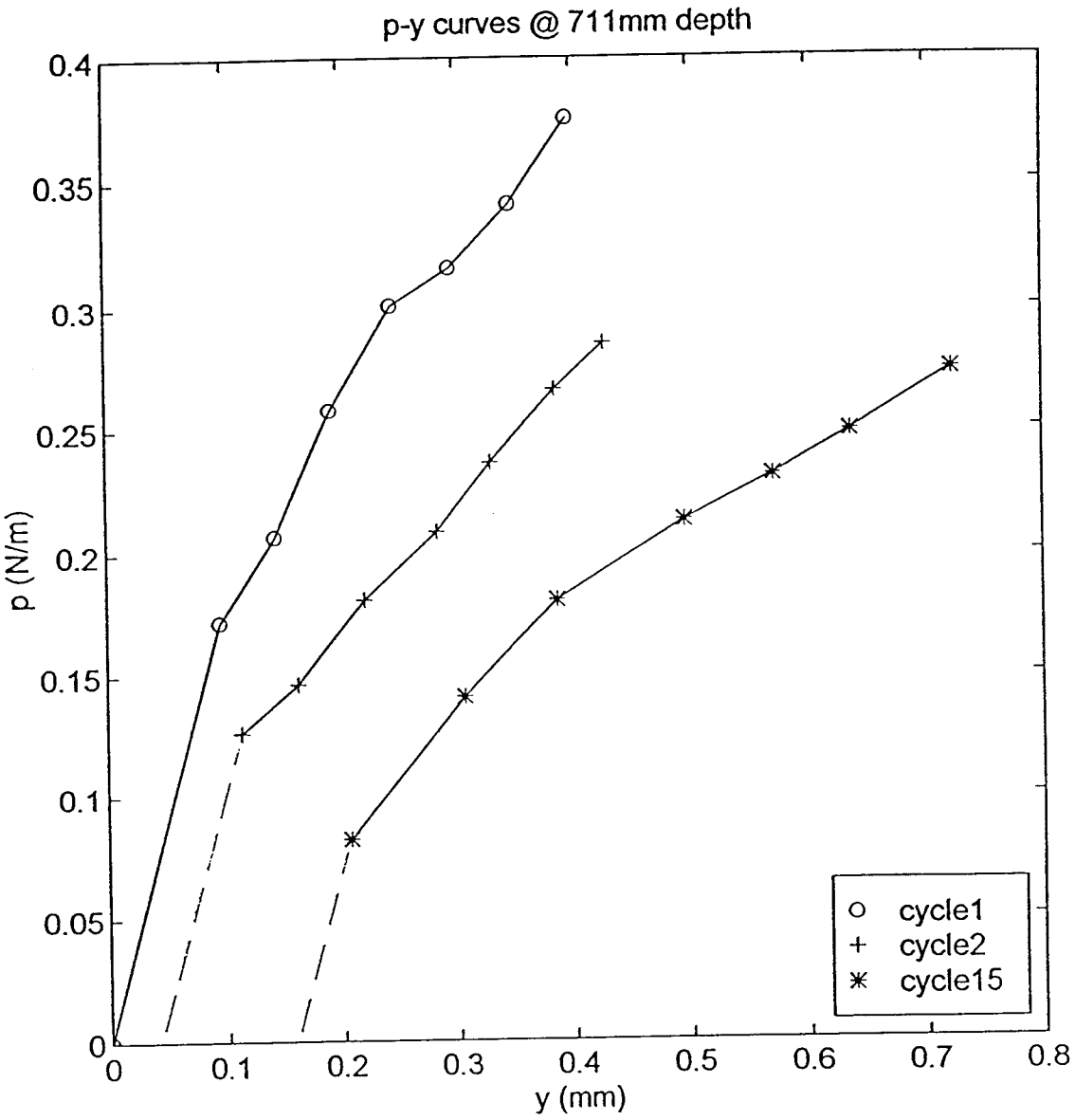

Figure 36. Lead pile p-y curves @ 711 mm depth.

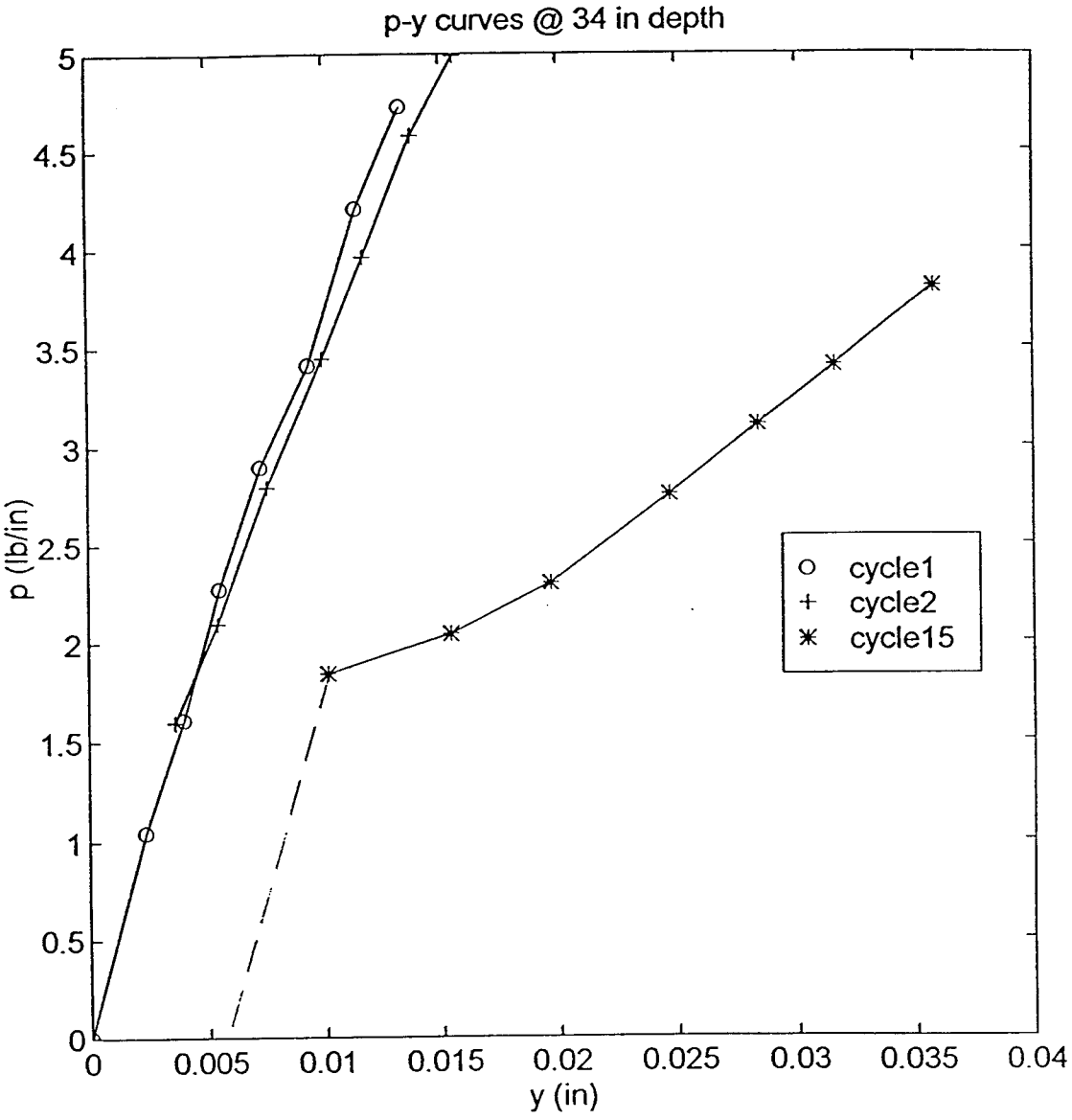

Figure 37. Lead pile p-y curves @ 34 in. depth.

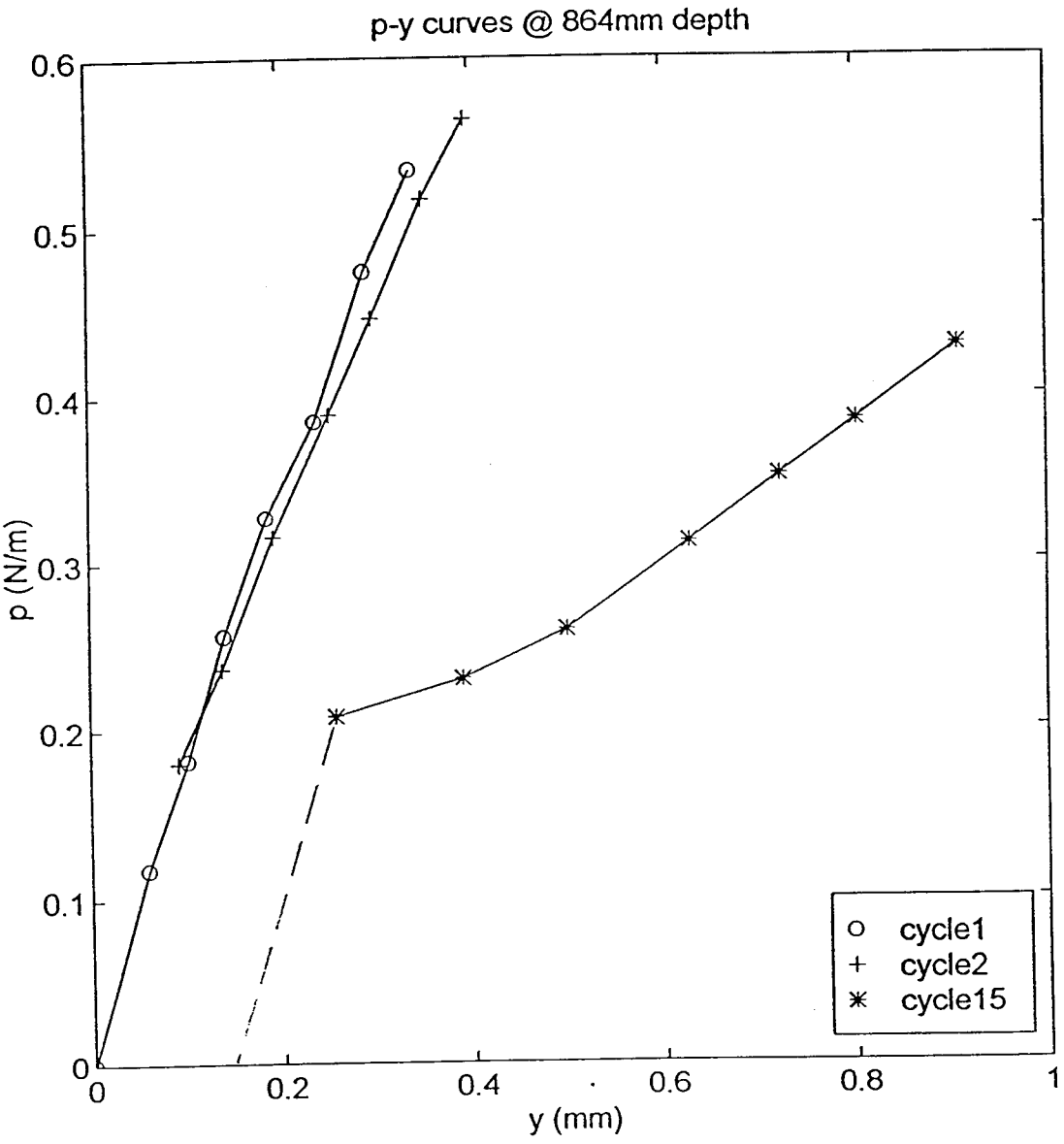

Figure 38. Lead pile p-y curves @ 864 mm depth.

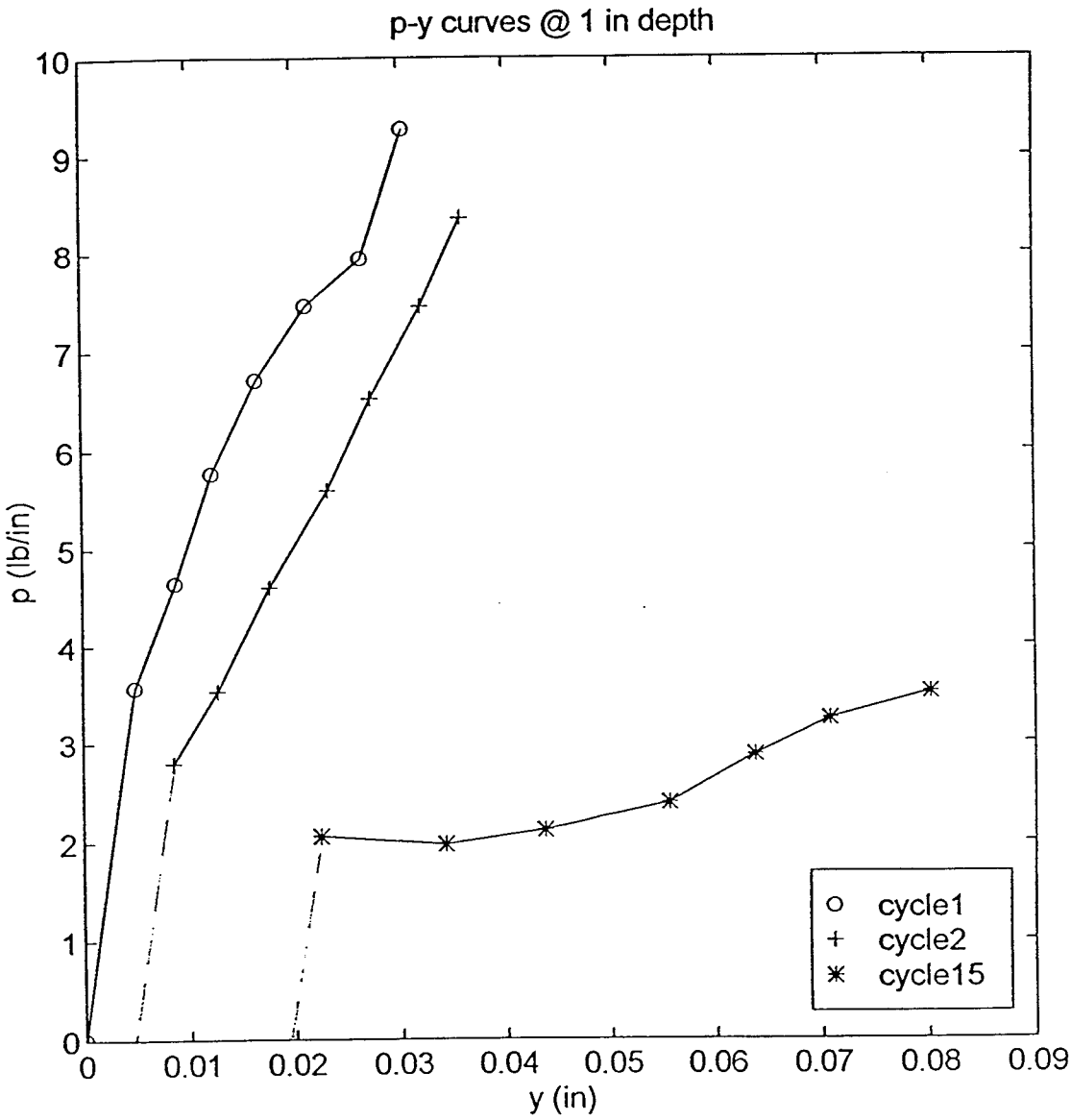

Figure 39. Second pile p-y curves @ 1 in. depth.

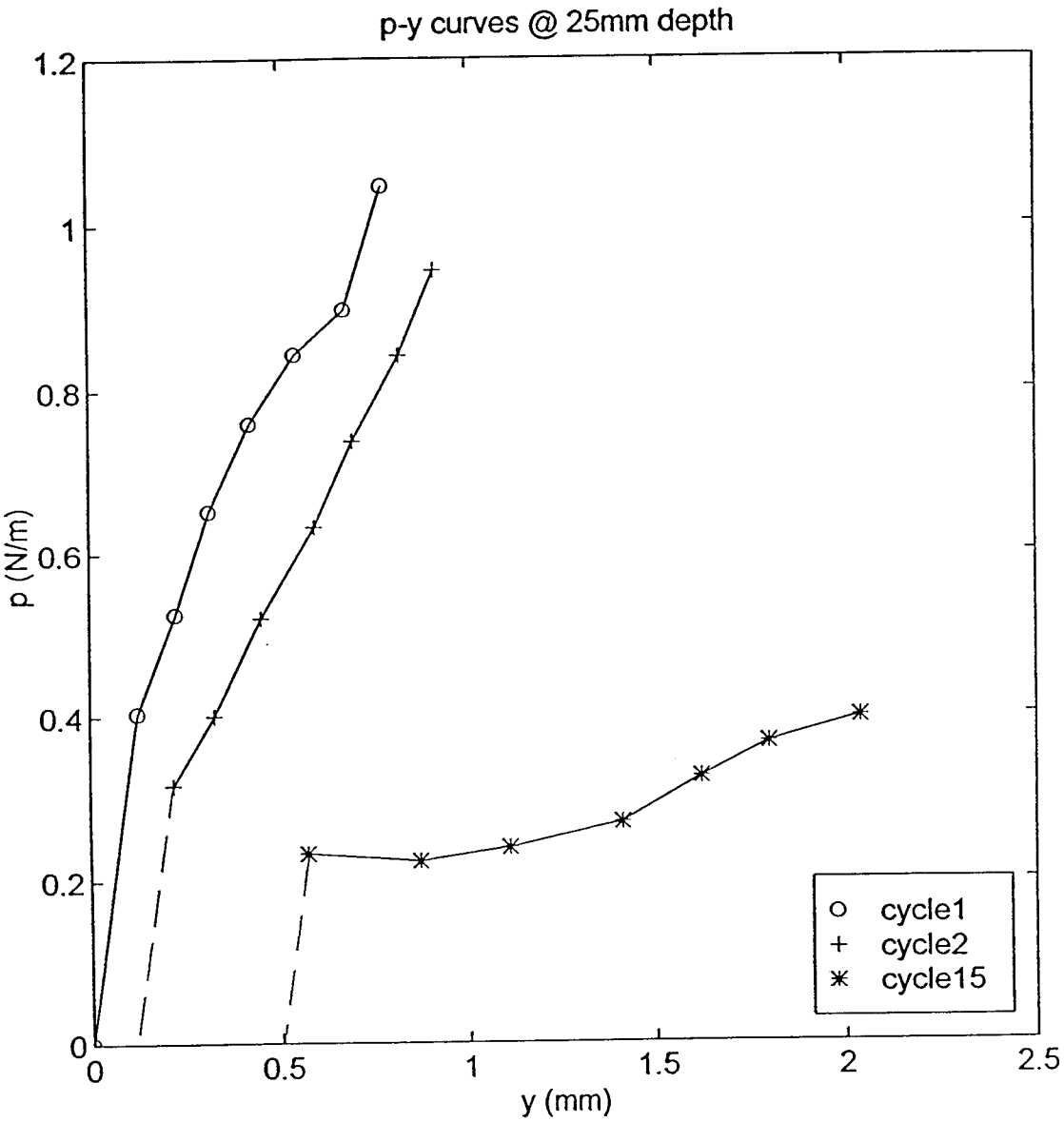

Figure 40. Second pile p-y curves @ 25 mm depth.

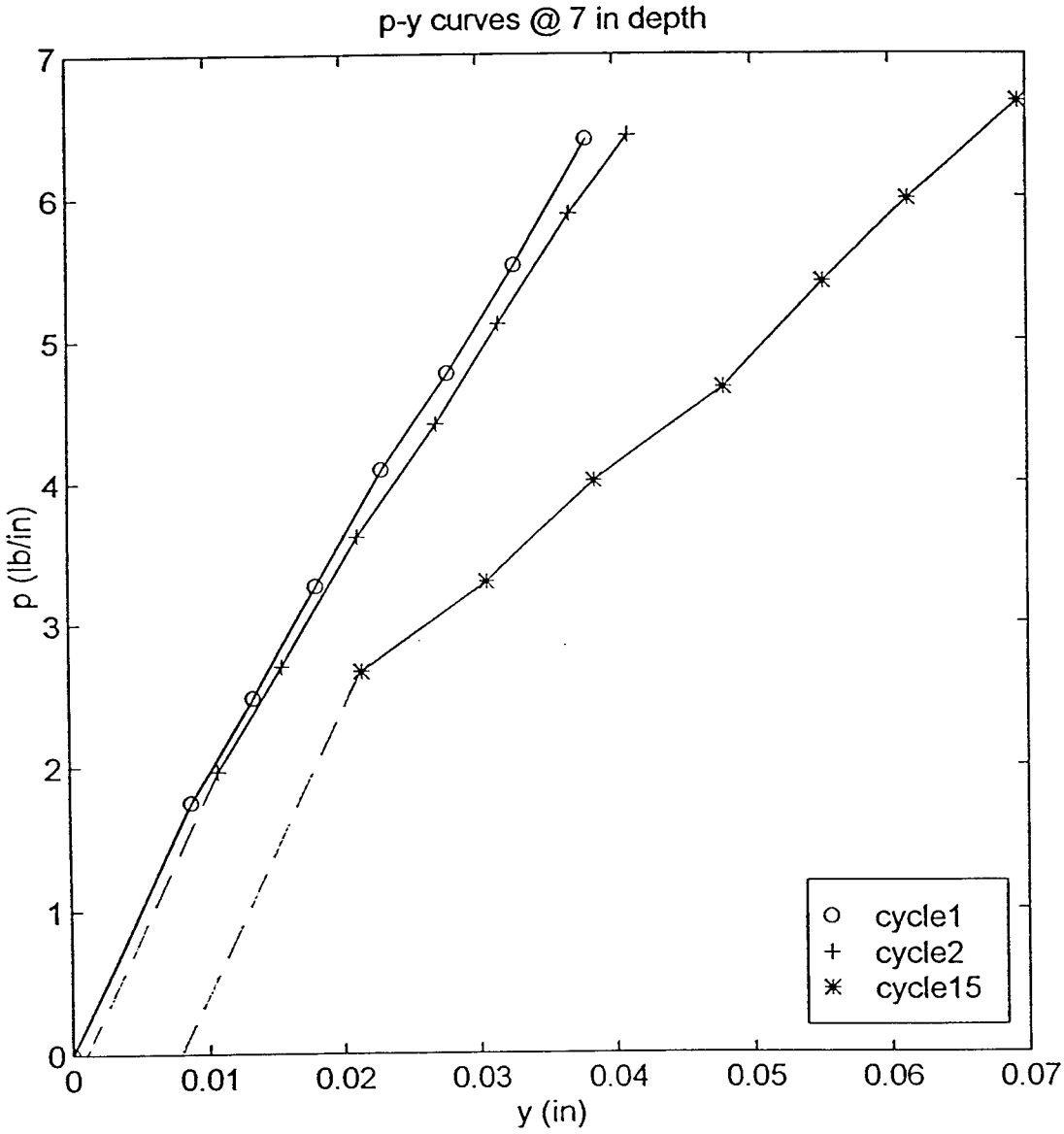

Figure 41. Second pile p-y curves @ 7 in. depth.

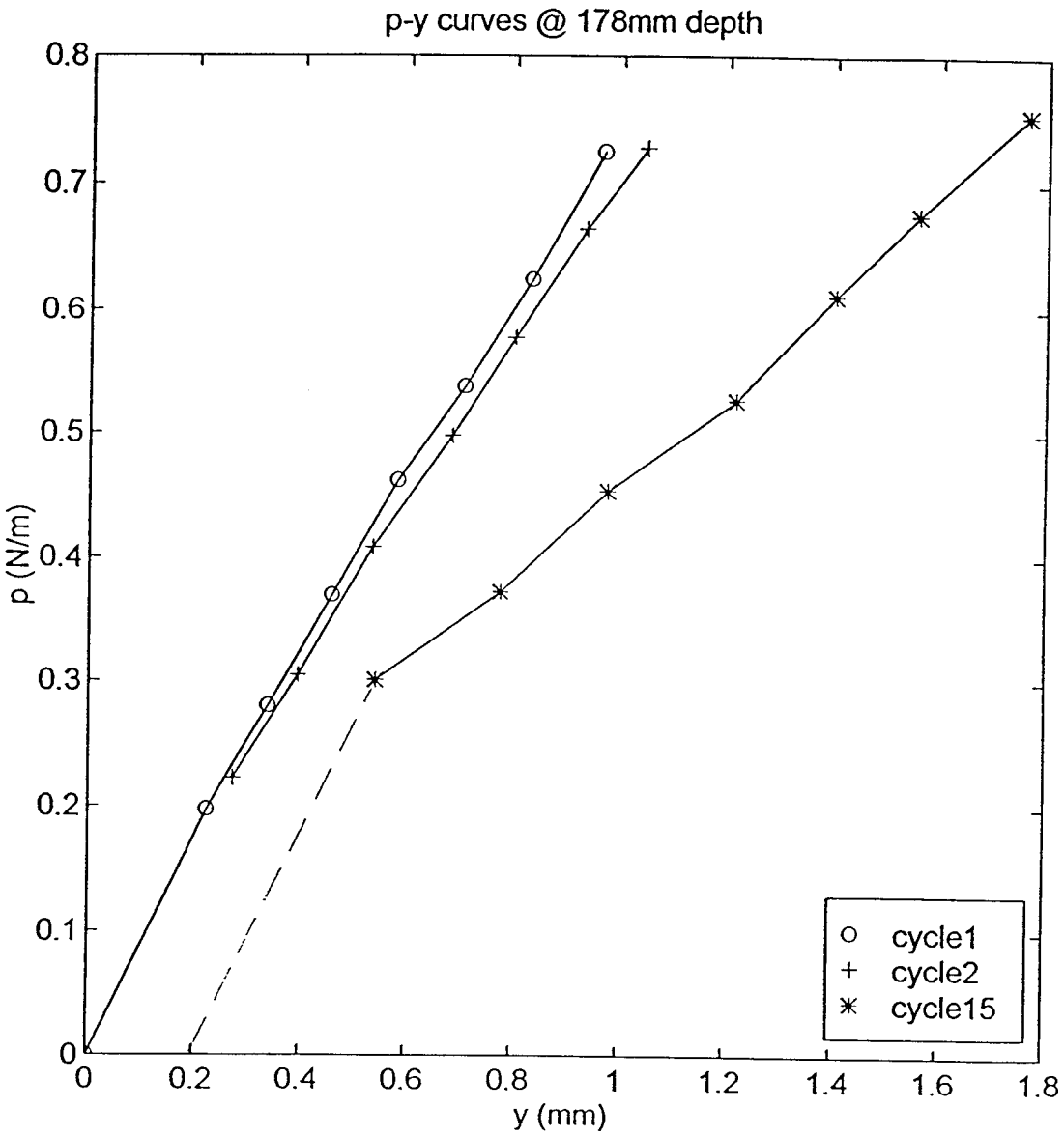

Figure 42. Second pile p-y curves @ 128 mm depth.

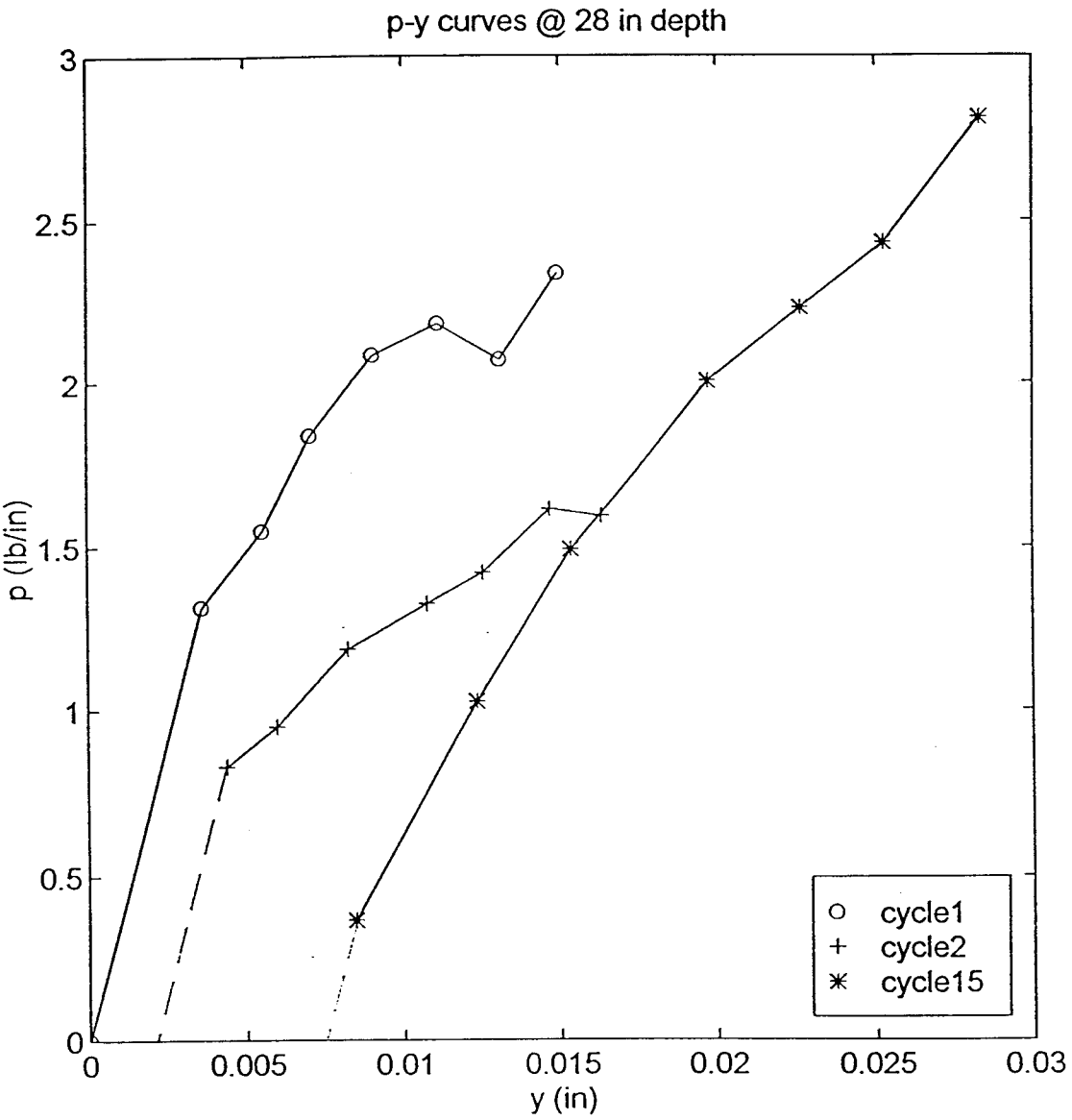

Figure 43. Second pile p-y curves @ 28 in. depth.

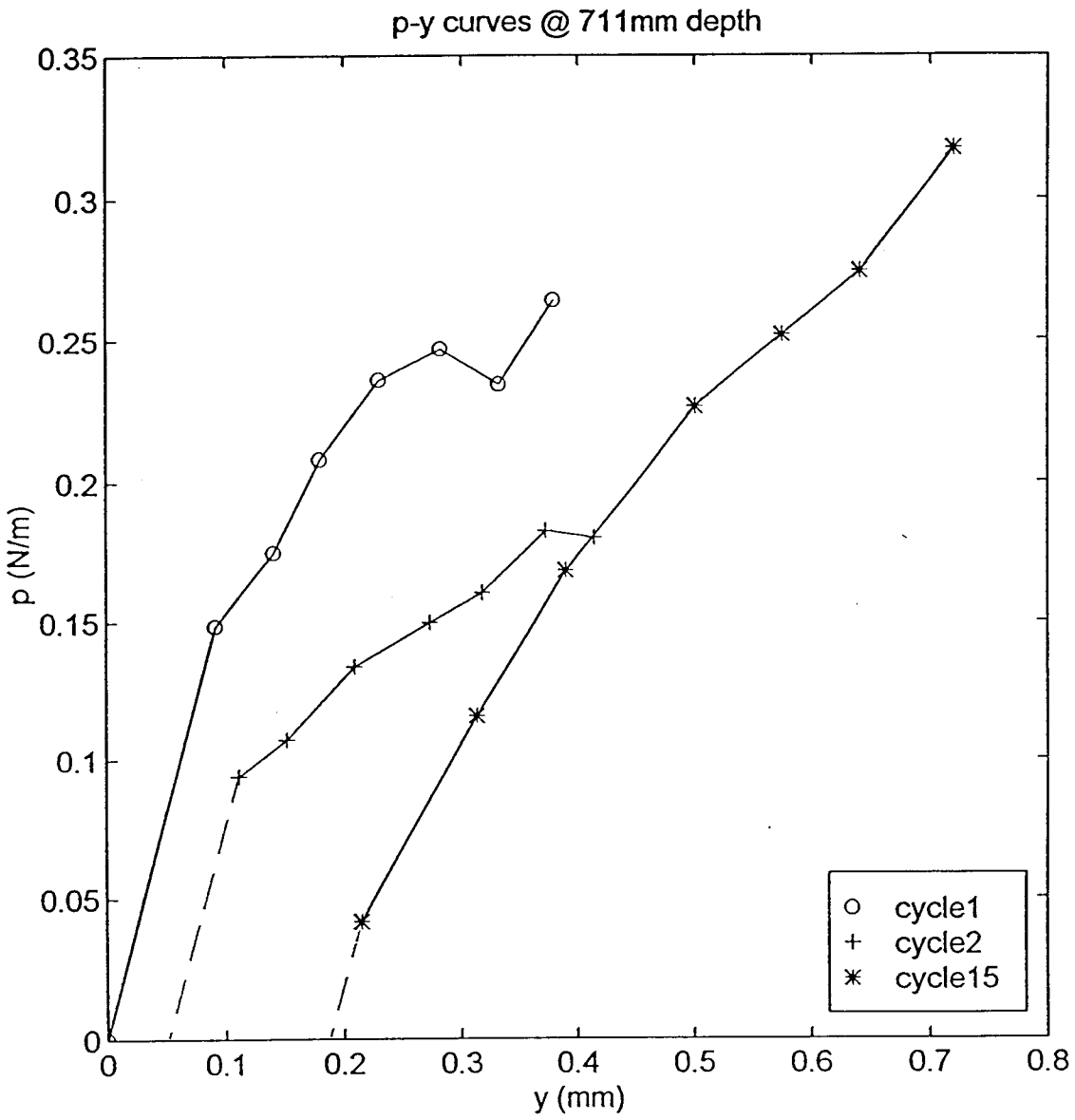

Figure 44. Second pile p-y curves @ 711 mm depth.

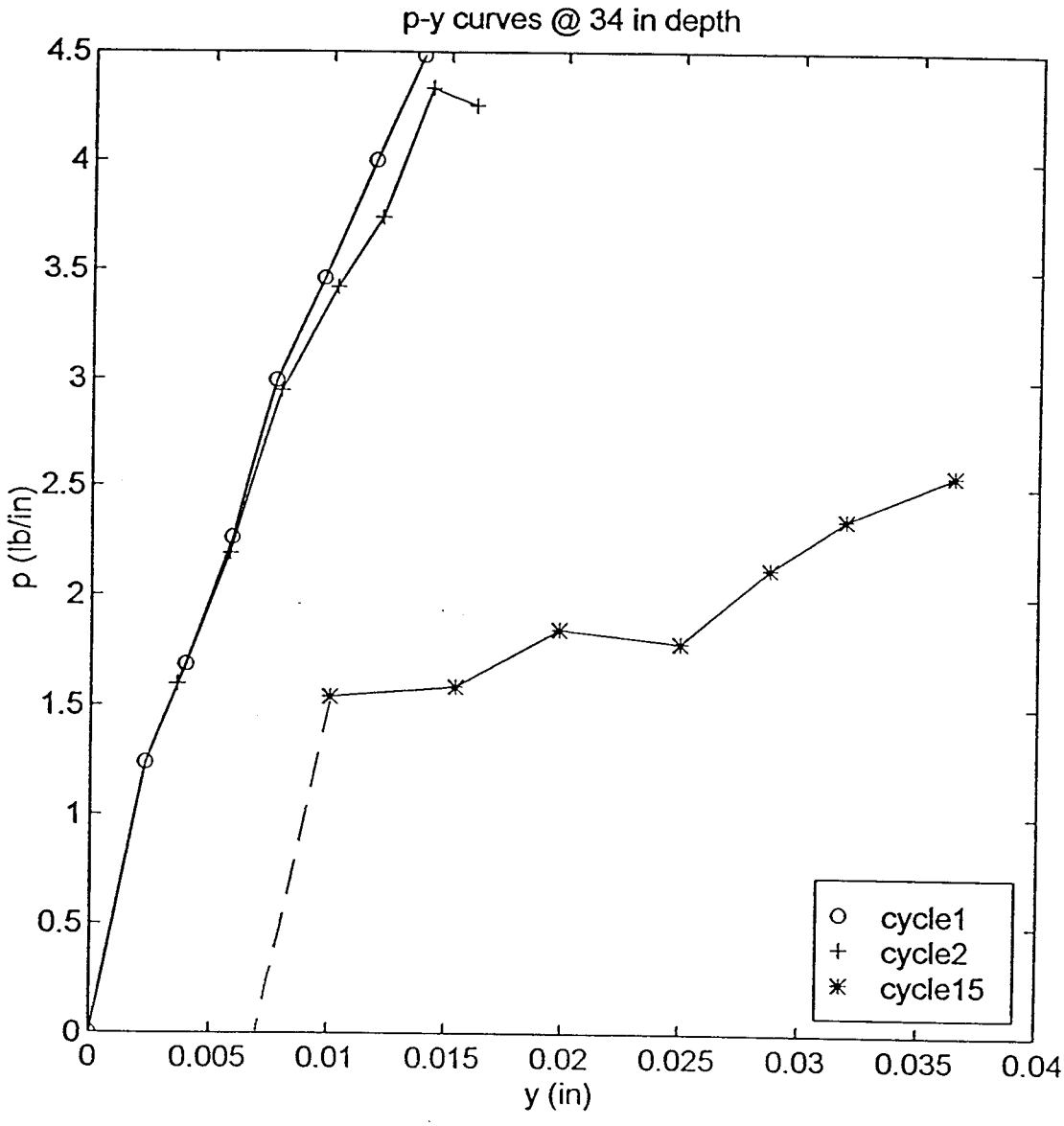

Figure 45. Second pile p-y curves @ 34 in. depth.

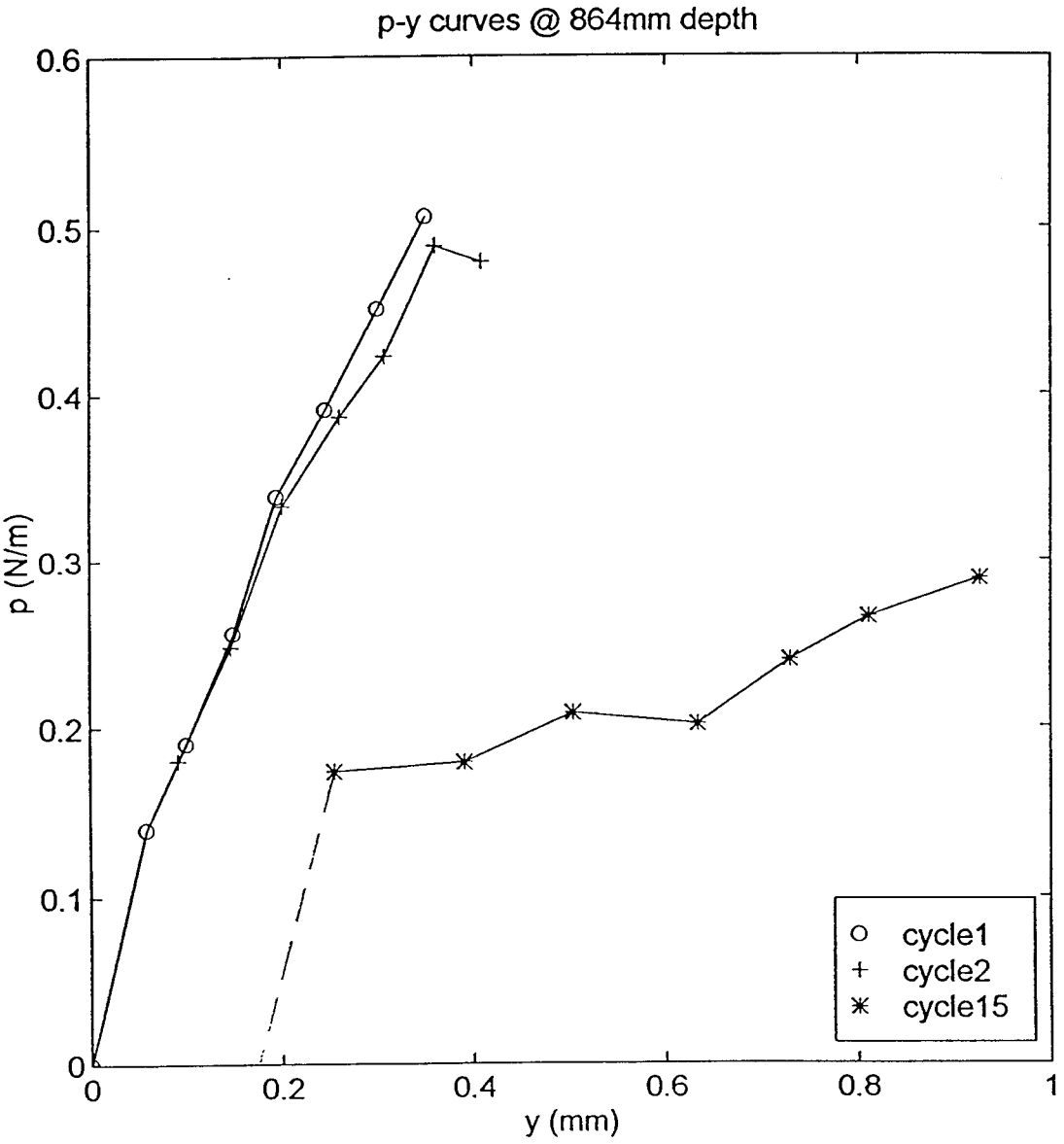

Figure 46. Second pile p-y curves @ 864 mm depth.

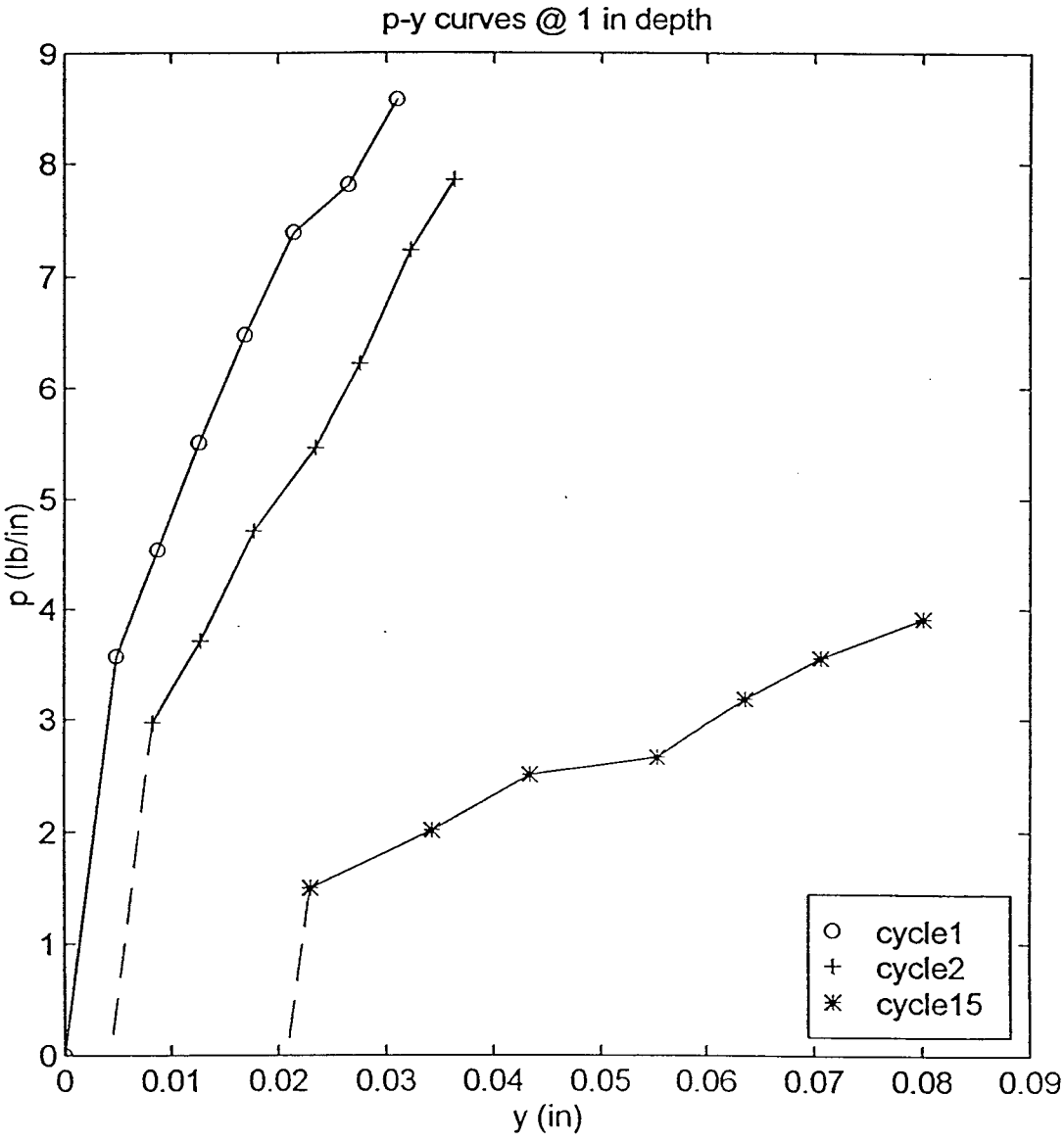

Figure 47. Third pile p-y curves @ 1 in. depth.

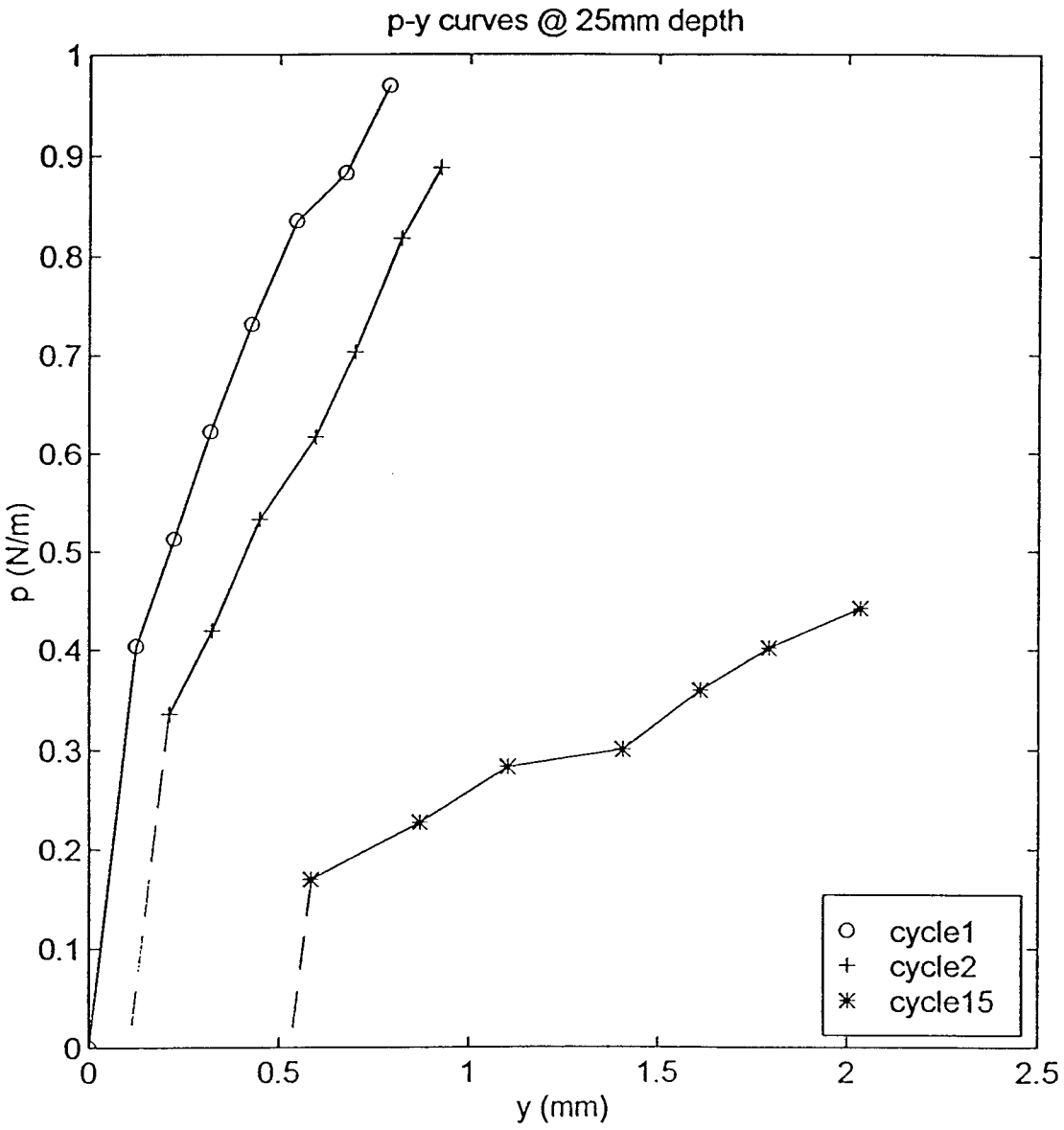

Figure 48. Third pile p-y curves @ 25 mm depth.

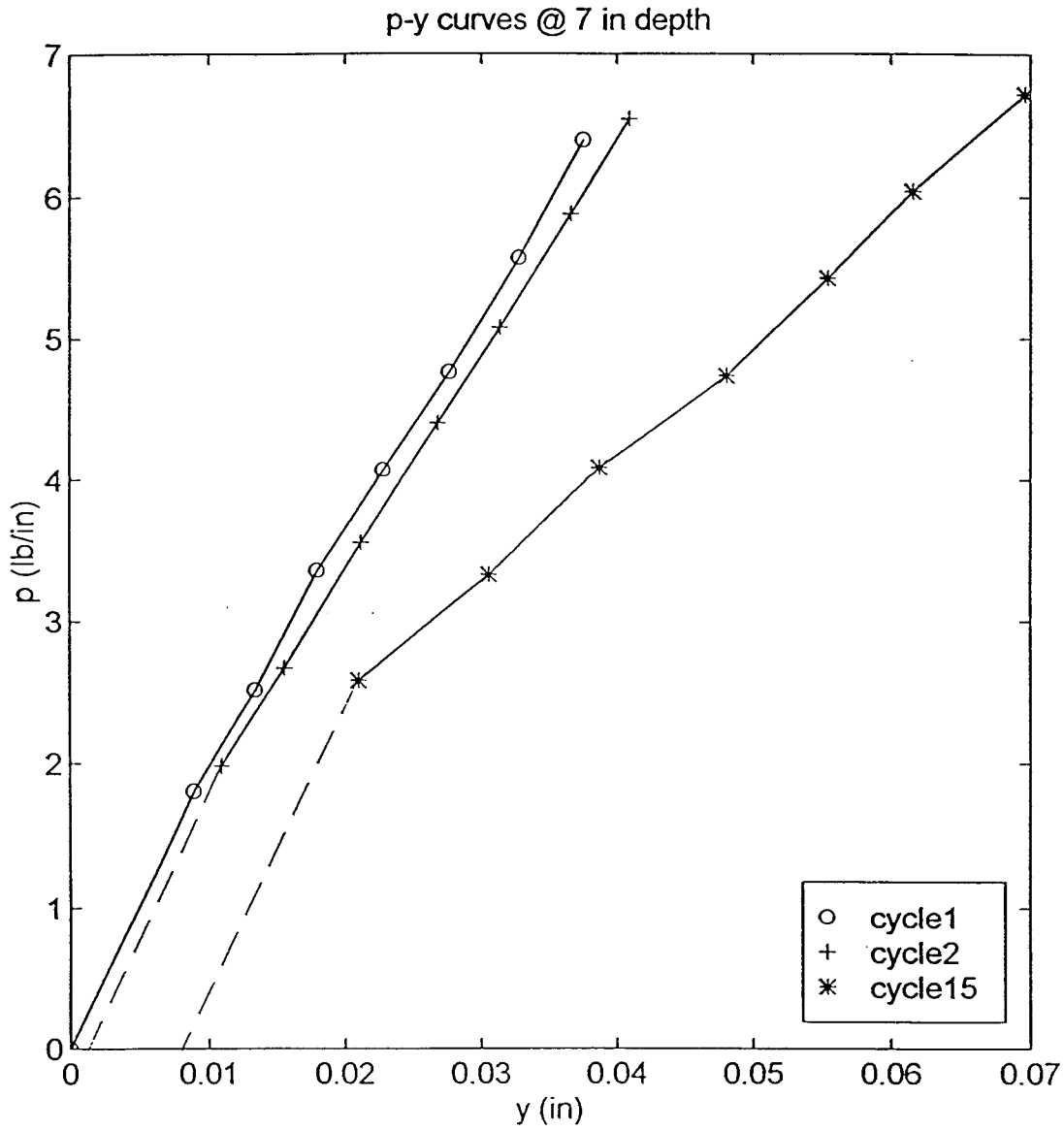

Figure 49. Third pile p-y curves @ 7 in. depth.

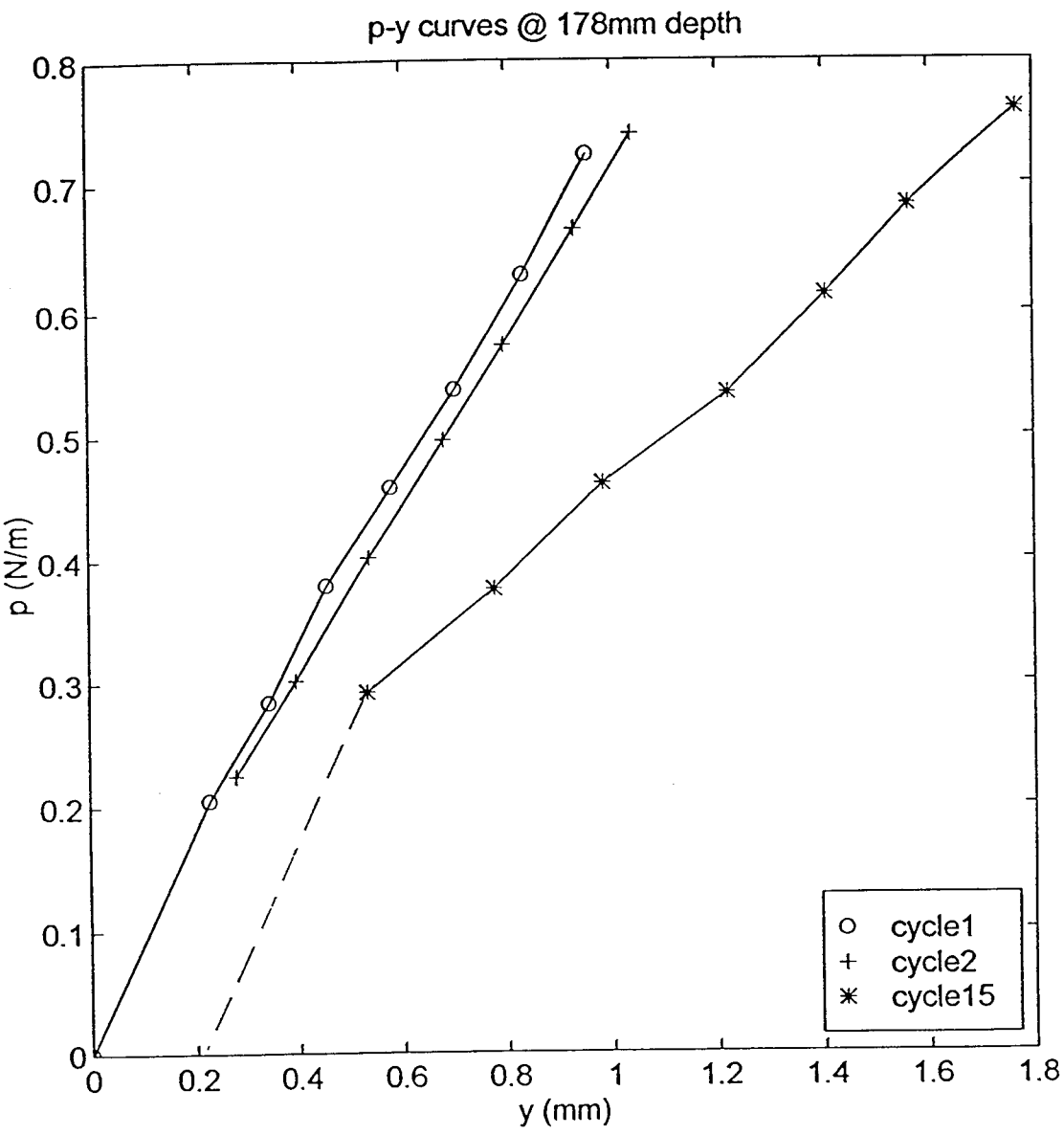

Figure 50. Third pile p-y curves @ 128 mm depth.

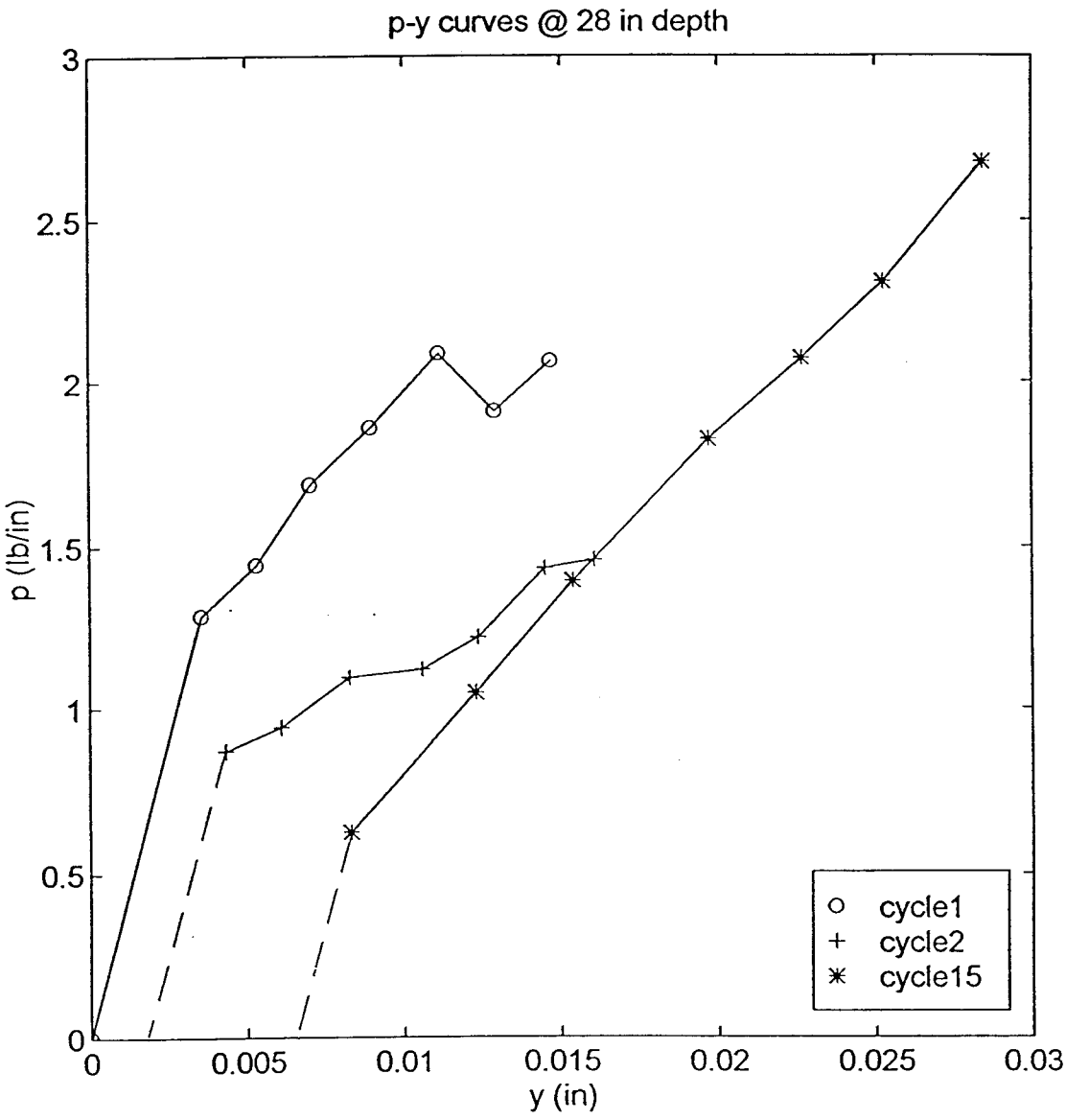

Figure 51. Third pile p-y curves @ 28 in. depth.

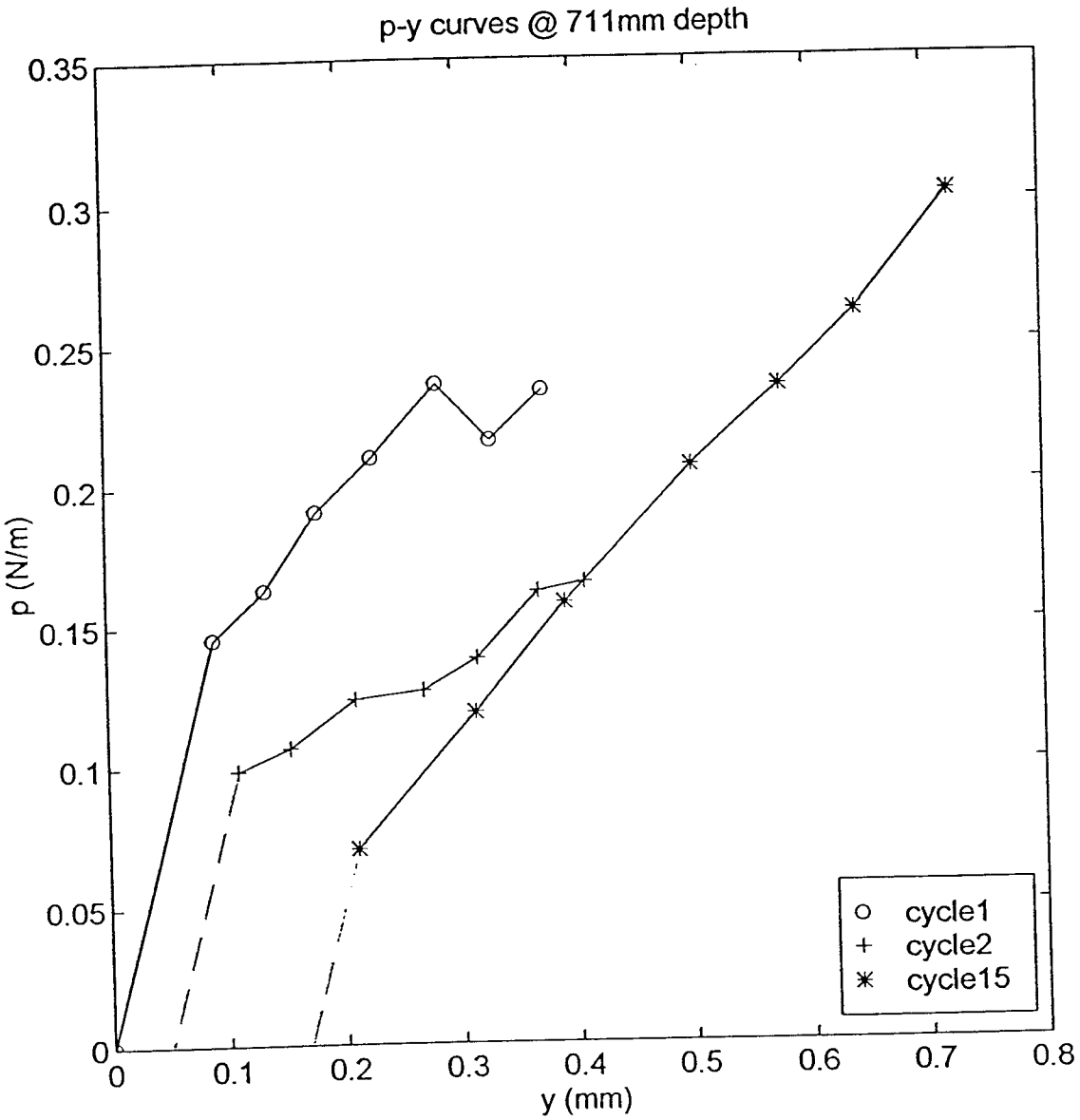

Figure 52. Third pile p-y curves @ 711 mm depth.

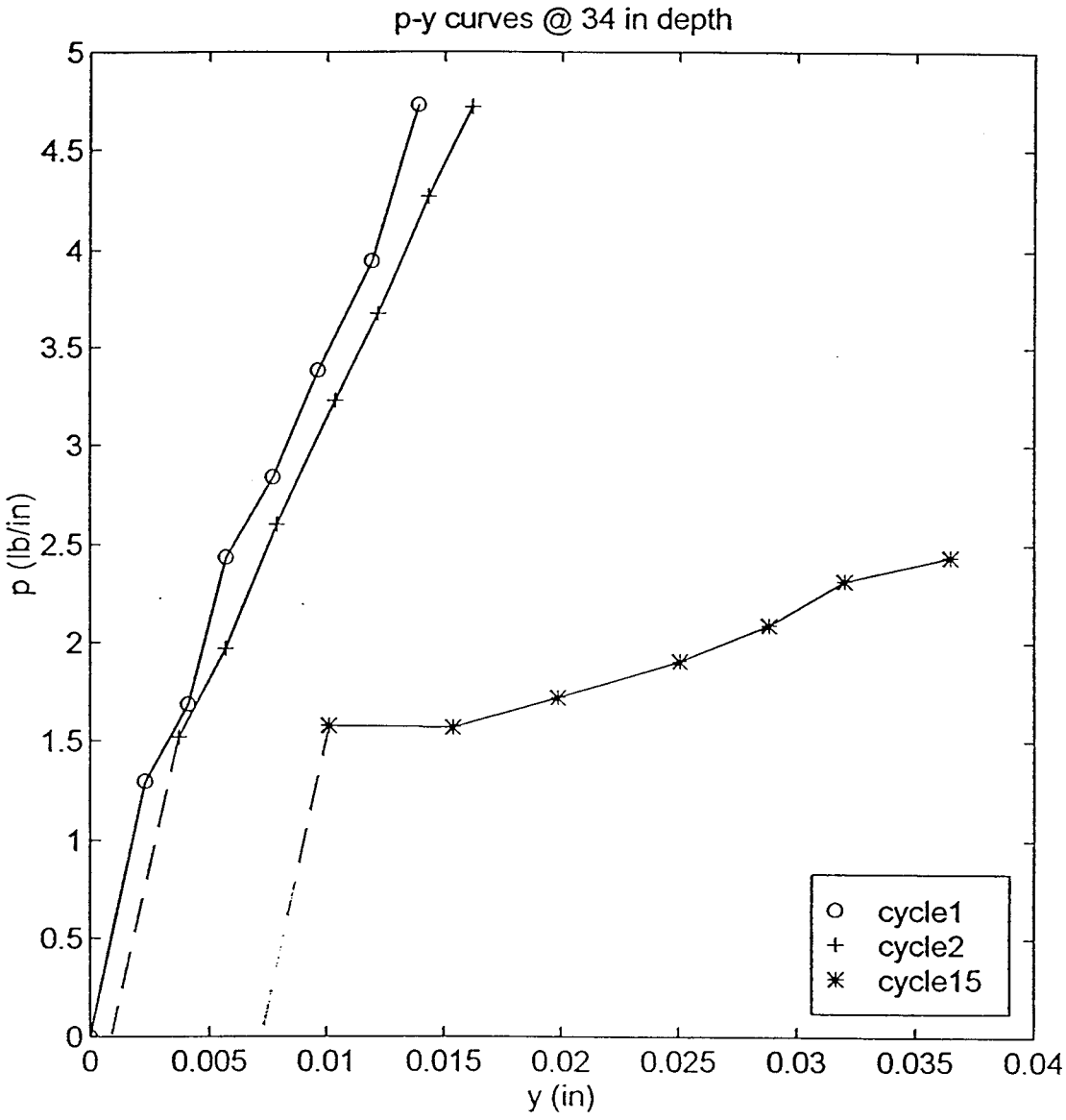

Figure 53. Third pile p-y curves @ 34 in. depth.

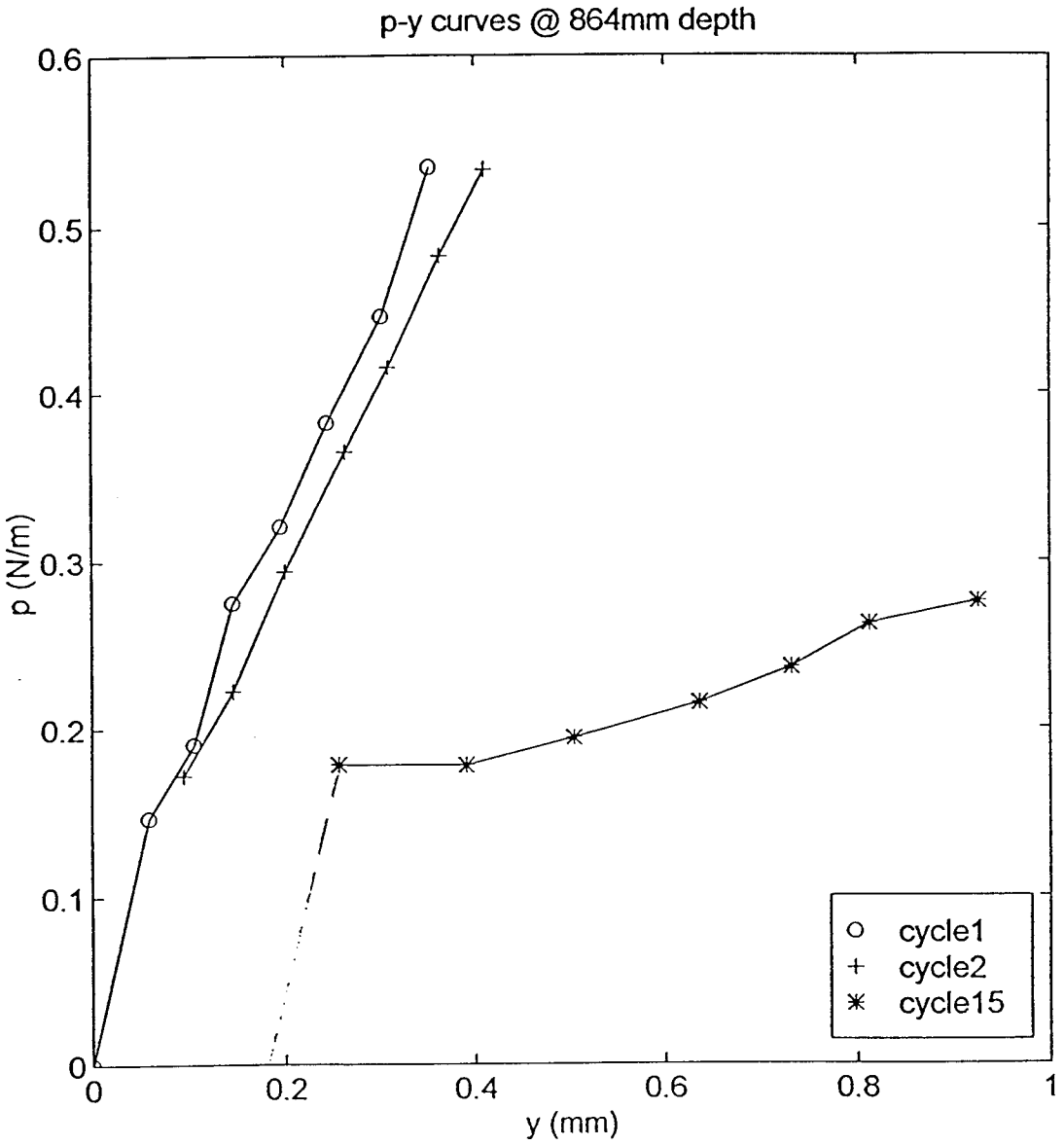

Figure 54. Third pile p-y curves @ 864 mm depth.

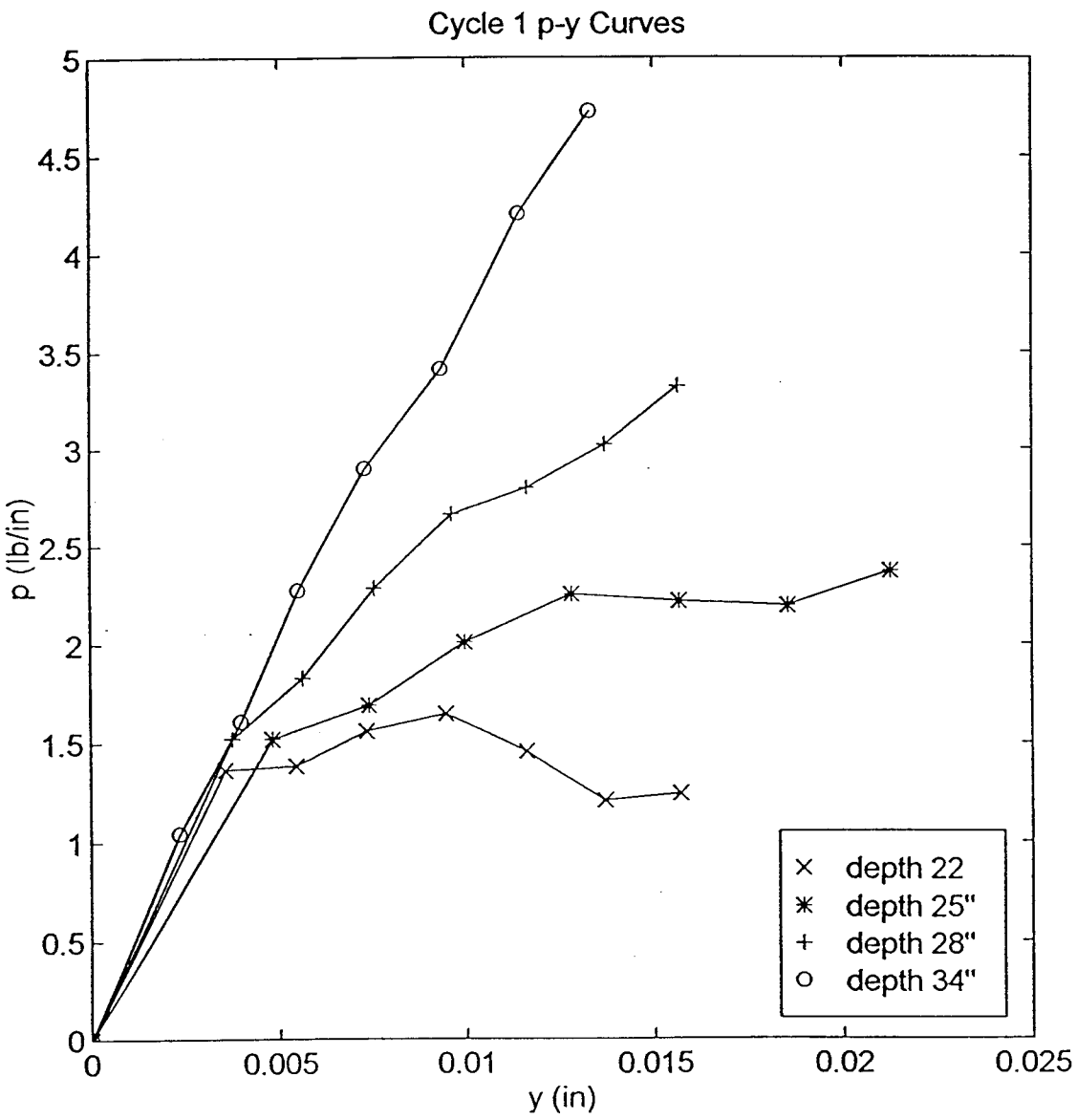

Figure 55. P-y curves for lead pile at various depths for cycle 1 (English units).

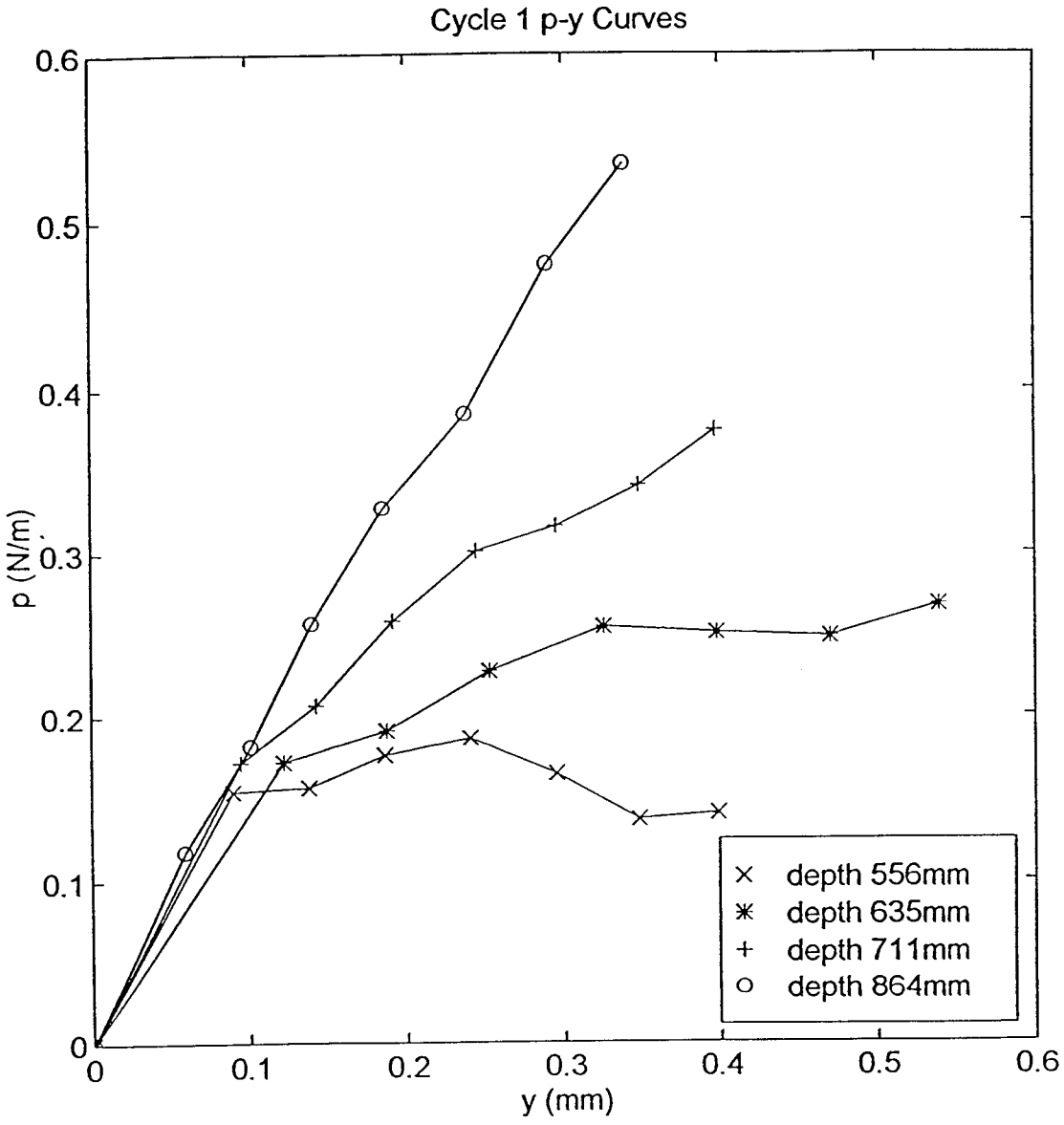

Figure 56. P-y curves for lead pile at various depths for cycle 1 (SI units).

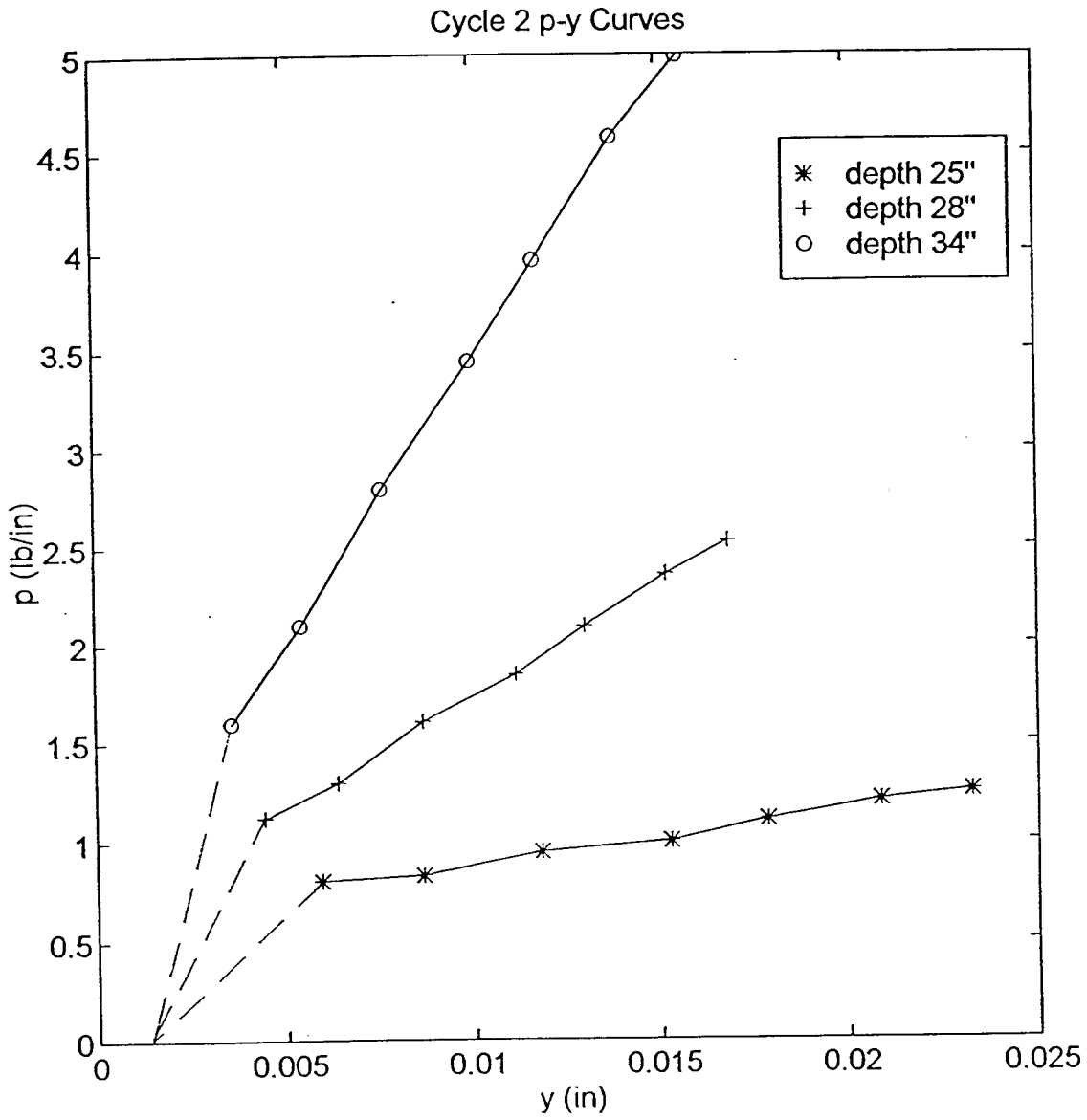

Figure 57. P-y curves for lead pile at various depths for cycle 2 (English units).

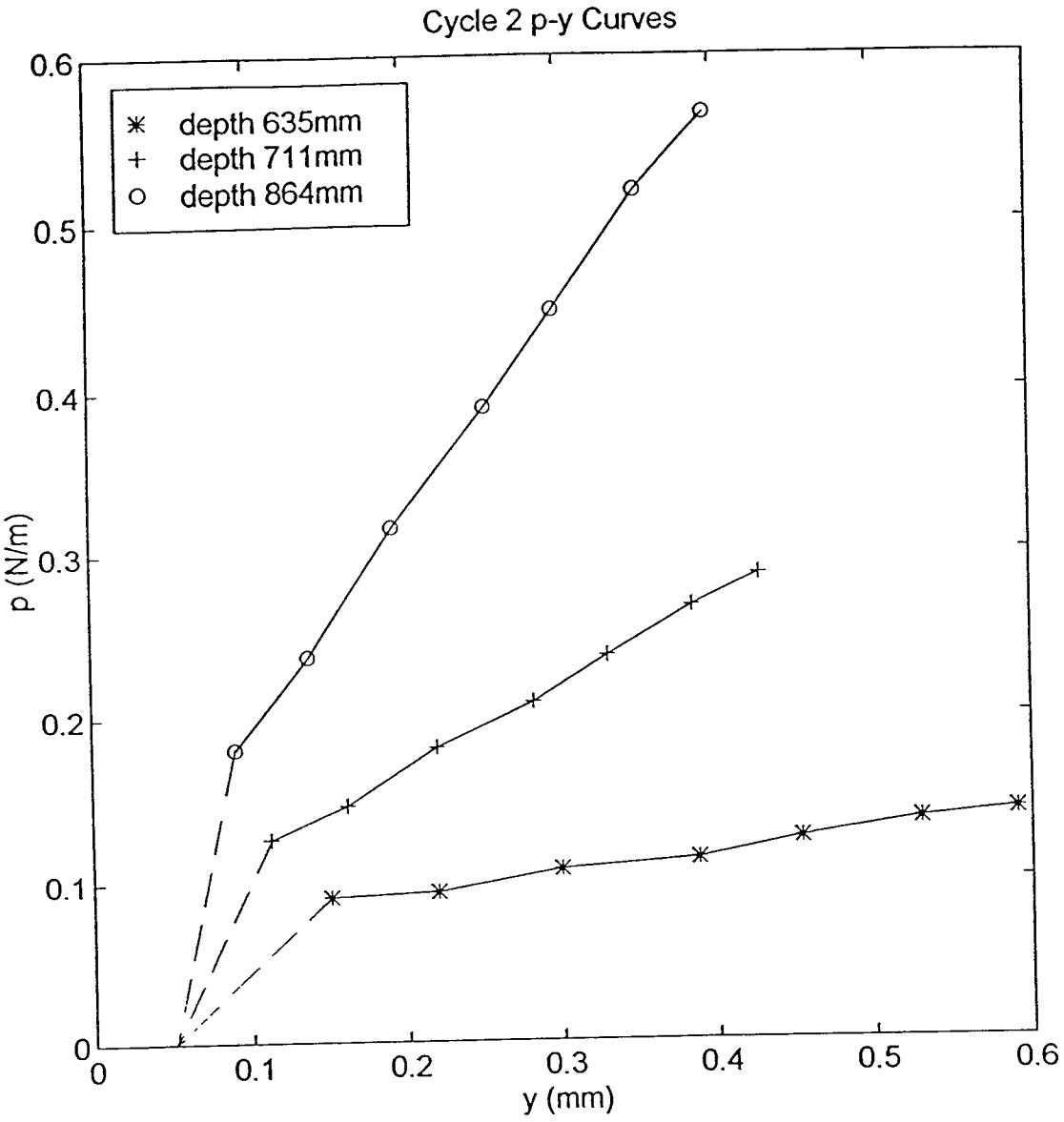

Figure 58. P-y curves for lead pile at various depths for cycle 2 (SI units).

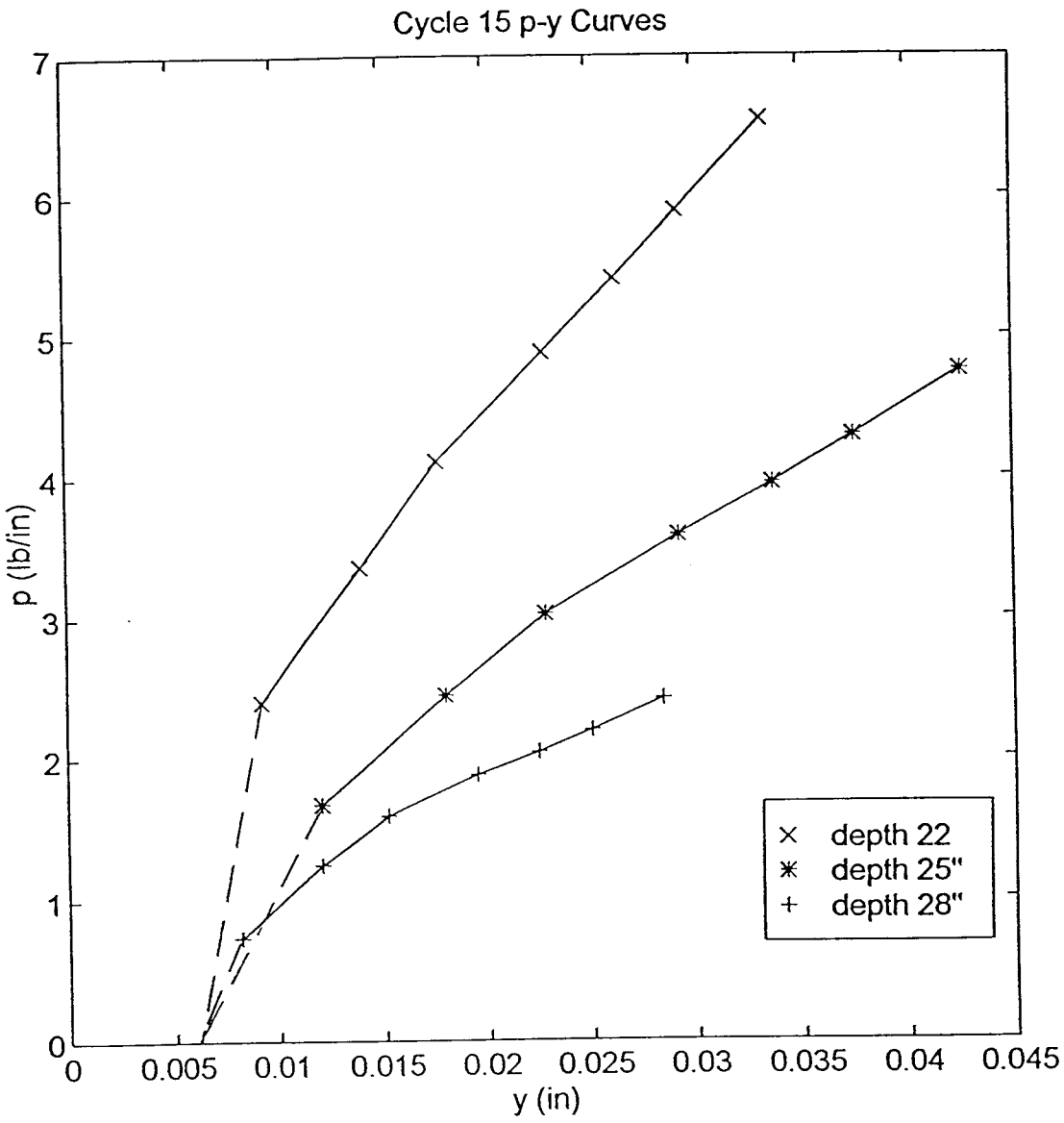

Figure 59. P-y curves for lead pile at various depths for cycle 15 (English units).

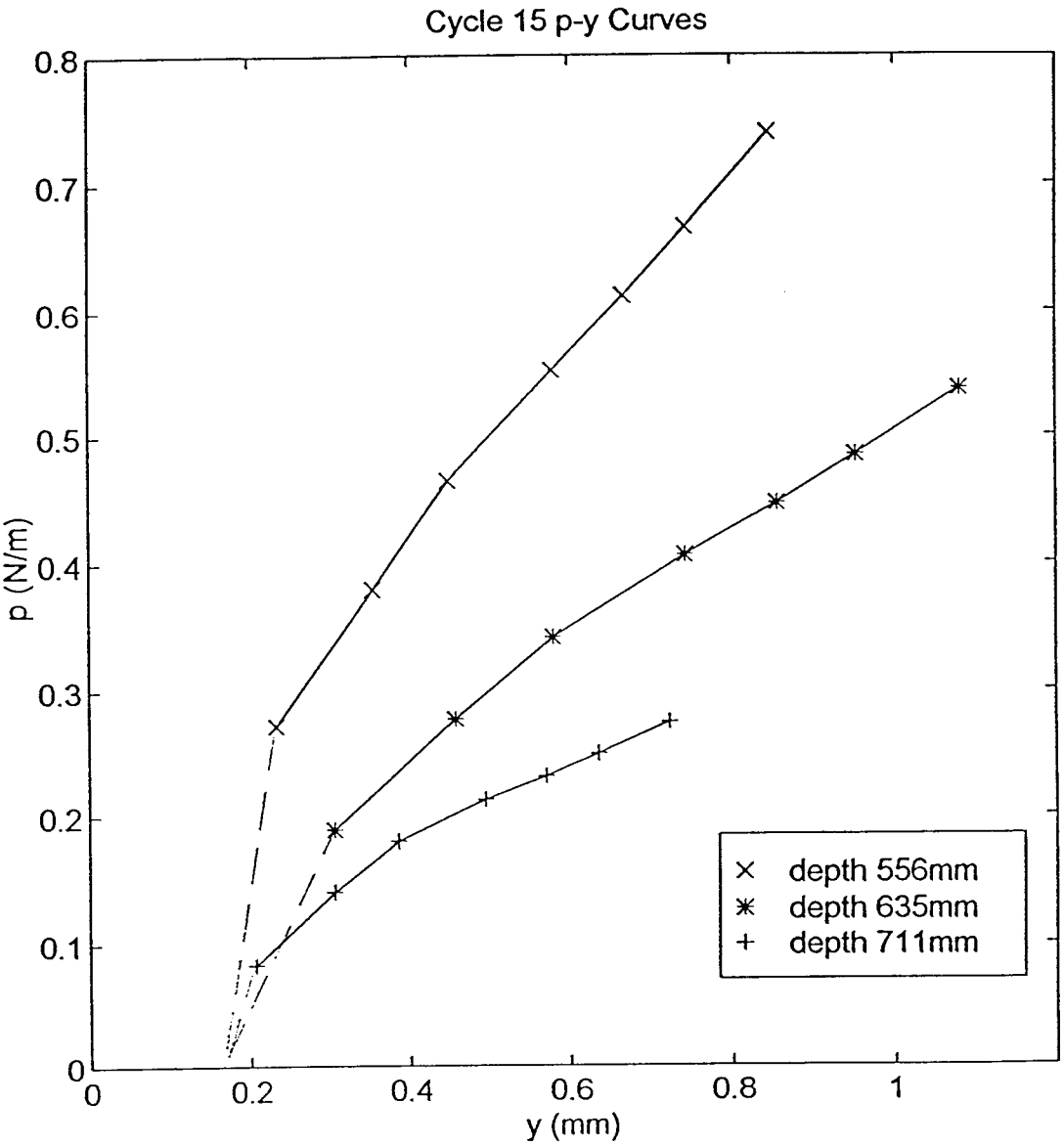

Figure 60. P-y curves for lead pile at various depths for cycle 15 (SI units).

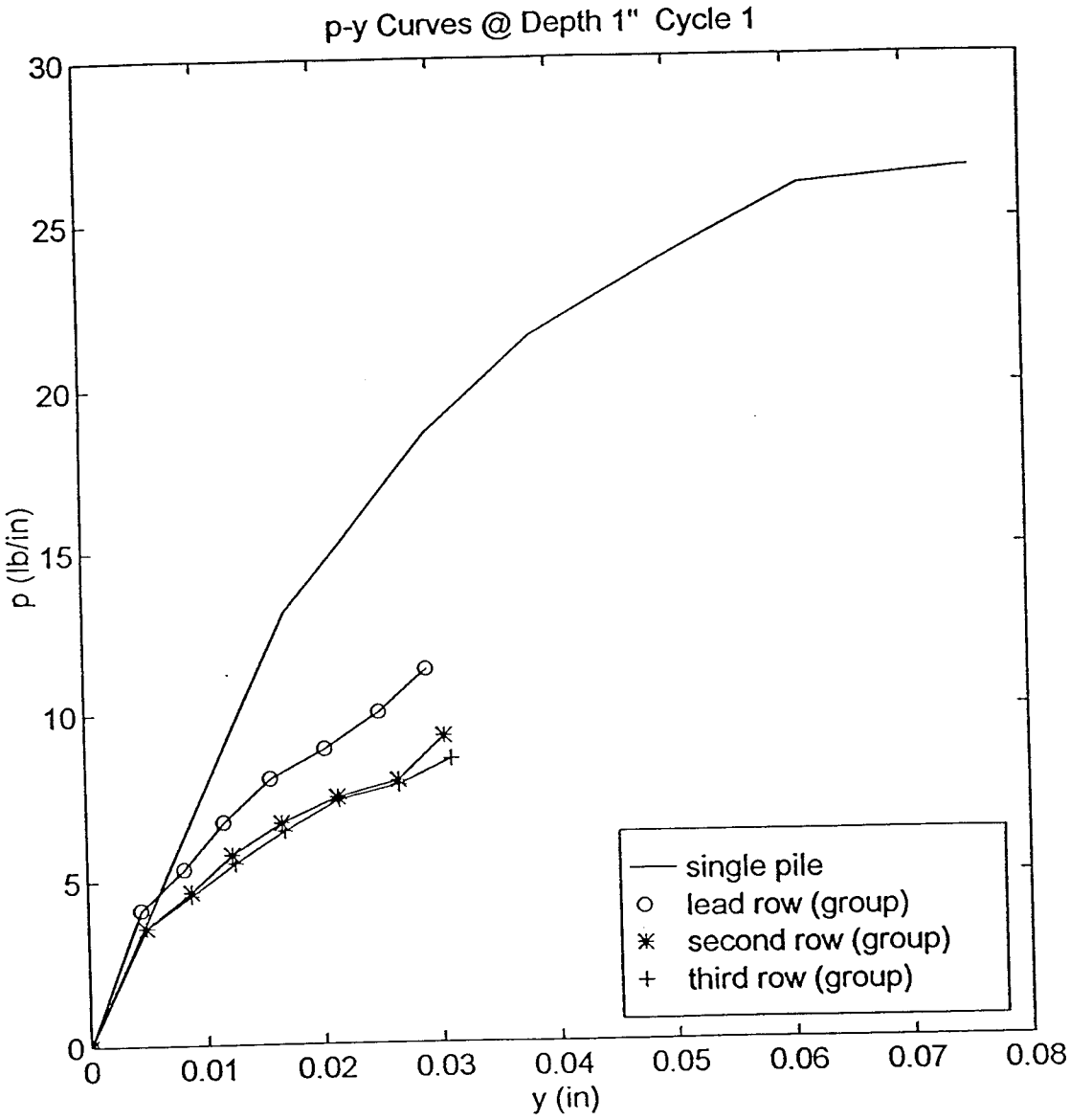

Figure 61. Comparison of single pile with group p-y curves @ 1 in. depth for cycle 1.

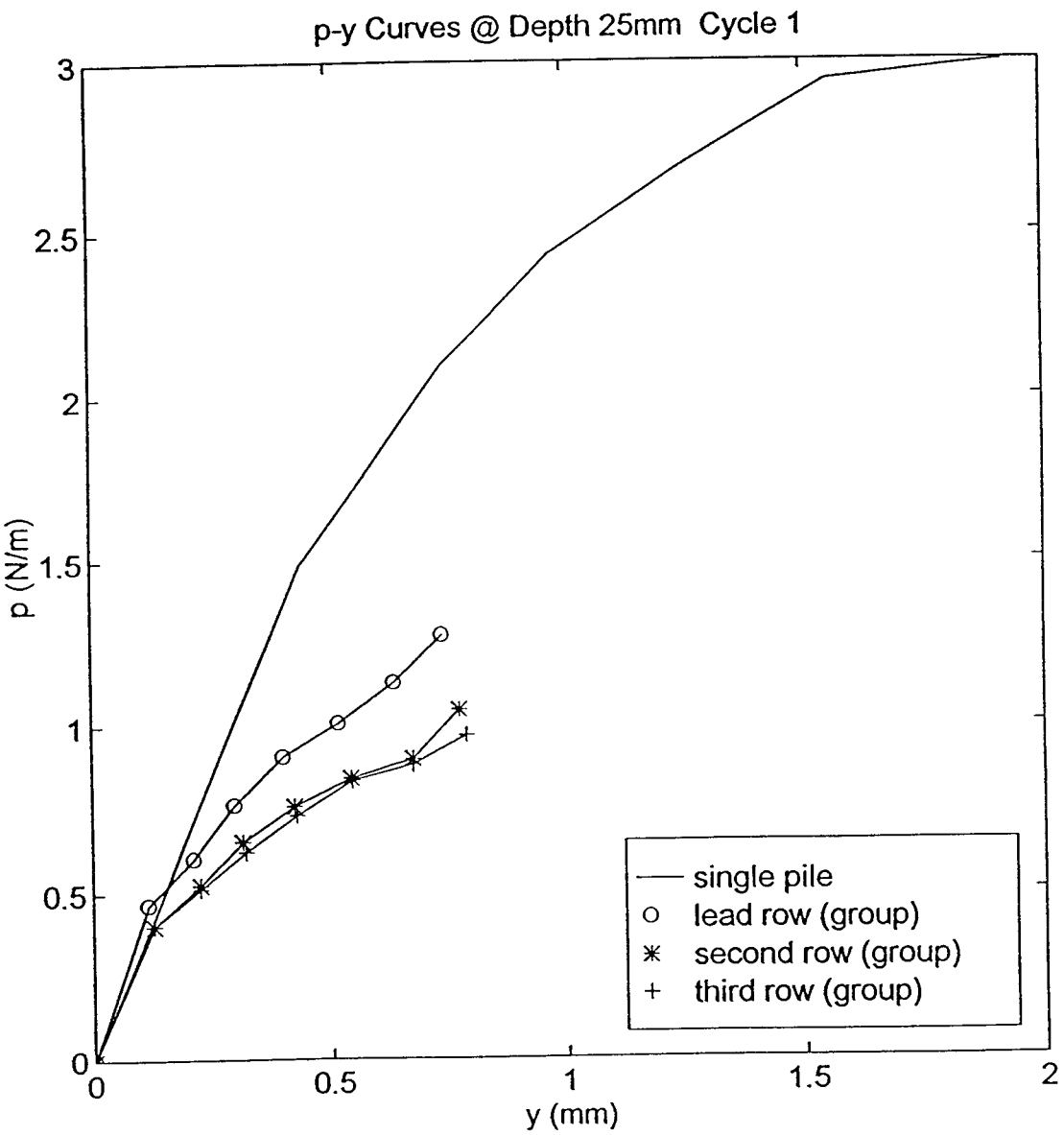

Figure 62. Comparison of single pile with group p-y curves @ 25 mm depth for cycle 1.

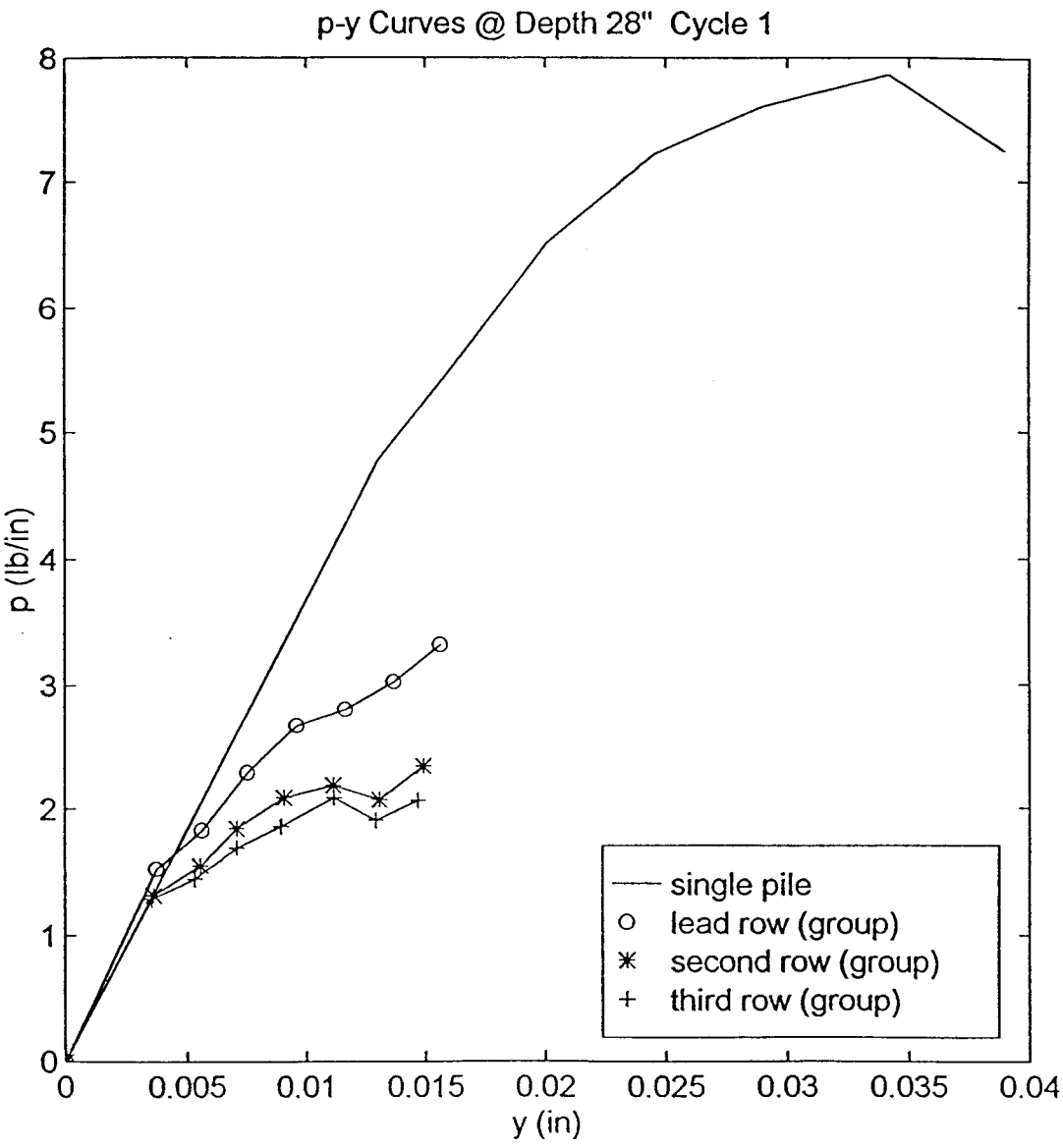

Figure 63. Comparison of single pile with group p-y curves @ 28 in. depth for cycle 1.

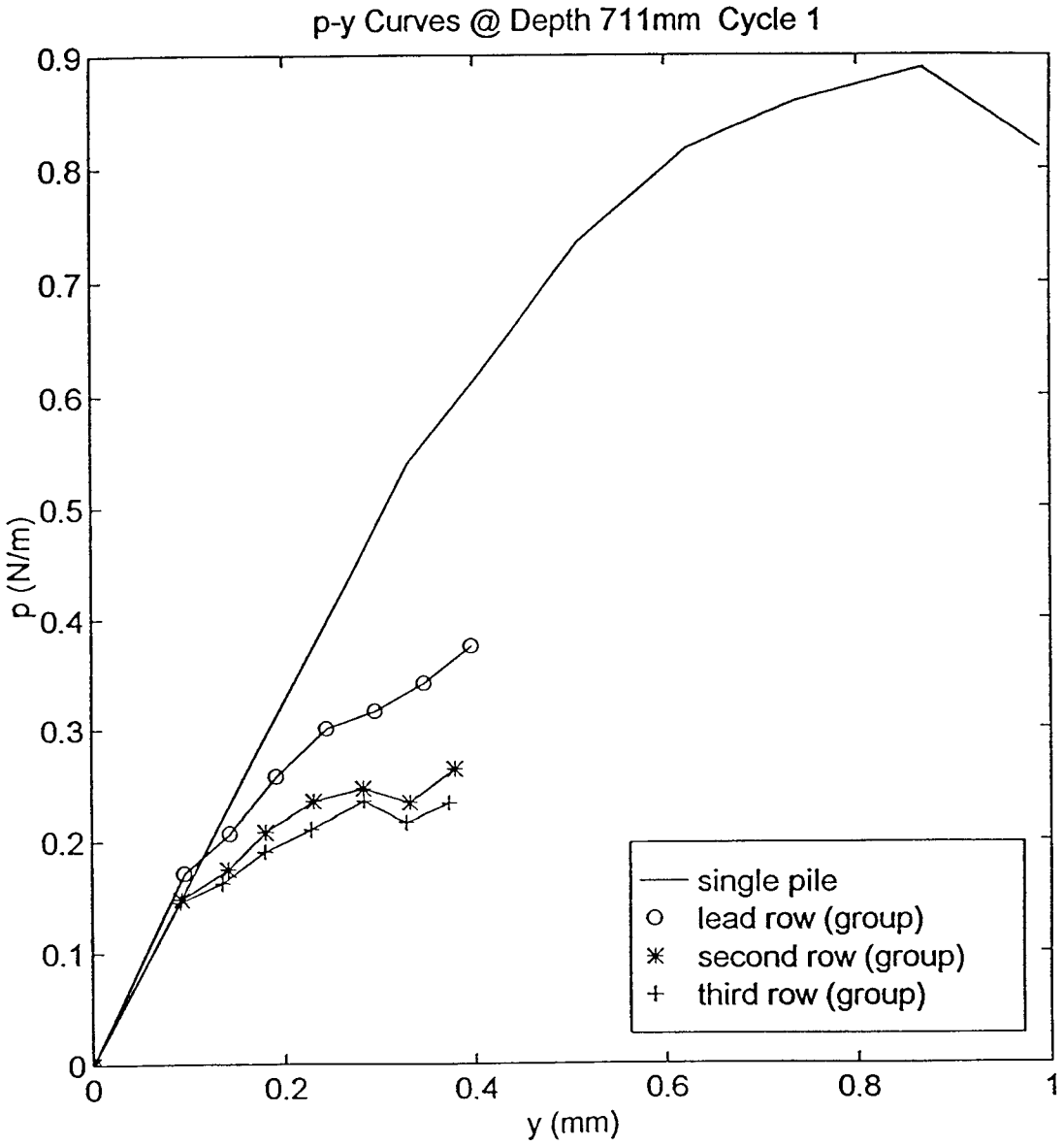

Figure 64. Comparison of single pile with group p-y curves @ 711 mm depth for cycle 1.

CHAPTER VII

CONCLUSIONS AND RECOMMENDATIONS

Conclusions

Many results were generated from the volumes of data acquired. The first group of results contain; load distribution, moment distribution per pile, moment distribution per cycle, and load vs. deflection. A comparison of test results with FLPIER predictions are provided showing load vs. deflection and maximum bending moment vs. deflection. The second group of results include normalized bending moment and deflection curves for use as design tools. The third group of results include p-y curves for different piles at different depths and different cycles, as well as accompanying graphs for explanation. These three groups of results were generated to define more clearly the response of pile groups in clay soils and ultimately mitigate seismic hazard by increasing the confidence in deep foundation design when cyclic loads are a concern.

The outcome of this research was a smashing success for a number of reasons. First, that an entire test facility and accompanying equipment was built from scratch and that the system produced such good results was a feat unto itself. Building a data acquisition system with no prior knowledge of the intricacies of electronic signal processing was a daunting task that seemed overwhelming at times. The author would recommend to anyone attempting the same foolishness again that it is not worth the effort. Second, results provided valuable insight into the mechanical response of lacustrian clays when imposed on by a deep foundation. This is an area where little research has been conducted and any empirical base is of great import. Third, the results are of some immediate use for design purposes when using similar piles and in similar soil profiles. The normalized design curves can be used to bolster confidence in design and the p-y curves can be used as input data for design software.

Recommendations For Further Research

he future of model testing looks promising for deep foundations in clay. The author believes that the model testing facility built at Utah State University is highly viable as an relatively inexpensive deep foundation testing tool. The results obtained from the first two tests (Phase 1 and Phase 2) sometimes looked so good they appeared to be textbook reproductions and not empirical data. As always in empirical research, there is room for improvement and modifications. The following is a list of recommendations for the next phase of model pile group testing:

1. The model piles should be installed with less free length (i.e. stick-up) than the previous two tests. This was a function of equipment limitations. To remedy this, the testing facility should contain a minimum of 60 in (1524 mm) of clay. A deeper embedded pile will result in less bending moment but more soil strain. Higher soil strains will define the p-y curves over a larger range making the determination of p-multipliers an easier objective.
2. The pile cap connecting rod should be re-manufactured. It should be redesigned so there is no bending moment incurred in it, only longitudinal stress. The rod also should be milled thinner to provide more sensitivity when measuring load. This also should be done for the load cells. Higher sensitivity when measuring loads should make interpreting load distribution results a much easier prospect.
3. A high speed run using the existing set up should be done: the model pile group loaded cyclically at the highest load possible with the cycling rate at maximum. This would entail pushing the air pressure generator to its maximum operating level and running the test continuously without specifically recording the unloading rate. This could be done using the LabView program named T1000. The objective would be to compare these results with the results from Phase 2, looking for any differences.

Further research can be performed using the current mass of data collected from Phase 2. The wealth of information that can be squeezed from the test results have only been touched on. Suggestions for further use of the Phase 2 data follow:

1. Results from Phase 2 should be compared with results from the full scale lateral load tests conducted by Rollins, Petersen, and Weaver (1996).
2. The p-y curves generated from the empirical data should be used as input p-y curves. These should be input into FLPIER and runs made to see how the deflections compare with the model group deflections.
3. A statistical analysis of the load distribution data should be done to determine load factors for pile row position.

REFERENCES

Broms, Bengt B. 1965. Design of laterally loaded piles. Journal of Soil Mechanics and Foundations Division, American Society of Civil Engineers, 91(SM3):79-99.

Brown, D. A. and H. T. Bollman. 1993. Pile-supported bridge foundations designed for Impact loading. Proceedings, Lateral and Rotational Stiffness of Highway Bridges, Federal Highway Administration, Crystal City, Virginia. 266-281p.

Brown, D. A., C. Morrison and L. C. Reese. 1988. Lateral load behavior of pile group in sand. Journal of Geotechnical Engineering, American Society of Civil Engineers, 114(11):1261-1276.

Brown, D. A. and L. C. Reese. 1985. Behavior of a Large-Scale Pile Group Subjected to Cyclic Lateral Loading. Geotechnical Engineering Report GR85-12, Geotechnical Engineering Center, Bureau of Engineering Research, Austin, Texas.

Caliendo, J. A. and L. R. Anderson. 1996. Lateral load testing of model piles, phase 1. Report to the Mountain Plains Consortium, Utah Transportation Center, Report MPC 96-60.

Desai, C. S. and G. C. Appel. 1976. 3-D analysis of laterally loaded structures. Proceedings, Second International Conference on Numerical Methods in Geomechanics, Blacksburg, Virginia, June.

Federal Highway Administration Manual. 1996. Design and construction of driven pile foundations. Federal Highway Administration Contract Number DTFH61-C- 00115, 1:9-128 to 9-133.

Hetenyi, M. 1946. Beams on elastic foundation. University of Michigan Press, Ann Arbor, Michigan.

Kramer, Steven L. 1996. Geotechnical Earthquake Engineering. Prentice-Hall, Inc., Upper Saddle River, New Jersey. 294-303p.

Matlock, H. and E. A. Ripperger. 1956. Procedures and instumentation for tests on a laterally loaded pile. Proceedings, Eighth Texas Conference on Soil Mechanics and Foundation Engineering, Austin, Texas.

McClelland, B. and J. A. Focht Jr. 1958. Soil Modulus for Laterally Loaded Piles. Transactions, American Society of Civil Engineers, 123:1049-1063.

O'Reilly, M. P. and S. F. Brown. 1991. Cyclic Loading of Soils: from theory to design. Van Nostrand Reinhold; New York. 313-366p.

Poulos, H. G. 1971. Behavior of laterally loaded piles: I and II. Journal of the Soil Mechanics and Foundations Division, American Society of Civil Engineers, 97(SM5):711-751.

Rawlings, Mark A. 1997. Cyclic lateral loading of model pile groups in clay. Masters Thesis. Civil and Environmental Engineering Department, Geotechnical Division, Utah State University, Logan, Utah.

Rollins, K., K. Peterson and T. Weaver. 1996. Full-scale group lateral load testing in soft clay. NCEER Bulletin, 10/96:9-11.

Seed, H. B. and I. M. Idriss. 1982. Ground motion and soil liquefaction during earthquakes. Earthquake Engineering Research Institute Monograph:97-119.

Terzaghi, K. 1955. Evaluation of coefficients of subgrade reaction. Geotechnique, 5:279-326.

Tomlinson, M. L. 1994. Pile design and construction practice, fourth edition. Chapman and Hall; London:227-232.

Winkler, E. 1876. Die lehre von elastizitat und festigkeit. (On Elasticity and Fixity), Prague.

APPENDIX A: EXTENDED BIBLIOGRAPHY

Badoni, D. and N. Makris. 1996. Modeling nonlinear pile-soil interaction: Inertial and Seismic Response. Proceedings, Fifth International Conference on the Application of Stress-Wave Theory to Piles, Orlando, Florida. 188-202p.

Blaney, G. W. and M. W. O'Neill. 1986. Measured lateral response of mass on single pile in clay. Journal of Geotechnical Engineering, American Society of Civil Engineers, 112(4):443-457.

Bollman, Henry T. 1993. Notes for discussion on designing deep foundations for lateral loads. Proceedings, Lateral and Rotational Stiffness of Highway Bridges, Federal Highway Administration , Crystal City, Virginia. 176-189p.

Broms, Bengt B. 1965. Design of laterally loaded piles. Journal of Soil Mechanics and Foundations Division, American Society of Civil Engineers, 91(SM3):79-99.

Broms, Bengt B. 1964. Lateral resistance of piles in cohesive soils. Journal of Soil Mechanics and Foundations Division, American Society of Civil Engineers, 90(SM2):27-63.

Brown, D. A. and H. T. Bollman. 1993. Pile-supported bridge foundations designed for impact loading. Proceedings, Lateral and Rotational Stiffness of Highway Bridges, Federal Highway Administration, Crystal City, Virginia.

Brown, D. A., C. Morrison and L. C. Reese. 1988. Lateral load behavior of pile group in sand. Journal of Geotechnical Engineering, American Society of Civil Engineers, 114(11):1261-1276.

Brown, D. A. and L. C. Reese. 1985. Behavior of a large-scale pile group subjected to cyclic lateral loading. Geotechnical Engineering Report GR85-12, Geotechnical Engineering Center, Bureau of Engineering Research, Austin, Texas.

Brown, D. A., L. C. Reese and M. W. O'Neill. 1987. Cyclic lateral loading of a large-scale pile group. Journal of Geotechnical Engineering, American Society of Civil Engineers, 113(11):1326-1343.

Boulanger, R. W., D. W. Wilson and B. L. Kutter. 1997. Soil-pile-superstructure interaction in liquefiable sand. Proceedings, Transportation Research Board, Washington D. C.

Caliendo, J. A. and L. R. Anderson. 1996. Lateral load testing of model piles, phase 1. Report to the Mountain Plains Consortium, Utah Transportation Center, Report MPC 96-60.

Clough, Ray W. 1993. P. Gulkan and R. W. Clough (Ed.). A structural engineer's view of soil-structure-interaction. Developments in Dynamic Soil-Structure Interaction, Kluwer Academic Publishers, Netherlands.

Desai, C. S. and G. C. Appel. 1976. 3-D Analysis of laterally loaded structures. Proceedings, Second International Conference on Numerical Methods in Geomechanics, Blacksburg, Virginia, June.

Federal Highway Administration Manual. 1996. Design and construction of driven pile foundations. Federal Highway Administration Contract Number DTFH61-C- 00115, 1:9-128 to 9-133.

Gaul, Roy D. 1958. Model study of a dynamically laterally loaded pile. Journal of Soil Mechanics and Foundations Division, American Society of Civil Engineers, 84(SM1), Paper 1535:1-33.

Hetenyi, M. 1946. Beams on elastic foundation. University of Michigan Press, Ann Arbor, Michigan.

Hoit, M., C. Hays and M. McVay. 1997. Pier analysis and design using Florida Pier. Proceedings, Transportation Research Board, Washington D. C.

Johnson, J. J. and A. P. Asfura. 1993. P. Gulkan and R. W. Clough (Ed.). Soil-structure interaction (SSI): Observations, data, and correlative analysis. Developments in Dynamic Soil-Structure Interaction, Kluwer Academic Publishers, Netherlands.

Kramer, Steven L. 1996. Geotechnical earthquake engineering. Prentice-Hall, Inc., Upper Saddle River, New Jersey.

Lam, I. P. and H. Law. 1994. Soil-foundation-structure-interaction-analytical considerations by empirical p-y methods. Proceedings, 3rd Annual Seismic Research Workshop, Caltrans, Sacramento, California.

Lin, San-Shyan 1997. Nonlinear analysis of laterally loaded reinforced concrete pile in stiff clay. Proceedings, Transportation Research Board, Washington D. C.

Long, James H. 1984. The Behavior of vertical piles in cohesive soil subjected to Repetitive horizontal loading. Dissertation for University of Texas at Austin.

Matlock, H. and E. A. Ripperger. 1956. Procedures and instumentation for tests on a Laterally-loaded pile. Proceedings, Eighth Texas Conference on Soil Mechanics and Foundation Engineering, Austin, Texas.

McClelland, B. and J. A. Focht Jr. 1958. Soil Modulus for laterally loaded piles. Transactions, American Society of Civil Engineers, 123:1049-1063.

Novak, M. 1993. P. Gulkan and R. W. Clough (Ed.). Pile-soil-pile interaction under small and large displacements. Developments in Dynamic Soil-Structure Interaction, Kluwer Academic Publishers, Netherlands.

O'Neill, M. W., D. A. Brown, F. C. Townsend and N. Abar, N. 1997. Innovative load testing of deep foundations. Proceedings, Transportation Research Board, Washington D. C.

O'Reilly, M. P. and S. F. Brown. 1991. Cyclic loading of soils: from theory to design. Van Nostrand Reinhold; New York.

Poulos, H. G. 1971. Behavior of laterally loaded piles: I and II. Journal of the Soil Mechanics and Foundations Division, American Society of Civil Engineers, 97(SM5).

Rawlings, Mark A. 1997. Cyclic lateral loading of model pile groups in clay: phase 2A. Masters Thesis. Civil and Environmental Engineering Department, Geotechnical Division, Utah State University, Logan, Utah.

Reese, Lymon C. 1993. A Perspective on the beginning of p-y curves. Pile-Supported Bridge Foundations Designed for Impact Loading. Proceedings, Lateral and Rotational Stiffness of Highway Bridges, Federal Highway Administration, Crystal City, Virginia.

Reese, L. C., D. A. Brown and Shin-Tower Wang. 1988. Experimental research into the behavior of piles and pile groups subjected to cyclic lateral loading. Misc. Paper GL-88-10, US Army Corps of Engineers, Vicksburg, Mississippi.

Rollins, Kyle. 1995. Notes on seismic deformation analysis. Prof. of Civil Engineering, Brigham Young University.

Rollins, K., K. Peterson and T. Weaver. 1996. Full-scale group lateral load testing in soft clay. NCEER Bulletin, 10/96:9-11.

Seed, H. B. and C. K. Chan. 1966. Clay strength under earthquake loading conditions. Journal of Soil Mechanics and Foundations Division, American Society of Civil Engineers, 92(SM2):53-78.

Seed, H. B. and I. M. Idriss. 1969. Influence of soil conditions on ground motions during earthquakes. Journal of Soil Mechanics and Foundations Division, American Society of Civil Engineers, 95(SM1):99-136.

Seed, H. B. and I. M. Idriss. 1982. Ground motion and soil liquefaction during earthquakes. Earthquake Engineering Research Institute Monograph.

Talaganov, K. and M. Cubrinovski. 1991. Soil-structure interaction effects based on recorded strong motions during earthquakes. Proceedings, Second International Conference on Recent Advances in Geotechnical Earthquake Engineering and Soil Dynamics, St. Louis, Missouri, March 11-15, Paper No. 5.67.

Terzaghi, K. 1955. Evaluation of coefficients of subgrade reaction. Geotechnique, 5:279-326.

Thiers, G. R. and H. B. Seed. 1968. Cyclic stress-strain characteristics of clay. Journal of the Soil Mechanics and Foundations Division, American Society of Civil Engineers, 94(SM2):555-569.

Tomlinson, M. L. 1994. Pile design and construction practice, fourth edition. Chapman and Hall; London.

Townsend, F., M. McVay, P. Ruesta and M. Hoyt. 1997. Prediction and evaluation of a laterally-loaded pile group at roosevelt bridge. Florida Department of Transportation, Report #WPI 0510663.

Veletsos, A. S. 1993. P. Gulkan and R. W. Clough (Ed.). Design concepts for dynamics of soil-structure interaction. Developments in Dynamic Soil-Structure Interaction, Kluwer Academic Publishers, Netherlands.

Winkler, E. 1876. Die lehre von elastizitat und festigkeit. (On elasticity and fixity), Prague.

APPENDIX B: PHASE 2A RESULTS

Figure B1. Moment distribution @ cycle 1 (next 14 plots)

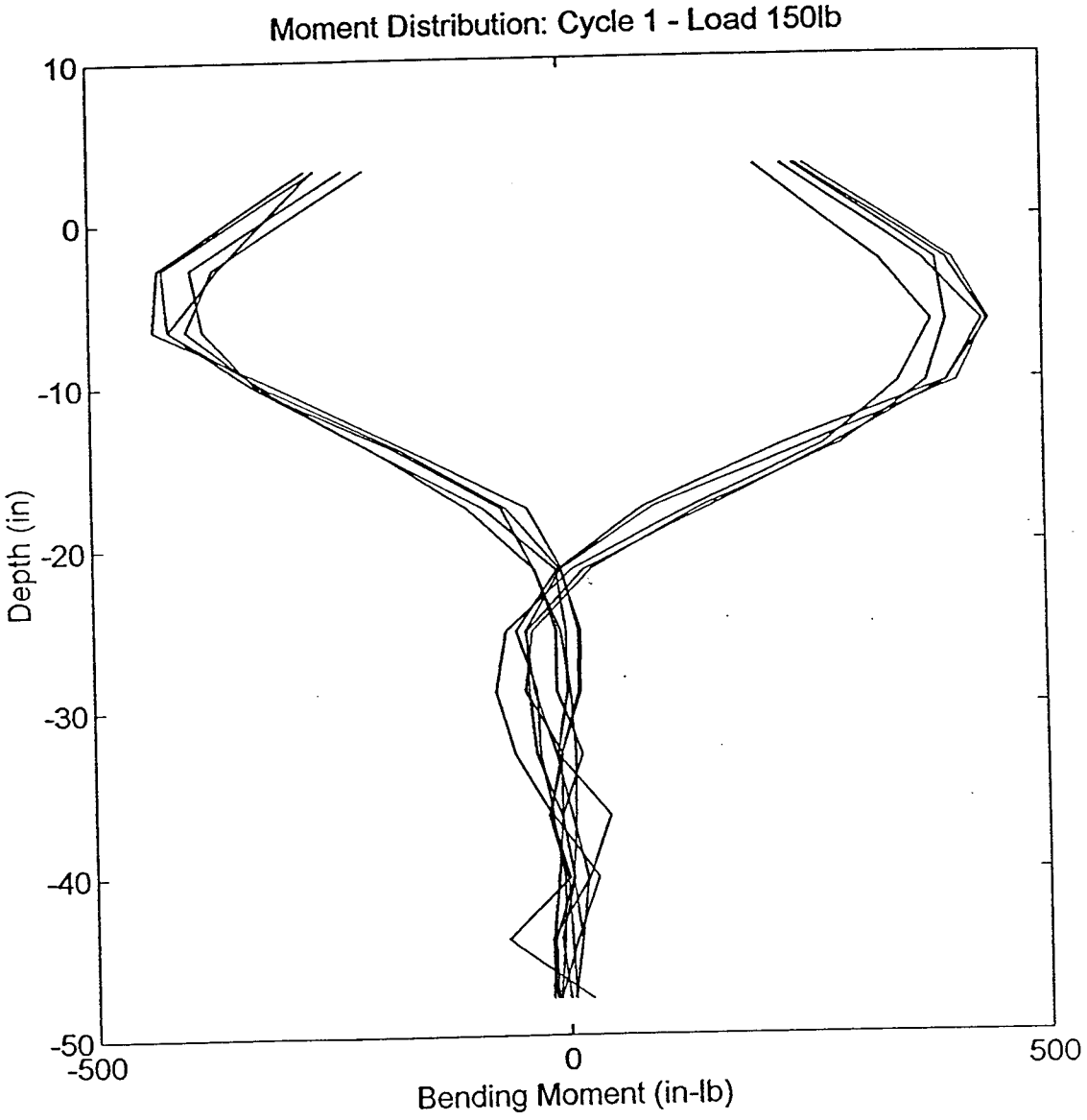
Moment Distribution: Cycle 1 - Load 150lb
10
0
-10
-20
-30
-40
-50
Depth (in)
-500
0
500
Bending Moment (in-lb)

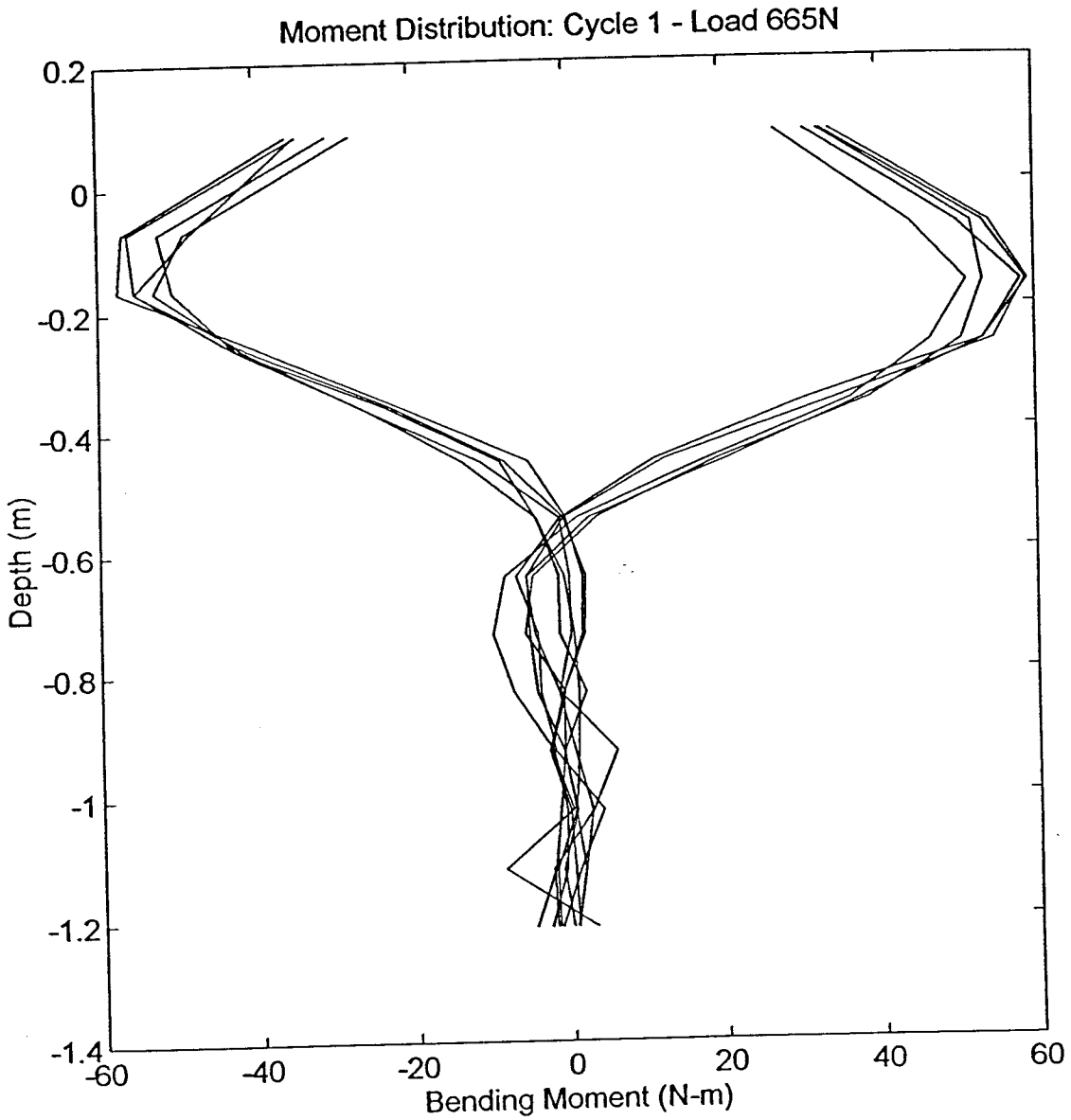
Moment Distribution: Cycle 1 - Load 665N
0.2
0
-0.2
-0.4
-0.6
-0.8
-1
-1.2
-1.4
Depth (m)
-60
-40
-20
0
20
40
60
Bending Moment (N-m)

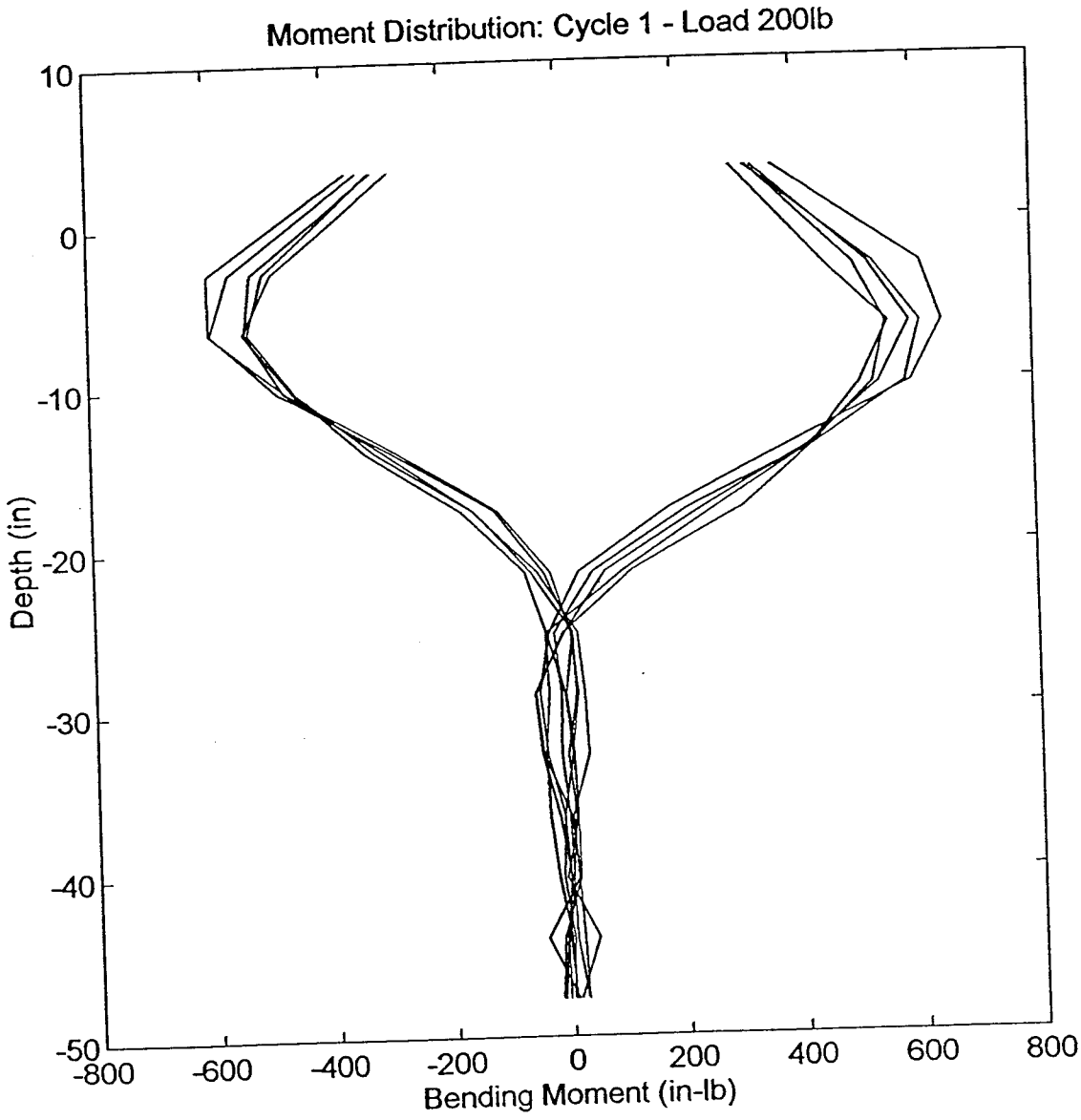
Moment Distribution: Cycle 1 - Load 200lb
10
0
-10
-20
-30
-40
-50
Depth (in)
-800
-600
-400
-200
0
200
400
600
800
Bending Moment (in-lb)

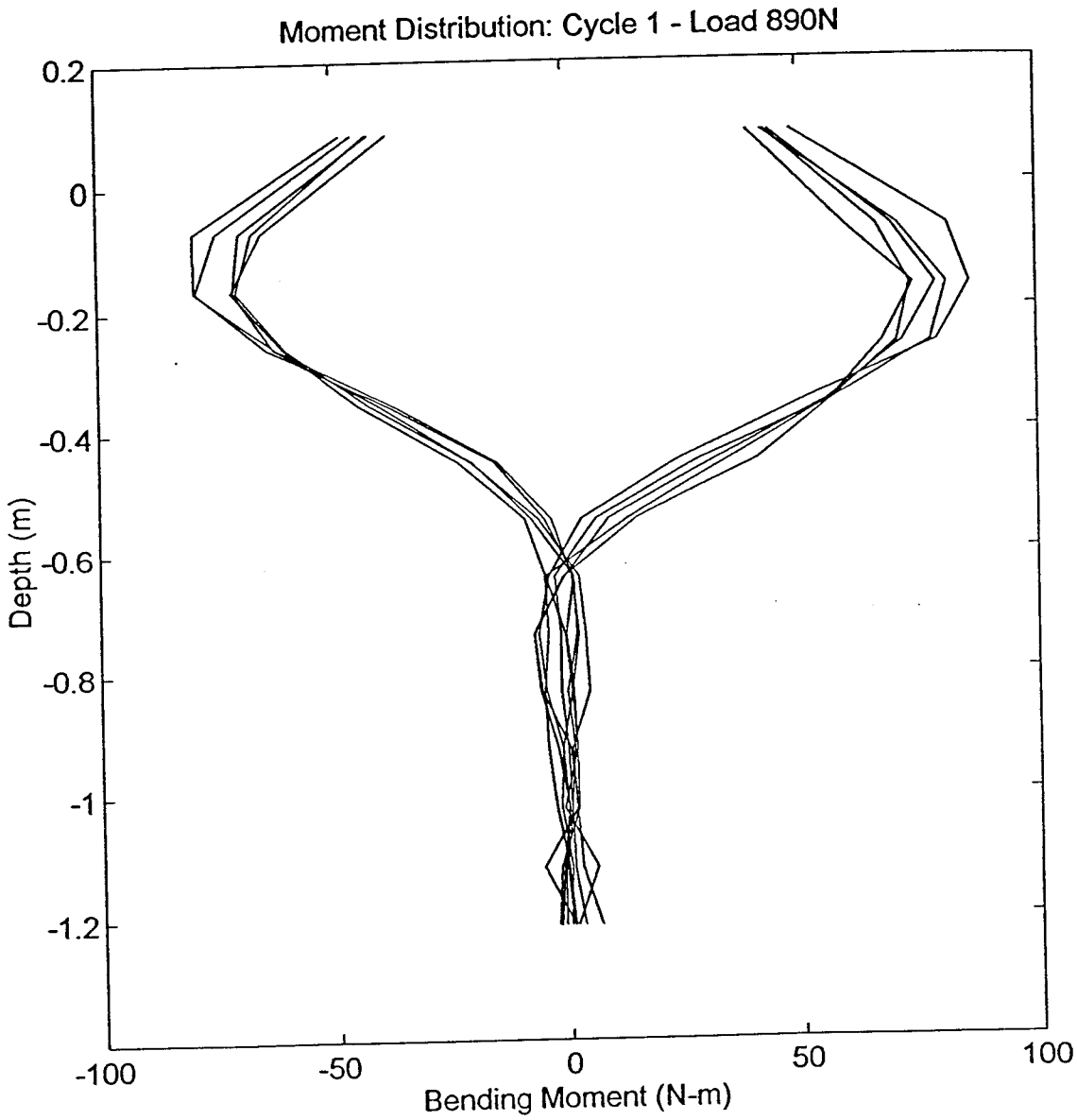
Moment Distribution: Cycle 1 - Load 890N
0.2
0
-0.2
-0.4
-0.6
-0.8
-1
-1.2
Depth (m)
-100
-50
0
50
100
Bending Moment (N-m)

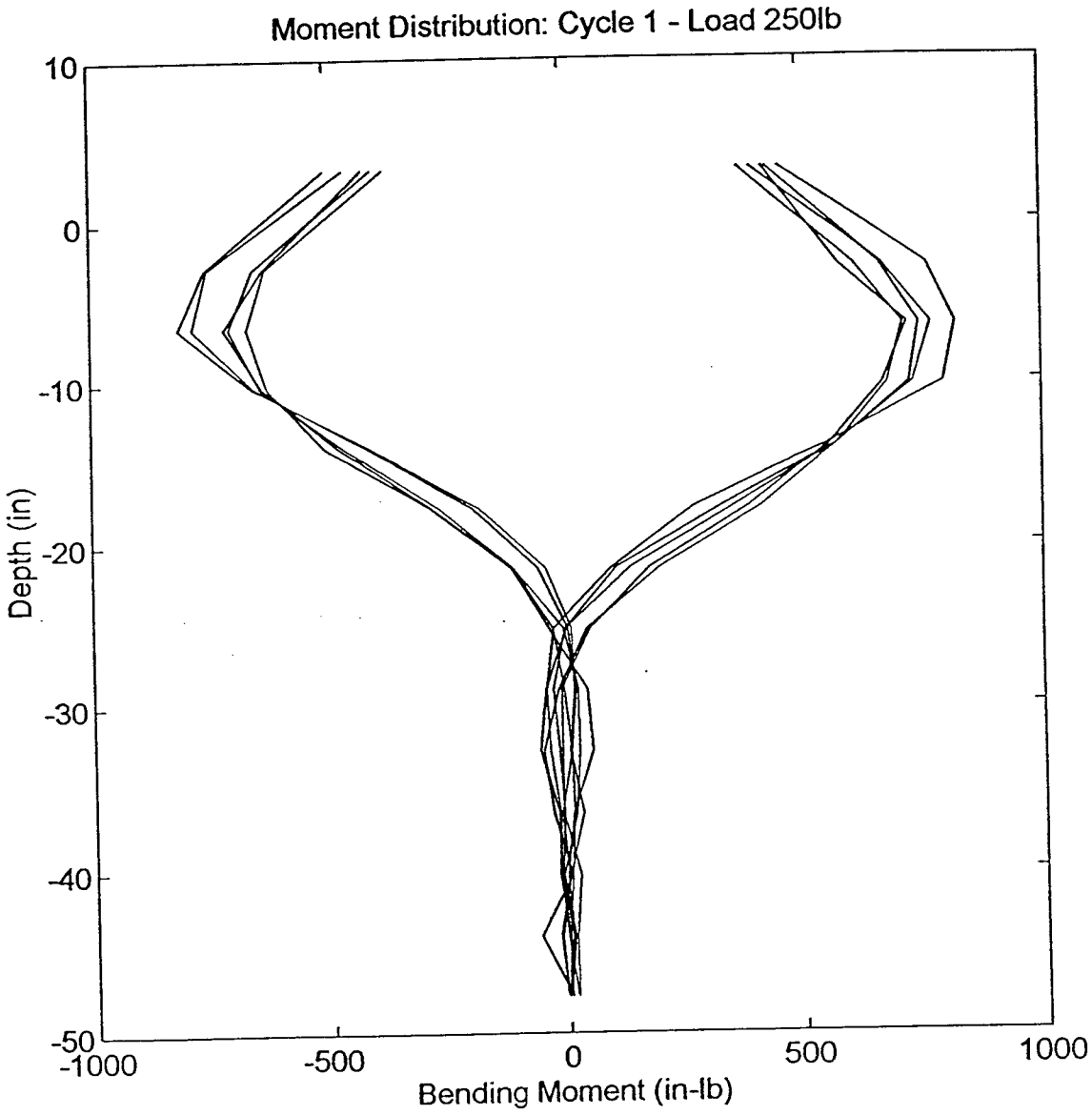
Moment Distribution: Cycle 1 - Load 250lb
10
0
-10
-20
-30
-40
-50
Depth (in)
-1000
-500
0
500
1000
Bending Moment (in-lb)

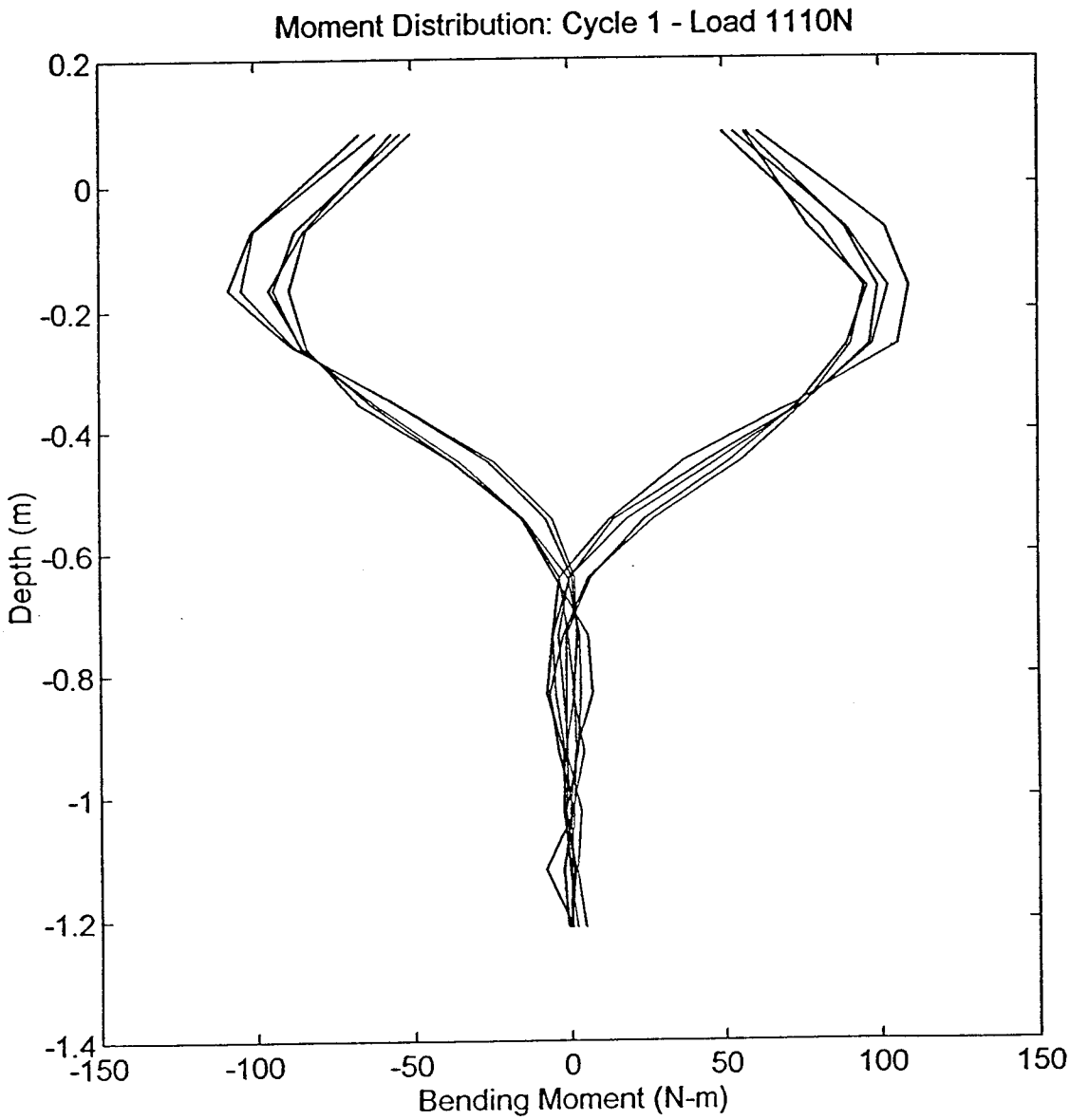
Moment Distribution: Cycle 1 - Load 1110N
0.2
0
-0.2
-0.4
-0.6
-0.8
-1
-1.2
-1.4
Depth (m)
-150
-100
-50
0
50
100
150
Bending Moment (N-m)

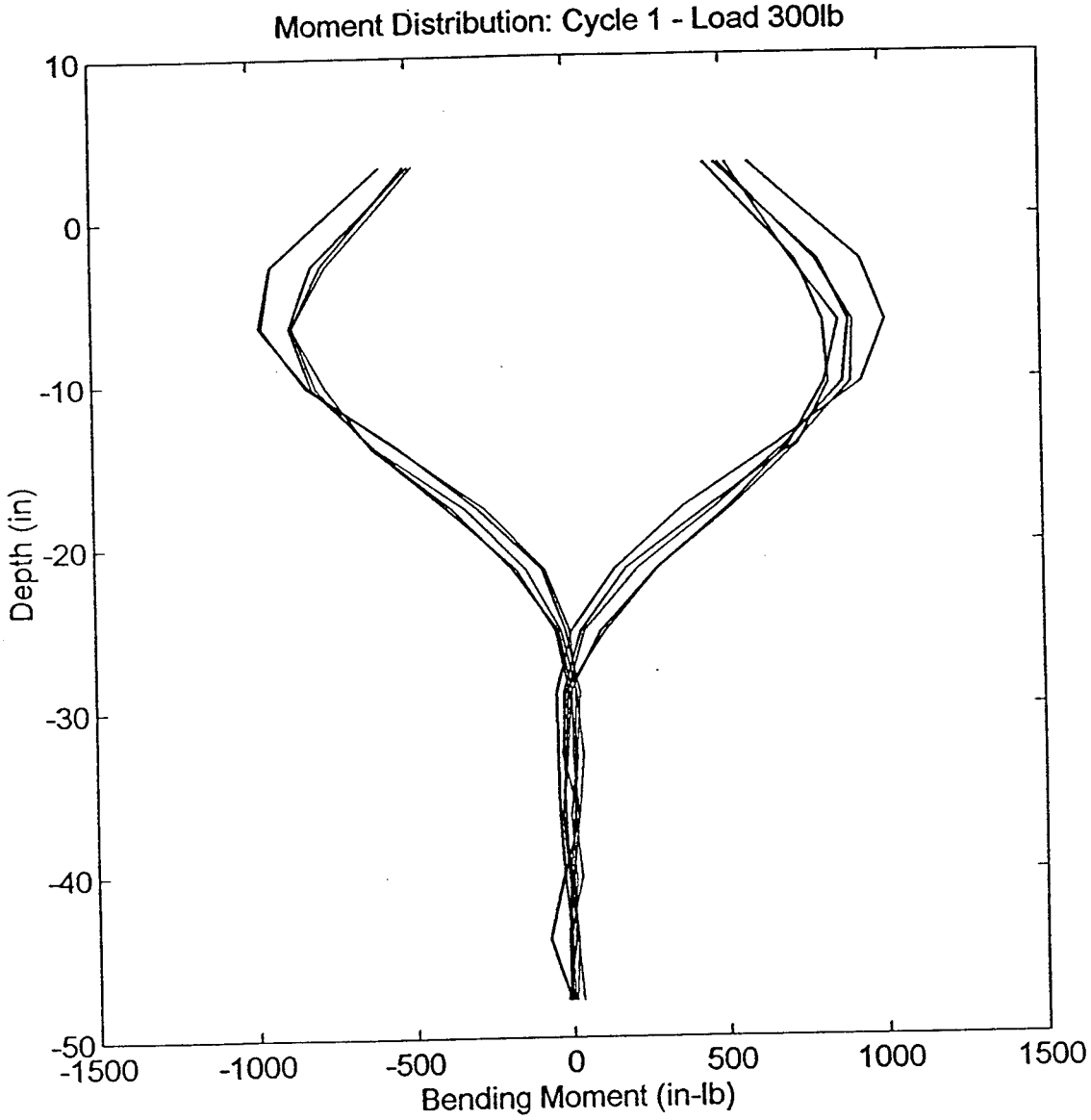
Moment Distribution: Cycle 1 - Load 300lb
10
0
-10
-20
-30
-40
-50
Depth (in)
-1500
-1000
-500
0
500
1000
1500
Bending Moment (in-lb)

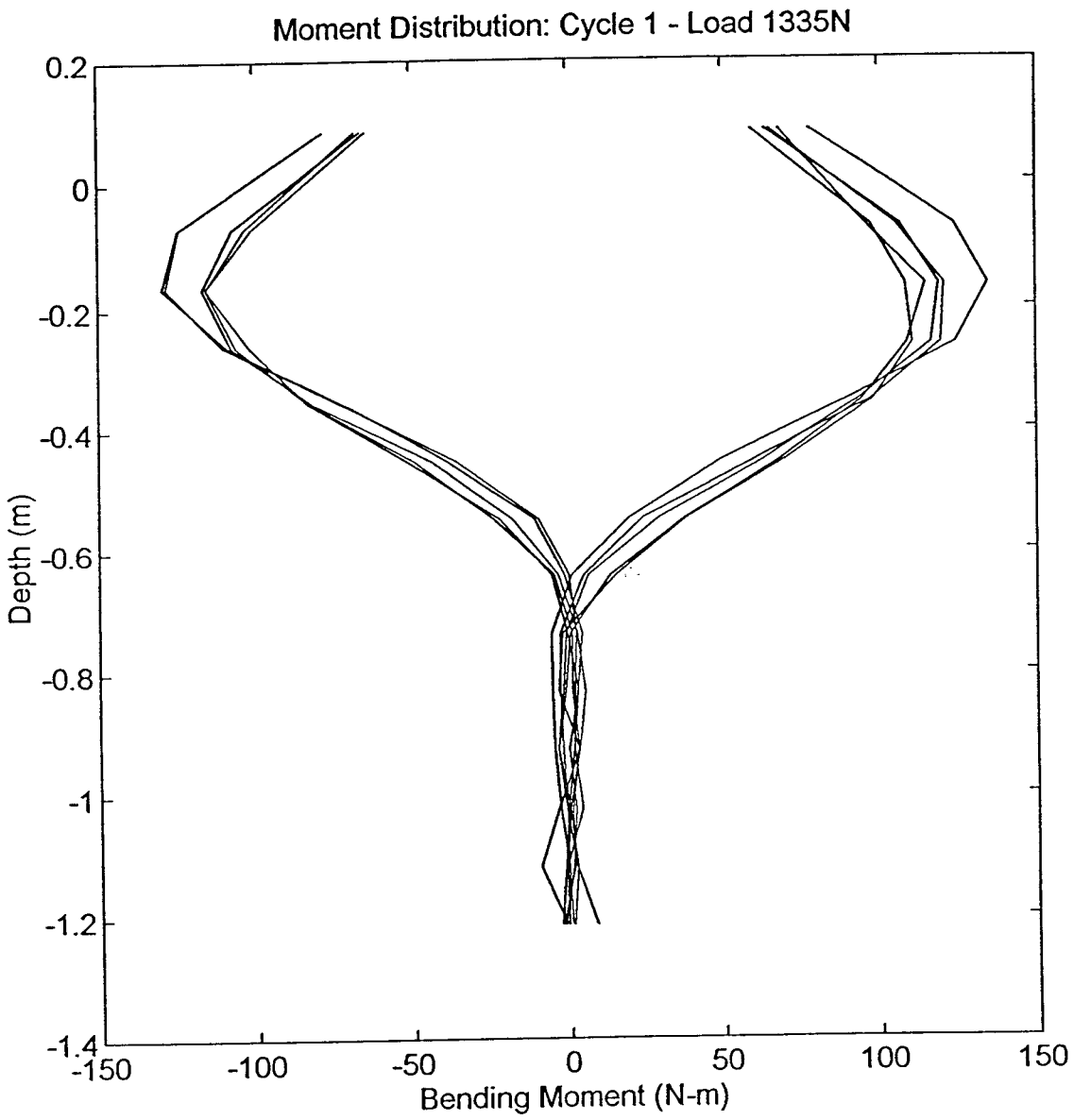
Moment Distribution: Cycle 1 - Load 1335N
0.2
0
-0.2
-0.4
-0.6
-0.8
-1
-1.2
-1.4
Depth (m)
-150
-100
-50
0
50
100
150
Bending Moment (N-m)

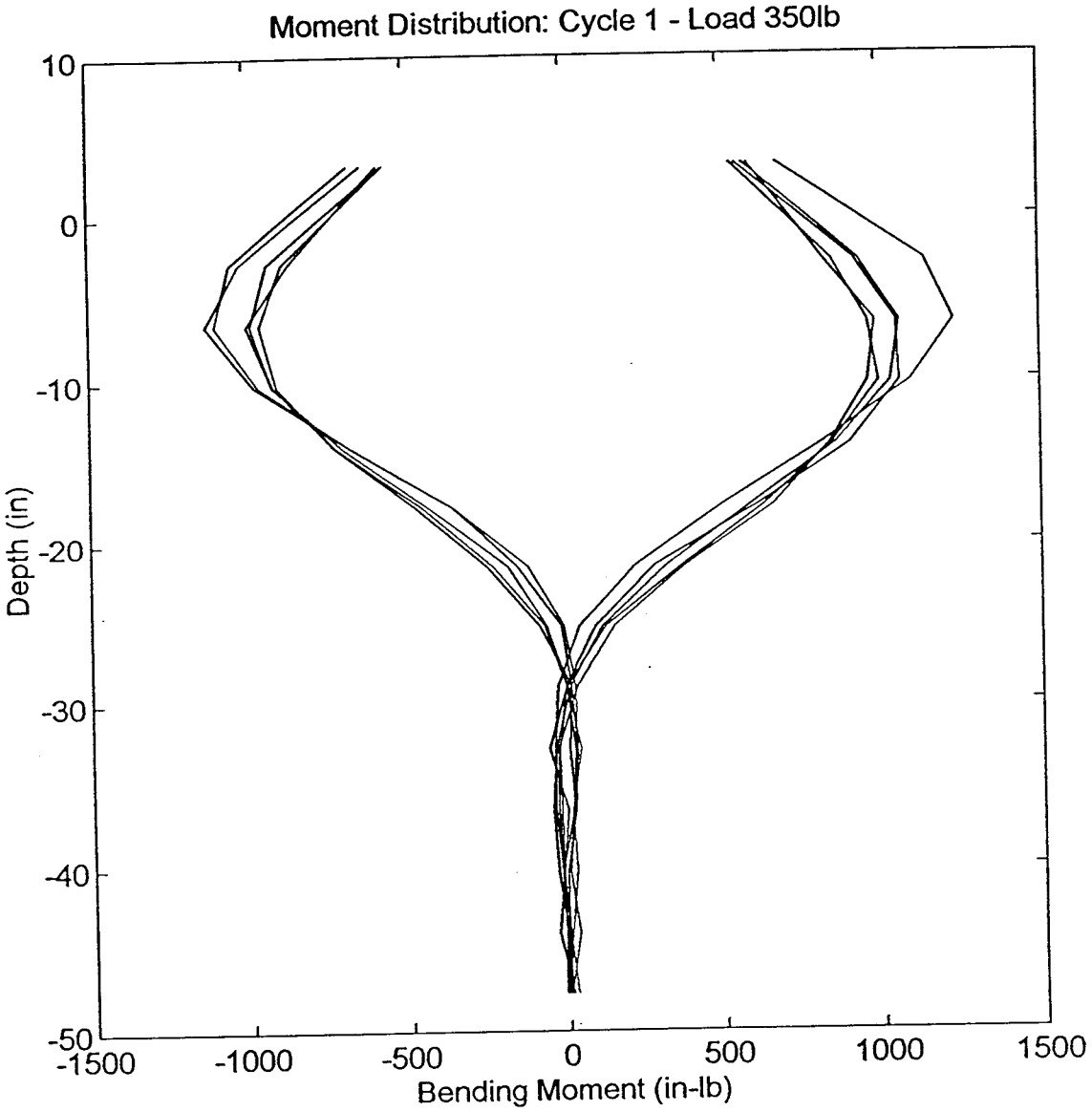
Moment Distribution: Cycle 1 - Load 350lb
10
0
-10
-20
-30
-40
-50
Depth (in)
-1500
-1000
-500
0
500
1000
1500
Bending Moment (in-lb)

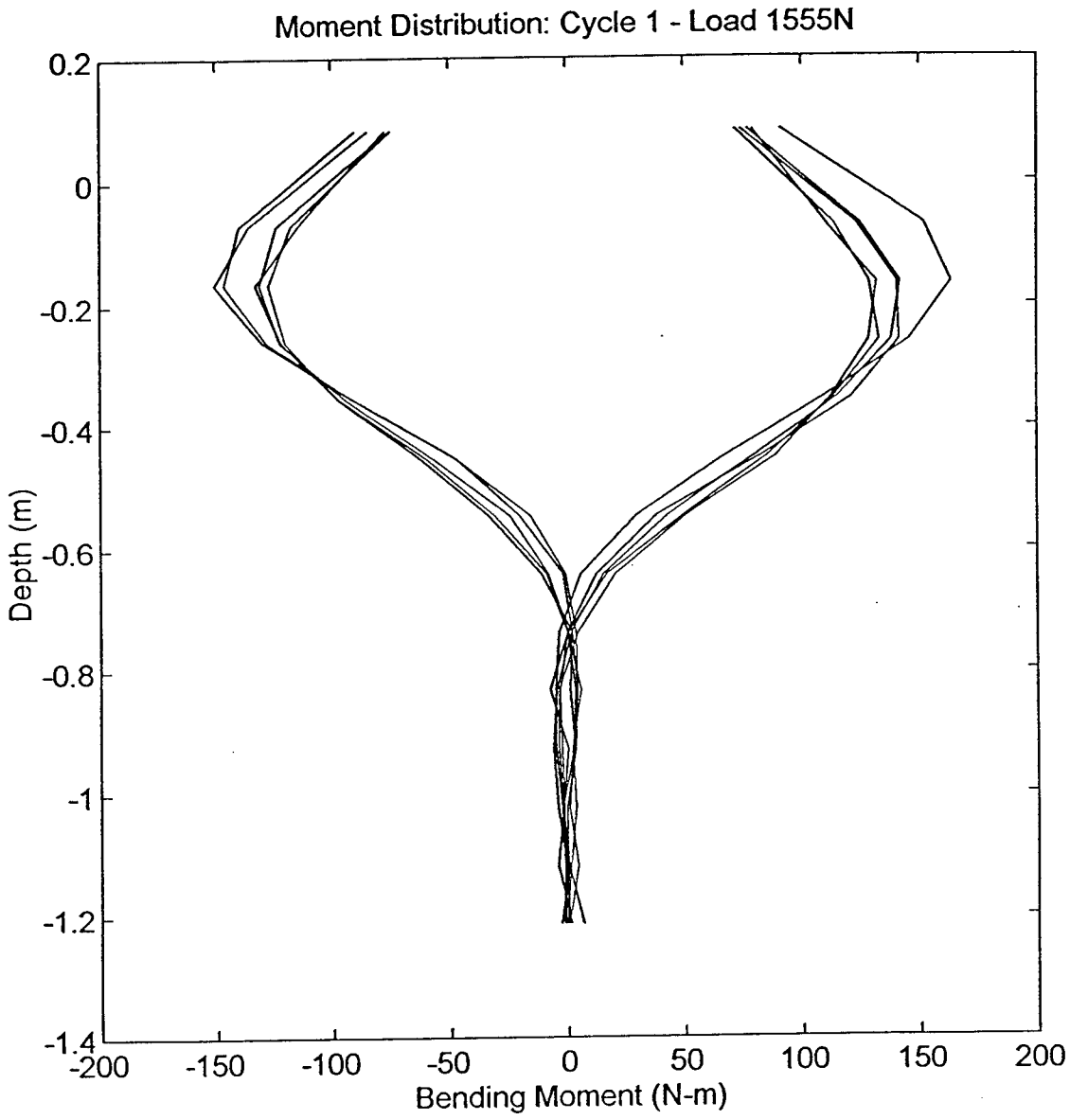
Moment Distribution: Cycle 1 - Load 1555N
0.2
0
-0.2
-0.4
-0.6
-0.8
-1
-1.2
-1.4
Depth (m)
-200
-150
-100
-50
0
50
100
150
200
Bending Moment (N-m)

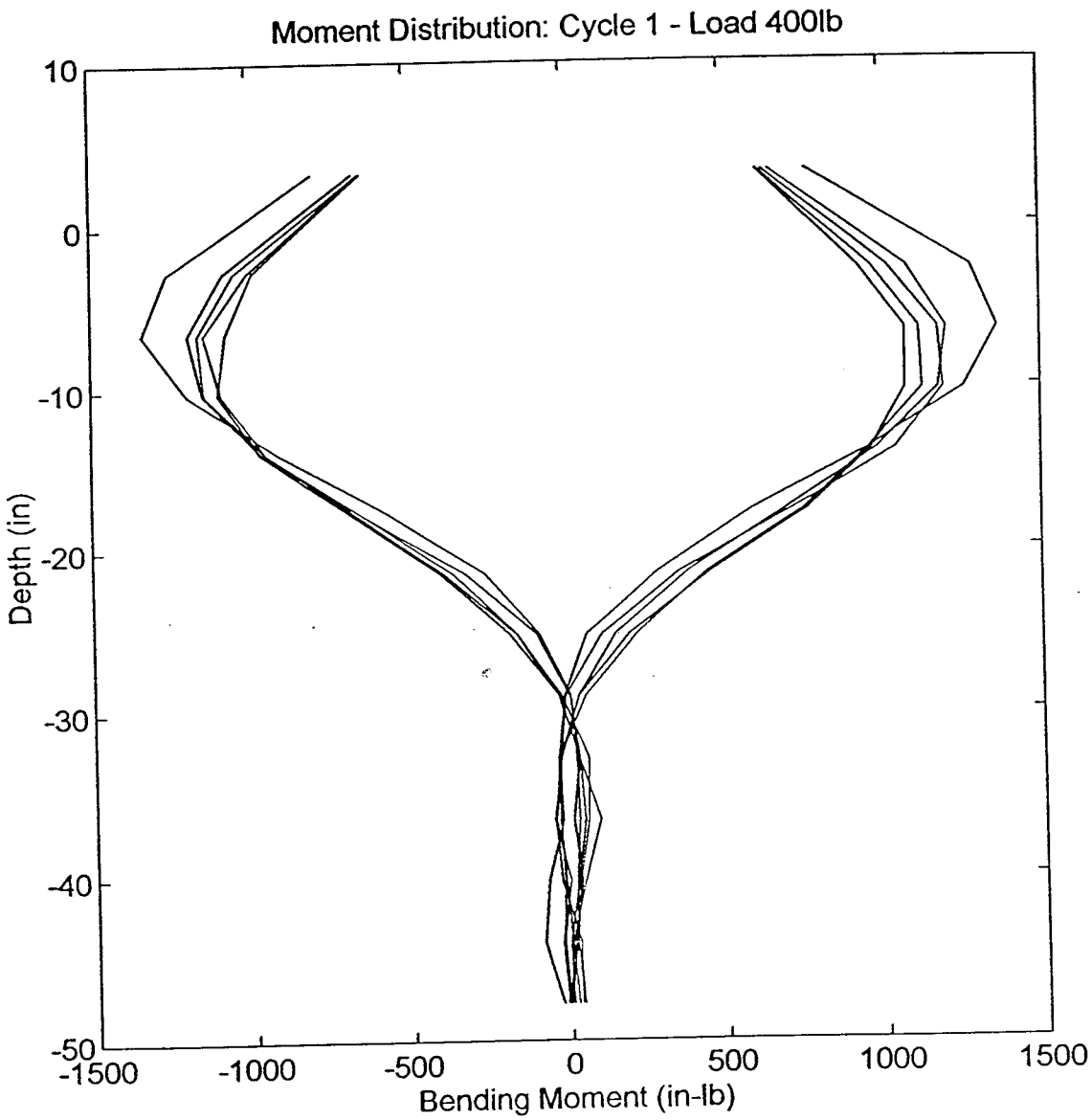
Moment Distribution: Cycle 1 - Load 400lb
10
0
-10
-20
-30
-40
-50
Depth (in)
-1500
-1000
-500
0
500
1000
1500
Bending Moment (in-lb)

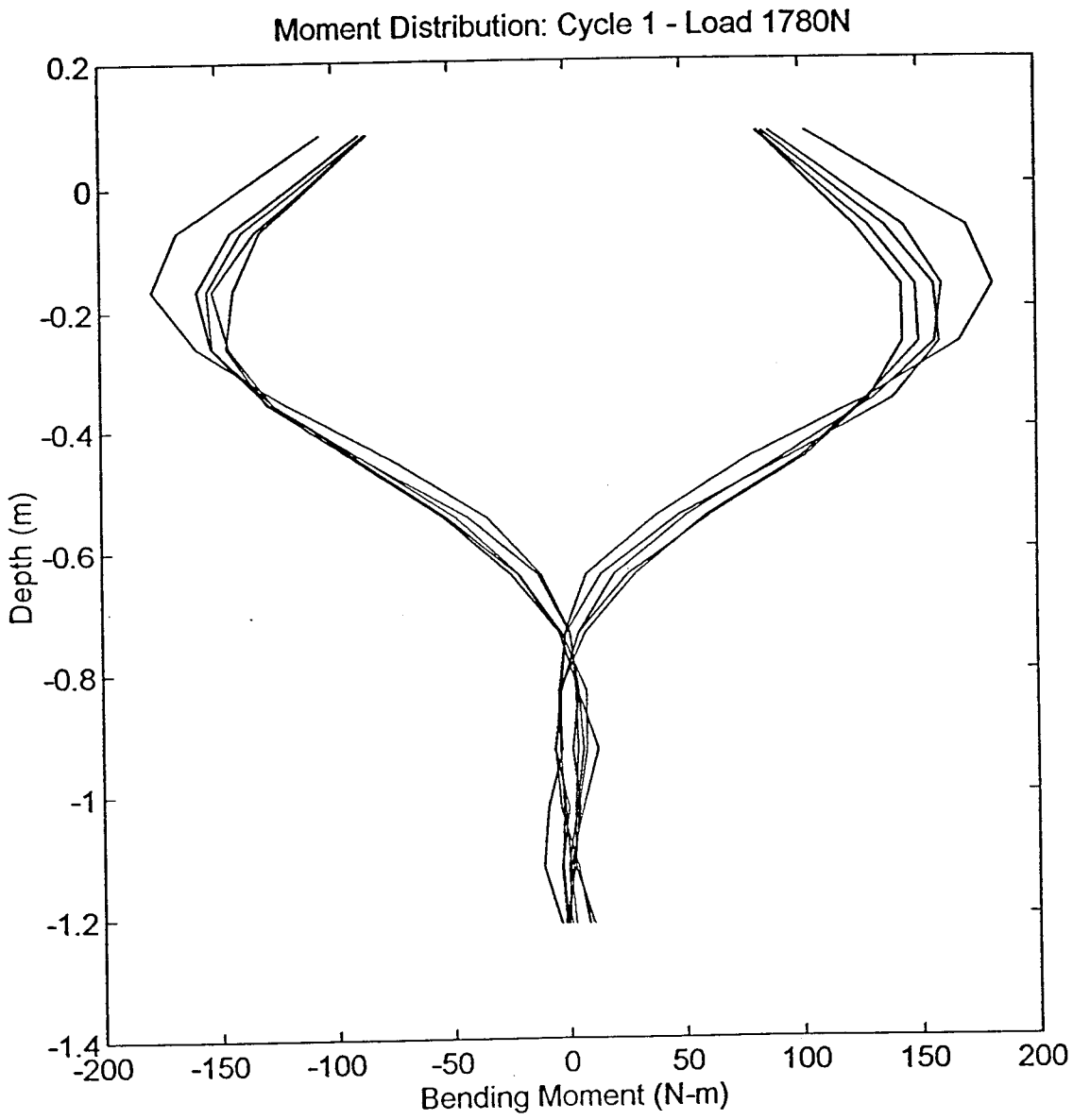
Moment Distribution: Cycle 1 - Load 1780N
0.2
0
-0.2
-0.4
-0.6
-0.8
-1
-1.2
-1.4
Depth (m)
-200
-150
-100
-50
0
50
100
150
200
Bending Moment (N-m)

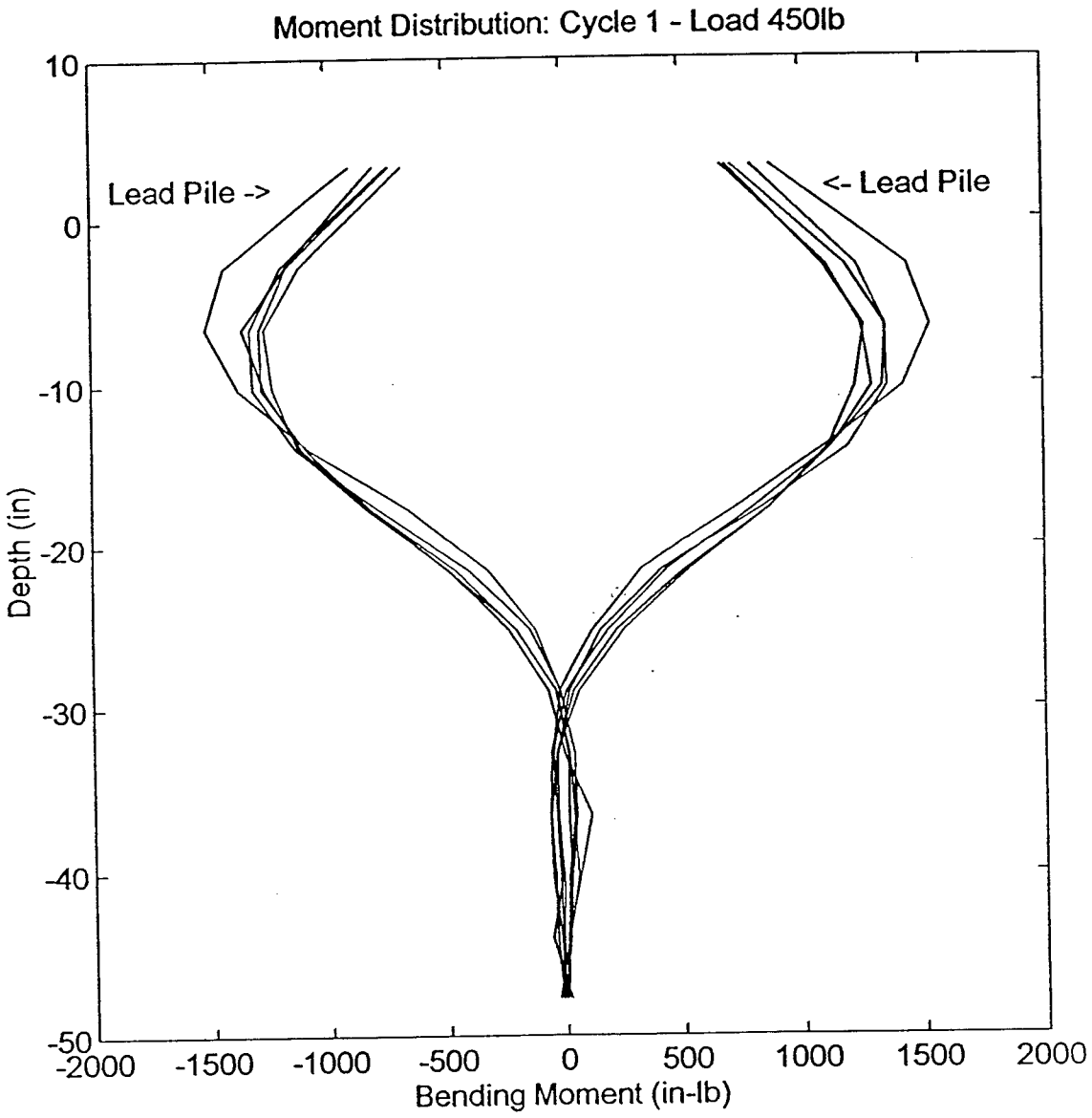
Moment Distribution: Cycle 1 - Load 450lb
Lead Pile ->
<- Lead Pile
Depth (in)
10
0
-10
-20
-30
-40
-50
-2000
-1500
-1000
-500
0
500
1000
1500
2000
Bending Moment (in-lb)

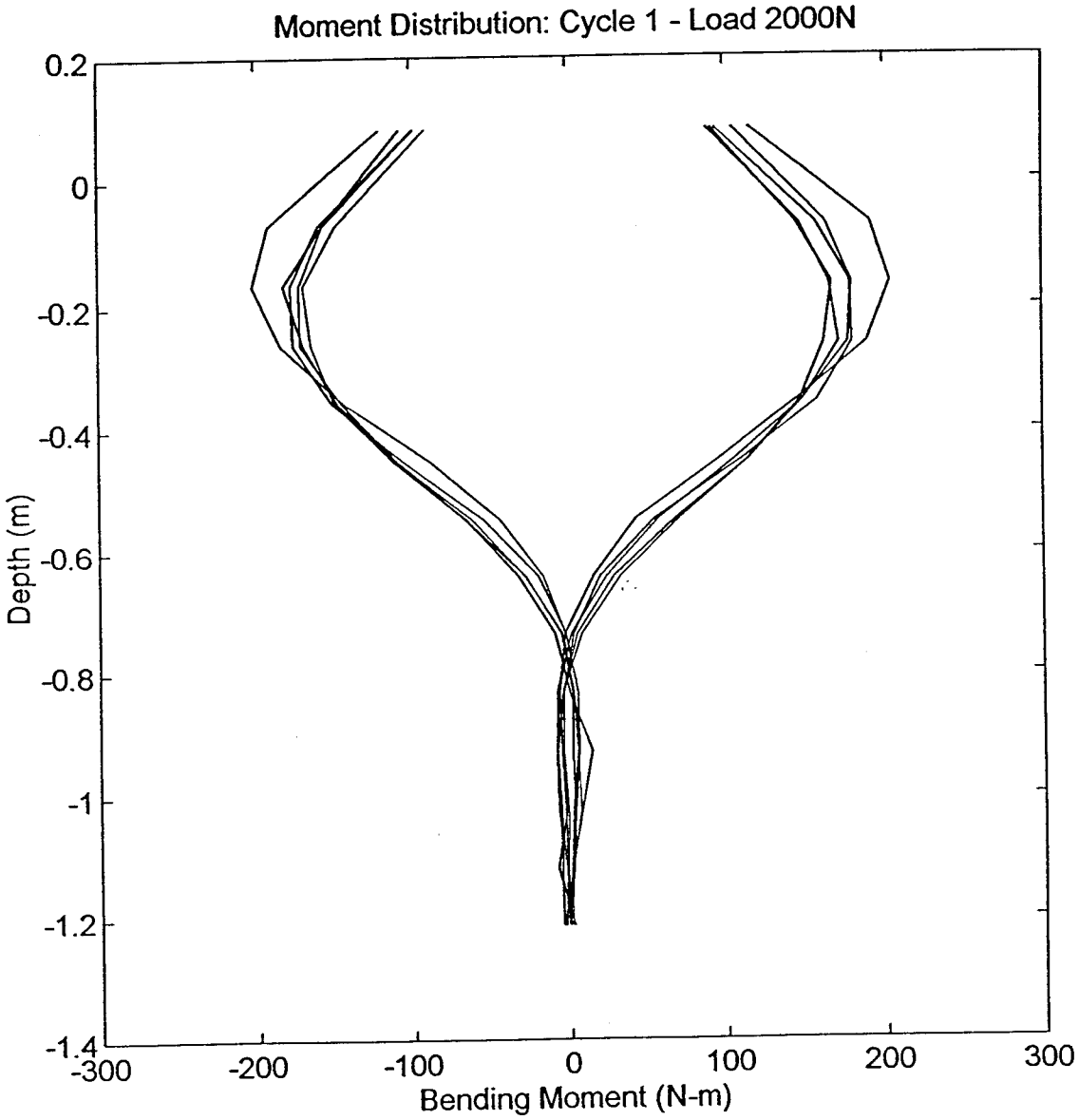
Moment Distribution: Cycle 1 - Load 2000N
0.2
0
-0.2
-0.4
-0.6
-0.8
-1
-1.2
-1.4
Depth (m)
-300
-200
-100
0
100
200
300
Bending Moment (N-m)

Figure B2. Moment distribution @ cycle 5 (next 14 plots).

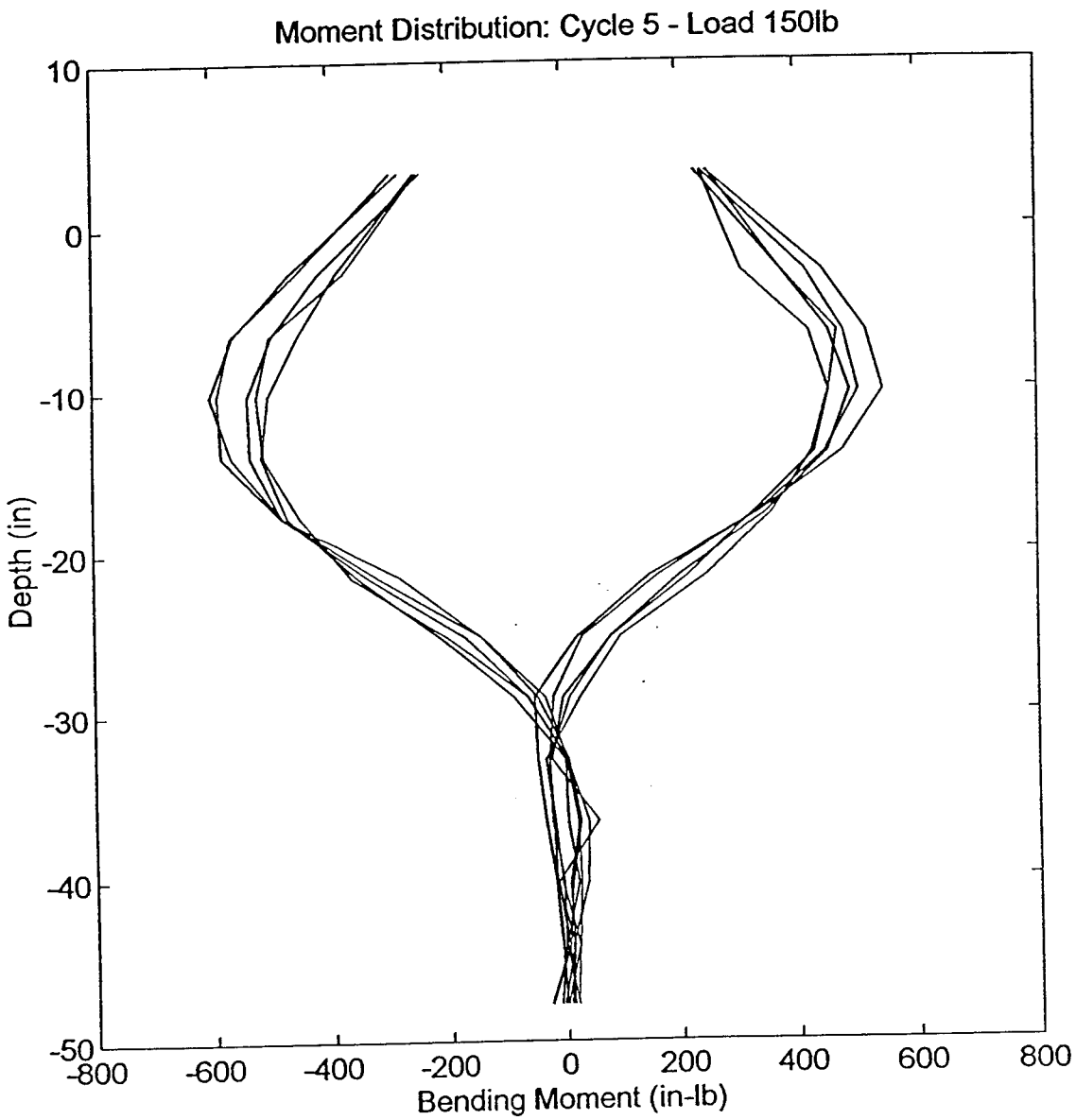
Moment Distribution: Cycle 5 - Load 150lb
10
0
-10
-20
-30
-40
-50
Depth (in)
-800
-600
-400
-200
0
200
400
600
800
Bending Moment (in-lb)

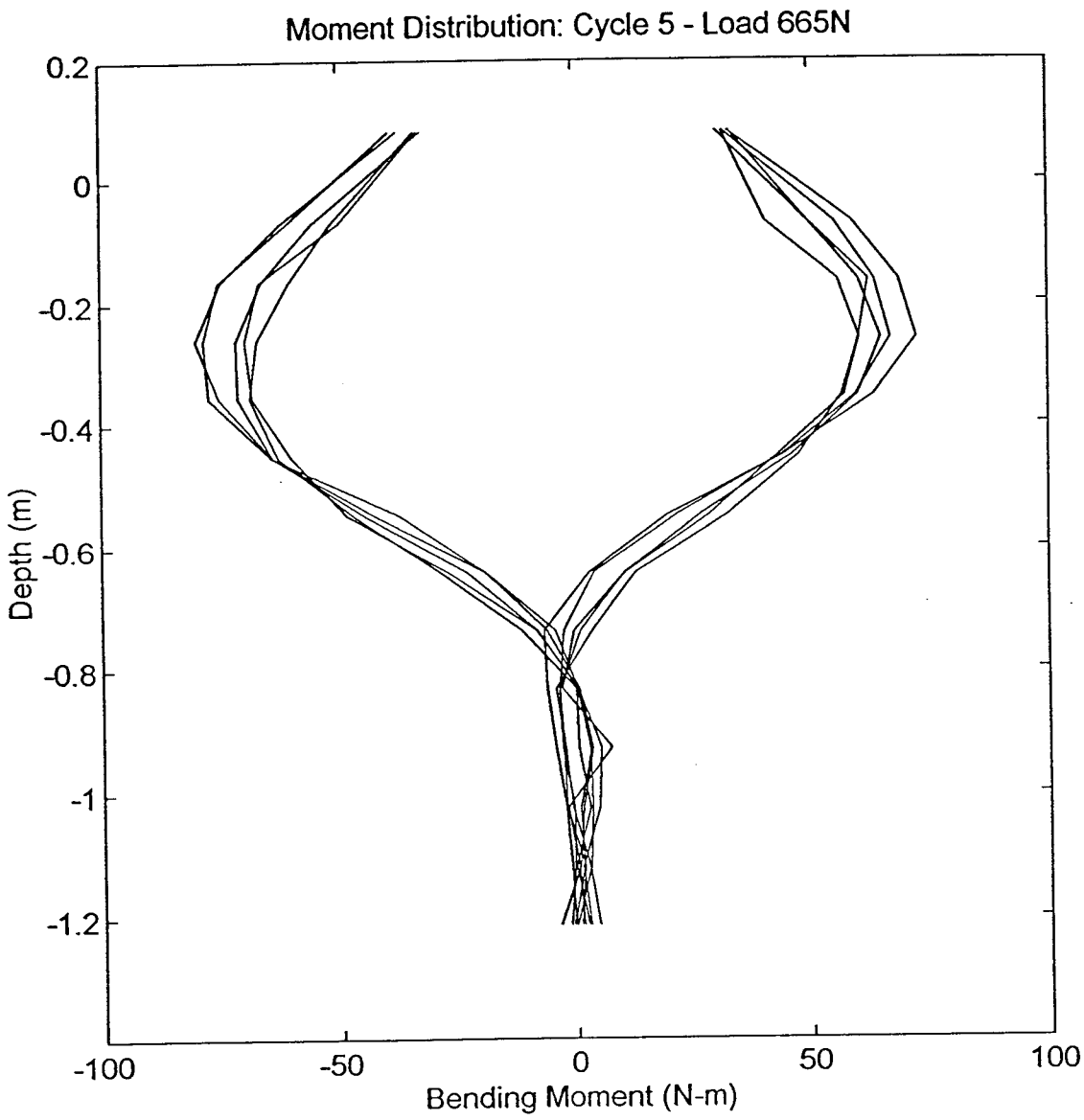
Moment Distribution: Cycle 5 - Load 665N
0.2
0
-0.2
-0.4
-0.6
-0.8
-1
-1.2
Depth (m)
-100
-50
0
50
100
Bending Moment (N-m)

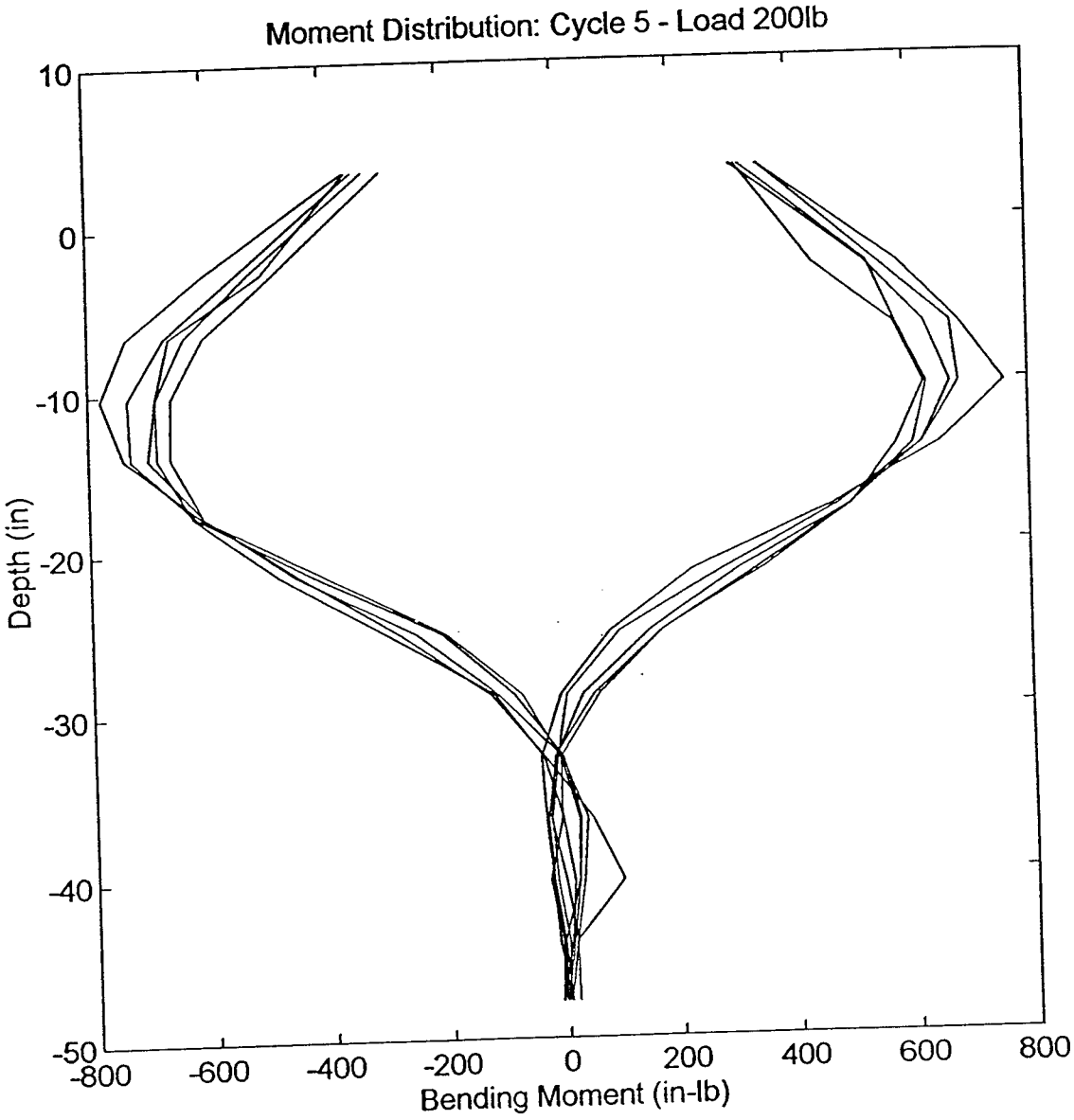
Moment Distribution: Cycle 5 - Load 200lb
Depth (in)
Bending Moment (in-lb)
10
0
-10
-20
-30
-40
-50
-800
-600
-400
-200
0
200
400
600
800

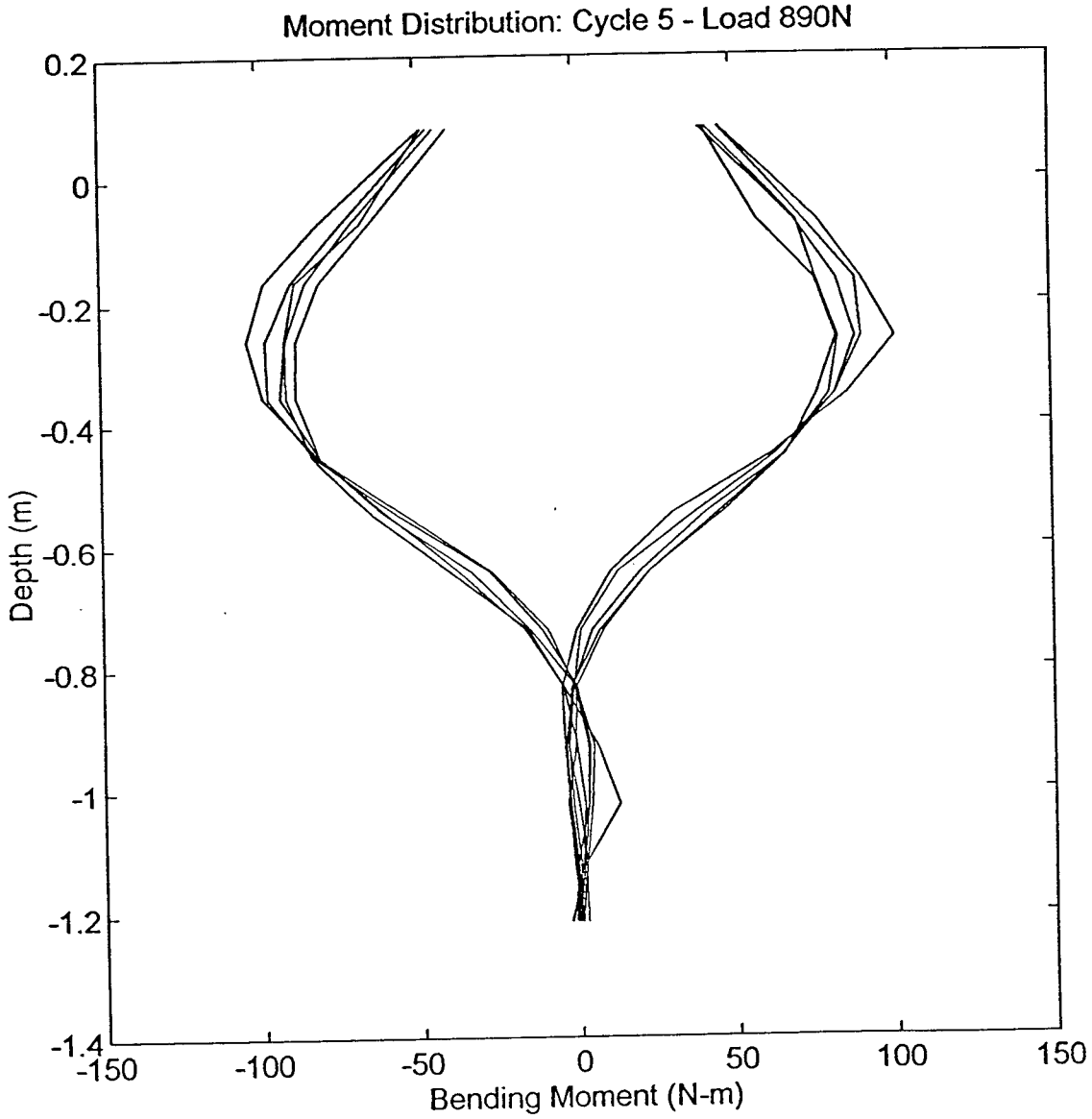
Moment Distribution: Cycle 5 - Load 890N
0.2
0
-0.2
-0.4
-0.6
-0.8
-1
-1.2
-1.4
Depth (m)
-150
-100
-50
0
50
100
150
Bending Moment (N-m)

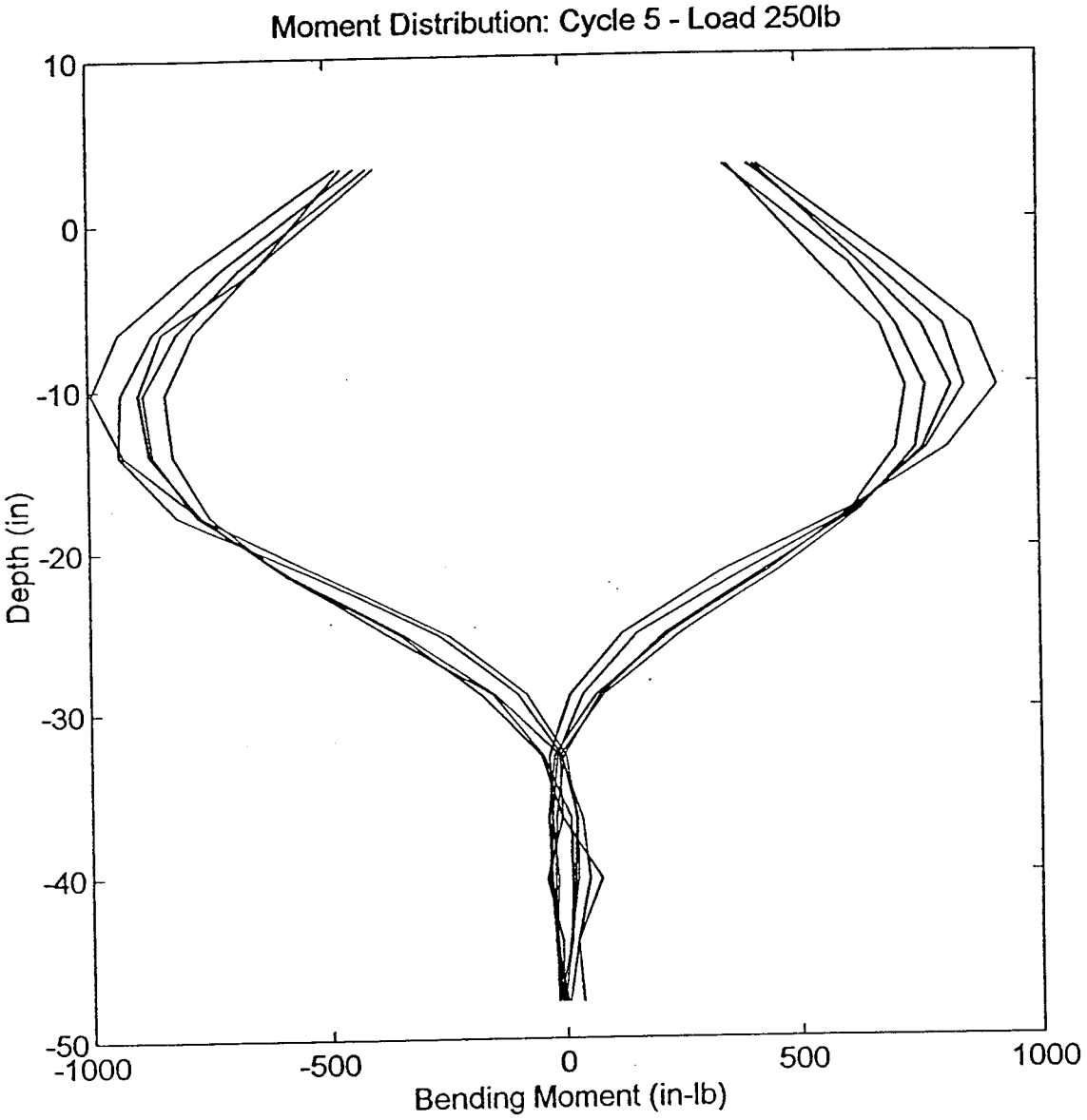
Moment Distribution: Cycle 5 - Load 250lb
10
0
-10
-20
-30
-40
-50
Depth (in)
-1000
-500
0
500
1000
Bending Moment (in-lb)

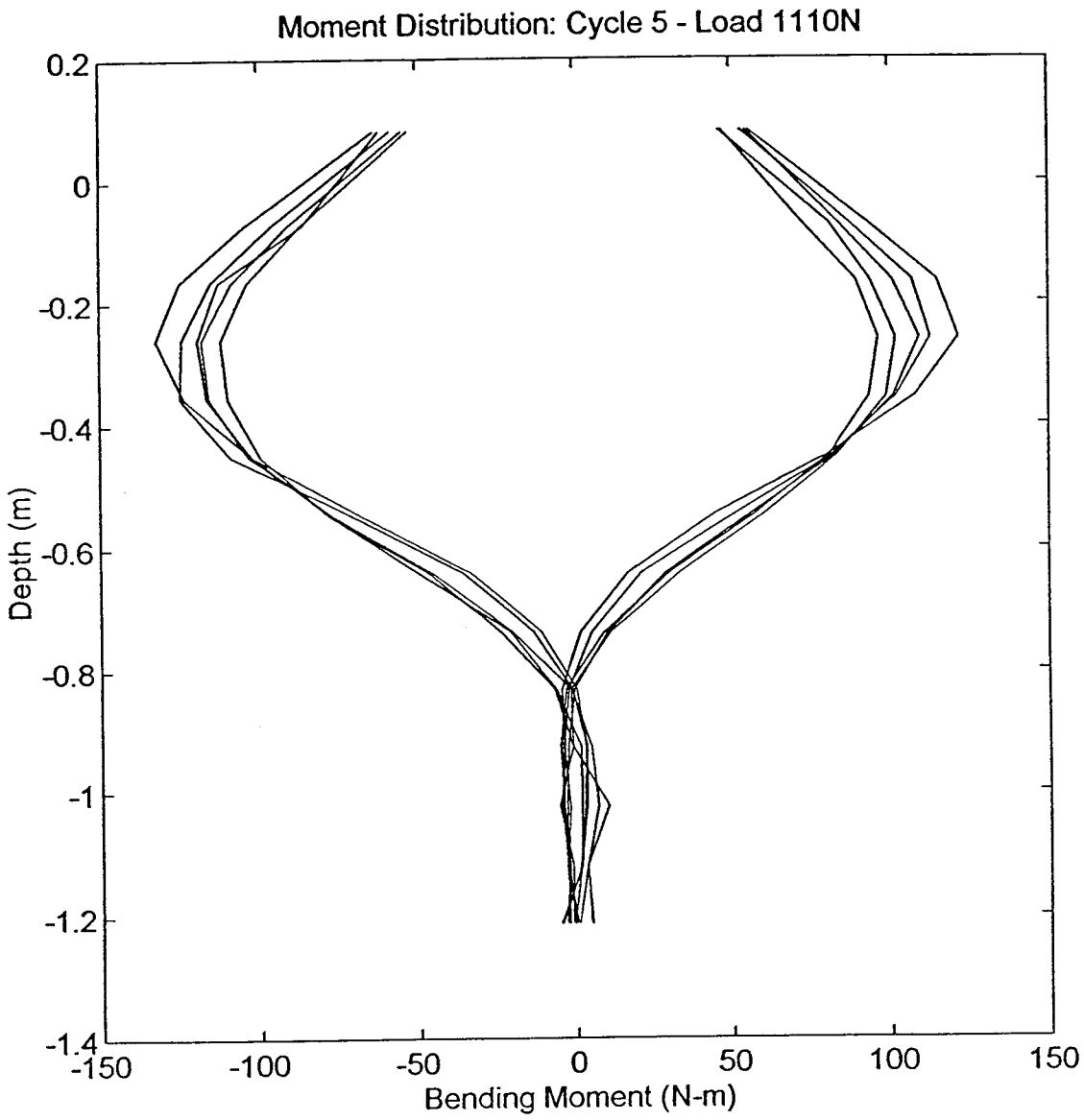
Moment Distribution: Cycle 5 - Load 1110N
0.2
0
-0.2
-0.4
-0.6
-0.8
-1
-1.2
-1.4
Depth (m)
-150
-100
-50
0
50
100
150
Bending Moment (N-m)

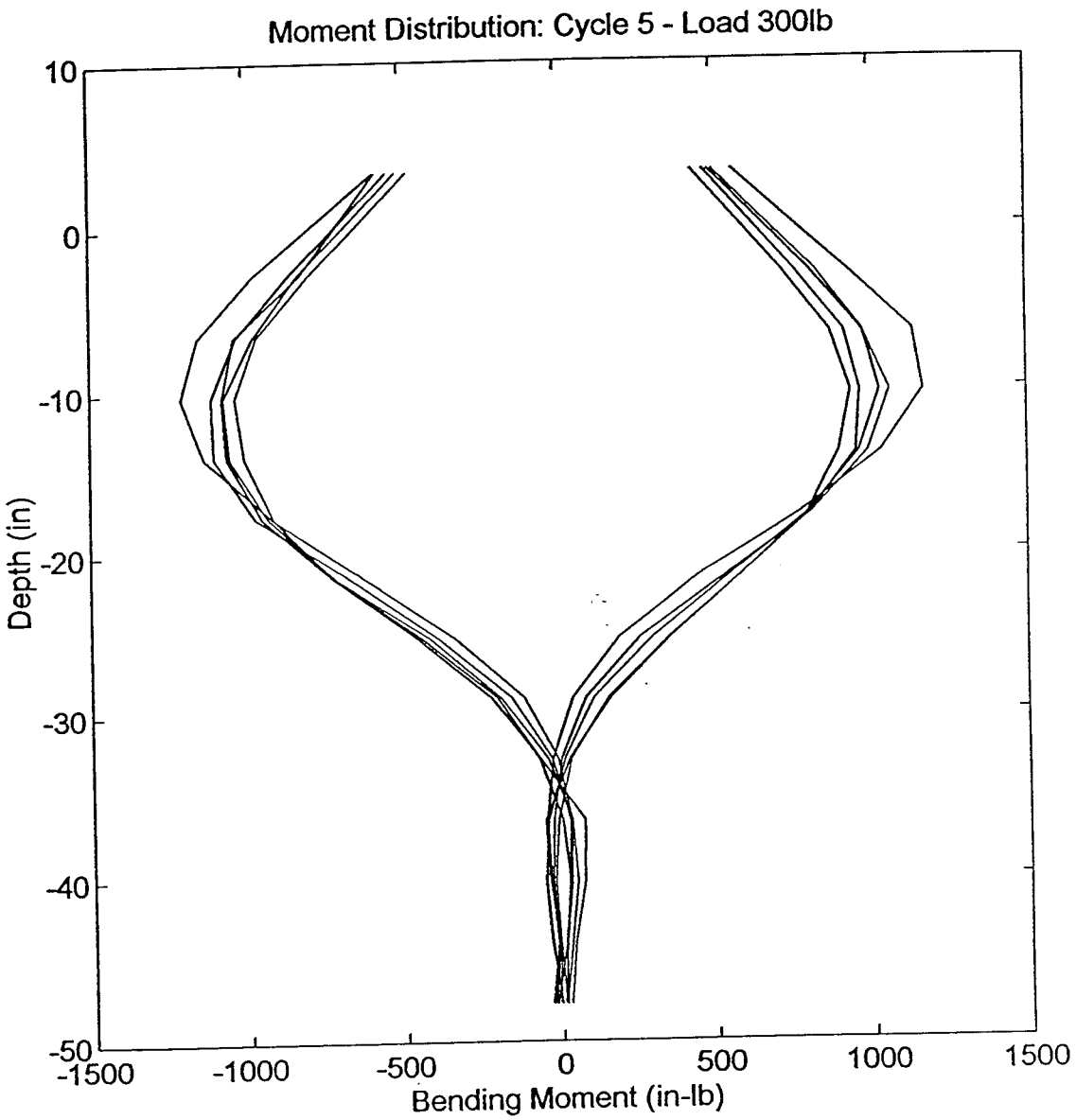
Moment Distribution: Cycle 5 - Load 300lb
10
0
-10
-20
-30
-40
-50
Depth (in)
-1500
-1000
-500
0
500
1000
1500
Bending Moment (in-lb)

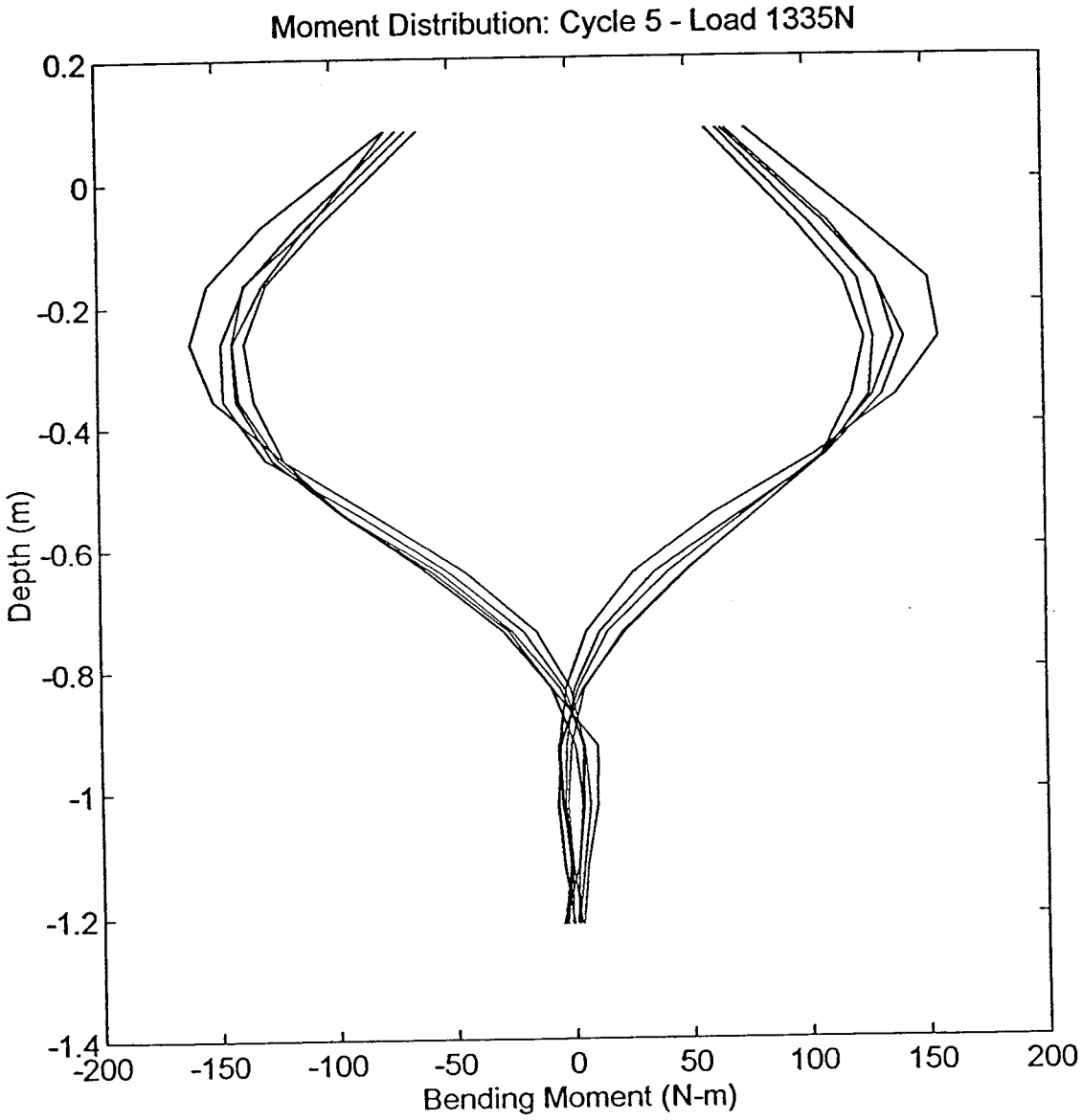
Moment Distribution: Cycle 5 - Load 1335N
0.2
0
-0.2
-0.4
-0.6
-0.8
-1
-1.2
-1.4
Depth (m)
-200
-150
-100
-50
0
50
100
150
200
Bending Moment (N-m)

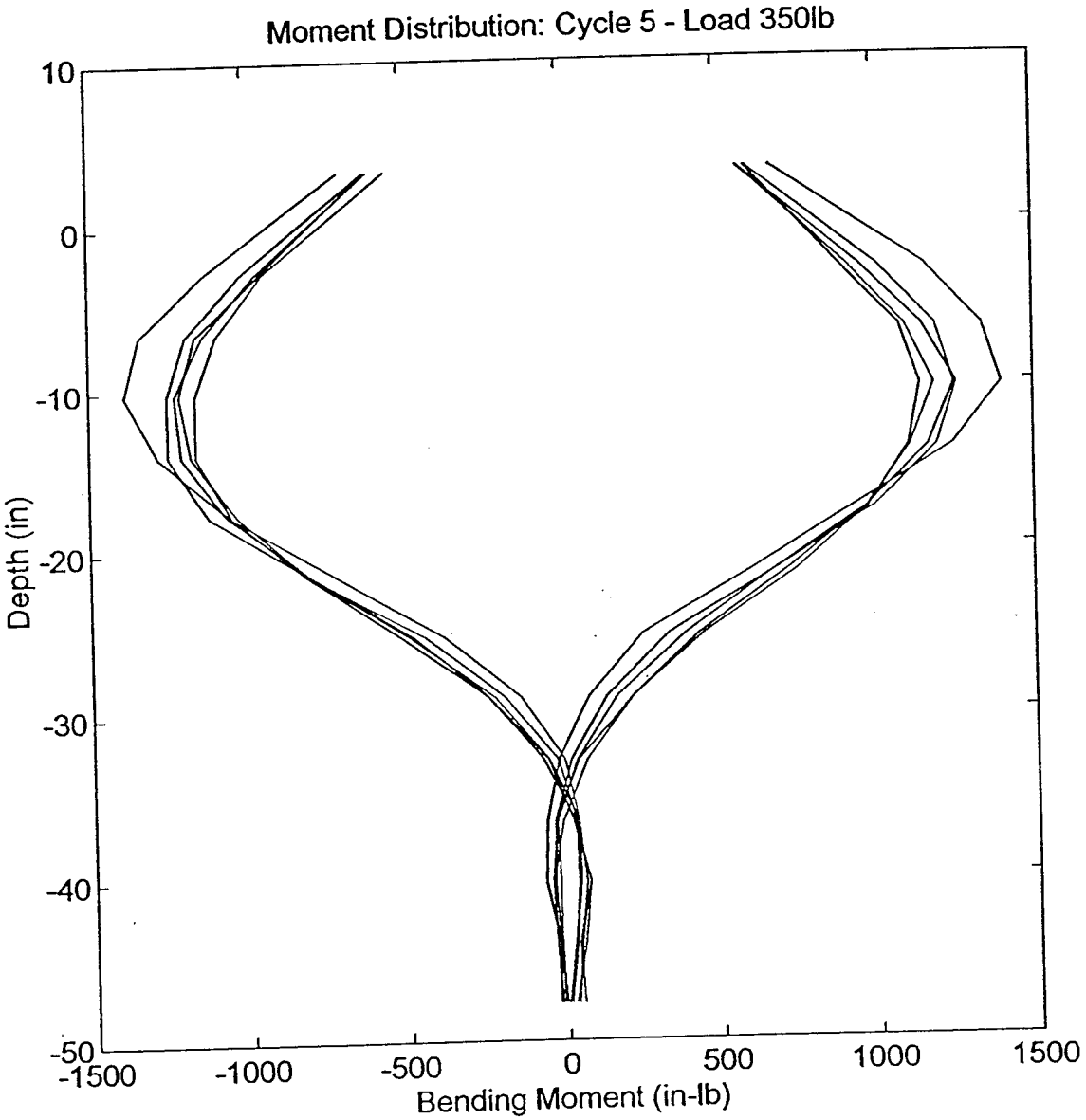
Moment Distribution: Cycle 5 - Load 350lb
10
0
-10
-20
-30
-40
-50
Depth (in)
-1500
-1000
-500
0
500
1000
1500
Bending Moment (in-lb)

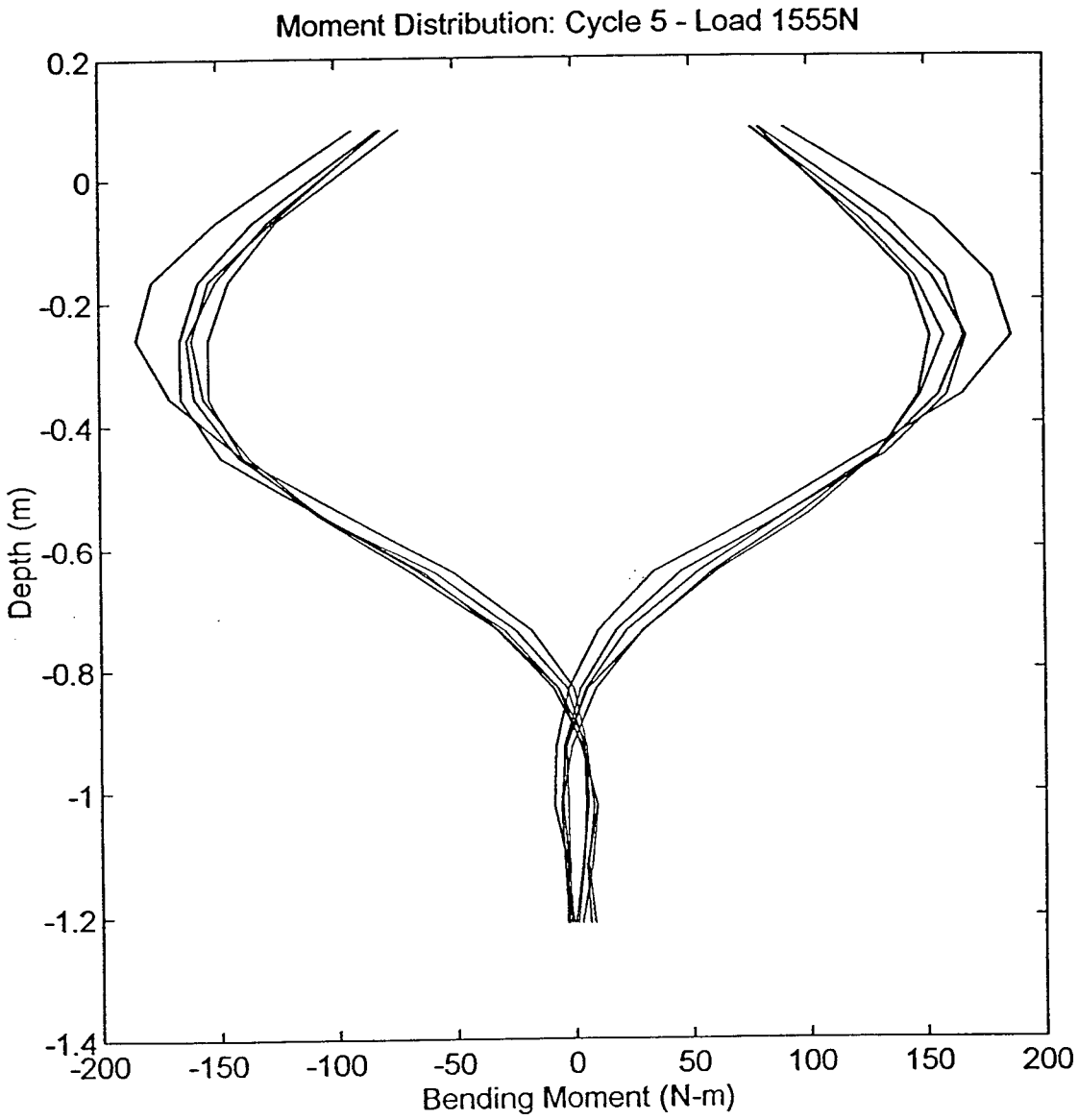
Moment Distribution: Cycle 5 - Load 1555N
0.2
0
-0.2
-0.4
-0.6
-0.8
-1
-1.2
-1.4
Depth (m)
-200
-150
-100
-50
0
50
100
150
200
Bending Moment (N-m)

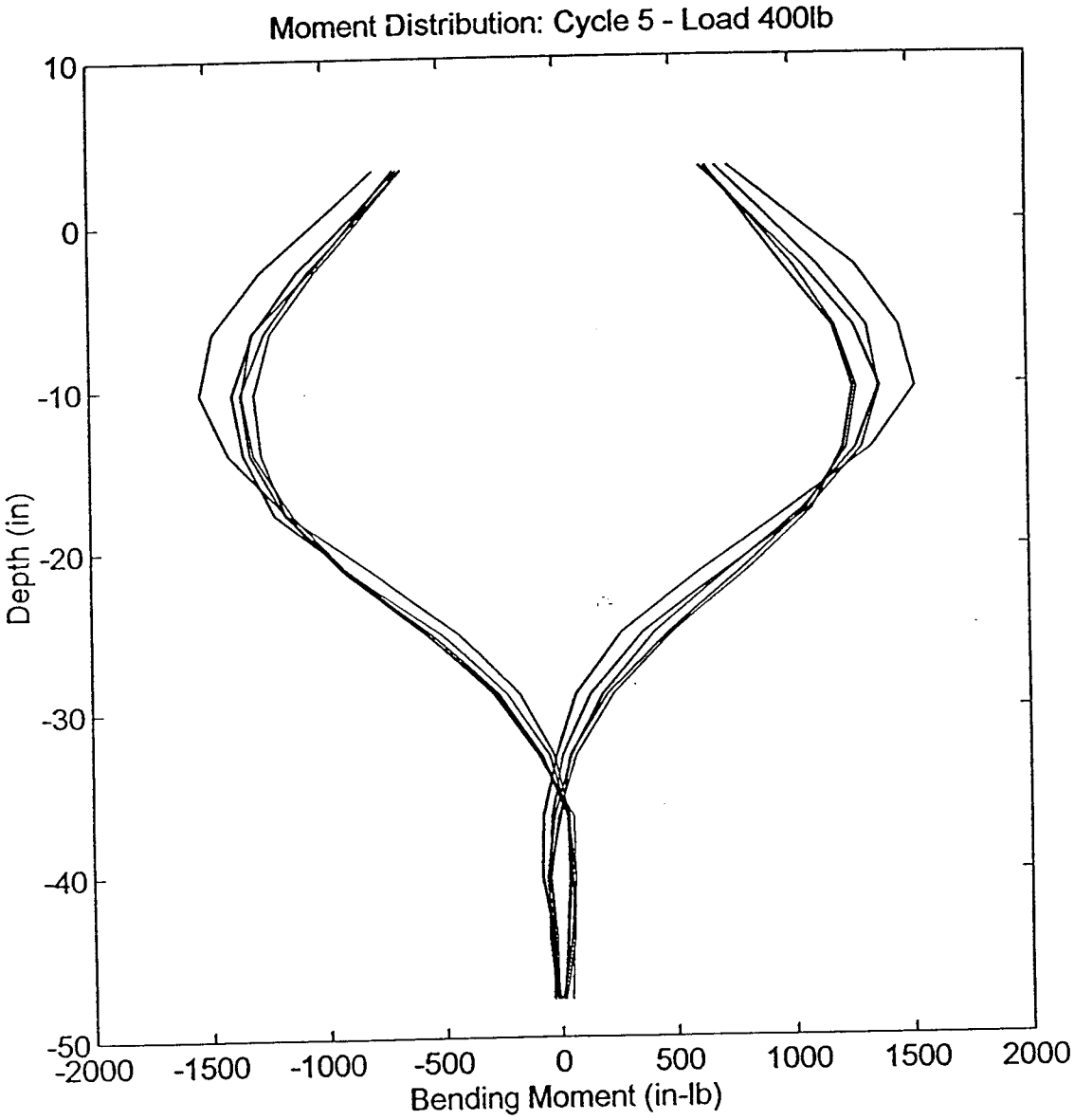
Moment Distribution: Cycle 5 - Load 400lb
10
0
-10
-20
-30
-40
-50
Depth (in)
-2000
-1500
-1000
-500
0
500
1000
1500
2000
Bending Moment (in-lb)

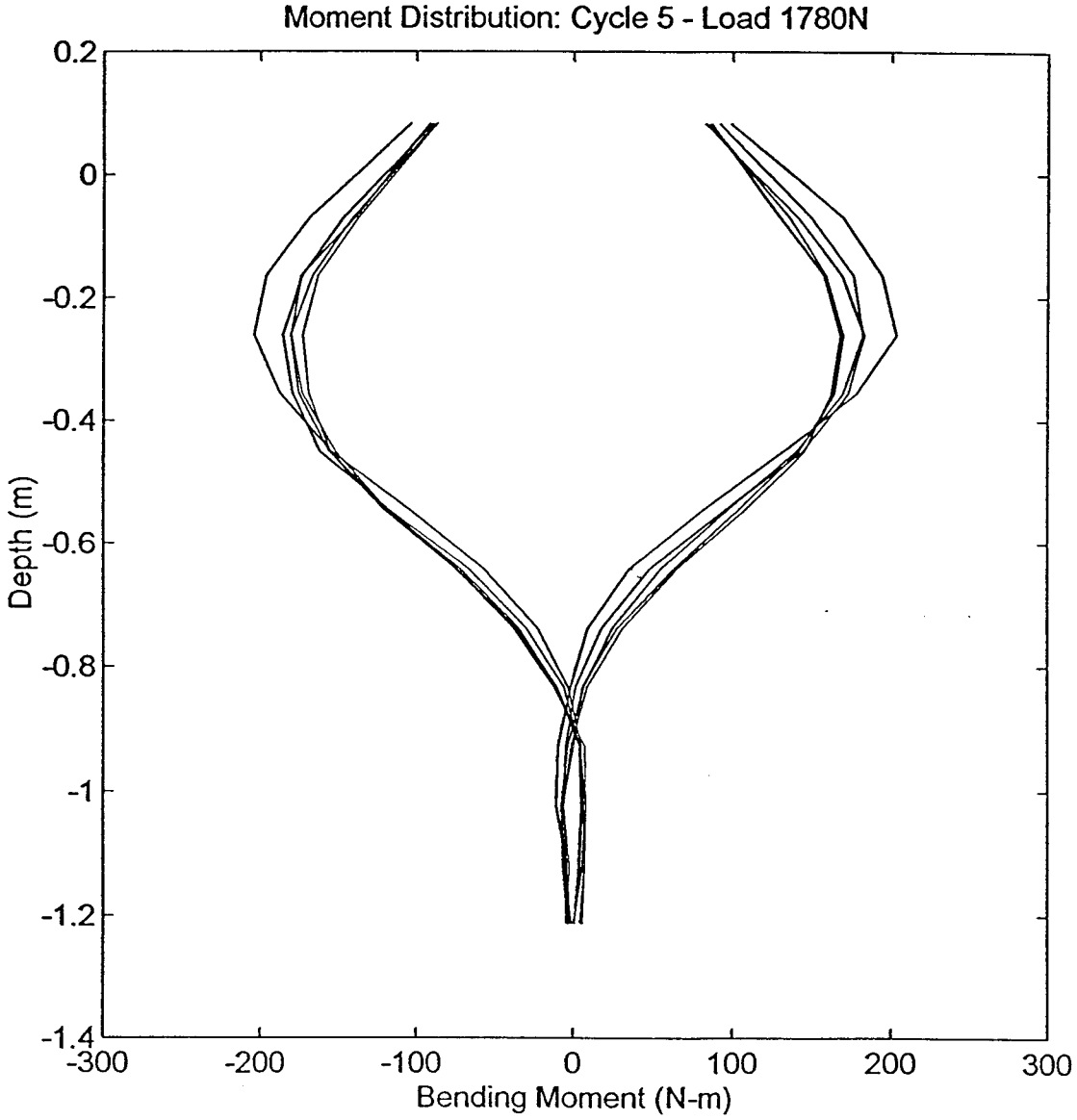
Moment Distribution: Cycle 5 - Load 1780N
0.2
0
-0.2
-0.4
-0.6
-0.8
-1
-1.2
-1.4
Depth (m)
-300
-200
-100
0
100
200
300
Bending Moment (N-m)

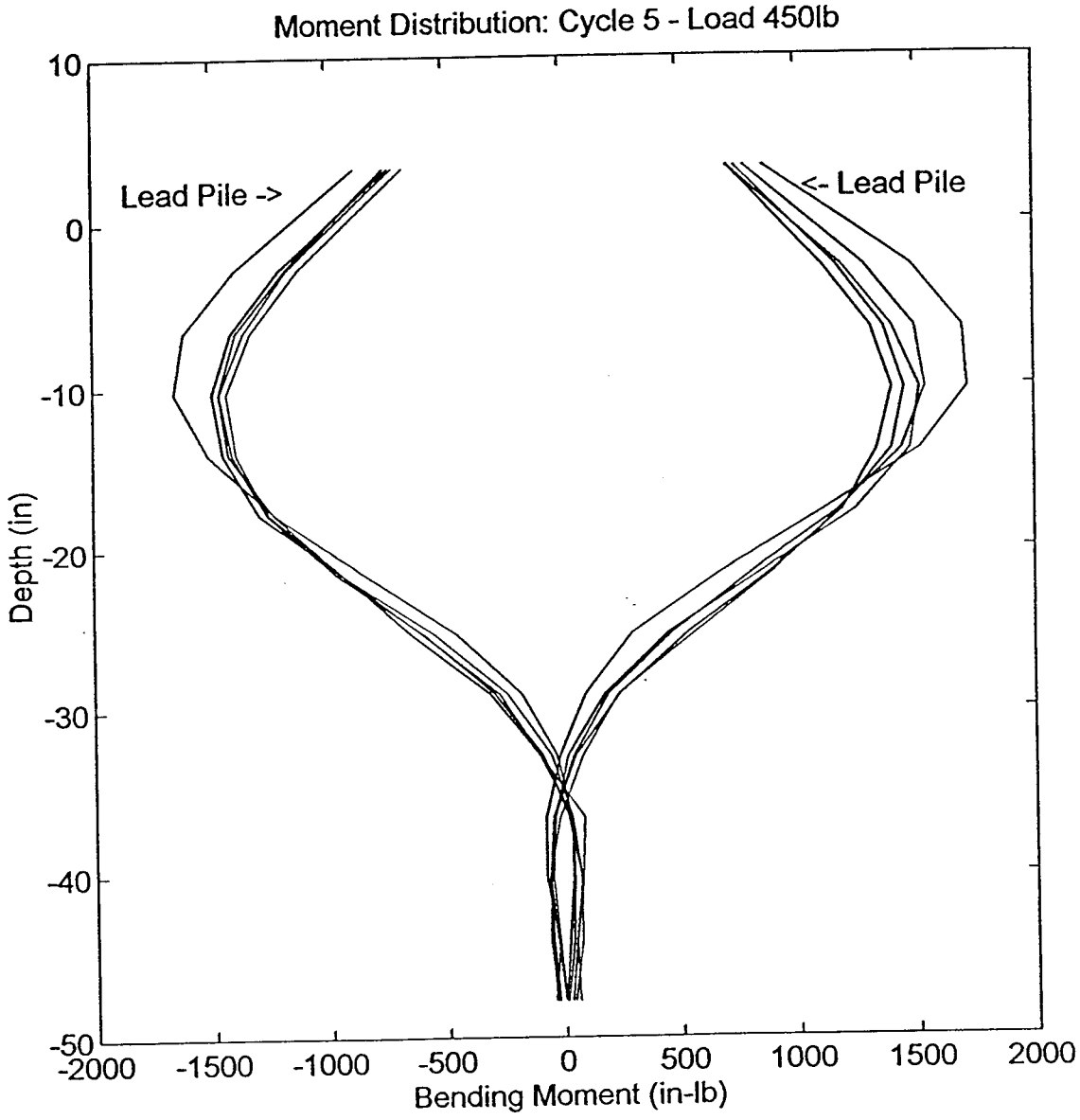
Moment Distribution: Cycle 5 - Load 450lb
Lead Pile ->
<- Lead Pile
Depth (in)
10
0
-10
-20
-30
-40
-50
-2000
-1500
-1000
-500
0
500
1000
1500
2000
Bending Moment (in-lb)

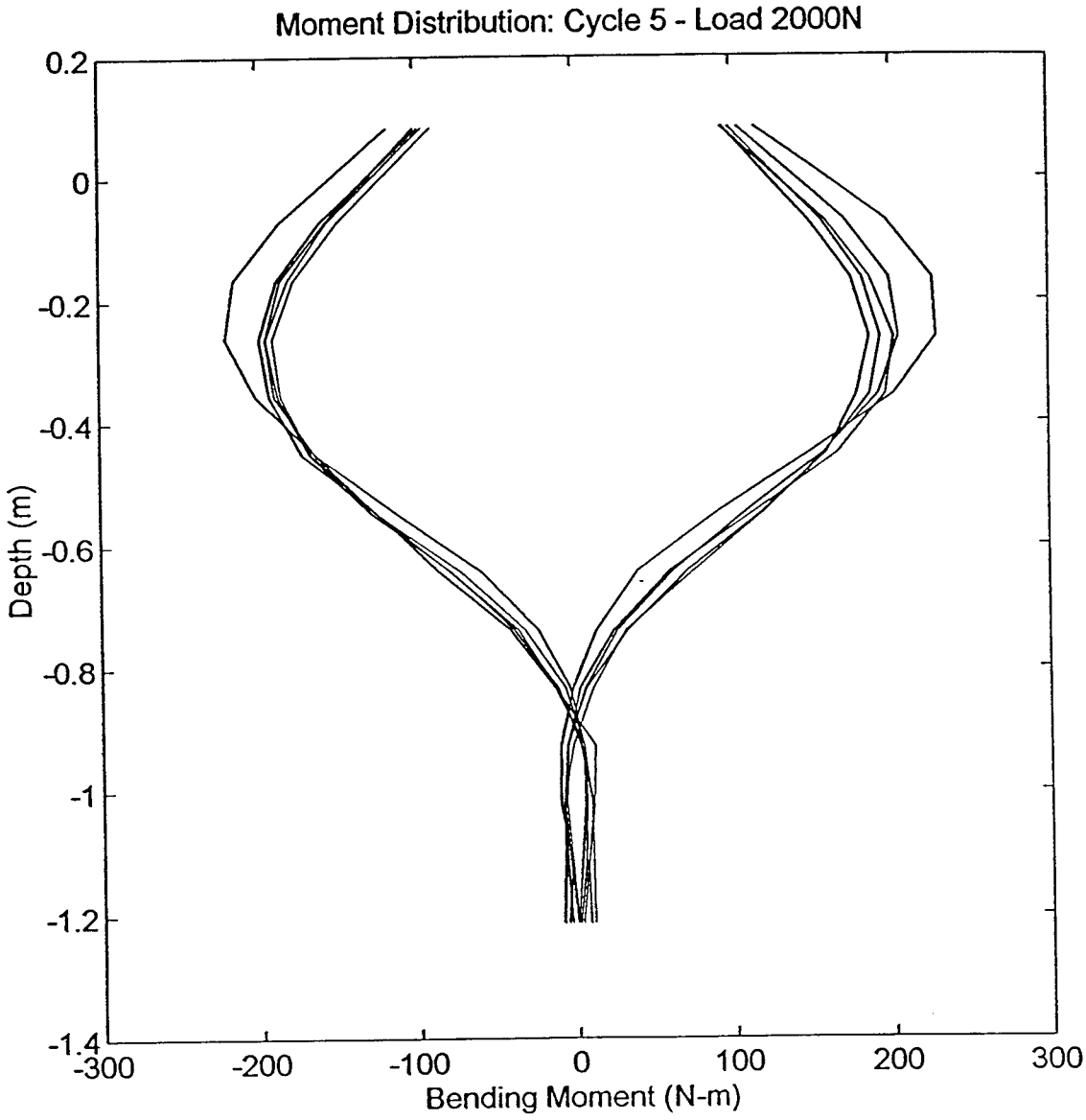
Moment Distribution: Cycle 5 - Load 2000N
0.2
0
-0.2
-0.4
-0.6
-0.8
-1
-1.2
-1.4
Depth (m)
-300
-200
-100
0
100
200
300
Bending Moment (N-m)

Figure B3. Moment distribution @ cycle 10 (next 14 plots).

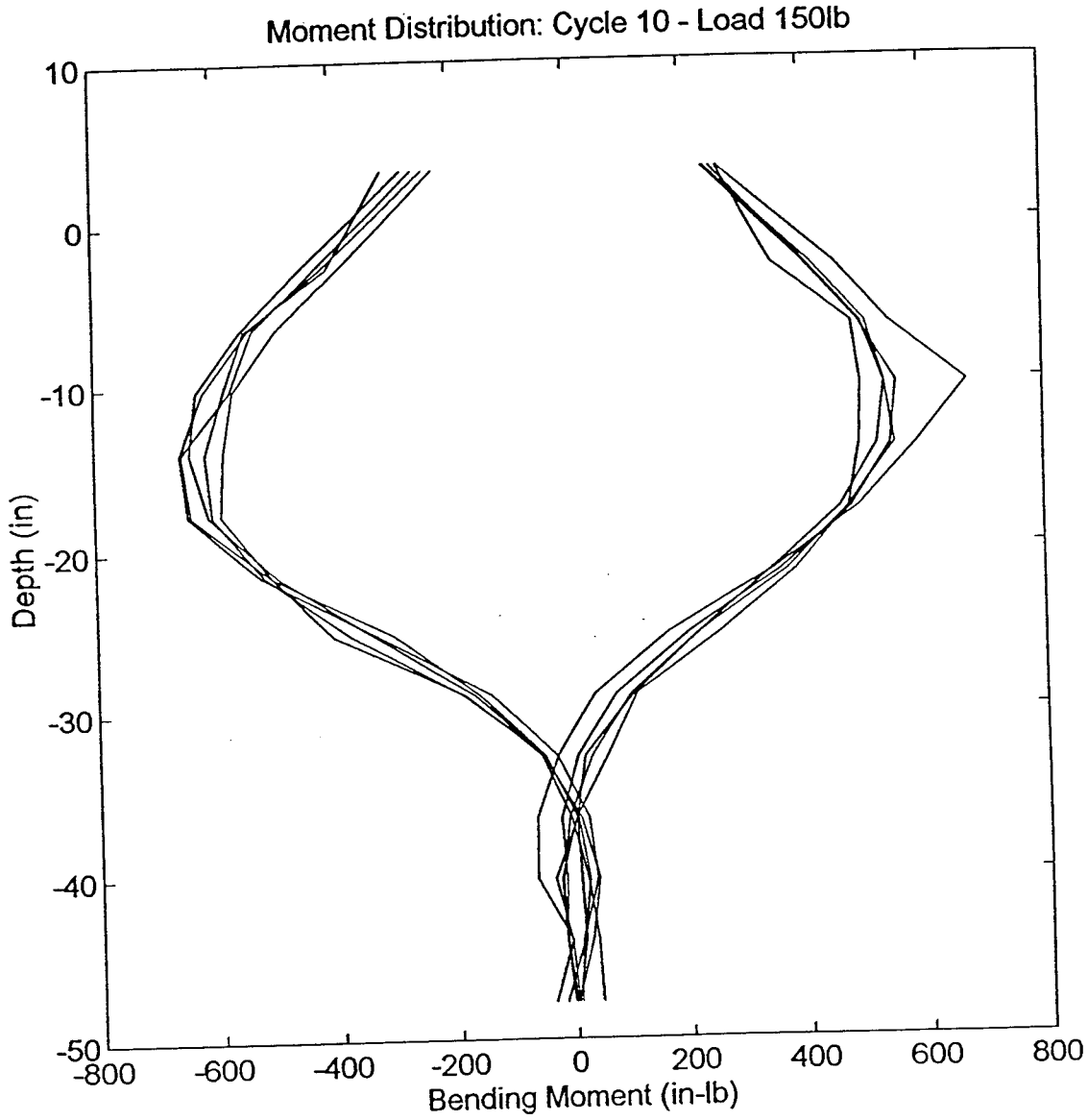
Moment Distribution: Cycle 10 - Load 150lb
10
0
-10
-20
-30
-40
-50
Depth (in)
-800
-600
-400
-200
0
200
400
600
800
Bending Moment (in-lb)

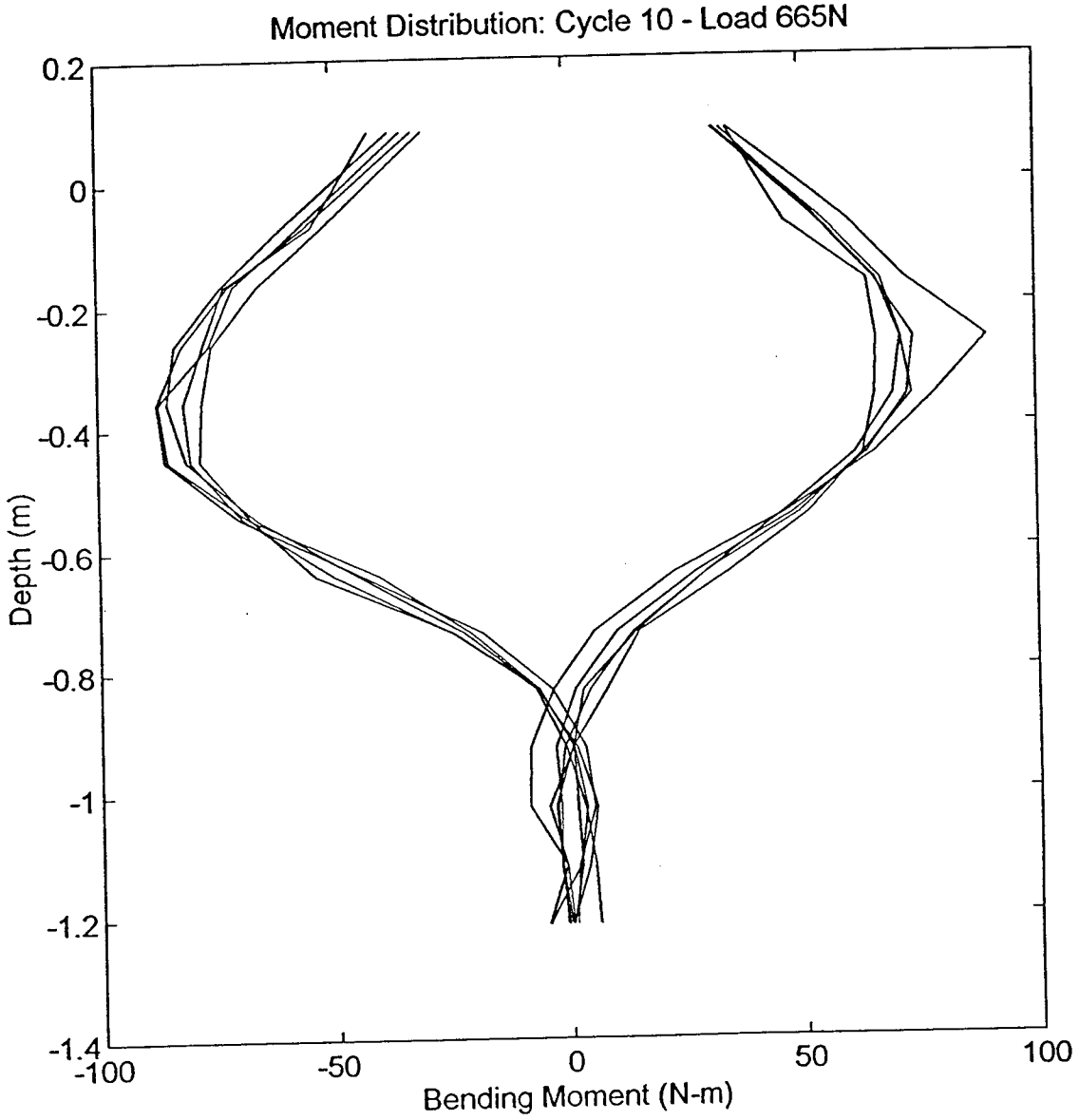
Moment Distribution: Cycle 10 - Load 665N
0.2
0
-0.2
-0.4
-0.6
-0.8
-1
-1.2
-1.4
Depth (m)
-100
-50
0
50
100
Bending Moment (N-m)

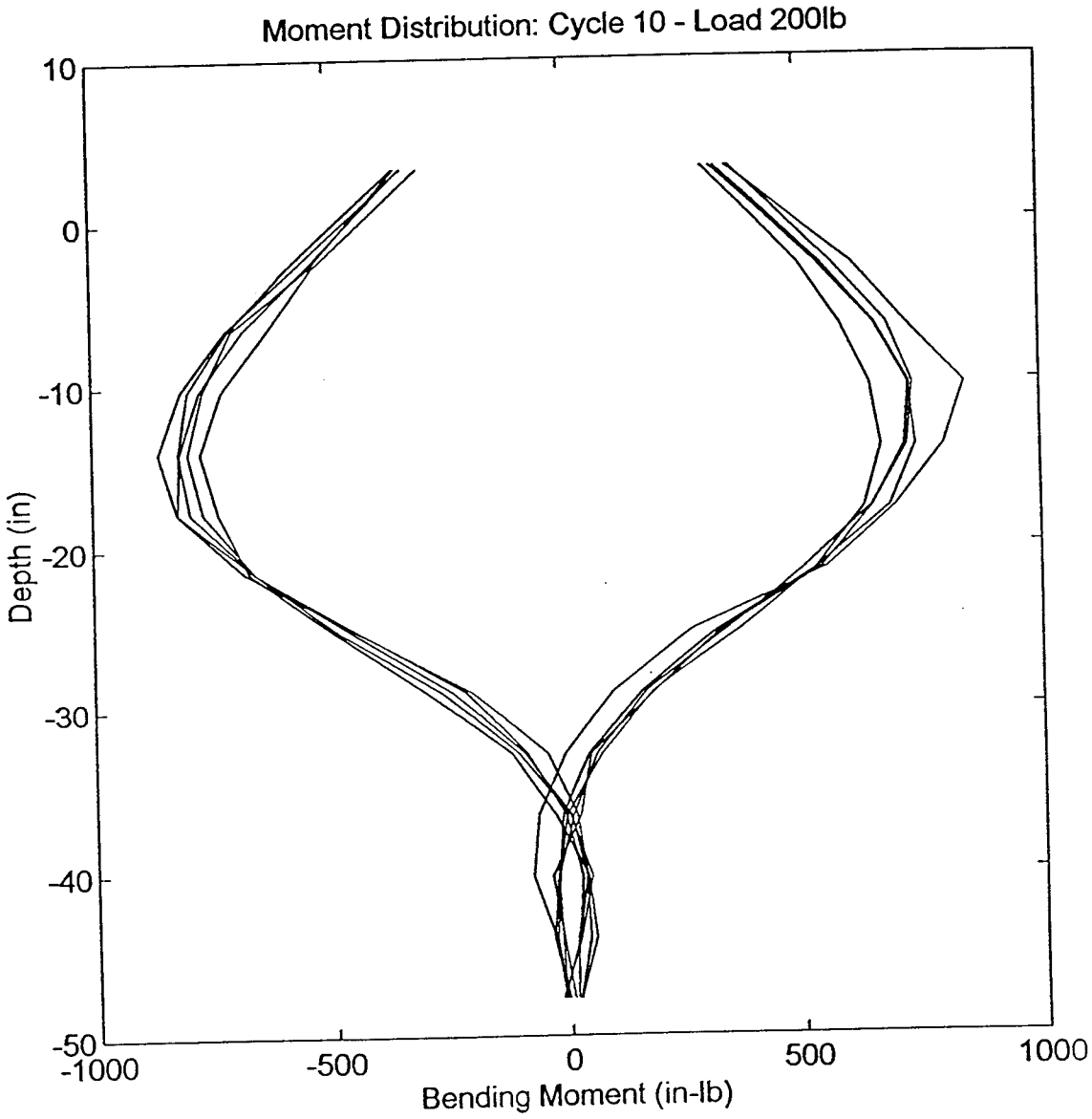
Moment Distribution: Cycle 10 - Load 200lb
10
0
-10
-20
-30
-40
-50
Depth (in)
-1000
-500
0
500
1000
Bending Moment (in-lb)

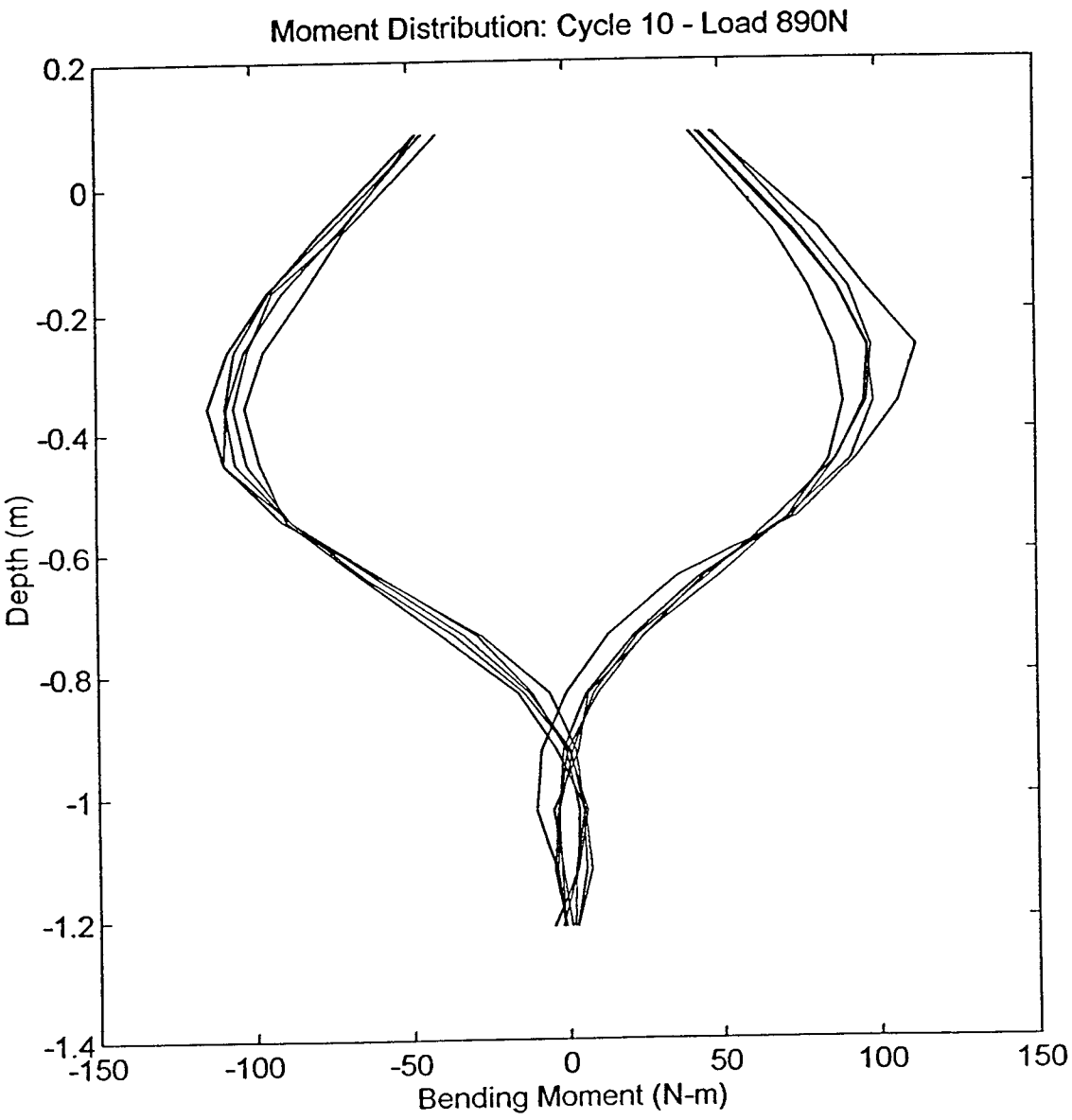
Moment Distribution: Cycle 10 - Load 890N
0.2
0
-0.2
-0.4
-0.6
-0.8
-1
-1.2
-1.4
Depth (m)
-150
-100
-50
0
50
100
150
Bending Moment (N-m)

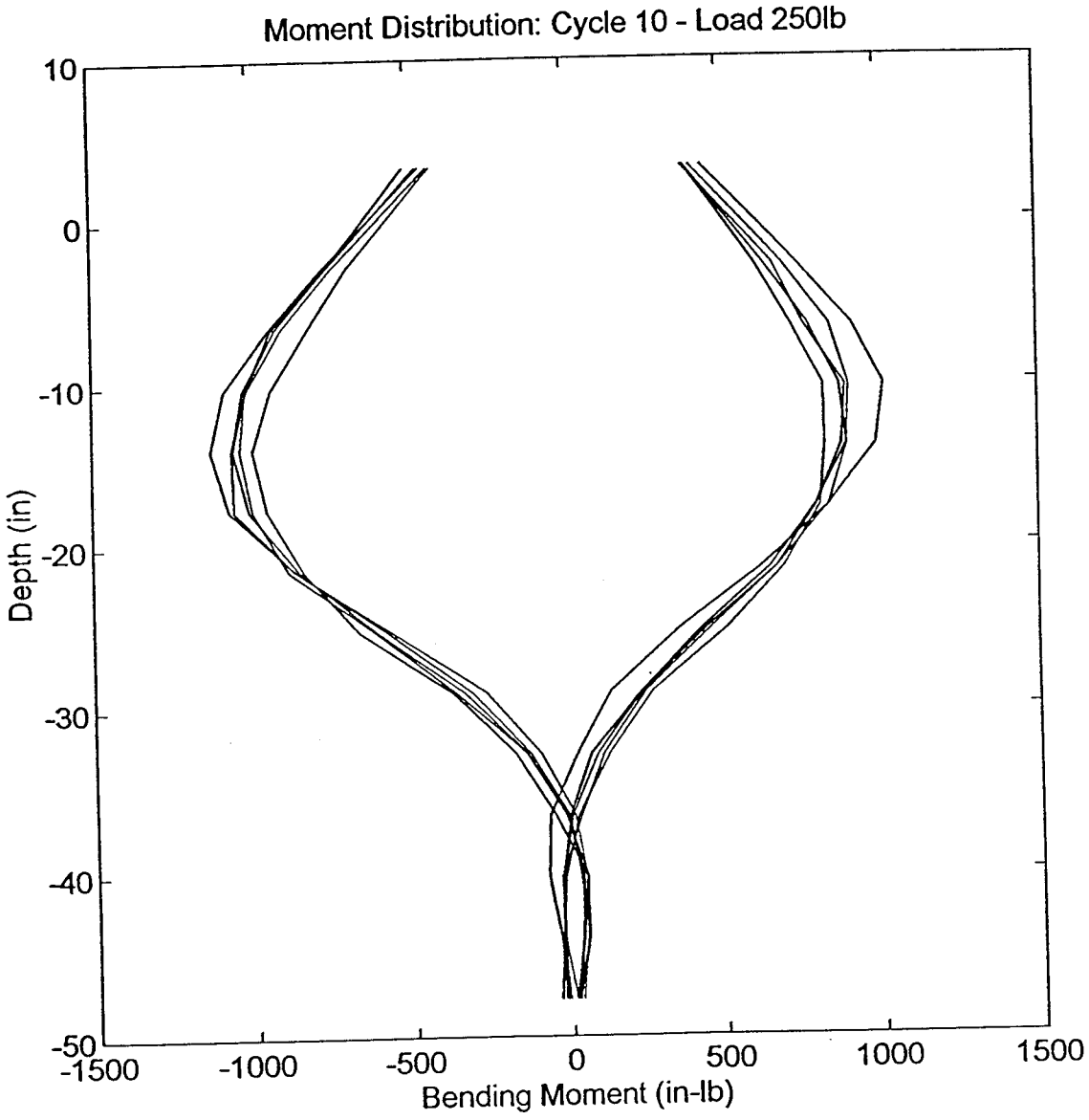
Moment Distribution: Cycle 10 - Load 250lb
10
0
-10
-20
-30
-40
-50
Depth (in)
-1500
-1000
-500
0
500
1000
1500
Bending Moment (in-lb)

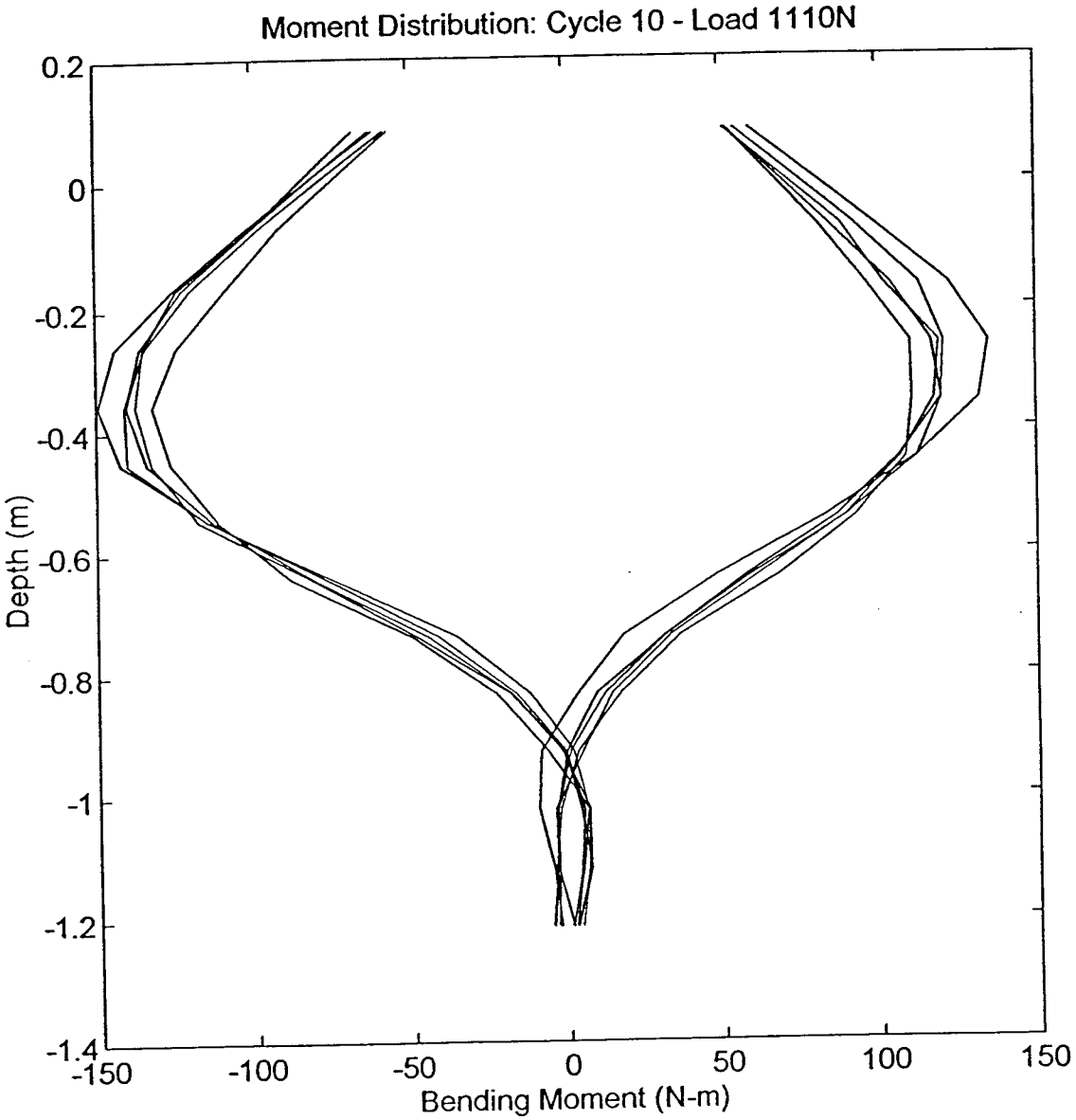
Moment Distribution: Cycle 10 - Load 1110N
0.2
0
-0.2
-0.4
-0.6
-0.8
-1
-1.2
-1.4
Depth (m)
-150
-100
-50
0
50
100
150
Bending Moment (N-m)

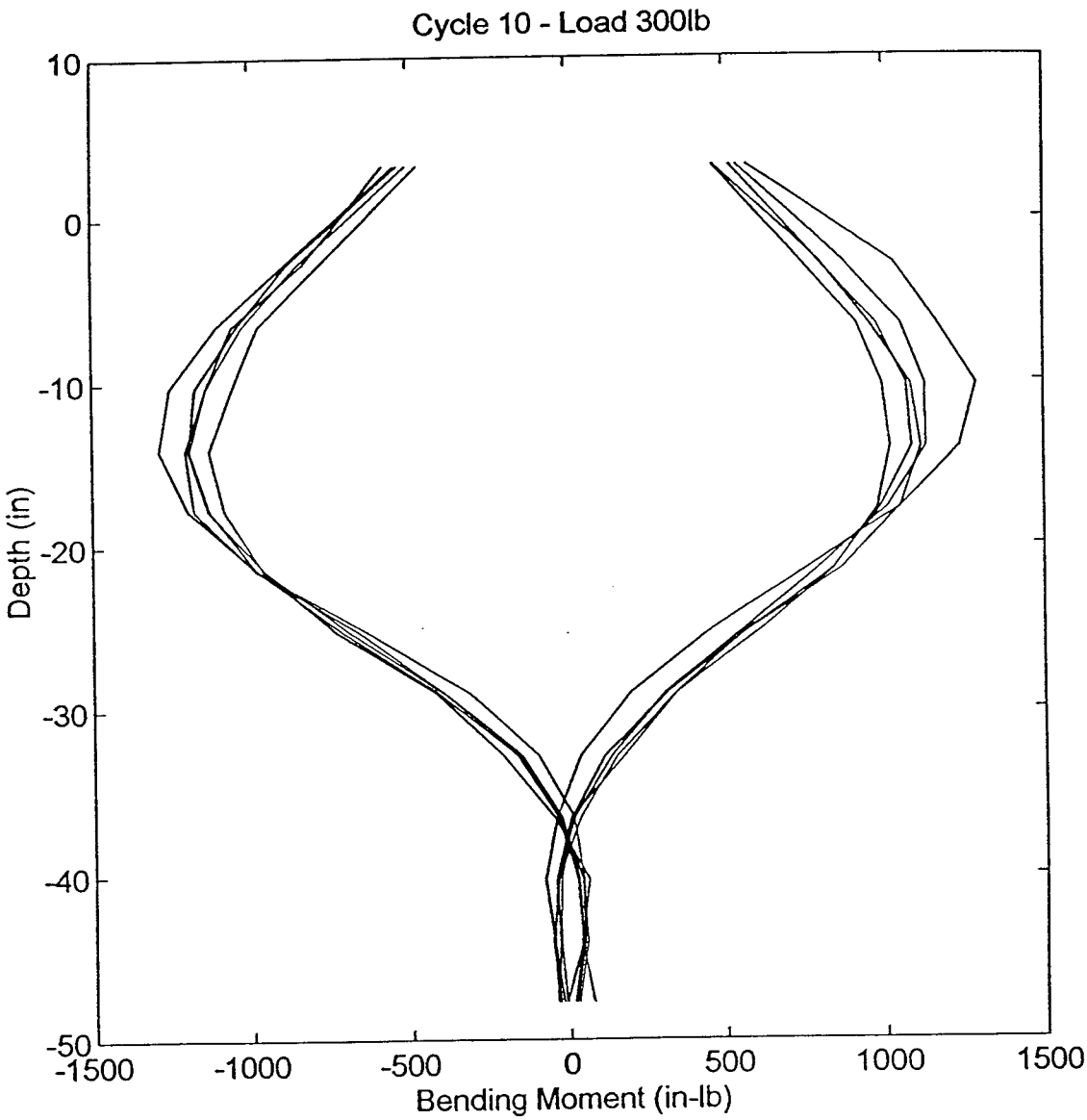
Cycle 10 - Load 300lb
10
0
-10
-20
-30
-40
-50
Depth (in)
-1500
-1000
-500
0
500
1000
1500
Bending Moment (in-lb)

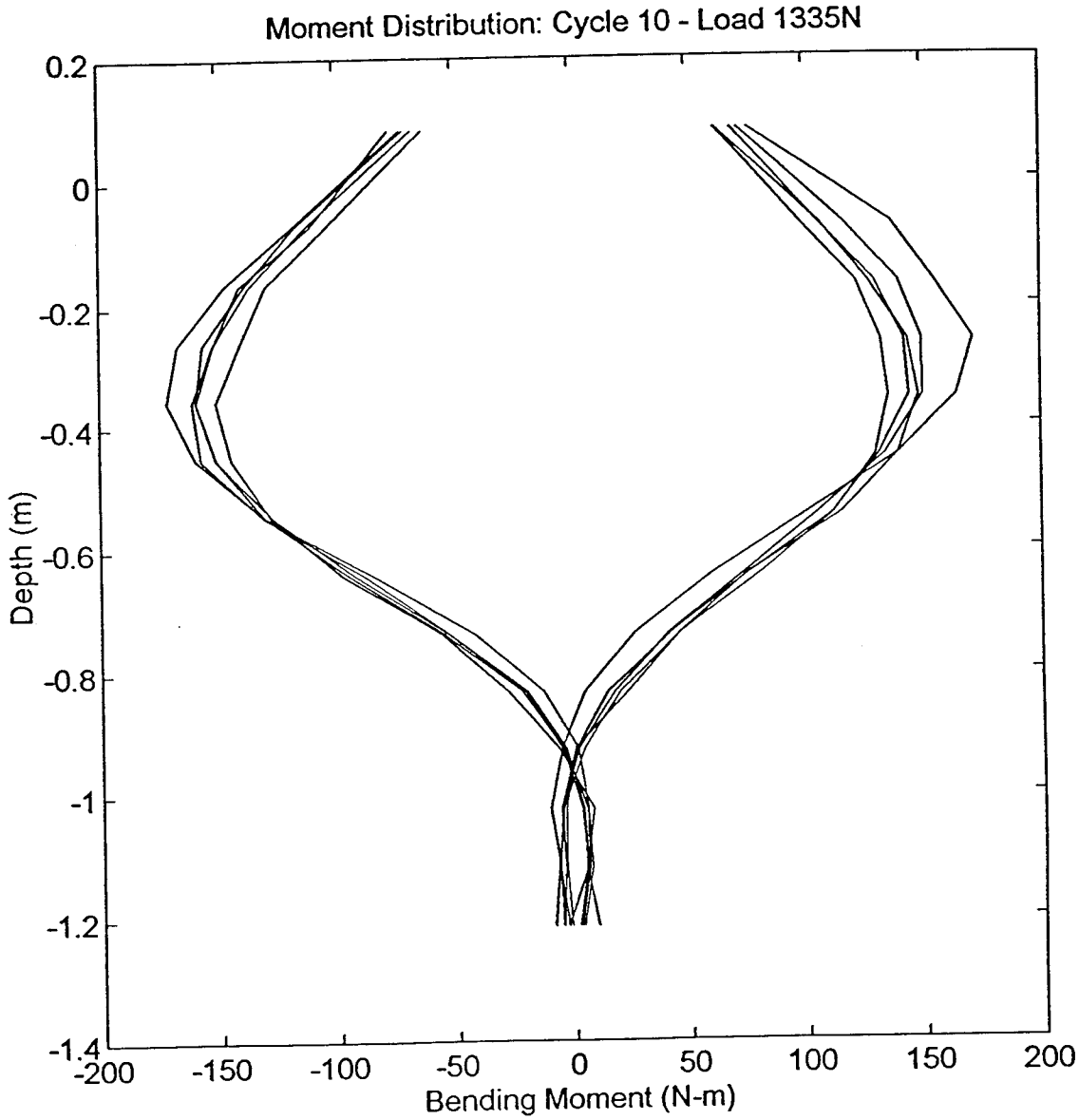
Moment Distribution: Cycle 10 - Load 1335N
0.2
0
-0.2
-0.4
-0.6
-0.8
-1
-1.2
-1.4
Depth (m)
-200
-150
-100
-50
0
50
100
150
200
Bending Moment (N-m)

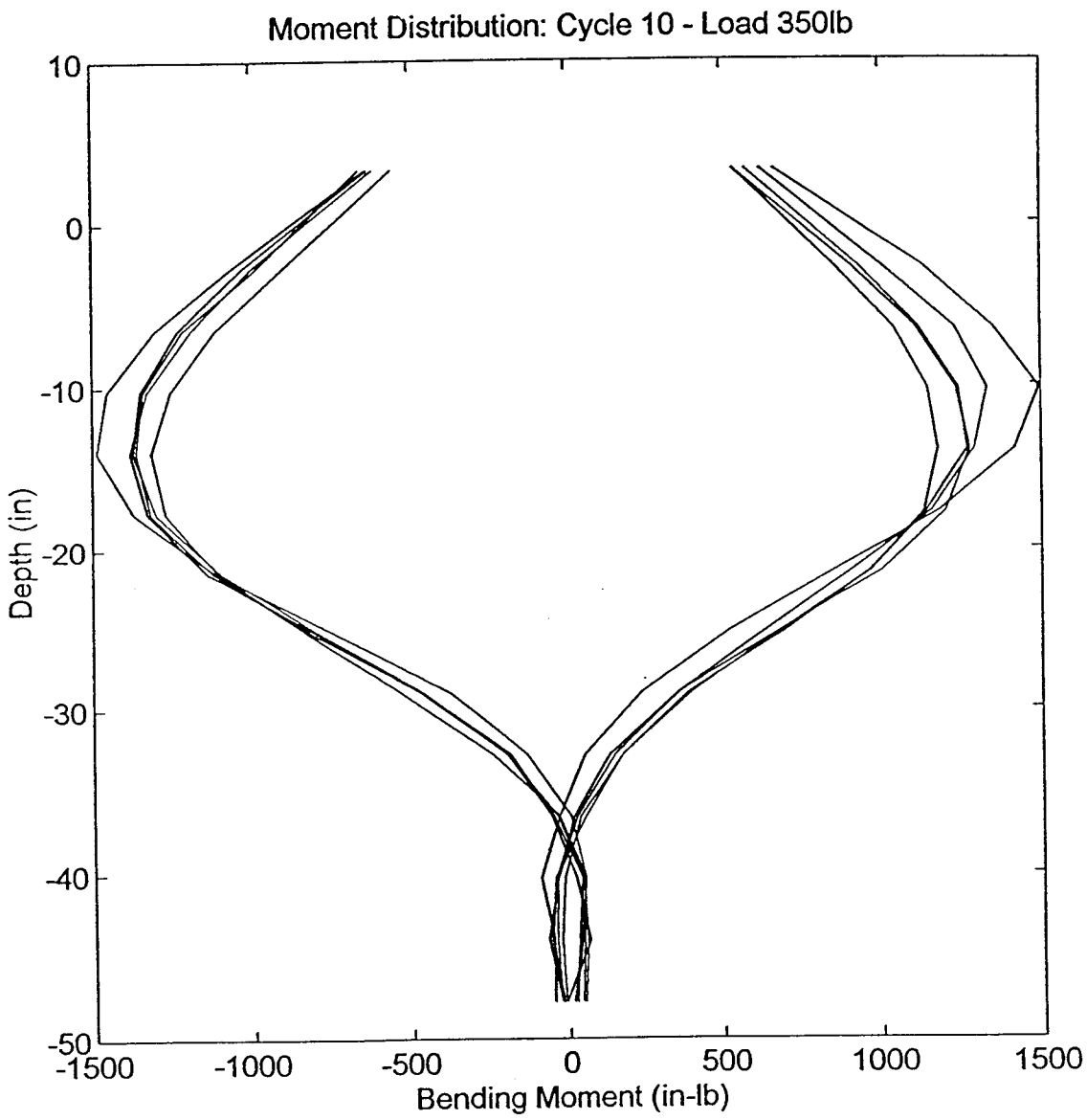
Moment Distribution: Cycle 10 - Load 350lb
10
0
-10
-20
-30
-40
-50
Depth (in)
-1500
-1000
-500
0
500
1000
1500
Bending Moment (in-lb)

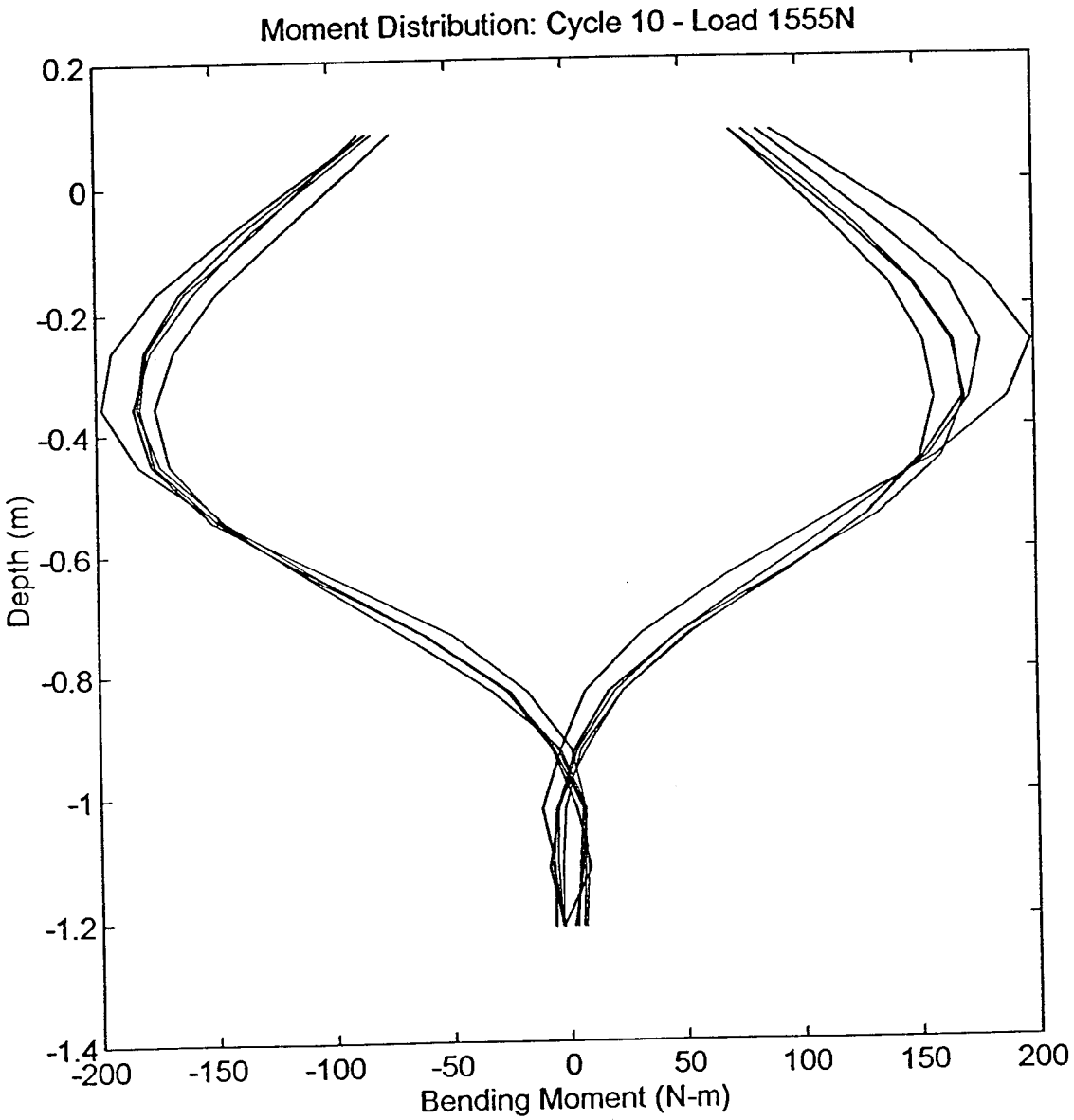
Moment Distribution: Cycle 10 - Load 1555N
0.2
0
-0.2
-0.4
-0.6
-0.8
-1
-1.2
-1.4
Depth (m)
-200
-150
-100
-50
0
50
100
150
200
Bending Moment (N-m)

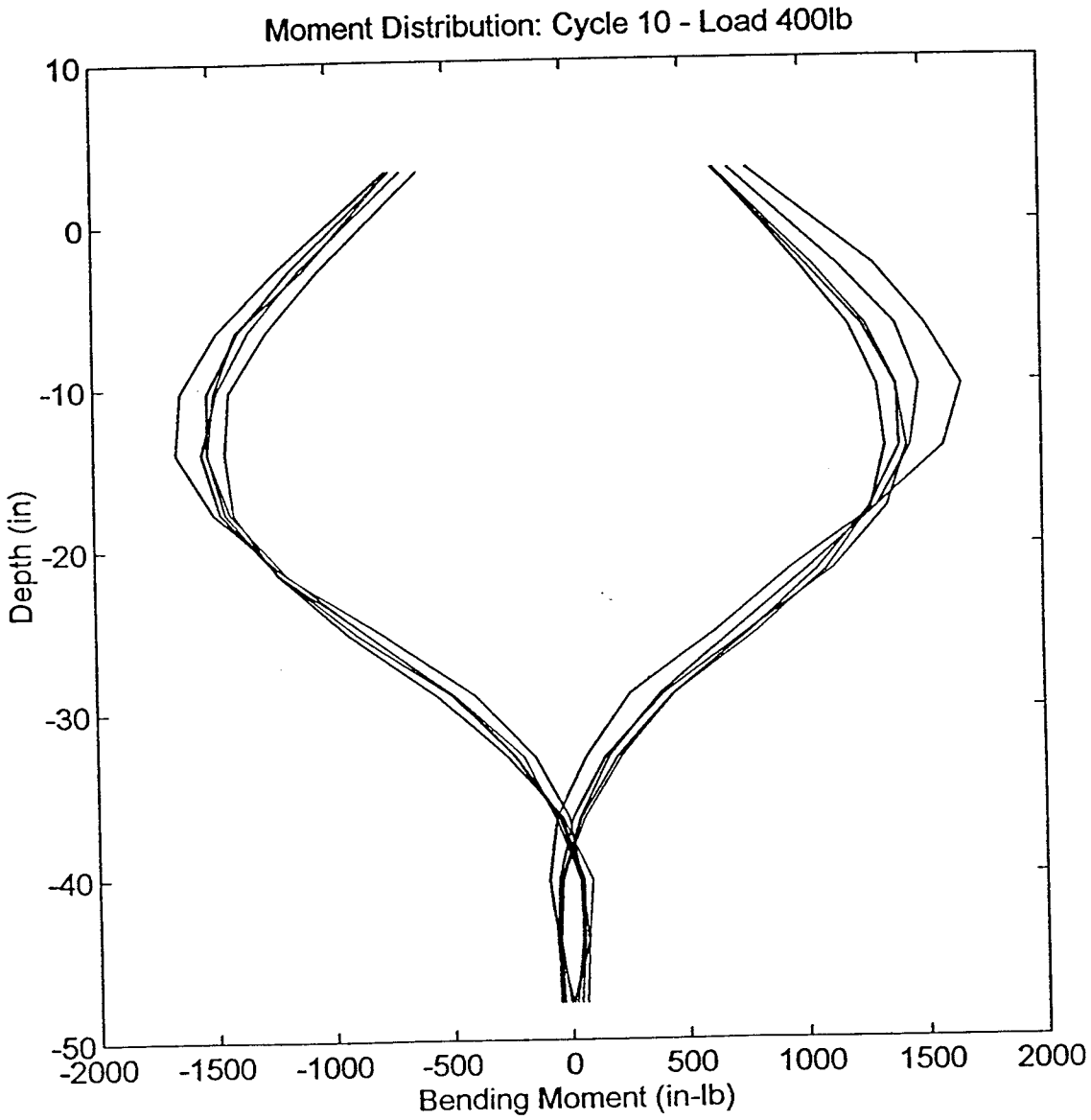
Moment Distribution: Cycle 10 - Load 400lb
10
0
-10
-20
-30
-40
-50
Depth (in)
-2000
-1500
-1000
-500
0
500
1000
1500
2000
Bending Moment (in-lb)

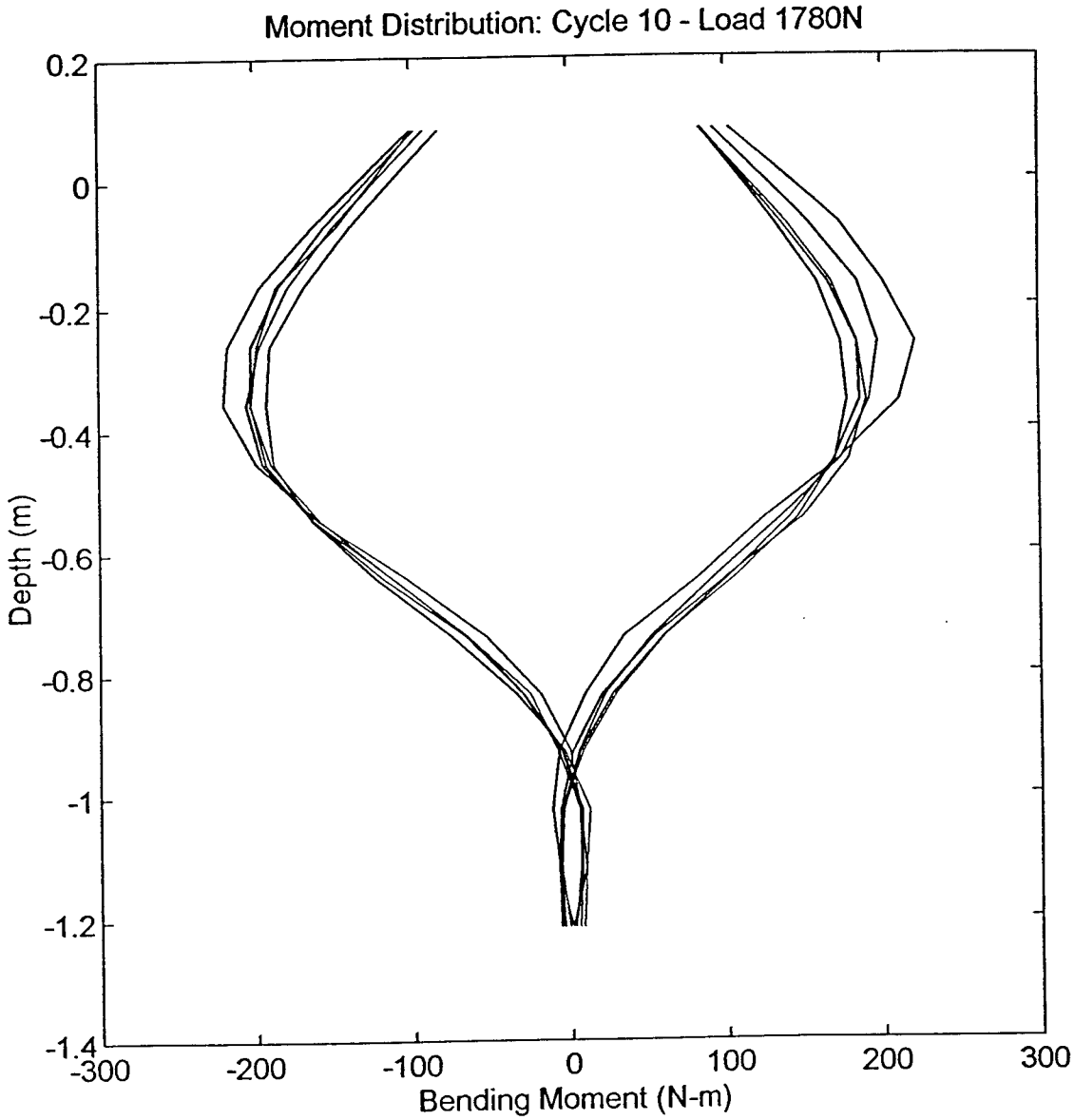
Moment Distribution: Cycle 10 - Load 1780N
0.2
0
-0.2
-0.4
-0.6
-0.8
-1
-1.2
-1.4
Depth (m)
-300
-200
-100
0
100
200
300
Bending Moment (N-m)

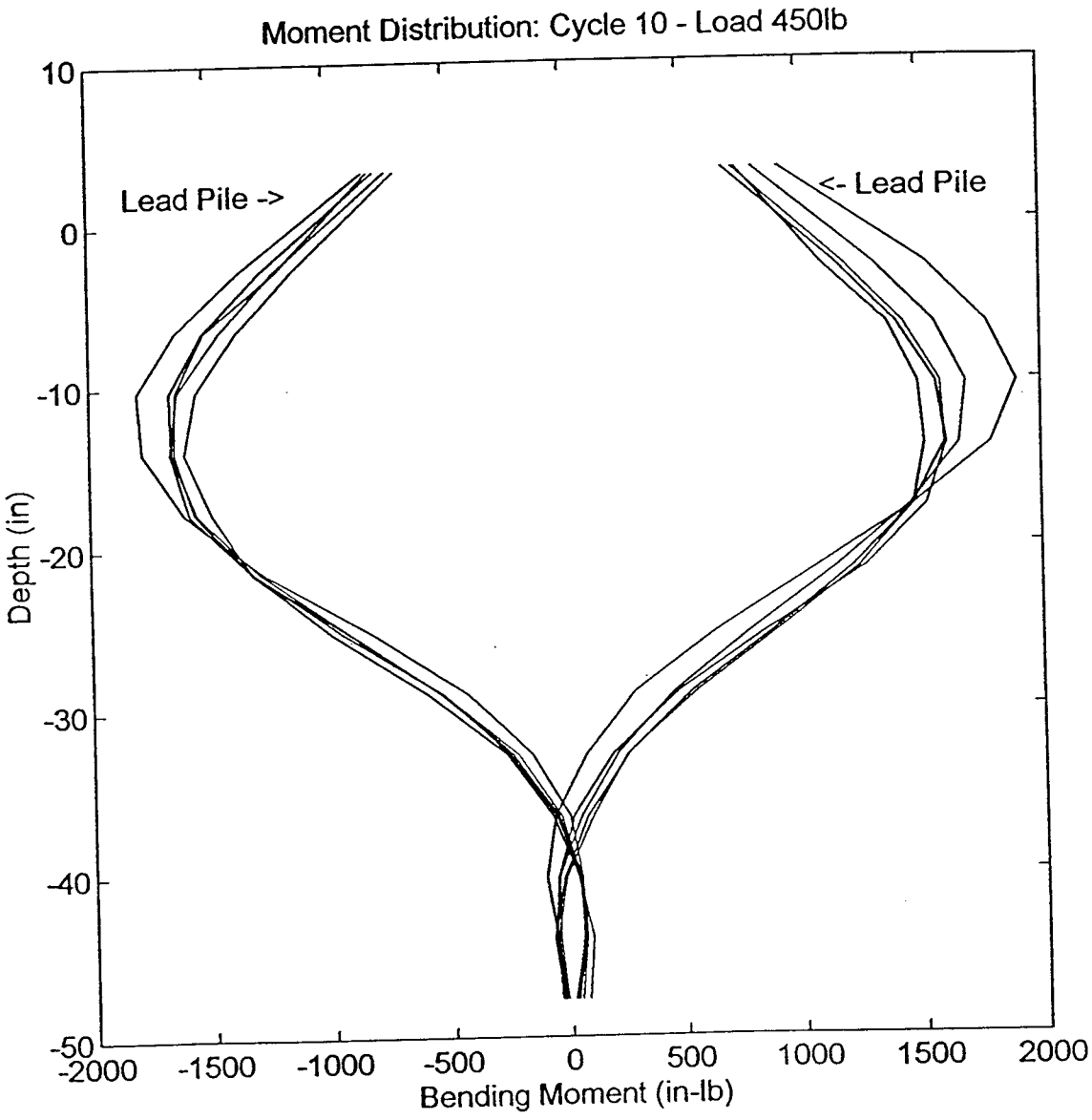
Moment Distribution: Cycle 10 - Load 450lb
Lead Pile ->
<- Lead Pile
Depth (in)
Bending Moment (in-lb)
10
0
-10
-20
-30
-40
-50
-2000
-1500
-1000
-500
0
500
1000
1500
2000

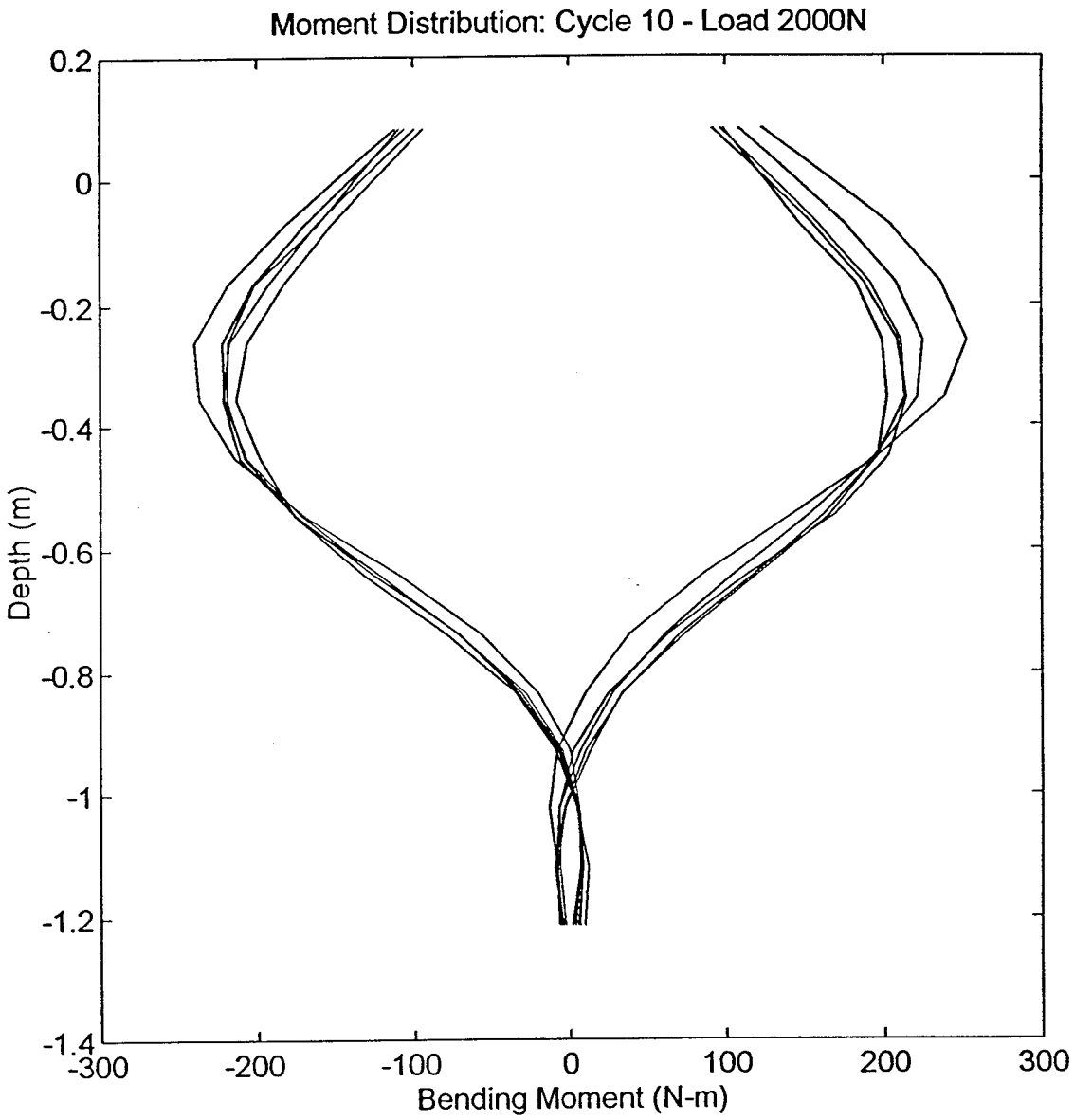
Moment Distribution: Cycle 10 - Load 2000N
0.2
0
-0.2
-0.4
-0.6
-0.8
-1
-1.2
-1.4
Depth (m)
-300
-200
-100
0
100
200
300
Bending Moment (N-m)

Figure B4. Moment distribution @ cycle 25 (next 14 plots).

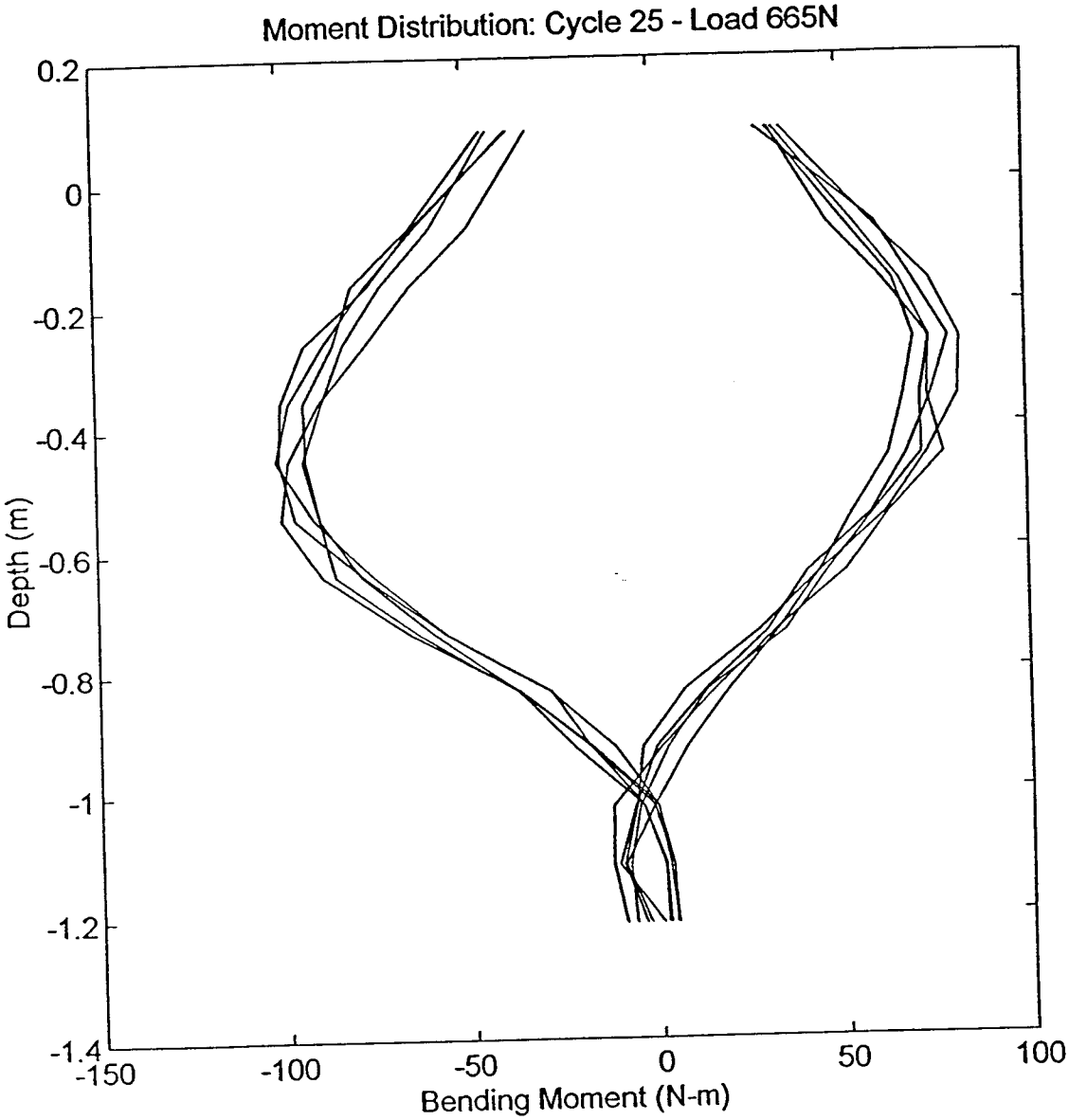
Moment Distribution: Cycle 25 - Load 665N
0.2
0
-0.2
-0.4
-0.6
-0.8
-1
-1.2
-1.4
Depth (m)
-150
-100
-50
0
50
100
Bending Moment (N-m)

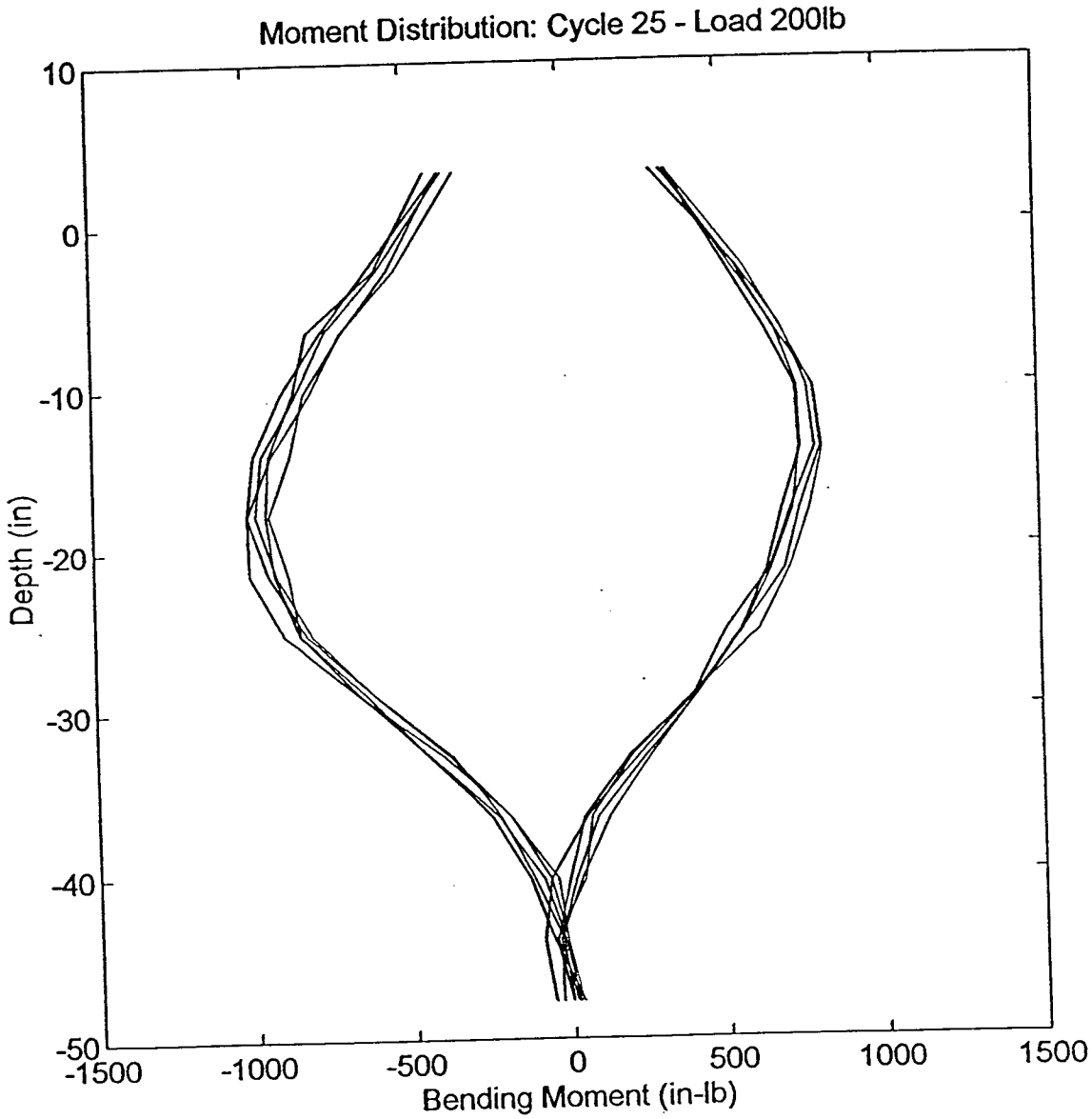
Moment Distribution: Cycle 25 - Load 200lb
10
0
-10
-20
-30
-40
-50
Depth (in)
-1500
-1000
-500
0
500
1000
1500
Bending Moment (in-lb)

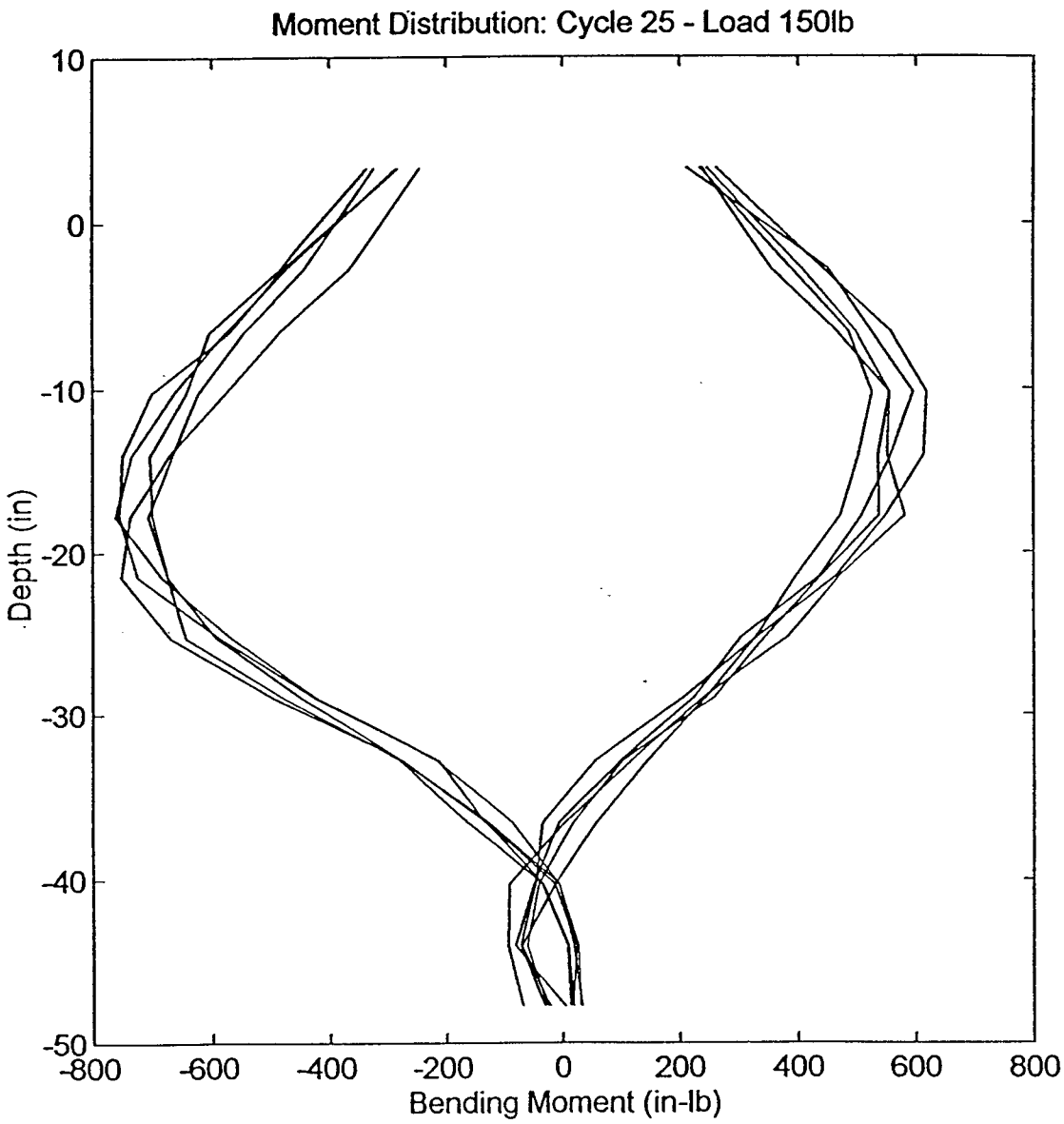
Moment Distribution: Cycle 25 - Load 150lb
10
0
-10
-20
-30
-40
-50
Depth (in)
-800
-600
-400
-200
0
200
400
600
800
Bending Moment (in-lb)

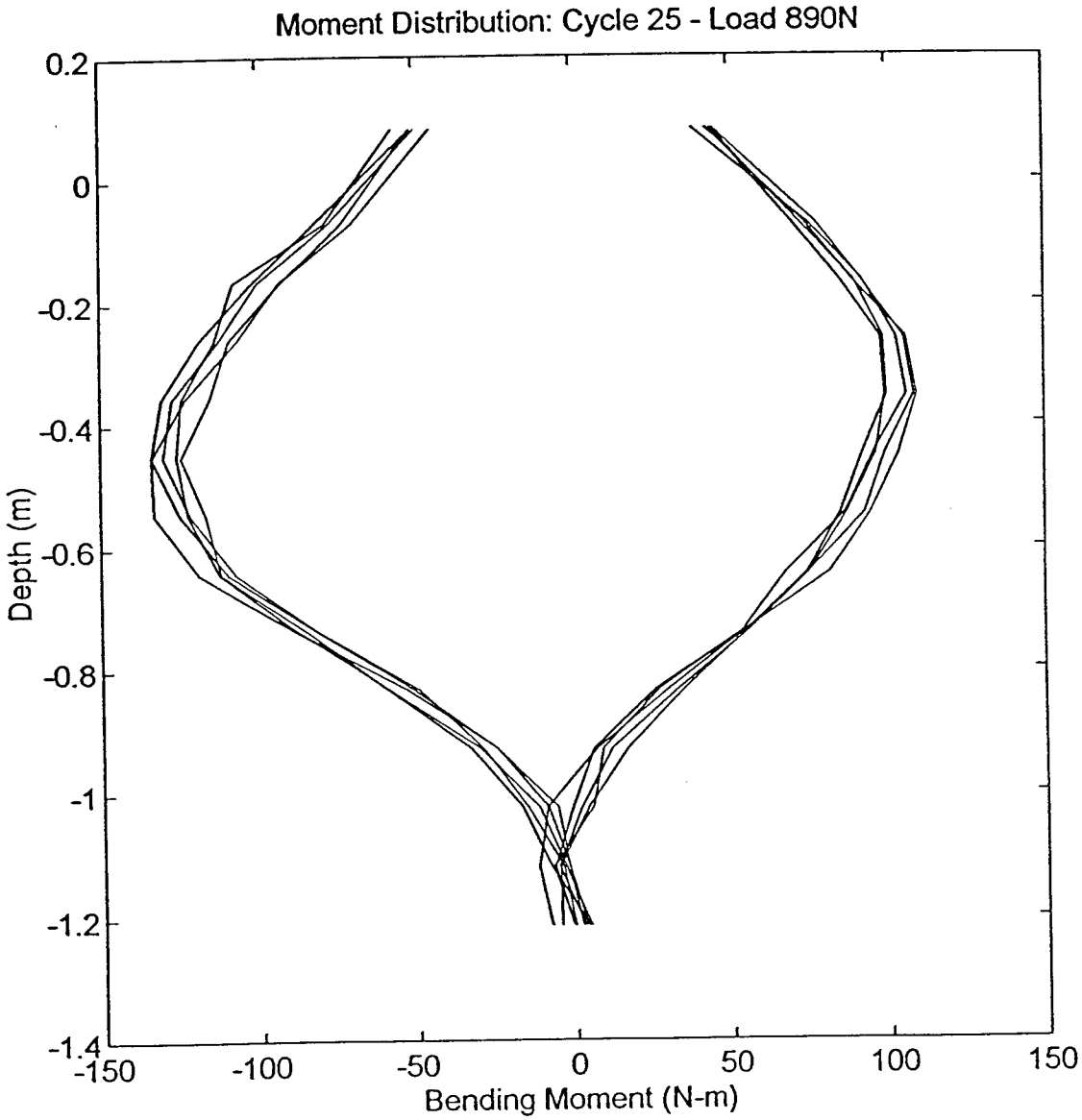
Moment Distribution: Cycle 25 - Load 890N
0.2
0
-0.2
-0.4
-0.6
-0.8
-1
-1.2
-1.4
Depth (m)
-150
-100
-50
0
50
100
150
Bending Moment (N-m)

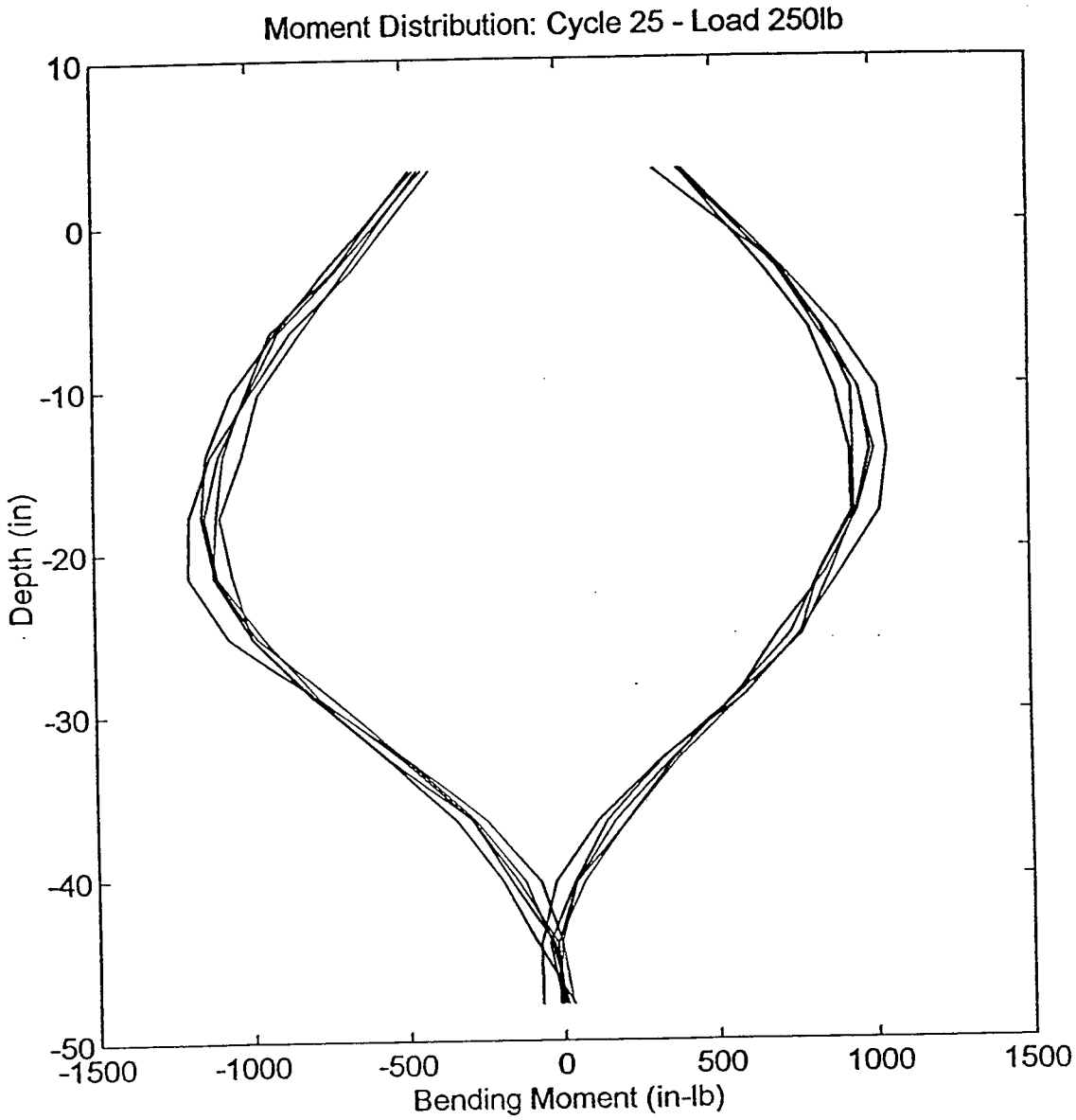
Moment Distribution: Cycle 25 - Load 250lb
10
0
-10
-20
-30
-40
-50
Depth (in)
-1500
-1000
-500
0
500
1000
1500
Bending Moment (in-lb)

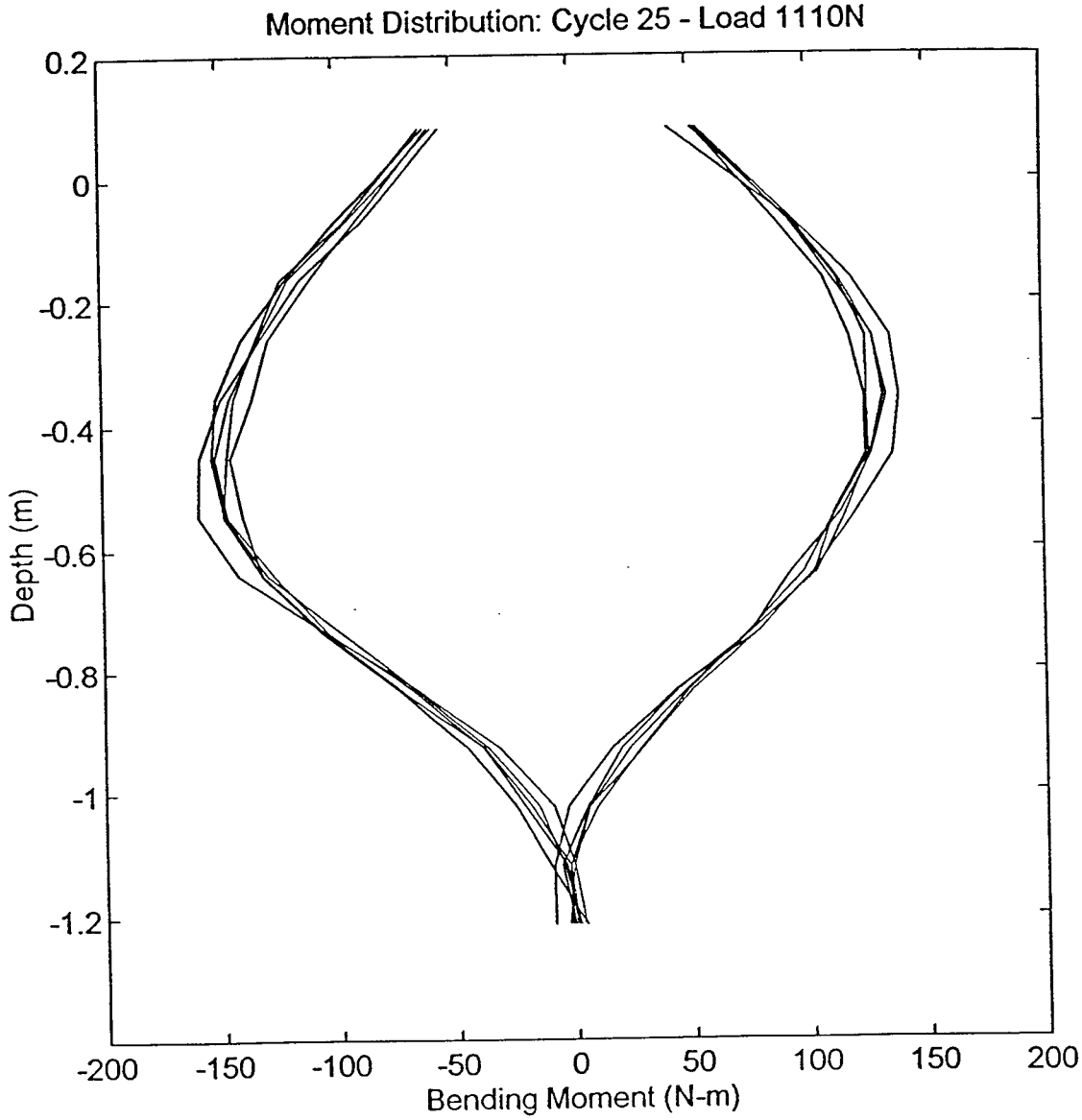
Moment Distribution: Cycle 25 - Load 1110N
0.2
0
-0.2
-0.4
-0.6
-0.8
-1
-1.2
Depth (m)
-200
-150
-100
-50
0
50
100
150
200
Bending Moment (N-m)

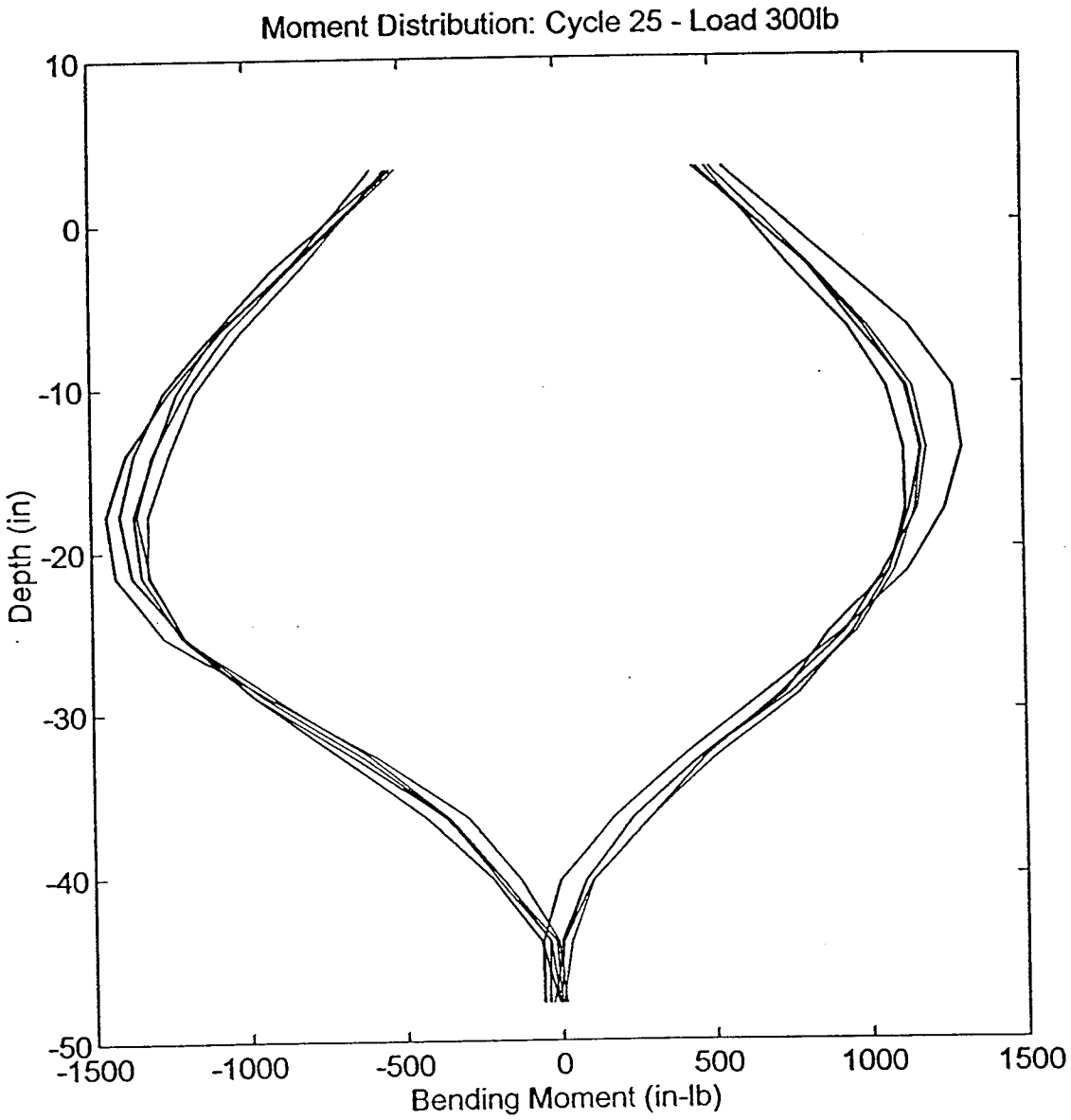
Moment Distribution: Cycle 25 - Load 300lb
10
0
-10
-20
-30
-40
-50
Depth (in)
-1500
-1000
-500
0
500
1000
1500
Bending Moment (in-lb)

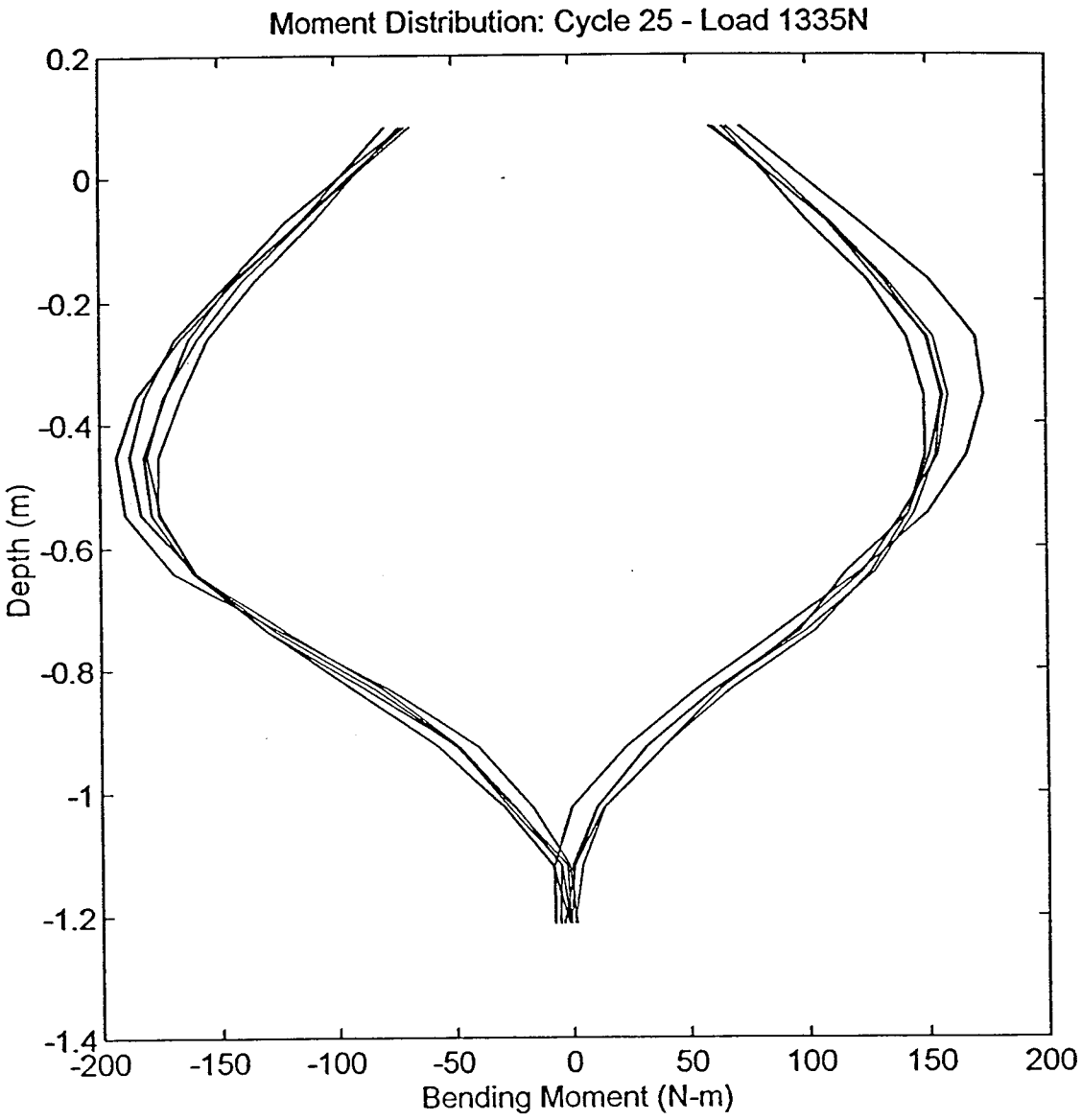
Moment Distribution: Cycle 25 - Load 1335N
0.2
0
-0.2
-0.4
-0.6
-0.8
-1
-1.2
-1.4
Depth (m)
-200
-150
-100
-50
0
50
100
150
200
Bending Moment (N-m)

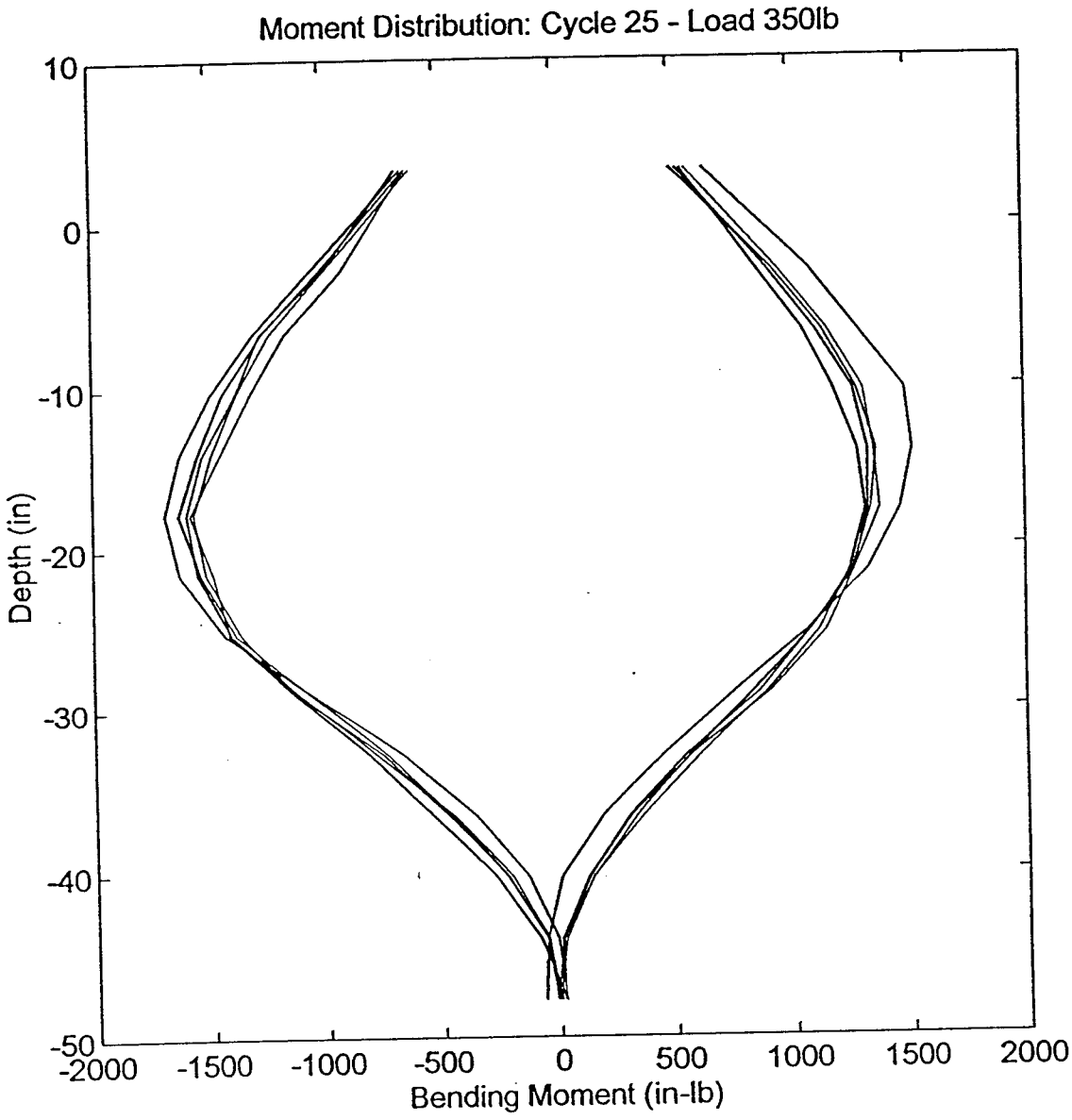
Moment Distribution: Cycle 25 - Load 350lb
10
0
-10
-20
-30
-40
-50
Depth (in)
-2000
-1500
-1000
-500
0
500
1000
1500
2000
Bending Moment (in-lb)

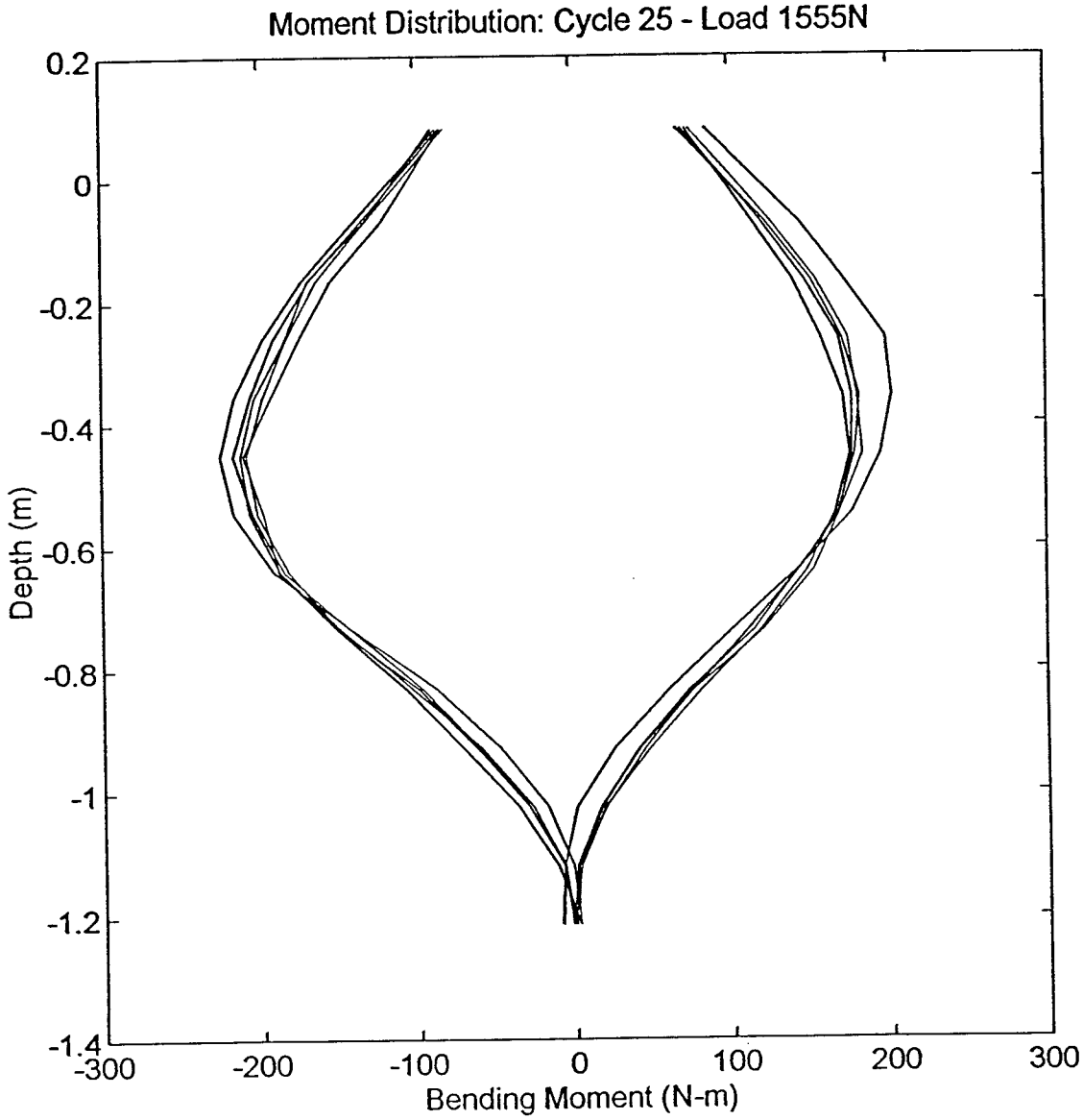
Moment Distribution: Cycle 25 - Load 1555N
0.2
0
-0.2
-0.4
-0.6
-0.8
-1
-1.2
-1.4
Depth (m)
-300
-200
-100
0
100
200
300
Bending Moment (N-m)

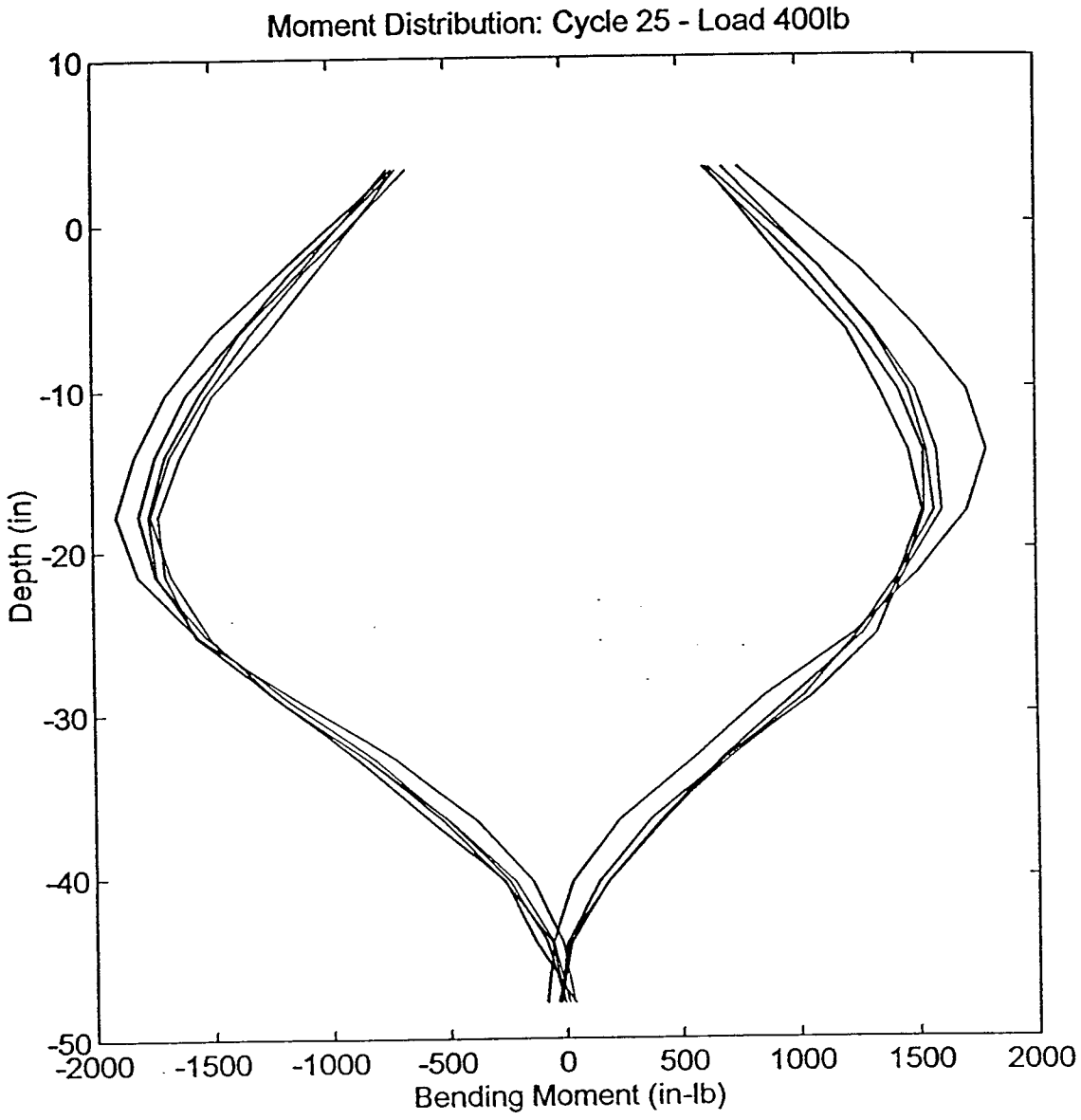
Moment Distribution: Cycle 25 - Load 400lb
10
0
-10
-20
-30
-40
-50
Depth (in)
-2000
-1500
-1000
-500
0
500
1000
1500
2000
Bending Moment (in-lb)

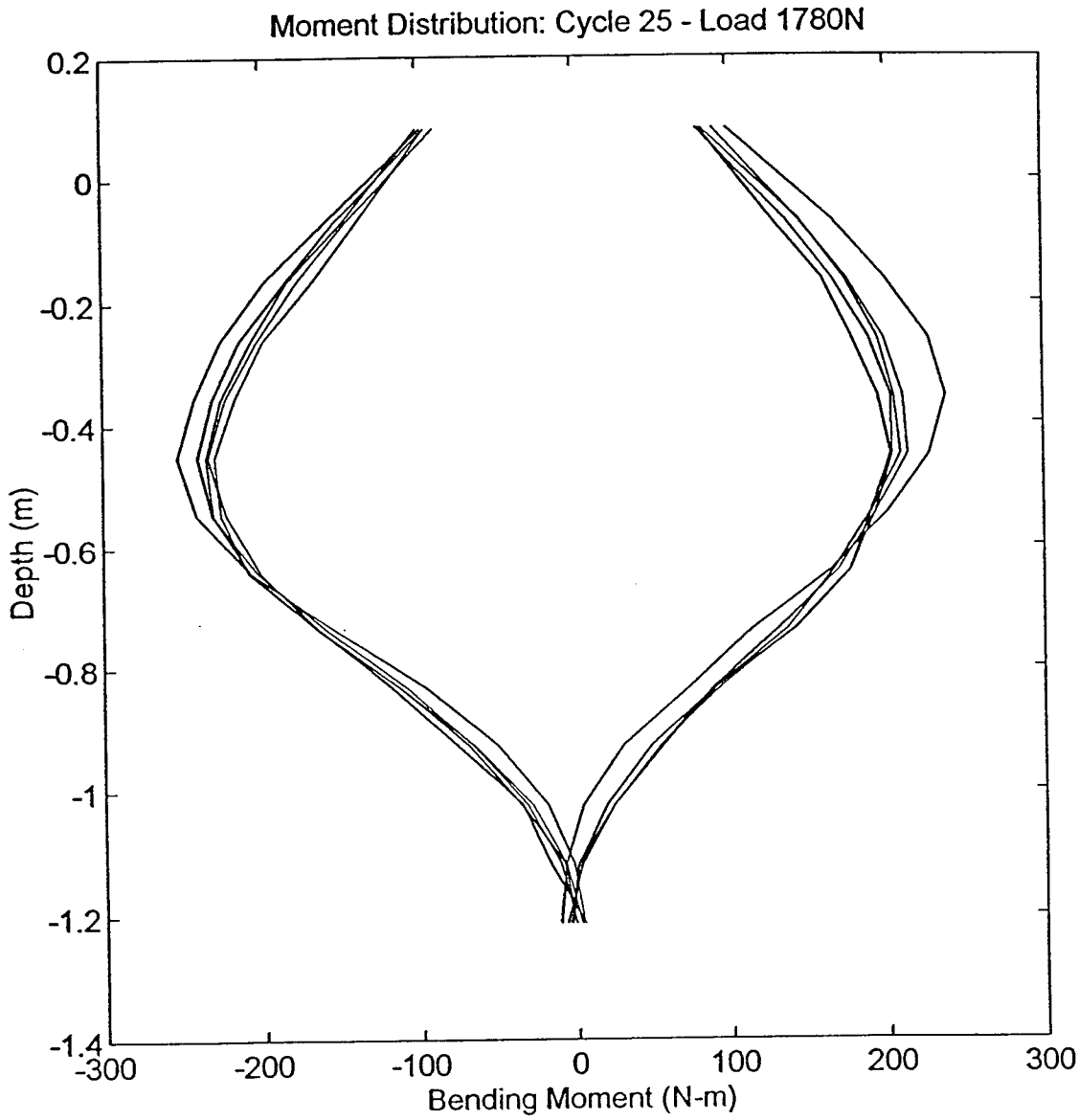
Moment Distribution: Cycle 25 - Load 1780N
0.2
0
-0.2
-0.4
-0.6
-0.8
-1
-1.2
-1.4
Depth (m)
-300
-200
-100
0
100
200
300
Bending Moment (N-m)

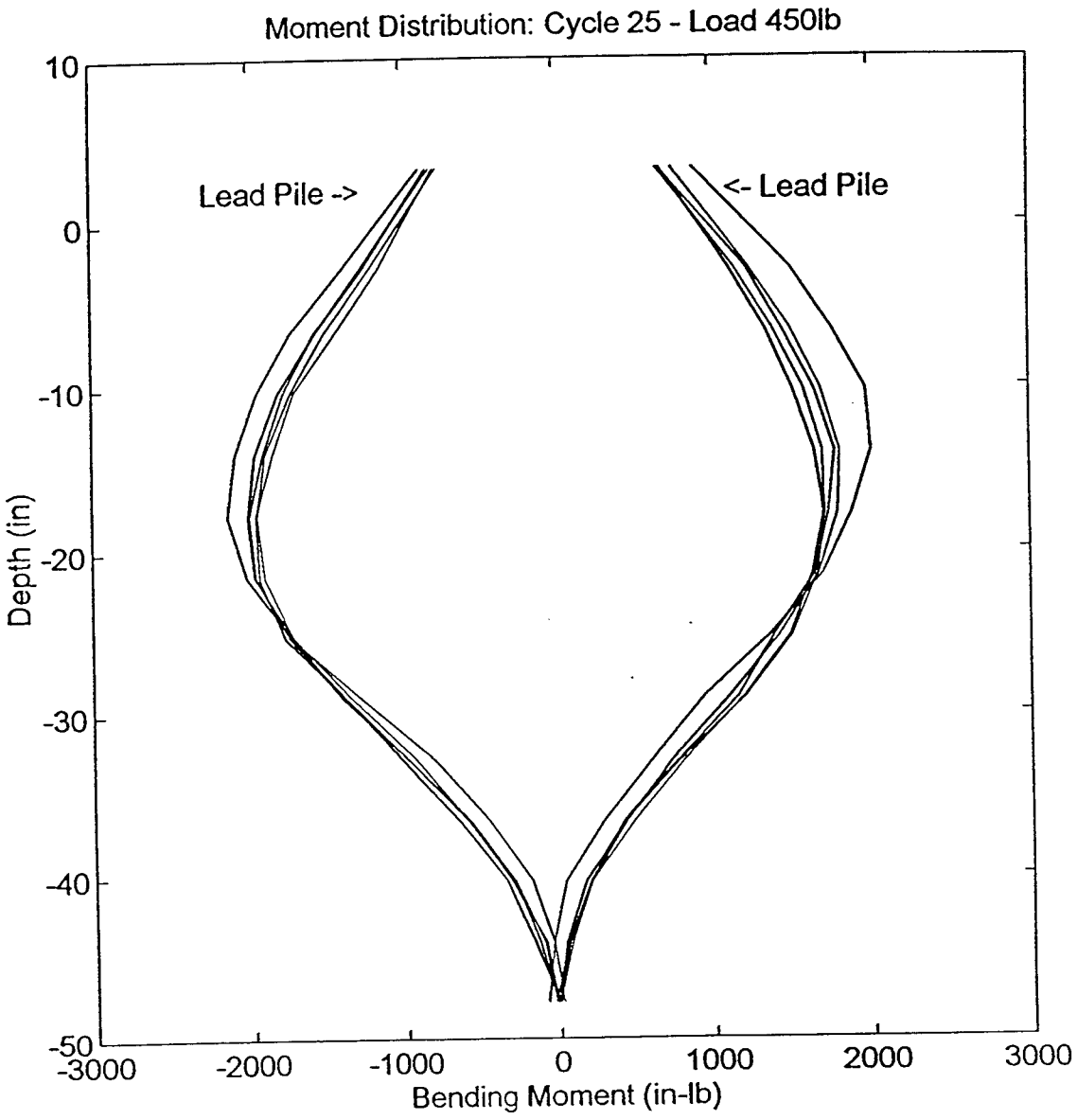
Moment Distribution: Cycle 25 - Load 450lb
Lead Pile ->
<- Lead Pile
Depth (in)
Bending Moment (in-lb)
10
0
-10
-20
-30
-40
-50
-3000
-2000
-1000
0
1000
2000
3000

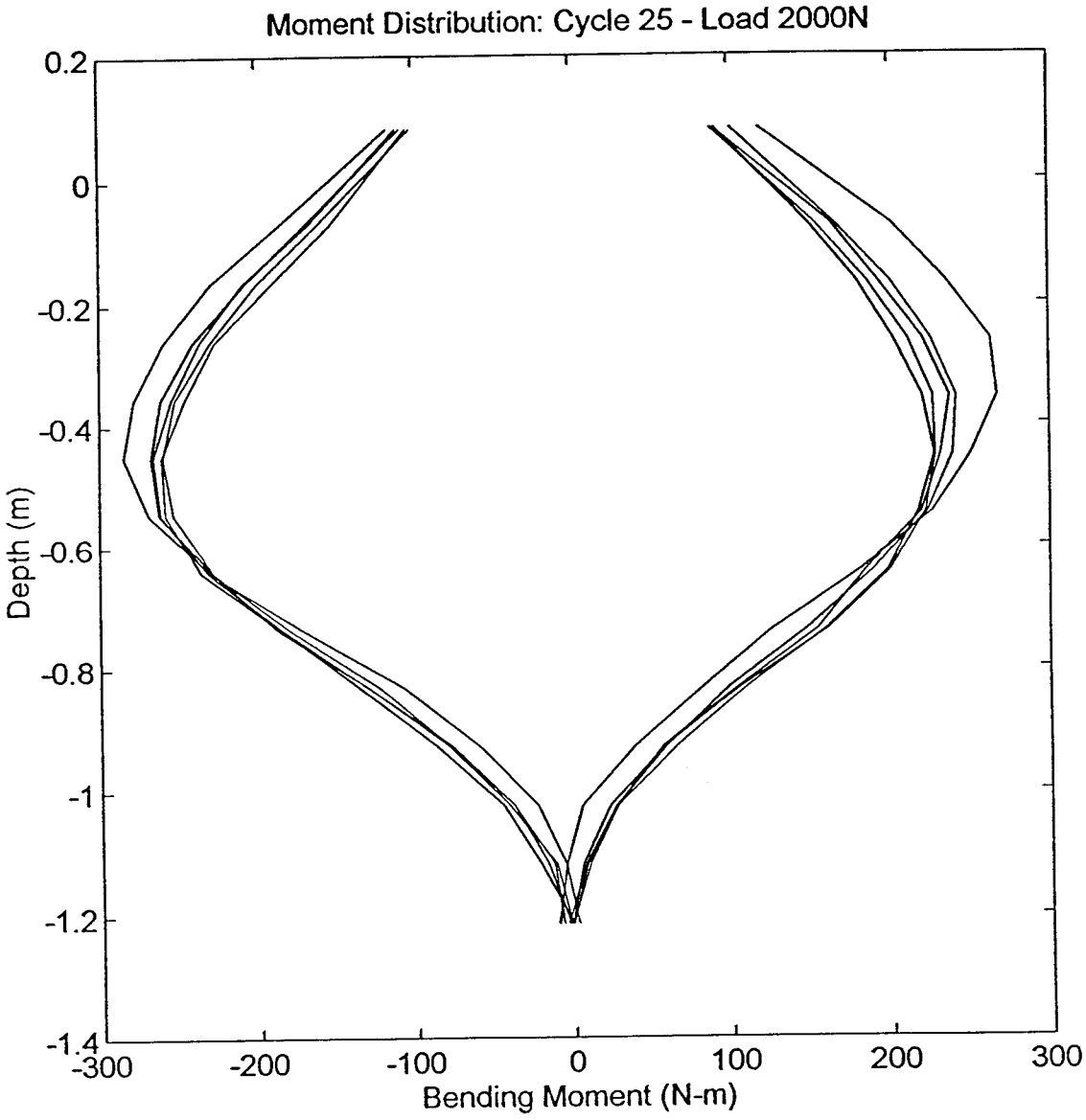
Moment Distribution: Cycle 25 - Load 2000N
0.2
0
-0.2
-0.4
-0.6
-0.8
-1
-1.2
-1.4
Depth (m)
-300
-200
-100
0
100
200
300
Bending Moment (N-m)

Figure B5. Moment distribution @ cycle 50 (next 14 plots).

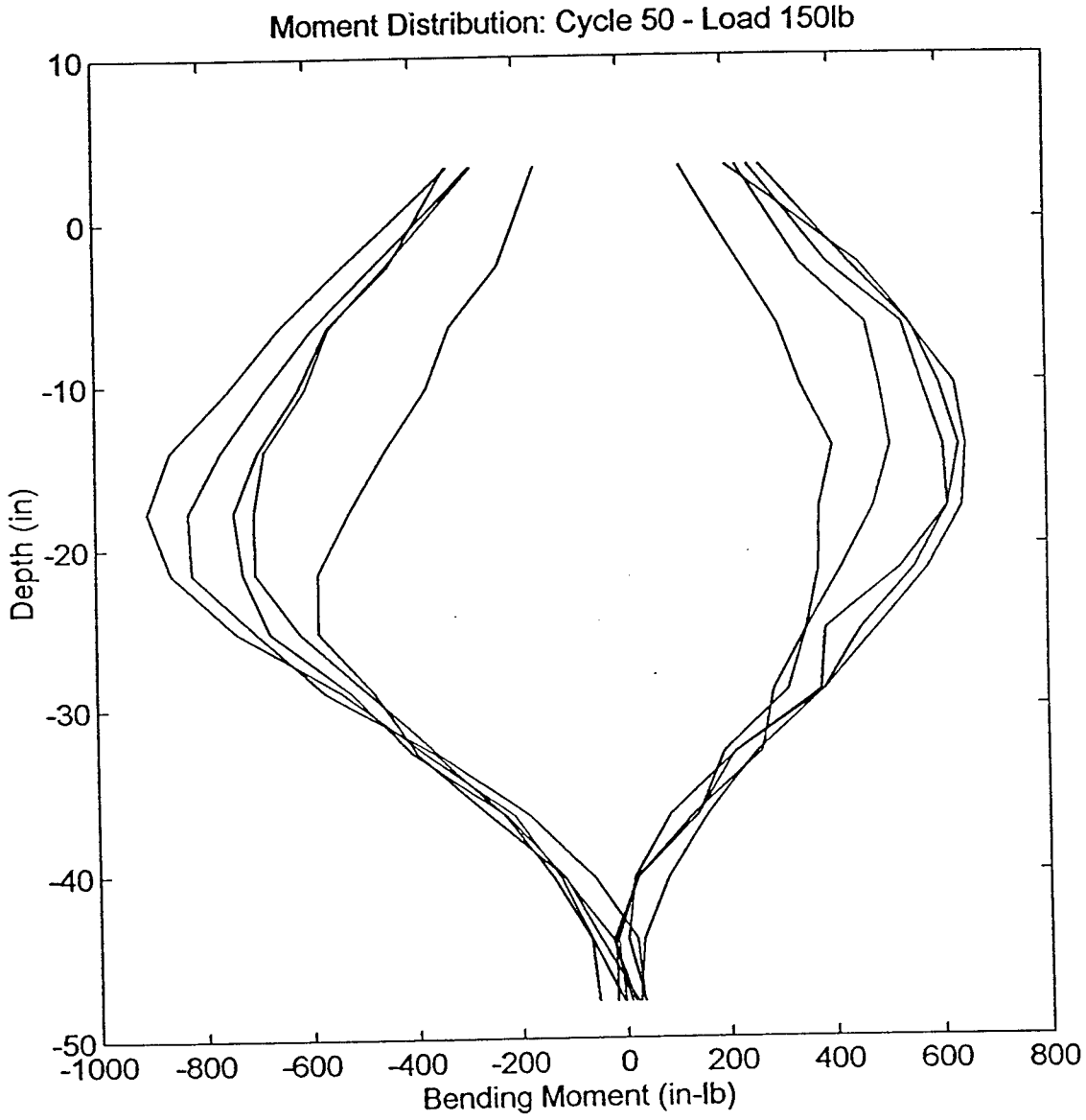
Moment Distribution: Cycle 50 - Load 150lb
10
0
-10
-20
-30
-40
-50
Depth (in)
-1000
-800
-600
-400
-200
0
200
400
600
800
Bending Moment (in-lb)

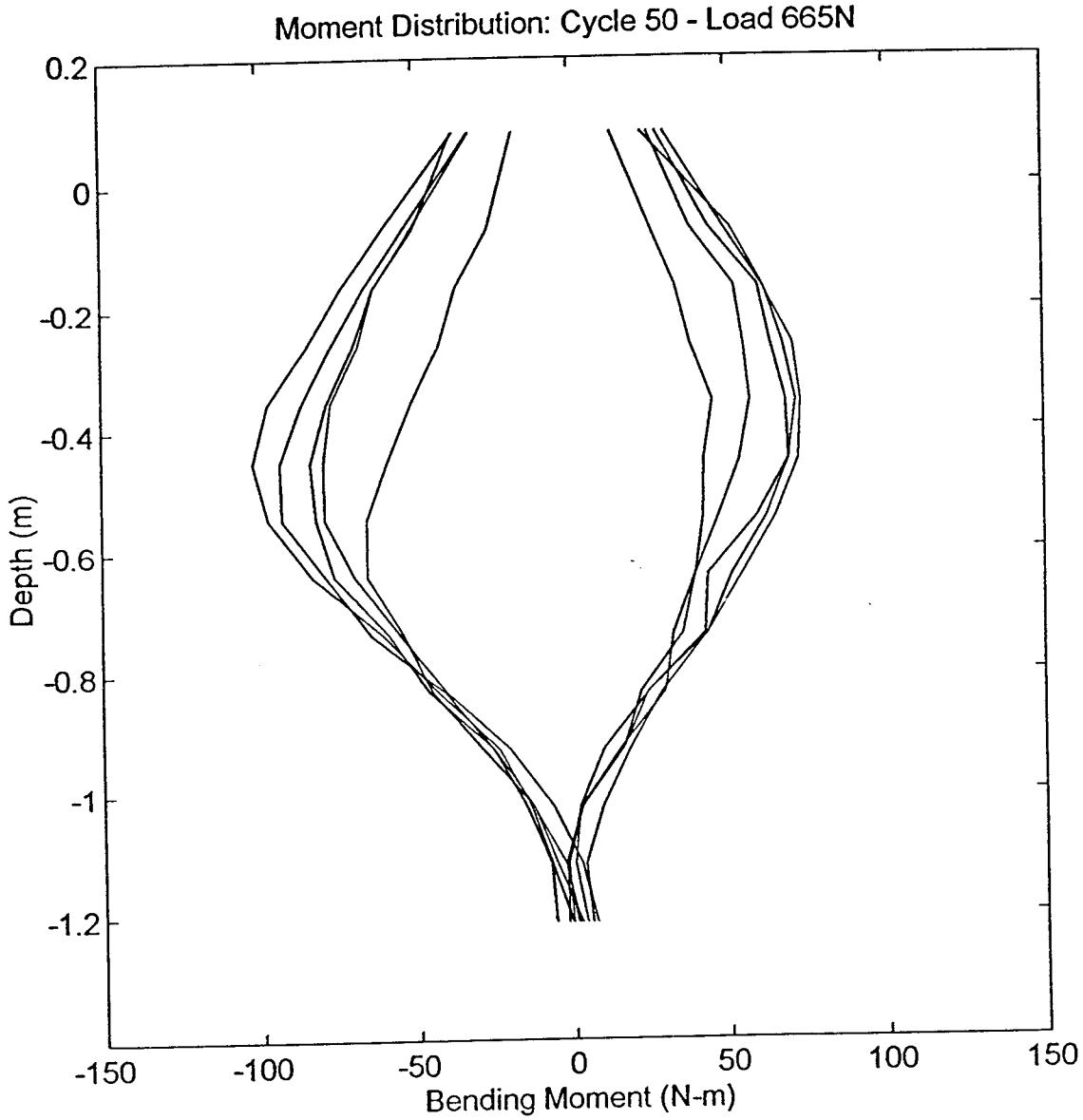
Moment Distribution: Cycle 50 - Load 665N
0.2
0
-0.2
-0.4
-0.6
-0.8
-1
-1.2
Depth (m)
-150
-100
-50
0
50
100
150
Bending Moment (N-m)

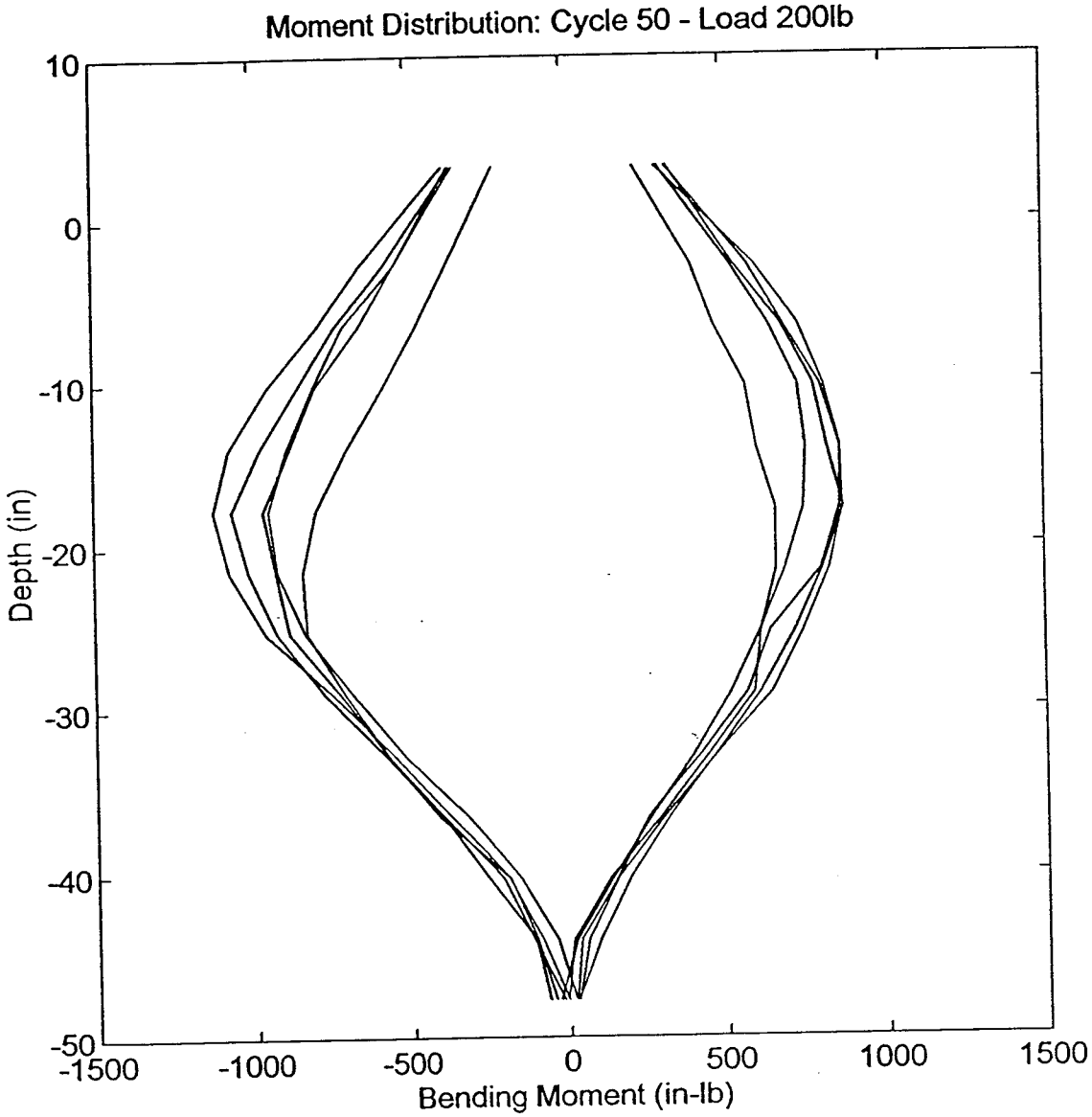
Moment Distribution: Cycle 50 - Load 200lb
10
0
-10
-20
-30
-40
-50
Depth (in)
-1500
-1000
-500
0
500
1000
1500
Bending Moment (in-lb)

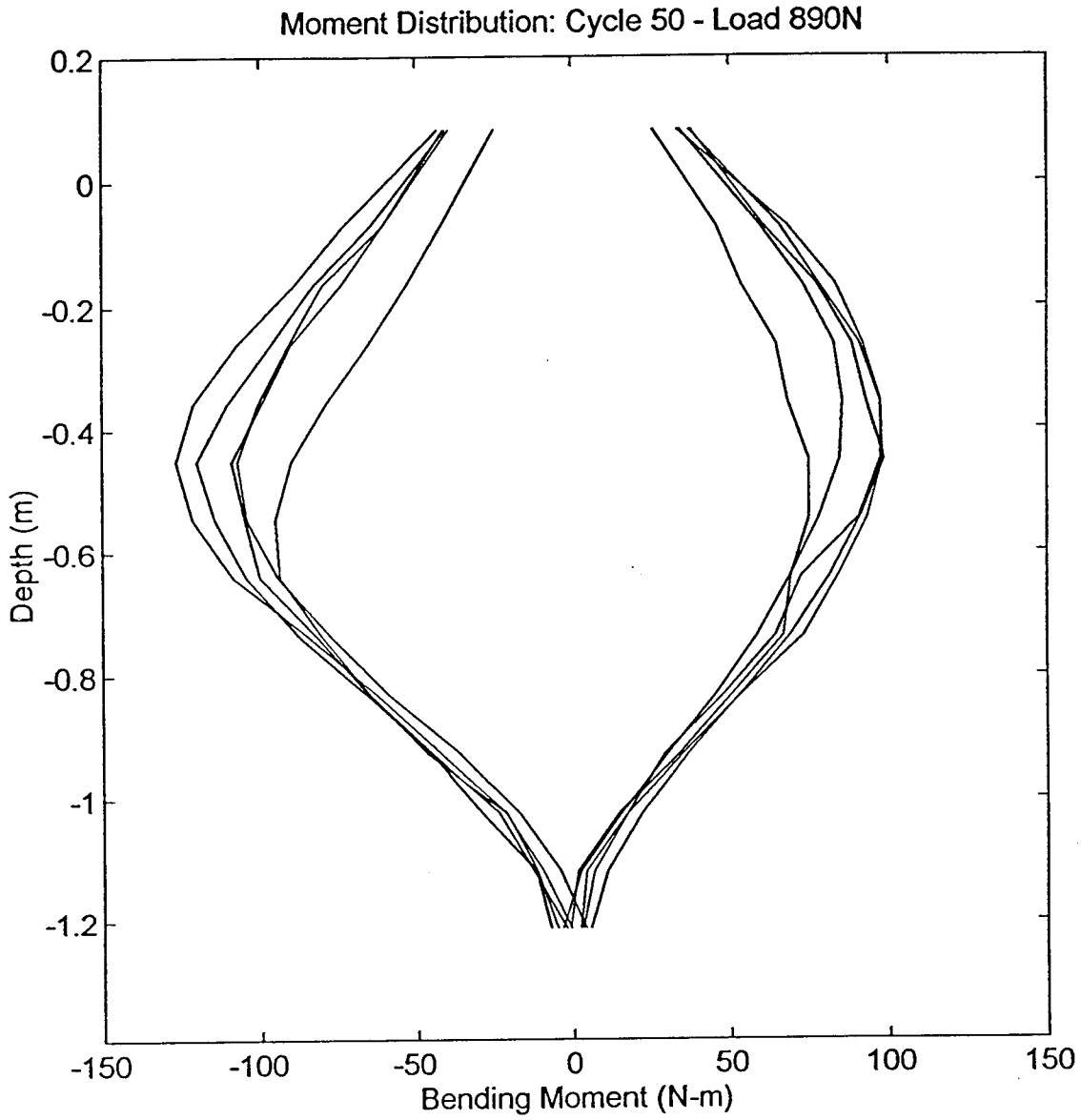
Moment Distribution: Cycle 50 - Load 890N
0.2
0
-0.2
-0.4
-0.6
-0.8
-1
-1.2
Depth (m)
-150
-100
-50
0
50
100
150
Bending Moment (N-m)

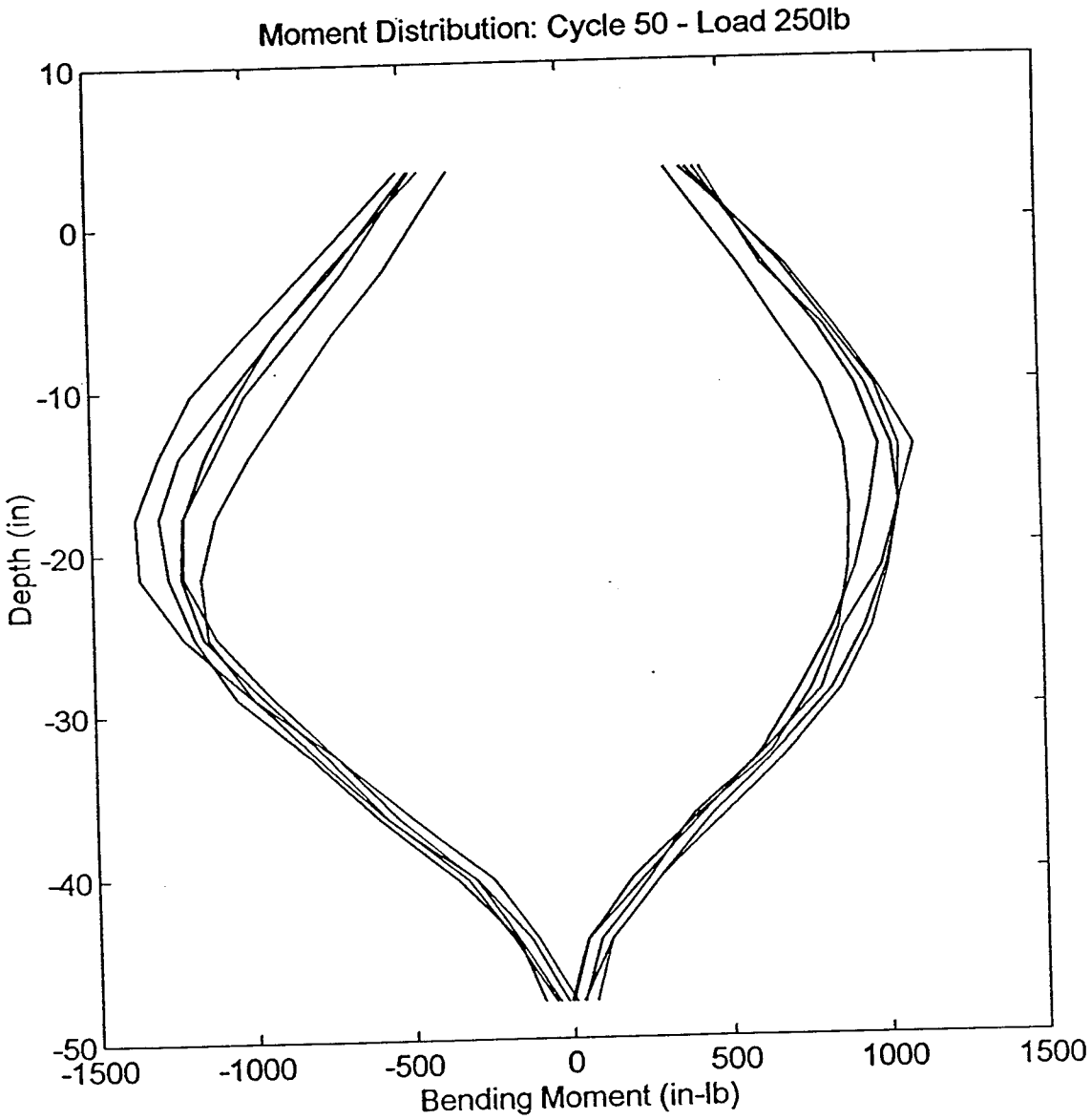
Moment Distribution: Cycle 50 - Load 250lb
10
0
-10
-20
-30
-40
-50
Depth (in)
-1500
-1000
-500
0
500
1000
1500
Bending Moment (in-lb)

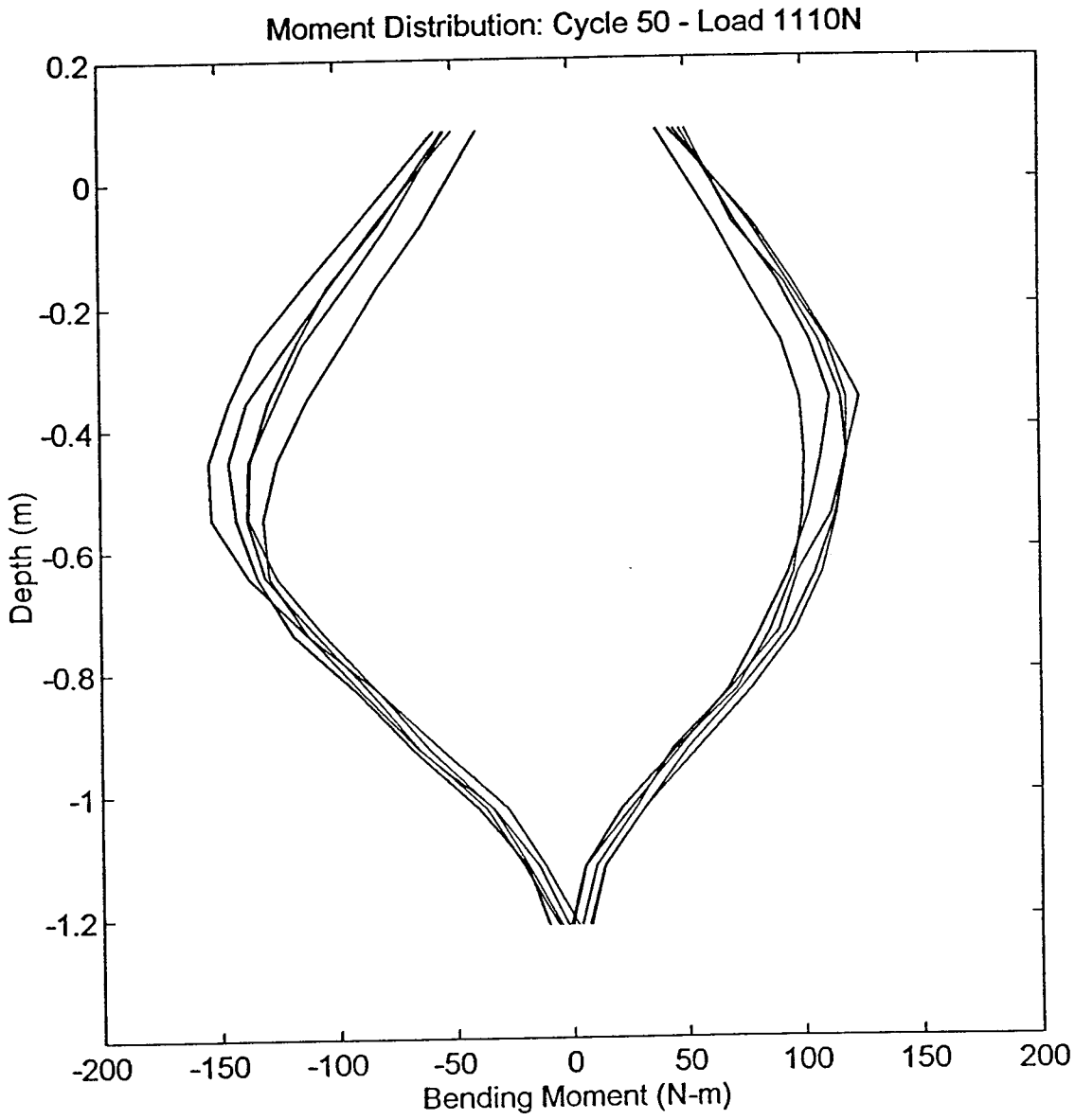
Moment Distribution: Cycle 50 - Load 1110N
0.2
0
-0.2
-0.4
-0.6
-0.8
-1
-1.2
Depth (m)
-200
-150
-100
-50
0
50
100
150
200
Bending Moment (N-m)

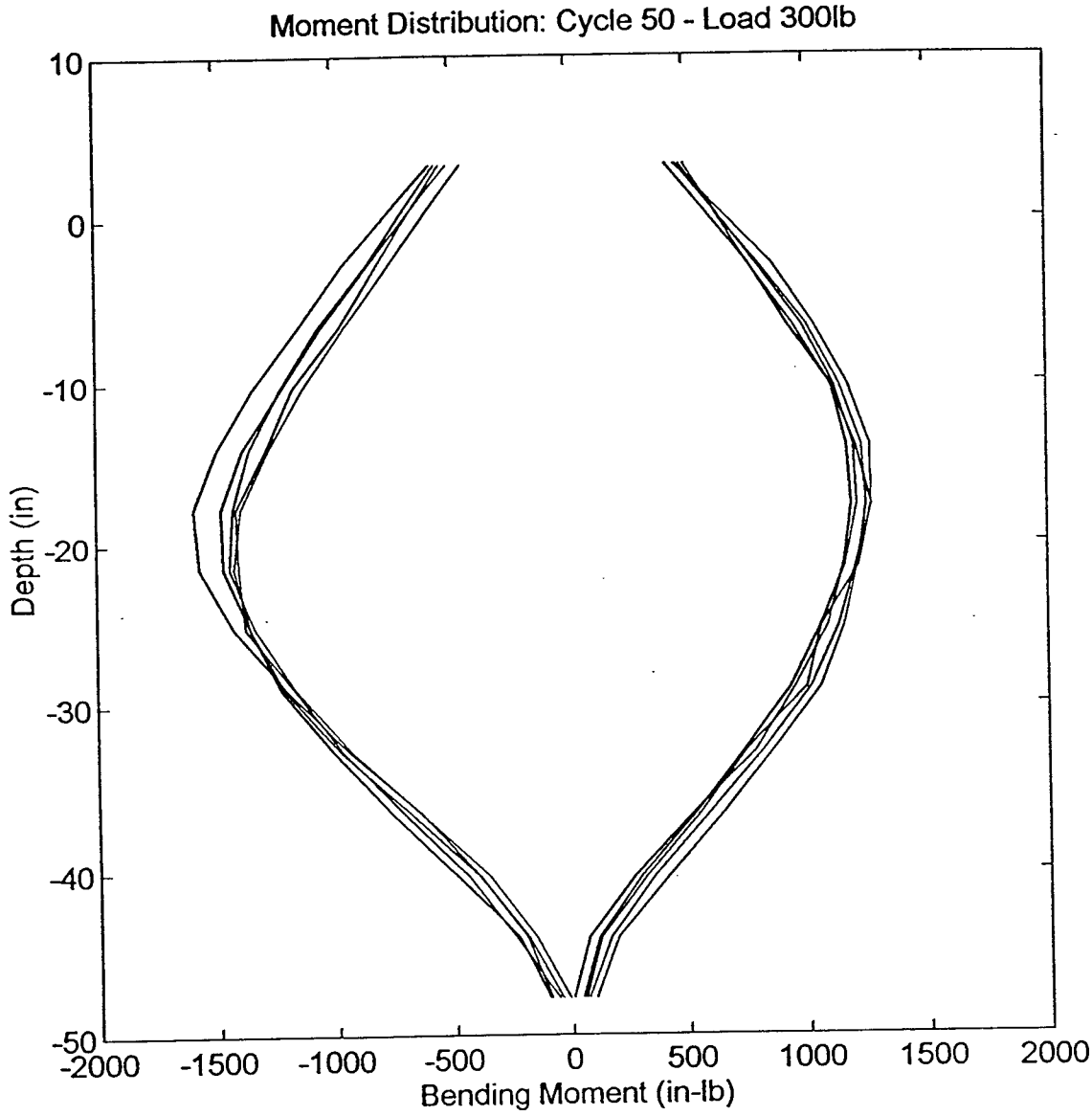
Moment Distribution: Cycle 50 - Load 300lb
10
0
-10
-20
-30
-40
-50
Depth (in)
-2000
-1500
-1000
-500
0
500
1000
1500
2000
Bending Moment (in-lb)

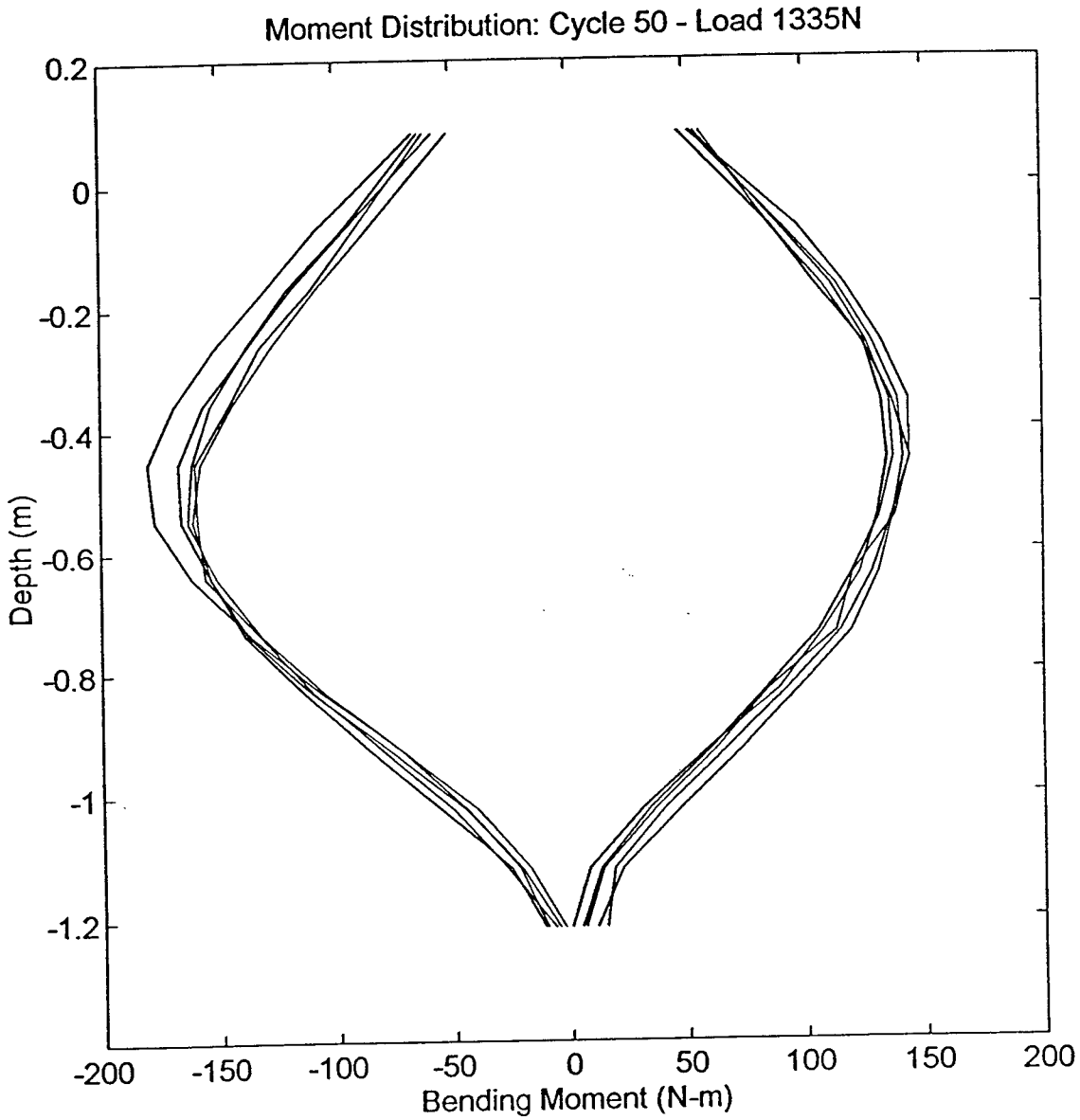
Moment Distribution: Cycle 50 - Load 1335N
0.2
0
-0.2
-0.4
-0.6
-0.8
-1
-1.2
Depth (m)
-200
-150
-100
-50
0
50
100
150
200
Bending Moment (N-m)

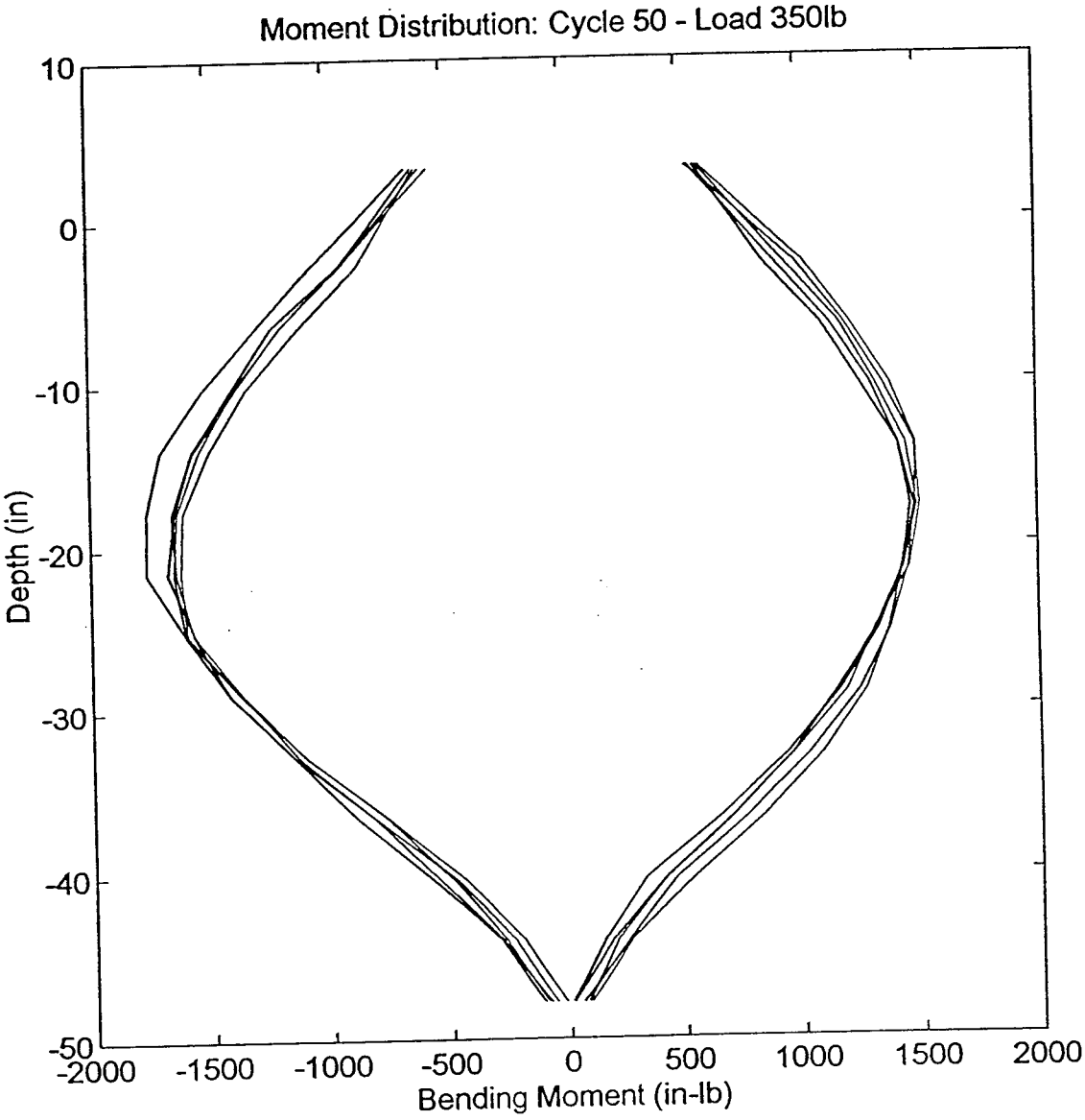
Moment Distribution: Cycle 50 - Load 350lb
10
0
-10
-20
-30
-40
-50
Depth (in)
-2000
-1500
-1000
-500
0
500
1000
1500
2000
Bending Moment (in-lb)

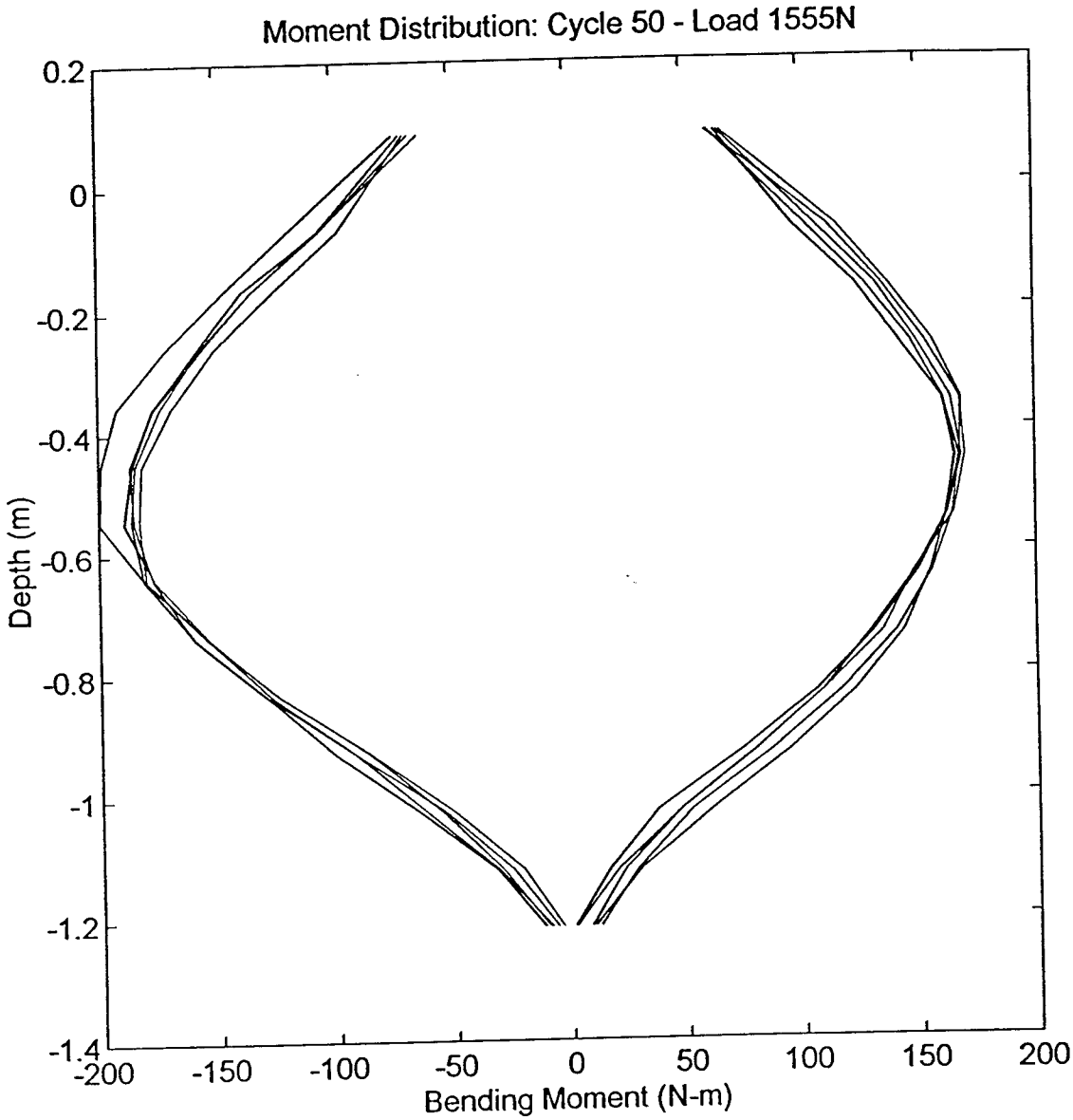
Moment Distribution: Cycle 50 - Load 1555N
0.2
0
-0.2
-0.4
-0.6
-0.8
-1
-1.2
-1.4
Depth (m)
-200
-150
-100
-50
0
50
100
150
200
Bending Moment (N-m)

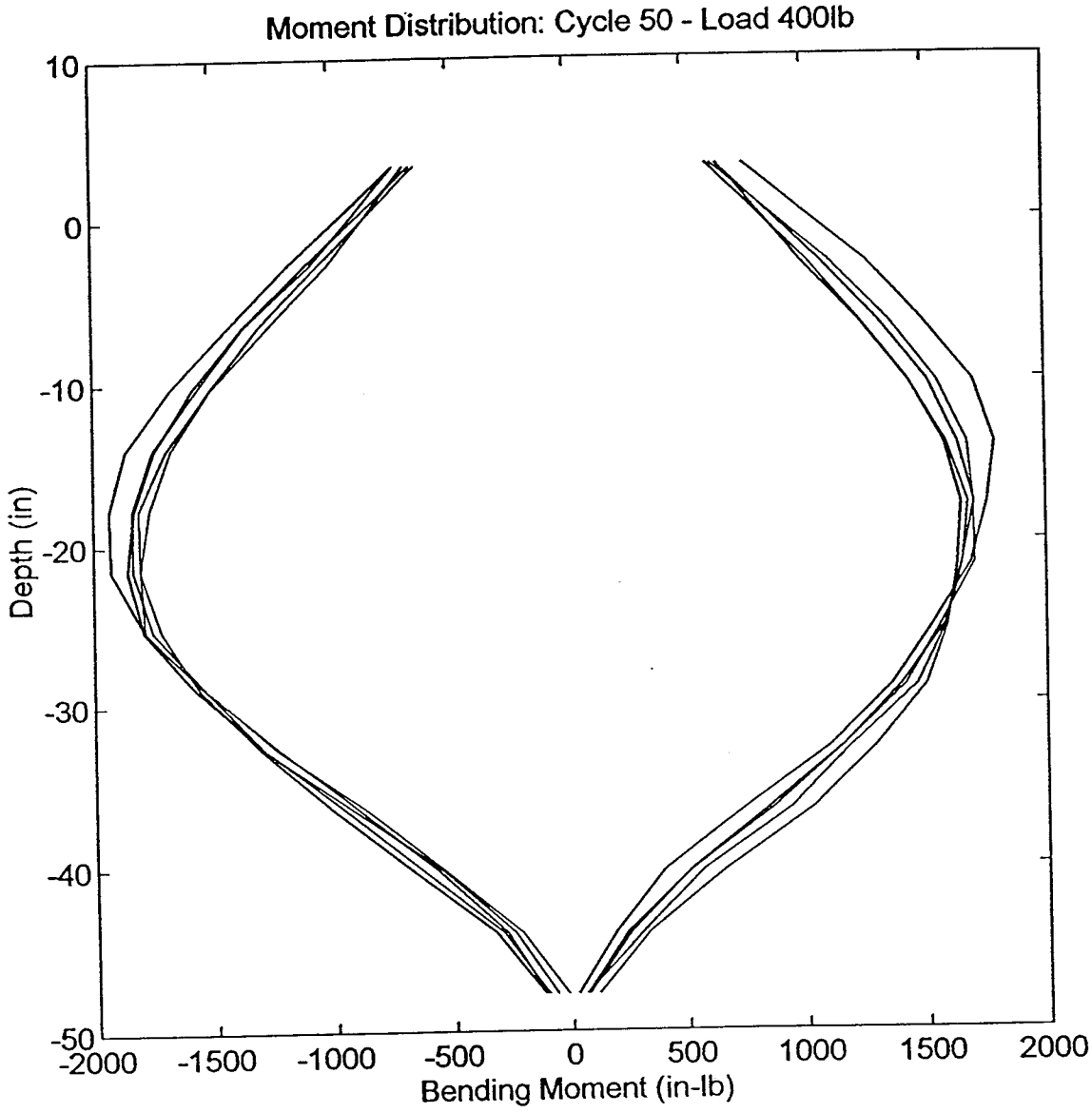
Moment Distribution: Cycle 50 - Load 400lb
10
0
-10
-20
-30
-40
-50
Depth (in)
-2000
-1500
-1000
-500
0
500
1000
1500
2000
Bending Moment (in-lb)

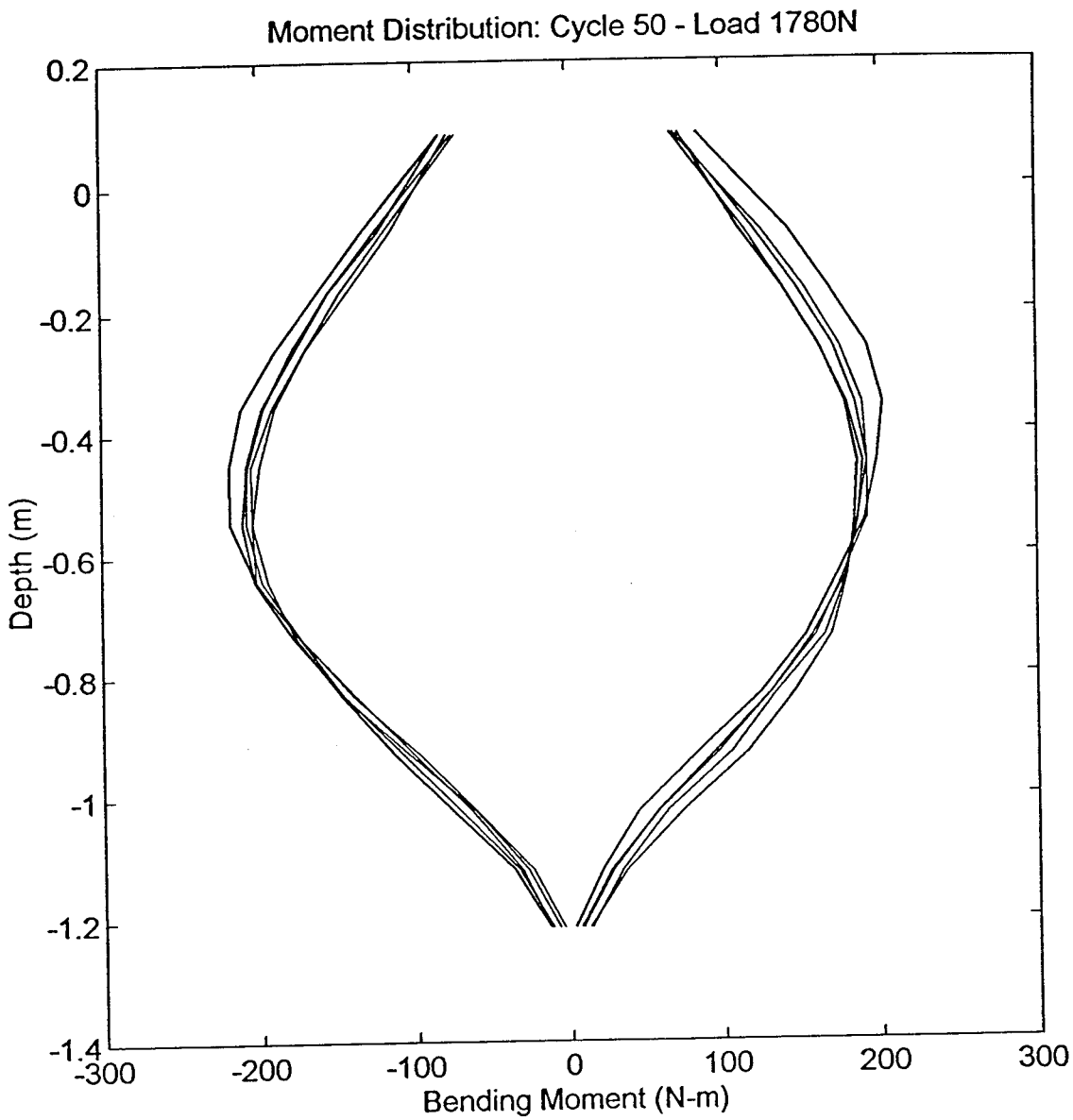
Moment Distribution: Cycle 50 - Load 1780N
0.2
0
-0.2
-0.4
-0.6
-0.8
-1
-1.2
-1.4
Depth (m)
-300
-200
-100
0
100
200
300
Bending Moment (N-m)

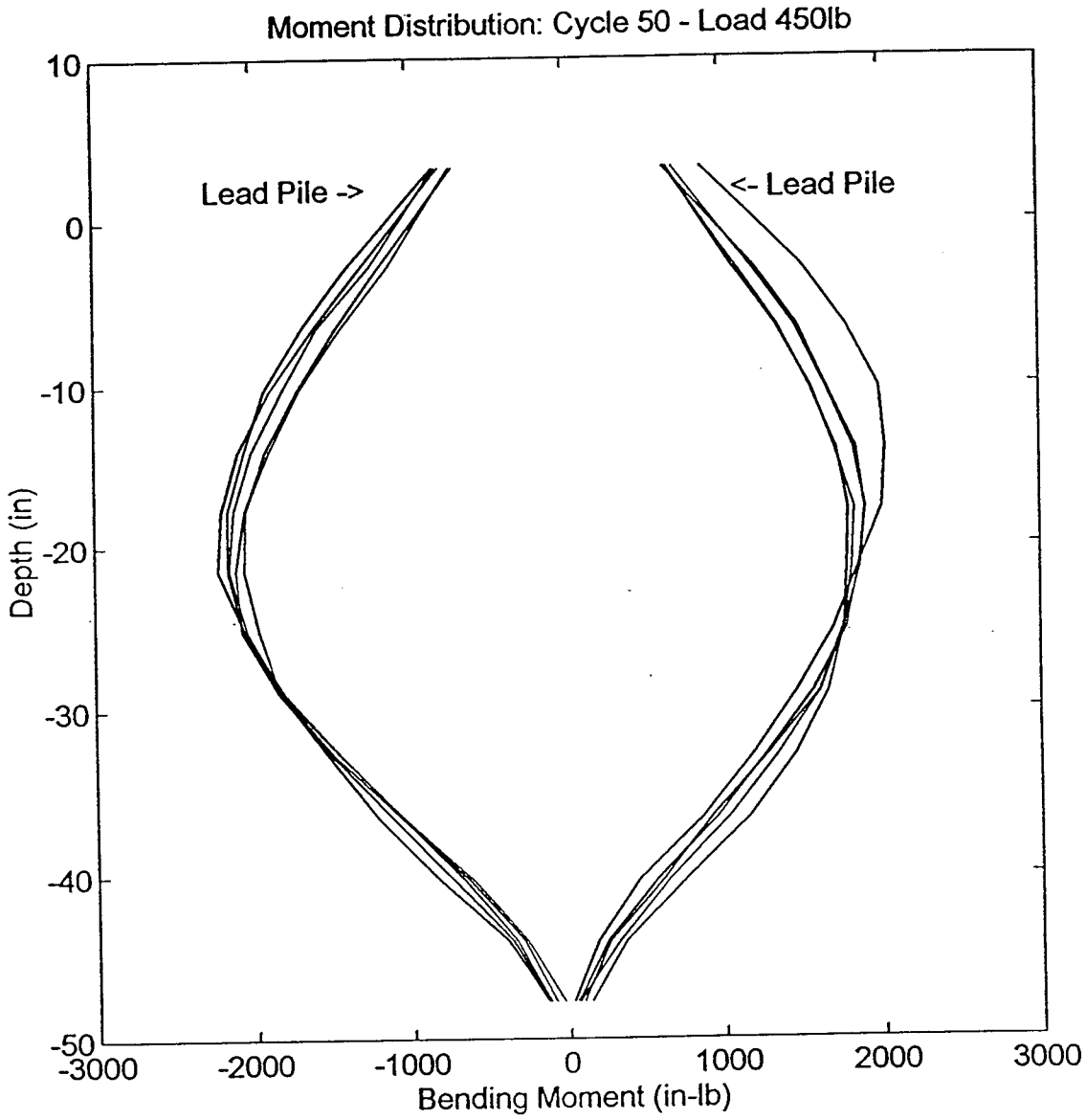
Moment Distribution: Cycle 50 - Load 450lb
Lead Pile ->
<- Lead Pile
Depth (in)
10
0
-10
-20
-30
-40
-50
-3000
-2000
-1000
0
1000
2000
3000
Bending Moment (in-lb)

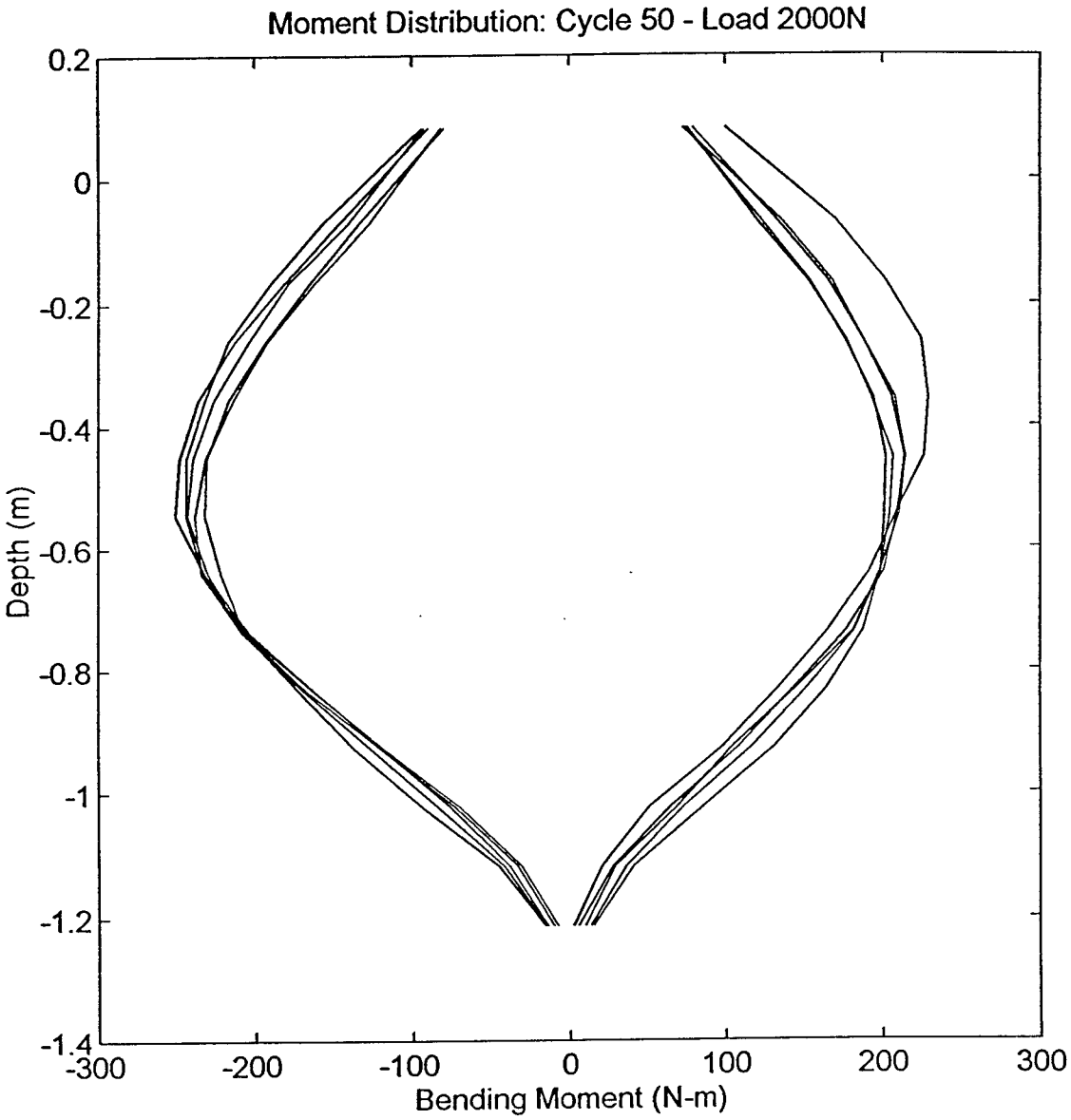
Moment Distribution: Cycle 50 - Load 2000N
0.2
0
-0.2
-0.4
-0.6
-0.8
-1
-1.2
-1.4
Depth (m)
-300
-200
-100
0
100
200
300
Bending Moment (N-m)

Figure B6. Moment distribution for pile 1 (next 14 plots).

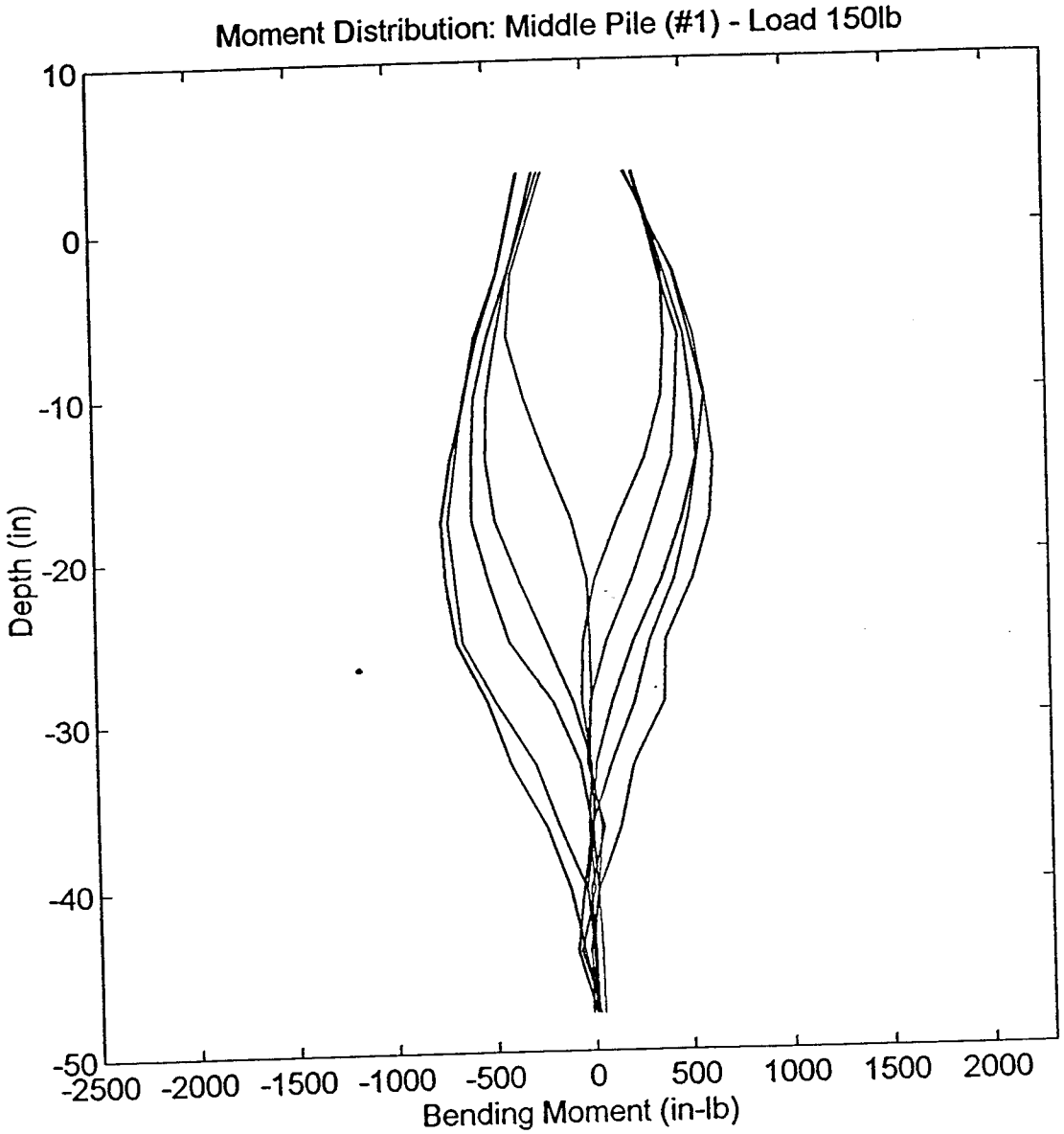
Moment Distribution: Middle Pile (#1) - Load 150lb
10
0
-10
-20
-30
-40
-50
Depth (in)
-2500
-2000
-1500
-1000
-500
0
500
1000
1500
2000
Bending Moment (in-lb)

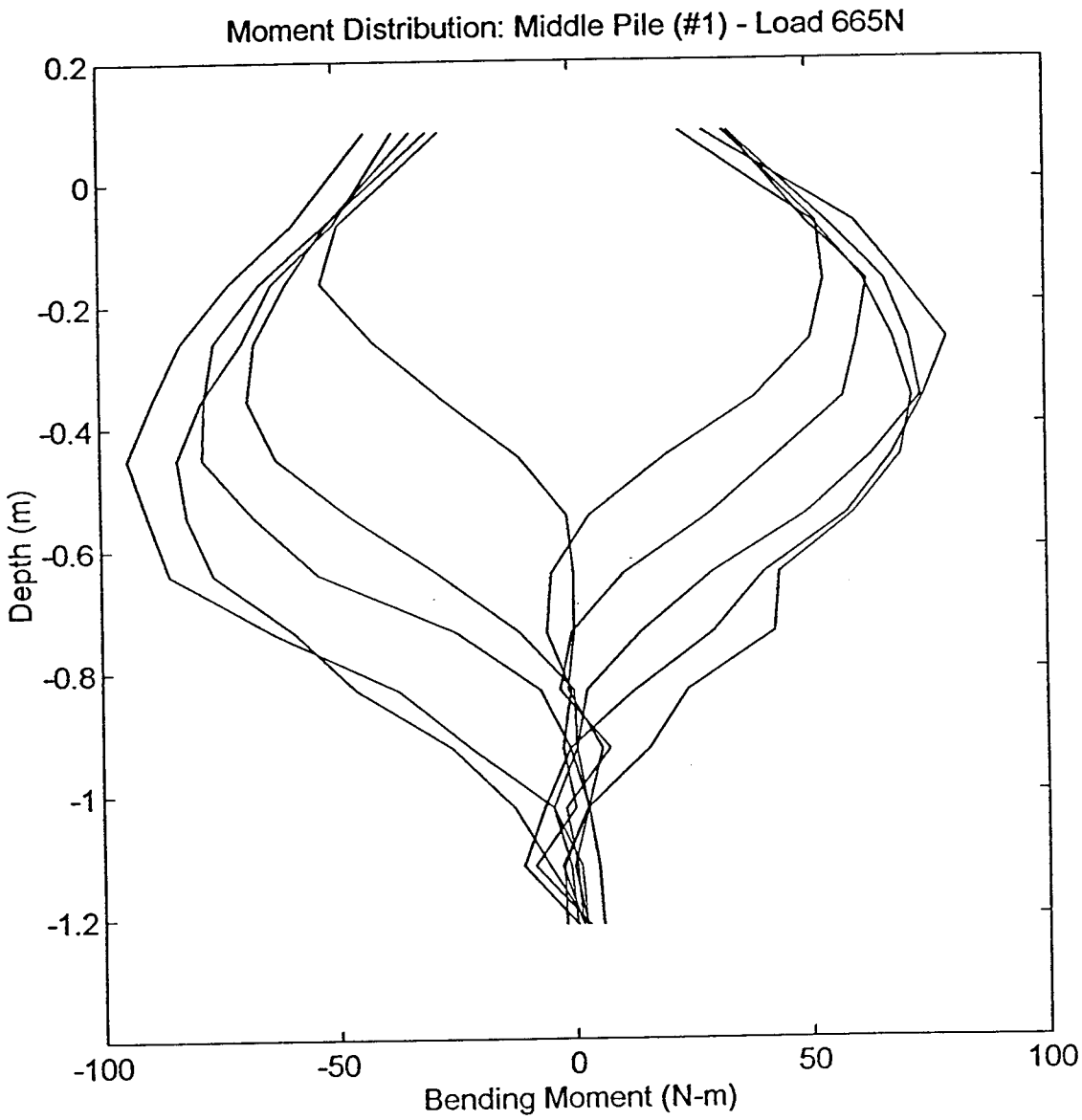
Moment Distribution: Middle Pile (#1) - Load 665N
0.2
0
-0.2
-0.4
-0.6
-0.8
-1
-1.2
Depth (m)
-100
-50
0
50
100
Bending Moment (N-m)

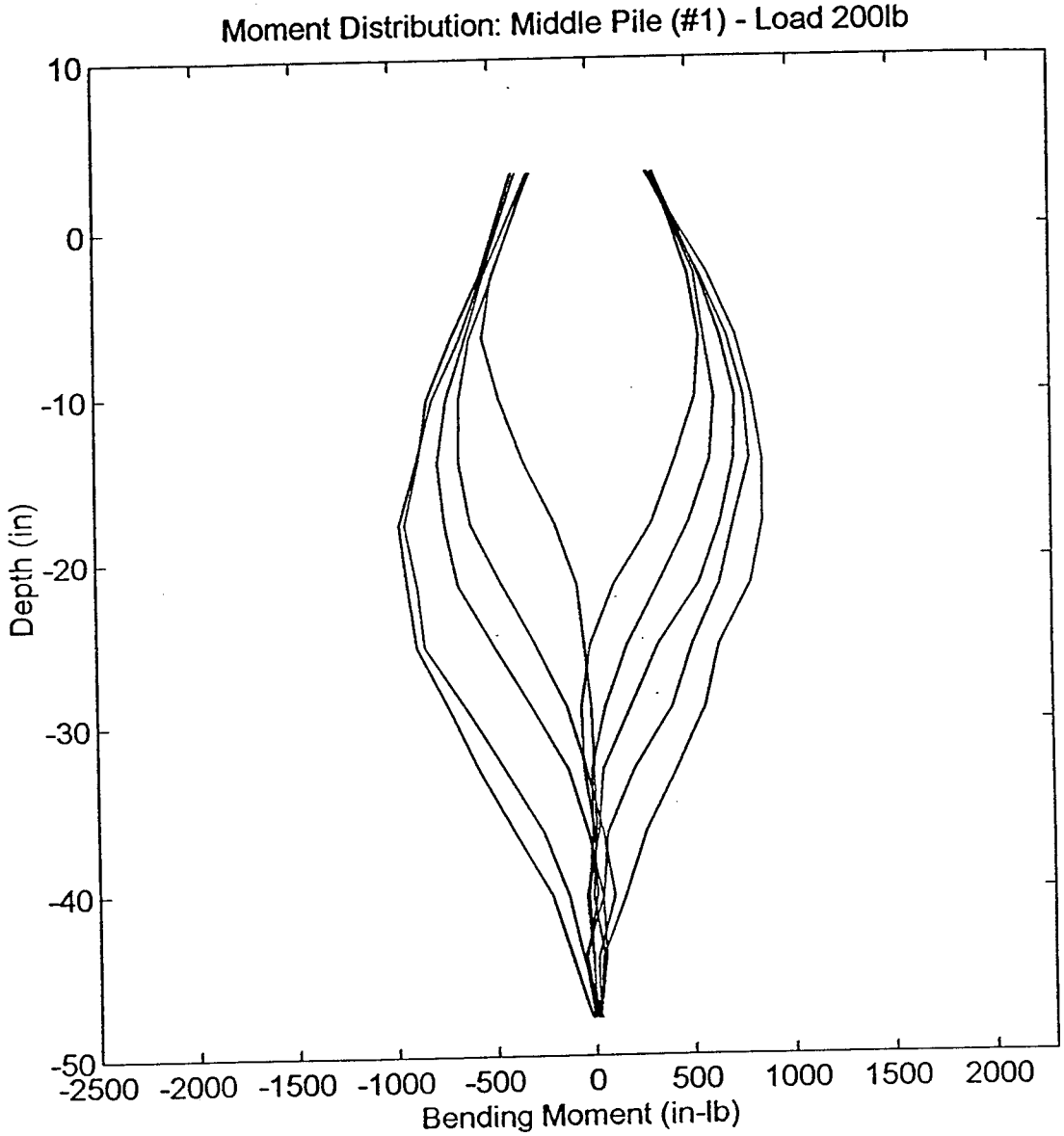
Moment Distribution: Middle Pile (#1) - Load 200lb
10
0
-10
-20
-30
-40
-50
Depth (in)
-2500
-2000
-1500
-1000
-500
0
500
1000
1500
2000
Bending Moment (in-lb)

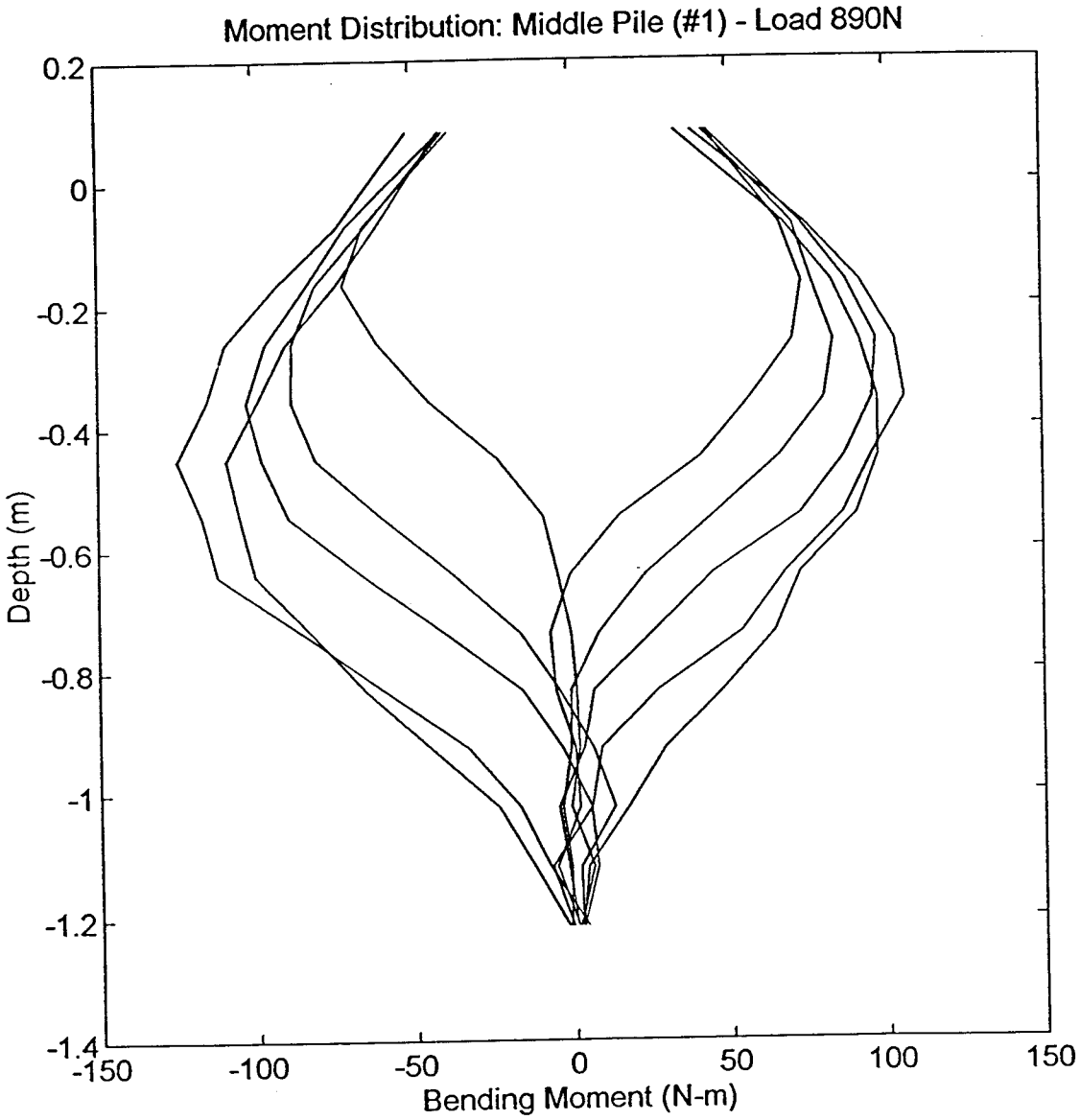
Moment Distribution: Middle Pile (#1) - Load 890N
0.2
0
-0.2
-0.4
-0.6
-0.8
-1
-1.2
-1.4
Depth (m)
-150
-100
-50
0
50
100
150
Bending Moment (N-m)

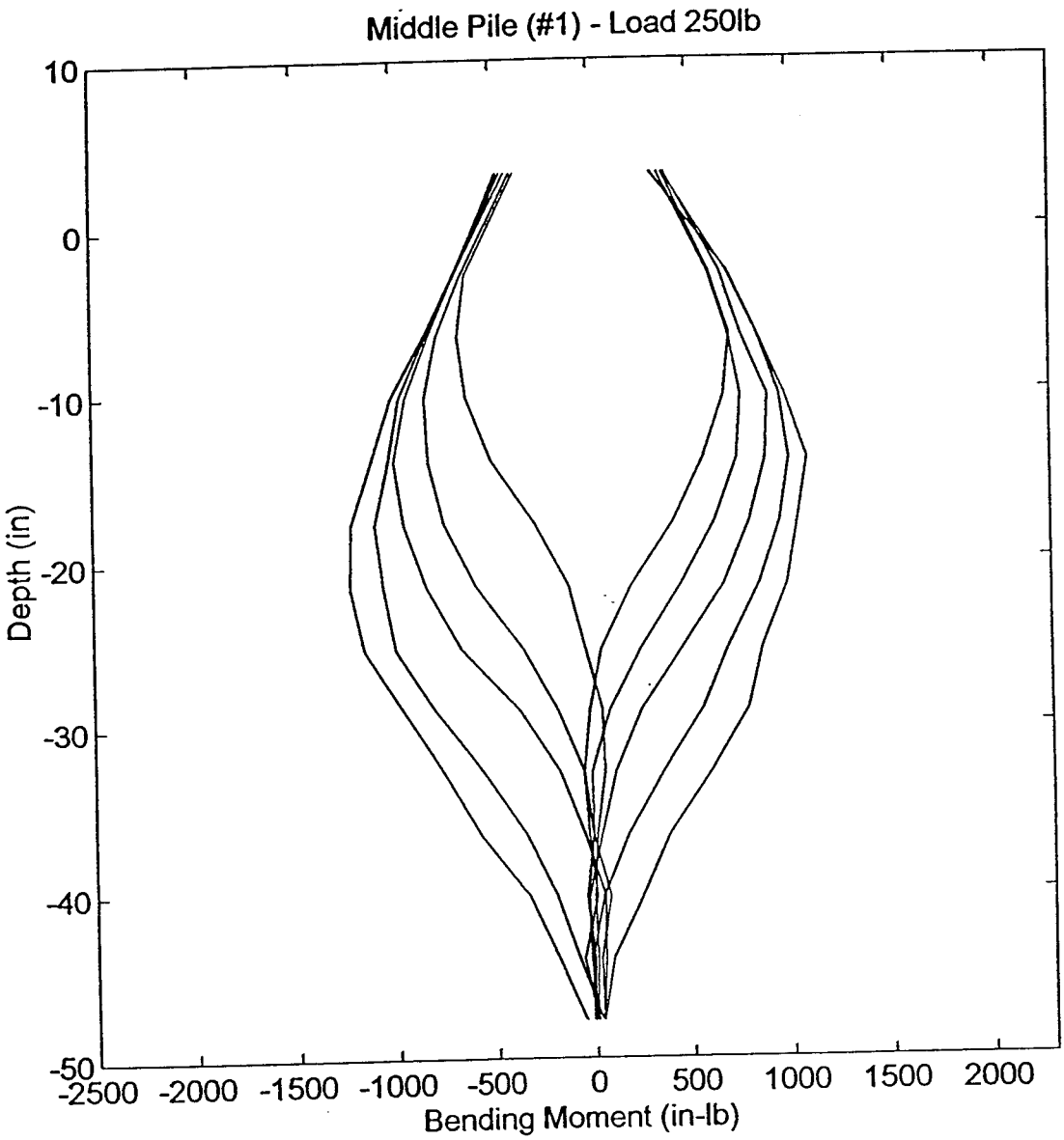
Middle Pile (#1) - Load 250lb
10
0
-10
-20
-30
-40
-50
Depth (in)
-2500
-2000
-1500
-1000
-500
0
500
1000
1500
2000
Bending Moment (in-lb)

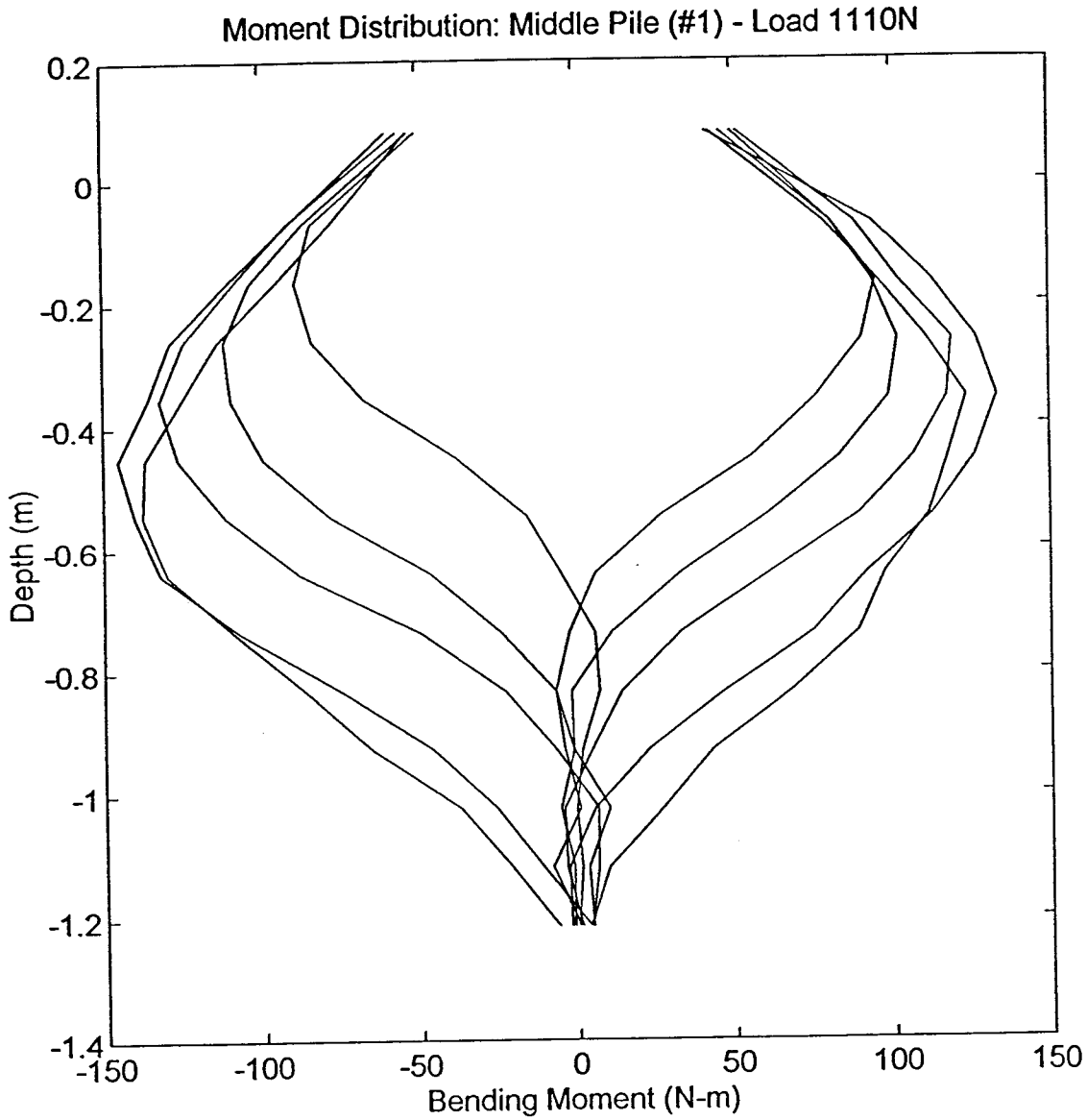
Moment Distribution: Middle Pile (#1) - Load 1110N
0.2
0
-0.2
-0.4
-0.6
-0.8
-1
-1.2
-1.4
Depth (m)
-150
-100
-50
0
50
100
150
Bending Moment (N-m)

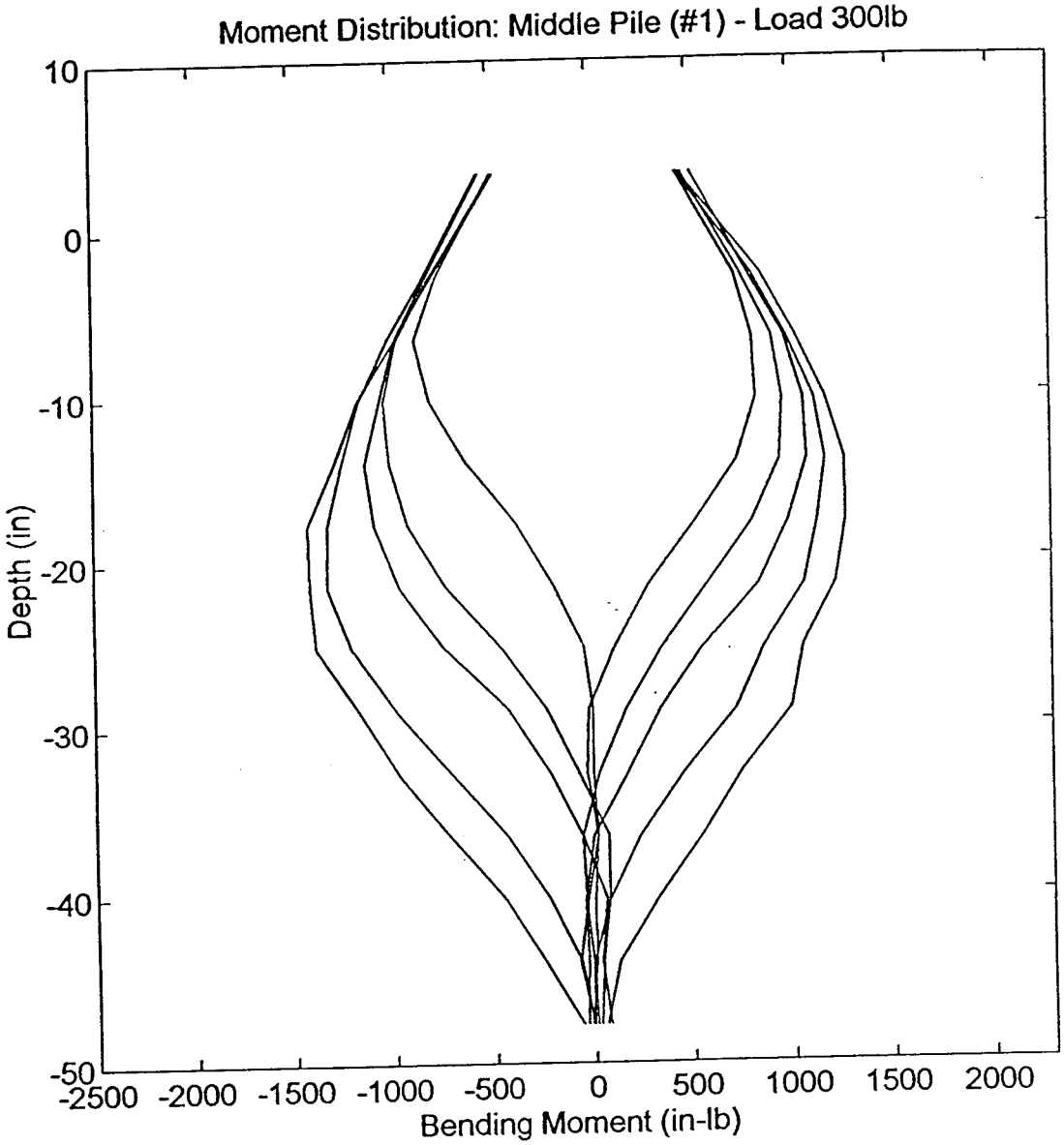
Moment Distribution: Middle Pile (#1) - Load 300lb
10
0
-10
-20
-30
-40
-50
Depth (in)
-2500
-2000
-1500
-1000
-500
0
500
1000
1500
2000
Bending Moment (in-lb)

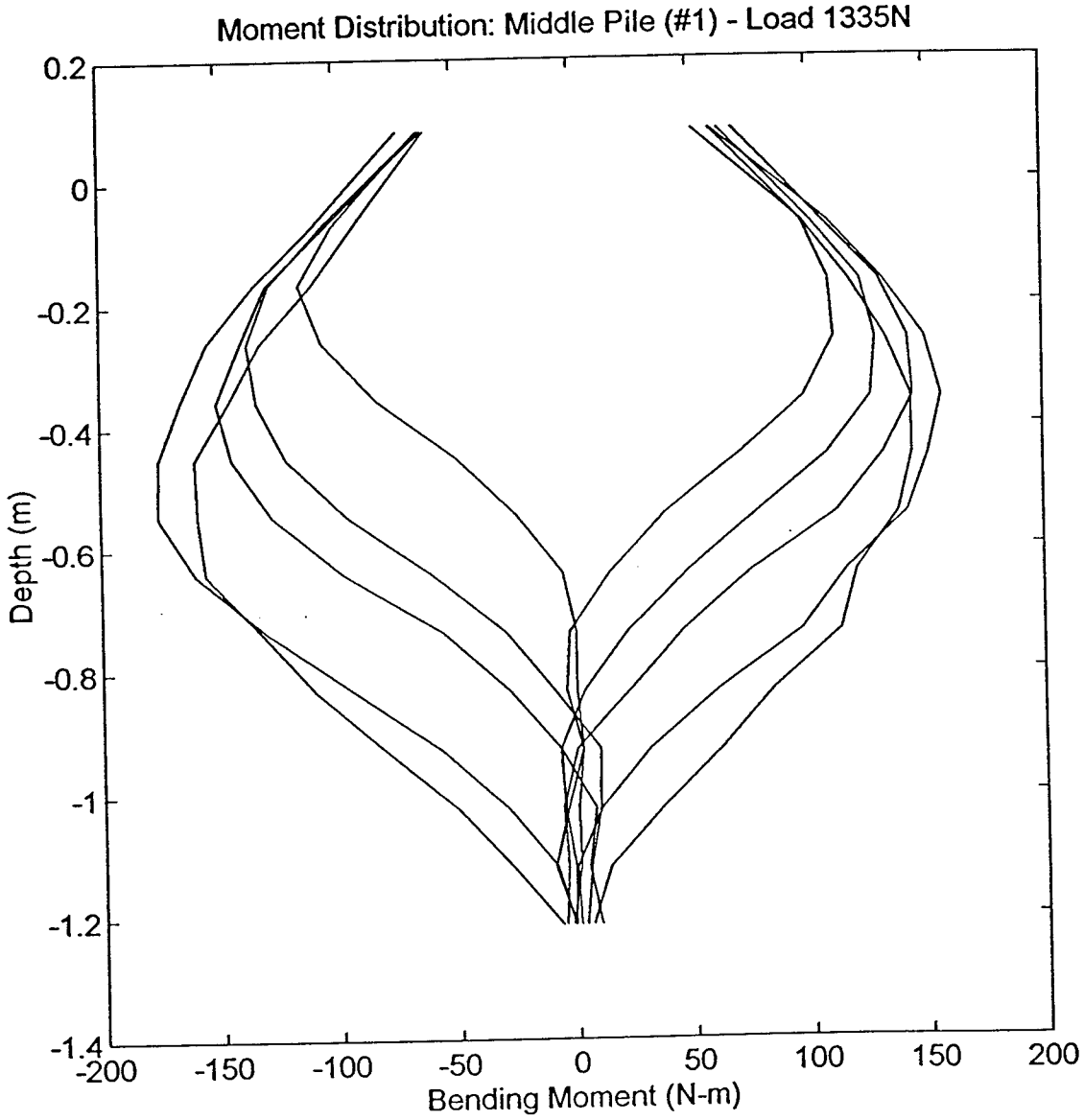
Moment Distribution: Middle Pile (#1) - Load 1335N
0.2
0
-0.2
-0.4
-0.6
-0.8
-1
-1.2
-1.4
Depth (m)
-200
-150
-100
-50
0
50
100
150
200
Bending Moment (N-m)

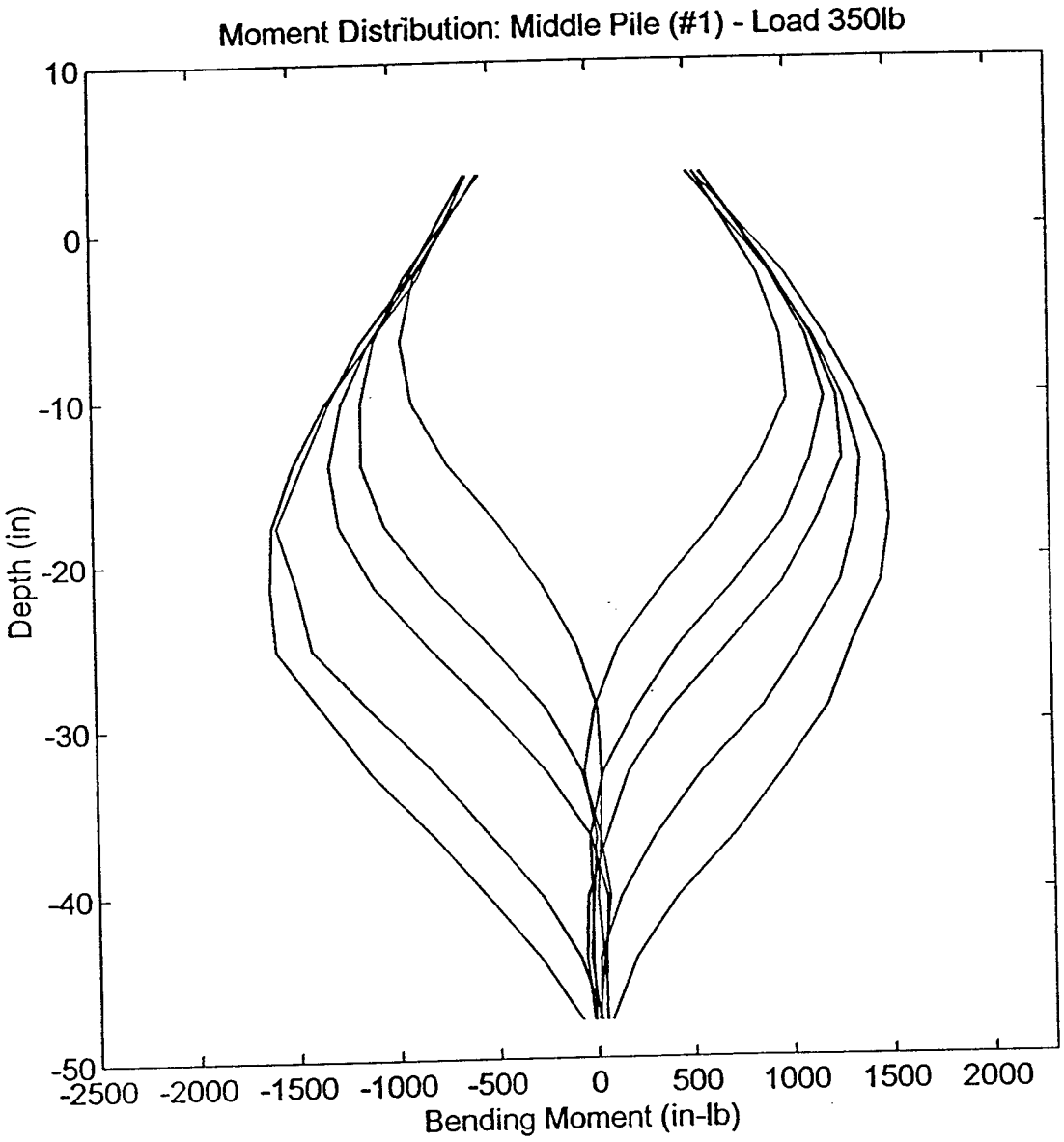
Moment Distribution: Middle Pile (#1) - Load 350lb
10
0
-10
-20
-30
-40
-50
Depth (in)
-2500
-2000
-1500
-1000
-500
0
500
1000
1500
2000
Bending Moment (in-lb)

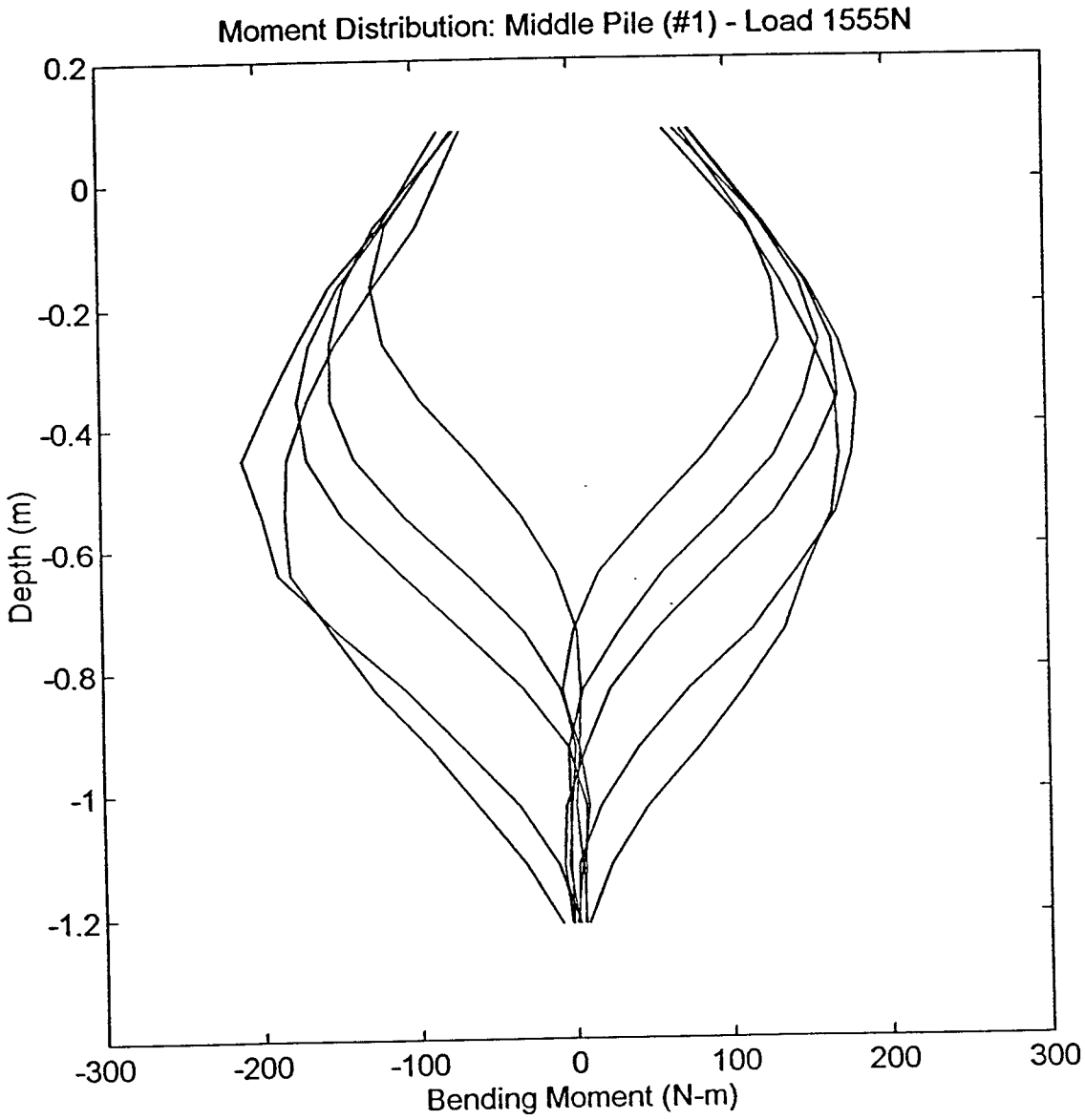
Moment Distribution: Middle Pile (#1) - Load 1555N
0.2
0
-0.2
-0.4
-0.6
-0.8
-1
-1.2
Depth (m)
-300
-200
-100
0
100
200
300
Bending Moment (N-m)

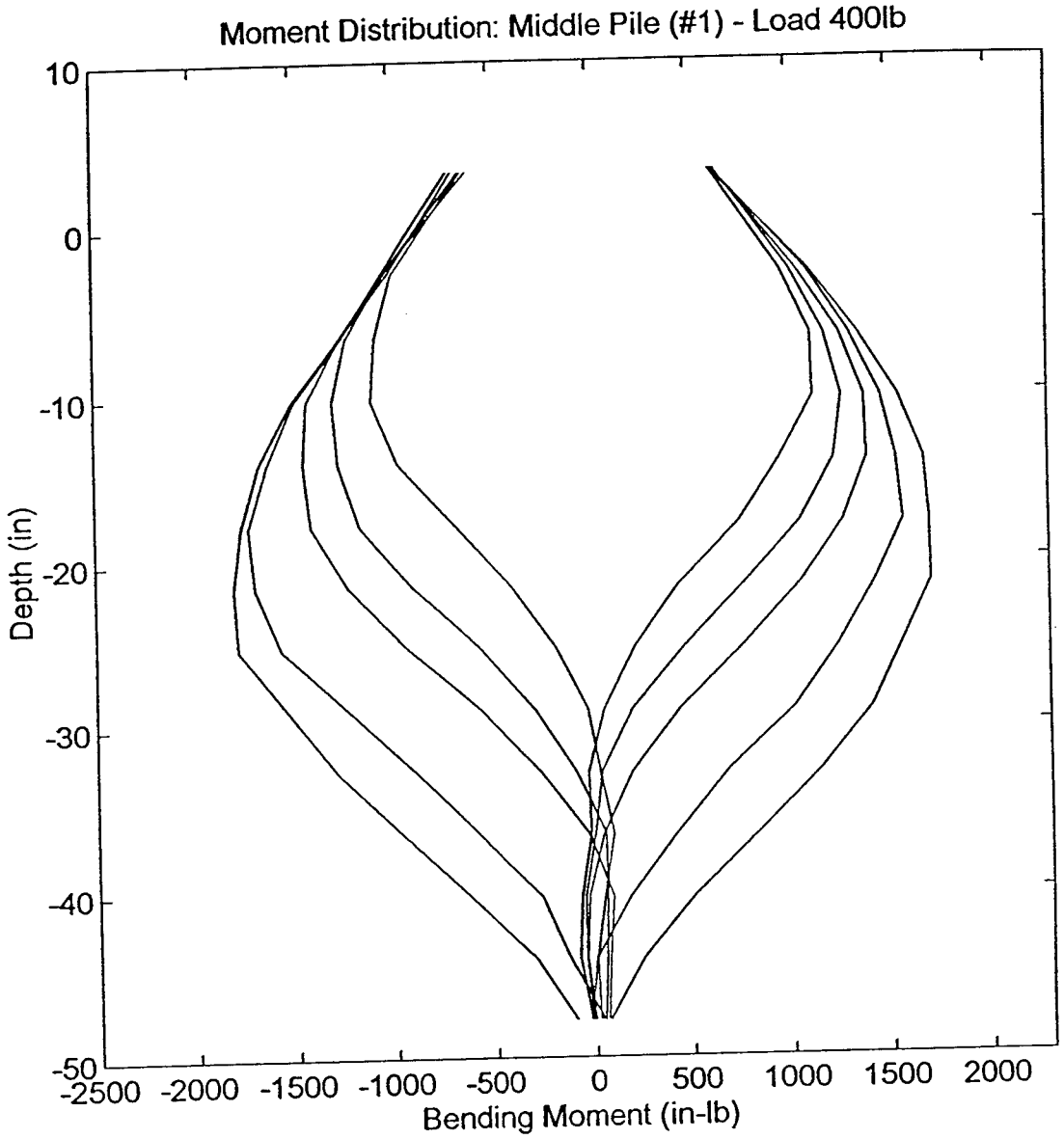
Moment Distribution: Middle Pile (#1) - Load 400lb
10
0
-10
-20
-30
-40
-50
Depth (in)
-2500
-2000
-1500
-1000
-500
0
500
1000
1500
2000
Bending Moment (in-lb)

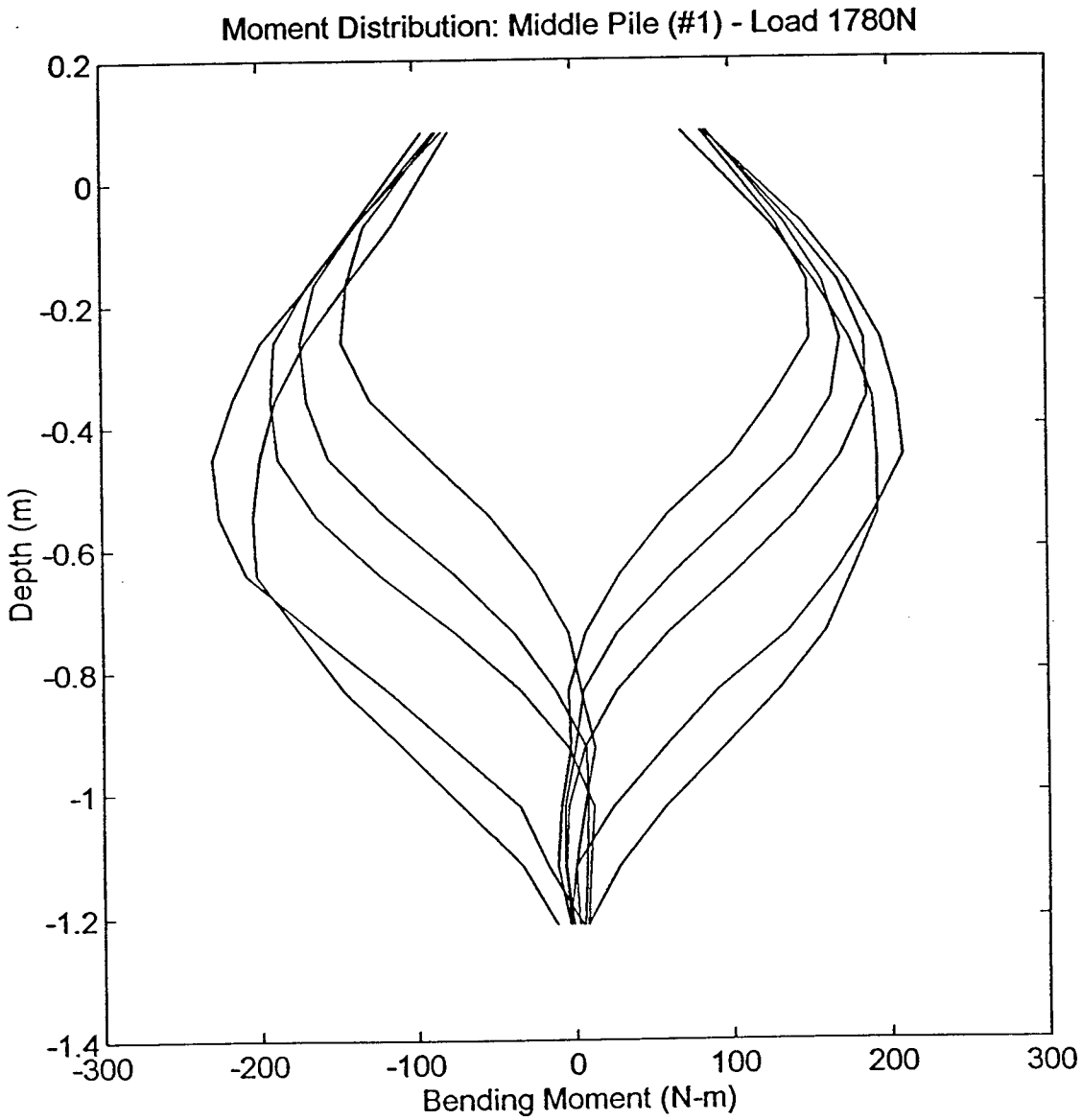
Moment Distribution: Middle Pile (#1) - Load 1780N
0.2
0
-0.2
-0.4
-0.6
-0.8
-1
-1.2
-1.4
Depth (m)
-300
-200
-100
0
100
200
300
Bending Moment (N-m)

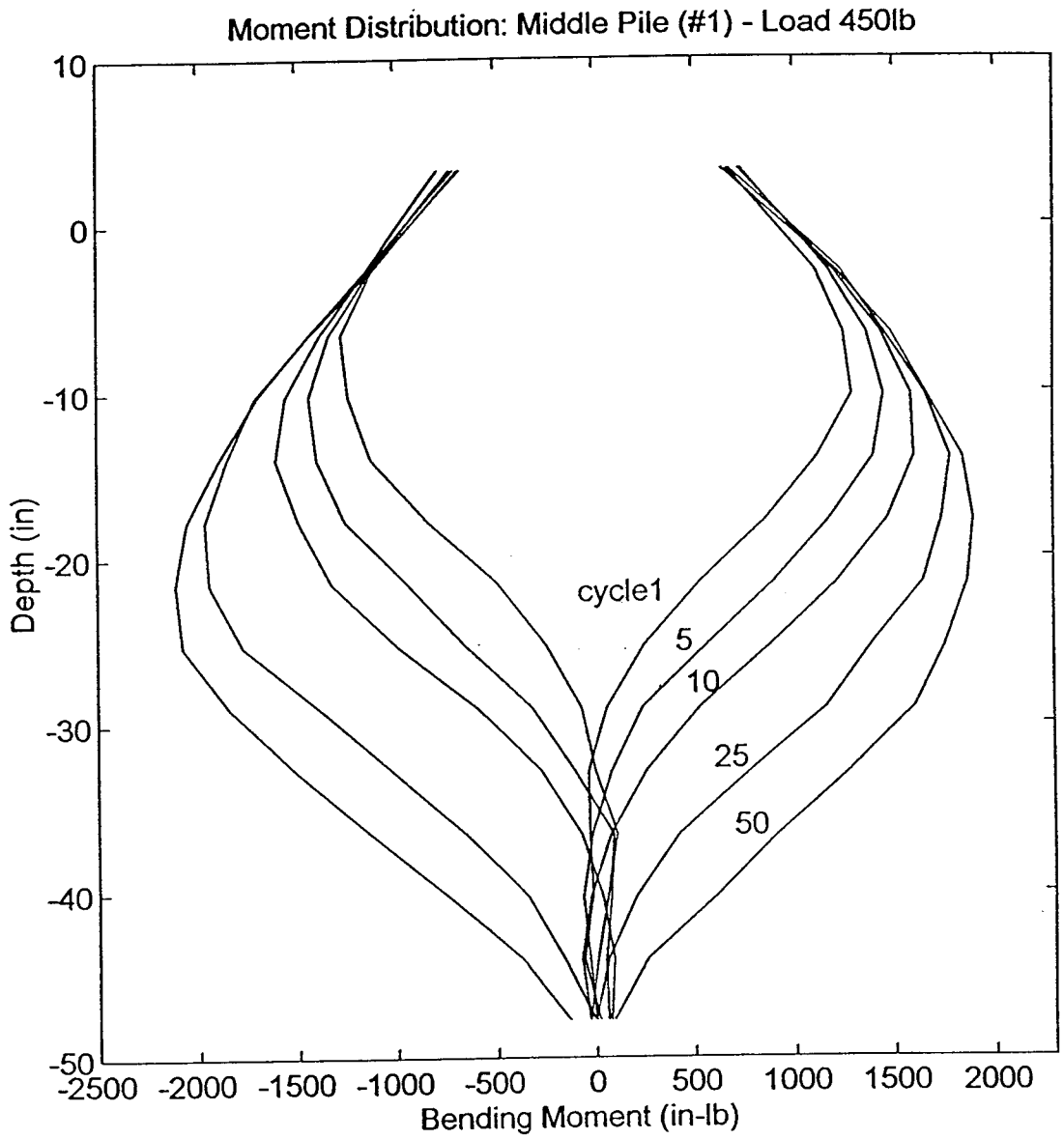
Moment Distribution: Middle Pile (#1) - Load 450lb
10
0
-10
-20
-30
-40
-50
Depth (in)
cycle1
5
10
25
50
-2500
-2000
-1500
-1000
-500
0
500
1000
1500
2000
Bending Moment (in-lb)

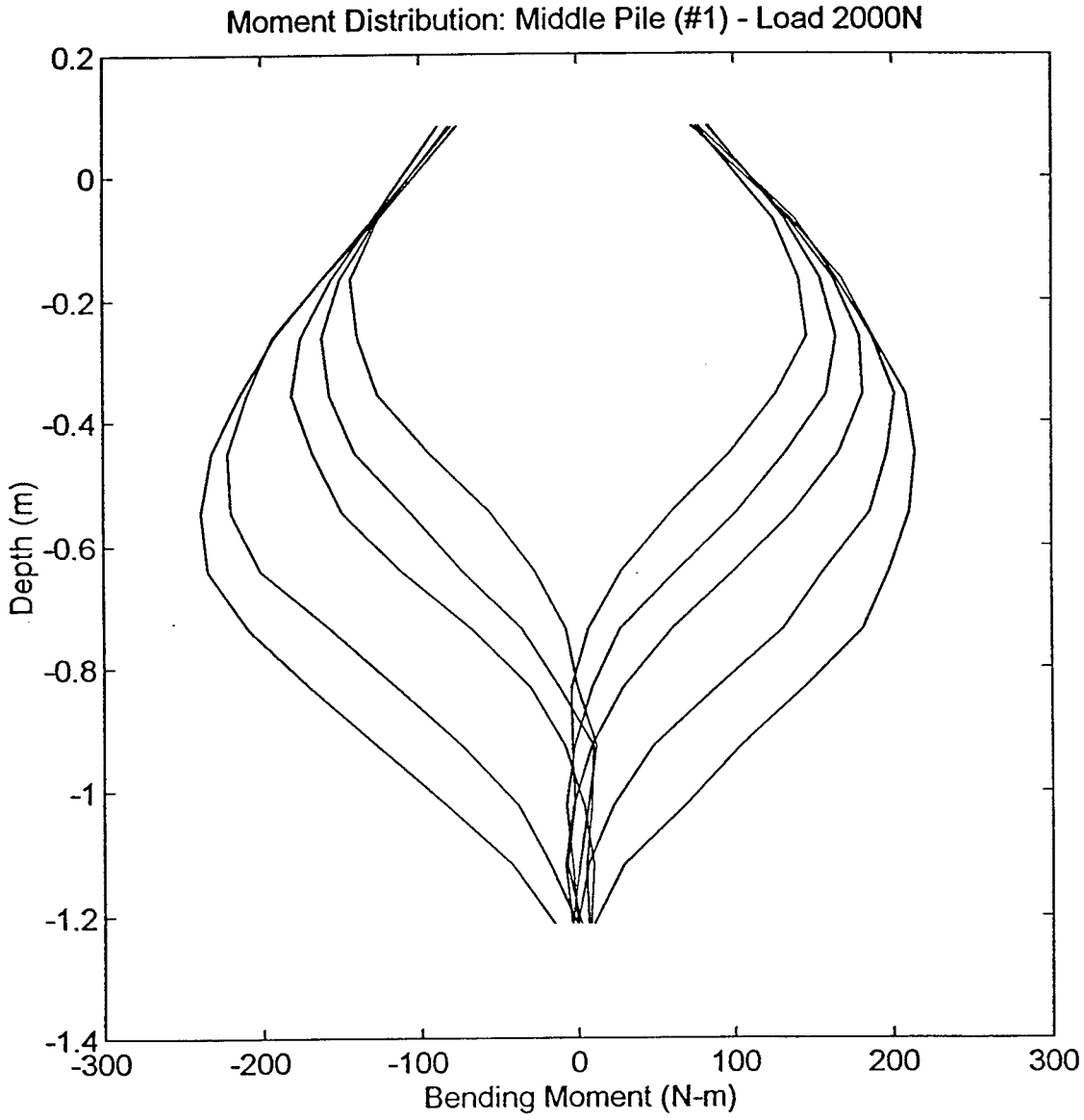
Moment Distribution: Middle Pile (#1) - Load 2000N
0.2
0
-0.2
-0.4
-0.6
-0.8
-1
-1.2
-1.4
Depth (m)
-300
-200
-100
0
100
200
300
Bending Moment (N-m)

Figure B7. Moment distribution for pile 2 (next 14 plots).

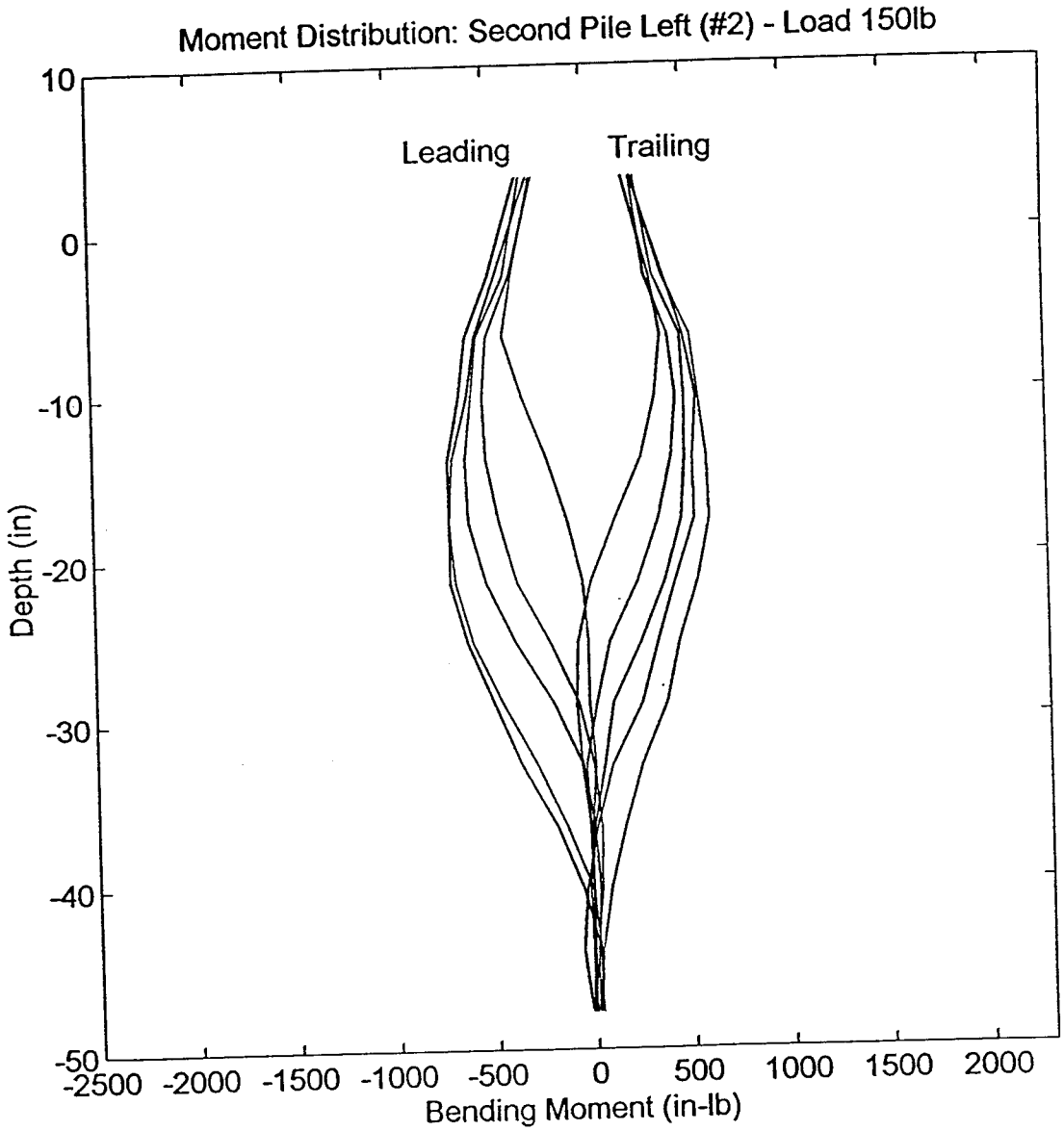
Moment Distribution: Second Pile Left (#2) - Load 150lb
Leading
Trailing
Depth (in)
10
0
-10
-20
-30
-40
-50
-2500
-2000
-1500
-1000
-500
0
500
1000
1500
2000
Bending Moment (in-lb)

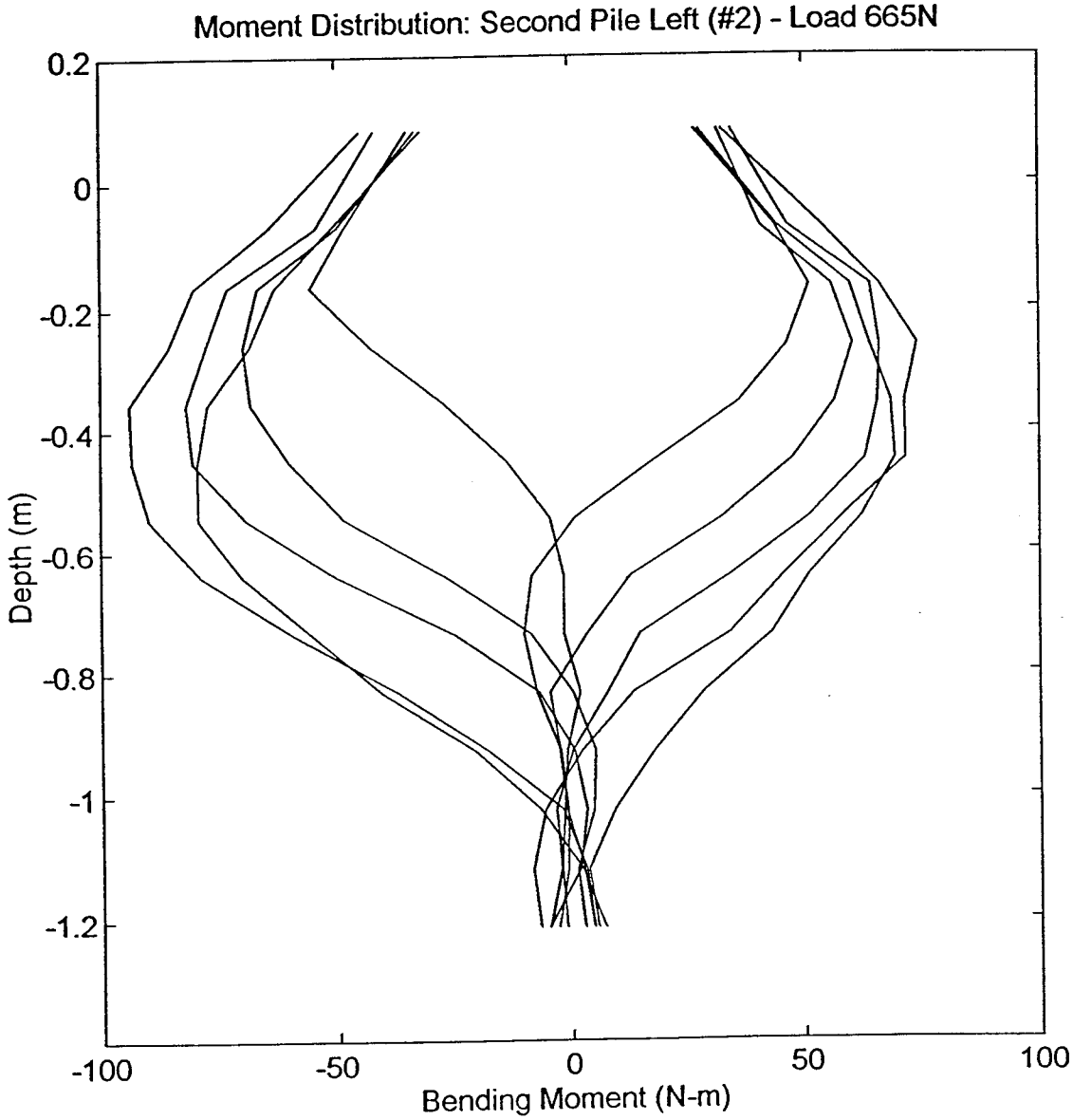
Moment Distribution: Second Pile Left (#2) - Load 665N
0.2
0
-0.2
-0.4
-0.6
-0.8
-1
-1.2
Depth (m)
-100
-50
0
50
100
Bending Moment (N-m)

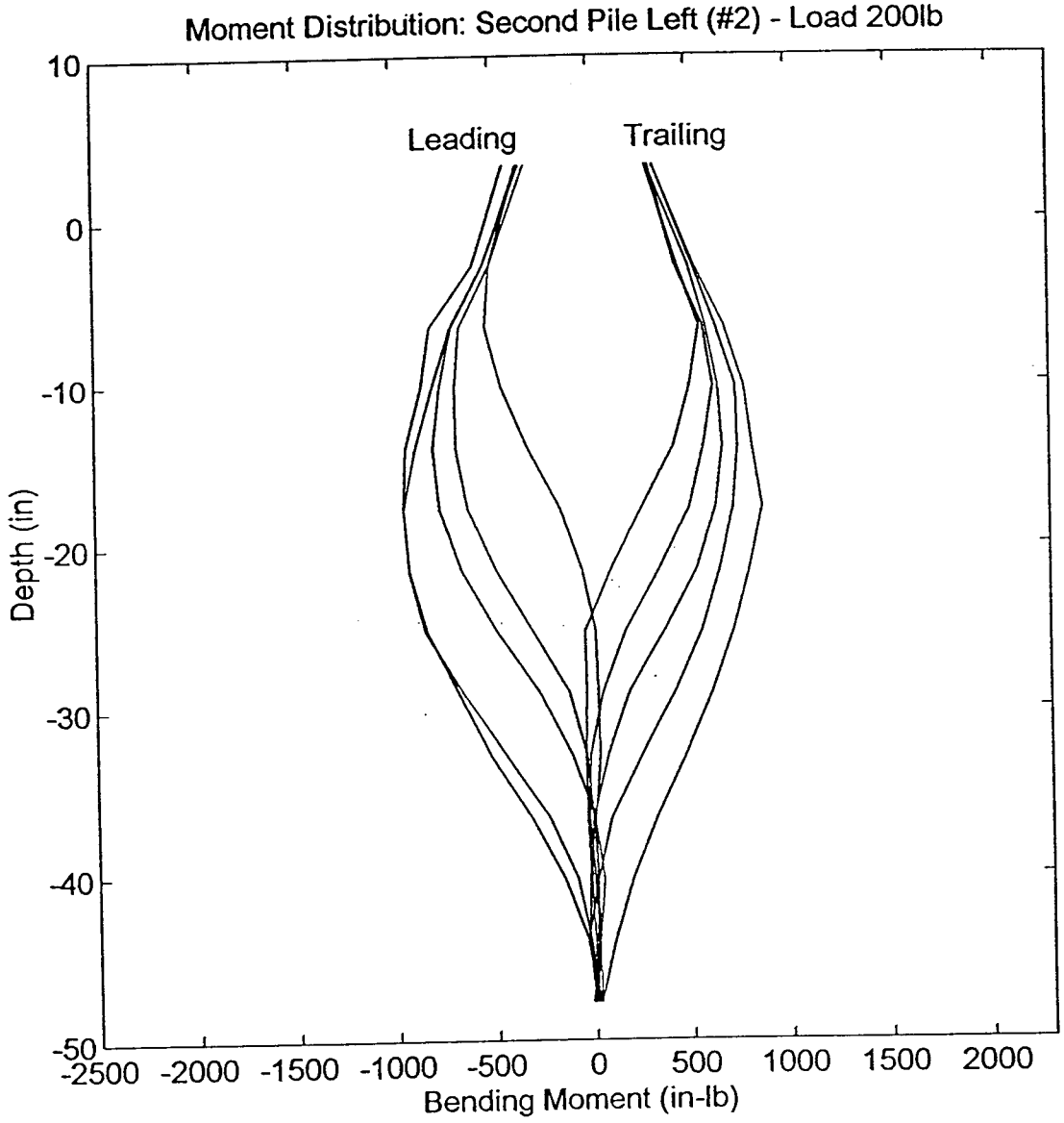
Moment Distribution: Second Pile Left (#2) - Load 200lb
Leading
Trailing
Depth (in)
10
0
-10
-20
-30
-40
-50
-2500
-2000
-1500
-1000
-500
0
500
1000
1500
2000
Bending Moment (in-lb)

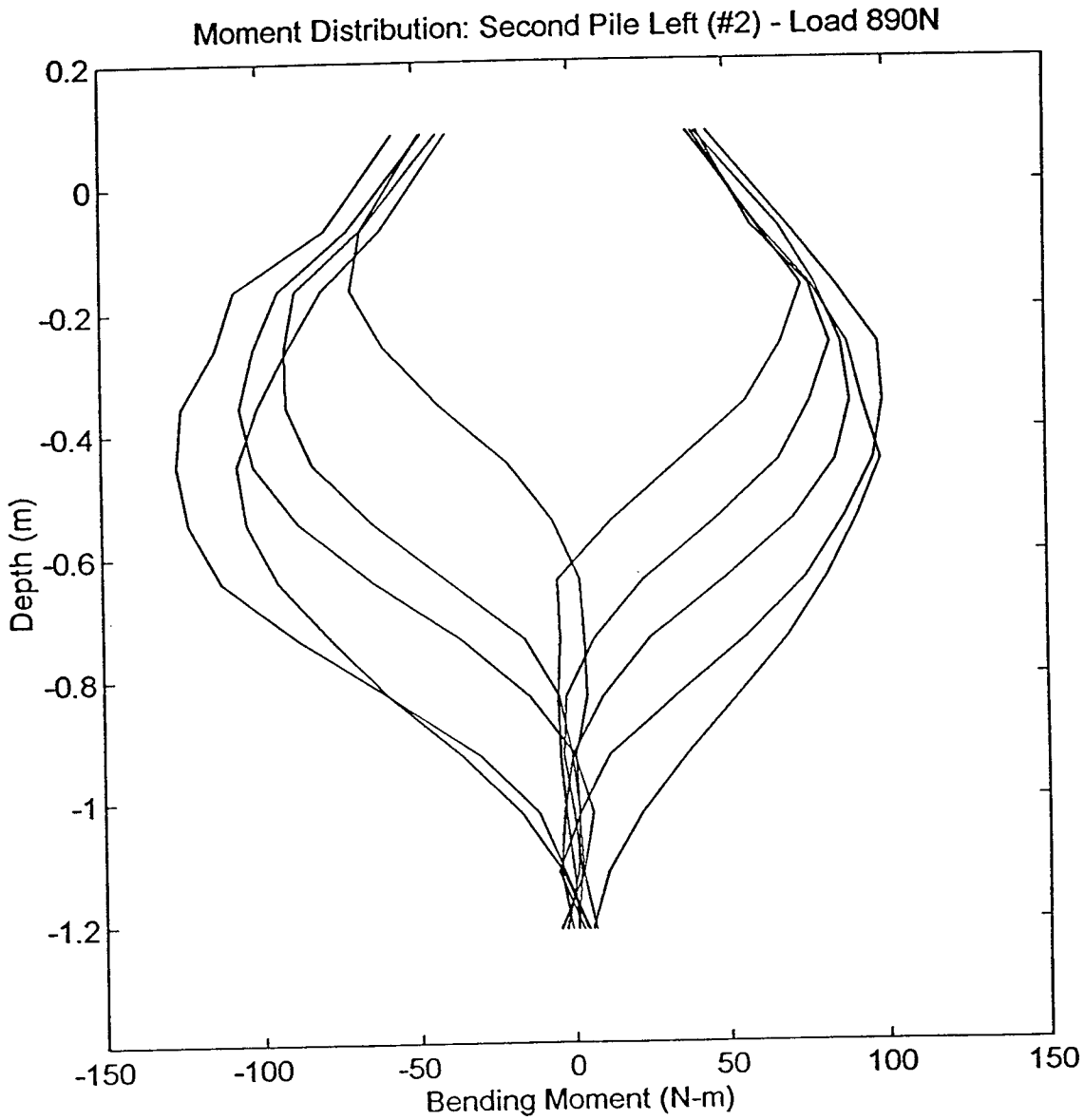
Moment Distribution: Second Pile Left (#2) - Load 890N
0.2
0
-0.2
-0.4
-0.6
-0.8
-1
-1.2
Depth (m)
-150
-100
-50
0
50
100
150
Bending Moment (N-m)

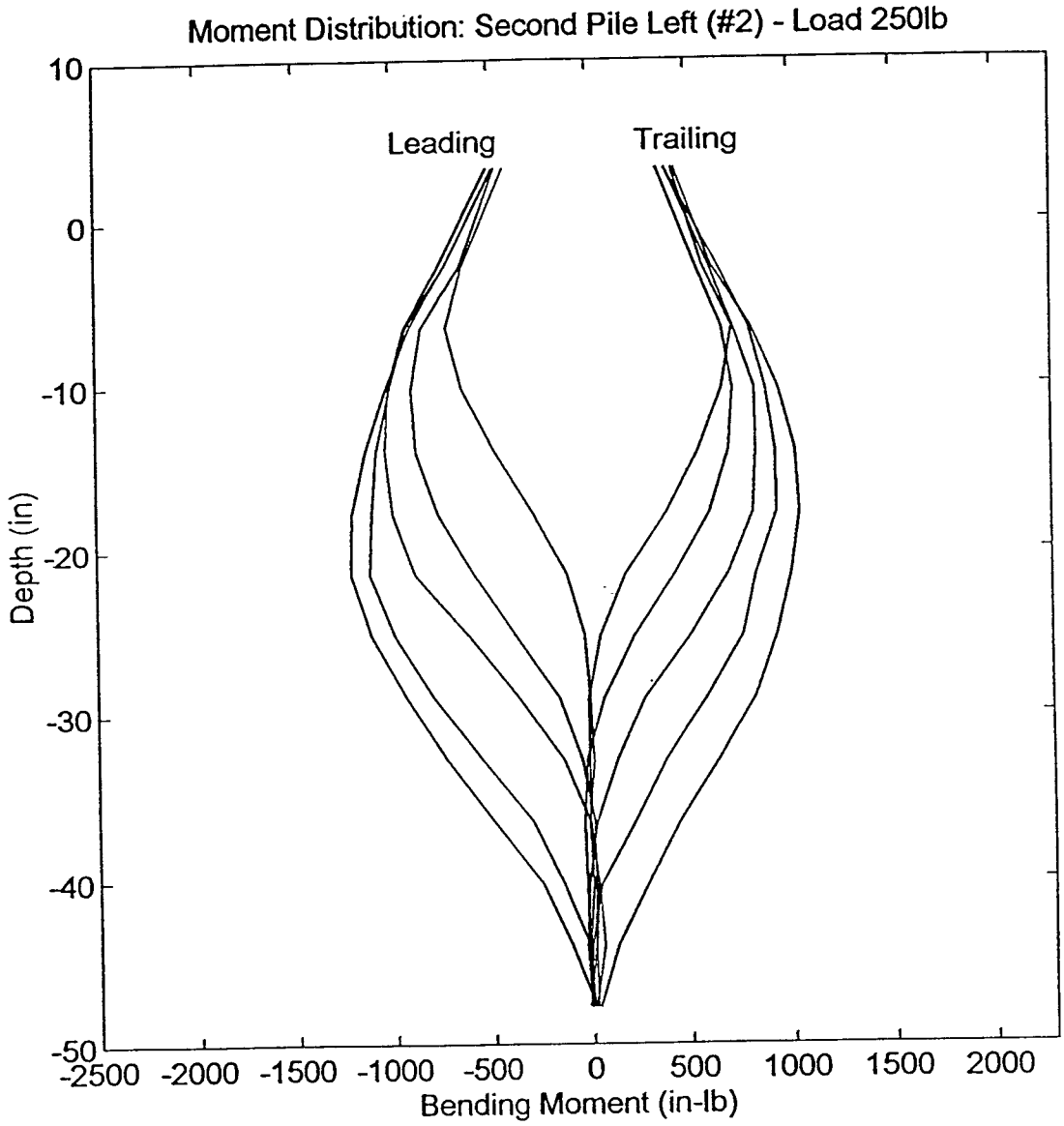
Moment Distribution: Second Pile Left (#2) - Load 250lb
Leading
Trailing
Depth (in)
10
0
-10
-20
-30
-40
-50
-2500
-2000
-1500
-1000
-500
0
500
1000
1500
2000
Bending Moment (in-lb)

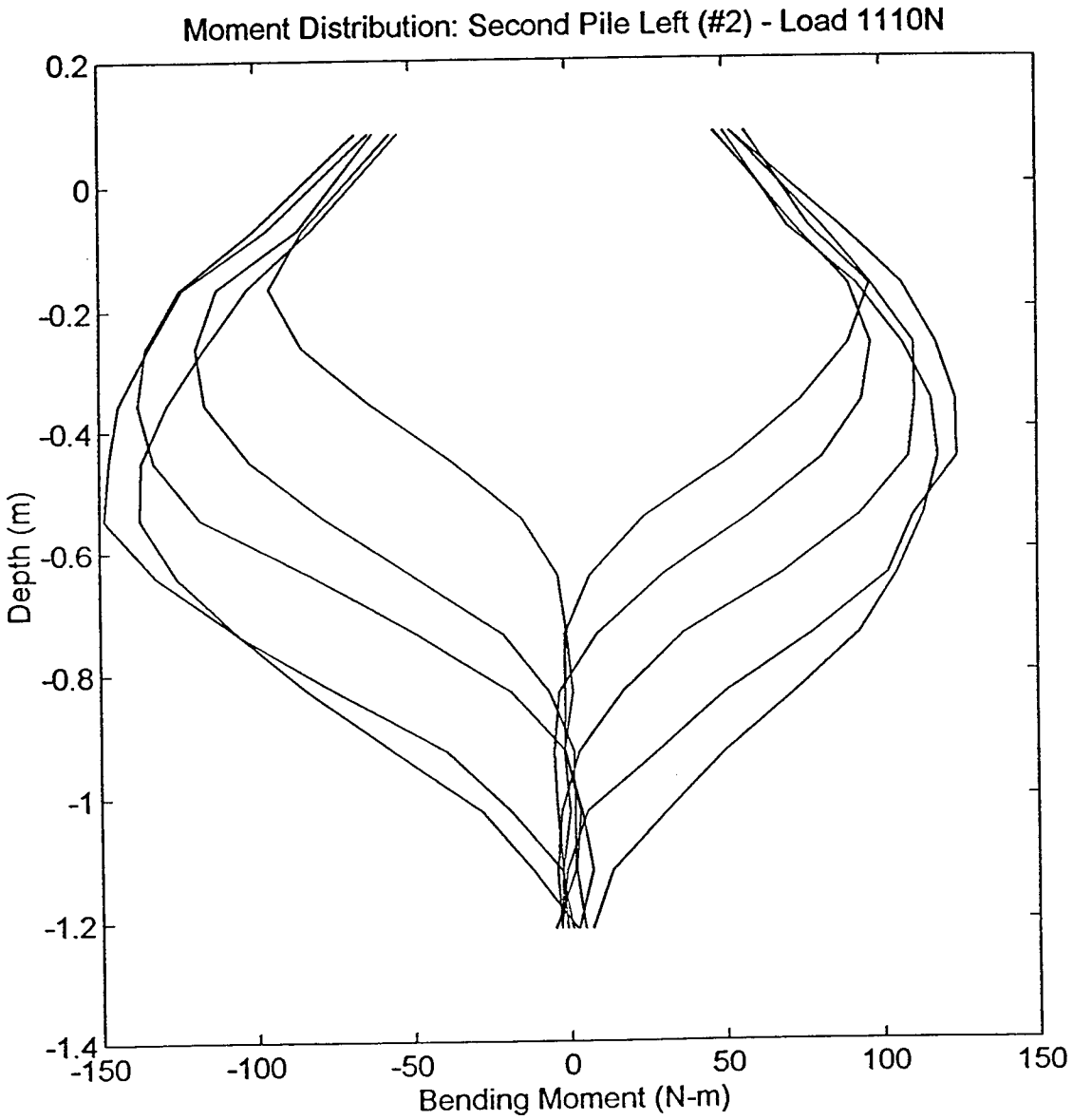
Moment Distribution: Second Pile Left (#2) - Load 1110N
0.2
0
-0.2
-0.4
-0.6
-0.8
-1
-1.2
-1.4
Depth (m)
-150
-100
-50
0
50
100
150
Bending Moment (N-m)

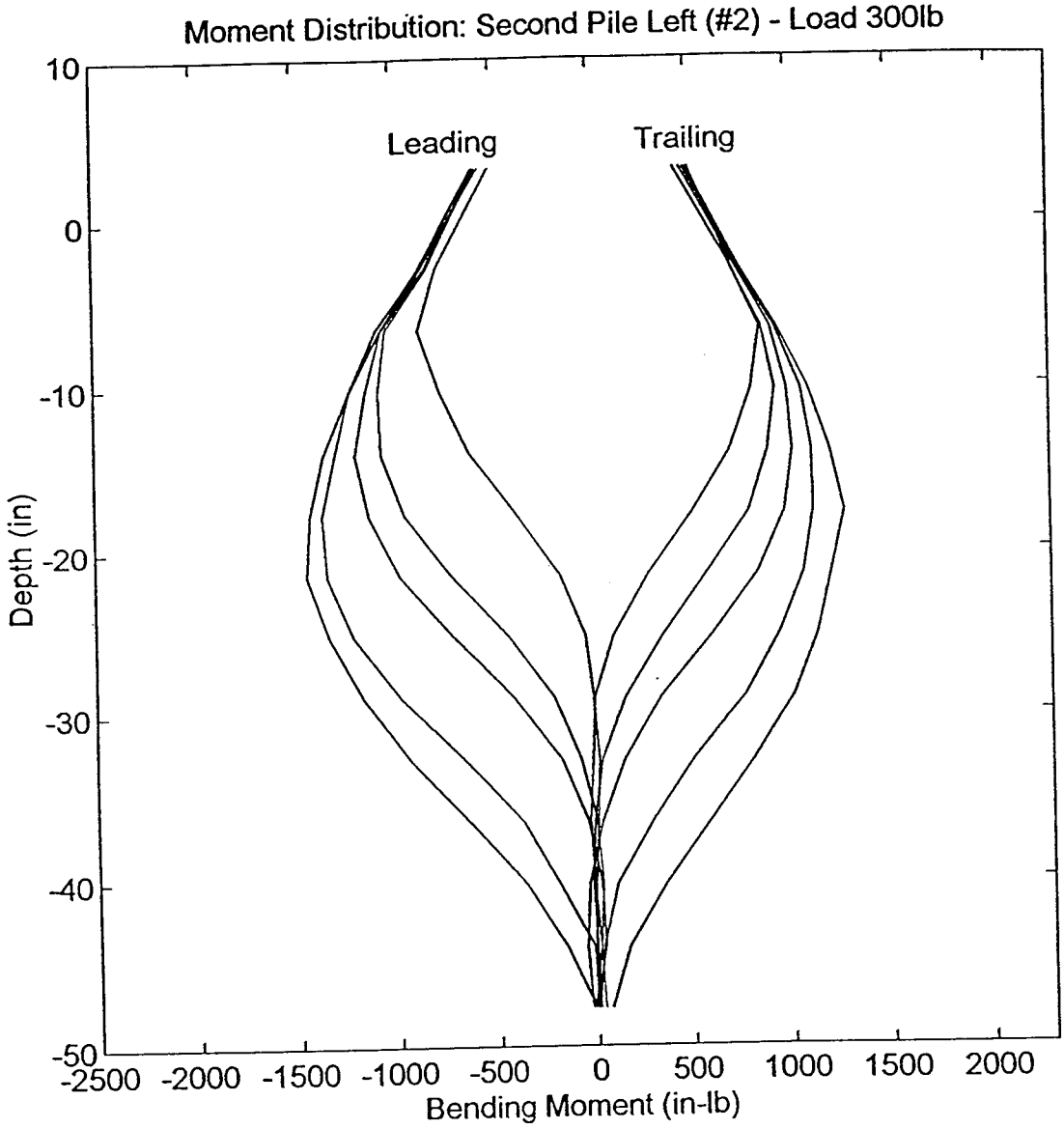
Moment Distribution: Second Pile Left (#2) - Load 300lb
Leading
Trailing
10
0
-10
-20
-30
-40
-50
Depth (in)
-2500
-2000
-1500
-1000
-500
0
500
1000
1500
2000
Bending Moment (in-lb)

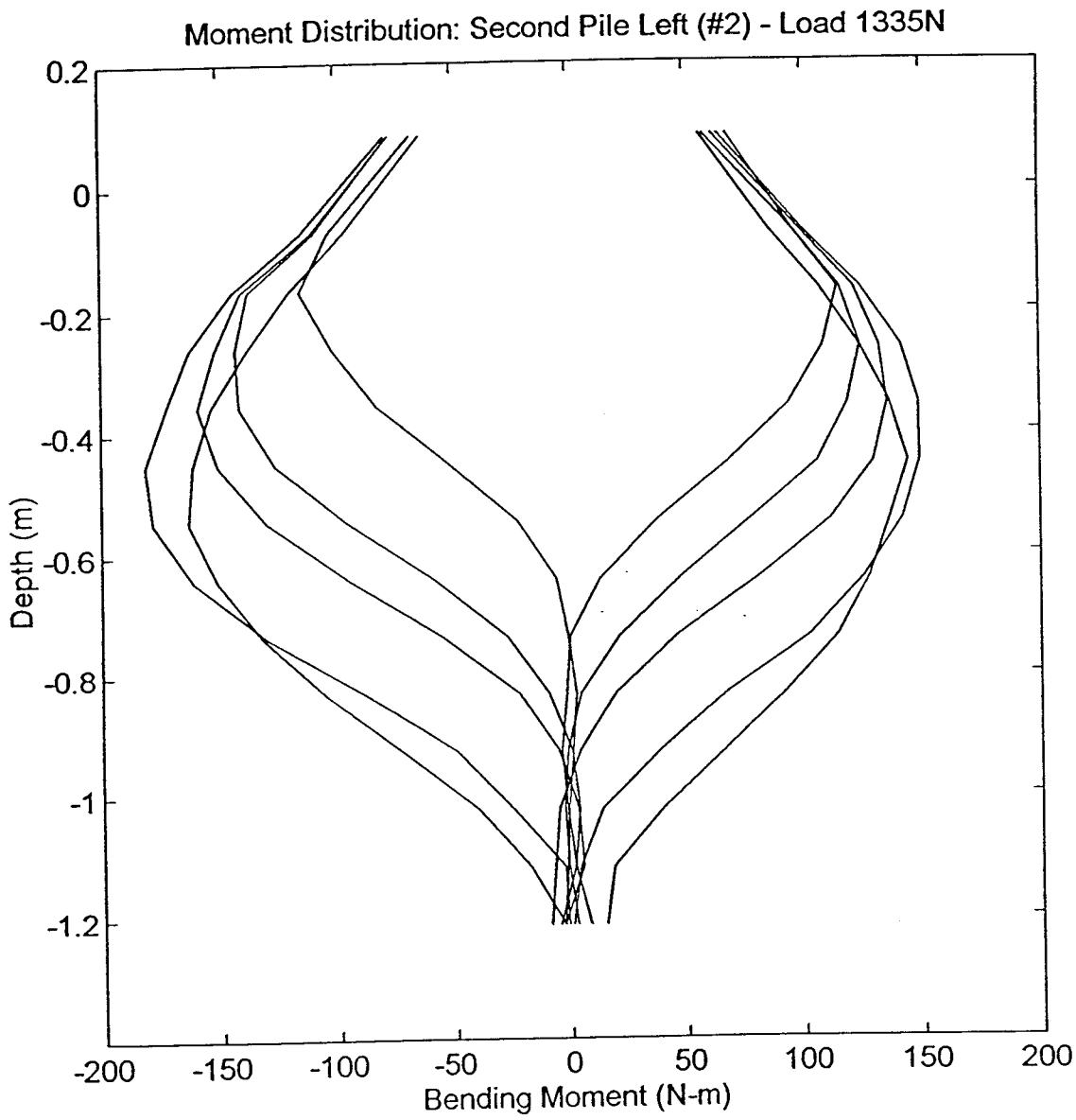
Moment Distribution: Second Pile Left (#2) - Load 1335N
0.2
0
-0.2
-0.4
-0.6
-0.8
-1
-1.2
Depth (m)
-200
-150
-100
-50
0
50
100
150
200
Bending Moment (N-m)

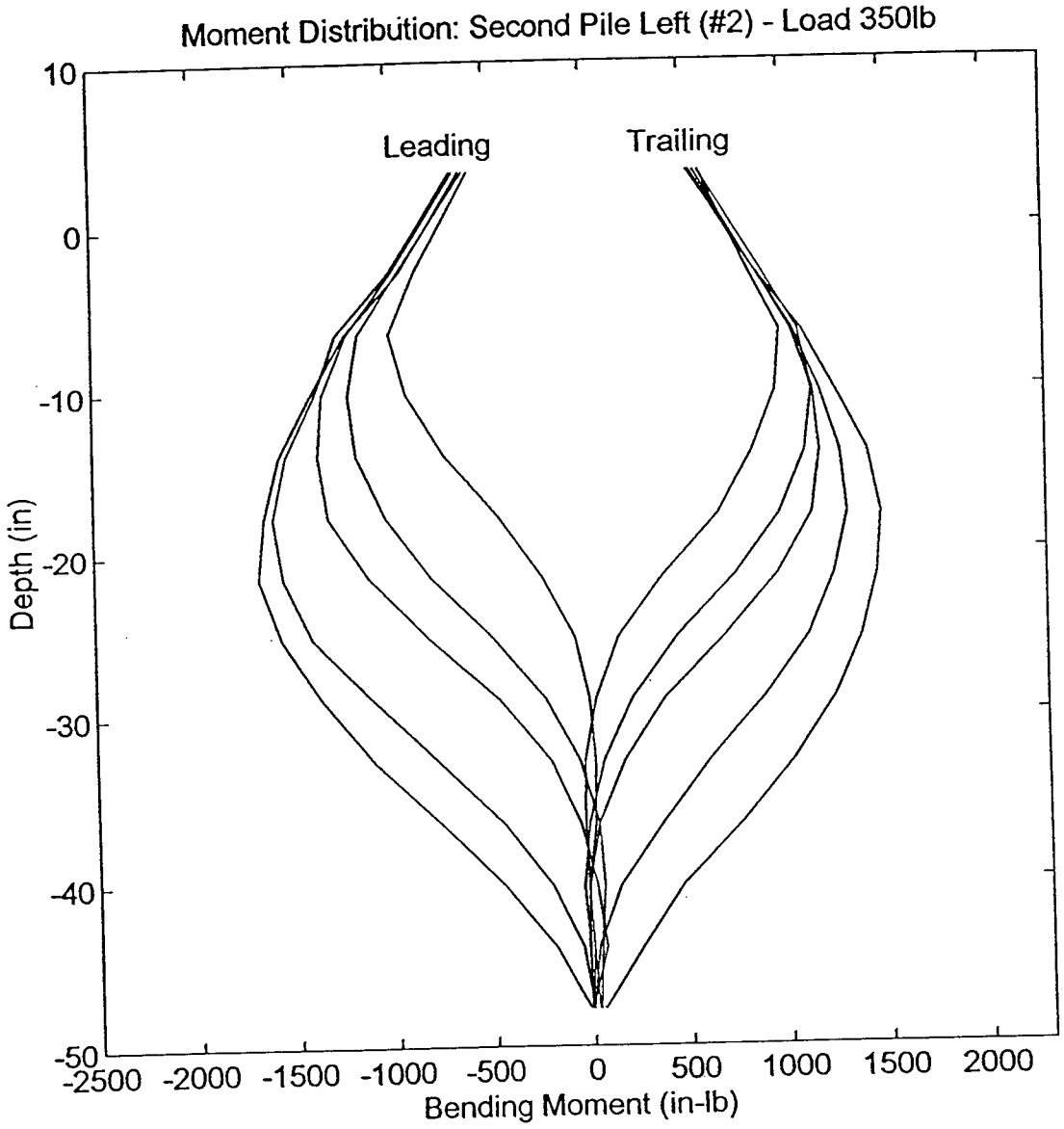
Moment Distribution: Second Pile Left (#2) - Load 350lb
Leading
Trailing
Depth (in)
10
0
-10
-20
-30
-40
-50
-2500
-2000
-1500
-1000
-500
0
500
1000
1500
2000
Bending Moment (in-lb)

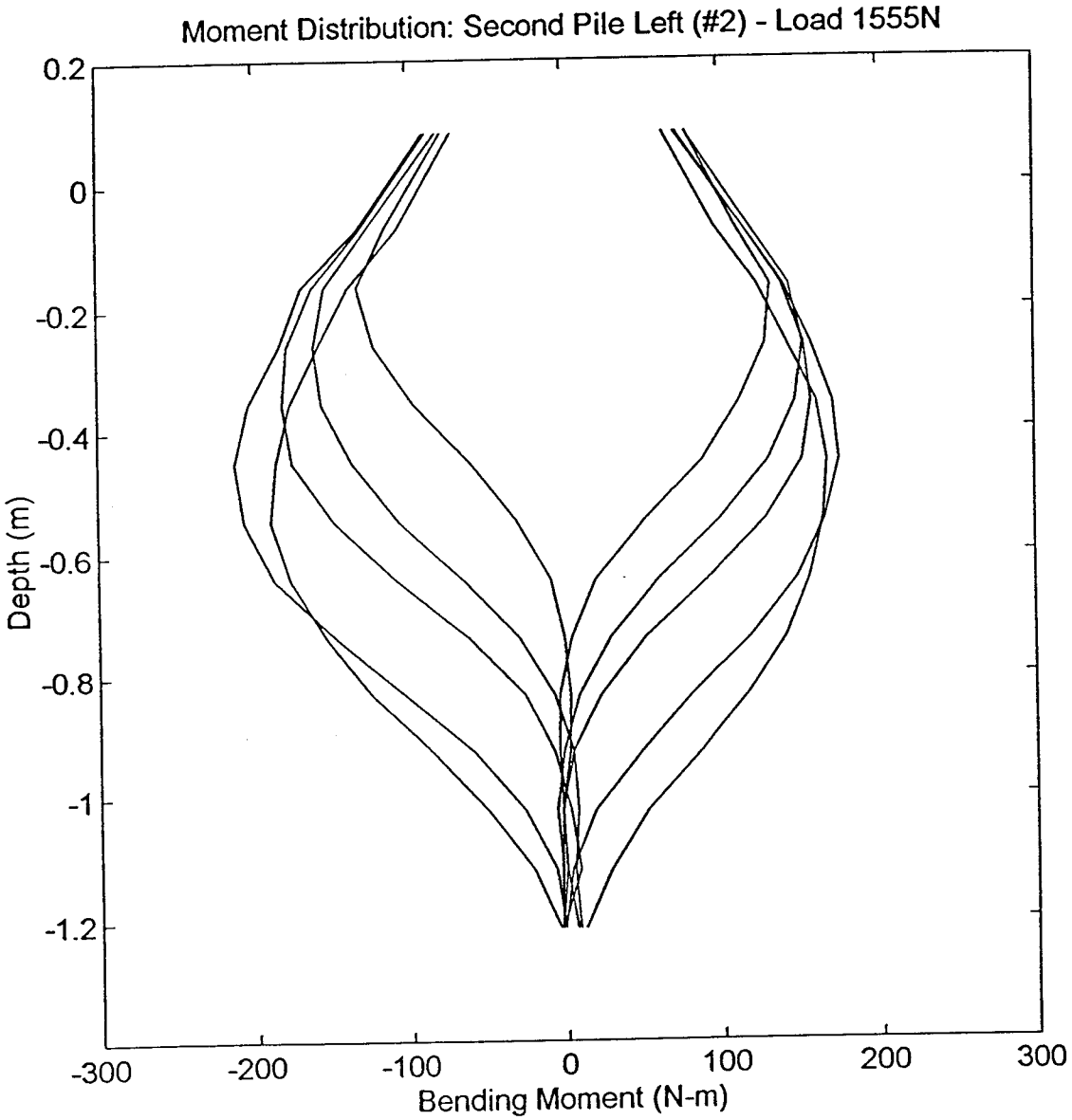
Moment Distribution: Second Pile Left (#2) - Load 1555N
0.2
0
-0.2
-0.4
-0.6
-0.8
-1
-1.2
Depth (m)
-300
-200
-100
0
100
200
300
Bending Moment (N-m)

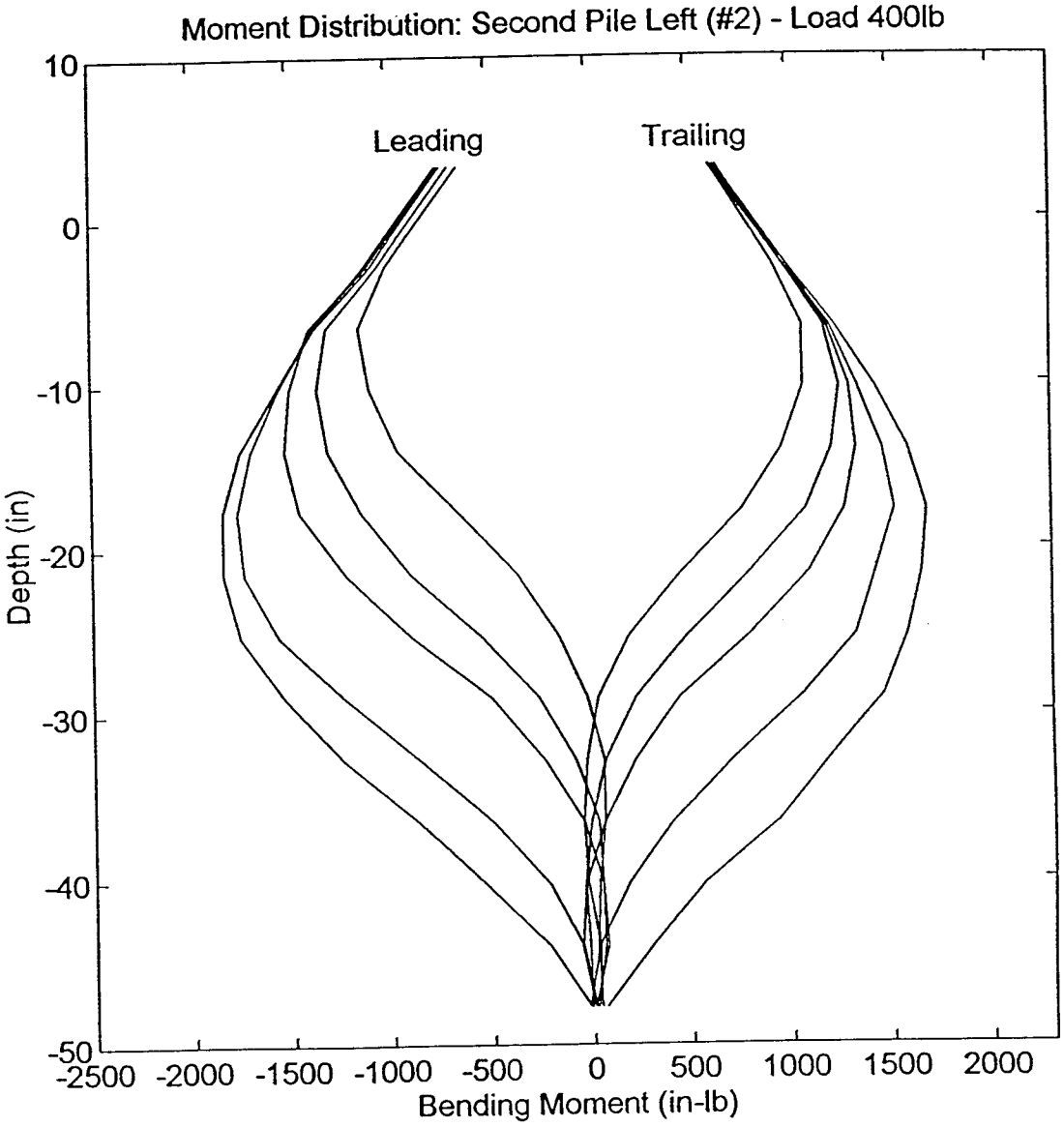
Moment Distribution: Second Pile Left (#2) - Load 400lb
Leading
Trailing
Depth (in)
Bending Moment (in-lb)
10
0
-10
-20
-30
-40
-50
-2500
-2000
-1500
-1000
-500
0
500
1000
1500
2000

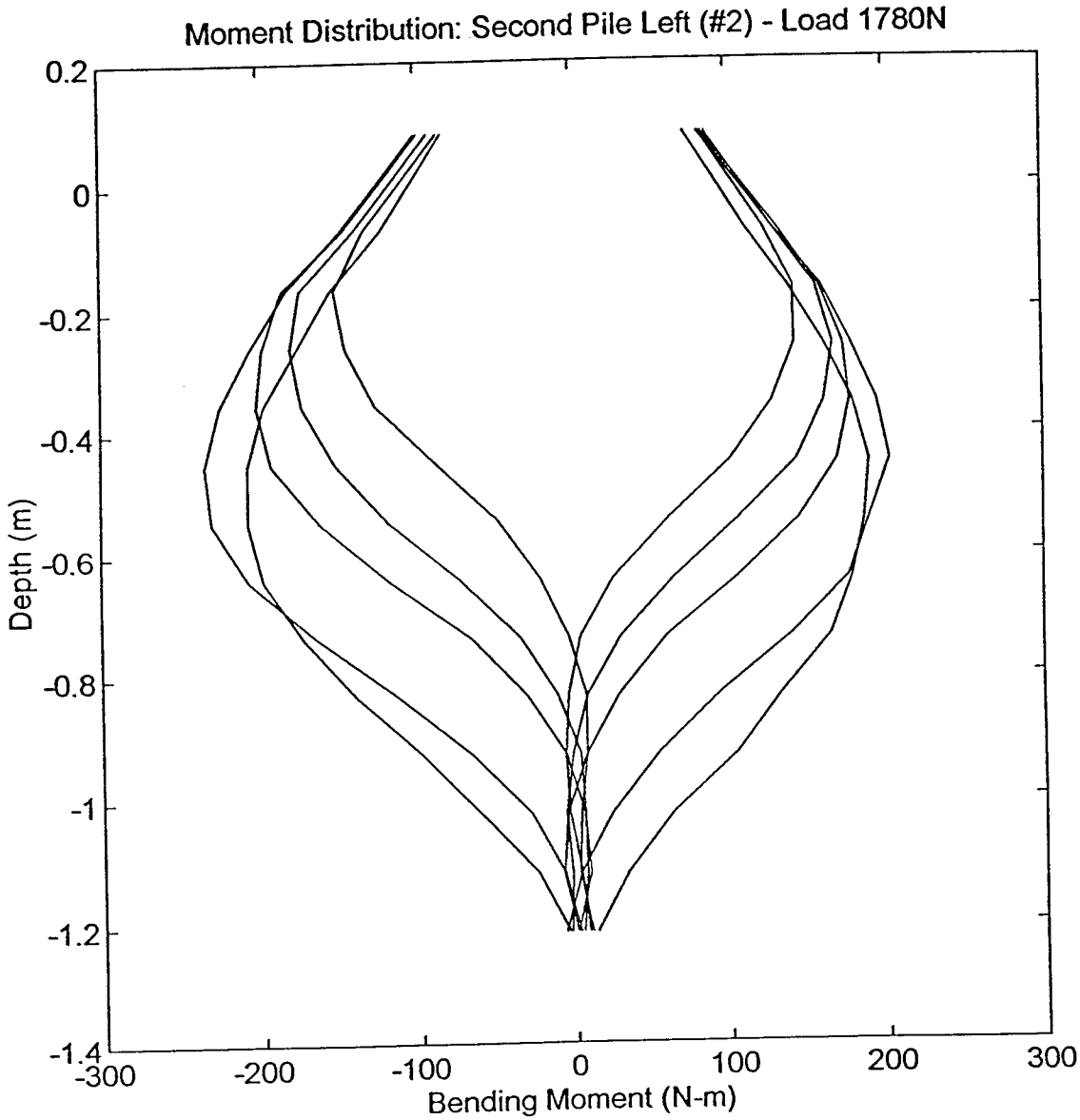
Moment Distribution: Second Pile Left (#2) - Load 1780N
0.2
0
-0.2
-0.4
-0.6
-0.8
-1
-1.2
-1.4
Depth (m)
-300
-200
-100
0
100
200
300
Bending Moment (N-m)

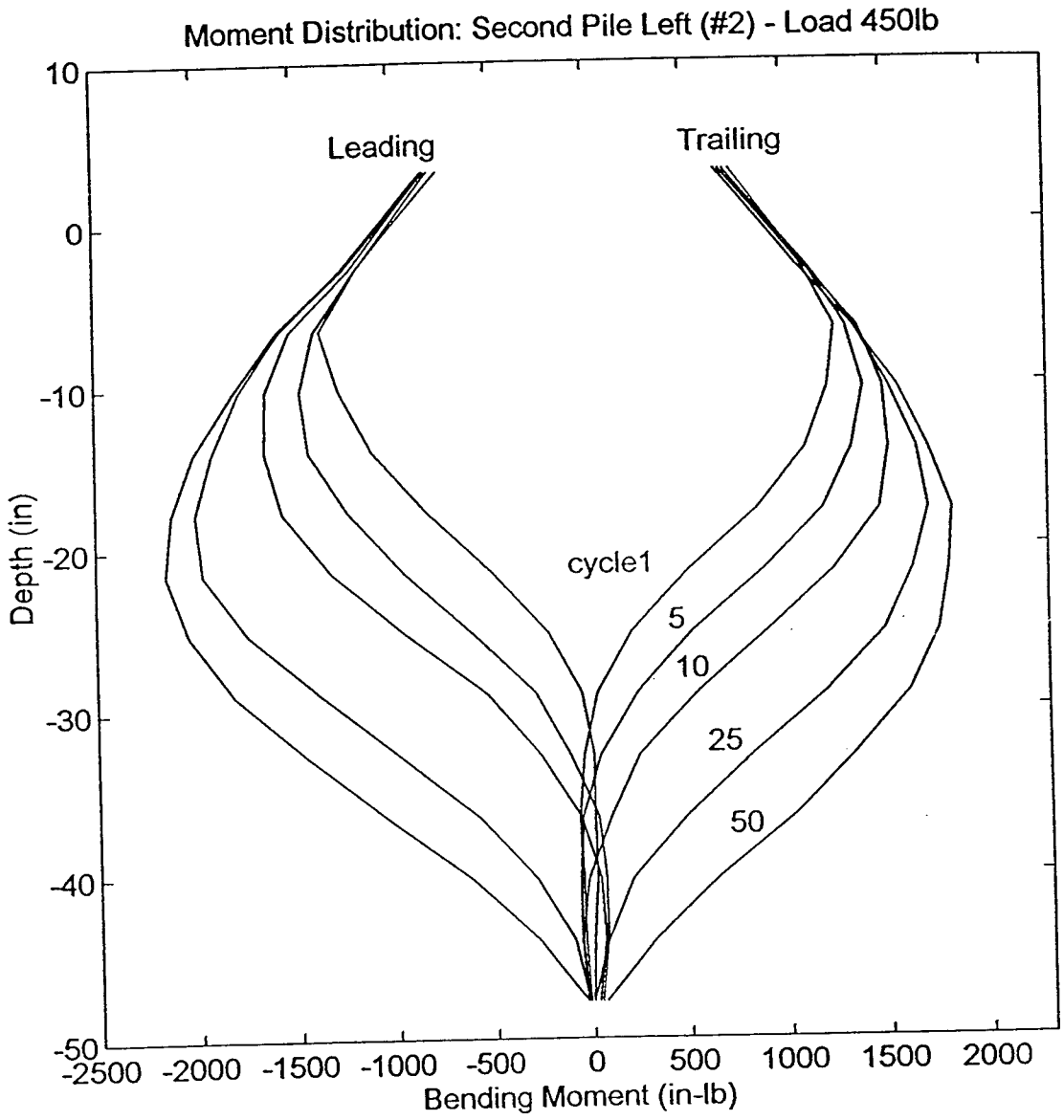
Moment Distribution: Second Pile Left (#2) - Load 450lb
Leading
Trailing
cycle1
5
10
25
50
Depth (in)
Bending Moment (in-lb)
10
0
-10
-20
-30
-40
-50
-2500
-2000
-1500
-1000
-500
0
500
1000
1500
2000

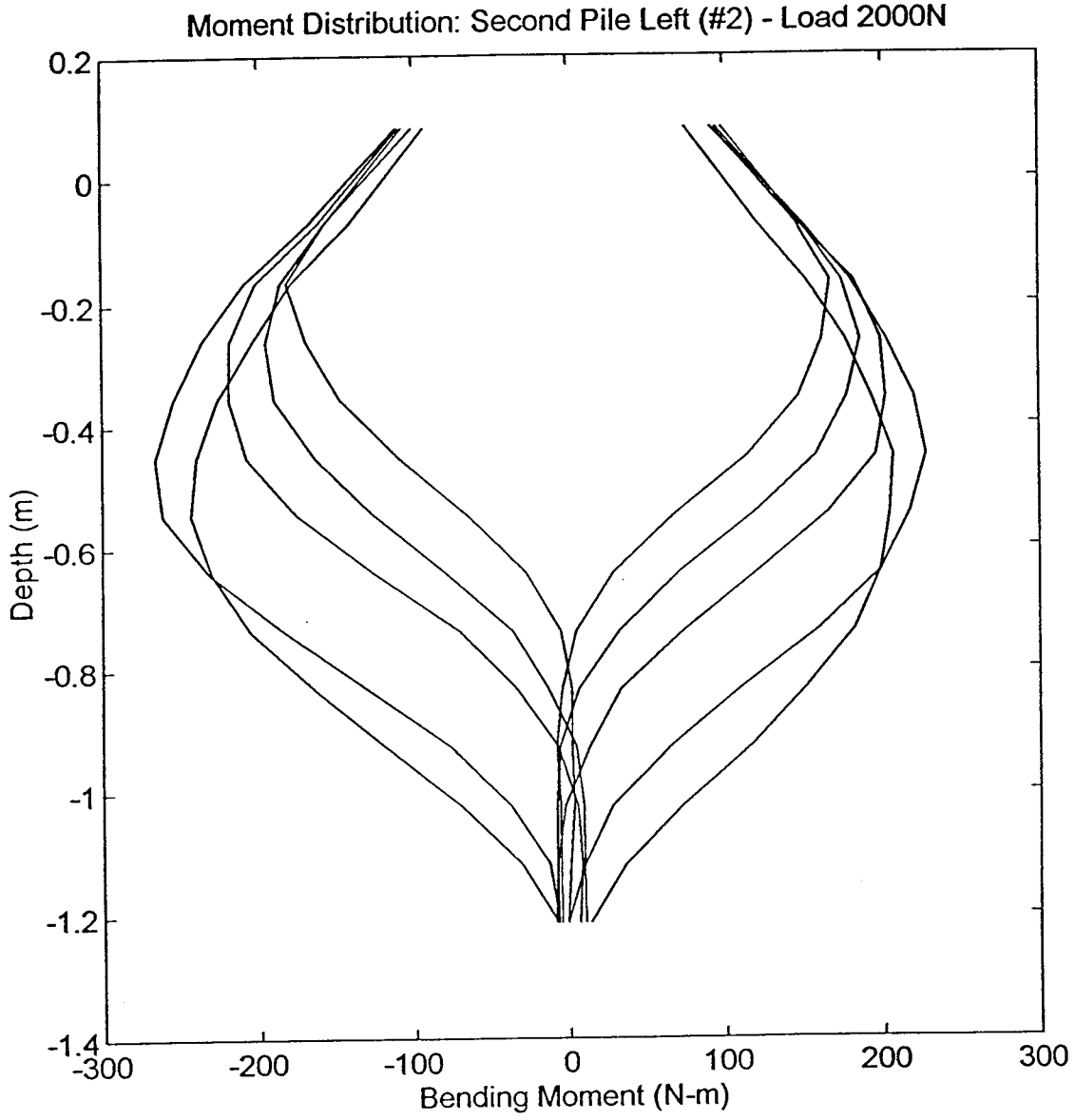
Moment Distribution: Second Pile Left (#2) - Load 2000N
0.2
0
-0.2
-0.4
-0.6
-0.8
-1
-1.2
-1.4
Depth (m)
-300
-200
-100
0
100
200
300
Bending Moment (N-m)

Figure B8. Moment distribution for pile 4 (next 14 plots).

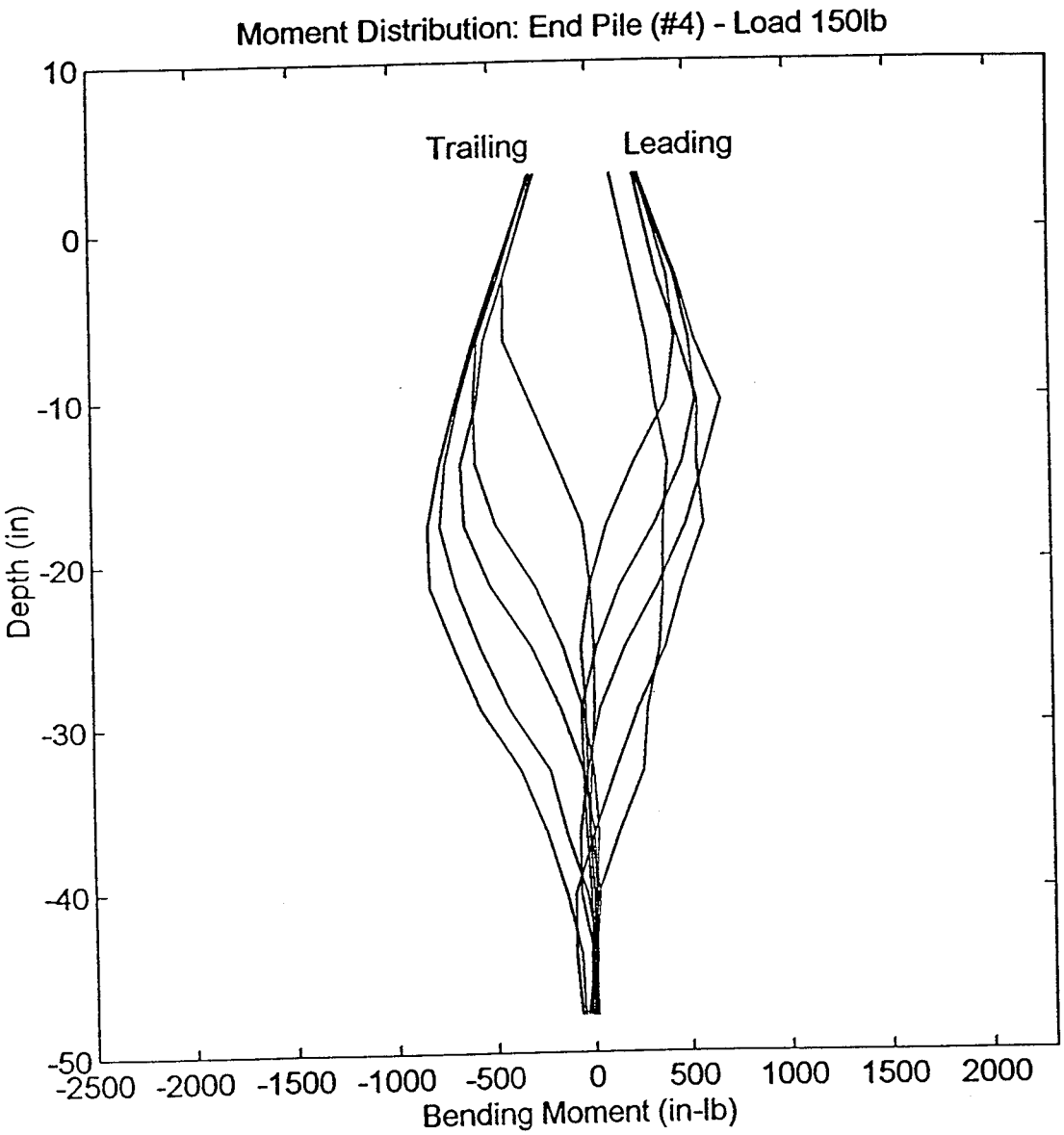
Moment Distribution: End Pile (#4) - Load 150lb
Trailing
Leading
Depth (in)
Bending Moment (in-lb)
10
0
-10
-20
-30
-40
-50
-2500
-2000
-1500
-1000
-500
0
500
1000
1500
2000

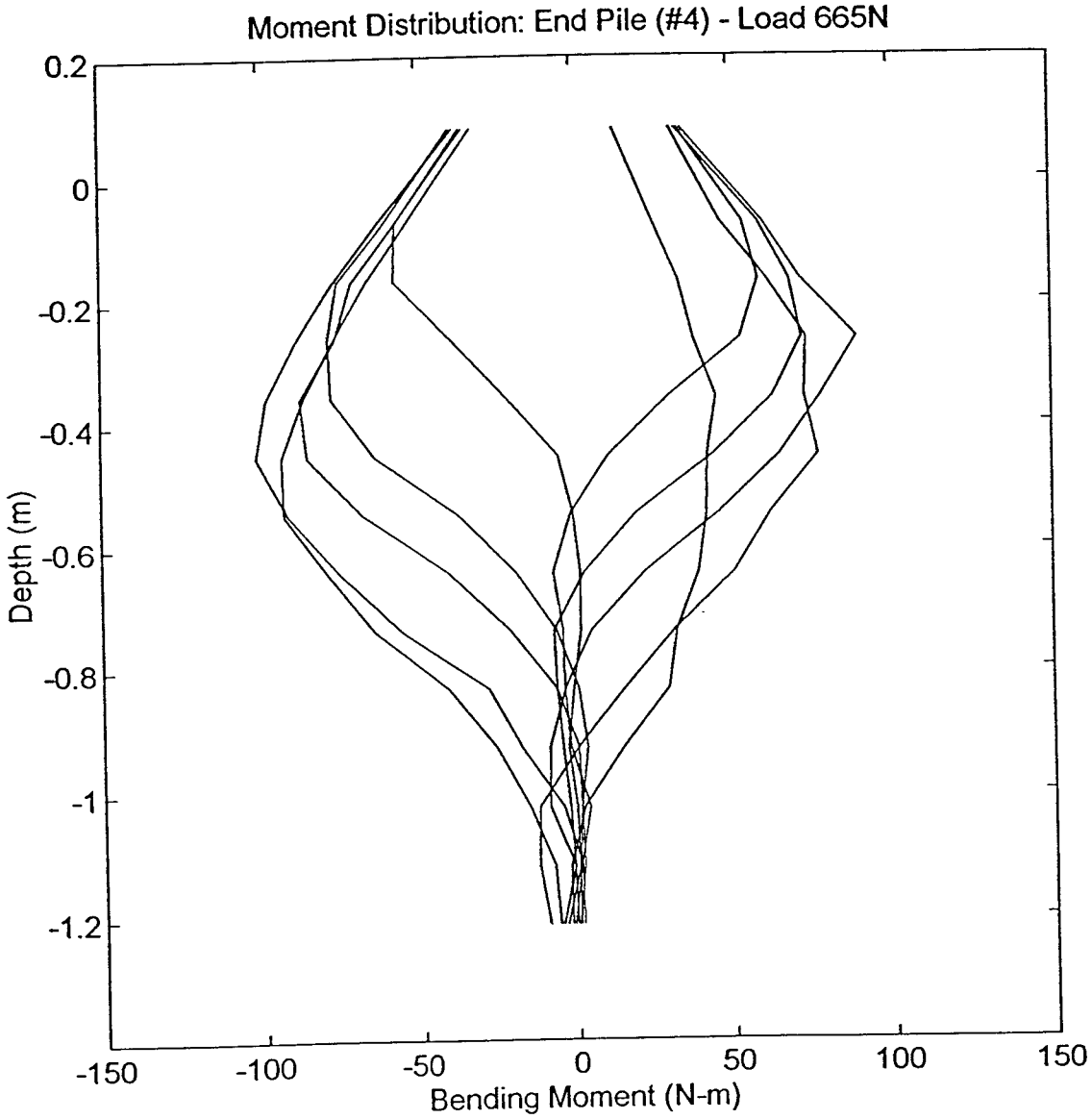
Moment Distribution: End Pile (#4) - Load 665N
0.2
0
-0.2
-0.4
-0.6
-0.8
-1
-1.2
Depth (m)
-150
-100
-50
0
50
100
150
Bending Moment (N-m)

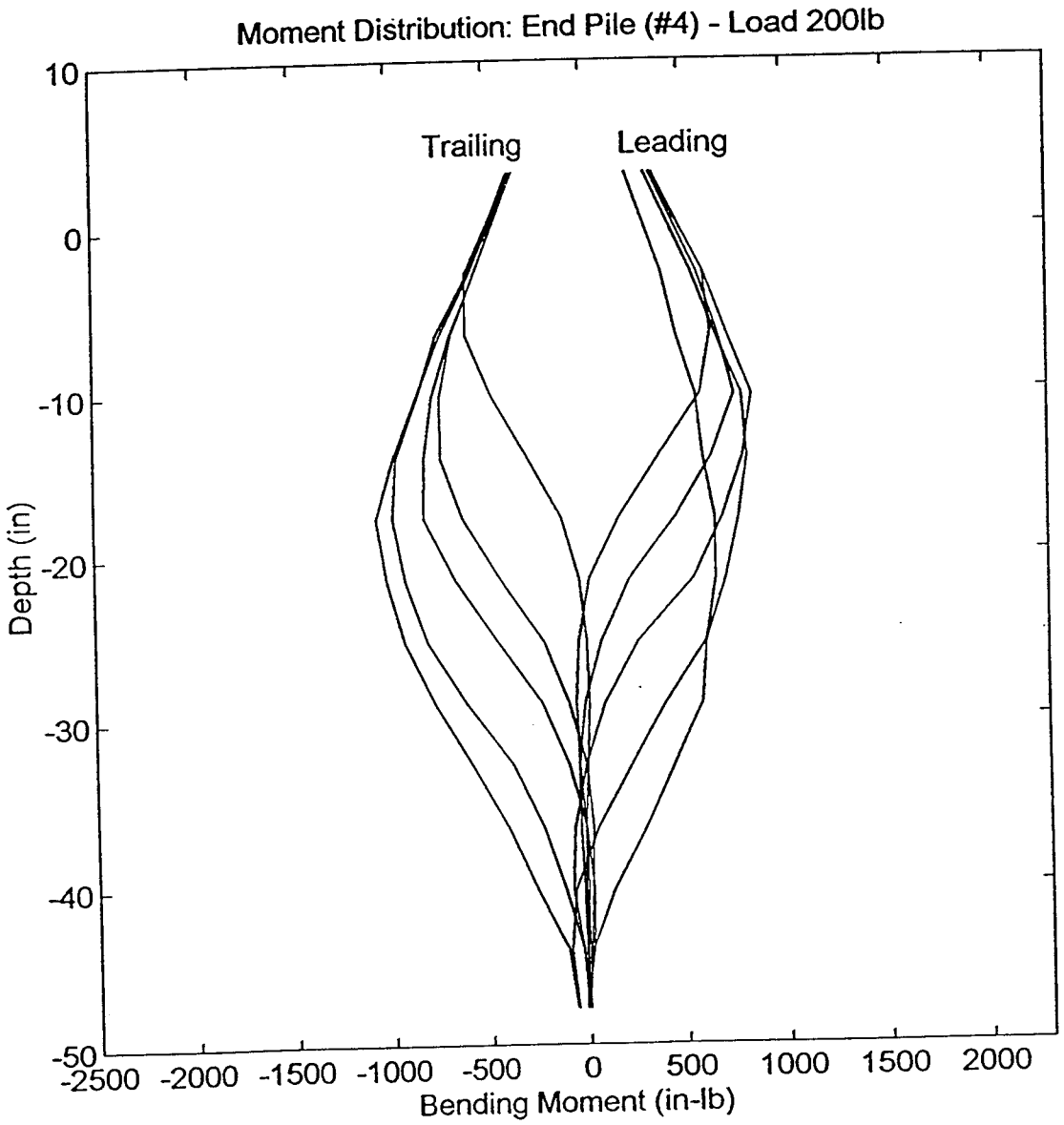
Moment Distribution: End Pile (#4) - Load 200lb
Trailing
Leading
Depth (in)
10
0
-10
-20
-30
-40
-50
-2500
-2000
-1500
-1000
-500
0
500
1000
1500
2000
Bending Moment (in-lb)

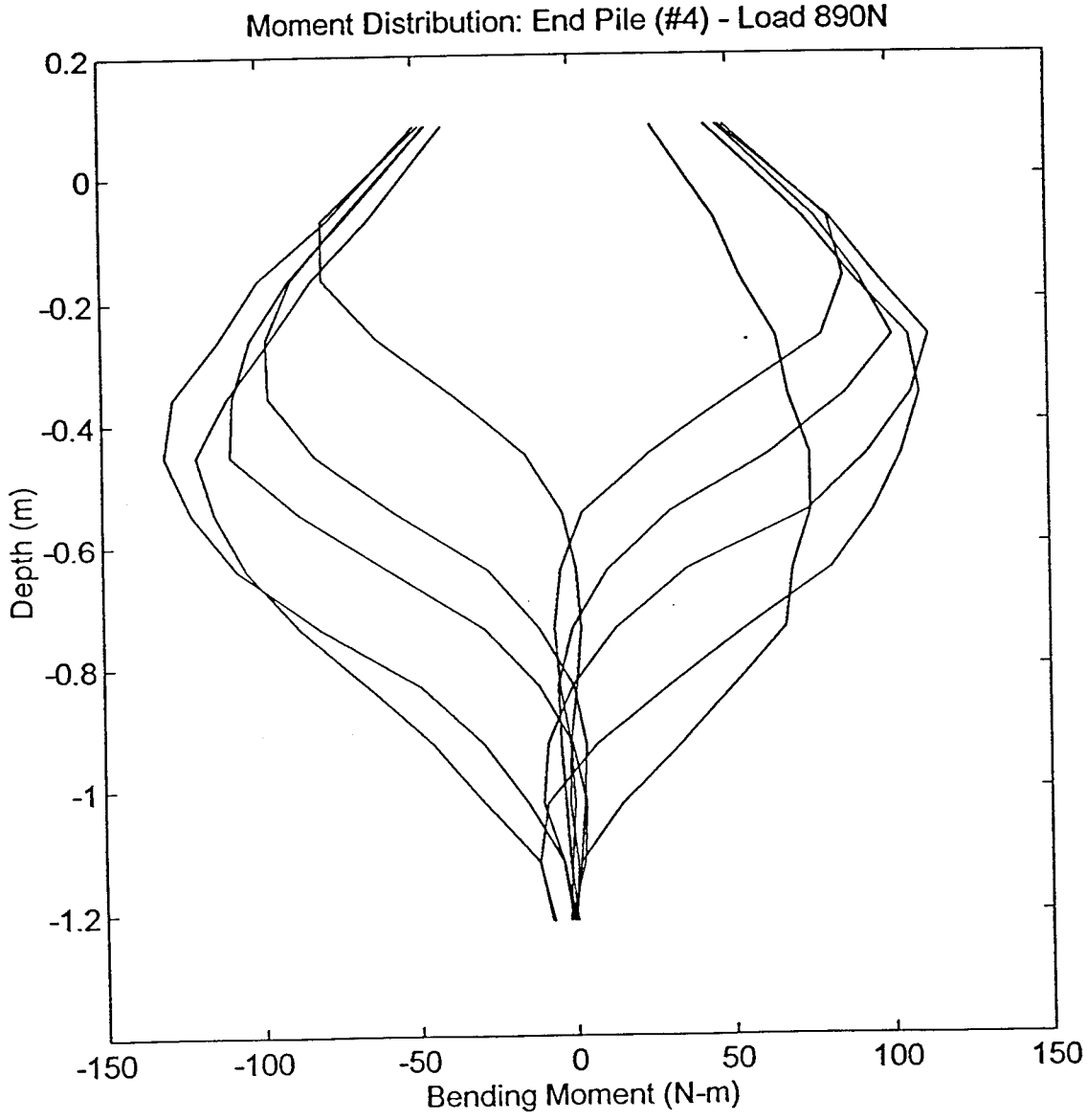
Moment Distribution: End Pile (#4) - Load 890N
0.2
0
-0.2
-0.4
-0.6
-0.8
-1
-1.2
Depth (m)
-150
-100
-50
0
50
100
150
Bending Moment (N-m)

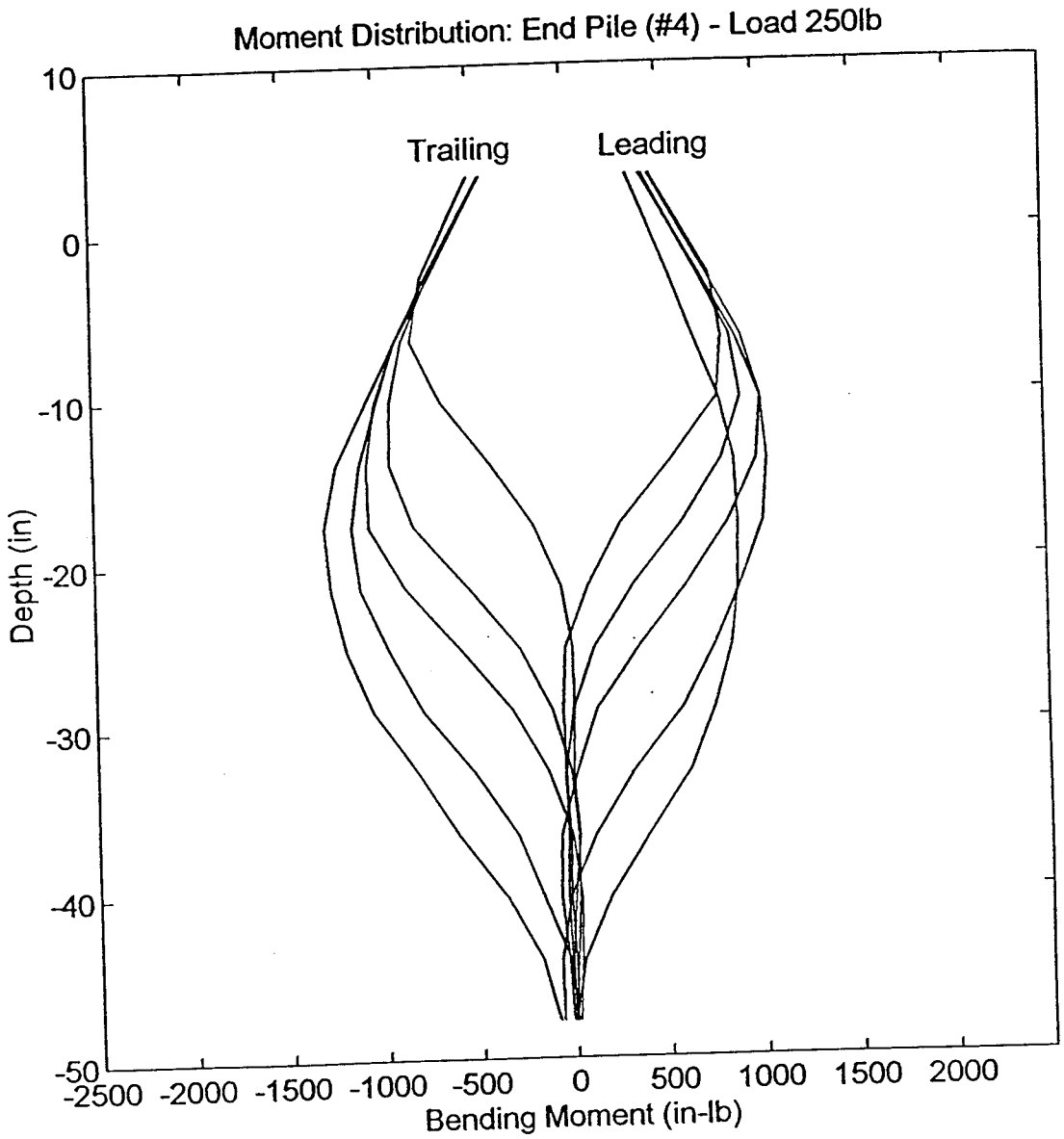
Moment Distribution: End Pile (#4) - Load 250lb
Trailing
Leading
10
0
-10
-20
-30
-40
-50
Depth (in)
-2500
-2000
-1500
-1000
-500
0
500
1000
1500
2000
Bending Moment (in-lb)

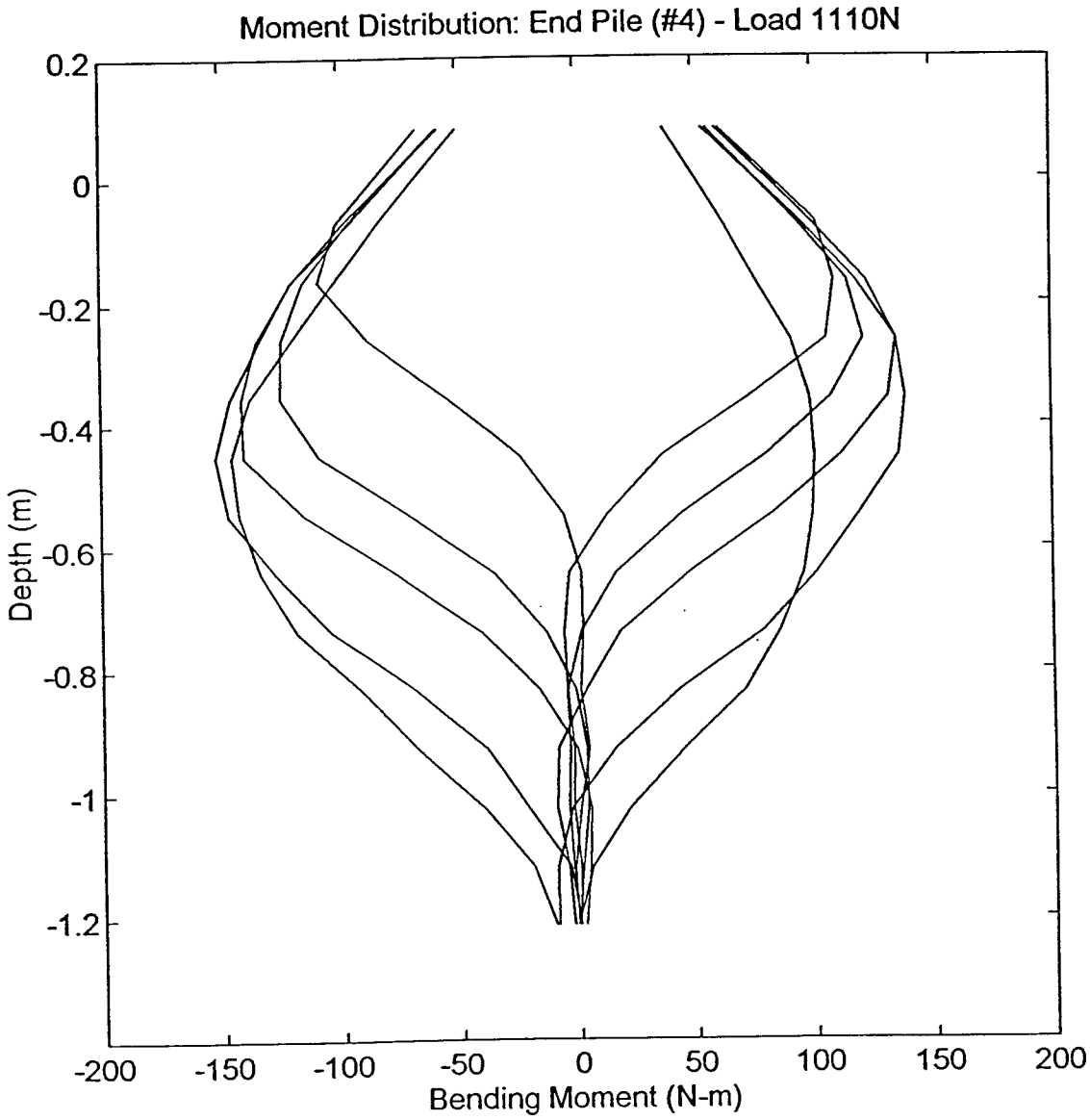
Moment Distribution: End Pile (#4) - Load 1110N
0.2
0
-0.2
-0.4
-0.6
-0.8
-1
-1.2
Depth (m)
-200
-150
-100
-50
0
50
100
150
200
Bending Moment (N-m)

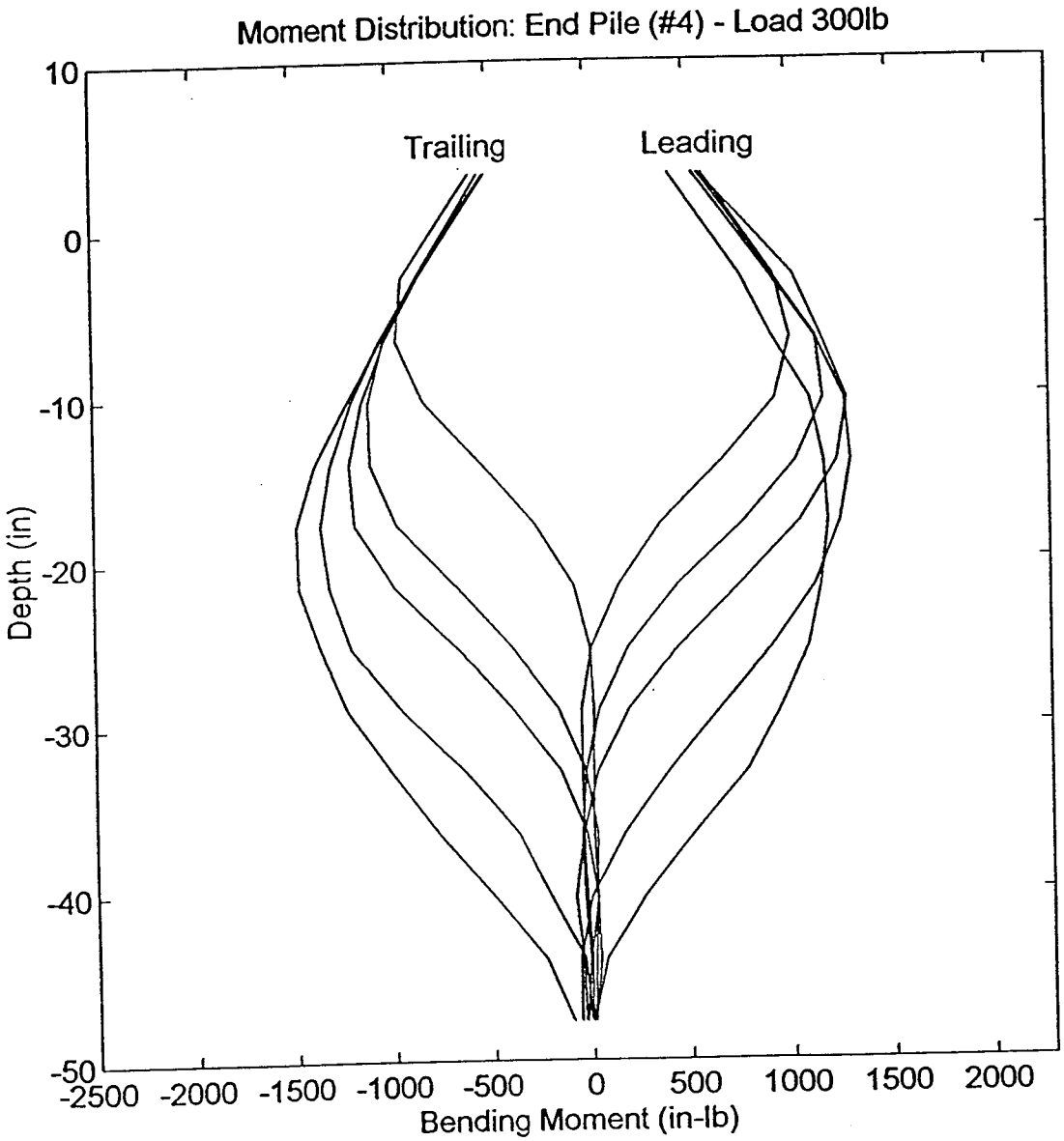
Moment Distribution: End Pile (#4) - Load 300lb
Trailing
Leading
Depth (in)
10
0
-10
-20
-30
-40
-50
-2500
-2000
-1500
-1000
-500
0
500
1000
1500
2000
Bending Moment (in-lb)

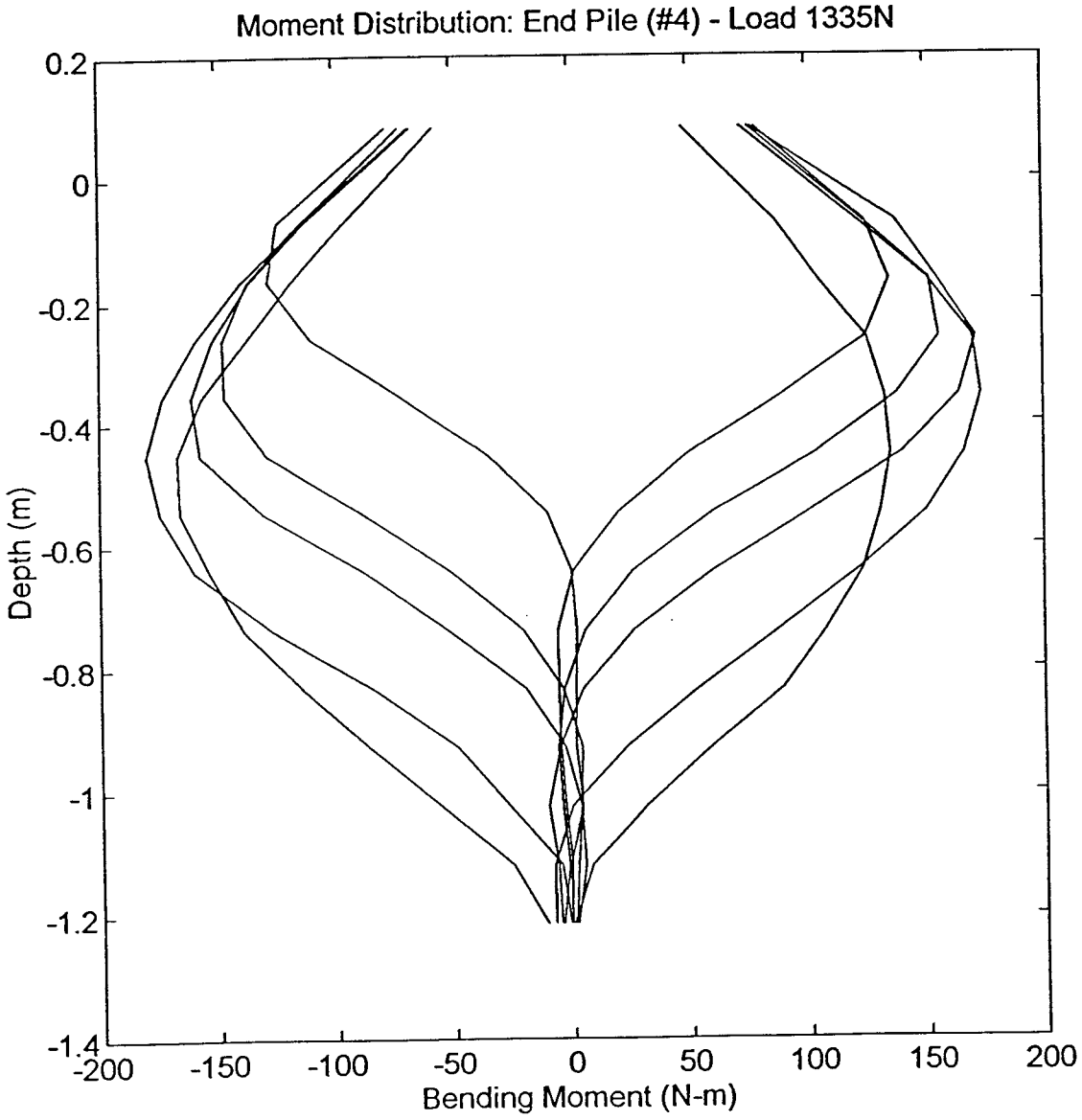
Moment Distribution: End Pile (#4) - Load 1335N
0.2
0
-0.2
-0.4
-0.6
-0.8
-1
-1.2
-1.4
Depth (m)
-200
-150
-100
-50
0
50
100
150
200
Bending Moment (N-m)

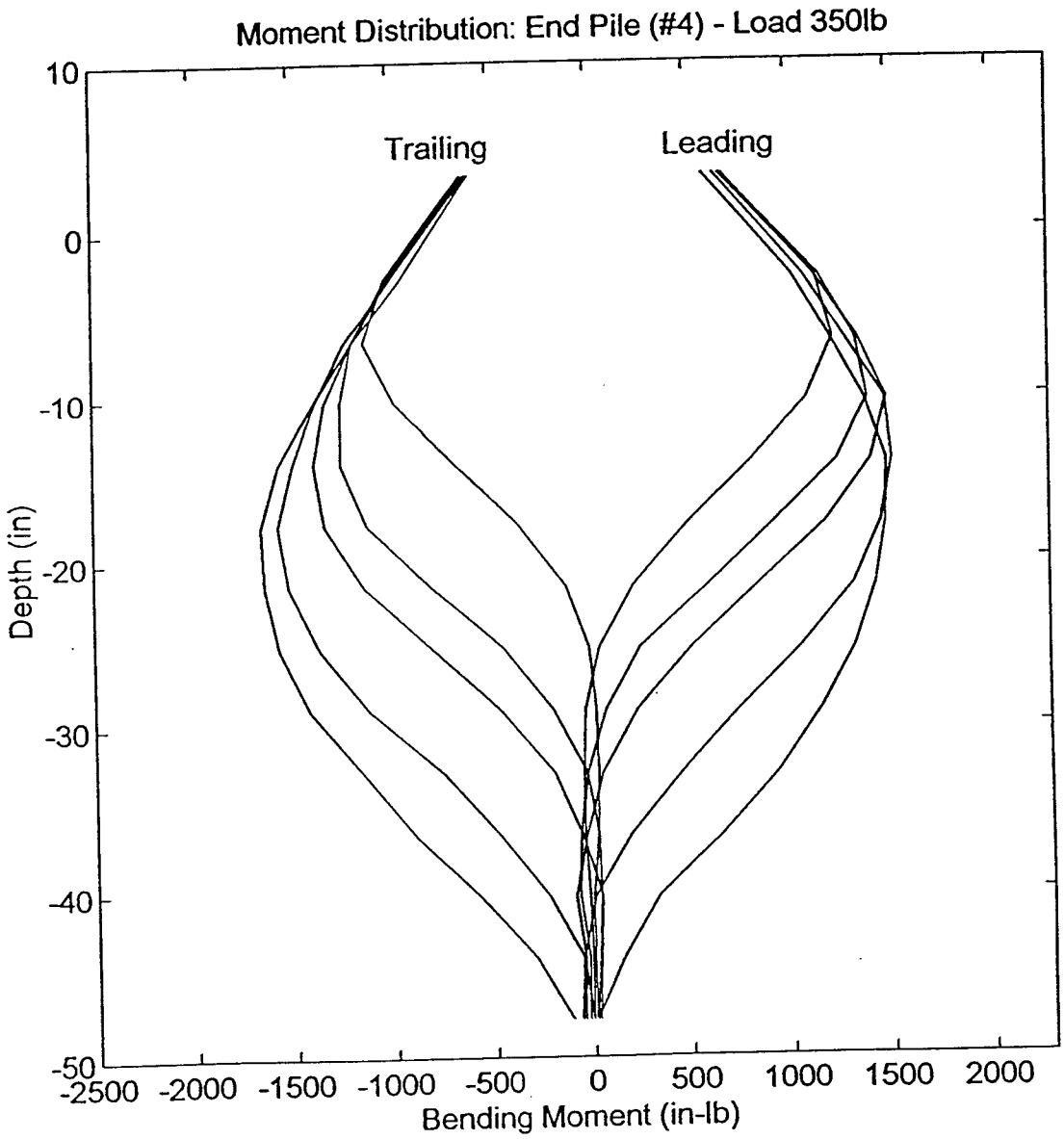
Moment Distribution: End Pile (#4) - Load 350lb
Trailing
Leading
Depth (in)
Bending Moment (in-lb)
10
0
-10
-20
-30
-40
-50
-2500
-2000
-1500
-1000
-500
0
500
1000
1500
2000

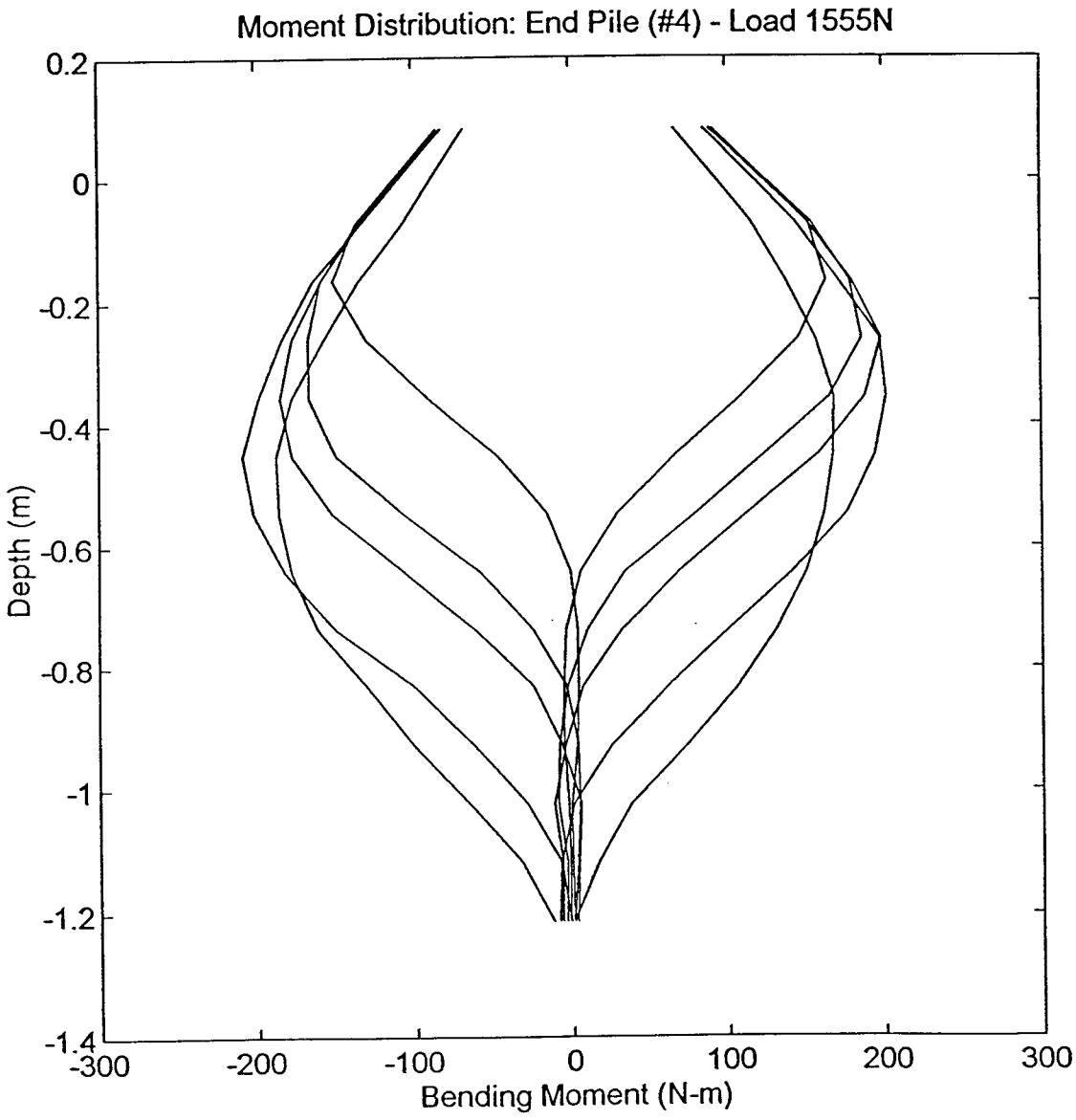
Moment Distribution: End Pile (#4) - Load 1555N
0.2
0
-0.2
-0.4
-0.6
-0.8
-1
-1.2
-1.4
Depth (m)
-300
-200
-100
0
100
200
300
Bending Moment (N-m)

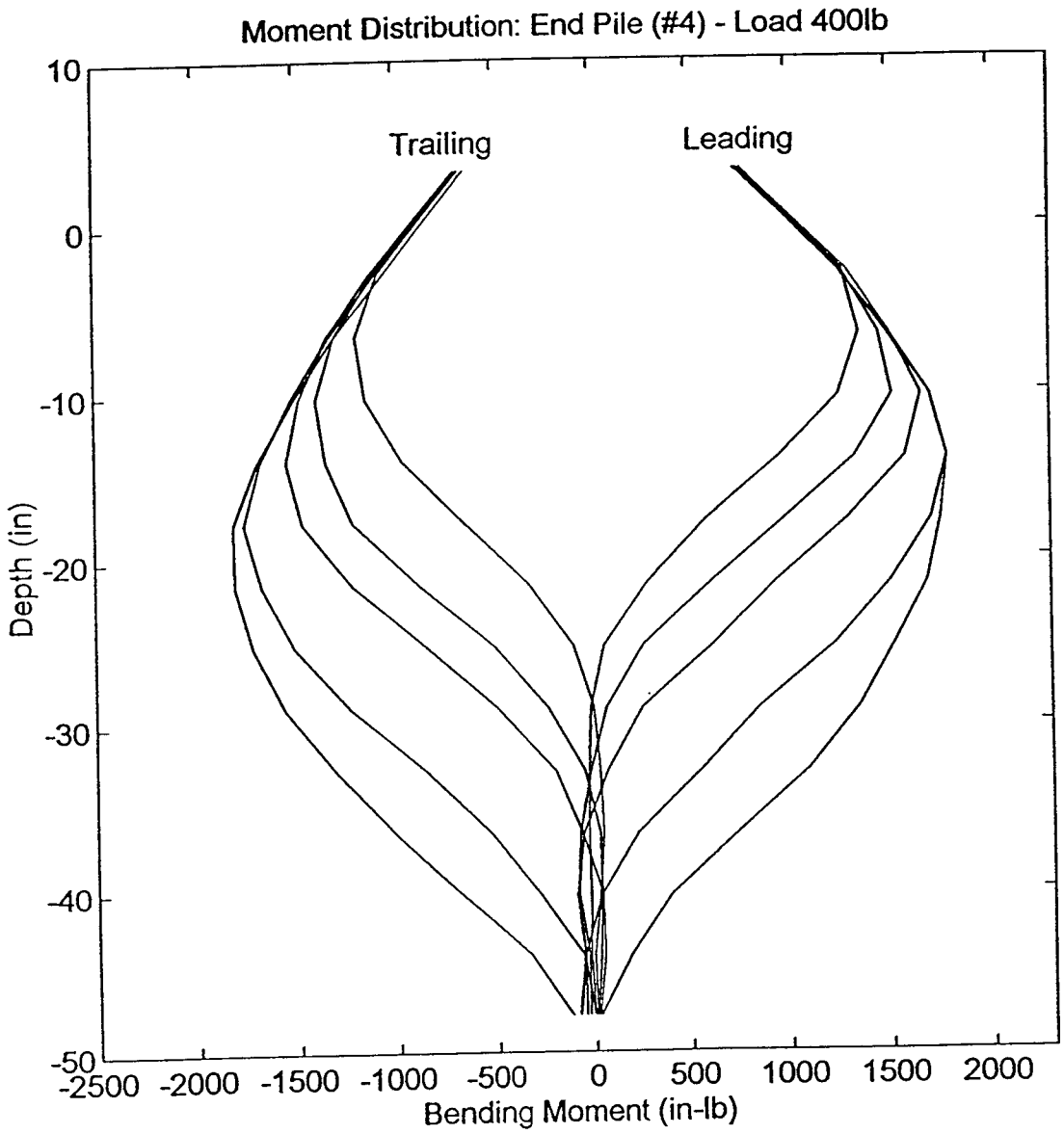
Moment Distribution: End Pile (#4) - Load 400lb
Trailing
Leading
Depth (in)
Bending Moment (in-lb)
10
0
-10
-20
-30
-40
-50
-2500
-2000
-1500
-1000
-500
0
500
1000
1500
2000

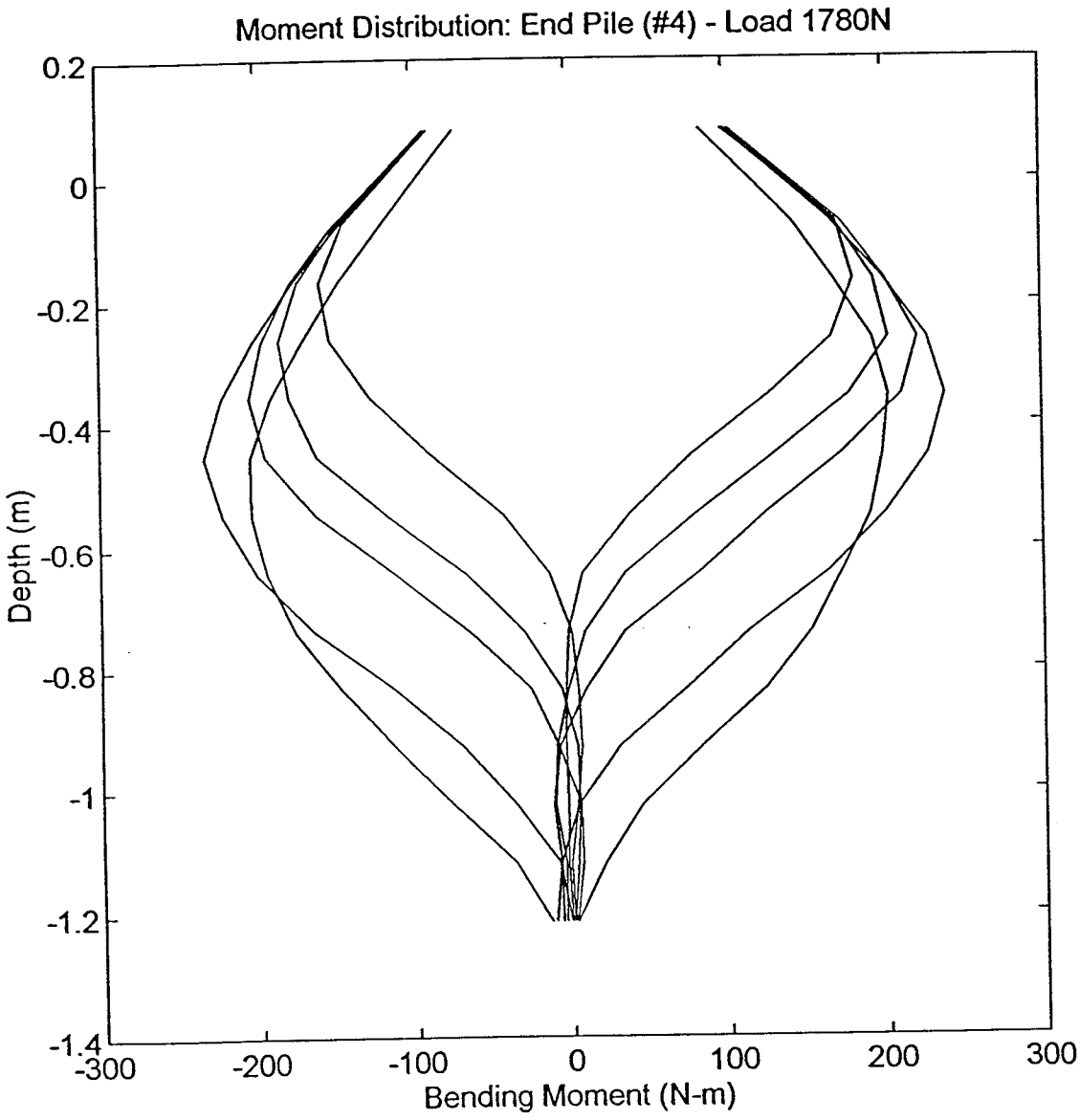
Moment Distribution: End Pile (#4) - Load 1780N
0.2
0
-0.2
-0.4
-0.6
-0.8
-1
-1.2
-1.4
Depth (m)
-300
-200
-100
0
100
200
300
Bending Moment (N-m)

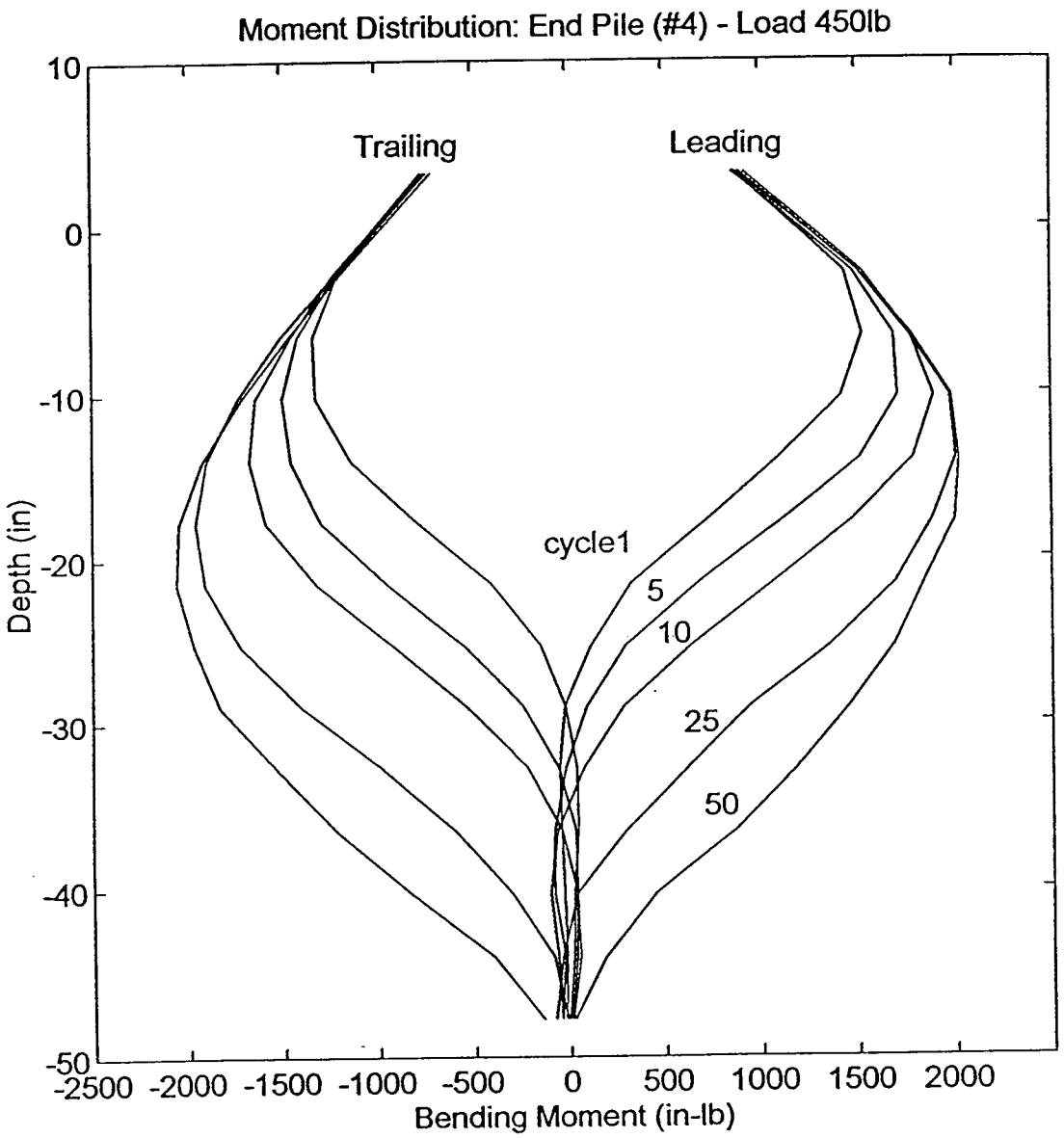
Moment Distribution: End Pile (#4) - Load 450lb
Trailing
Leading
cycle1
5
10
25
50
Depth (in)
Bending Moment (in-lb)
10
0
-10
-20
-30
-40
-50
-2500
-2000
-1500
-1000
-500
0
500
1000
1500
2000

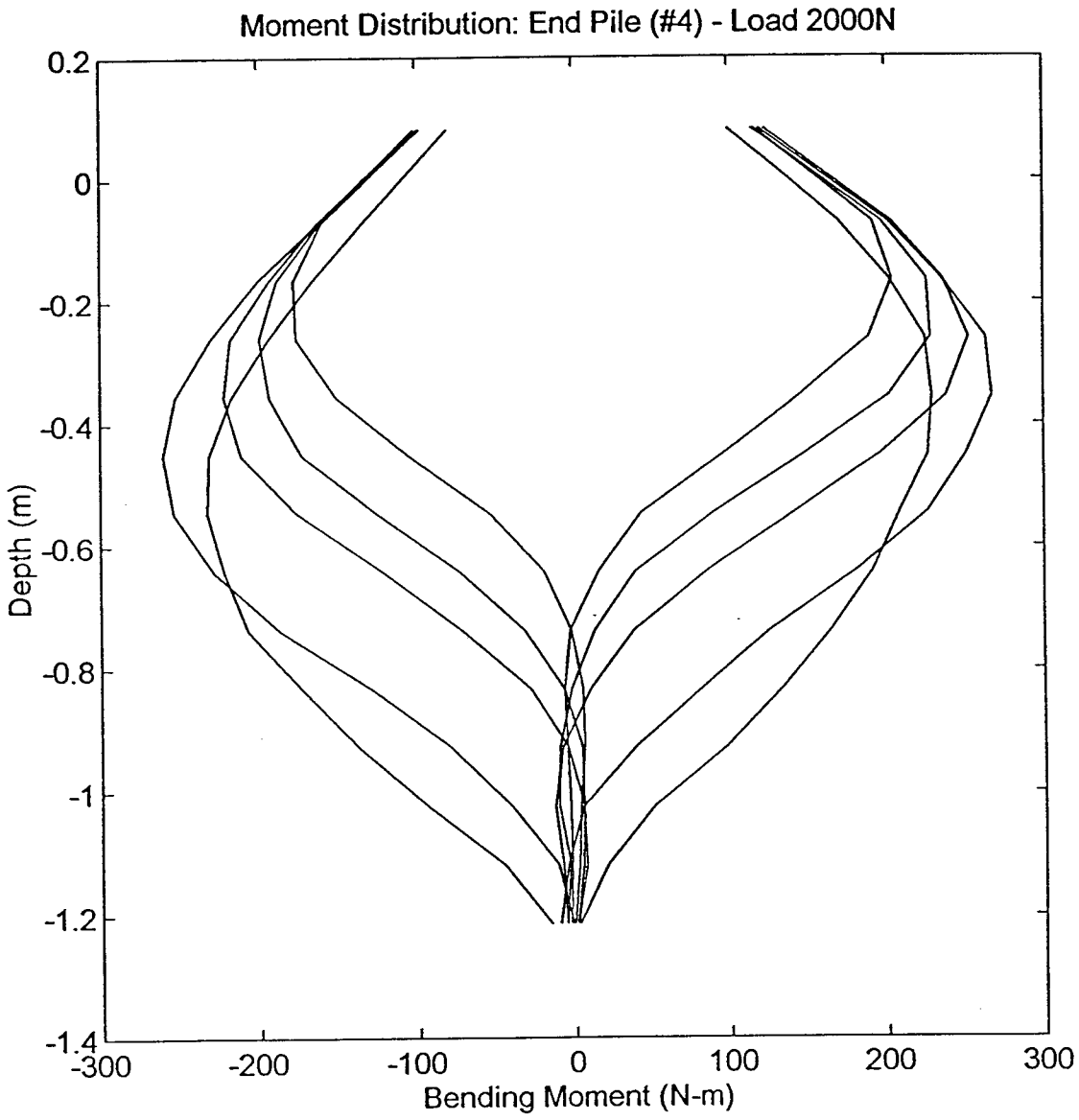
Moment Distribution: End Pile (#4) - Load 2000N
0.2
0
-0.2
-0.4
-0.6
-0.8
-1
-1.2
-1.4
Depth (m)
-300
-200
-100
0
100
200
300
Bending Moment (N-m)

Figure B9. Moment distribution for pile 5 (next 14 plots).

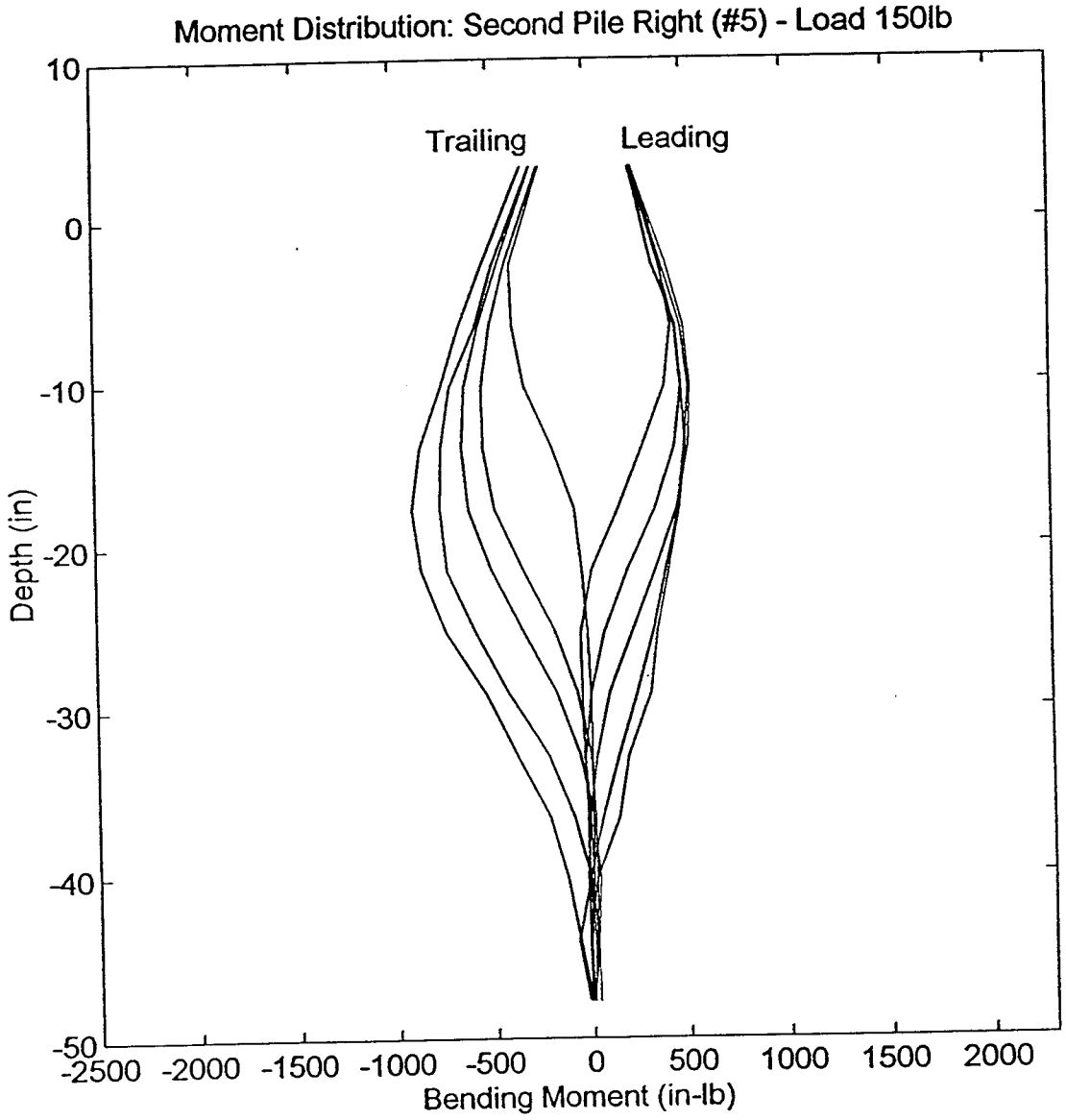
Moment Distribution: Second Pile Right (#5) - Load 150lb
Trailing
Leading
Depth (in)
10
0
-10
-20
-30
-40
-50
-2500
-2000
-1500
-1000
-500
0
500
1000
1500
2000
Bending Moment (in-lb)

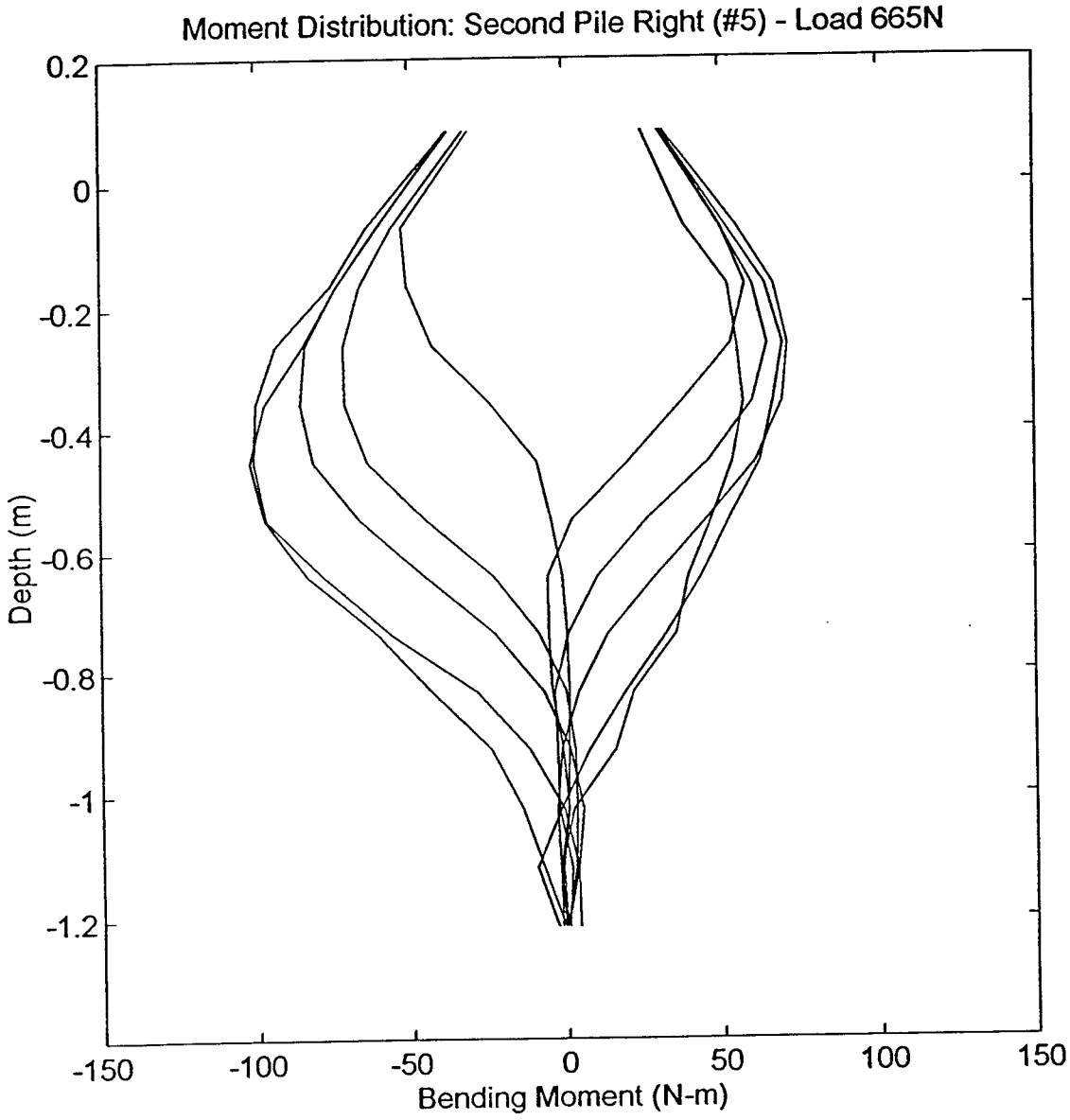
Moment Distribution: Second Pile Right (#5) - Load 665N
0.2
0
-0.2
-0.4
-0.6
-0.8
-1
-1.2
Depth (m)
-150
-100
-50
0
50
100
150
Bending Moment (N-m)

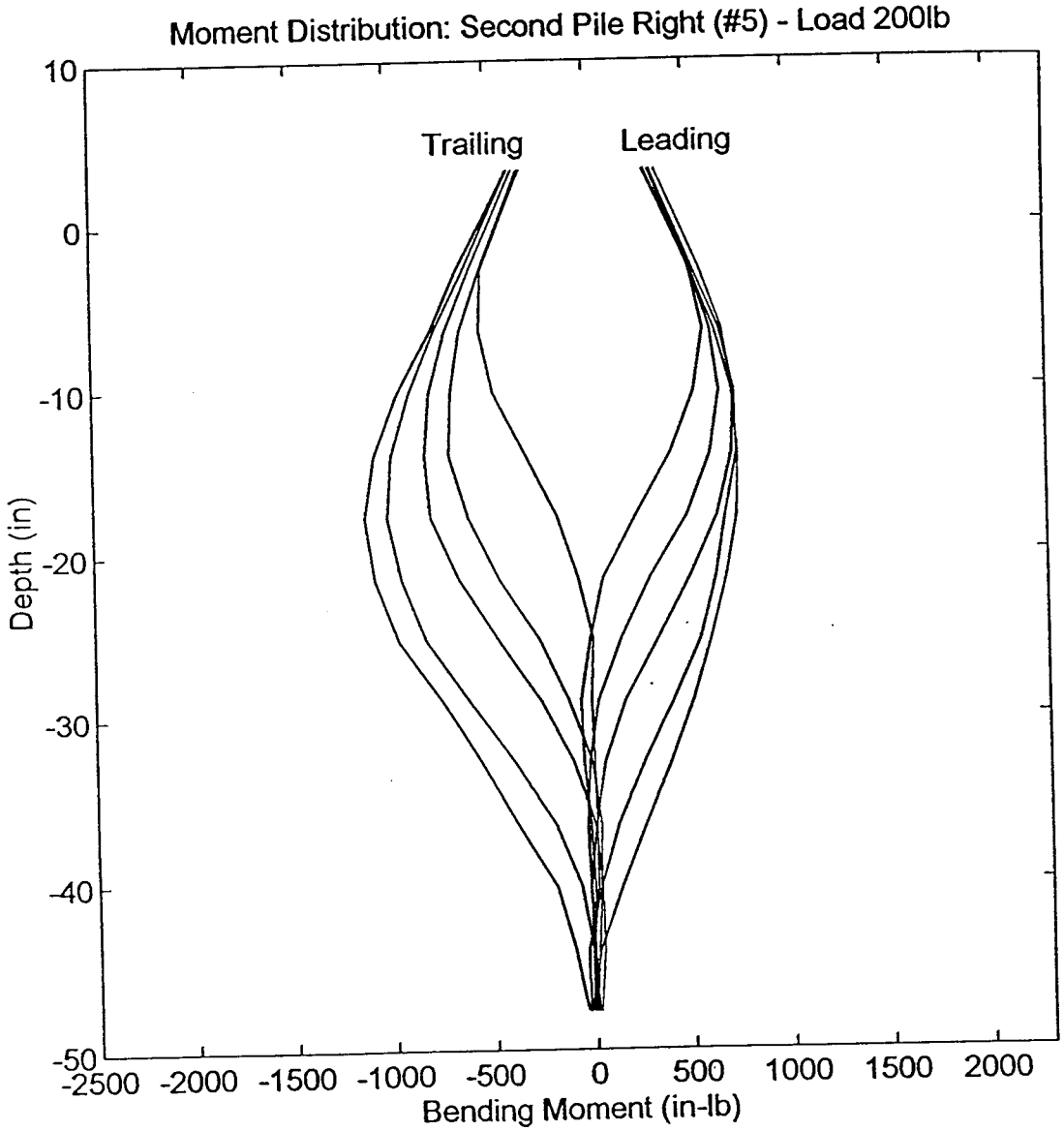
Moment Distribution: Second Pile Right (#5) - Load 200lb
Trailing
Leading
Depth (in)
10
0
-10
-20
-30
-40
-50
-2500
-2000
-1500
-1000
-500
0
500
1000
1500
2000
Bending Moment (in-lb)

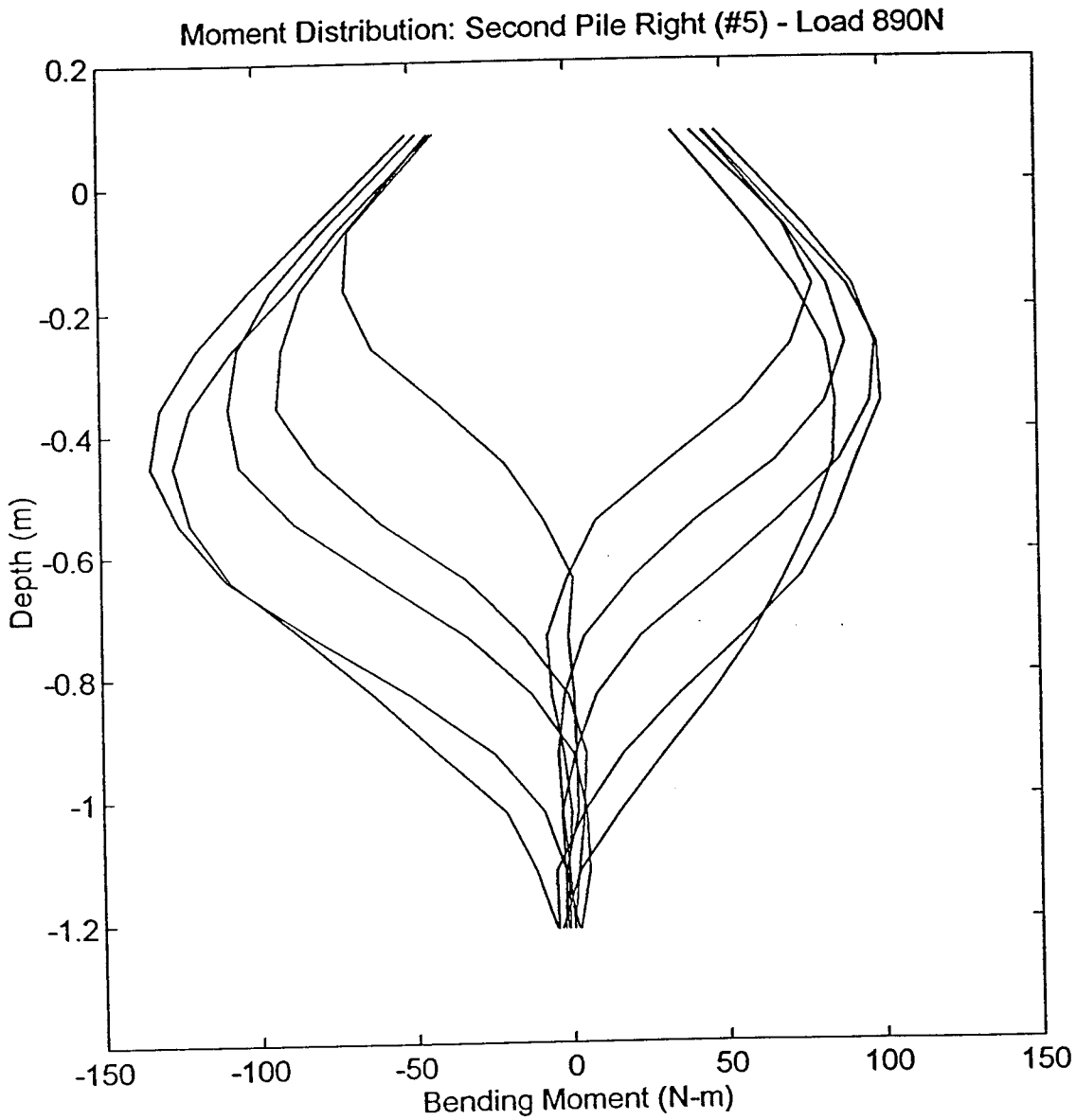
Moment Distribution: Second Pile Right (#5) - Load 890N
0.2
0
-0.2
-0.4
-0.6
-0.8
-1
-1.2
Depth (m)
-150
-100
-50
0
50
100
150
Bending Moment (N-m)

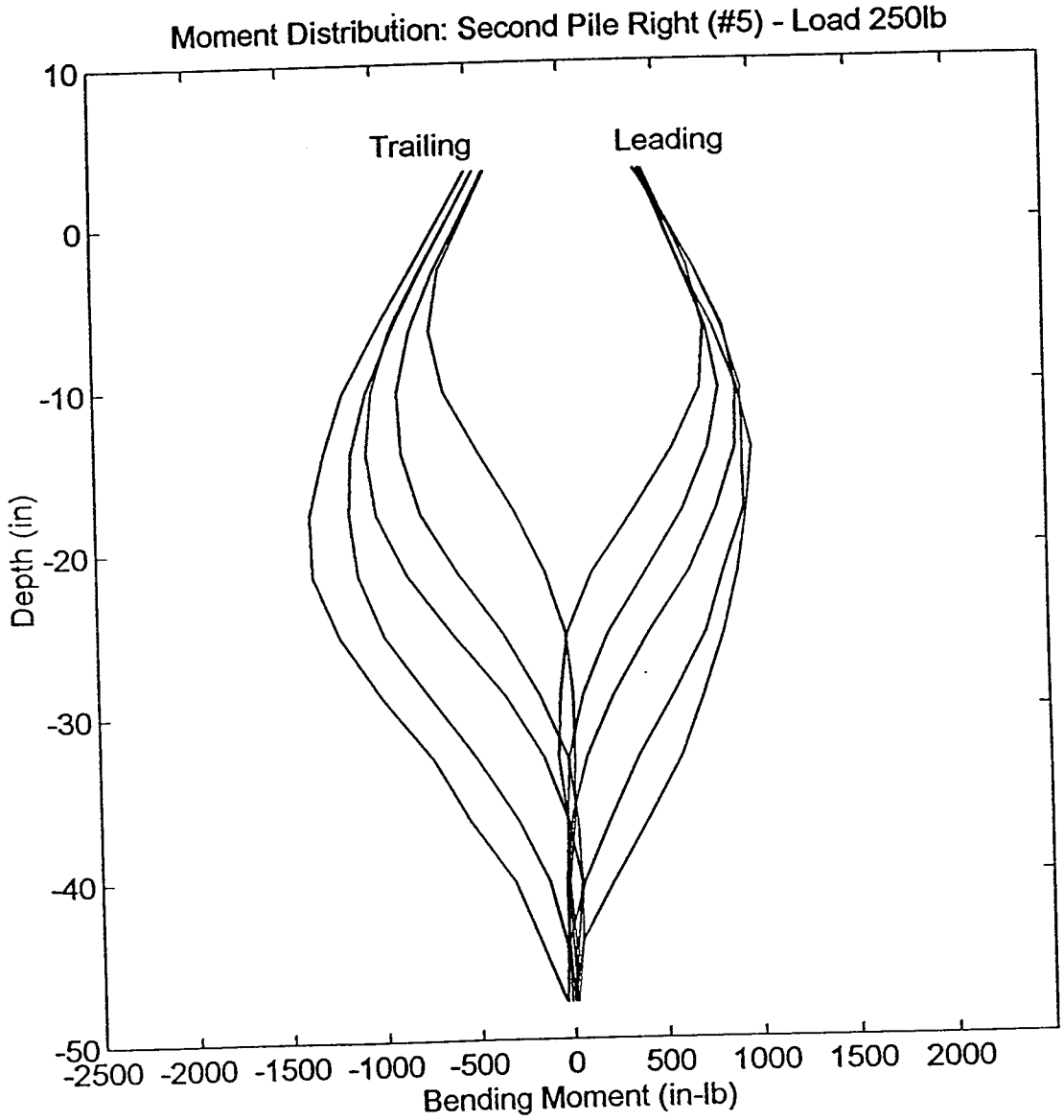
Moment Distribution: Second Pile Right (#5) - Load 250lb
Trailing
Leading
Depth (in)
10
0
-10
-20
-30
-40
-50
-2500
-2000
-1500
-1000
-500
0
500
1000
1500
2000
Bending Moment (in-lb)

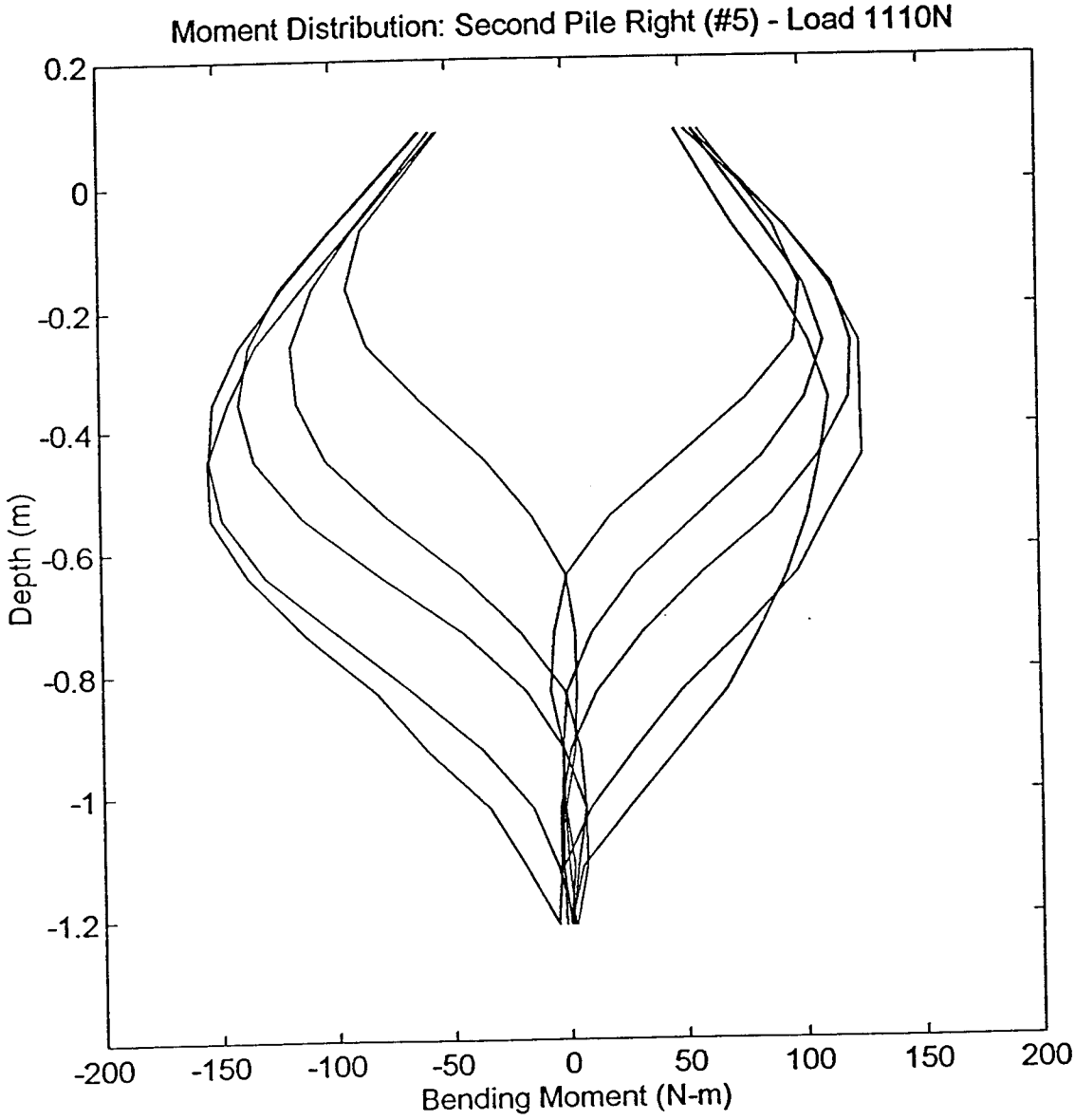
Moment Distribution: Second Pile Right (#5) - Load 1110N
0.2
0
-0.2
-0.4
-0.6
-0.8
-1
-1.2
Depth (m)
-200
-150
-100
-50
0
50
100
150
200
Bending Moment (N-m)

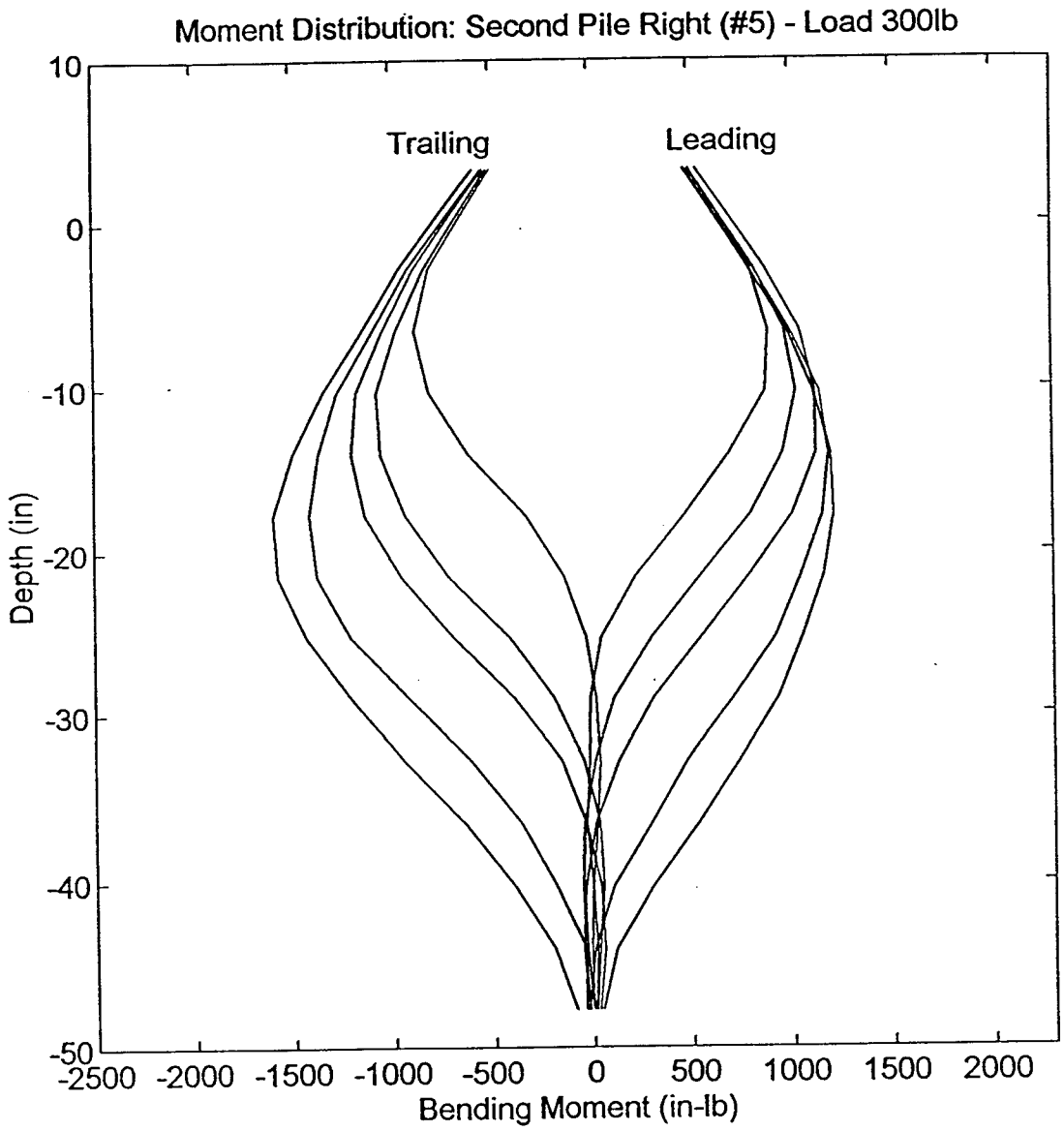
Moment Distribution: Second Pile Right (#5) - Load 300lb
Trailing
Leading
Depth (in)
10
0
-10
-20
-30
-40
-50
-2500
-2000
-1500
-1000
-500
0
500
1000
1500
2000
Bending Moment (in-lb)

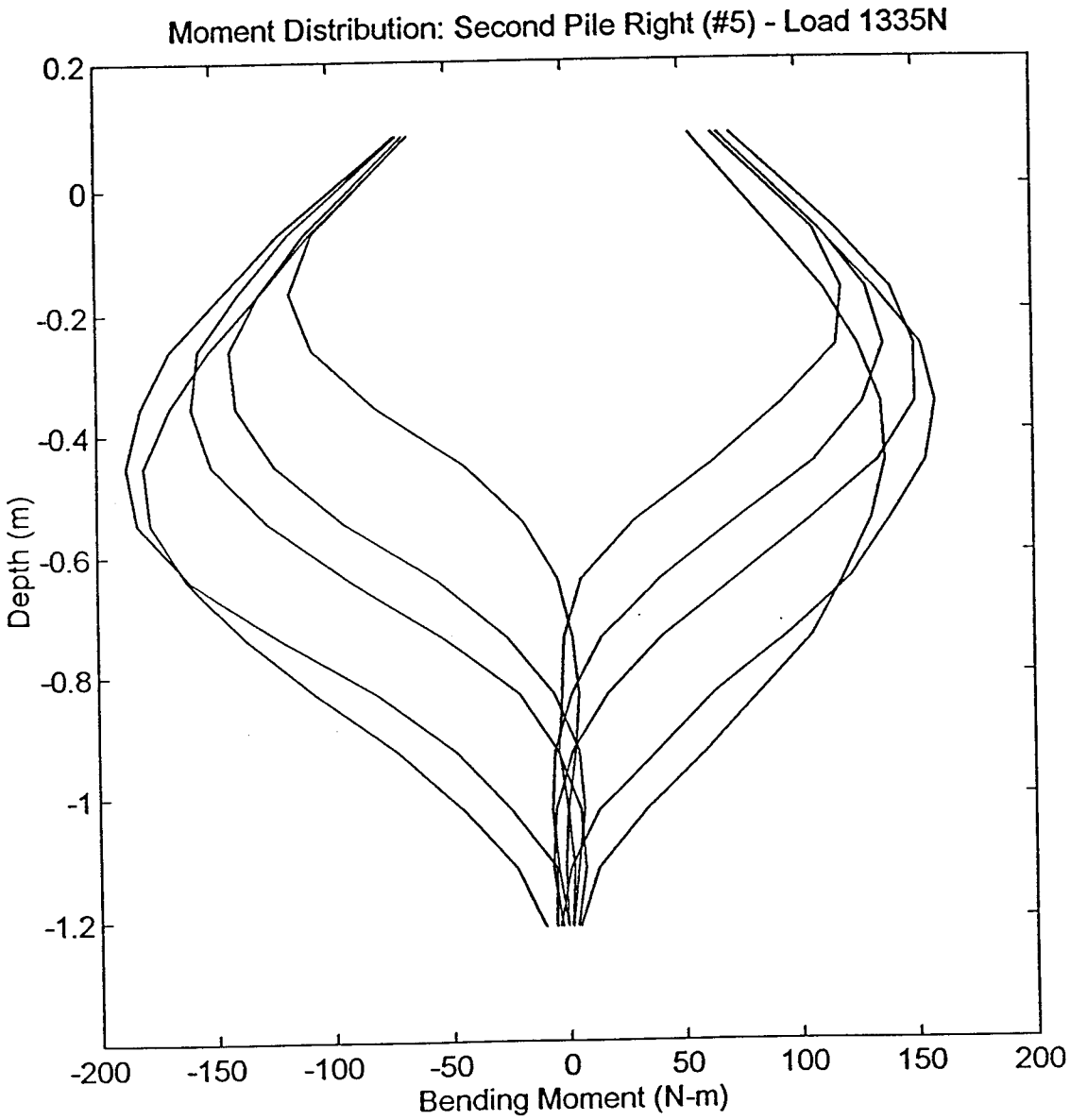
Moment Distribution: Second Pile Right (#5) - Load 1335N
0.2
0
-0.2
-0.4
-0.6
-0.8
-1
-1.2
Depth (m)
-200
-150
-100
-50
0
50
100
150
200
Bending Moment (N-m)

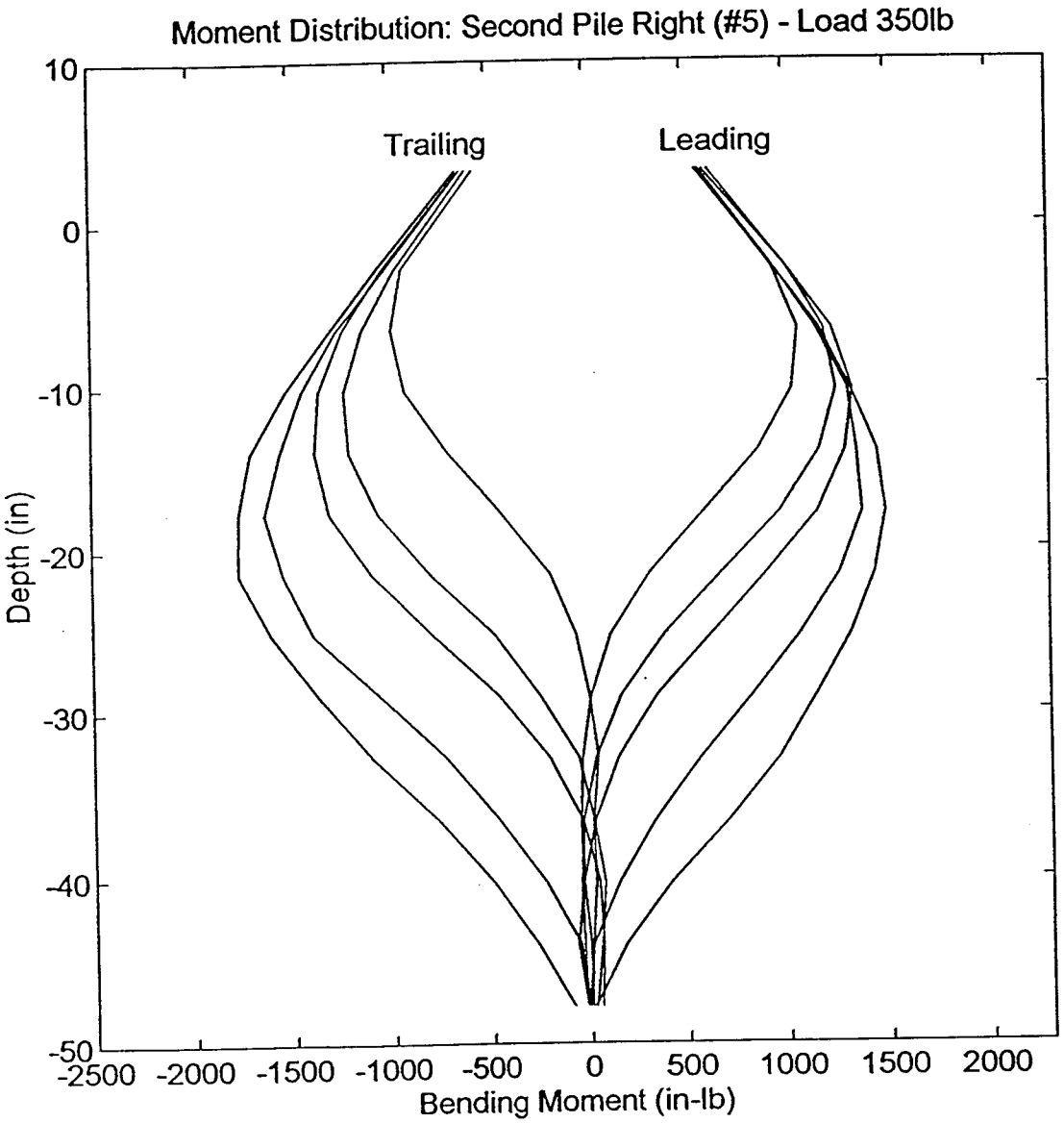
Moment Distribution: Second Pile Right (#5) - Load 350lb
Trailing
Leading
Depth (in)
10
0
-10
-20
-30
-40
-50
-2500
-2000
-1500
-1000
-500
0
500
1000
1500
2000
Bending Moment (in-lb)

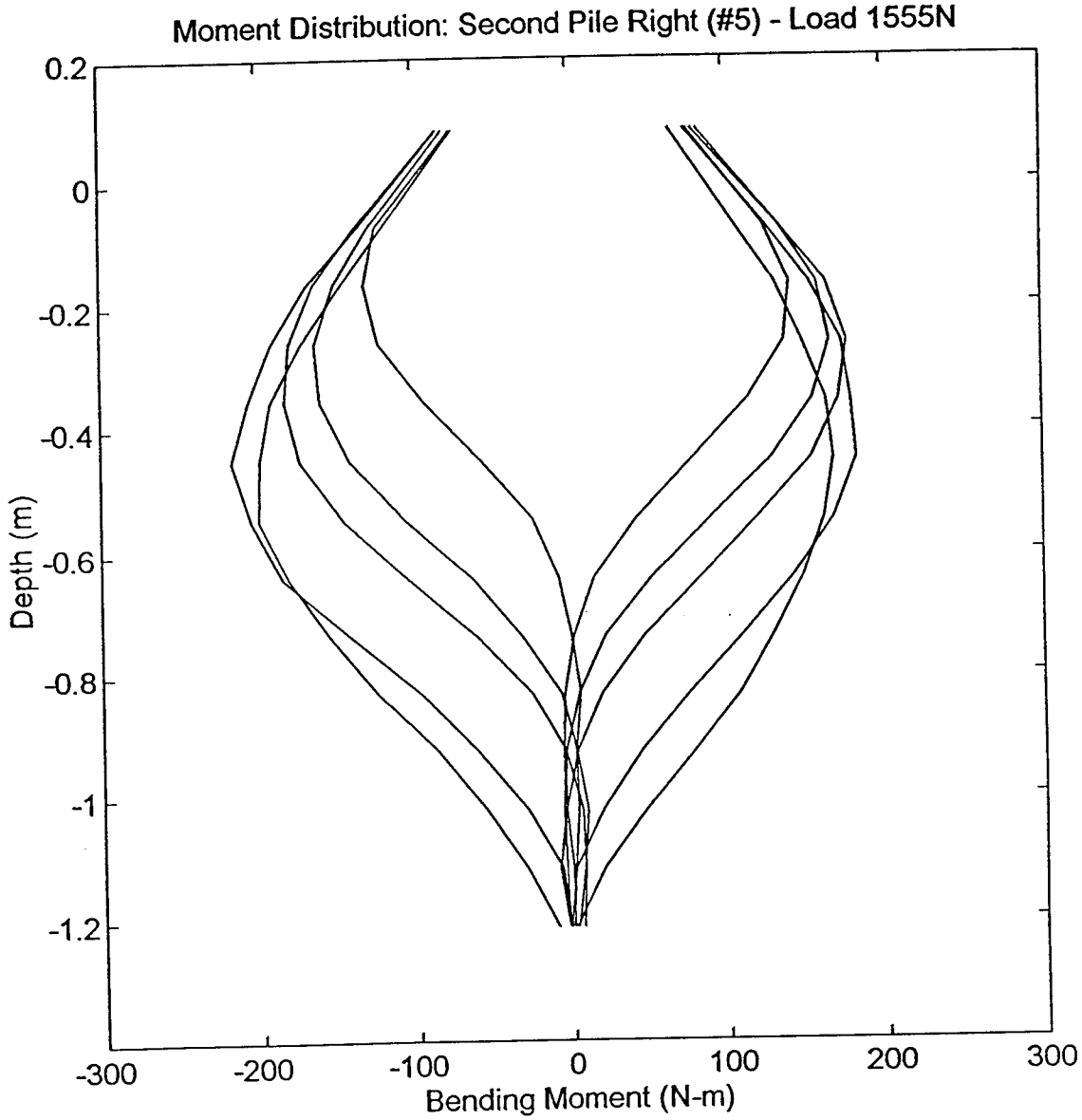
Moment Distribution: Second Pile Right (#5) - Load 1555N
0.2
0
-0.2
-0.4
-0.6
-0.8
-1
-1.2
Depth (m)
-300
-200
-100
0
100
200
300
Bending Moment (N-m)

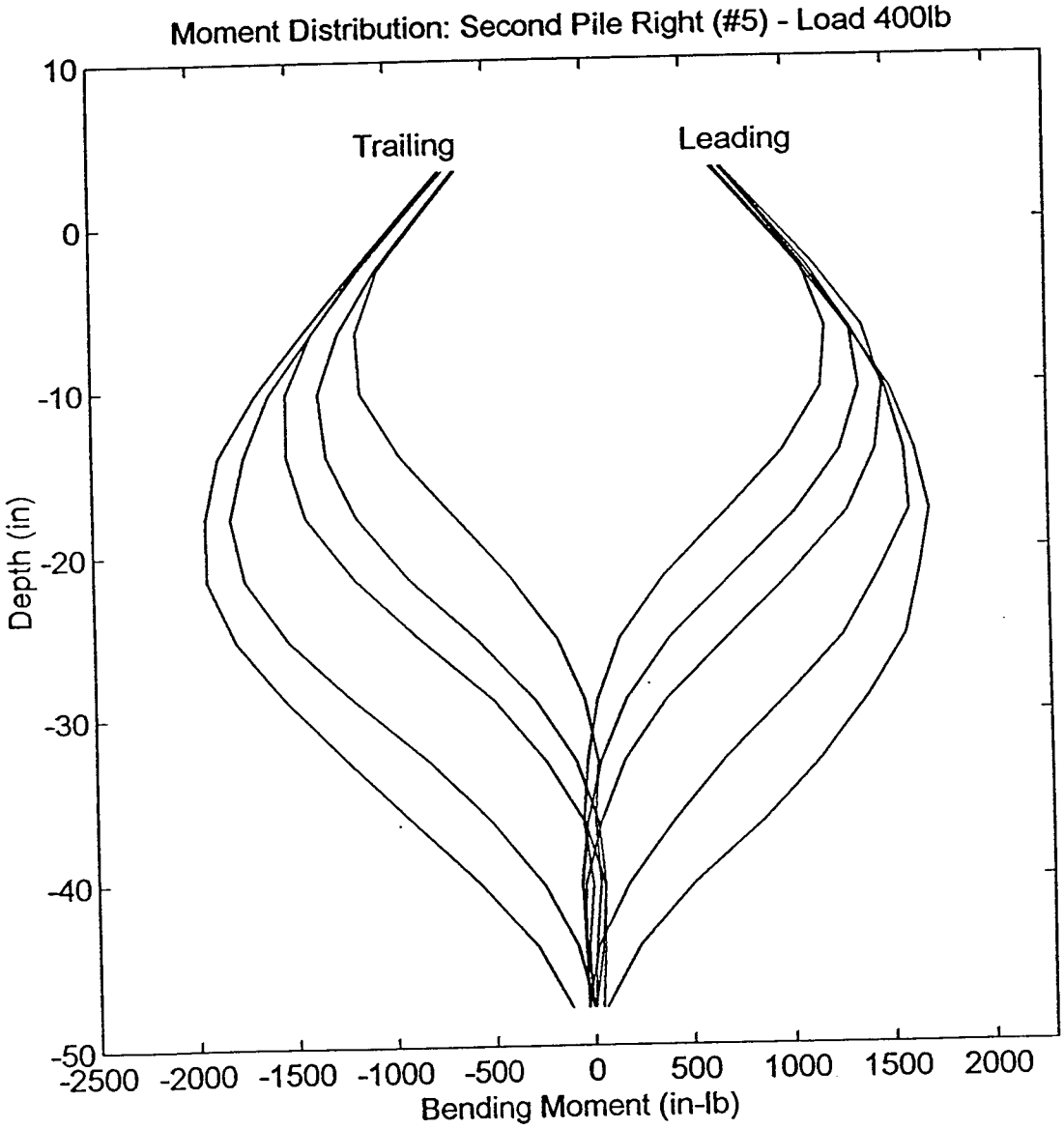
Moment Distribution: Second Pile Right (#5) - Load 400lb
Trailing
Leading
Depth (in)
10
0
-10
-20
-30
-40
-50
-2500
-2000
-1500
-1000
-500
0
500
1000
1500
2000
Bending Moment (in-lb)

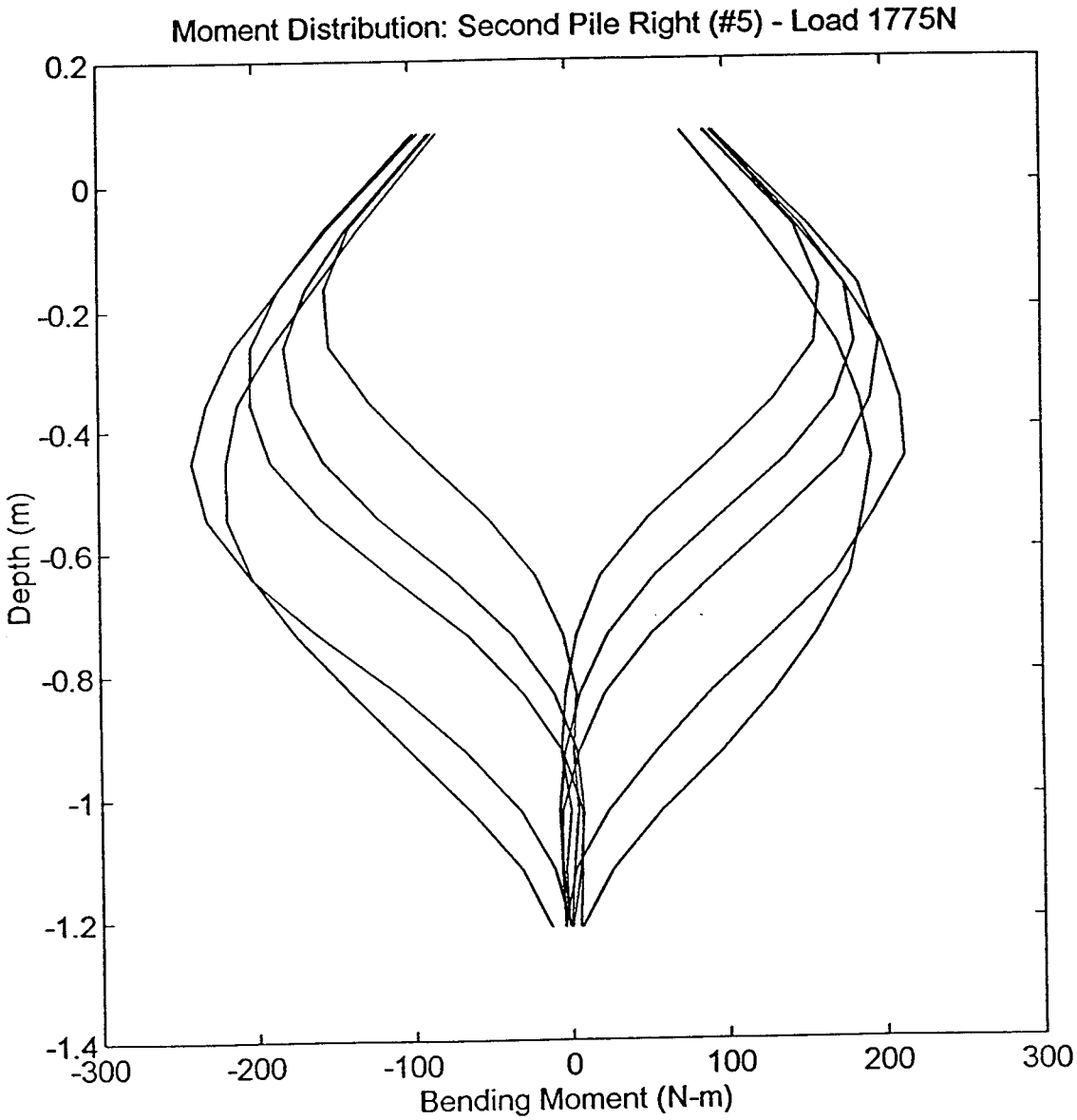
Moment Distribution: Second Pile Right (#5) - Load 1775N
0.2
0
-0.2
-0.4
-0.6
-0.8
-1
-1.2
-1.4
Depth (m)
-300
-200
-100
0
100
200
300
Bending Moment (N-m)

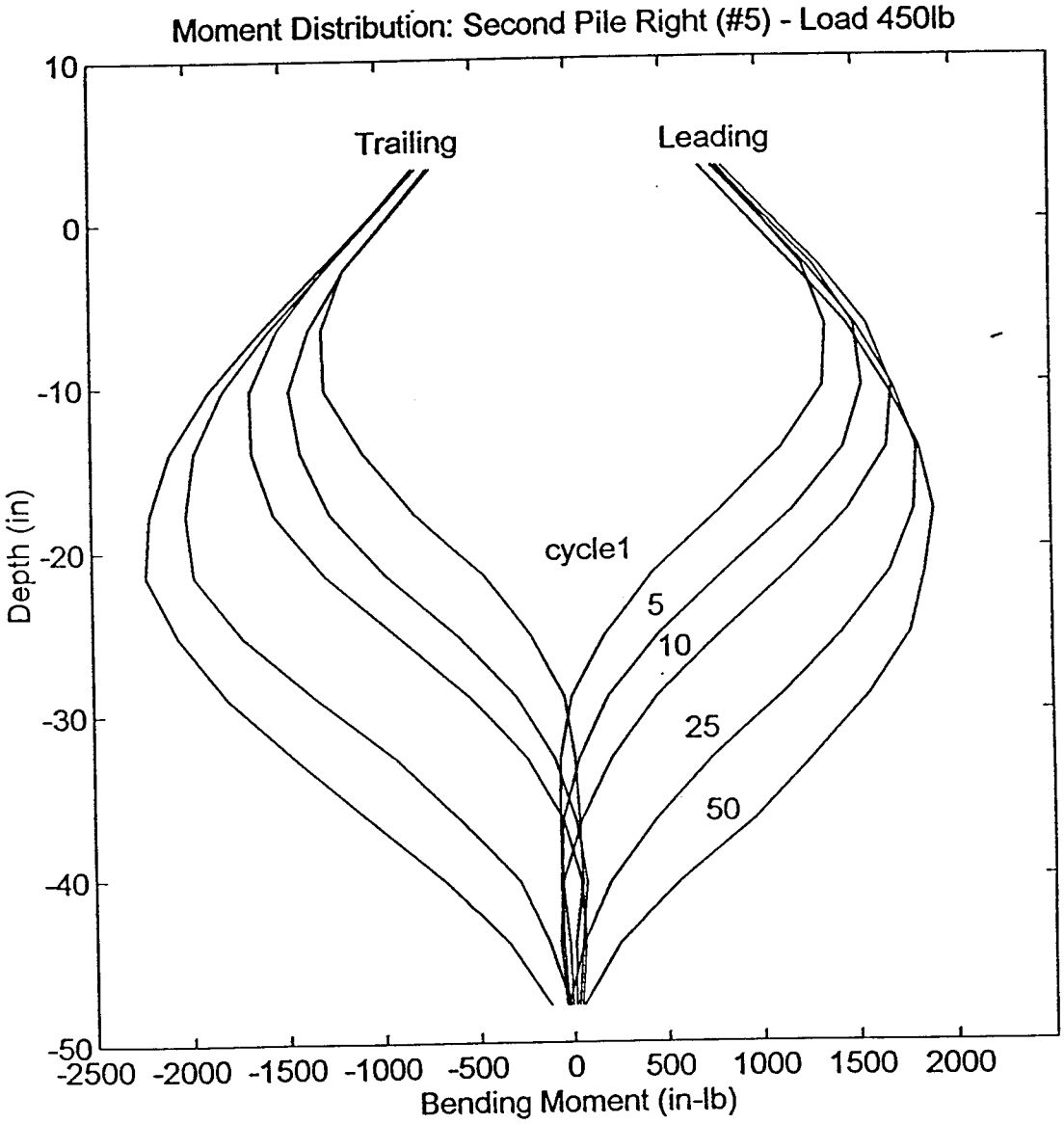
Moment Distribution: Second Pile Right (#5) - Load 450lb
Trailing
Leading
cycle1
5
10
25
50
Depth (in)
Bending Moment (in-lb)
10
0
-10
-20
-30
-40
-50
-2500
-2000
-1500
-1000
-500
0
500
1000
1500
2000

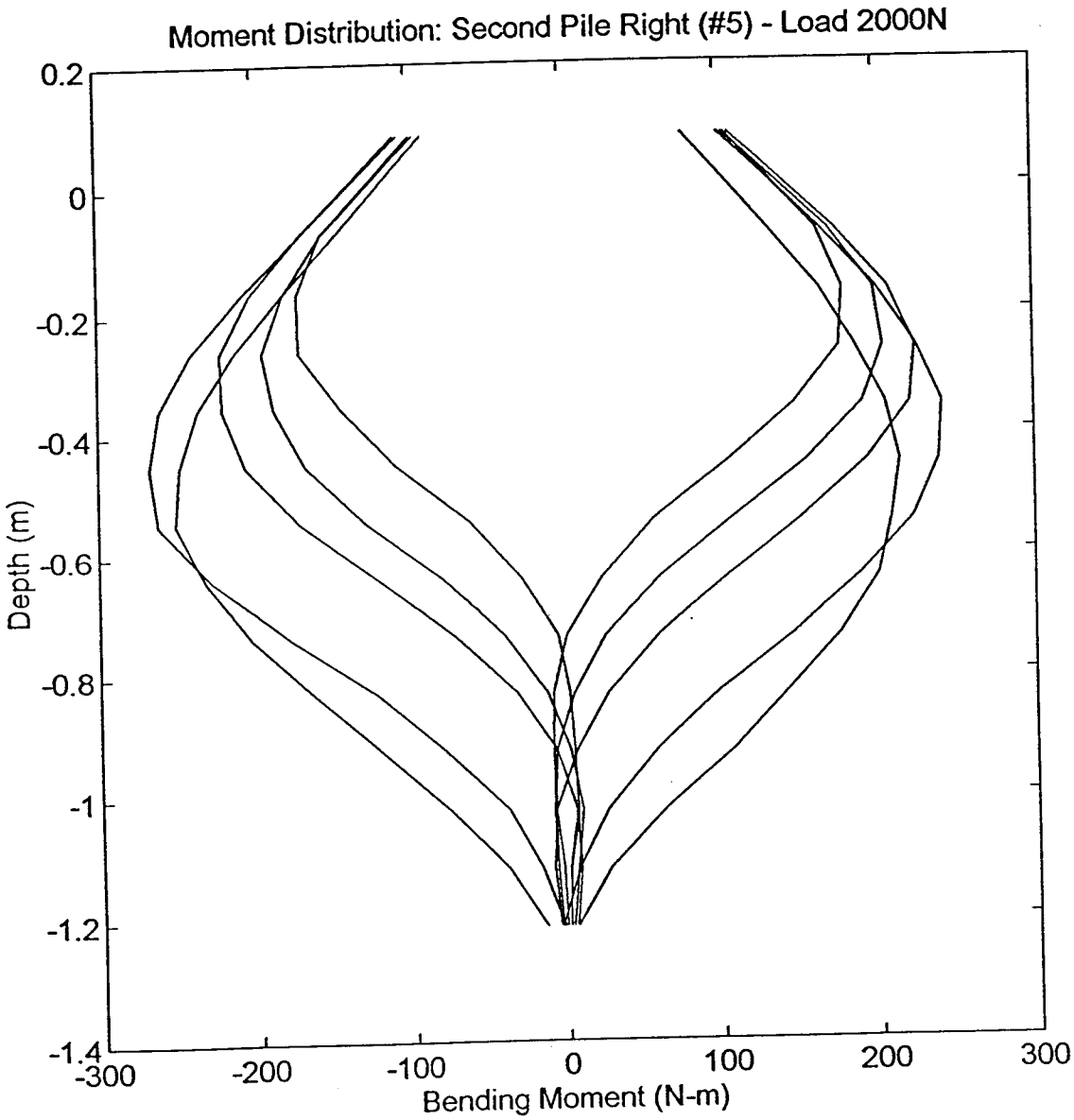
Moment Distribution: Second Pile Right (#5) - Load 2000N
0.2
0
-0.2
-0.4
-0.6
-0.8
-1
-1.2
-1.4
Depth (m)
-300
-200
-100
0
100
200
300
Bending Moment (N-m)

Figure B10. Moment distribution for pile 6 (next 14 plots).

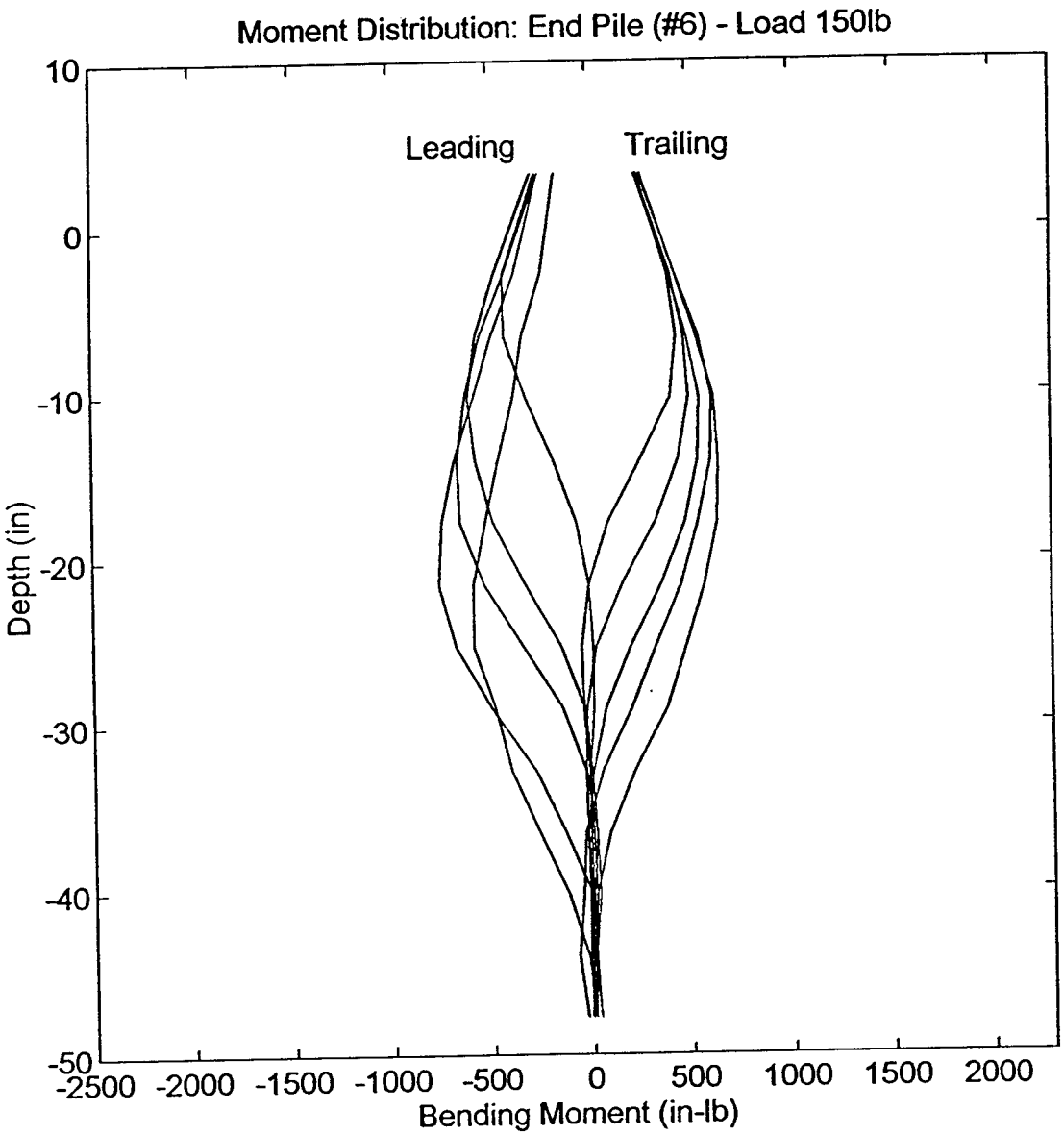
Moment Distribution: End Pile (#6) - Load 150lb
Leading
Trailing
10
0
-10
-20
-30
-40
-50
Depth (in)
-2500
-2000
-1500
-1000
-500
0
500
1000
1500
2000
Bending Moment (in-lb)

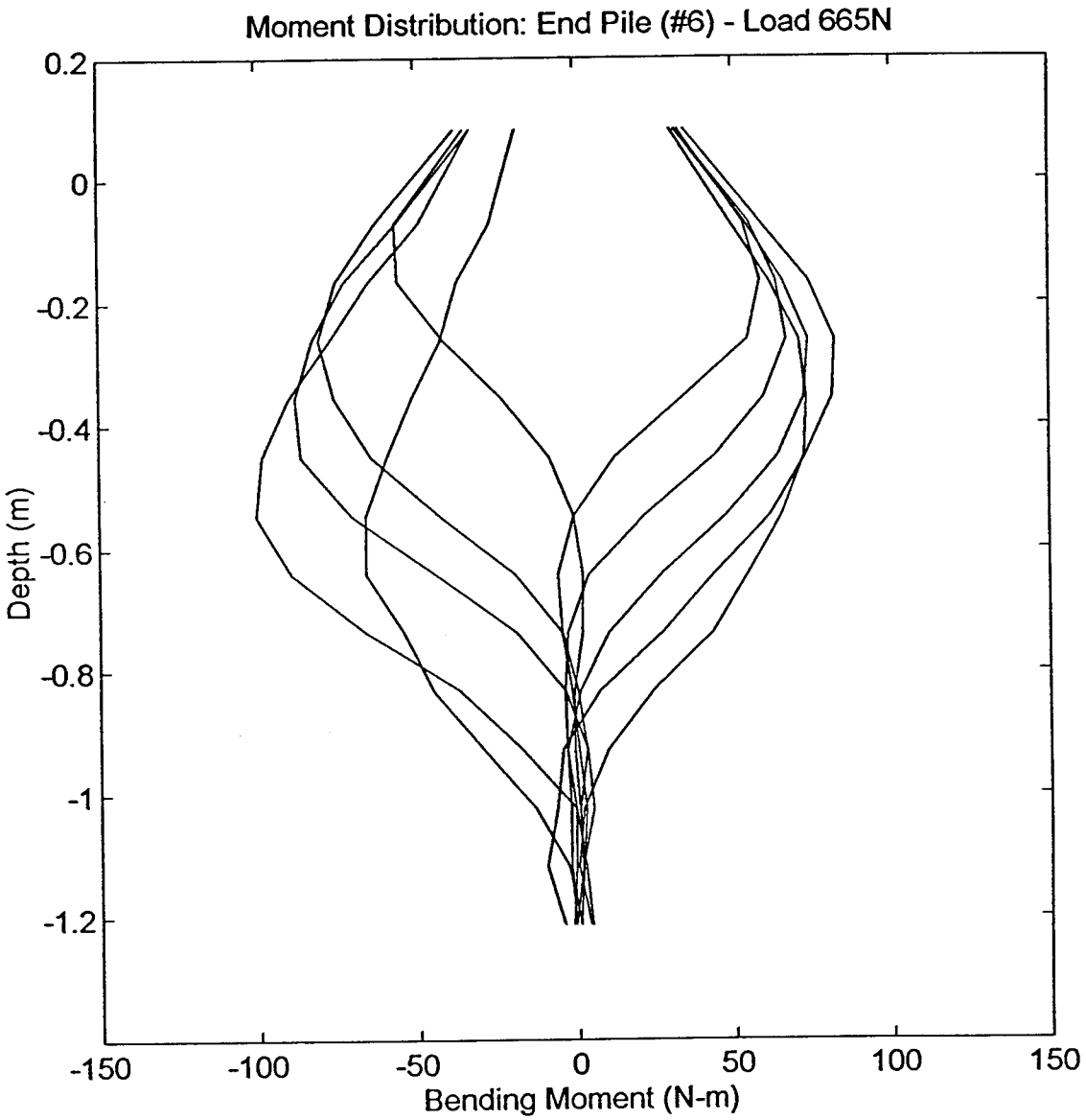
Moment Distribution: End Pile (#6) - Load 665N
0.2
0
-0.2
-0.4
-0.6
-0.8
-1
-1.2
Depth (m)
-150
-100
-50
0
50
100
150
Bending Moment (N-m)

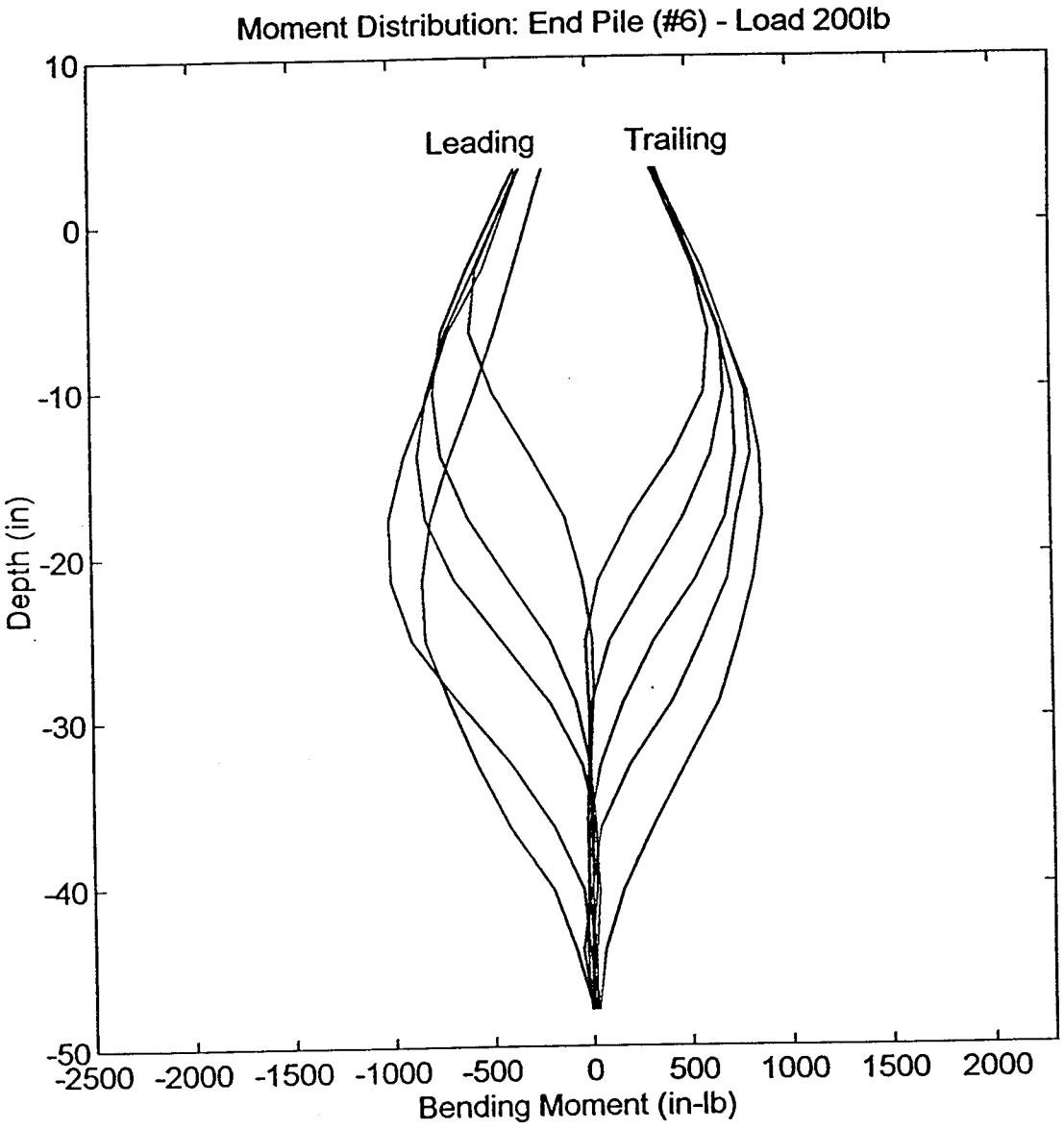
Moment Distribution: End Pile (#6) - Load 200lb
Leading
Trailing
10
0
-10
-20
-30
-40
-50
Depth (in)
-2500
-2000
-1500
-1000
-500
0
500
1000
1500
2000
Bending Moment (in-lb)

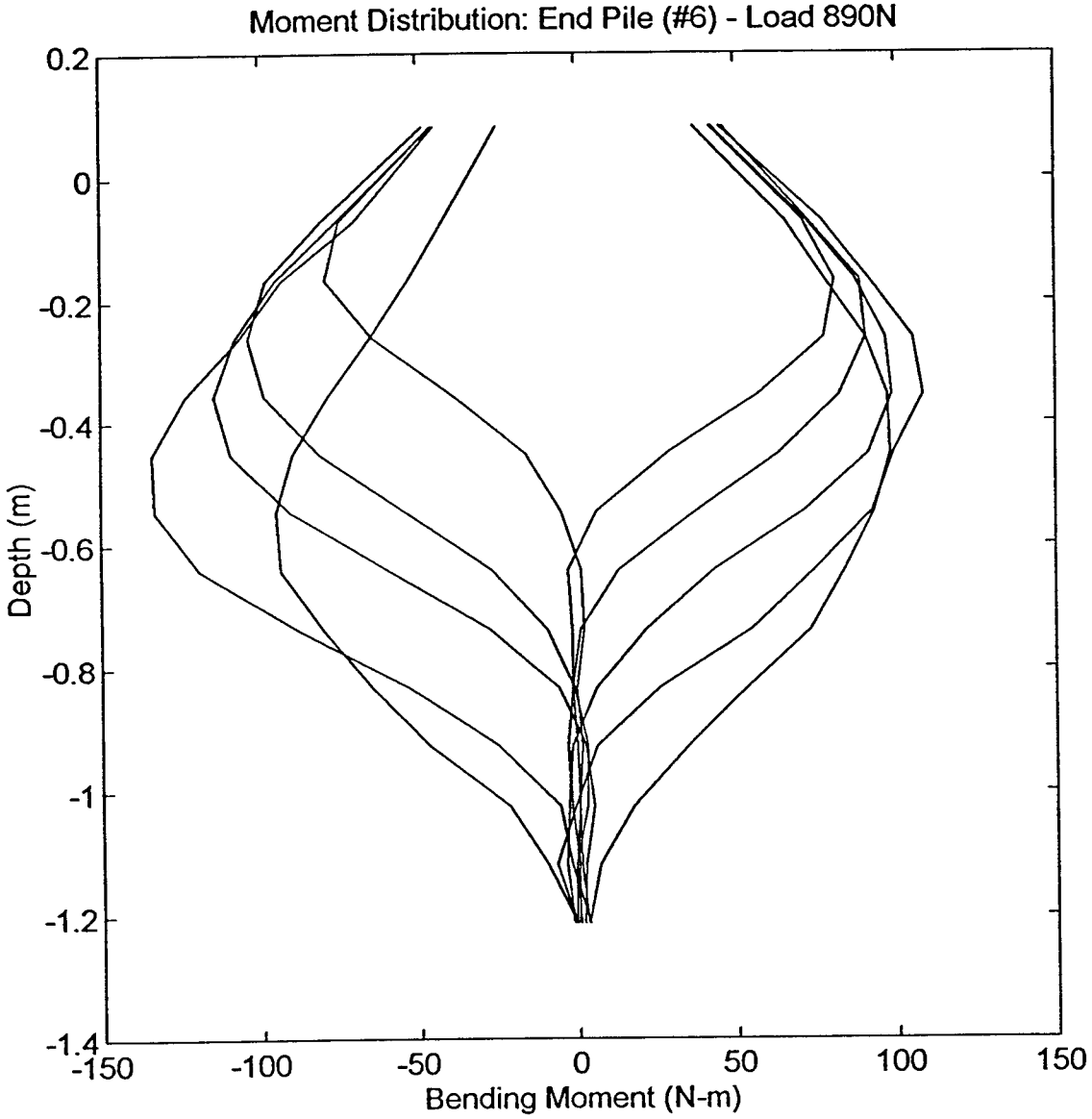
Moment Distribution: End Pile (#6) - Load 890N
0.2
0
-0.2
-0.4
-0.6
-0.8
-1
-1.2
-1.4
Depth (m)
-150
-100
-50
0
50
100
150
Bending Moment (N-m)

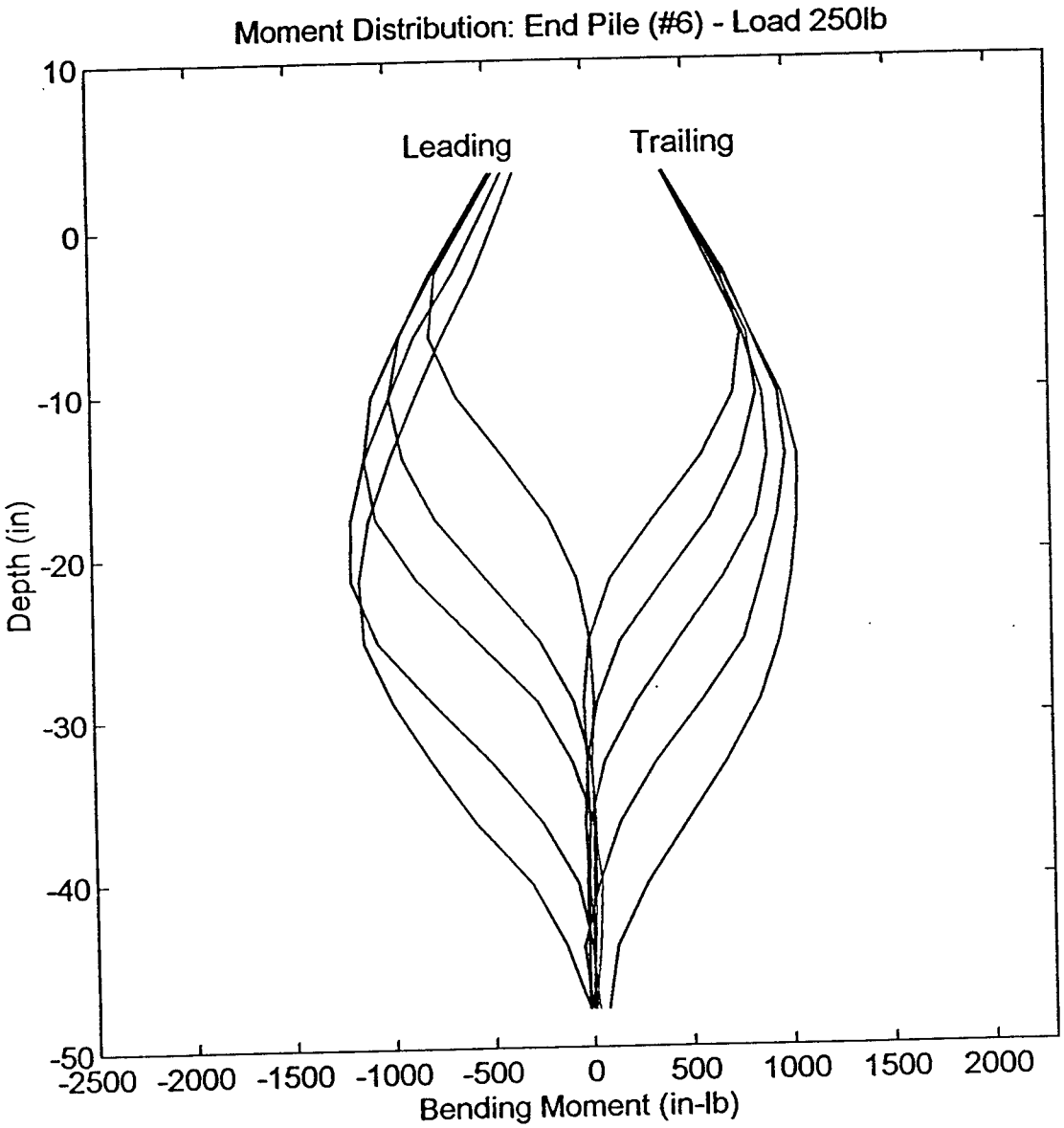
Moment Distribution: End Pile (#6) - Load 250lb
Leading
Trailing
Depth (in)
10
0
-10
-20
-30
-40
-50
-2500
-2000
-1500
-1000
-500
0
500
1000
1500
2000
Bending Moment (in-lb)

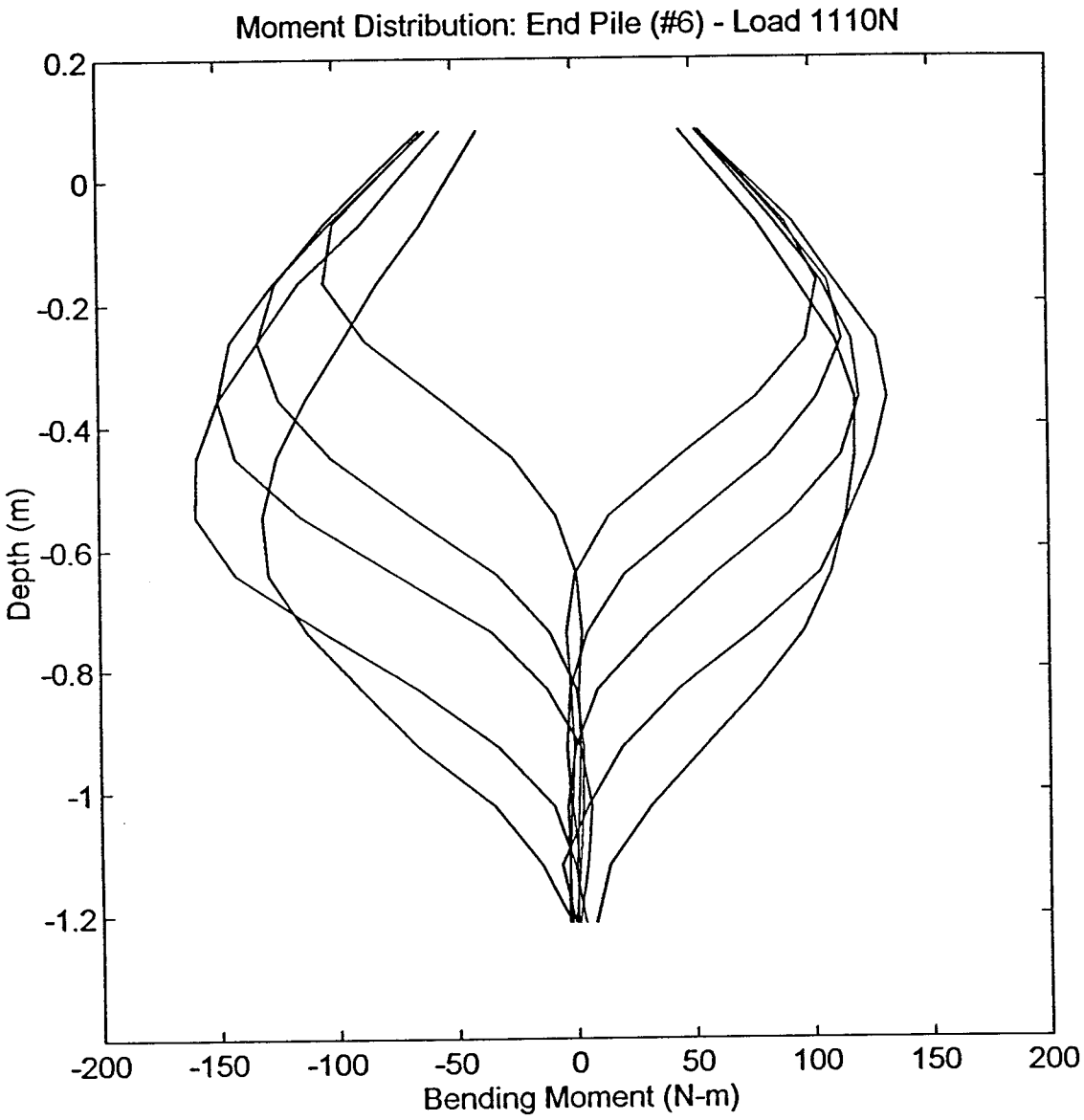
Moment Distribution: End Pile (#6) - Load 1110N
0.2
0
-0.2
-0.4
-0.6
-0.8
-1
-1.2
Depth (m)
-200
-150
-100
-50
0
50
100
150
200
Bending Moment (N-m)

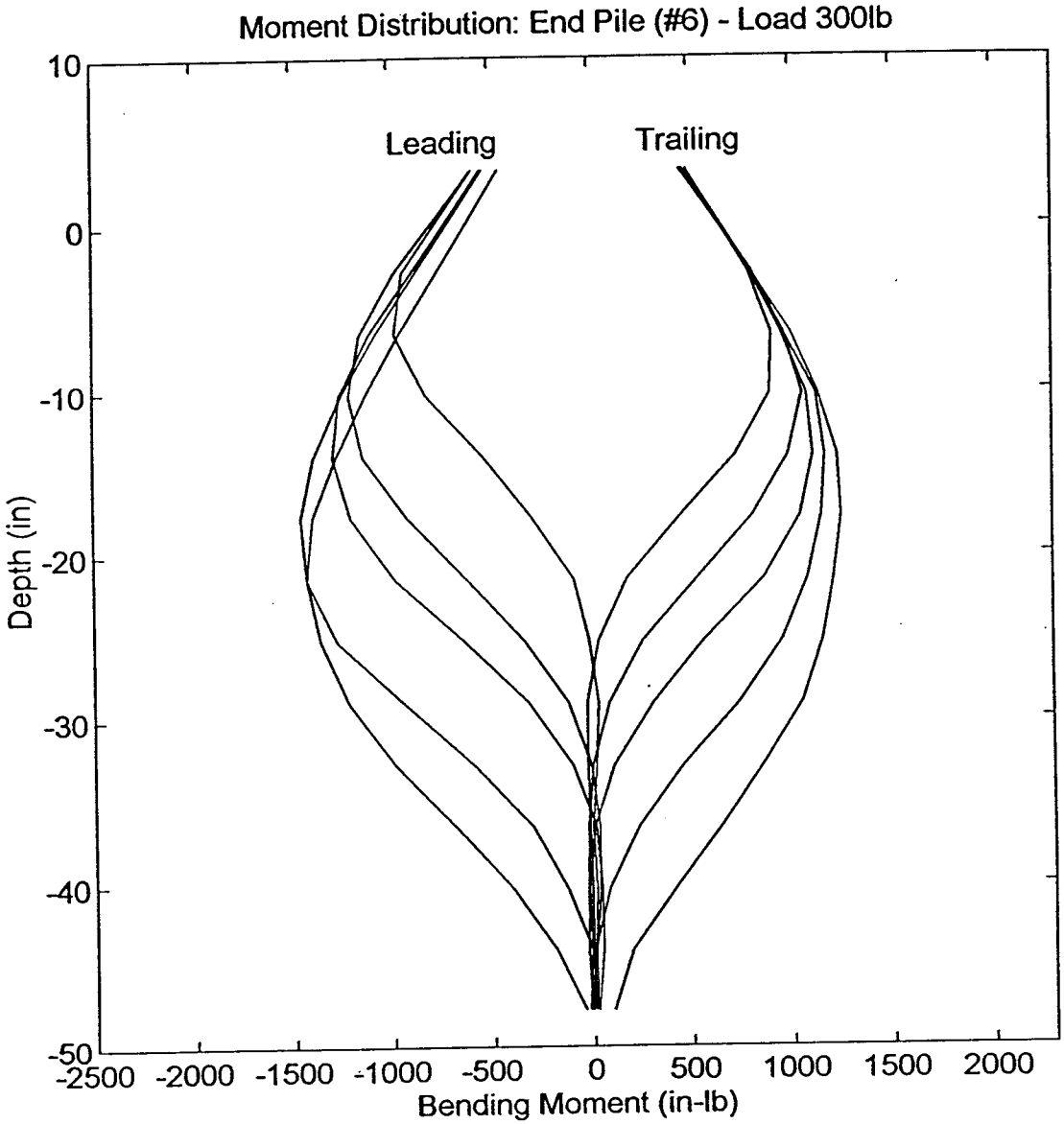
Moment Distribution: End Pile (#6) - Load 300lb
Leading
Trailing
Depth (in)
10
0
-10
-20
-30
-40
-50
-2500
-2000
-1500
-1000
-500
0
500
1000
1500
2000
Bending Moment (in-lb)

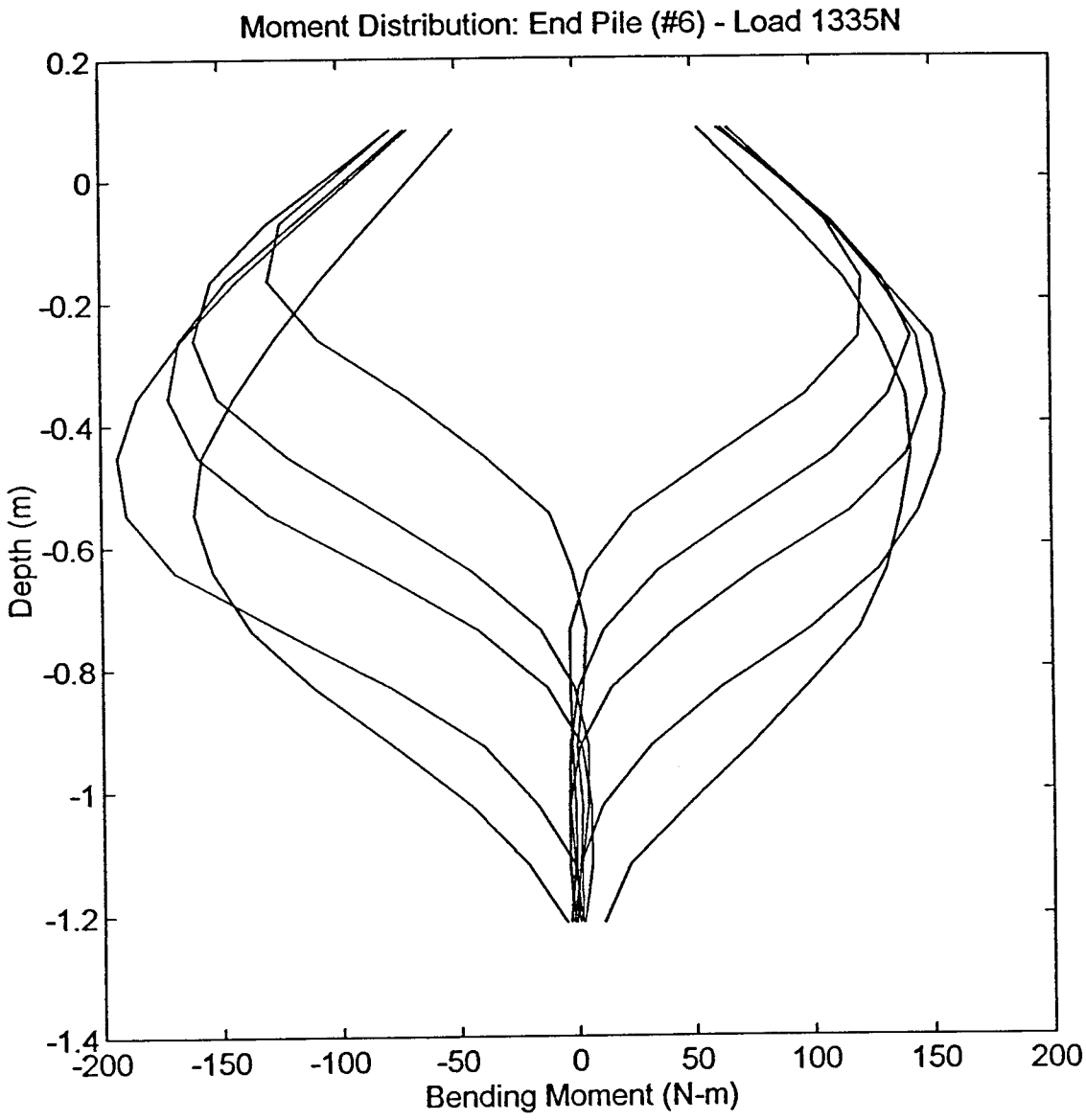
Moment Distribution: End Pile (#6) - Load 1335N
0.2
0
-0.2
-0.4
-0.6
-0.8
-1
-1.2
-1.4
Depth (m)
-200
-150
-100
-50
0
50
100
150
200
Bending Moment (N-m)

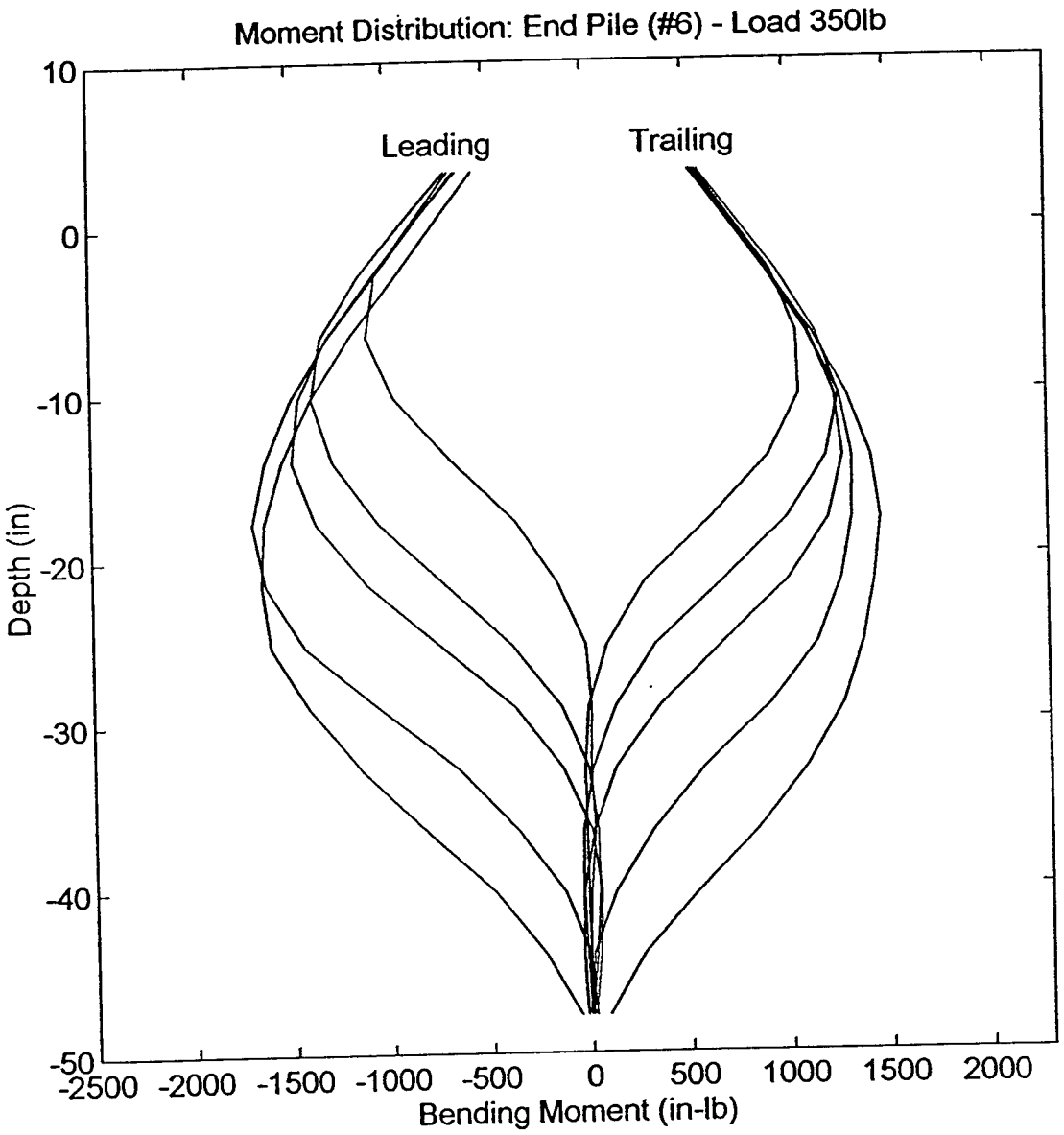
Moment Distribution: End Pile (#6) - Load 350lb
Leading
Trailing
10
0
-10
-20
-30
-40
-50
Depth (in)
-2500
-2000
-1500
-1000
-500
0
500
1000
1500
2000
Bending Moment (in-lb)

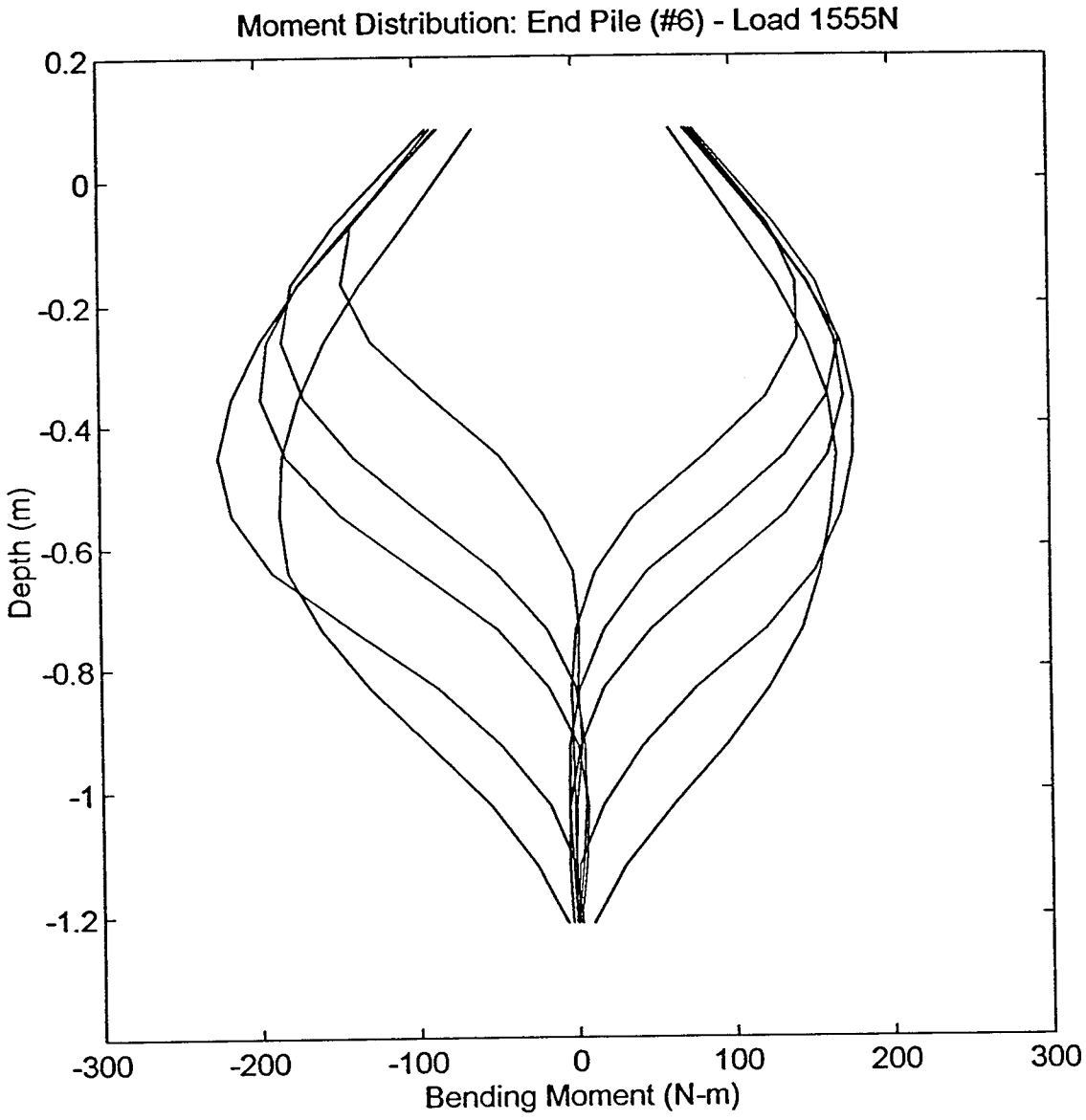
Moment Distribution: End Pile (#6) - Load 1555N
0.2
0
-0.2
-0.4
-0.6
-0.8
-1
-1.2
Depth (m)
-300
-200
-100
0
100
200
300
Bending Moment (N-m)

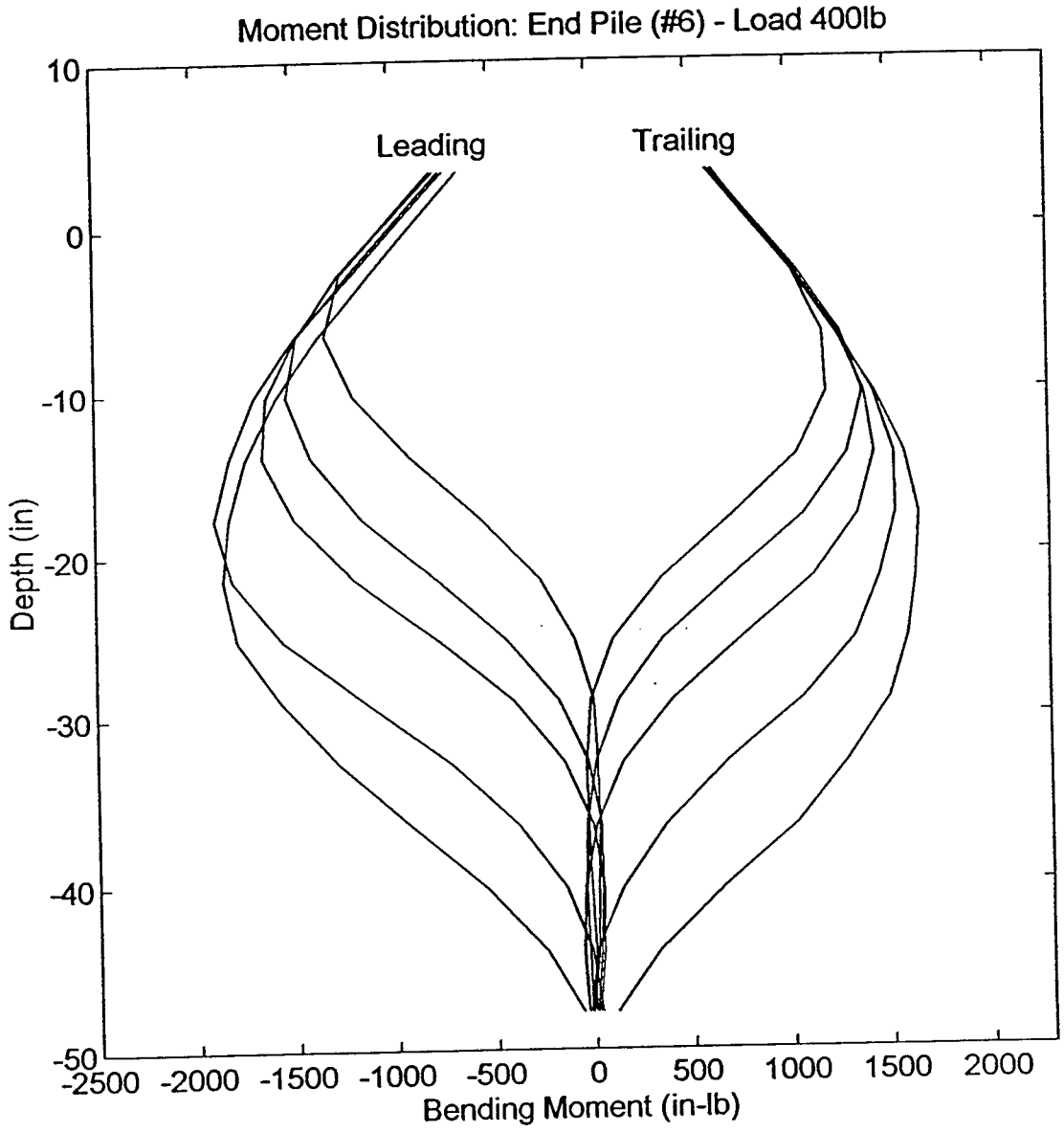
Moment Distribution: End Pile (#6) - Load 400lb
Leading
Trailing
10
0
-10
-20
-30
-40
-50
Depth (in)
-2500
-2000
-1500
-1000
-500
0
500
1000
1500
2000
Bending Moment (in-lb)

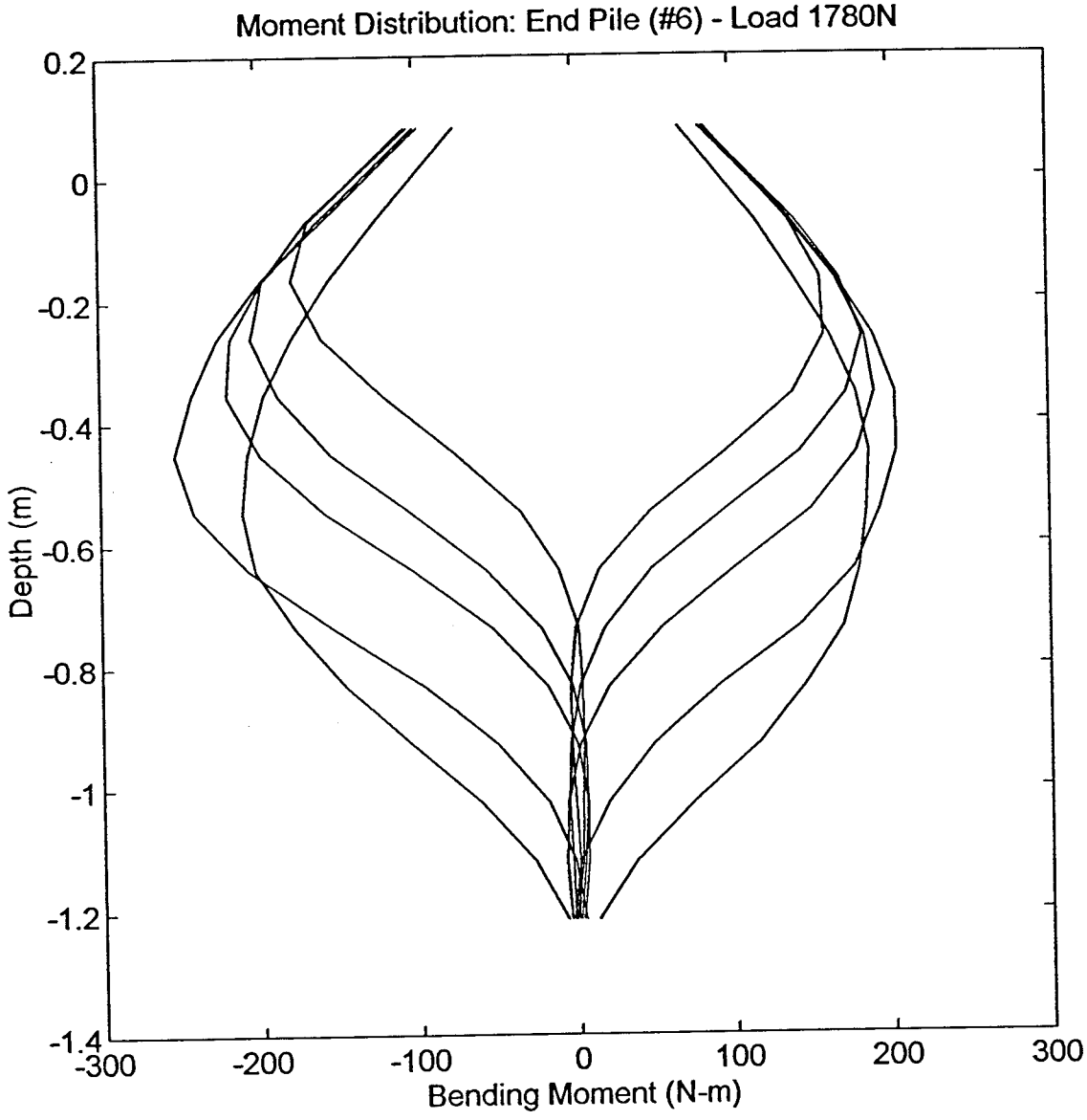
Moment Distribution: End Pile (#6) - Load 1780N
0.2
0
-0.2
-0.4
-0.6
-0.8
-1
-1.2
-1.4
Depth (m)
-300
-200
-100
0
100
200
300
Bending Moment (N-m)

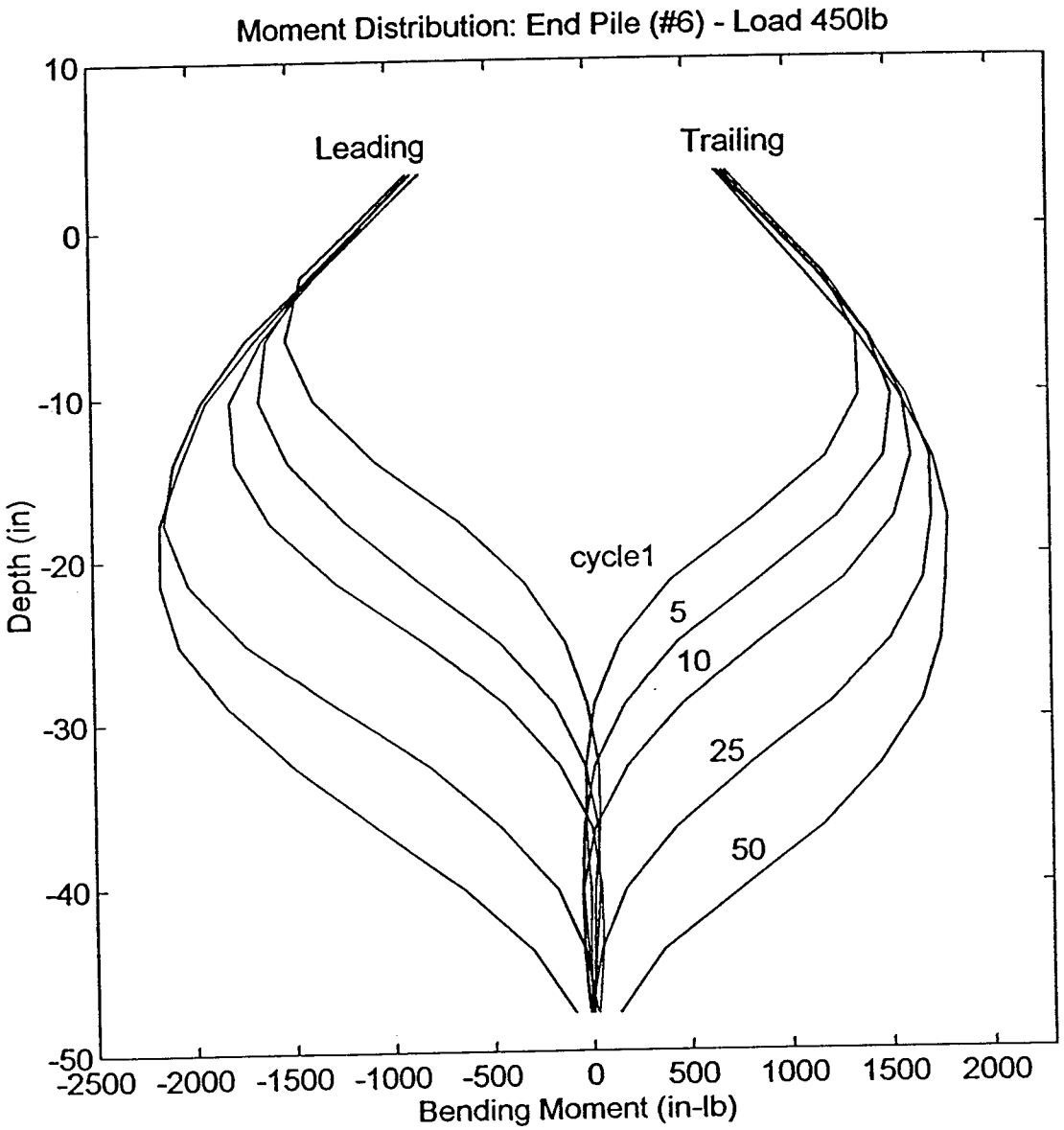
Moment Distribution: End Pile (#6) - Load 450lb
Leading
Trailing
cycle1
5
10
25
50
Depth (in)
Bending Moment (in-lb)
10
0
-10
-20
-30
-40
-50
-2500
-2000
-1500
-1000
-500
0
500
1000
1500
2000

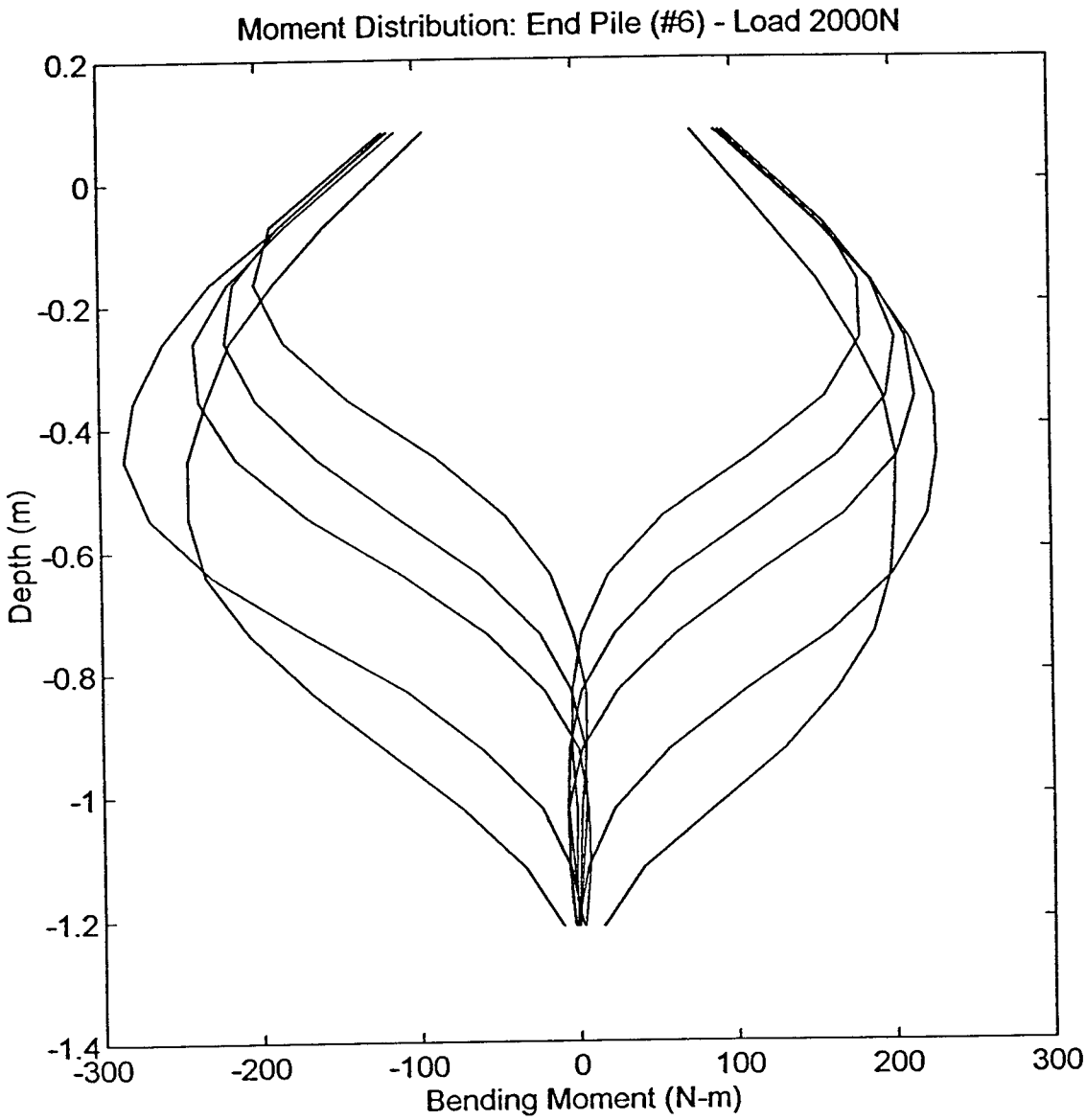
Moment Distribution: End Pile (#6) - Load 2000N
0.2
0
-0.2
-0.4
-0.6
-0.8
-1
-1.2
-1.4
Depth (m)
-300
-200
-100
0
100
200
300
Bending Moment (N-m)

Figure B11. Load distribution @ cycle 1 (next 14 plots).

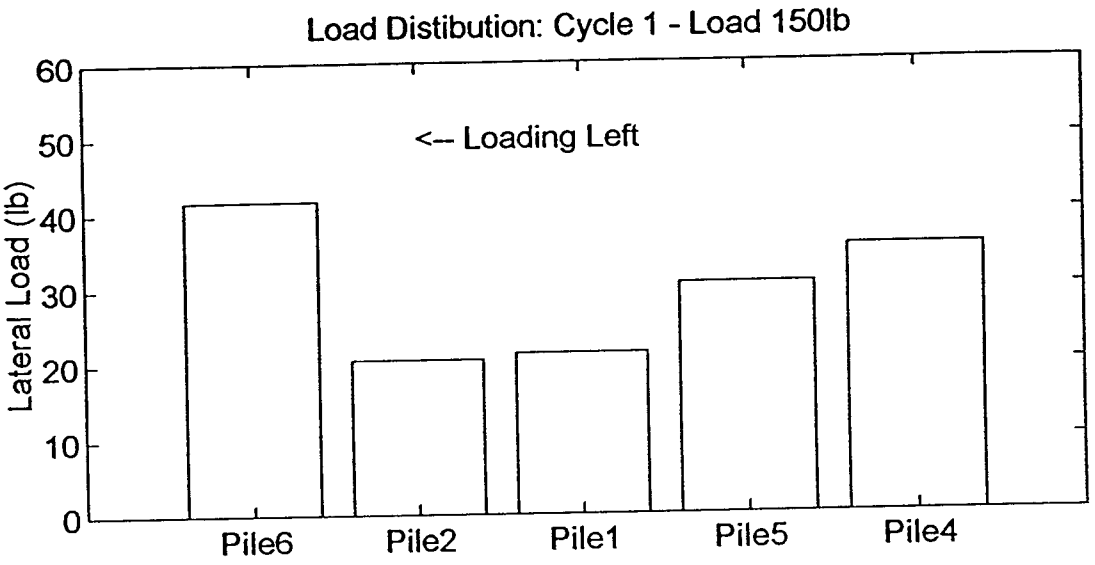
Load Distibution: Cycle 1 - Load 150lb
<-- Loading Left
Lateral Load (lb)
60
50
40
30
20
10
0
Pile6
Pile2
Pile1
Pile5
Pile4

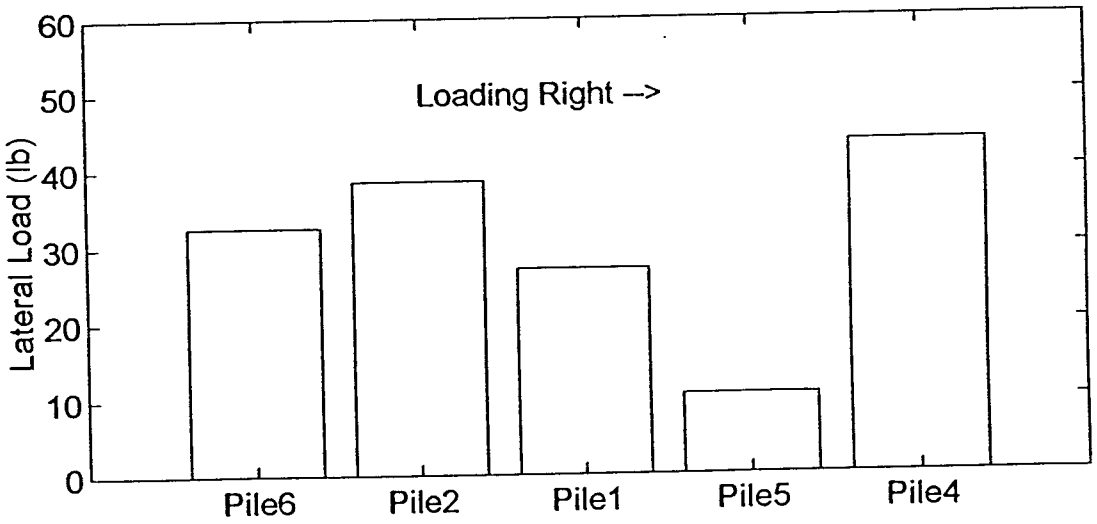
Loading Right -->
Lateral Load (lb)
60
50
40
30
20
10
0
Pile6
Pile2
Pile1
Pile5
Pile4

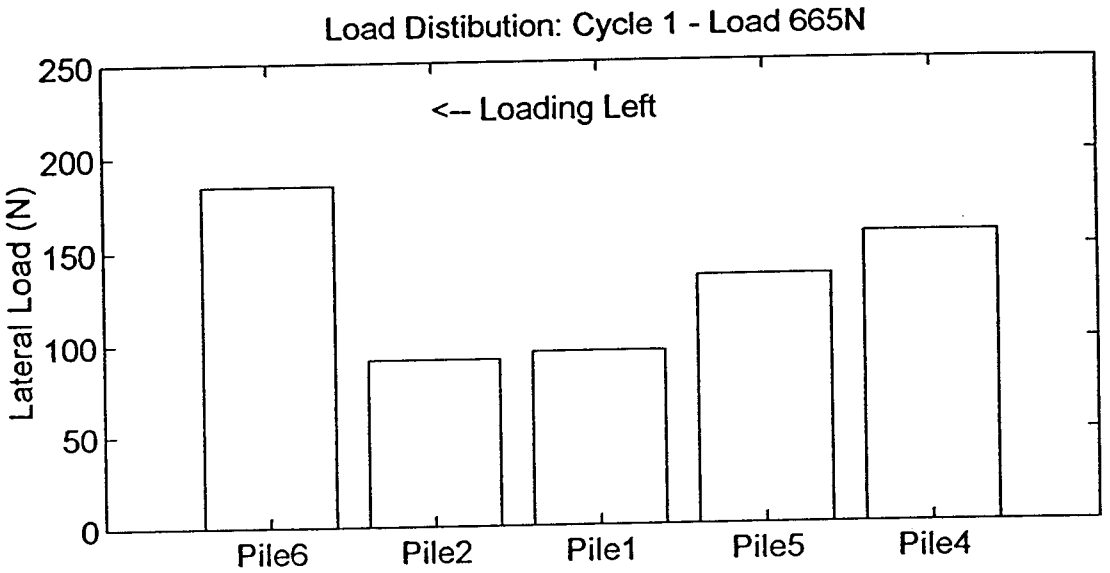
Load Distibution: Cycle 1 - Load 665N
<-- Loading Left
Lateral Load (N)
250
200
150
100
50
0
Pile6
Pile2
Pile1
Pile5
Pile4

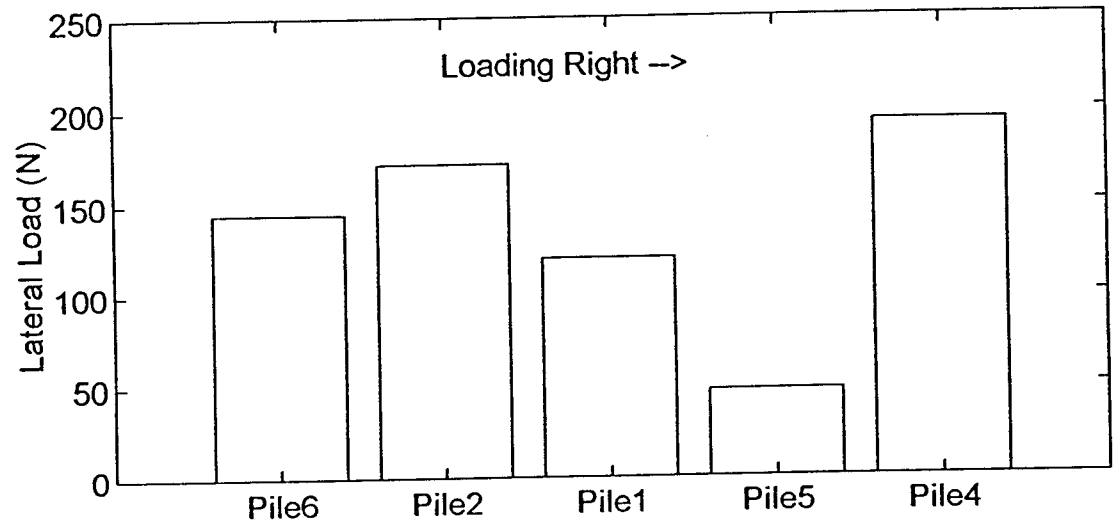
Loading Right -->
Lateral Load (N)
250
200
150
100
50
0
Pile6
Pile2
Pile1
Pile5
Pile4

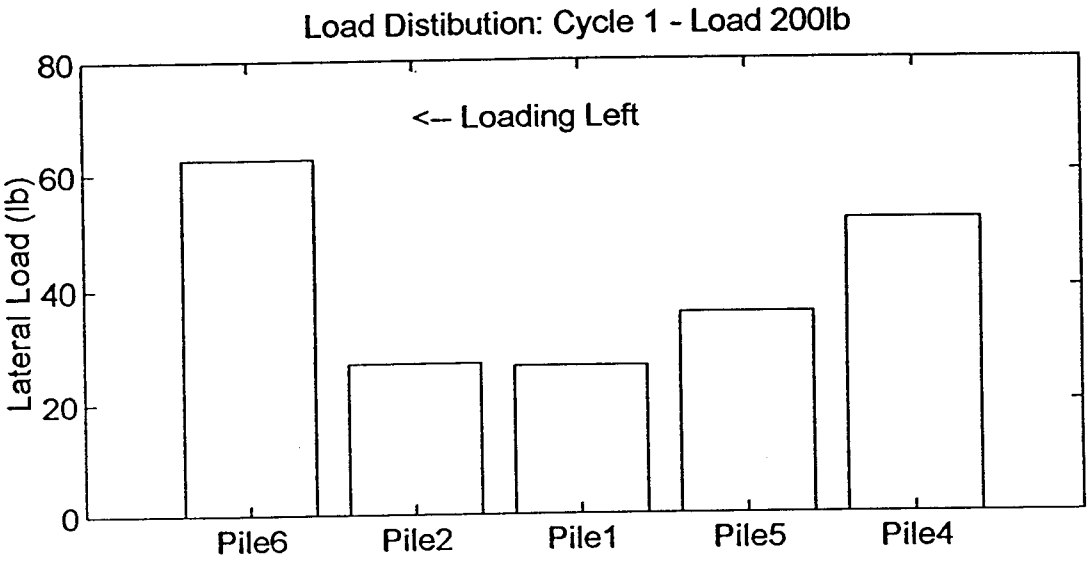
Load Distibution: Cycle 1 - Load 200lb
<-- Loading Left
Lateral Load (lb)
80
60
40
20
0
Pile6
Pile2
Pile1
Pile5
Pile4

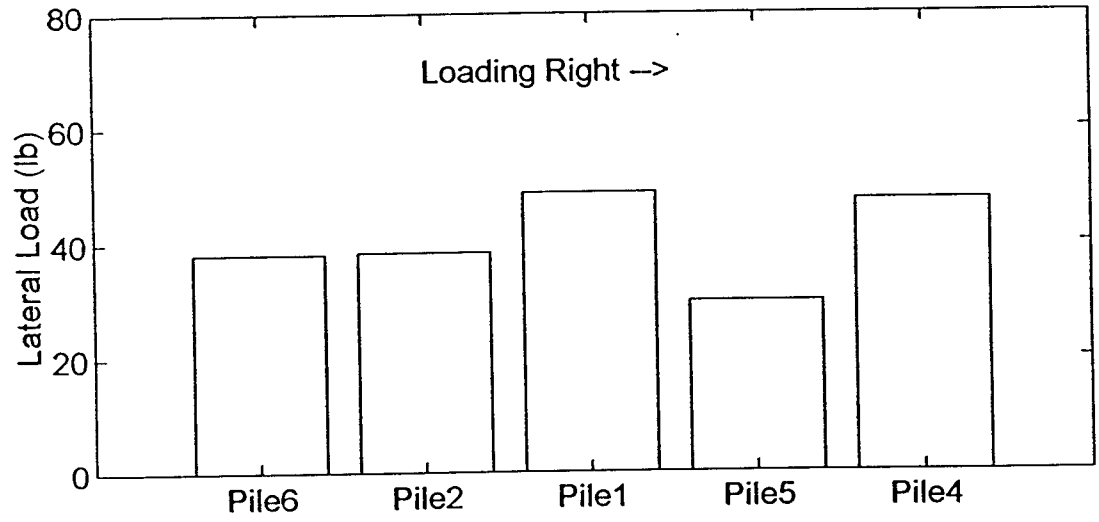
Loading Right -->
Lateral Load (lb)
80
60
40
20
0
Pile6
Pile2
Pile1
Pile5
Pile4

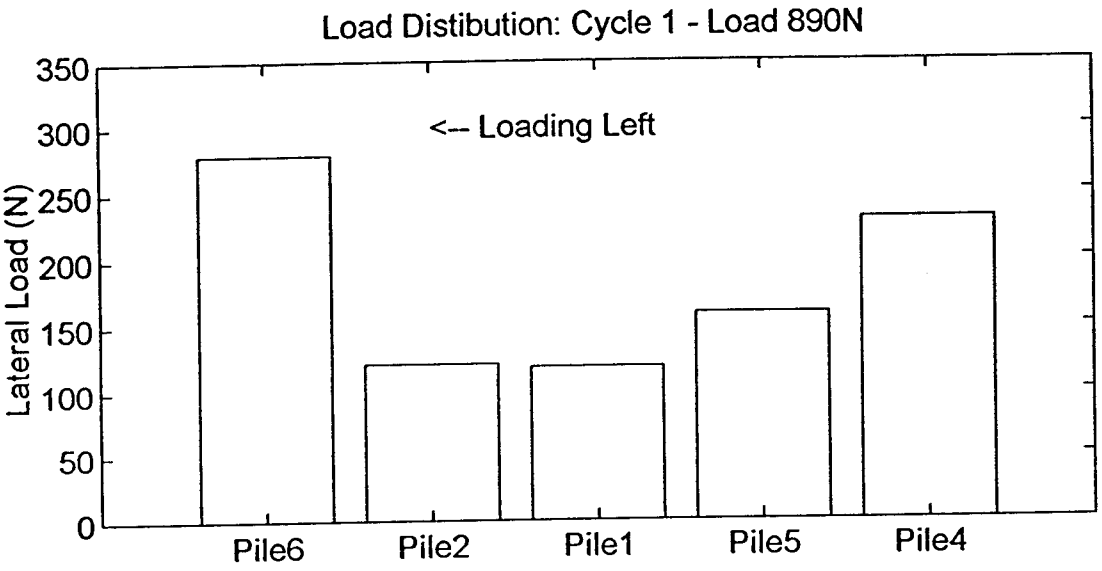
Load Distibution: Cycle 1 - Load 890N
<-- Loading Left
Lateral Load (N)
350
300
250
200
150
100
50
0
Pile6
Pile2
Pile1
Pile5
Pile4

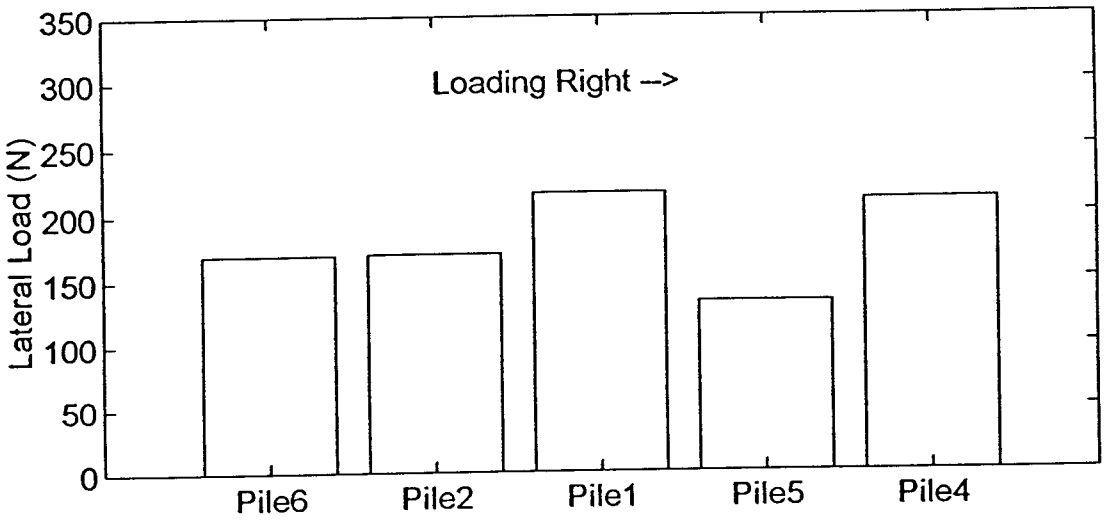
Loading Right -->
Lateral Load (N)
350
300
250
200
150
100
50
0
Pile6
Pile2
Pile1
Pile5
Pile4

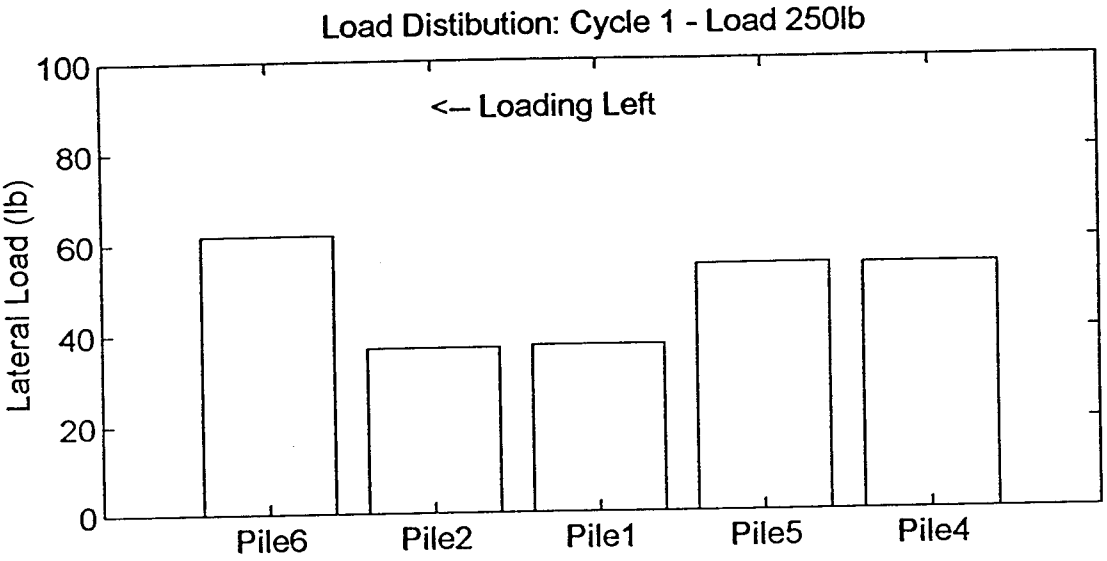
Load Distibution: Cycle 1 - Load 250lb
<-- Loading Left
Lateral Load (lb)
100
80
60
40
20
0
Pile6
Pile2
Pile1
Pile5
Pile4

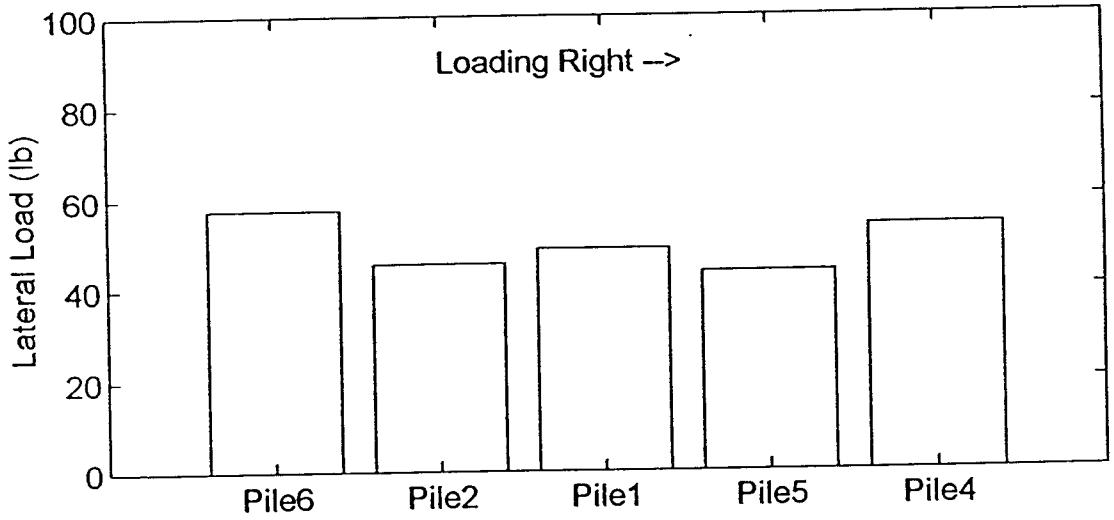
Loading Right -->
Lateral Load (lb)
100
80
60
40
20
0
Pile6
Pile2
Pile1
Pile5
Pile4

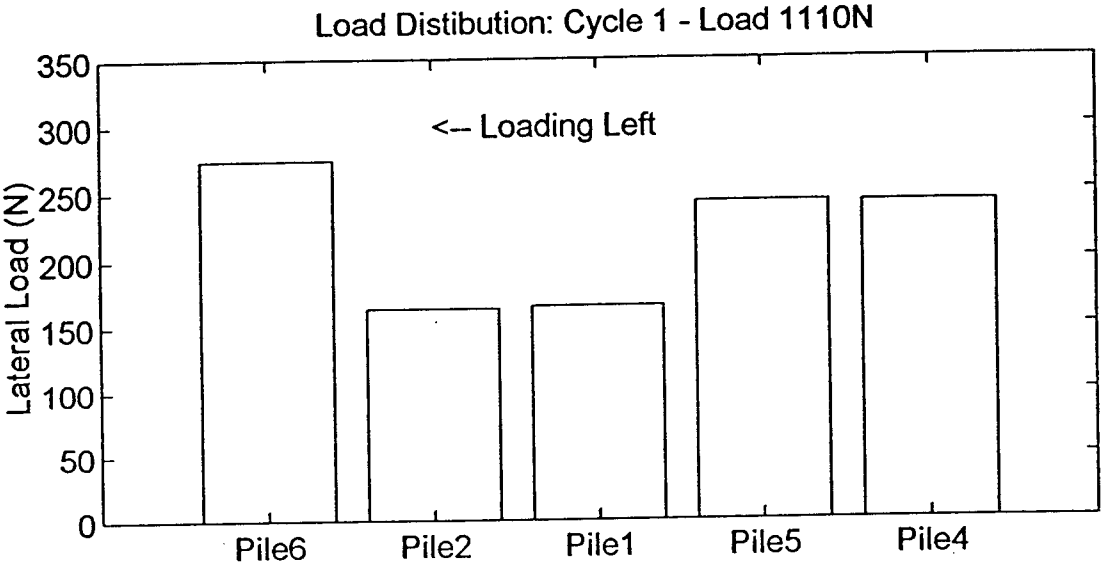
Load Distibution: Cycle 1 - Load 1110N
<-- Loading Left
Lateral Load (N)
350
300
250
200
150
100
50
0
Pile6
Pile2
Pile1
Pile5
Pile4

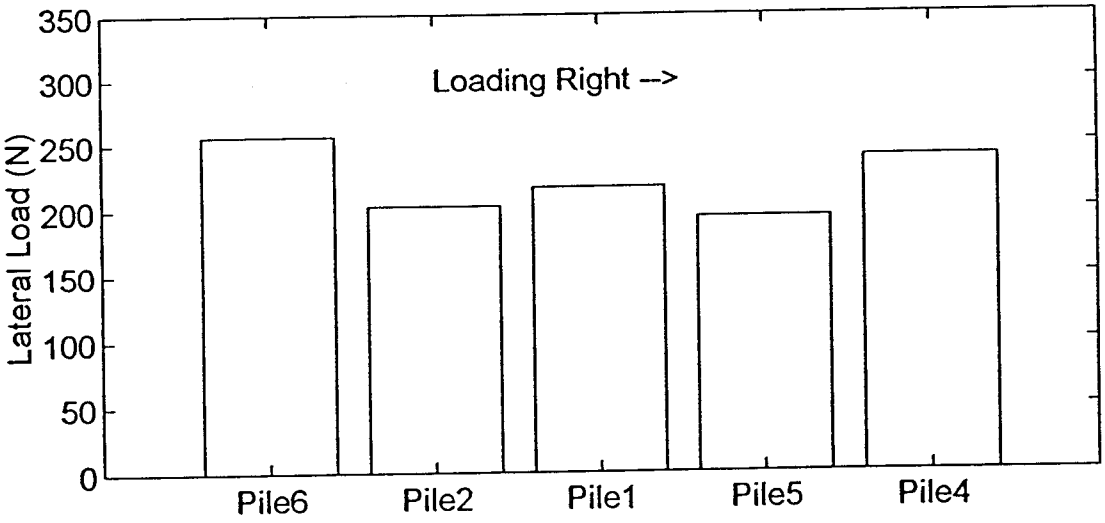
Loading Right -->
Lateral Load (N)
350
300
250
200
150
100
50
0
Pile6
Pile2
Pile1
Pile5
Pile4

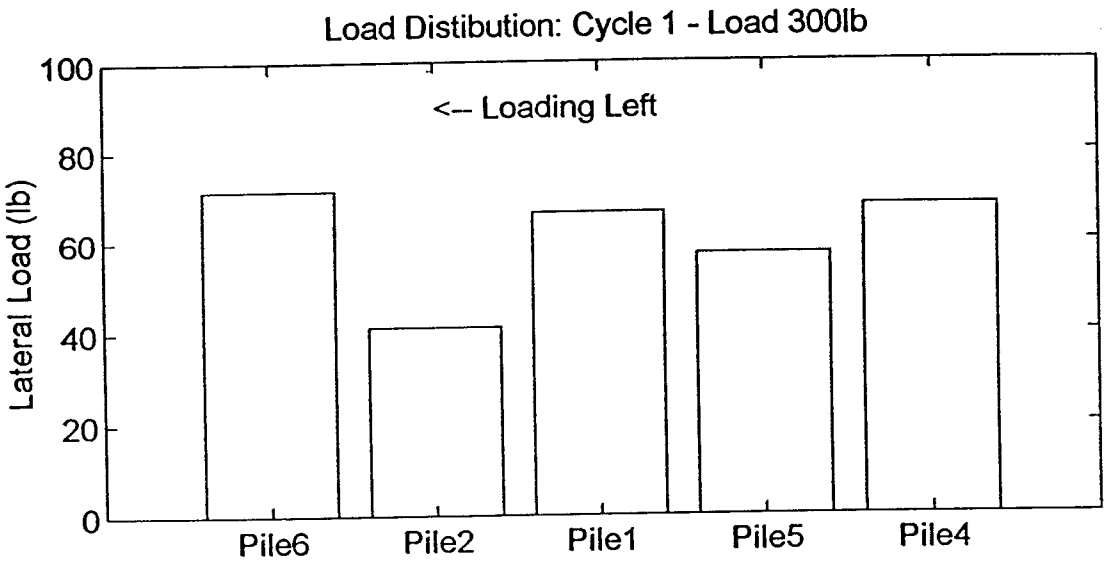
Load Distibution: Cycle 1 - Load 300lb
<-- Loading Left
Lateral Load (lb)
100
80
60
40
20
0
Pile6
Pile2
Pile1
Pile5
Pile4

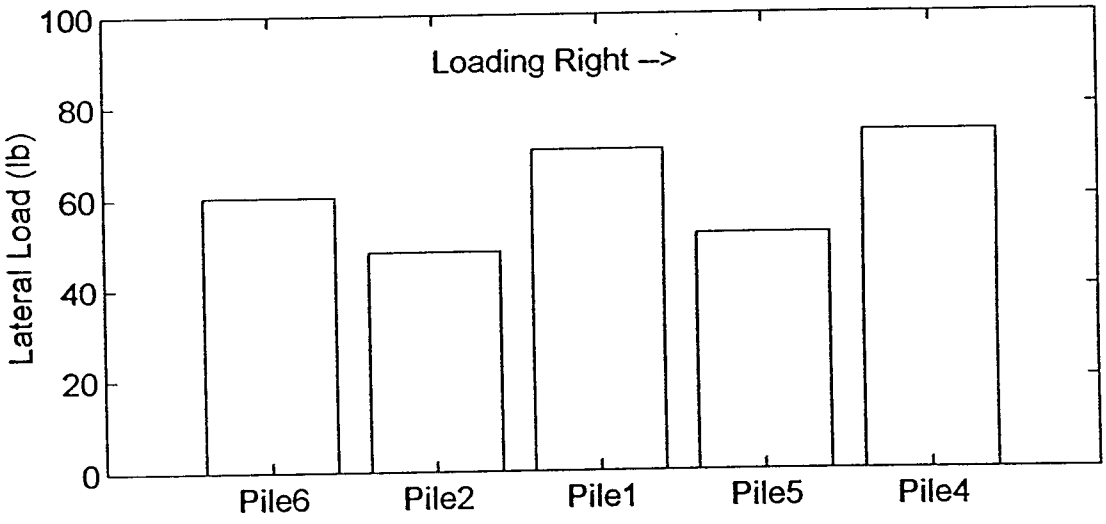
Loading Right -->
Lateral Load (lb)
100
80
60
40
20
0
Pile6
Pile2
Pile1
Pile5
Pile4

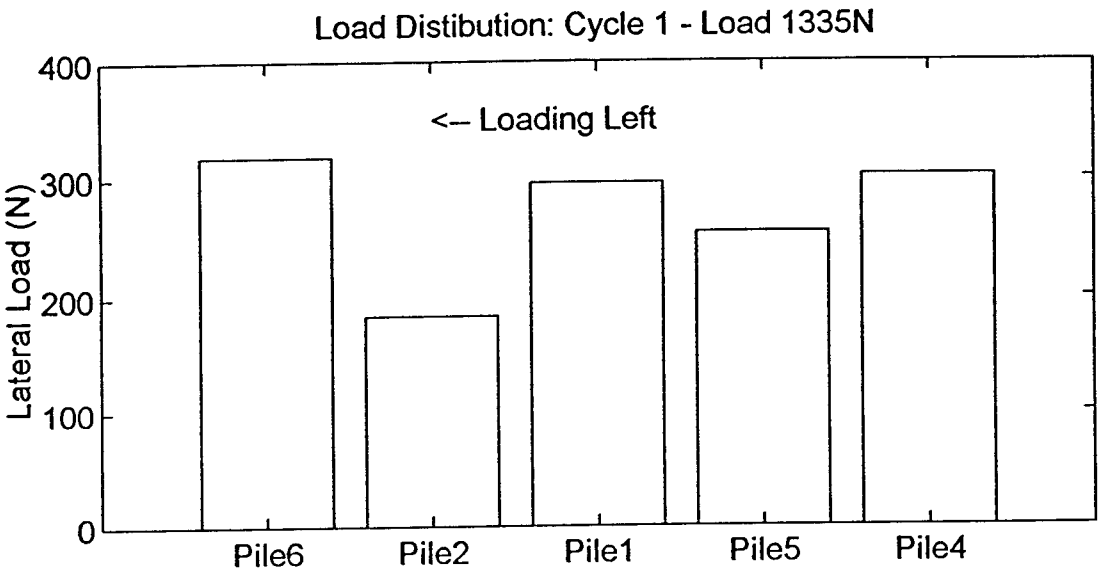
Load Distibution: Cycle 1 - Load 1335N
<-- Loading Left
Lateral Load (N)
400
300
200
100
0
Pile6
Pile2
Pile1
Pile5
Pile4

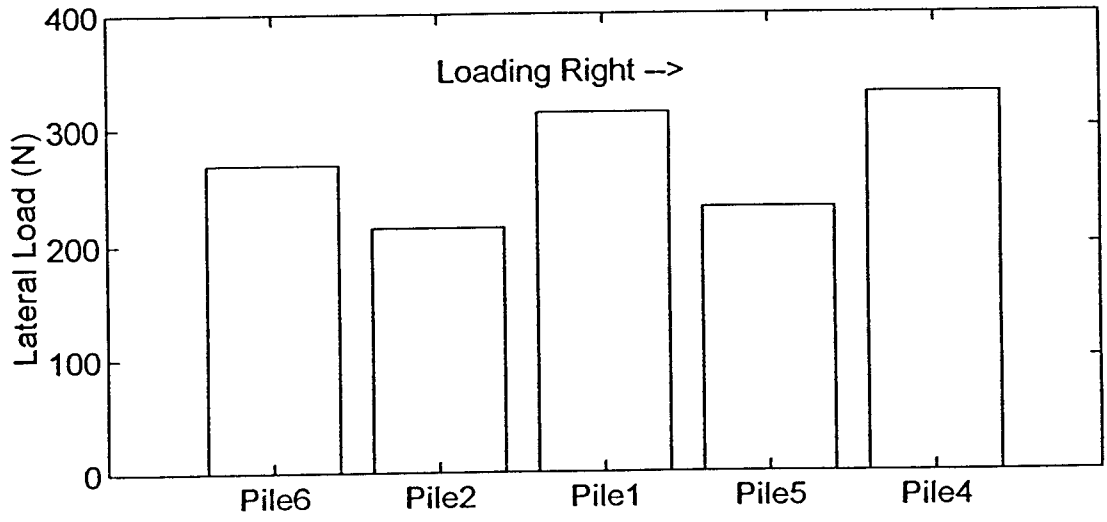
Loading Right -->
Lateral Load (N)
400
300
200
100
0
Pile6
Pile2
Pile1
Pile5
Pile4

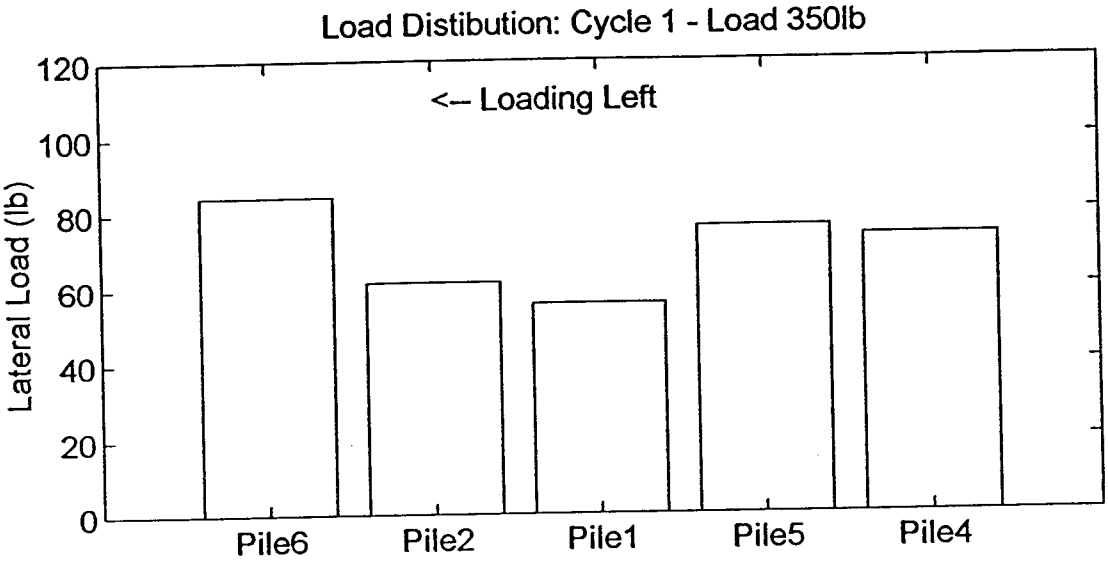
Load Distibution: Cycle 1 - Load 350lb
<-- Loading Left
Lateral Load (lb)
120
100
80
60
40
20
0
Pile6
Pile2
Pile1
Pile5
Pile4

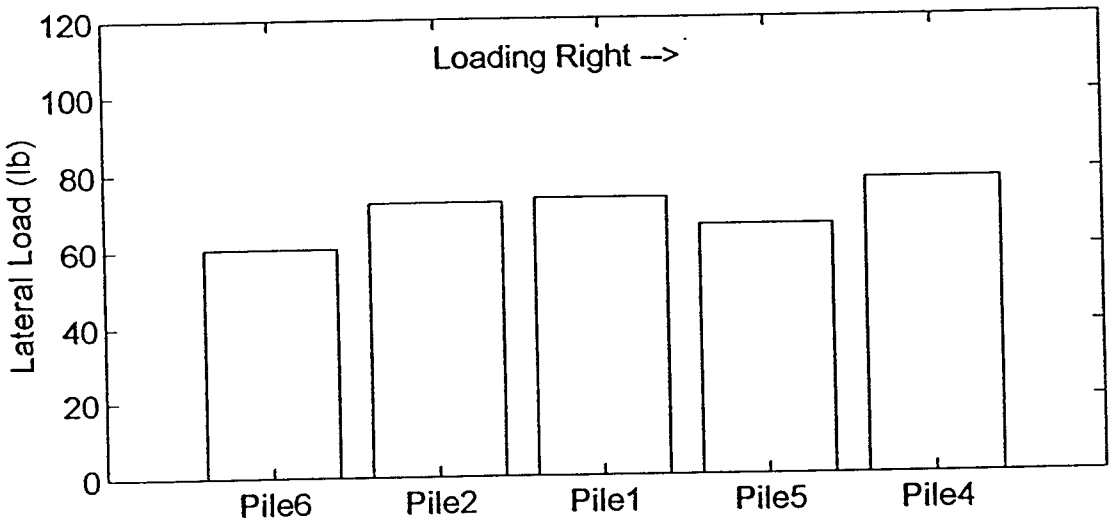
Loading Right -->
Lateral Load (lb)
120
100
80
60
40
20
0
Pile6
Pile2
Pile1
Pile5
Pile4

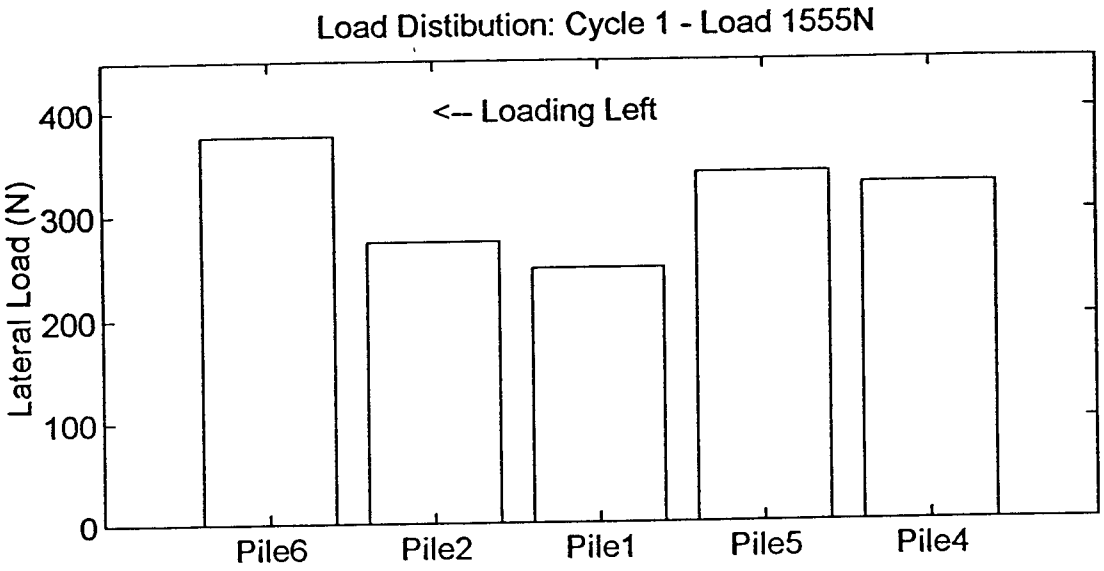
Load Distibution: Cycle 1 - Load 1555N
<-- Loading Left
Lateral Load (N)
400
300
200
100
0
Pile6
Pile2
Pile1
Pile5
Pile4

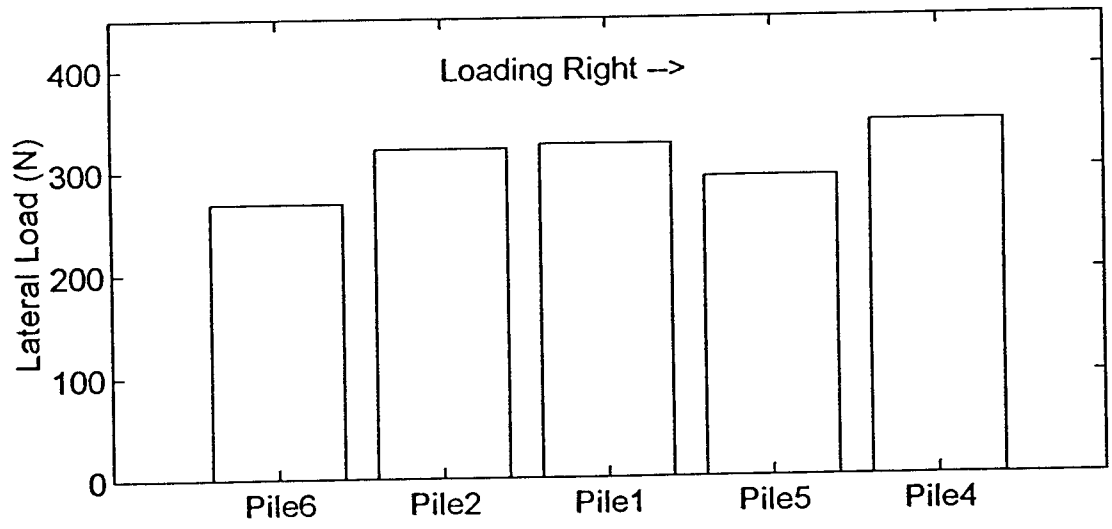
Loading Right -->
Lateral Load (N)
400
300
200
100
0
Pile6
Pile2
Pile1
Pile5
Pile4

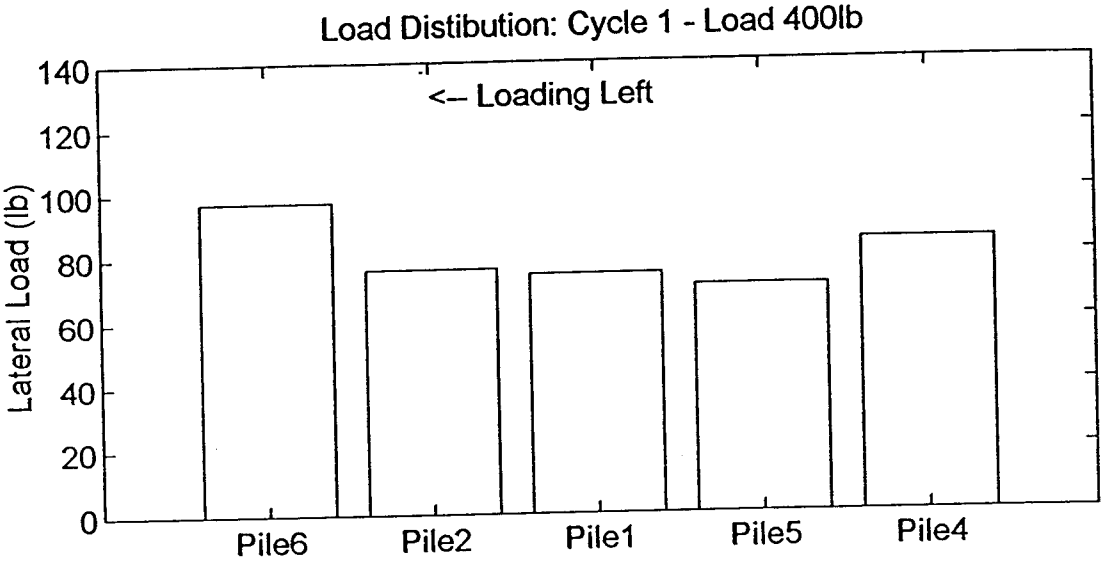
Load Distibution: Cycle 1 - Load 400lb
<-- Loading Left
Lateral Load (lb)
140
120
100
80
60
40
20
0
Pile6
Pile2
Pile1
Pile5
Pile4

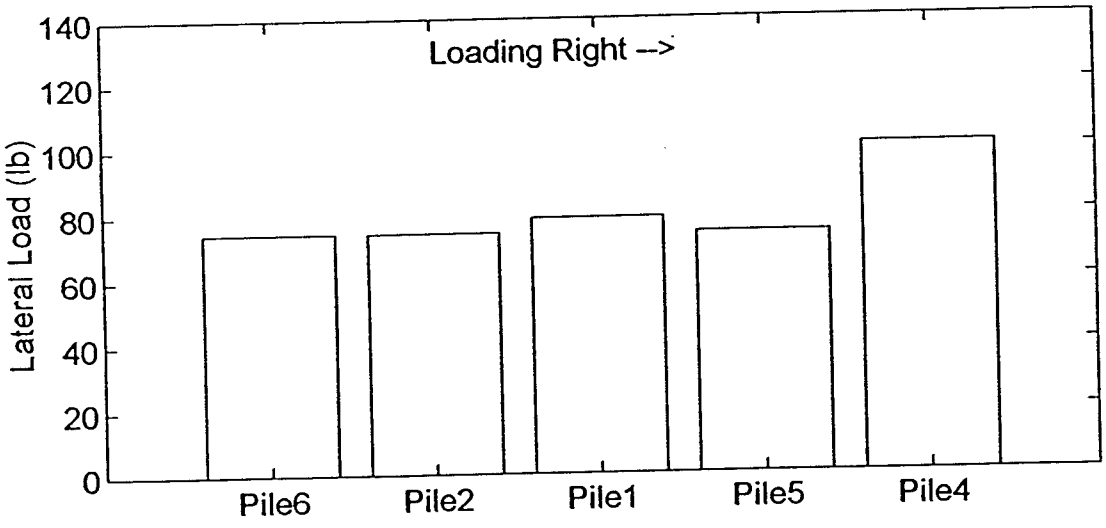
Loading Right -->
Lateral Load (lb)
140
120
100
80
60
40
20
0
Pile6
Pile2
Pile1
Pile5
Pile4

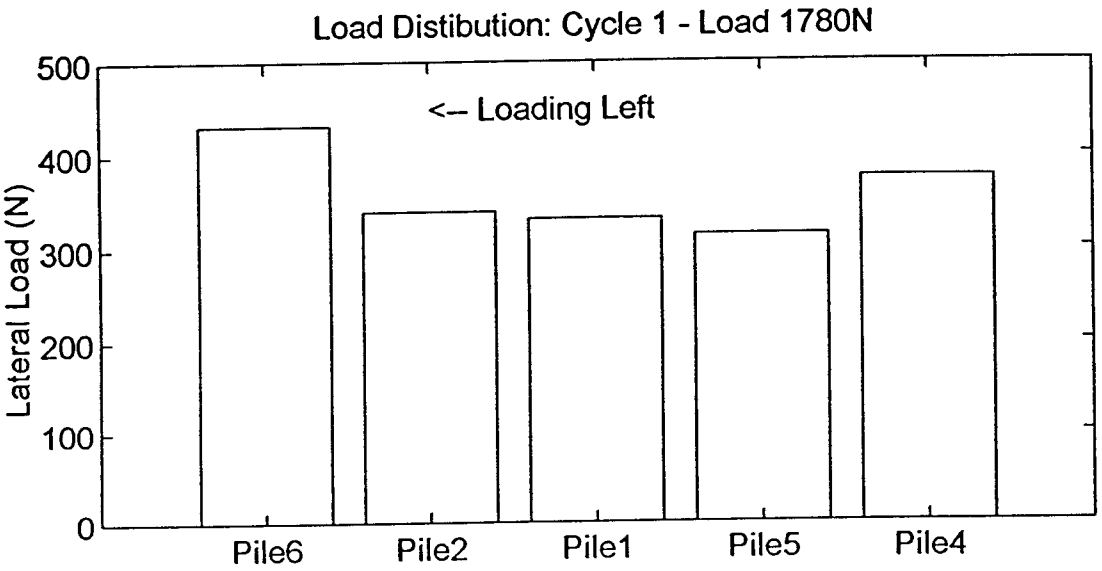
Load Distibution: Cycle 1 - Load 1780N
<-- Loading Left
Lateral Load (N)
500
400
300
200
100
0
Pile6
Pile2
Pile1
Pile5
Pile4

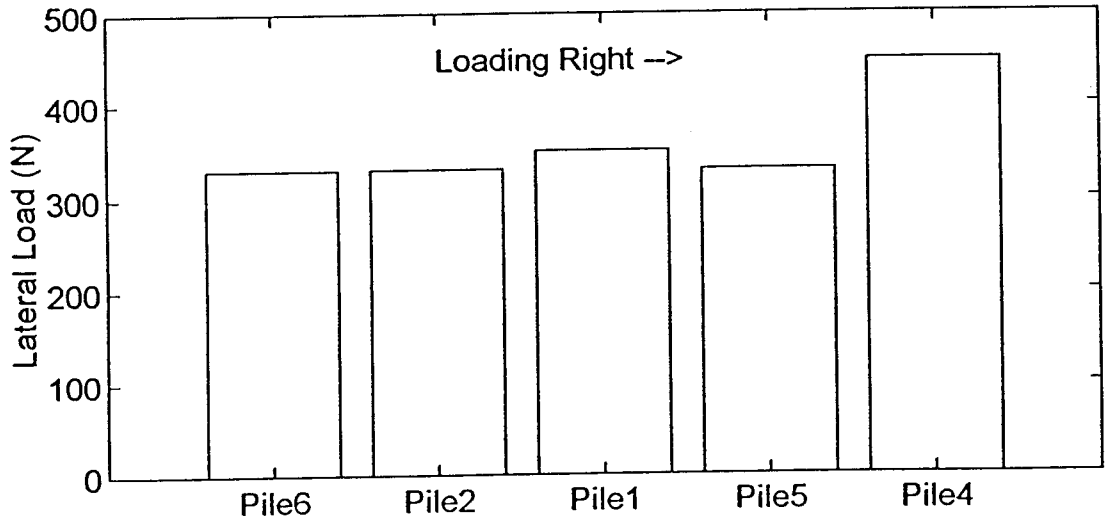
Loading Right -->
Lateral Load (N)
500
400
300
200
100
0
Pile6
Pile2
Pile1
Pile5
Pile4

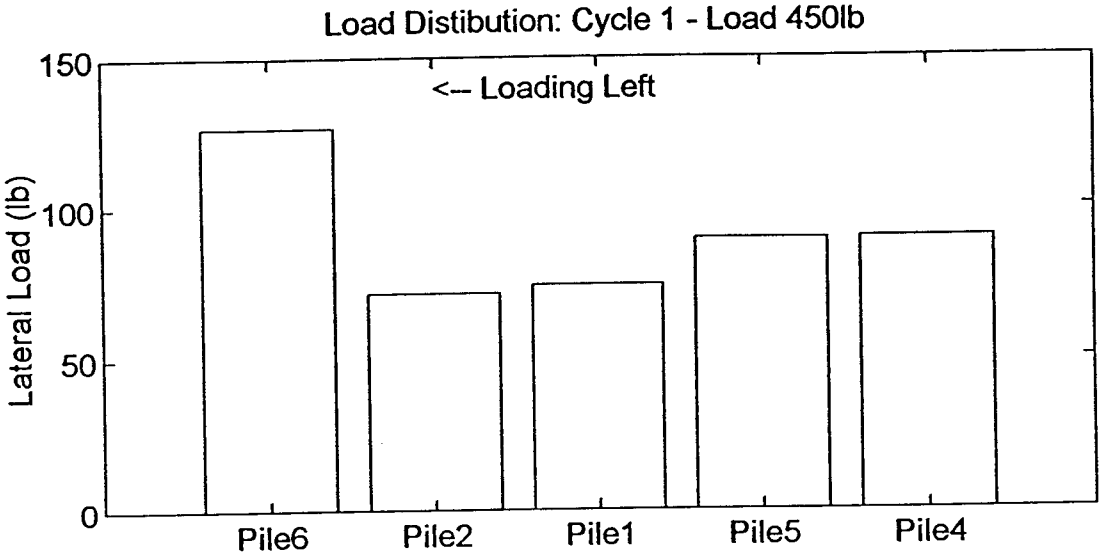
Load Distibution: Cycle 1 - Load 450lb
<-- Loading Left
Lateral Load (lb)
150
100
50
0
Pile6
Pile2
Pile1
Pile5
Pile4

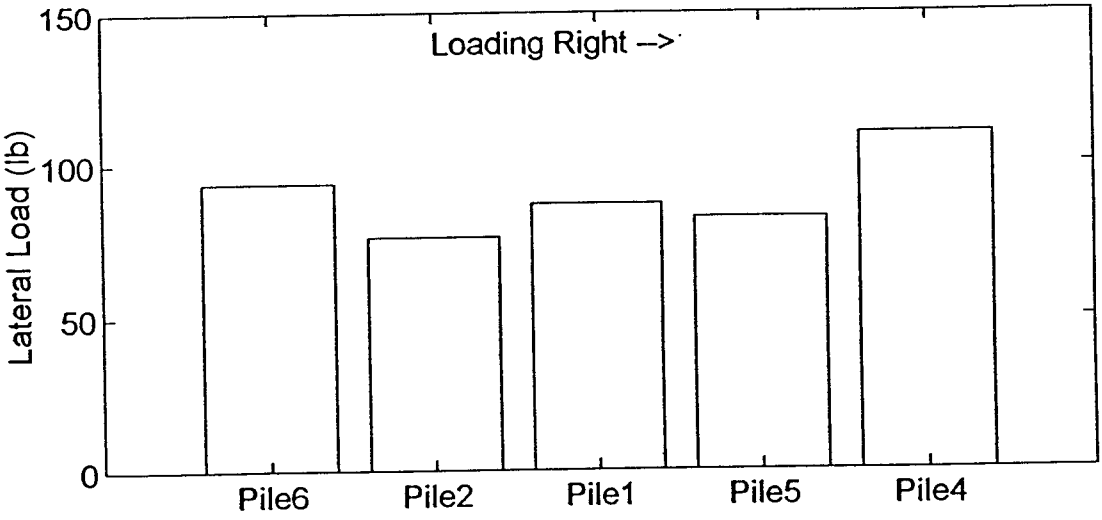
Loading Right -->
Lateral Load (lb)
150
100
50
0
Pile6
Pile2
Pile1
Pile5
Pile4

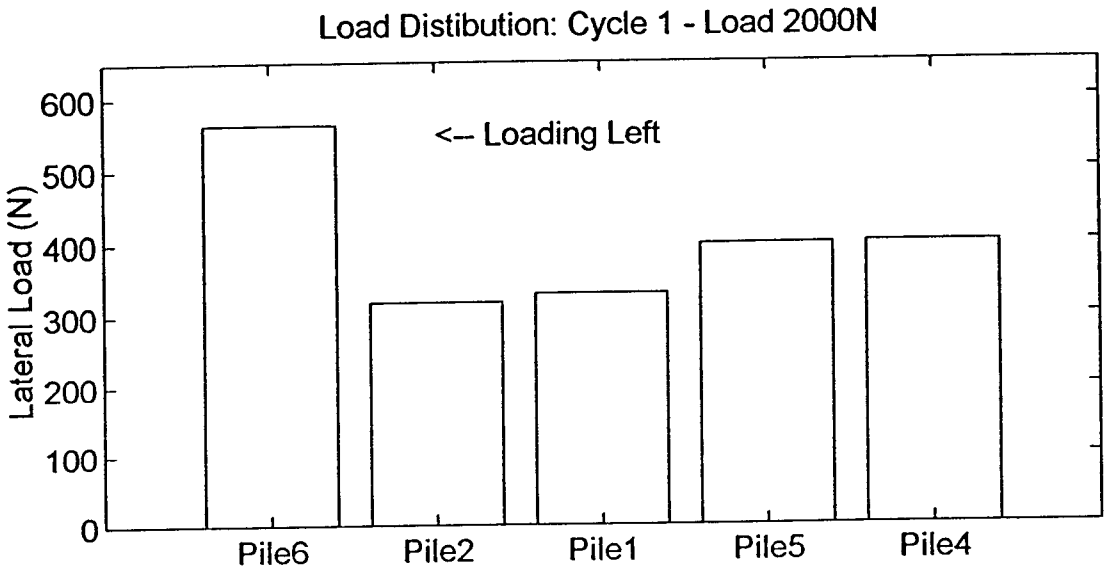
Load Distibution: Cycle 1 - Load 2000N
<-- Loading Left
Lateral Load (N)
600
500
400
300
200
100
0
Pile6
Pile2
Pile1
Pile5
Pile4

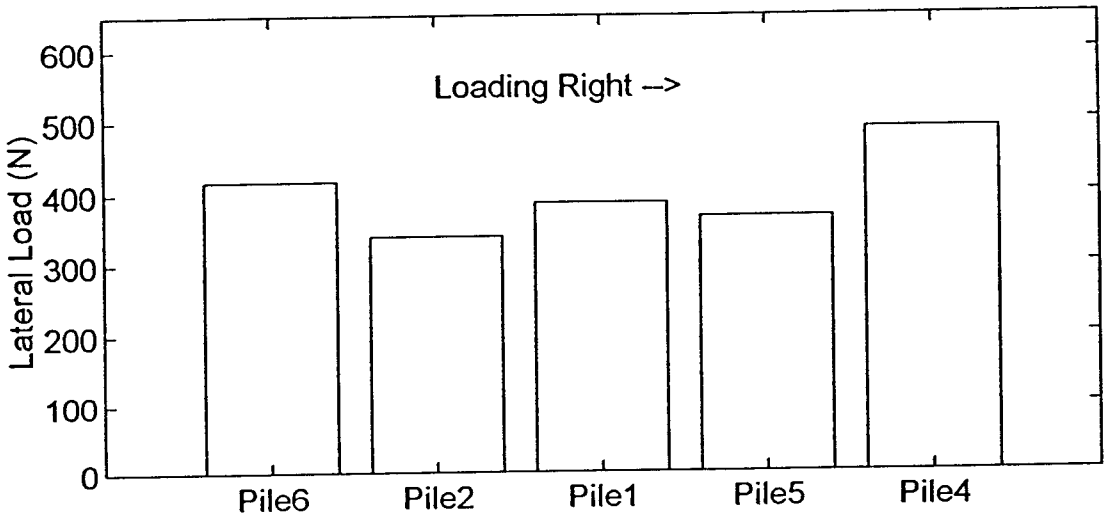
Loading Right -->
Lateral Load (N)
600
500
400
300
200
100
0
Pile6
Pile2
Pile1
Pile5
Pile4

Figure B12. Load distribution @ cycle 5 (next 14 plots).

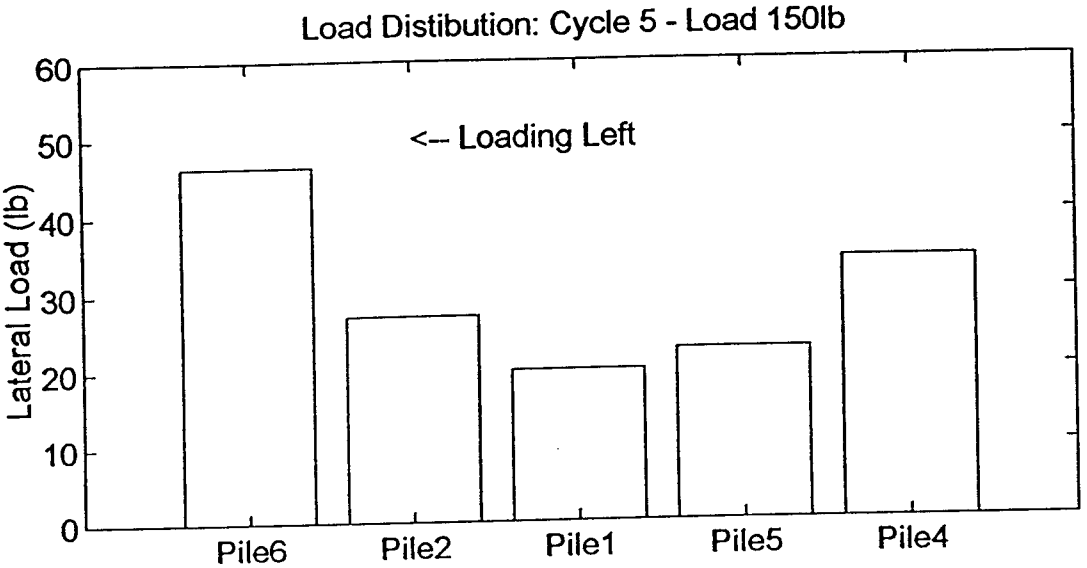
Load Distibution: Cycle 5 - Load 150lb
<-- Loading Left
Lateral Load (lb)
60
50
40
30
20
10
0
Pile6
Pile2
Pile1
Pile5
Pile4

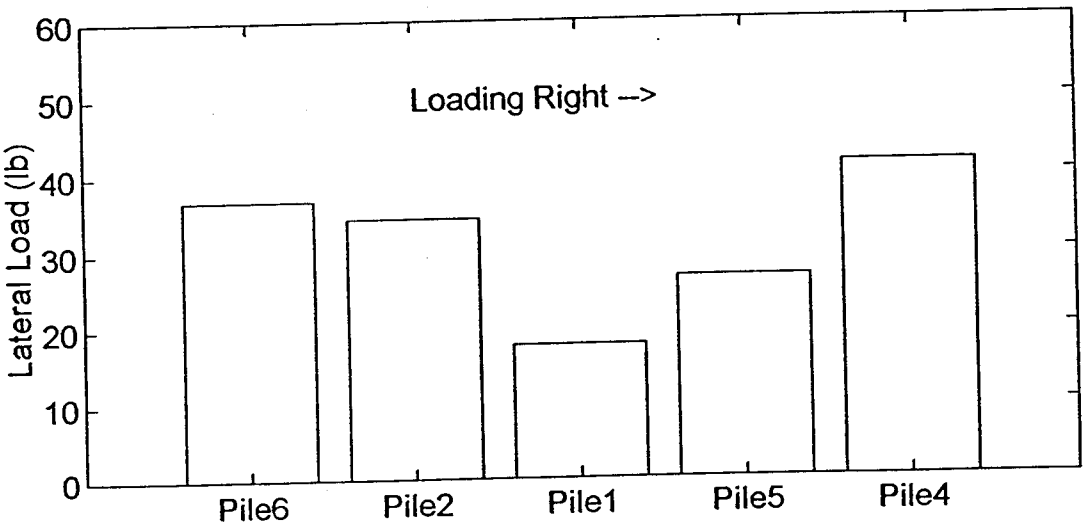
Loading Right -->
Lateral Load (lb)
60
50
40
30
20
10
0
Pile6
Pile2
Pile1
Pile5
Pile4

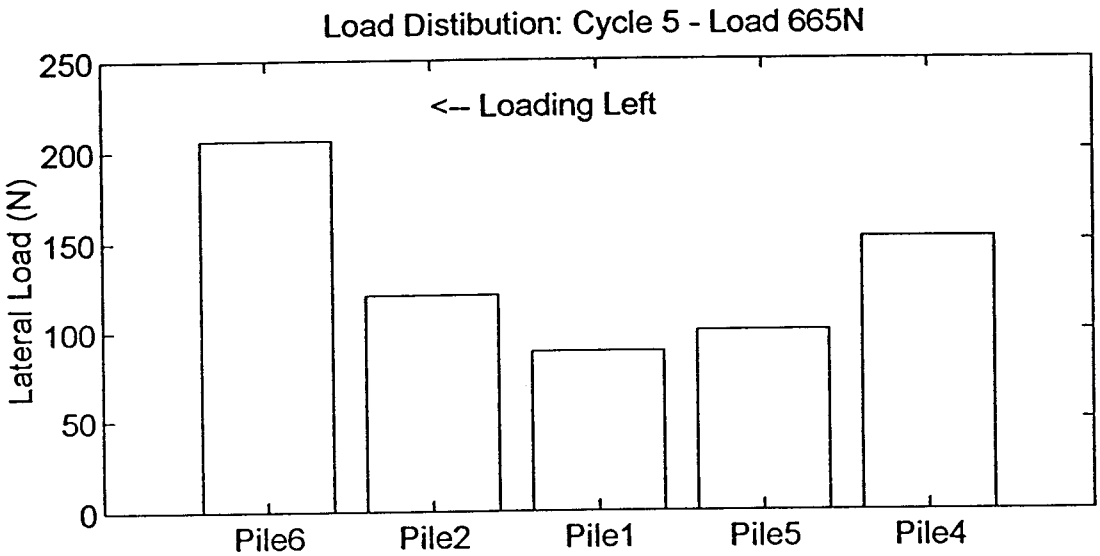
Load Distibution: Cycle 5 - Load 665N
<-- Loading Left
Lateral Load (N)
250
200
150
100
50
0
Pile6
Pile2
Pile1
Pile5
Pile4

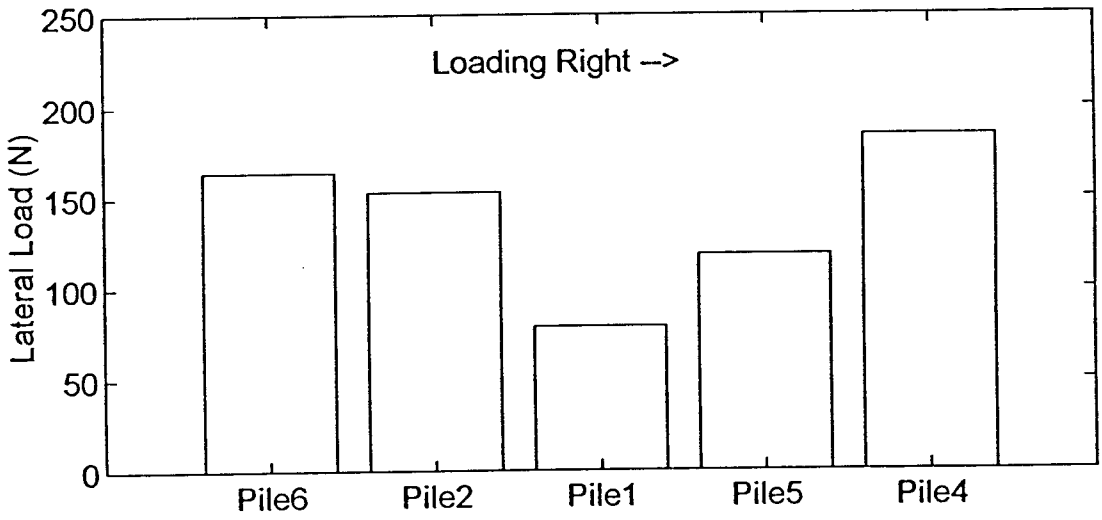
Loading Right -->
Lateral Load (N)
250
200
150
100
50
0
Pile6
Pile2
Pile1
Pile5
Pile4

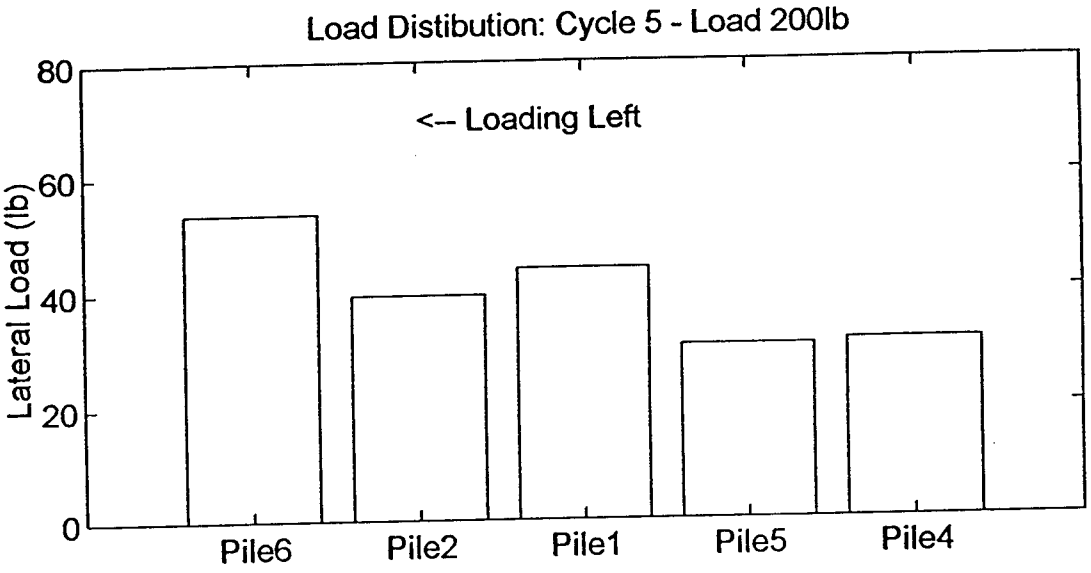
Load Distibution: Cycle 5 - Load 200lb
<-- Loading Left
Lateral Load (lb)
0
20
40
60
80
Pile6
Pile2
Pile1
Pile5
Pile4

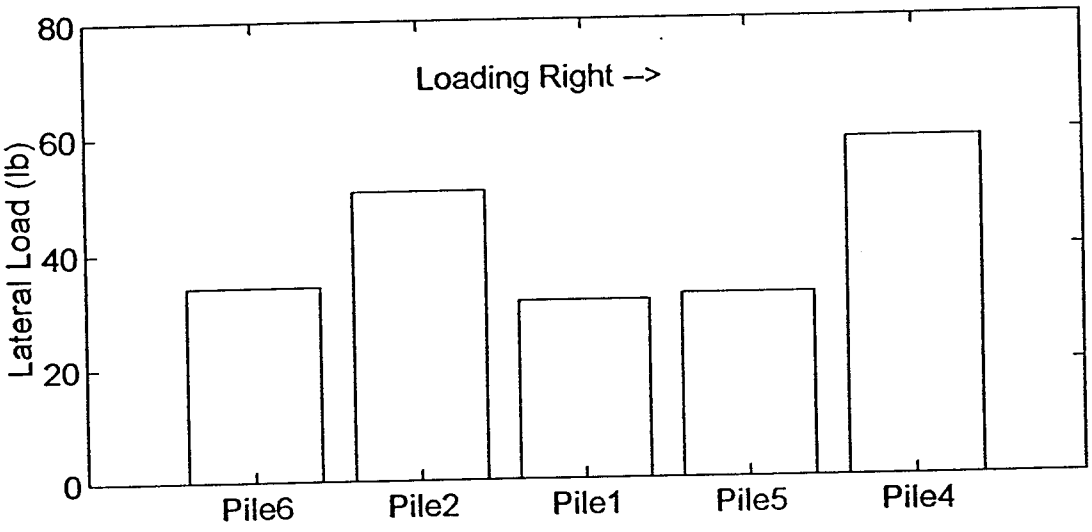
Loading Right -->
Lateral Load (lb)
0
20
40
60
80
Pile6
Pile2
Pile1
Pile5
Pile4

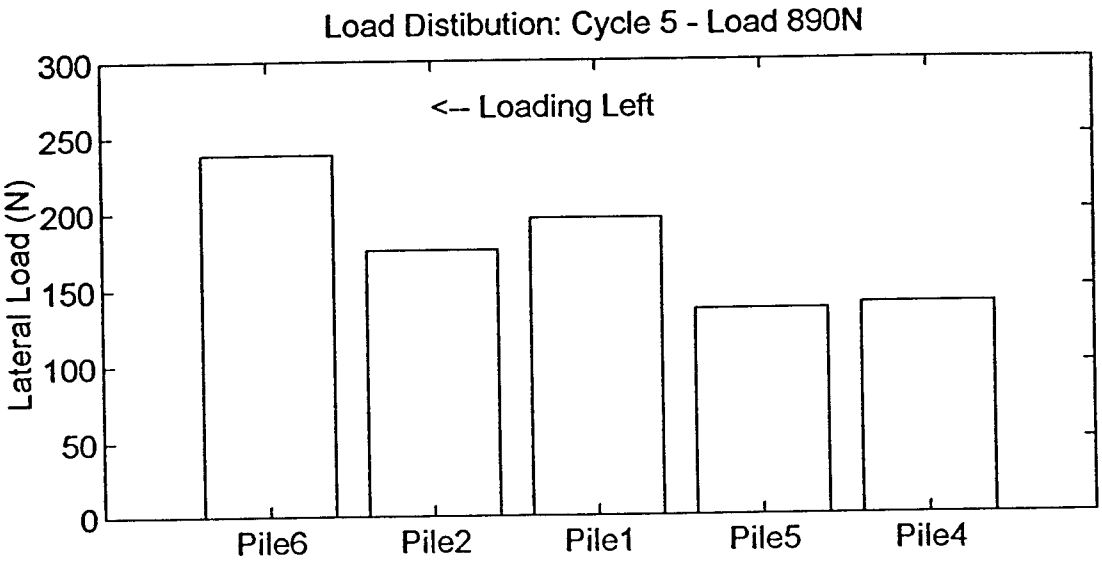
Load Distibution: Cycle 5 - Load 890N
<-- Loading Left
Lateral Load (N)
300
250
200
150
100
50
0
Pile6
Pile2
Pile1
Pile5
Pile4

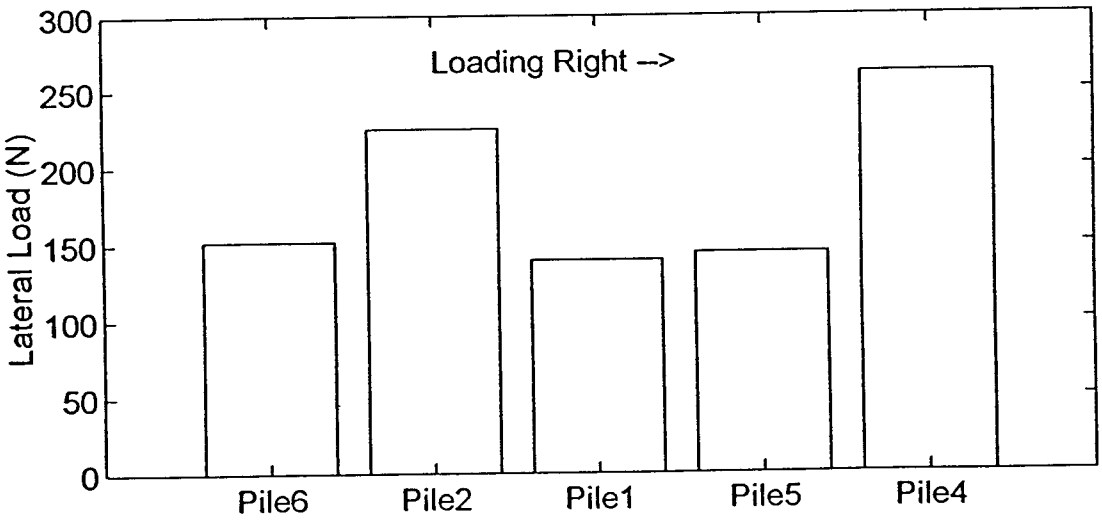
Loading Right -->
Lateral Load (N)
300
250
200
150
100
50
0
Pile6
Pile2
Pile1
Pile5
Pile4

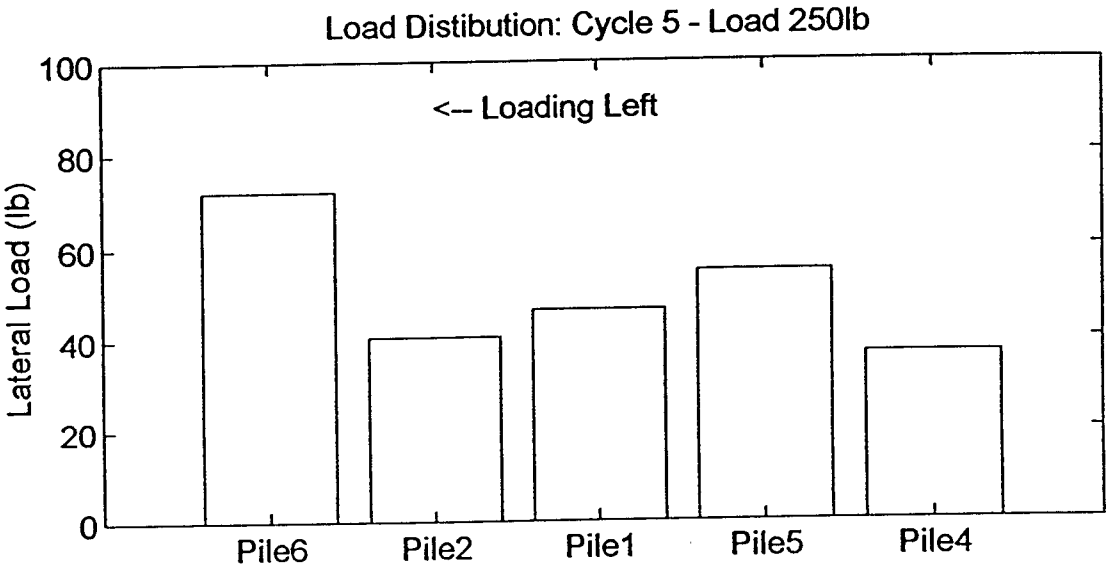
Load Distibution: Cycle 5 - Load 250lb
<-- Loading Left
Lateral Load (lb)
100
80
60
40
20
0
Pile6
Pile2
Pile1
Pile5
Pile4

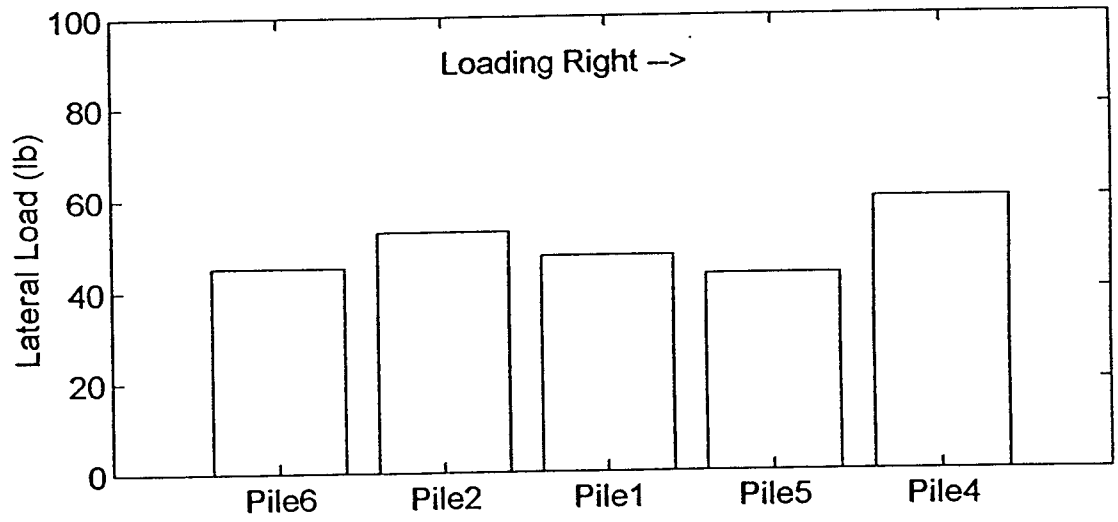
Loading Right -->
Lateral Load (lb)
100
80
60
40
20
0
Pile6
Pile2
Pile1
Pile5
Pile4

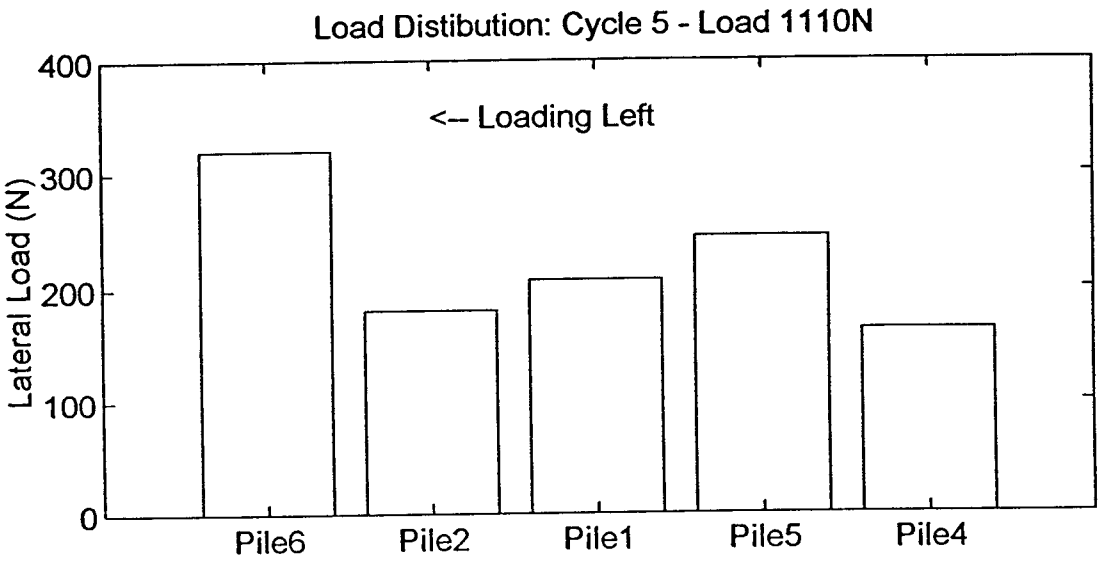
Load Distibution: Cycle 5 - Load 1110N
<-- Loading Left
Lateral Load (N)
400
300
200
100
0
Pile6
Pile2
Pile1
Pile5
Pile4

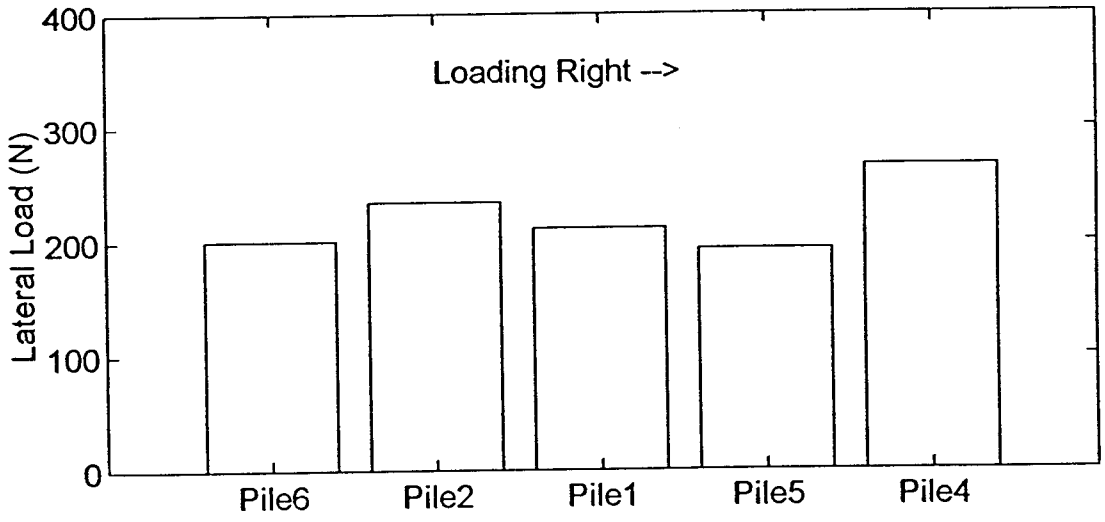
Loading Right -->
Lateral Load (N)
400
300
200
100
0
Pile6
Pile2
Pile1
Pile5
Pile4

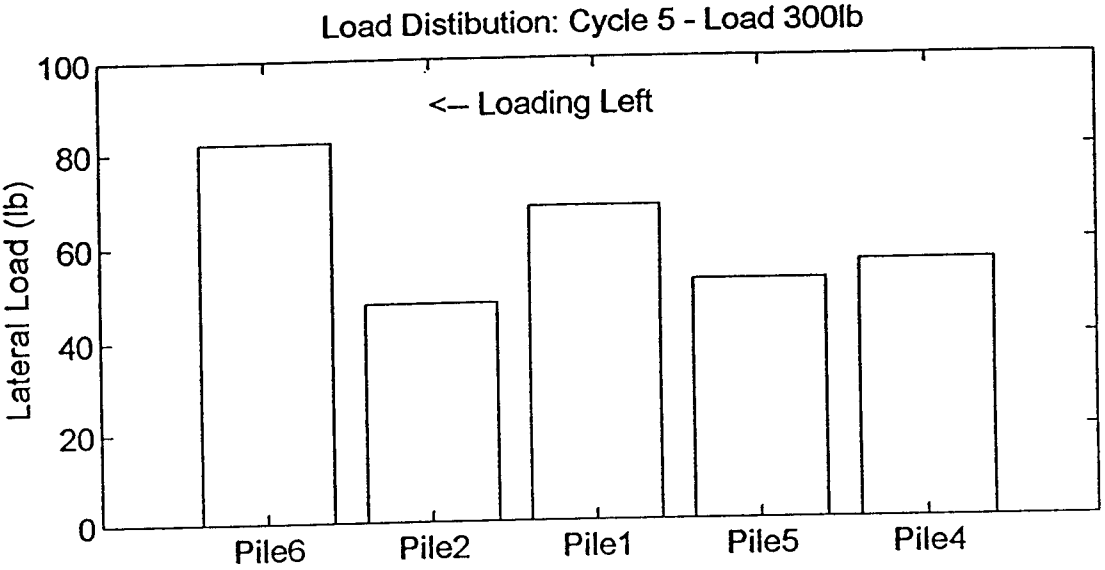
Load Distibution: Cycle 5 - Load 300lb
<-- Loading Left
Lateral Load (lb)
100
80
60
40
20
0
Pile6
Pile2
Pile1
Pile5
Pile4

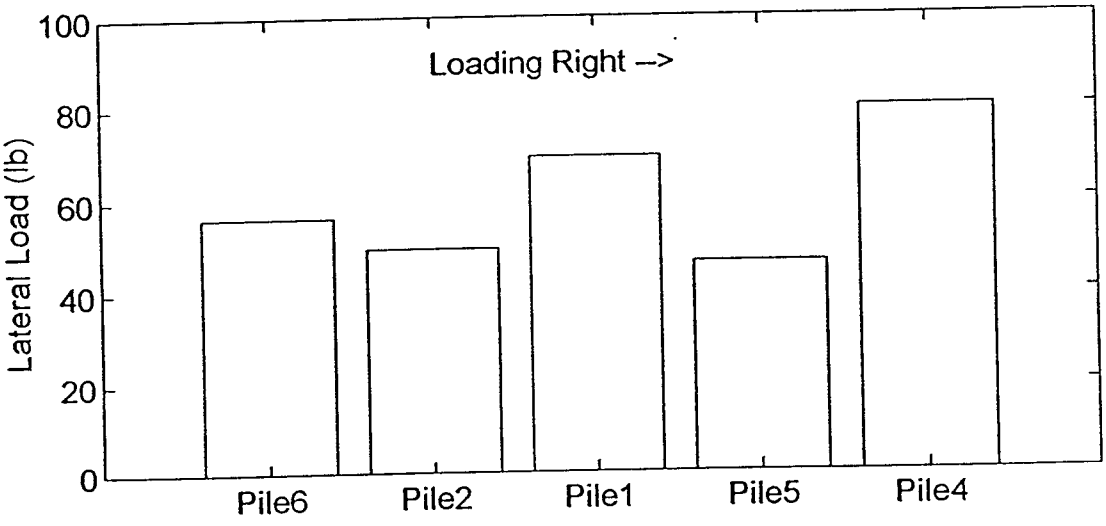
Loading Right -->
Lateral Load (lb)
100
80
60
40
20
0
Pile6
Pile2
Pile1
Pile5
Pile4

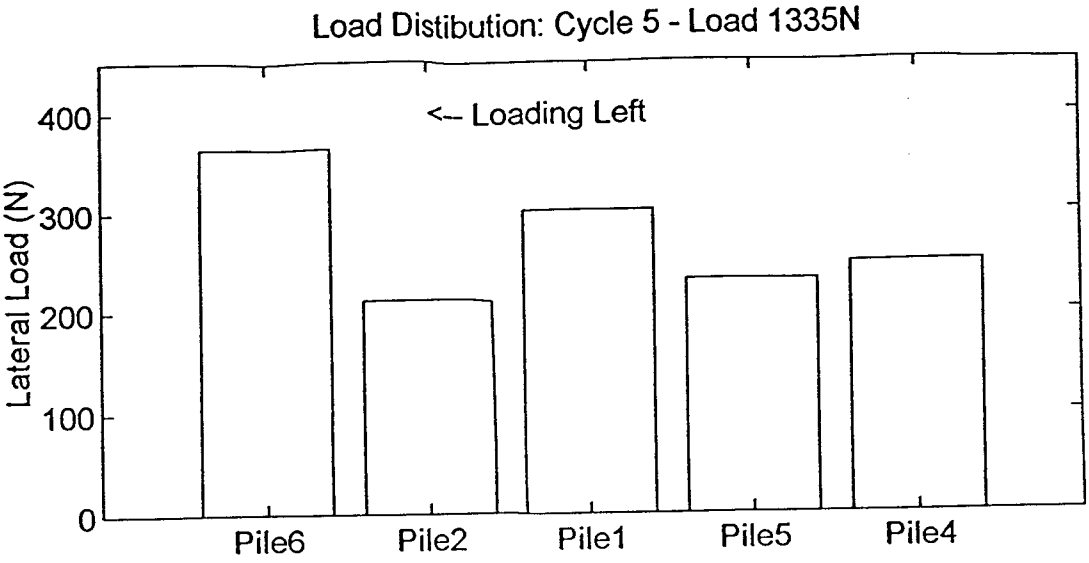
Load Distibution: Cycle 5 - Load 1335N
<-- Loading Left
Lateral Load (N)
400
300
200
100
0
Pile6
Pile2
Pile1
Pile5
Pile4

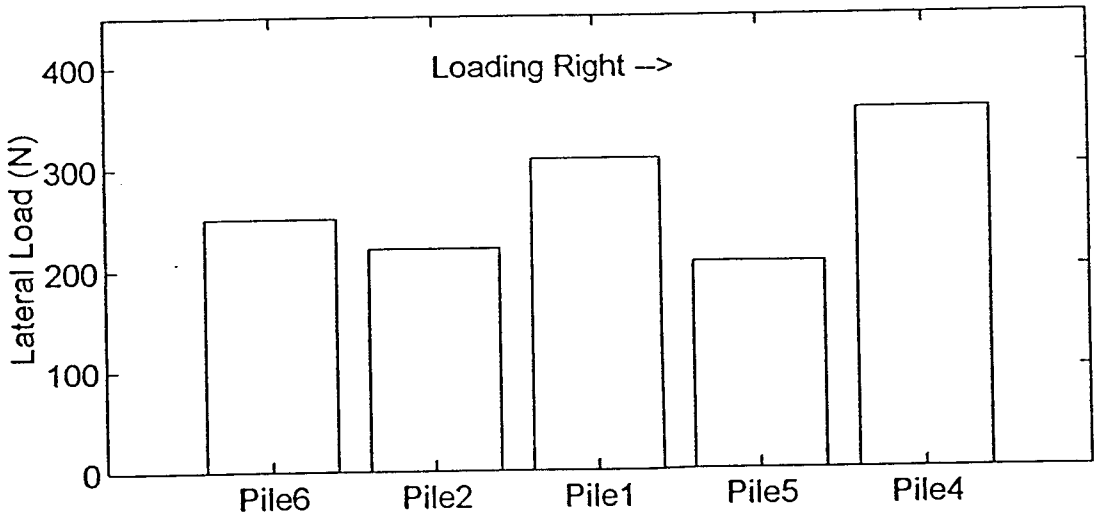
Loading Right -->
Lateral Load (N)
400
300
200
100
0
Pile6
Pile2
Pile1
Pile5
Pile4

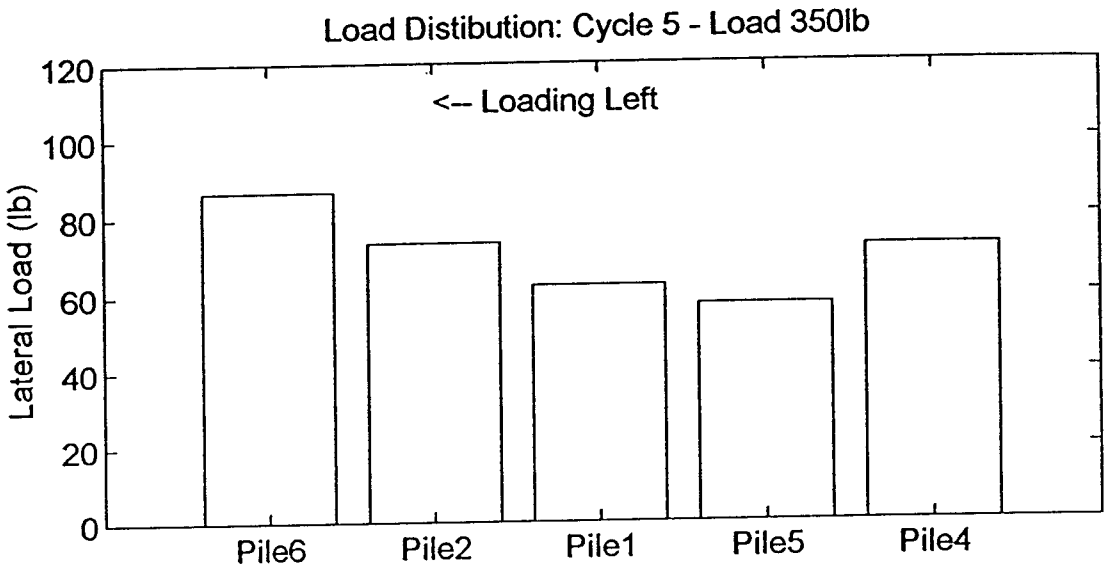
Load Distibution: Cycle 5 - Load 350lb
<-- Loading Left
Lateral Load (lb)
120
100
80
60
40
20
0
Pile6
Pile2
Pile1
Pile5
Pile4

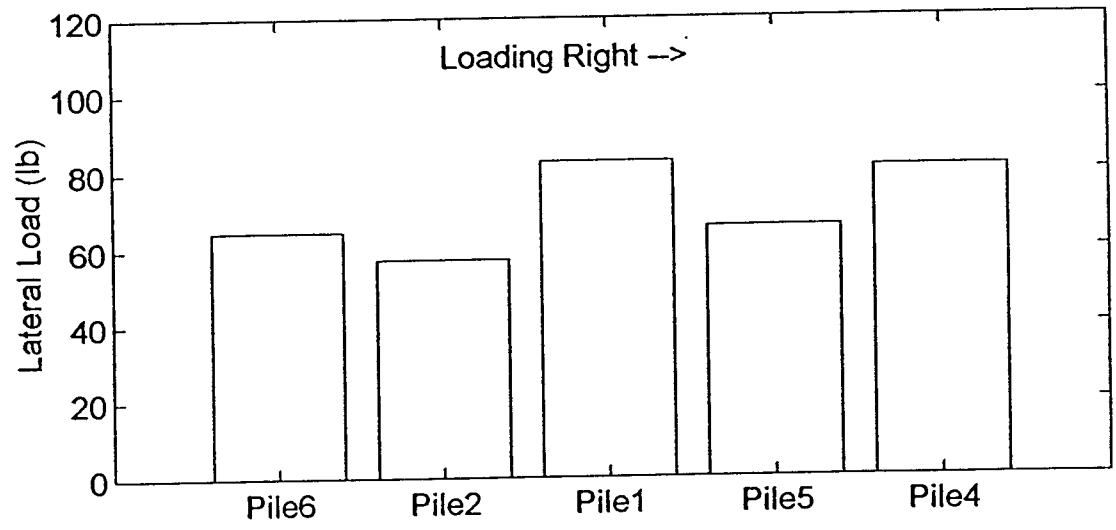
Loading Right -->
Lateral Load (lb)
120
100
80
60
40
20
0
Pile6
Pile2
Pile1
Pile5
Pile4

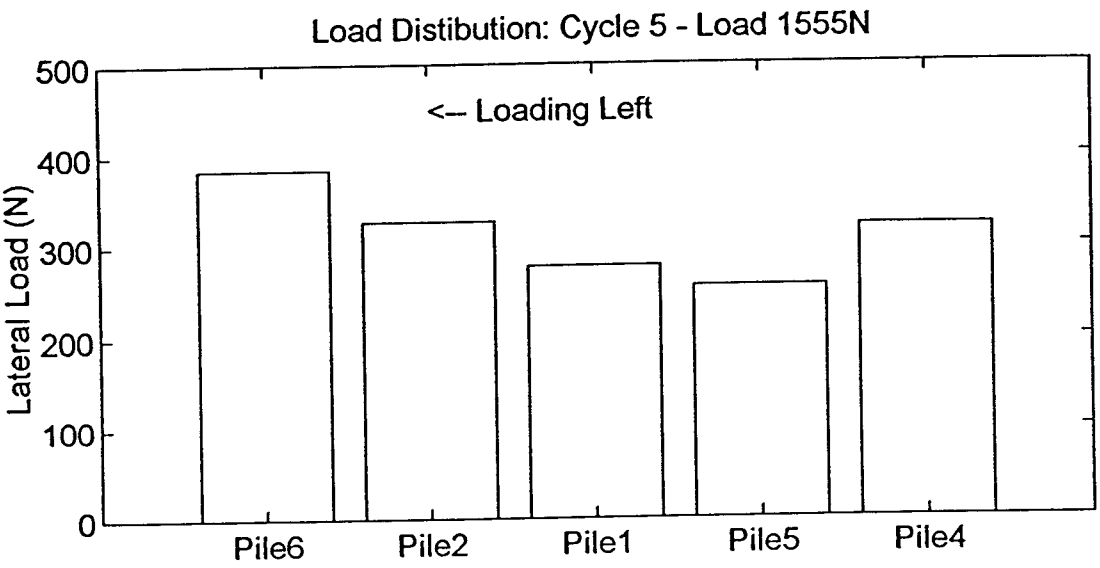
Load Distibution: Cycle 5 - Load 1555N
<-- Loading Left
Lateral Load (N)
500
400
300
200
100
0
Pile6
Pile2
Pile1
Pile5
Pile4

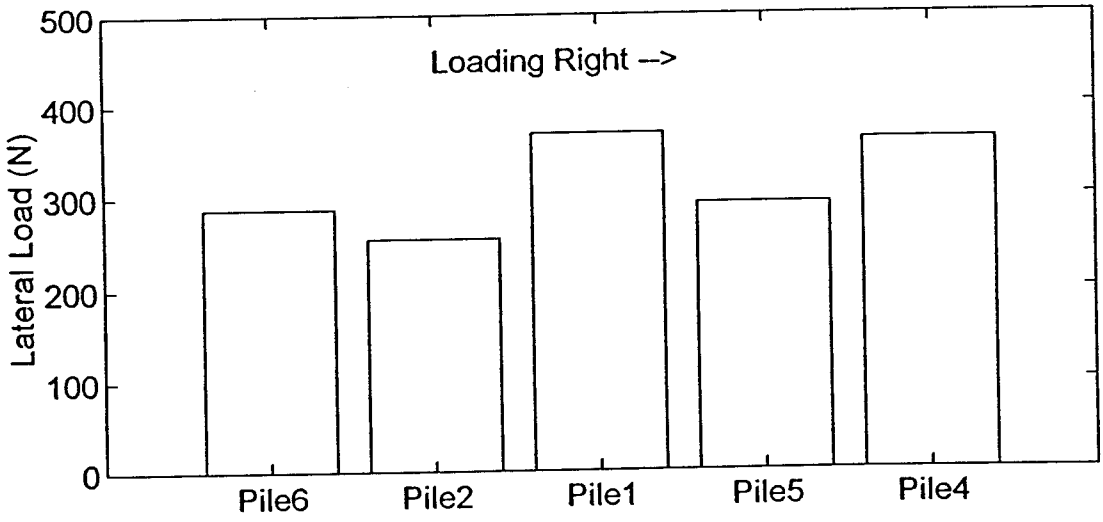
Loading Right -->
Lateral Load (N)
500
400
300
200
100
0
Pile6
Pile2
Pile1
Pile5
Pile4

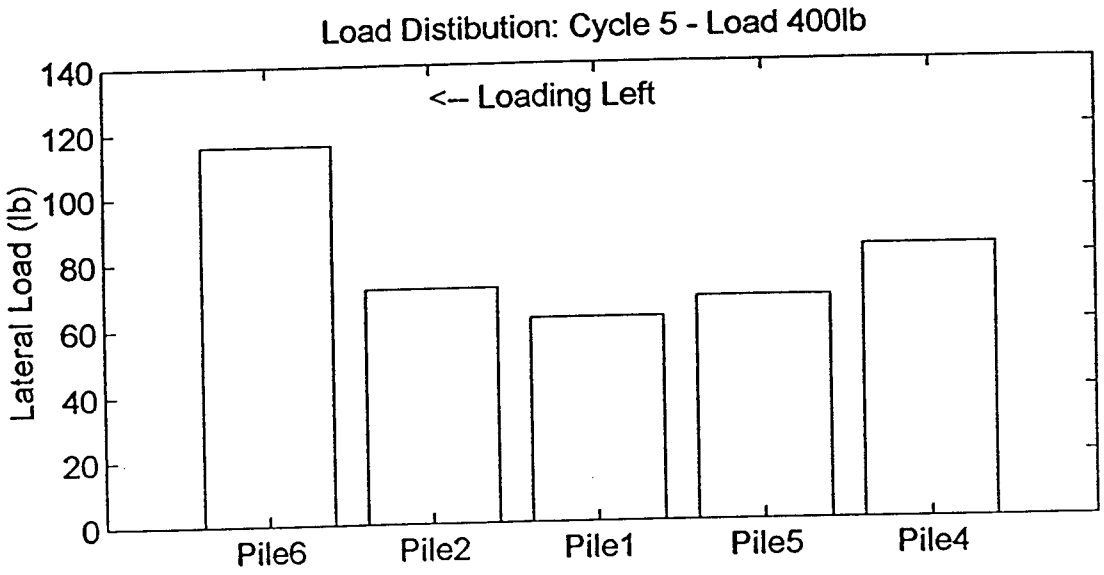
Load Distibution: Cycle 5 - Load 400lb
<-- Loading Left
Lateral Load (lb)
140
120
100
80
60
40
20
0
Pile6
Pile2
Pile1
Pile5
Pile4

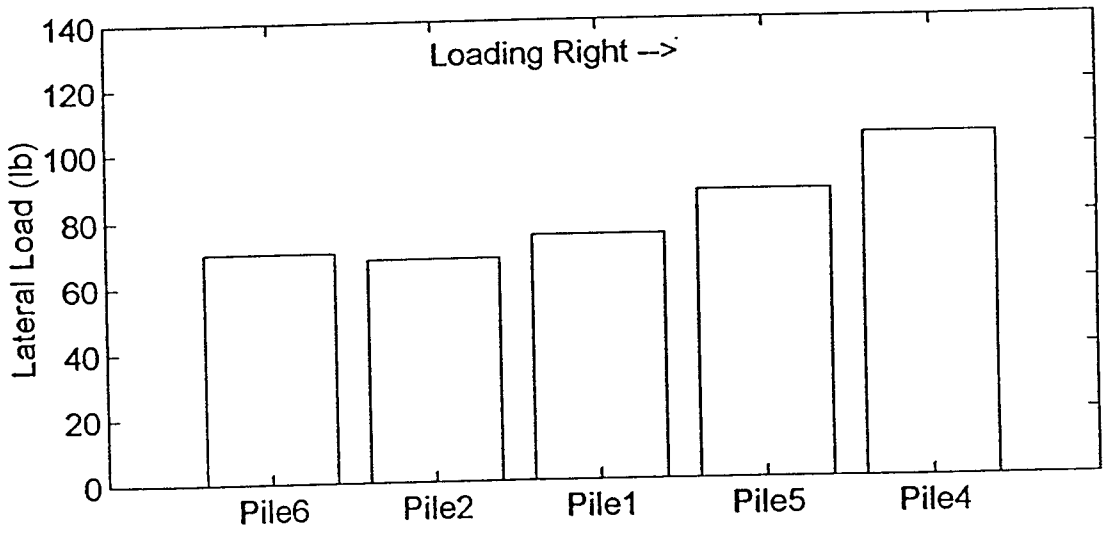
Loading Right -->
Lateral Load (lb)
140
120
100
80
60
40
20
0
Pile6
Pile2
Pile1
Pile5
Pile4

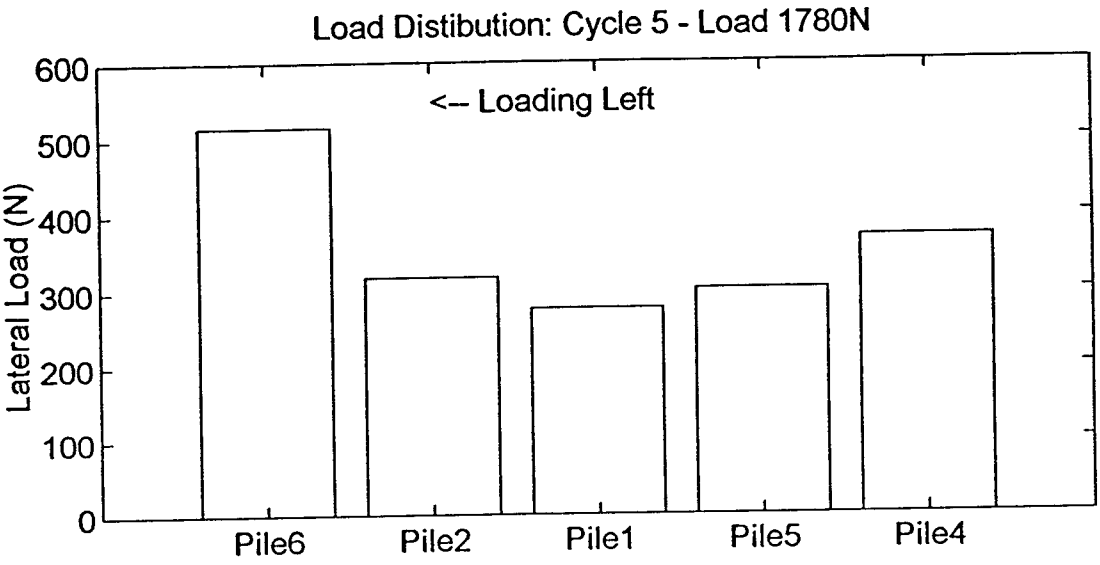
Load Distibution: Cycle 5 - Load 1780N
<-- Loading Left
Lateral Load (N)
600
500
400
300
200
100
0
Pile6
Pile2
Pile1
Pile5
Pile4

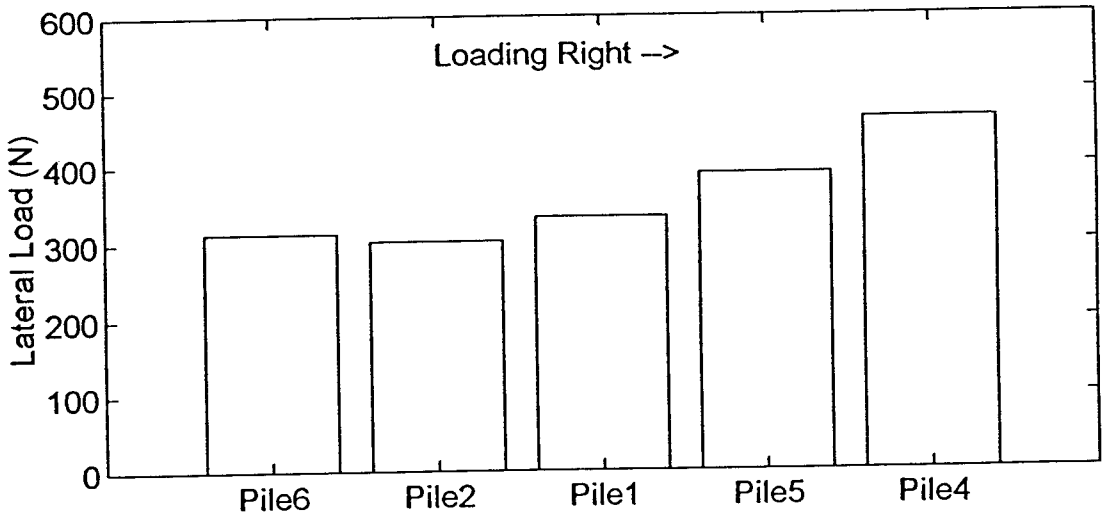
Loading Right -->
Lateral Load (N)
600
500
400
300
200
100
0
Pile6
Pile2
Pile1
Pile5
Pile4

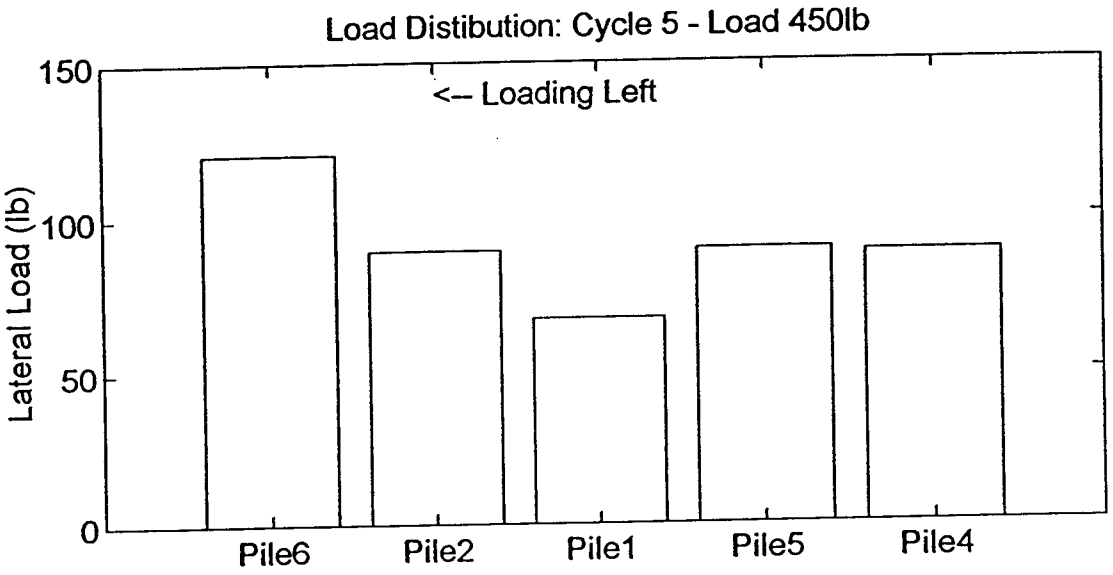
Load Distibution: Cycle 5 - Load 450lb
<-- Loading Left
Lateral Load (lb)
150
100
50
0
Pile6
Pile2
Pile1
Pile5
Pile4

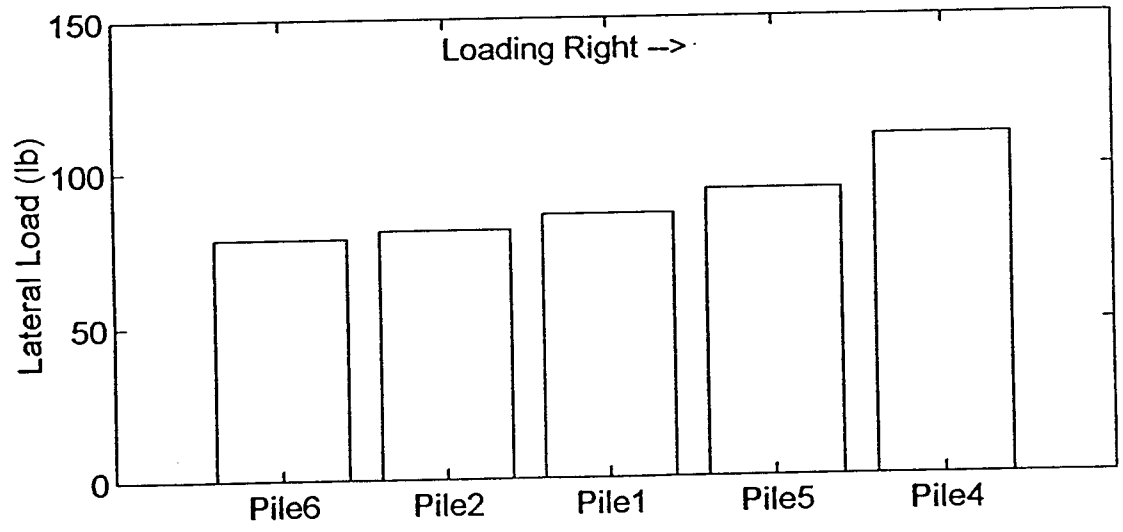
Loading Right -->
Lateral Load (lb)
150
100
50
0
Pile6
Pile2
Pile1
Pile5
Pile4

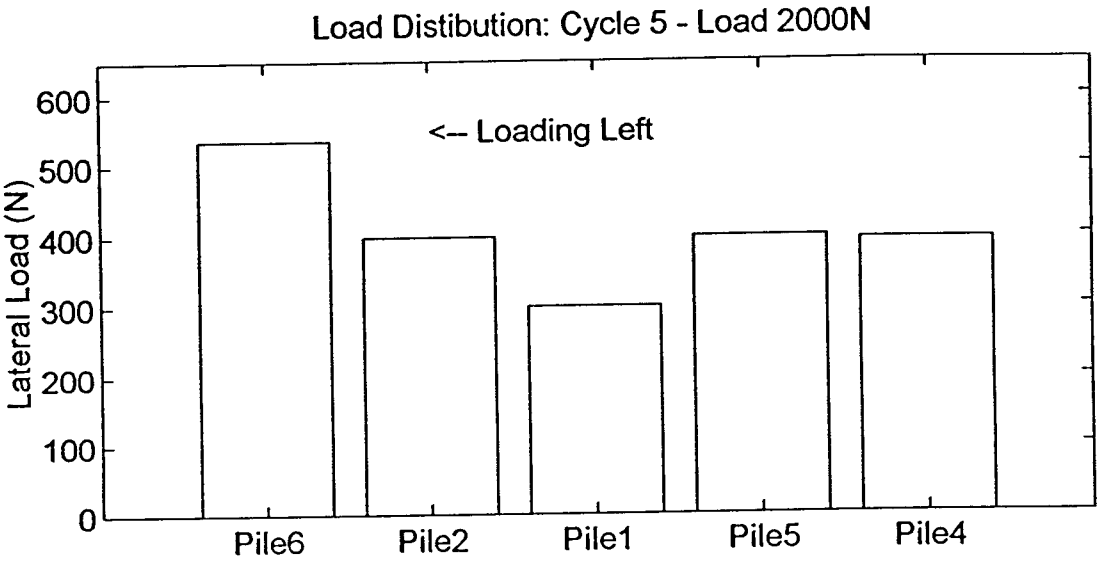
Load Distibution: Cycle 5 - Load 2000N
<-- Loading Left
Lateral Load (N)
600
500
400
300
200
100
0
Pile6
Pile2
Pile1
Pile5
Pile4

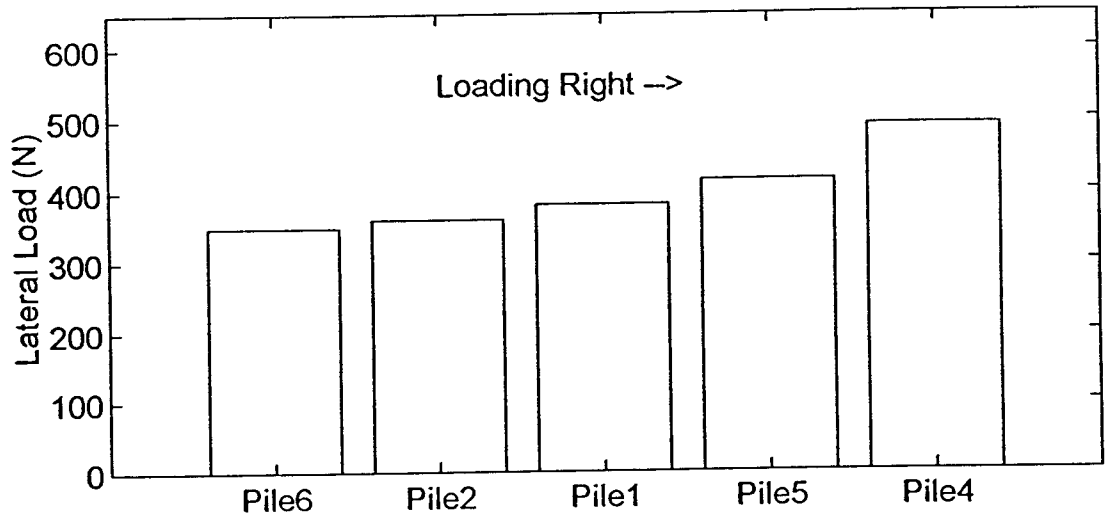
Loading Right -->
Lateral Load (N)
600
500
400
300
200
100
0
Pile6
Pile2
Pile1
Pile5
Pile4

Figure B13. Load distribution @ cycle 10 (next 14 plots).

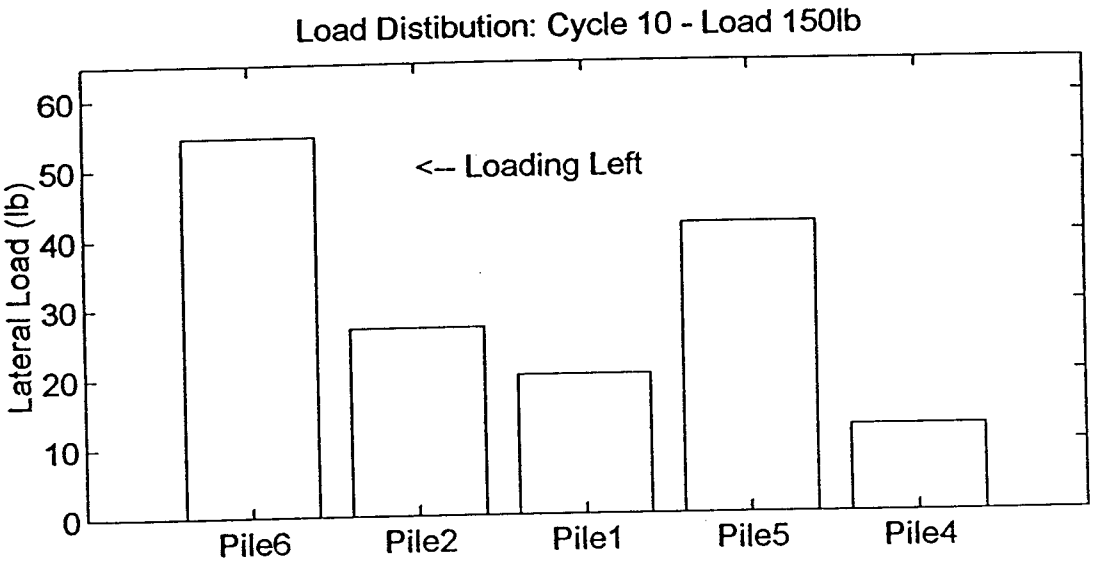
Load Distibution: Cycle 10 - Load 150lb
<-- Loading Left
Lateral Load (lb)
0
10
20
30
40
50
60
Pile6
Pile2
Pile1
Pile5
Pile4

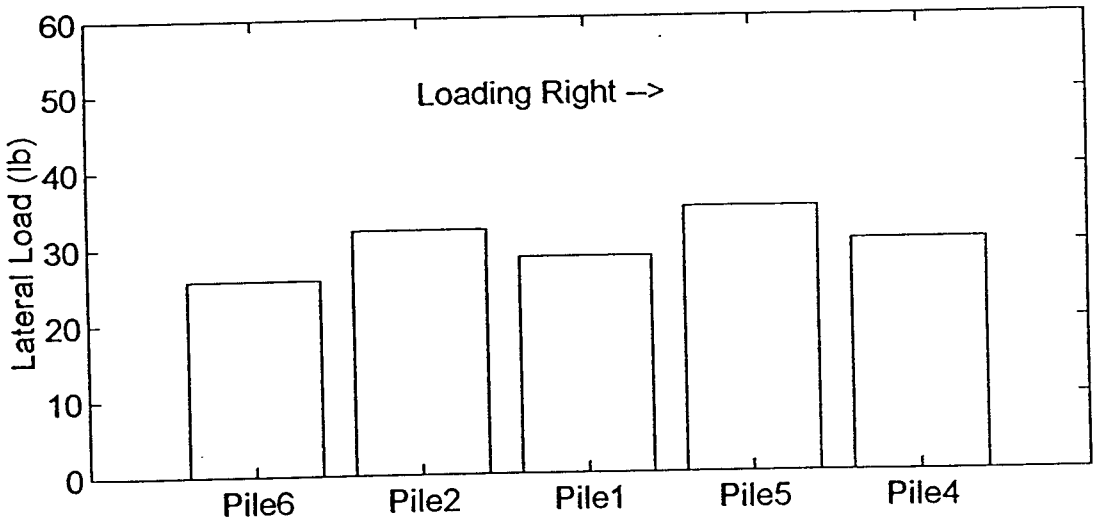
Loading Right -->
Lateral Load (lb)
0
10
20
30
40
50
60
Pile6
Pile2
Pile1
Pile5
Pile4

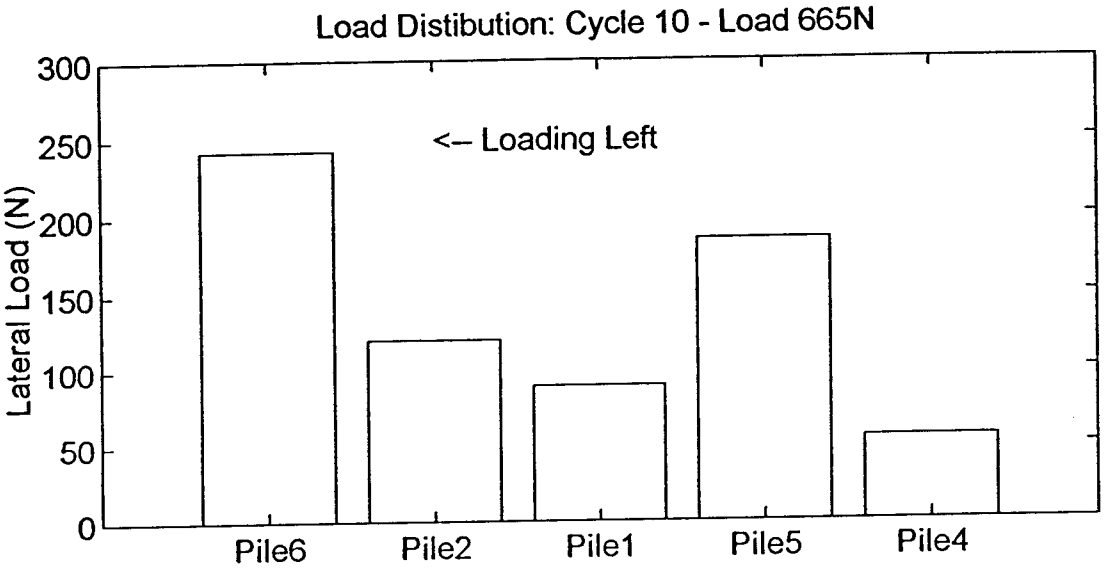
Load Distibution: Cycle 10 - Load 665N
<-- Loading Left
Lateral Load (N)
300
250
200
150
100
50
0
Pile6
Pile2
Pile1
Pile5
Pile4

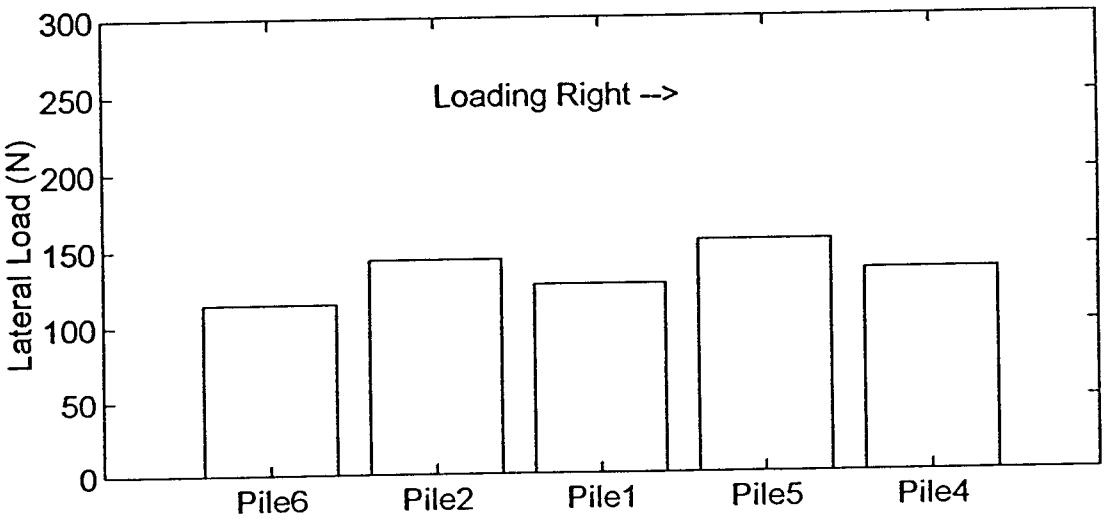
Loading Right -->
Lateral Load (N)
300
250
200
150
100
50
0
Pile6
Pile2
Pile1
Pile5
Pile4

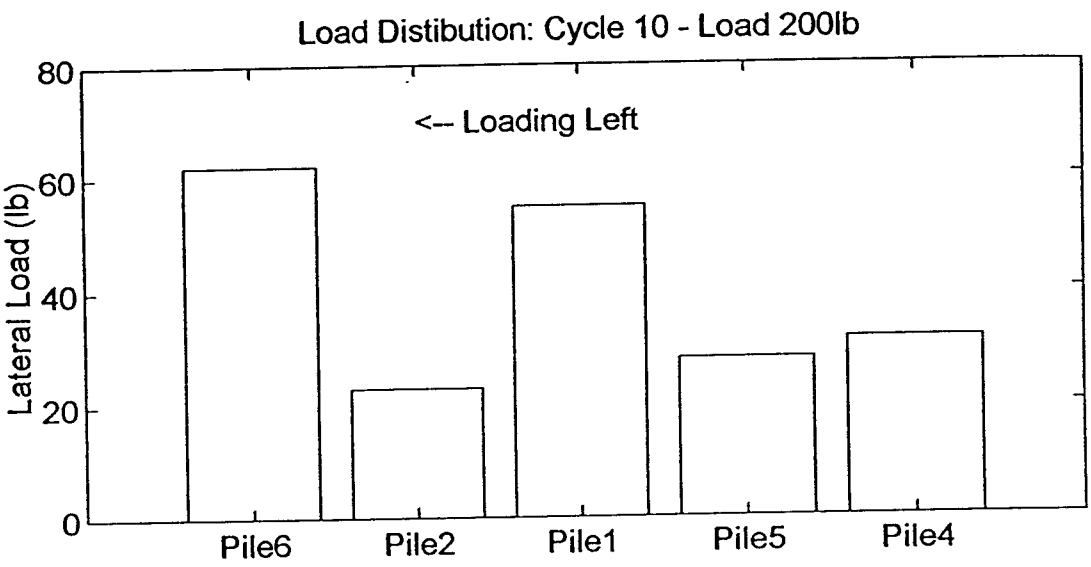
Load Distibution: Cycle 10 - Load 200lb
<-- Loading Left
Lateral Load (lb)
80
60
40
20
0
Pile6
Pile2
Pile1
Pile5
Pile4

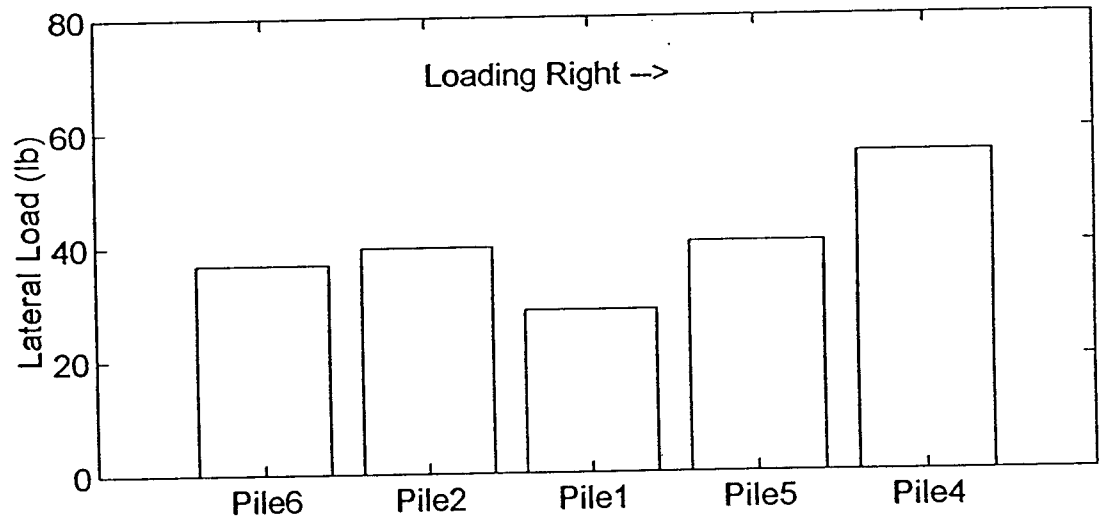
Loading Right -->
Lateral Load (lb)
80
60
40
20
0
Pile6
Pile2
Pile1
Pile5
Pile4

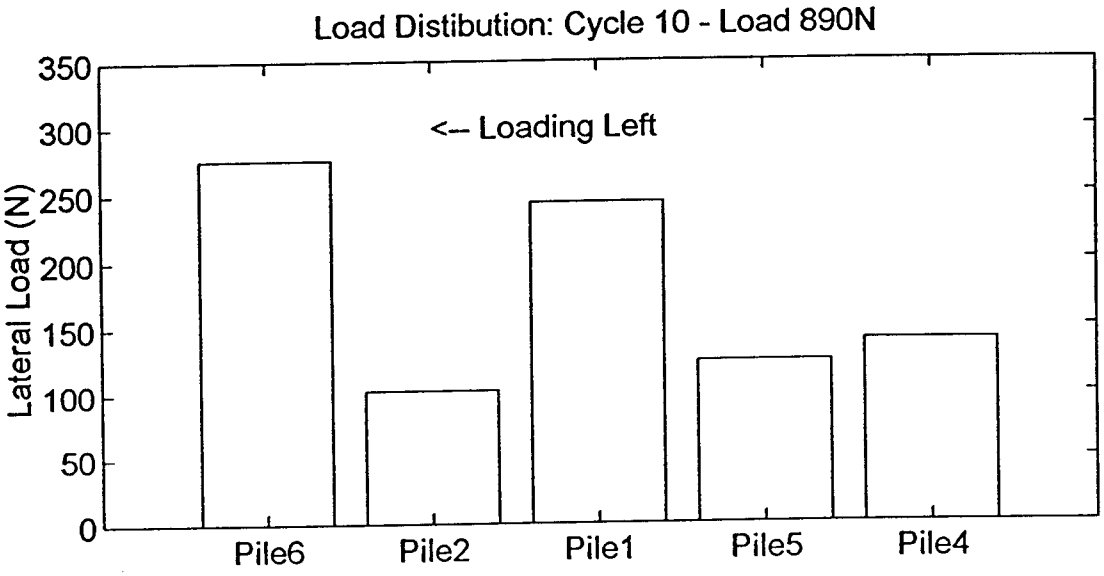
Load Distibution: Cycle 10 - Load 890N
<-- Loading Left
Lateral Load (N)
350
300
250
200
150
100
50
0
Pile6
Pile2
Pile1
Pile5
Pile4

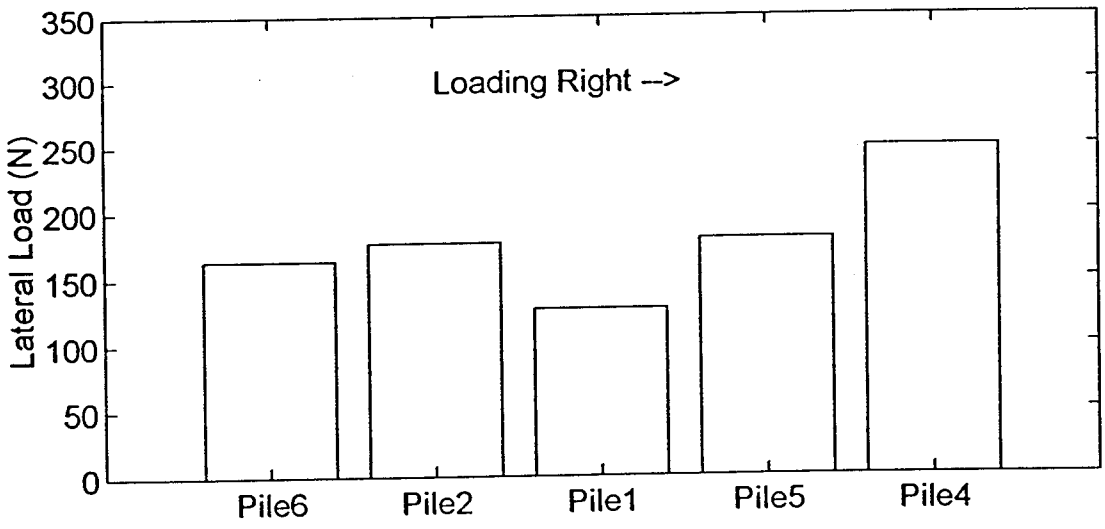
Loading Right -->
Lateral Load (N)
350
300
250
200
150
100
50
0
Pile6
Pile2
Pile1
Pile5
Pile4

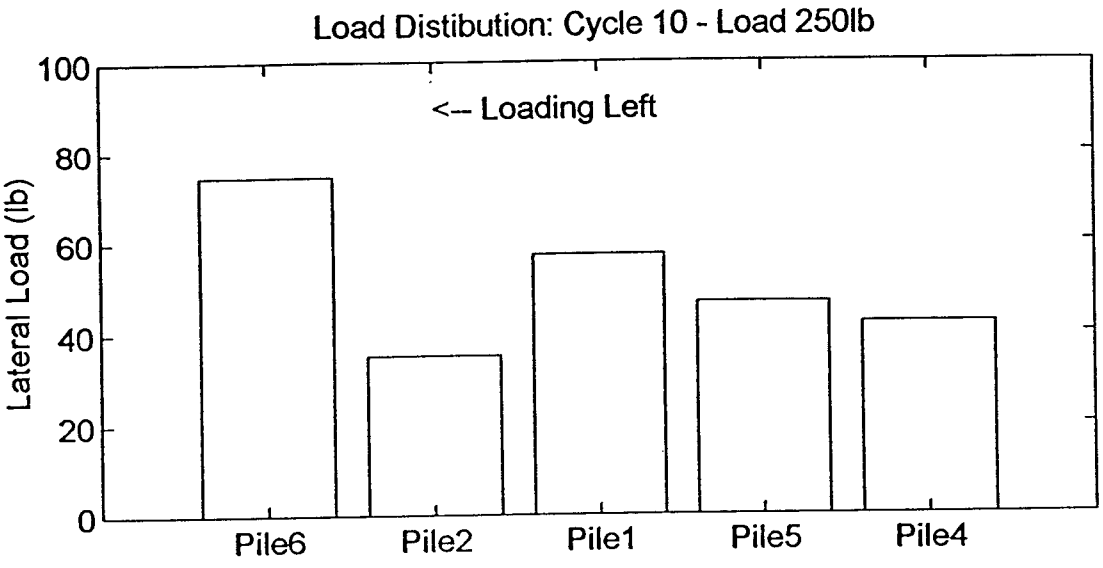
Load Distibution: Cycle 10 - Load 250lb
<-- Loading Left
Lateral Load (lb)
100
80
60
40
20
0
Pile6
Pile2
Pile1
Pile5
Pile4

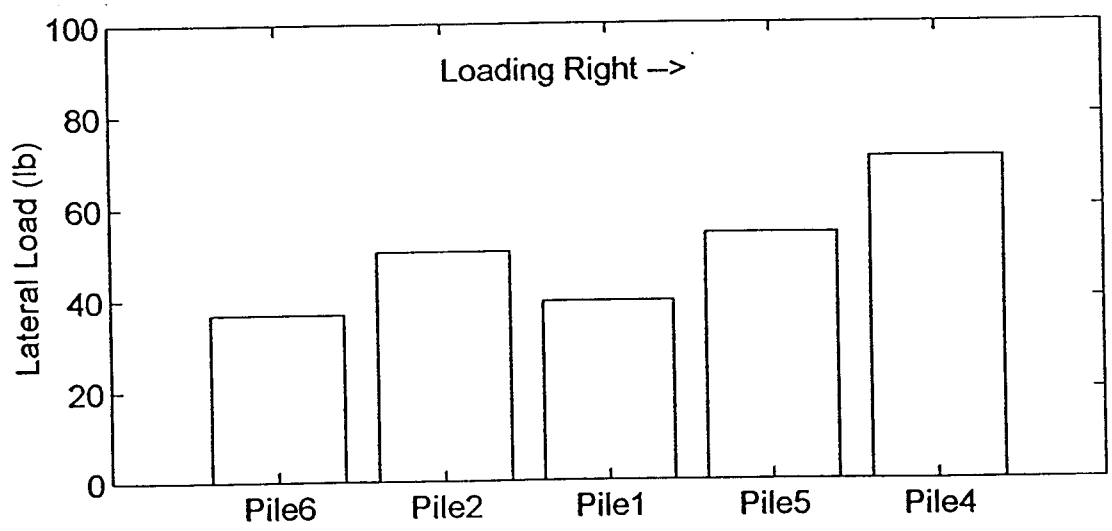
Loading Right -->
Lateral Load (lb)
100
80
60
40
20
0
Pile6
Pile2
Pile1
Pile5
Pile4

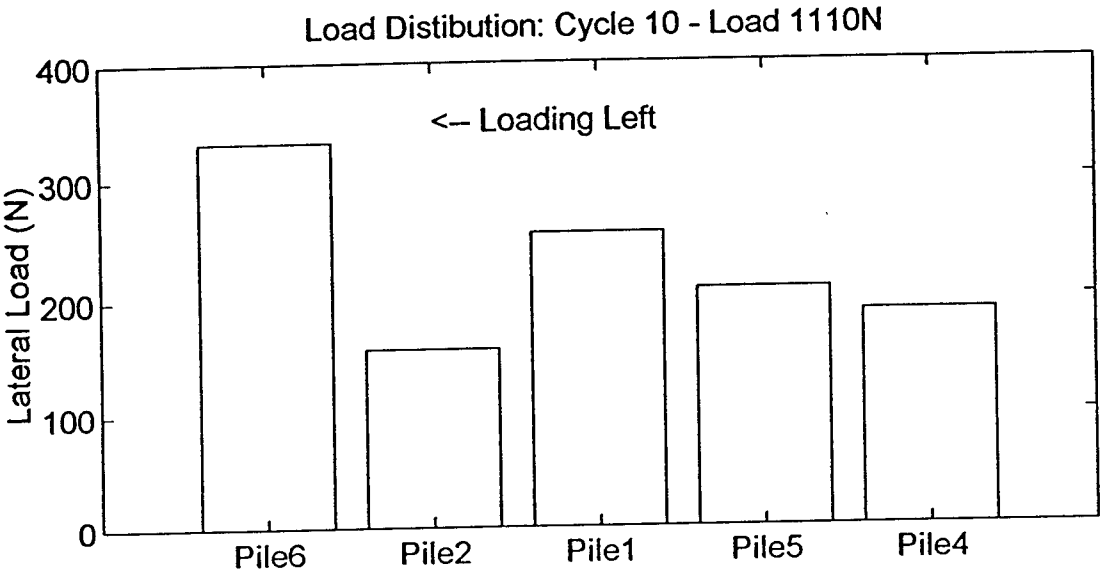
Load Distibution: Cycle 10 - Load 1110N
<-- Loading Left
Lateral Load (N)
400
300
200
100
0
Pile6
Pile2
Pile1
Pile5
Pile4

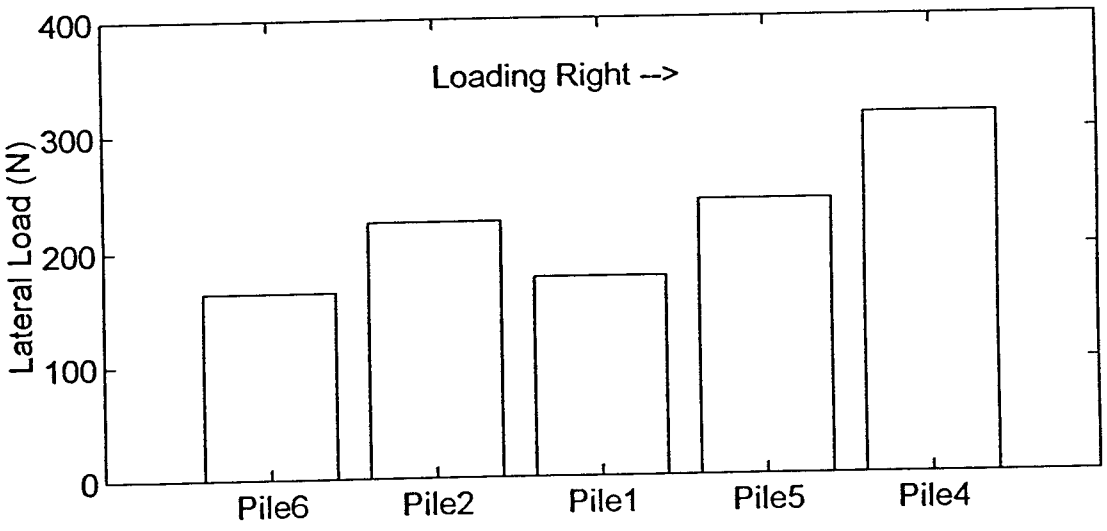
Loading Right -->
Lateral Load (N)
400
300
200
100
0
Pile6
Pile2
Pile1
Pile5
Pile4

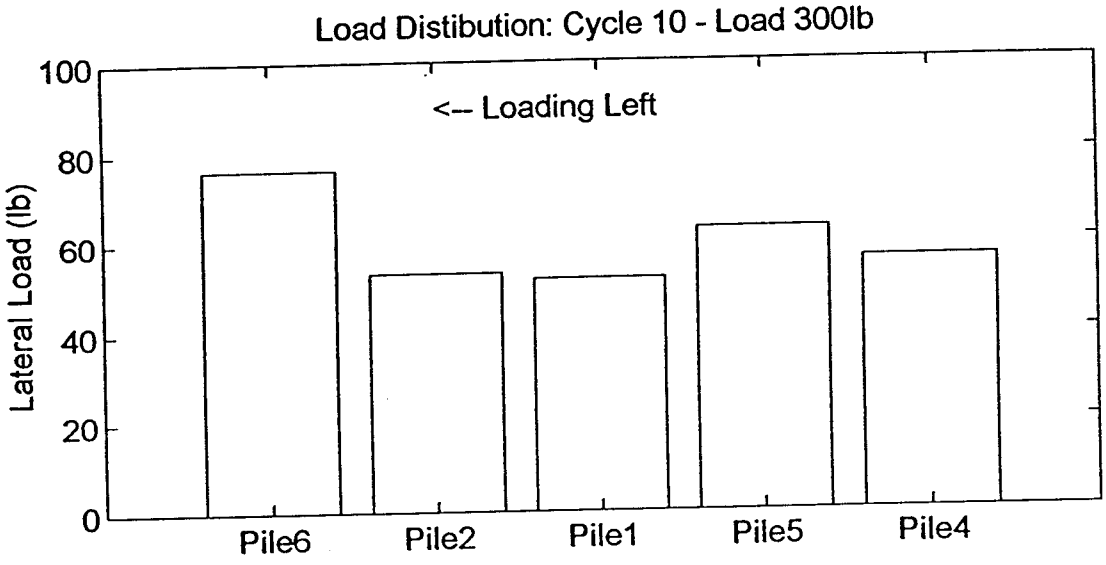
Load Distibution: Cycle 10 - Load 300lb
<-- Loading Left
Lateral Load (lb)
100
80
60
40
20
0
Pile6
Pile2
Pile1
Pile5
Pile4

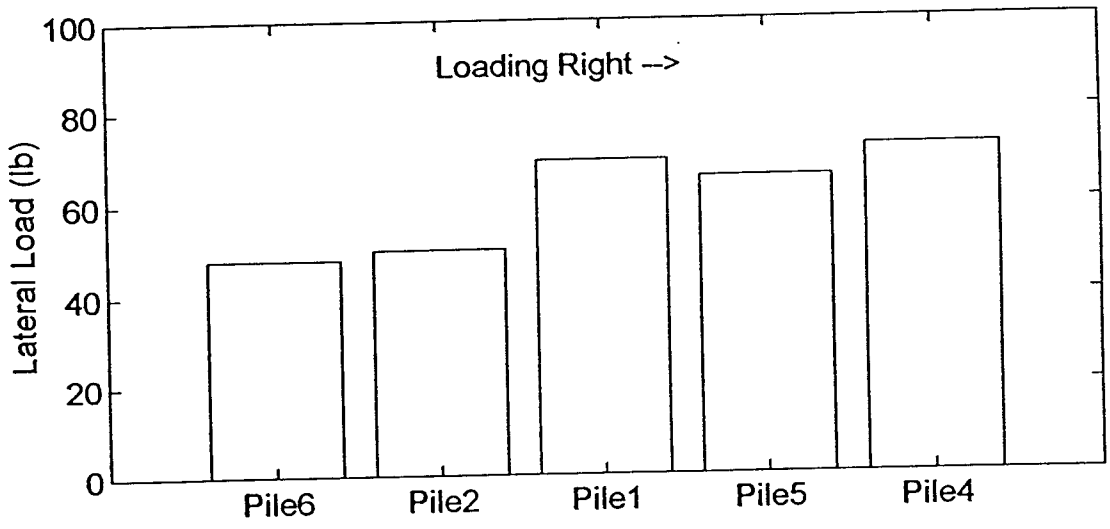
Loading Right -->
Lateral Load (lb)
100
80
60
40
20
0
Pile6
Pile2
Pile1
Pile5
Pile4

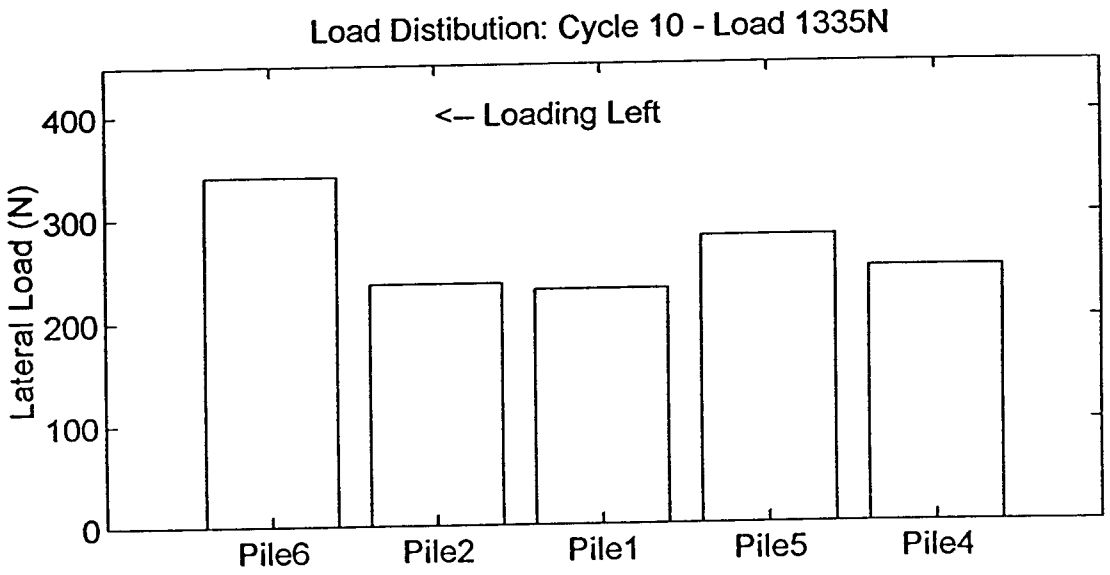
Load Distibution: Cycle 10 - Load 1335N
<-- Loading Left
Lateral Load (N)
400
300
200
100
0
Pile6
Pile2
Pile1
Pile5
Pile4

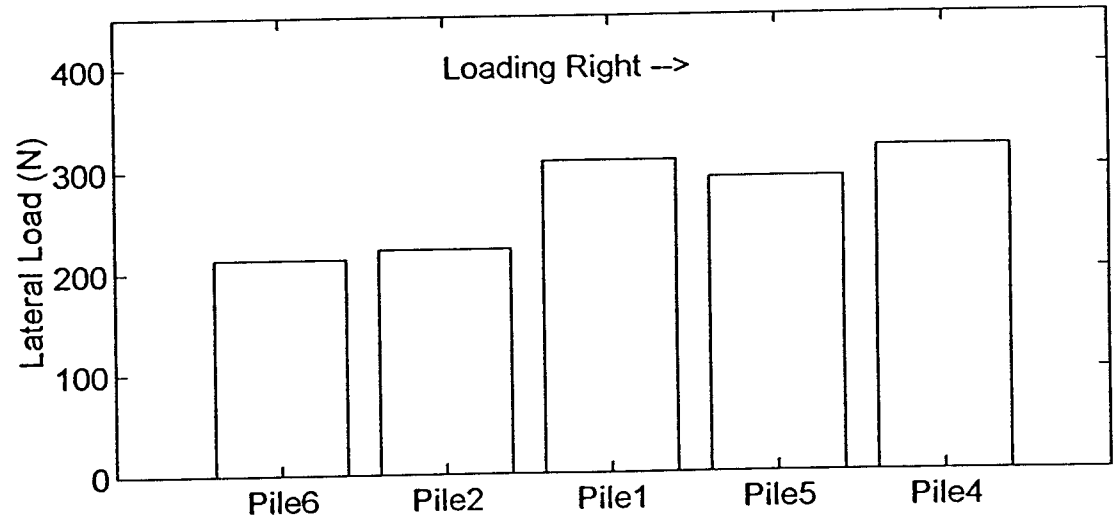
Loading Right -->
Lateral Load (N)
400
300
200
100
0
Pile6
Pile2
Pile1
Pile5
Pile4

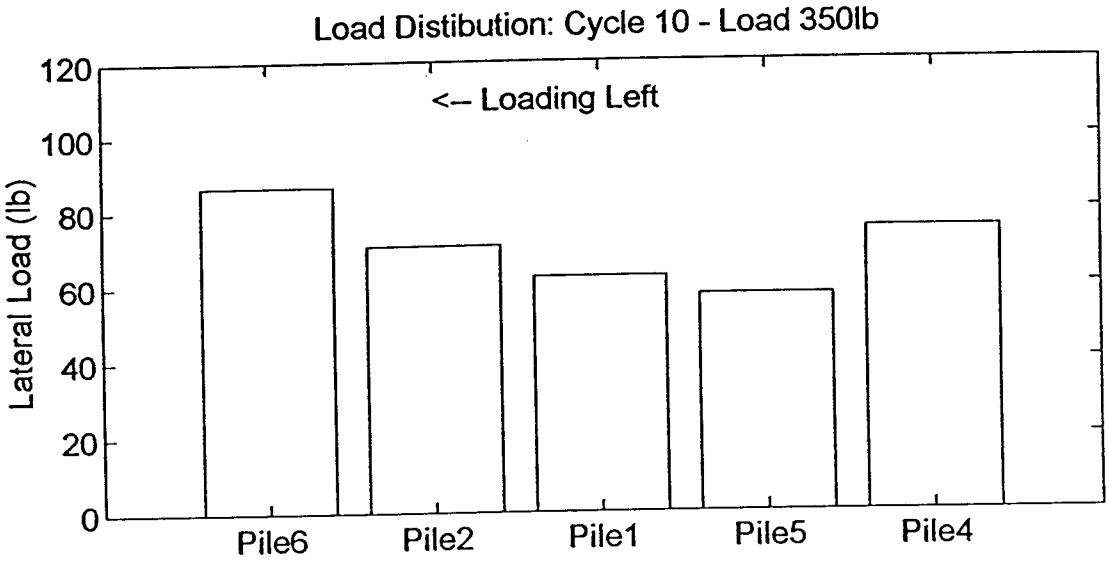
Load Distibution: Cycle 10 - Load 350lb
<-- Loading Left
Lateral Load (lb)
120
100
80
60
40
20
0
Pile6
Pile2
Pile1
Pile5
Pile4

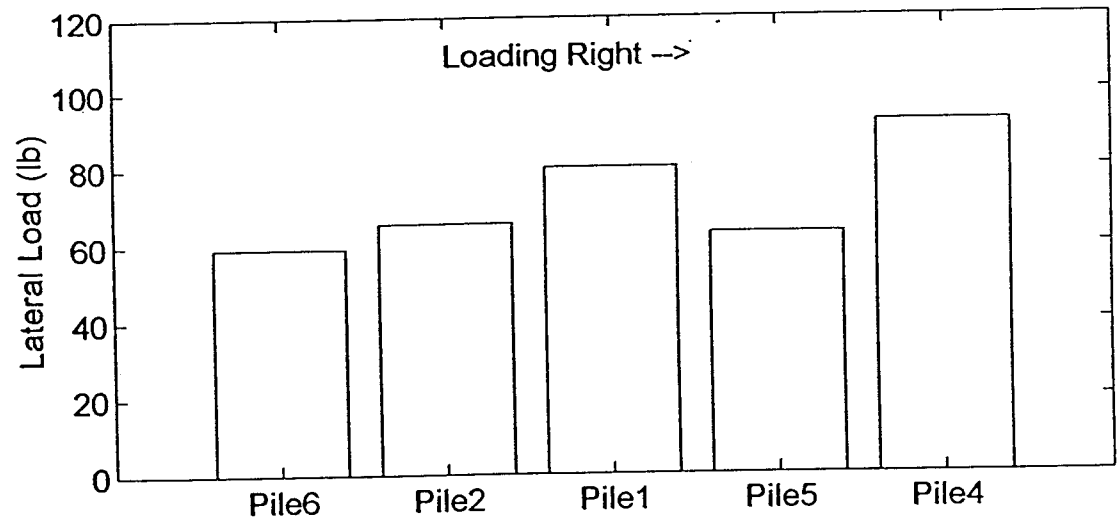
Loading Right -->
Lateral Load (lb)
120
100
80
60
40
20
0
Pile6
Pile2
Pile1
Pile5
Pile4

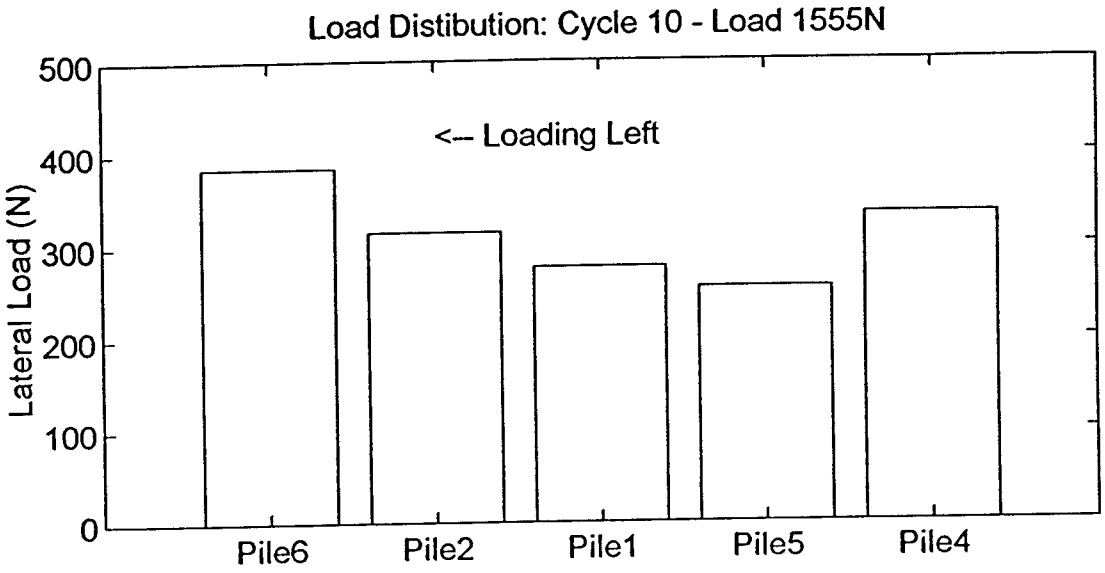
Load Distibution: Cycle 10 - Load 1555N
<-- Loading Left
Lateral Load (N)
500
400
300
200
100
0
Pile6
Pile2
Pile1
Pile5
Pile4

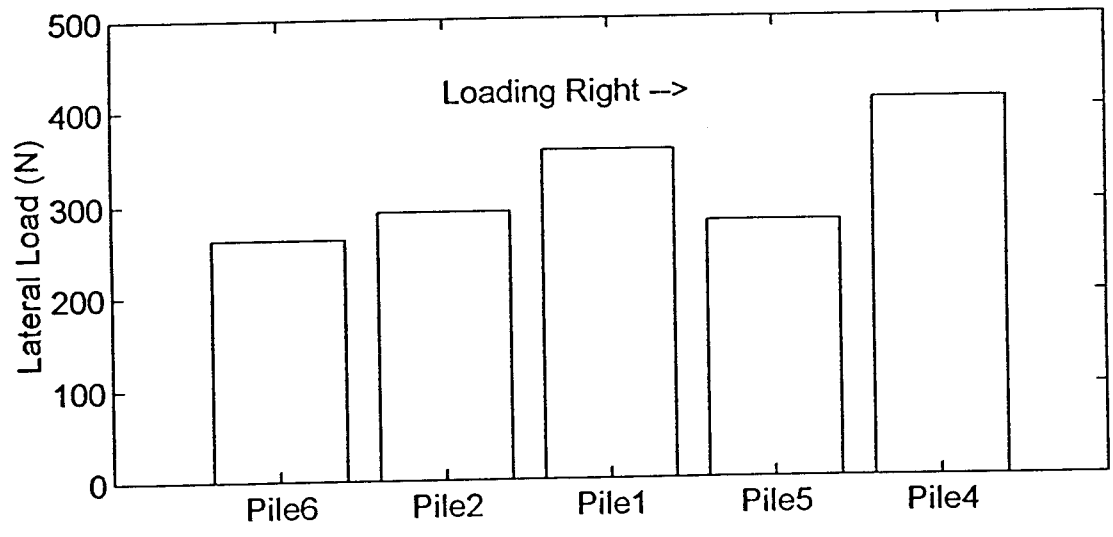
Loading Right -->
Lateral Load (N)
500
400
300
200
100
0
Pile6
Pile2
Pile1
Pile5
Pile4

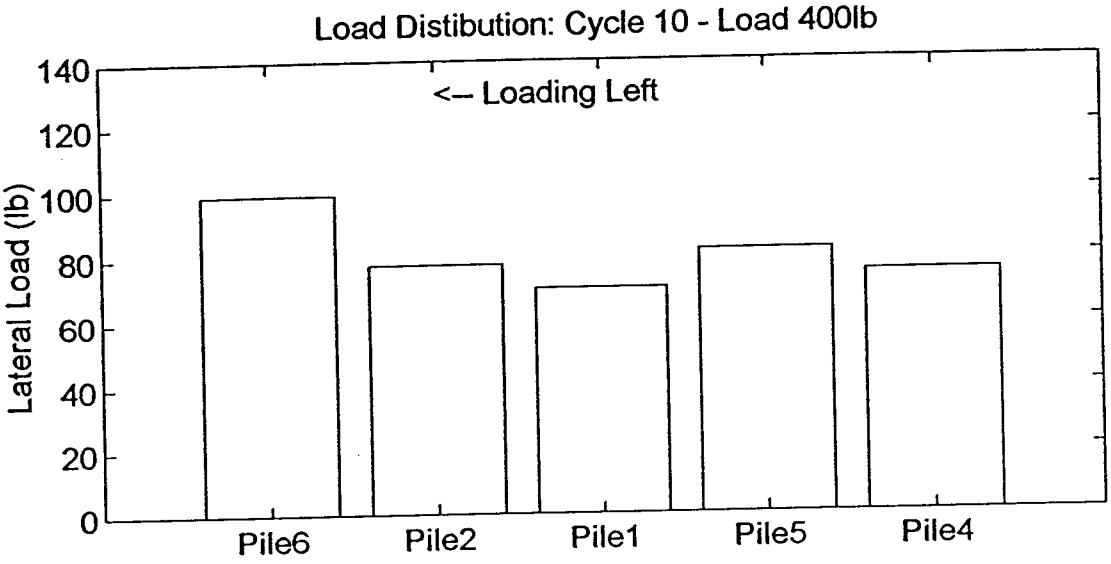
Load Distibution: Cycle 10 - Load 400lb
<-- Loading Left
Lateral Load (lb)
140
120
100
80
60
40
20
0
Pile6
Pile2
Pile1
Pile5
Pile4

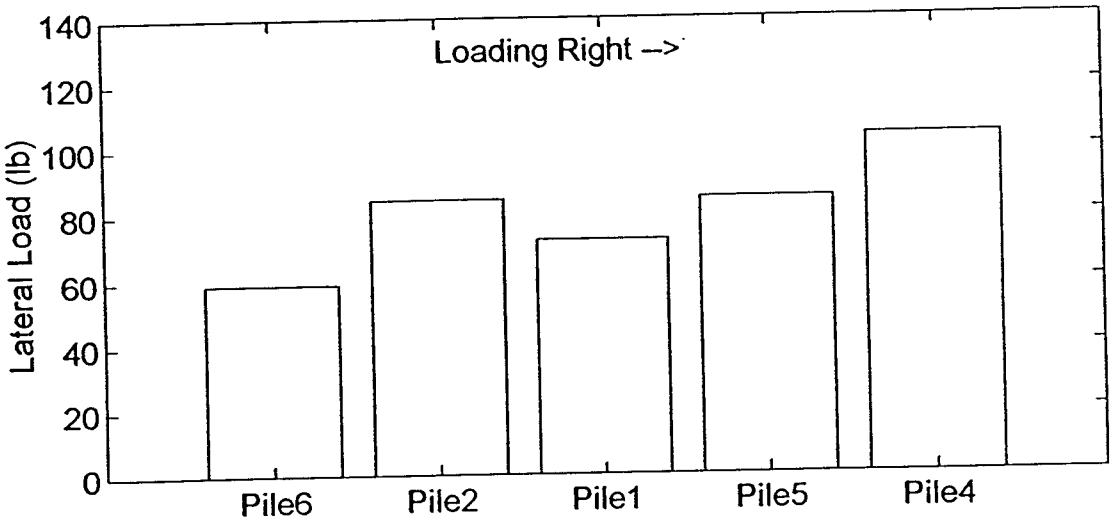
Loading Right -->
Lateral Load (lb)
140
120
100
80
60
40
20
0
Pile6
Pile2
Pile1
Pile5
Pile4

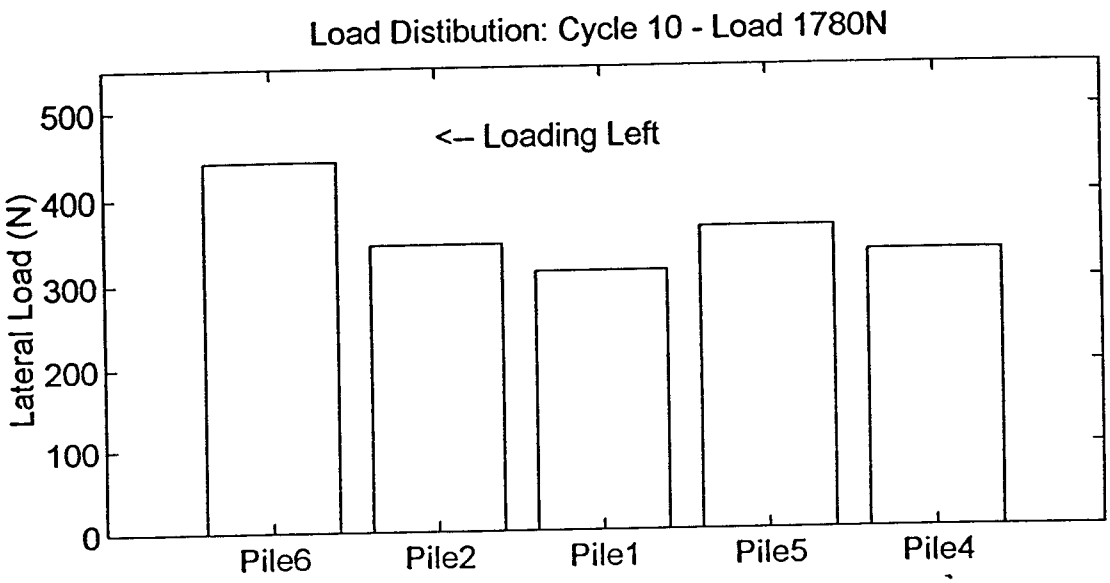
Load Distibution: Cycle 10 - Load 1780N
<-- Loading Left
Lateral Load (N)
500
400
300
200
100
0
Pile6
Pile2
Pile1
Pile5
Pile4

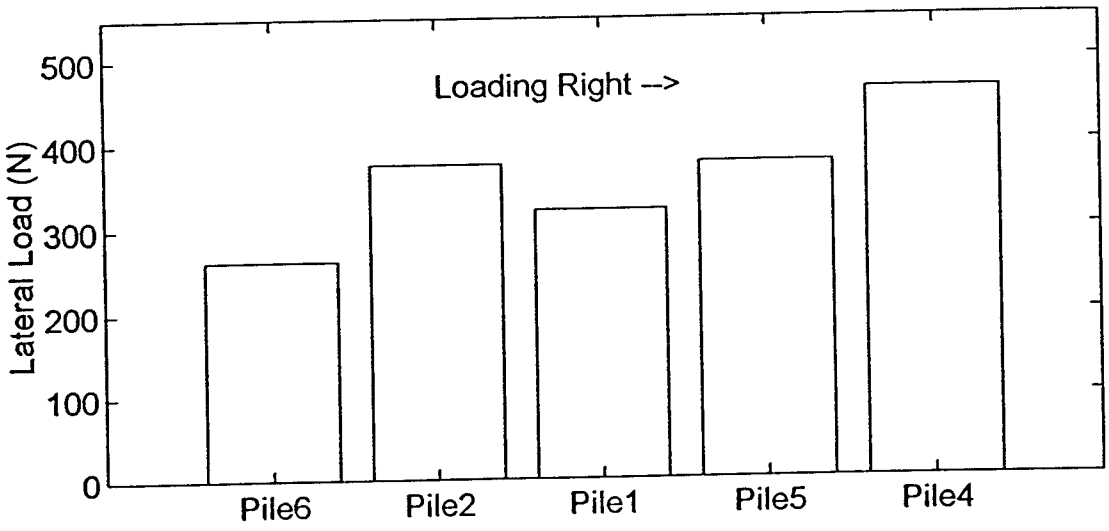
Loading Right -->
Lateral Load (N)
500
400
300
200
100
0
Pile6
Pile2
Pile1
Pile5
Pile4

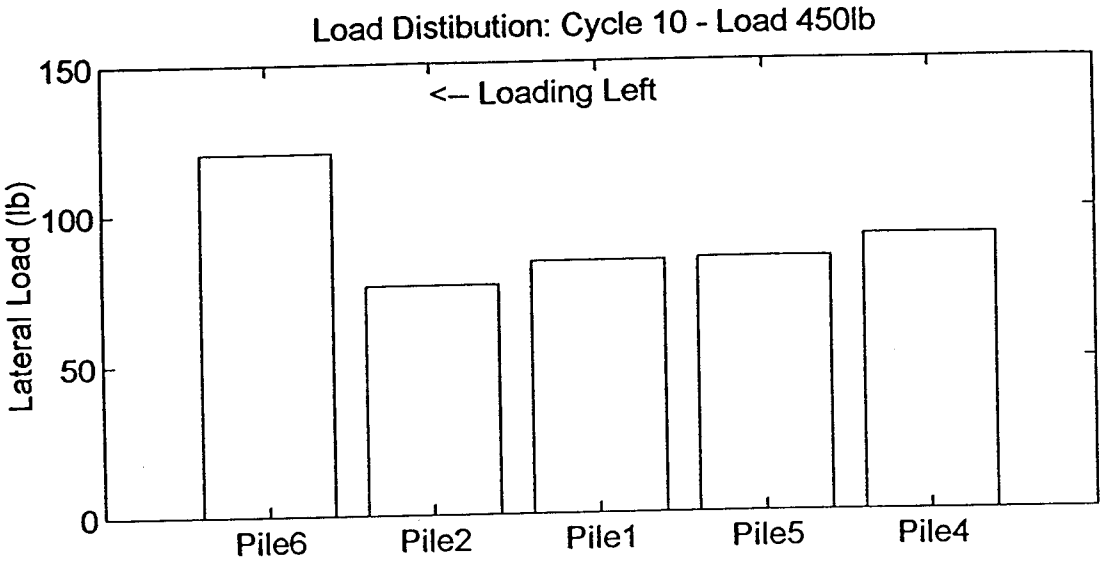
Load Distibution: Cycle 10 - Load 450lb
<-- Loading Left
Lateral Load (lb)
150
100
50
0
Pile6
Pile2
Pile1
Pile5
Pile4

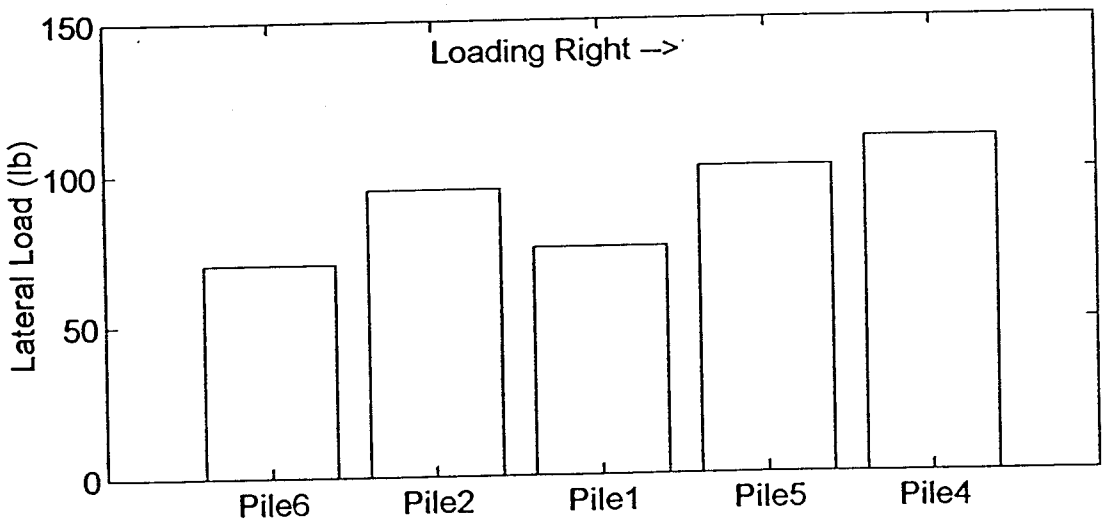
Loading Right -->
Lateral Load (lb)
150
100
50
0
Pile6
Pile2
Pile1
Pile5
Pile4

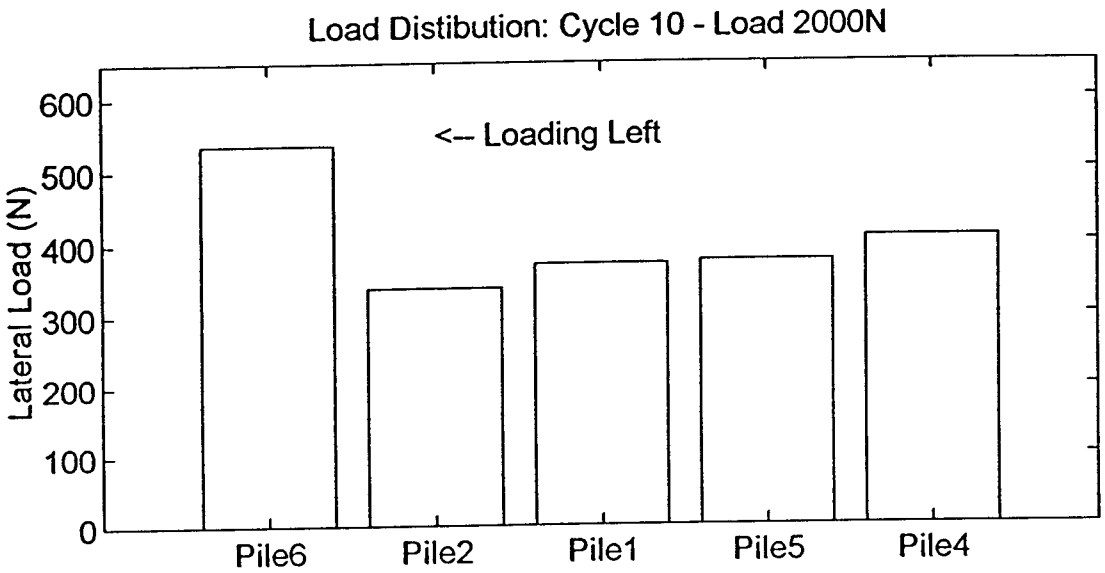
Load Distibution: Cycle 10 - Load 2000N
<-- Loading Left
Lateral Load (N)
600
500
400
300
200
100
0
Pile6
Pile2
Pile1
Pile5
Pile4

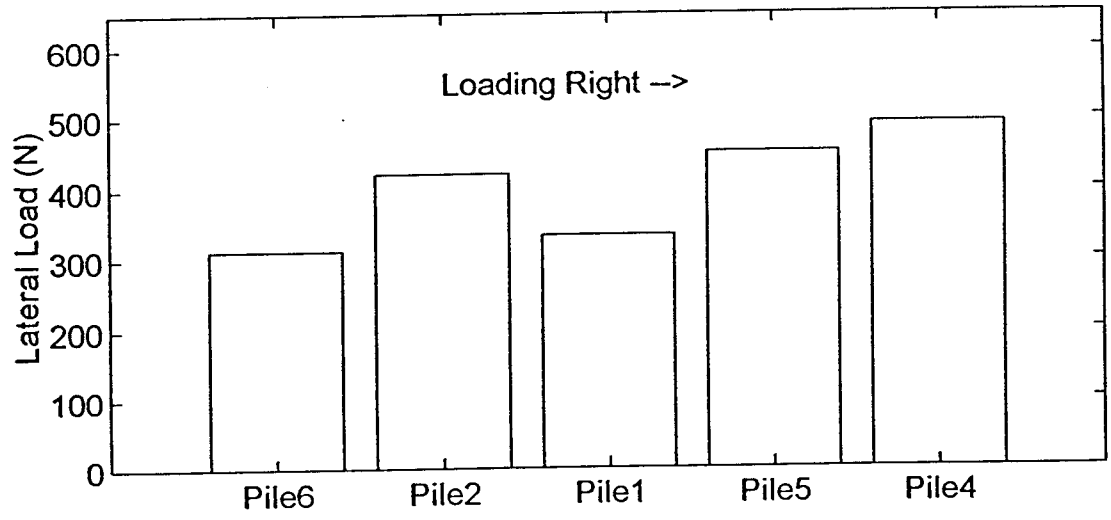
Loading Right -->
Lateral Load (N)
600
500
400
300
200
100
0
Pile6
Pile2
Pile1
Pile5
Pile4

Figure B14. Load distribution @ cycle 25 (next 14 plots).

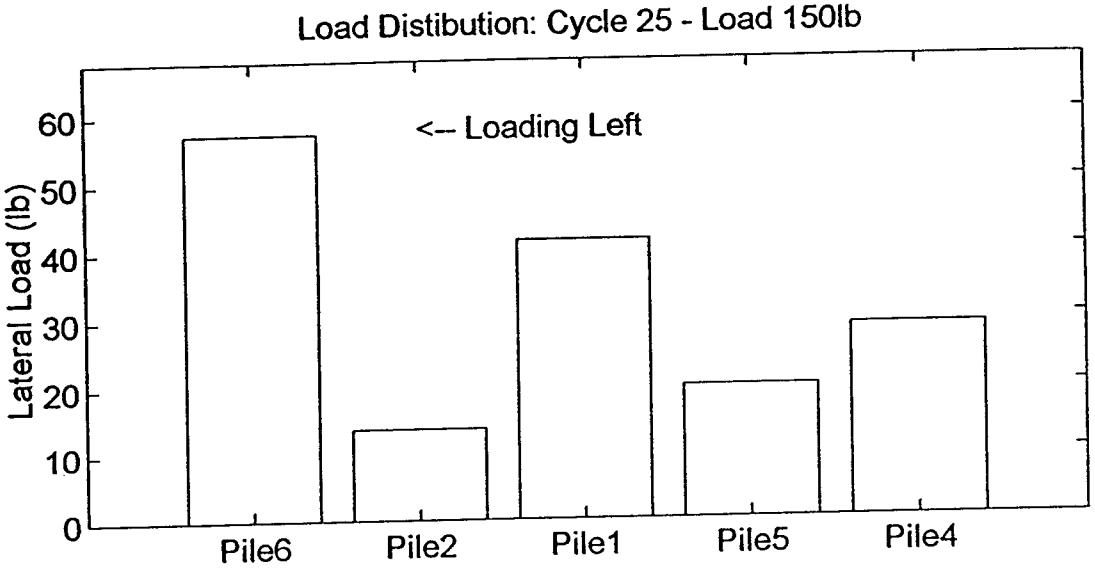
Load Distibution: Cycle 25 - Load 150lb
<-- Loading Left
Lateral Load (lb)
60
50
40
30
20
10
0
Pile6
Pile2
Pile1
Pile5
Pile4

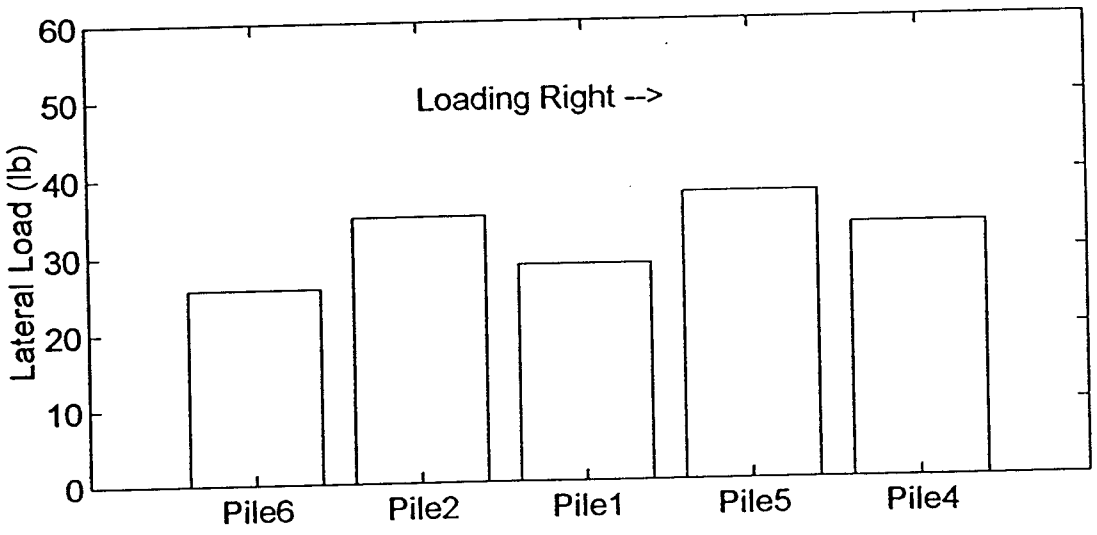
Loading Right -->
Lateral Load (lb)
60
50
40
30
20
10
0
Pile6
Pile2
Pile1
Pile5
Pile4

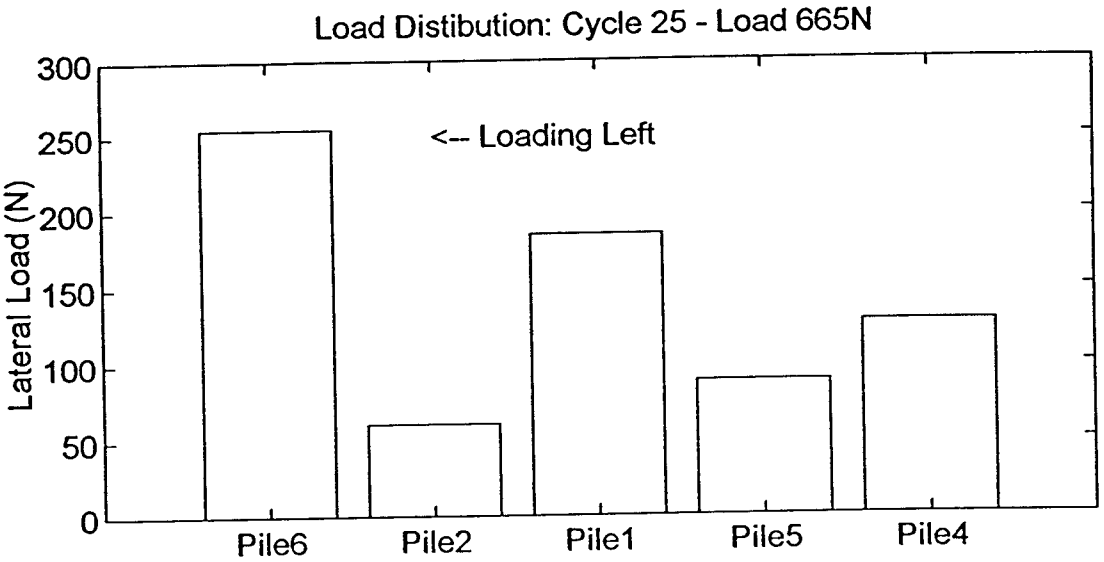
Load Distibution: Cycle 25 - Load 665N
<-- Loading Left
Lateral Load (N)
300
250
200
150
100
50
0
Pile6
Pile2
Pile1
Pile5
Pile4

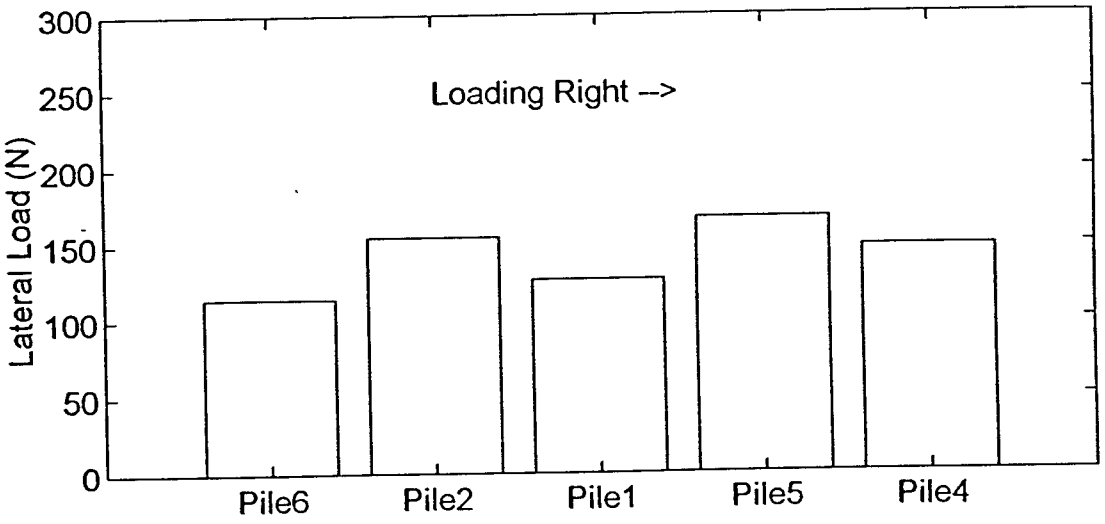
Loading Right -->
Lateral Load (N)
300
250
200
150
100
50
0
Pile6
Pile2
Pile1
Pile5
Pile4

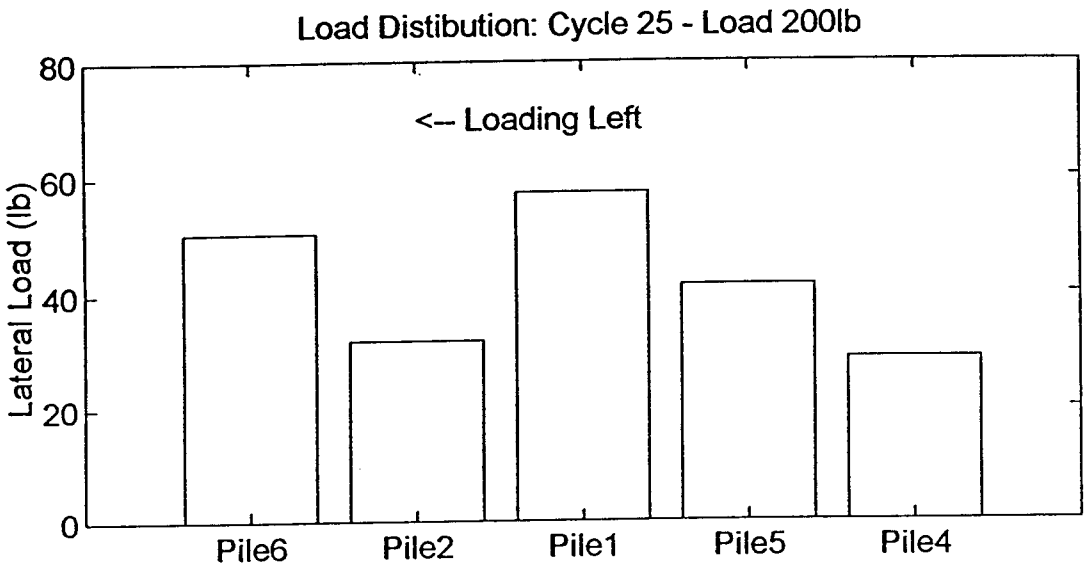
Load Distibution: Cycle 25 - Load 200lb
<-- Loading Left
Lateral Load (lb)
80
60
40
20
0
Pile6
Pile2
Pile1
Pile5
Pile4

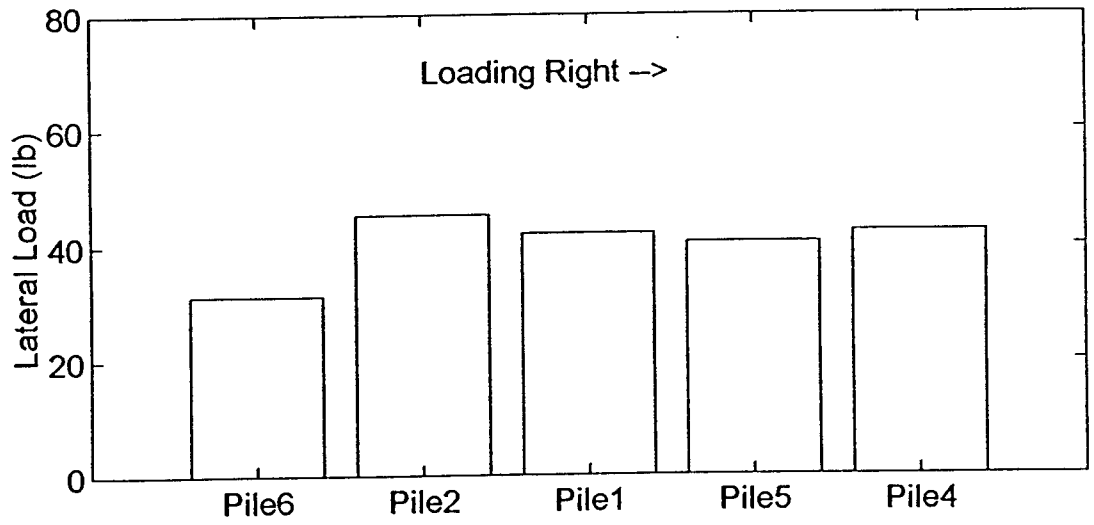
Loading Right -->
Lateral Load (lb)
80
60
40
20
0
Pile6
Pile2
Pile1
Pile5
Pile4

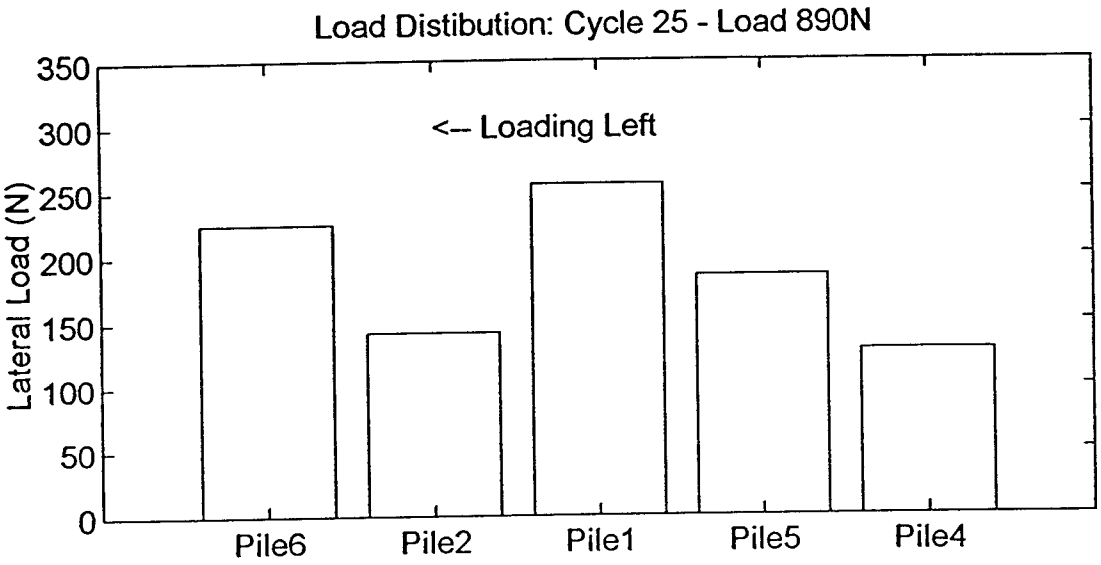
Load Distibution: Cycle 25 - Load 890N
<-- Loading Left
Lateral Load (N)
350
300
250
200
150
100
50
0
Pile6
Pile2
Pile1
Pile5
Pile4

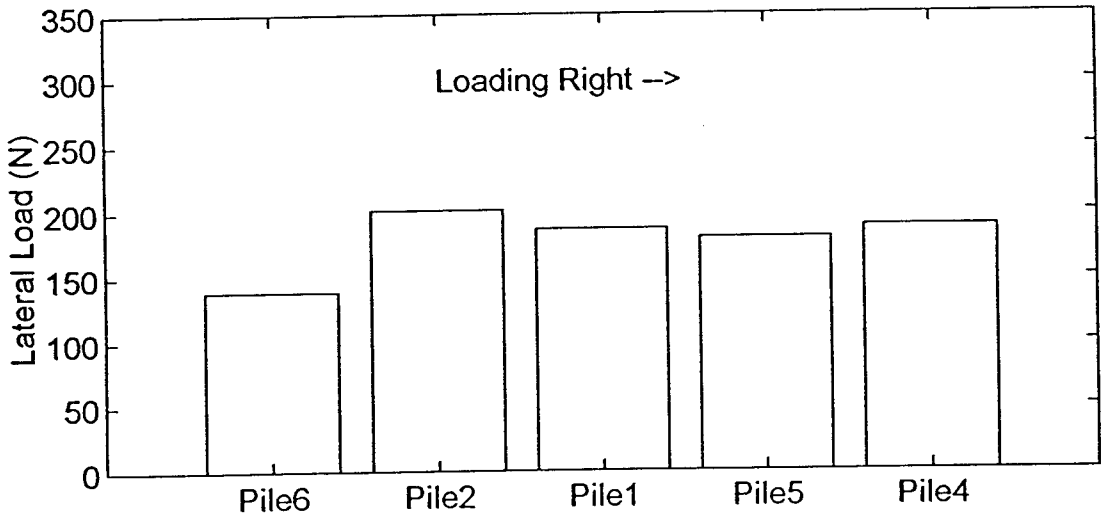
Loading Right -->
Lateral Load (N)
350
300
250
200
150
100
50
0
Pile6
Pile2
Pile1
Pile5
Pile4

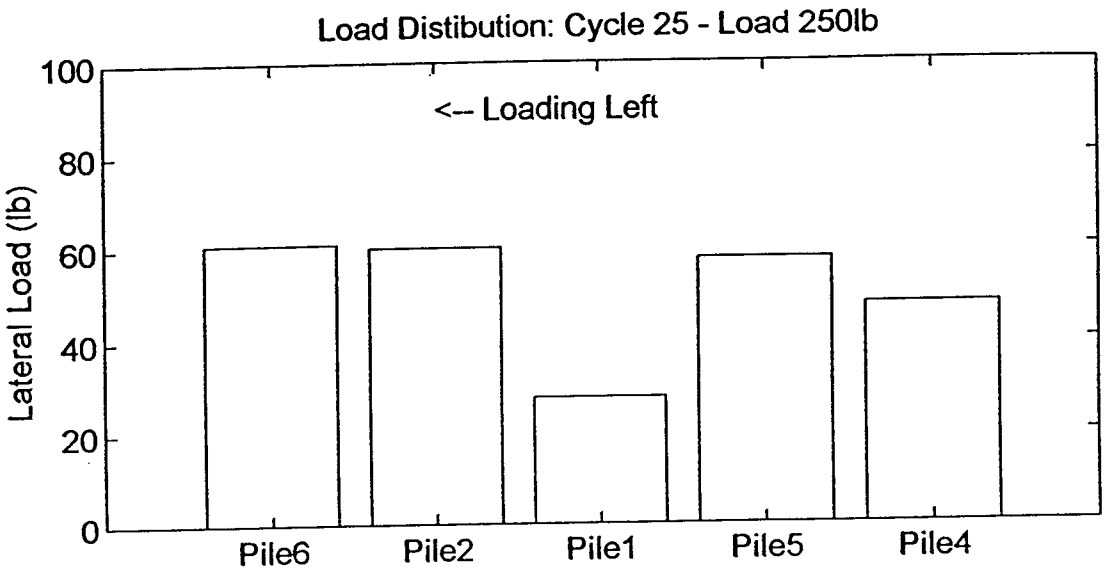
Load Distibution: Cycle 25 - Load 250lb
<-- Loading Left
Lateral Load (lb)
100
80
60
40
20
0
Pile6
Pile2
Pile1
Pile5
Pile4

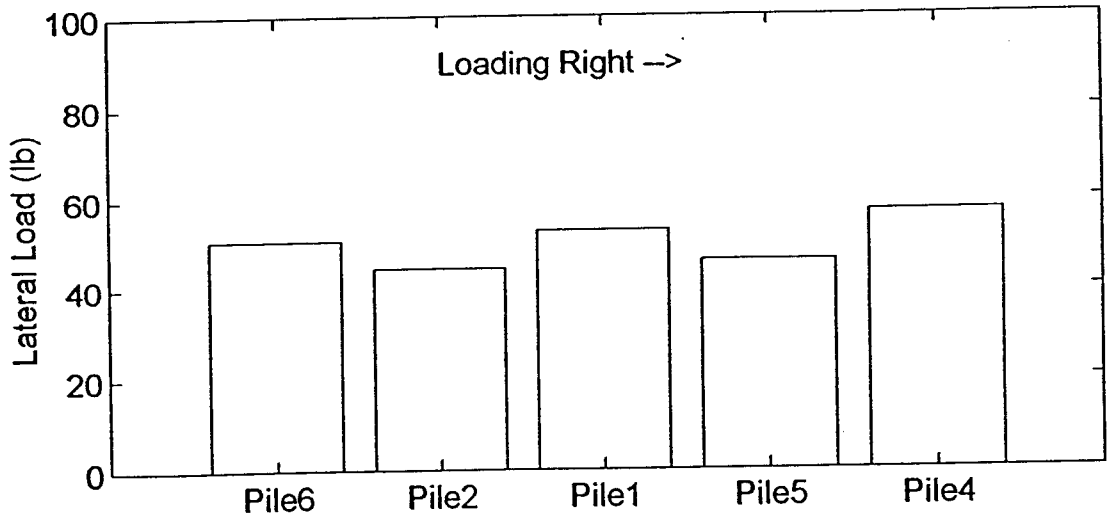
Loading Right -->
Lateral Load (lb)
100
80
60
40
20
0
Pile6
Pile2
Pile1
Pile5
Pile4

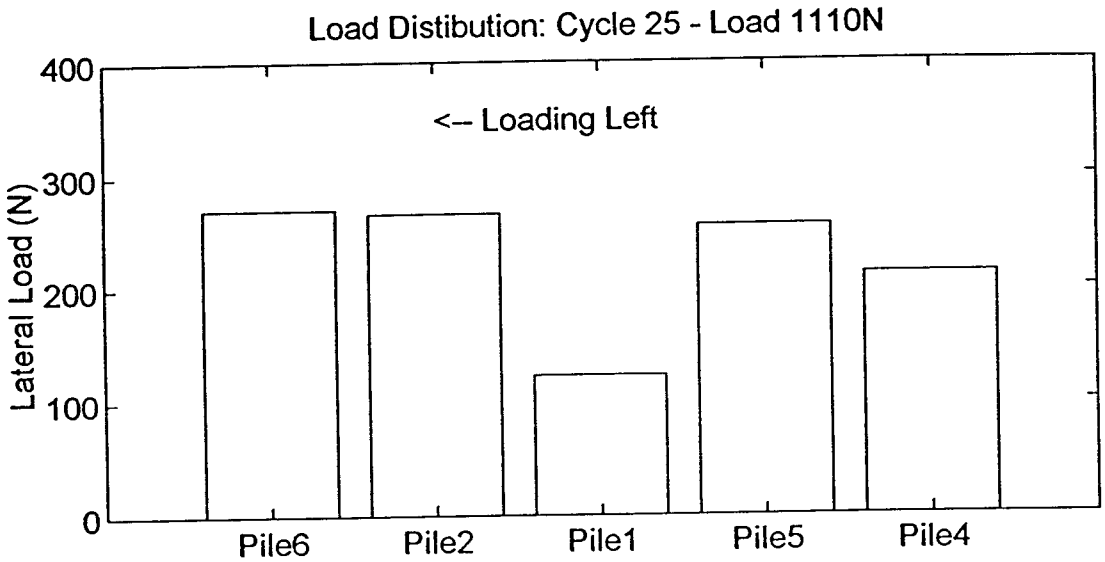
Load Distibution: Cycle 25 - Load 1110N
<-- Loading Left
Lateral Load (N)
400
300
200
100
0
Pile6
Pile2
Pile1
Pile5
Pile4

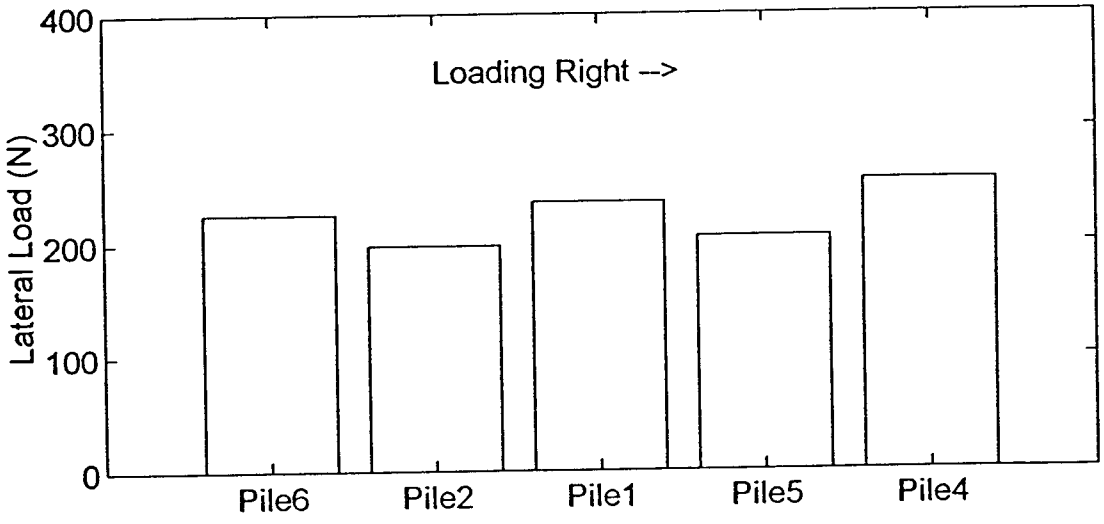
Loading Right -->
Lateral Load (N)
400
300
200
100
0
Pile6
Pile2
Pile1
Pile5
Pile4

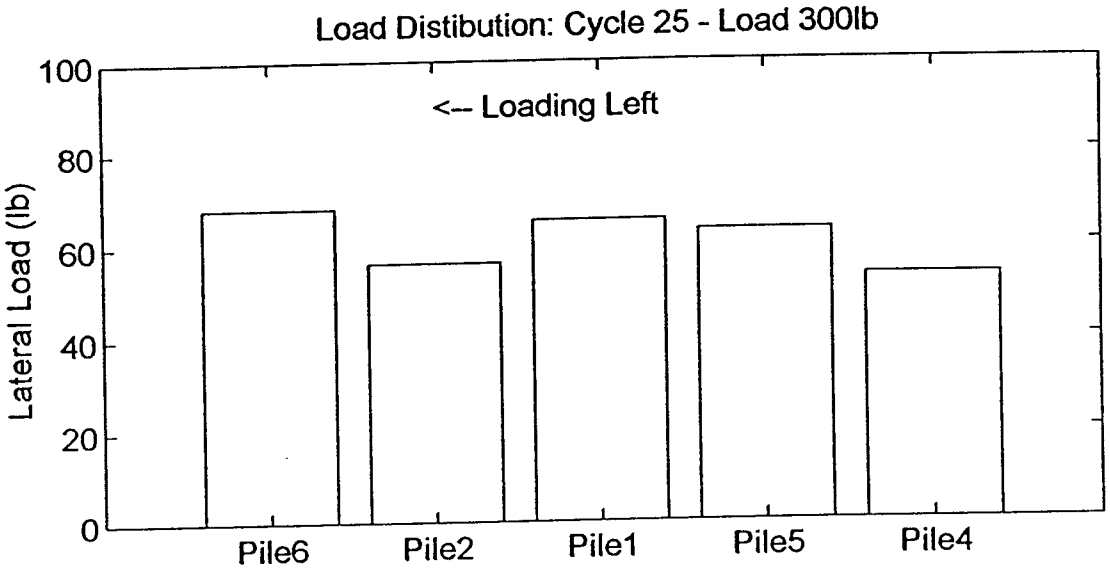
Load Distibution: Cycle 25 - Load 300lb
<-- Loading Left
Lateral Load (lb)
100
80
60
40
20
0
Pile6
Pile2
Pile1
Pile5
Pile4

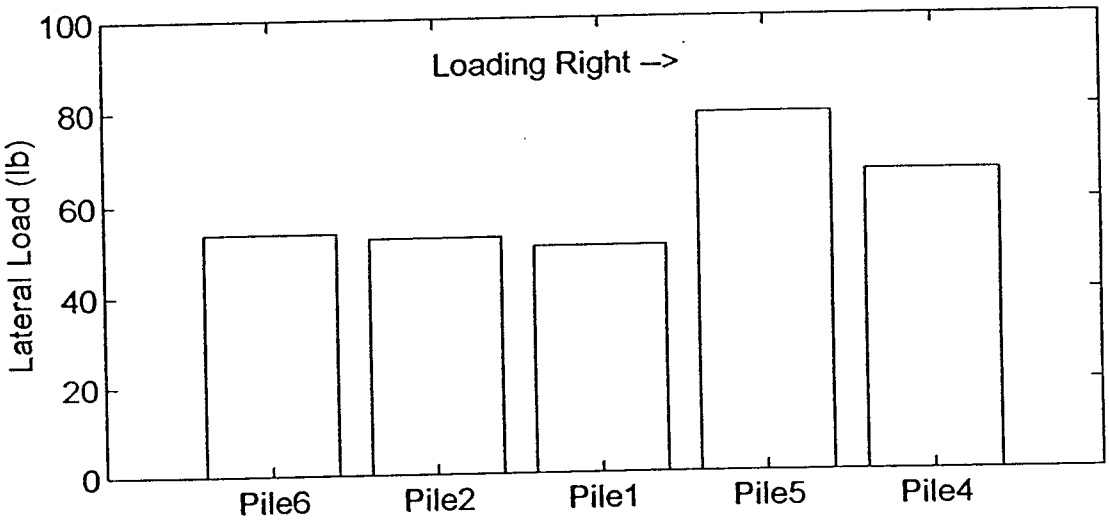
Loading Right -->
Lateral Load (lb)
100
80
60
40
20
0
Pile6
Pile2
Pile1
Pile5
Pile4

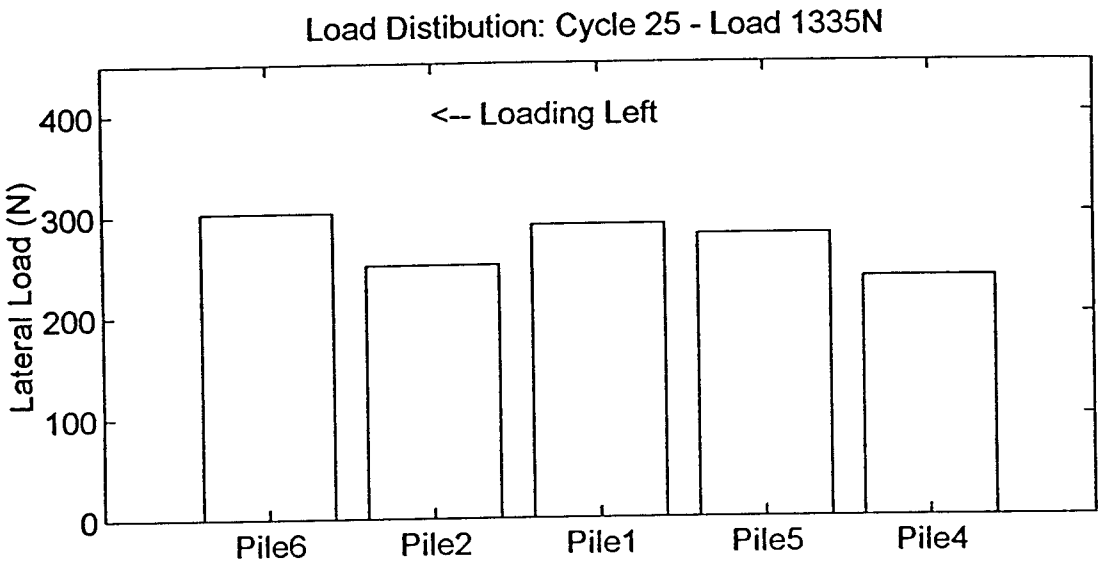
Load Distibution: Cycle 25 - Load 1335N
<-- Loading Left
Lateral Load (N)
400
300
200
100
0
Pile6
Pile2
Pile1
Pile5
Pile4

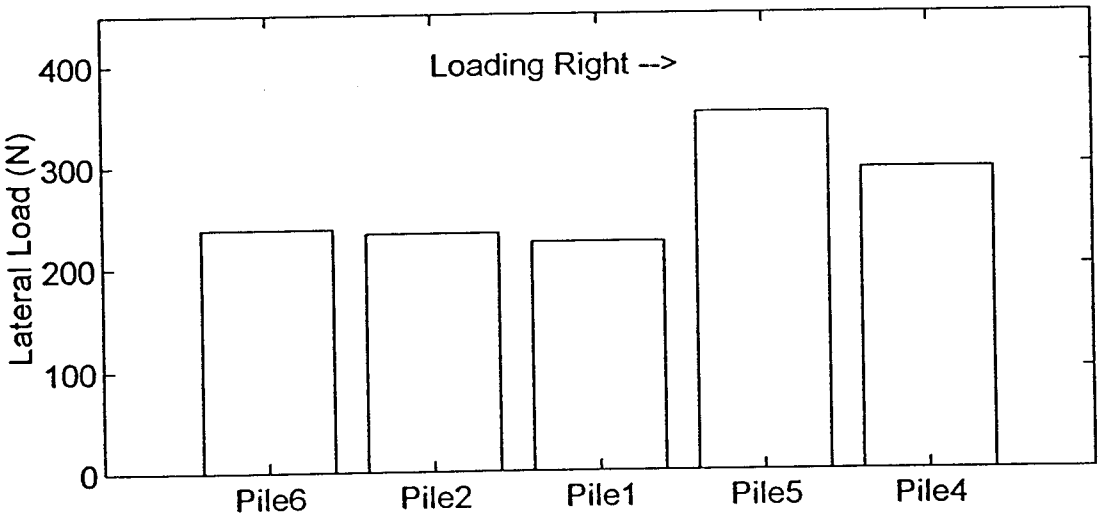
Loading Right -->
Lateral Load (N)
400
300
200
100
0
Pile6
Pile2
Pile1
Pile5
Pile4

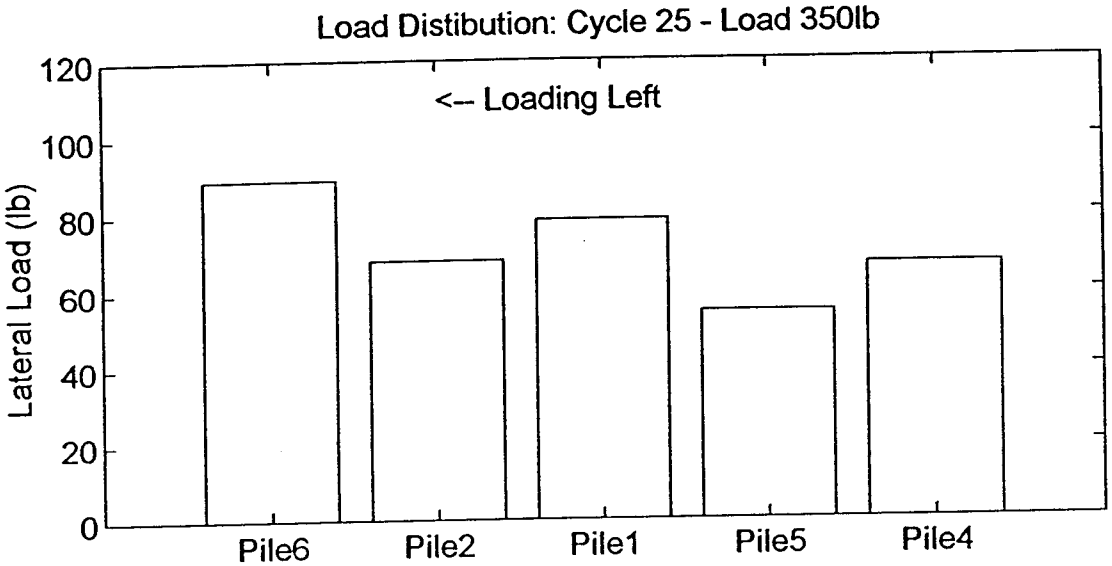
Load Distibution: Cycle 25 - Load 350lb
<-- Loading Left
Lateral Load (lb)
120
100
80
60
40
20
0
Pile6
Pile2
Pile1
Pile5
Pile4

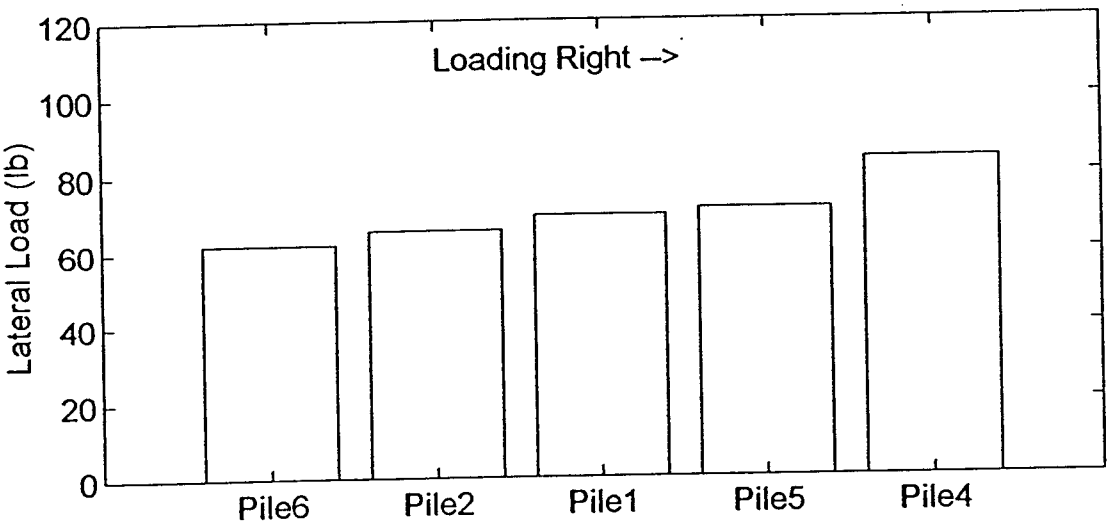
Loading Right -->
Lateral Load (lb)
120
100
80
60
40
20
0
Pile6
Pile2
Pile1
Pile5
Pile4

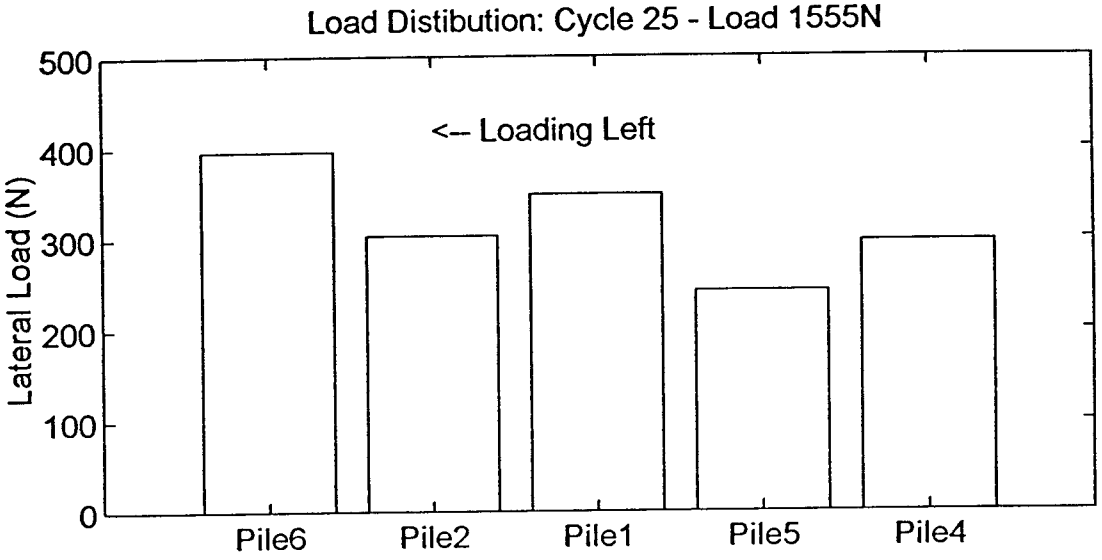
Load Distibution: Cycle 25 - Load 1555N
<-- Loading Left
Lateral Load (N)
500
400
300
200
100
0
Pile6
Pile2
Pile1
Pile5
Pile4

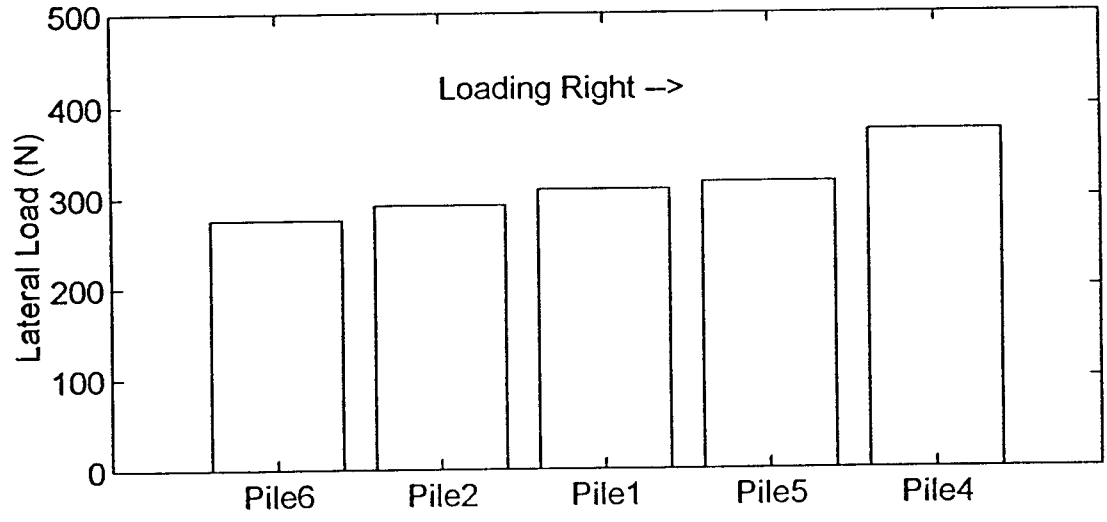
Loading Right -->
Lateral Load (N)
500
400
300
200
100
0
Pile6
Pile2
Pile1
Pile5
Pile4

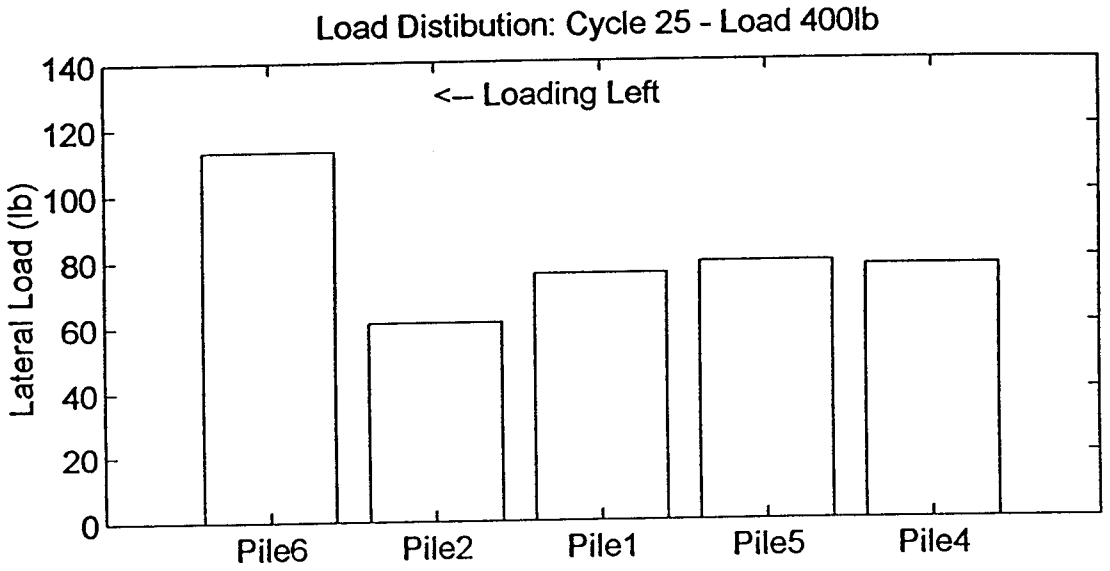
Load Distibution: Cycle 25 - Load 400lb
<-- Loading Left
Lateral Load (lb)
140
120
100
80
60
40
20
0
Pile6
Pile2
Pile1
Pile5
Pile4

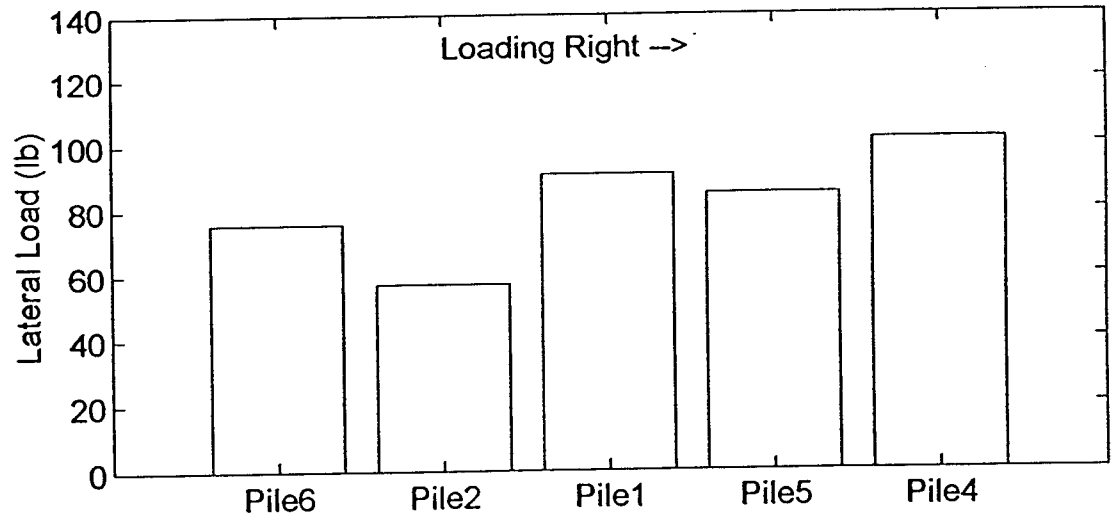
Loading Right -->
Lateral Load (lb)
140
120
100
80
60
40
20
0
Pile6
Pile2
Pile1
Pile5
Pile4

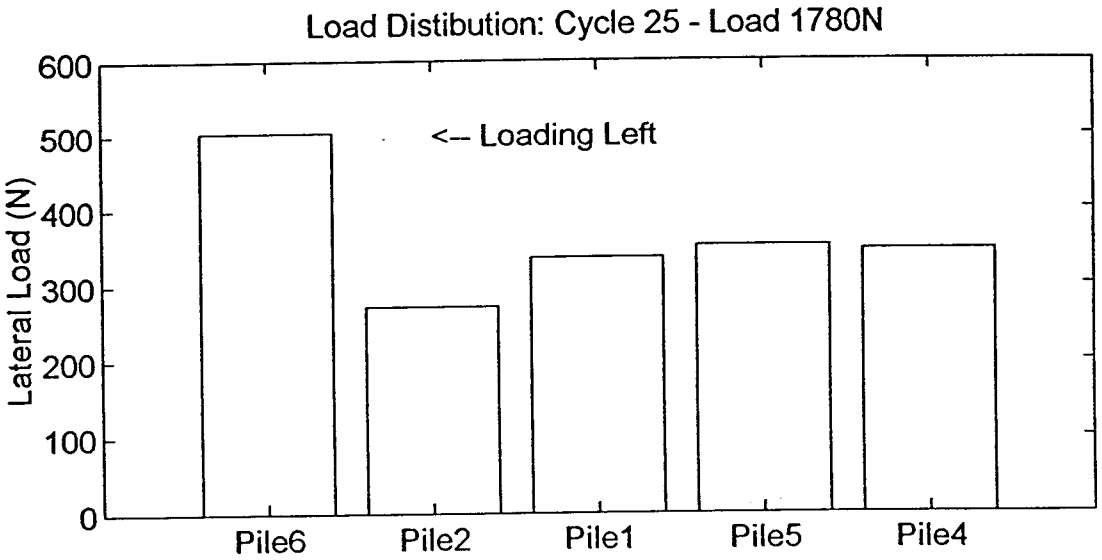
Load Distibution: Cycle 25 - Load 1780N
<-- Loading Left
Lateral Load (N)
600
500
400
300
200
100
0
Pile6
Pile2
Pile1
Pile5
Pile4

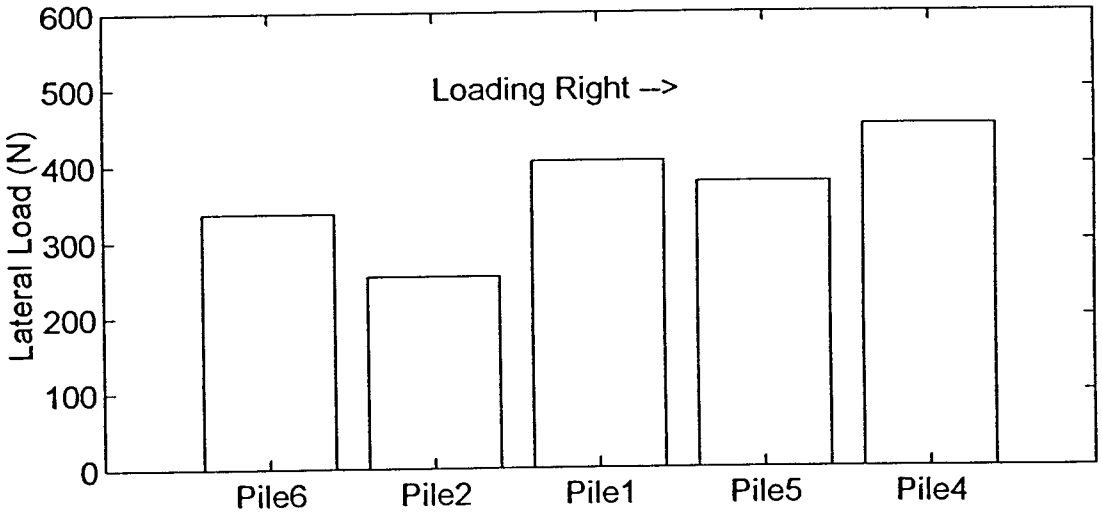
Loading Right -->
Lateral Load (N)
600
500
400
300
200
100
0
Pile6
Pile2
Pile1
Pile5
Pile4

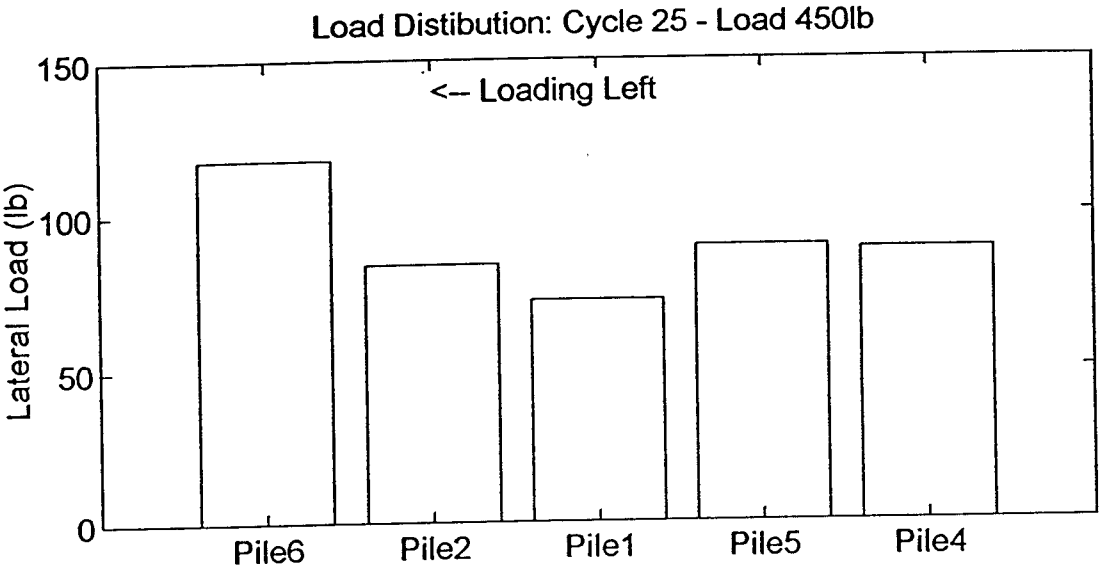
Load Distibution: Cycle 25 - Load 450lb
<-- Loading Left
Lateral Load (lb)
150
100
50
0
Pile6
Pile2
Pile1
Pile5
Pile4

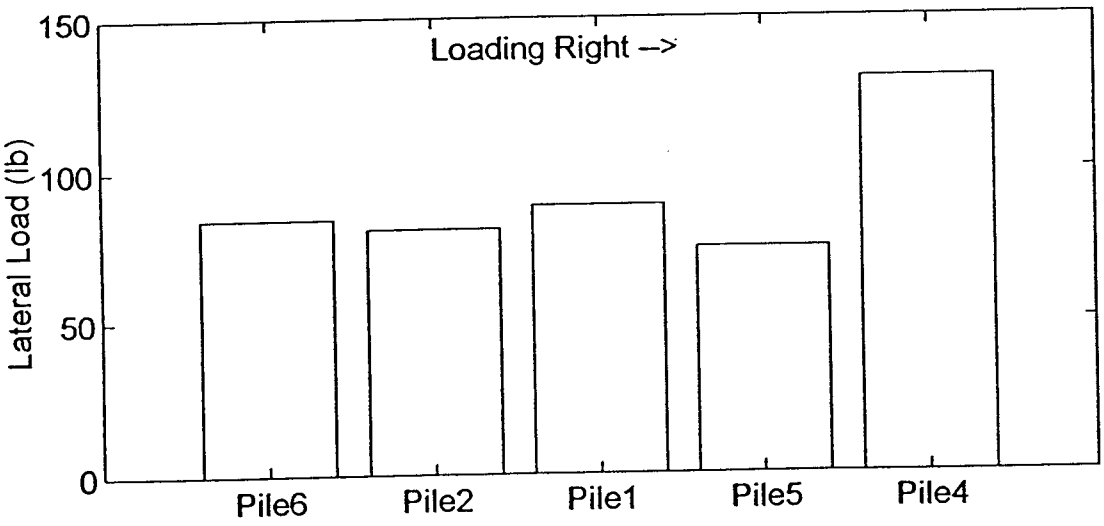
Loading Right -->
Lateral Load (lb)
150
100
50
0
Pile6
Pile2
Pile1
Pile5
Pile4

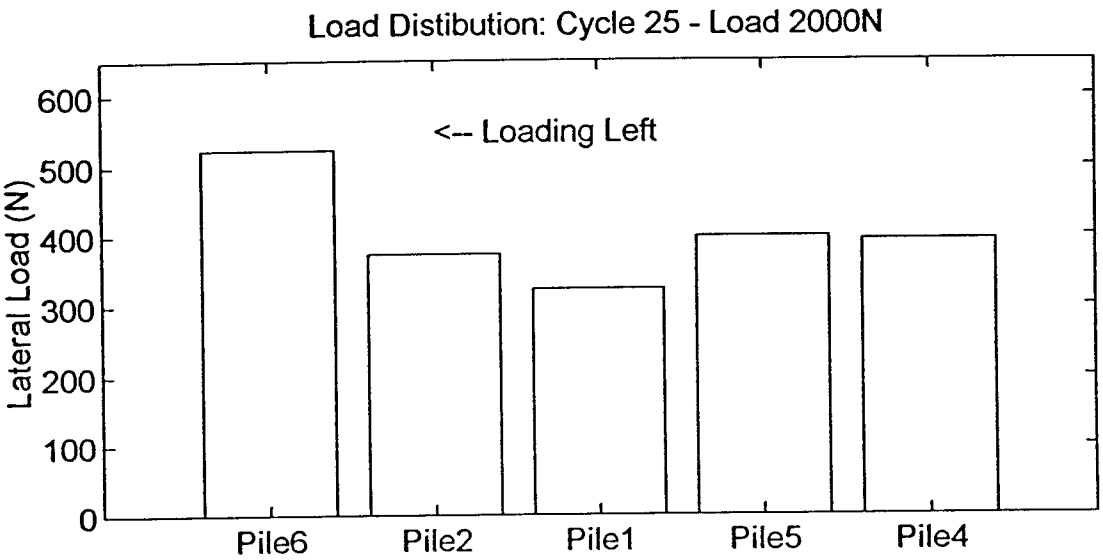
Load Distibution: Cycle 25 - Load 2000N
<-- Loading Left
Lateral Load (N)
600
500
400
300
200
100
0
Pile6
Pile2
Pile1
Pile5
Pile4

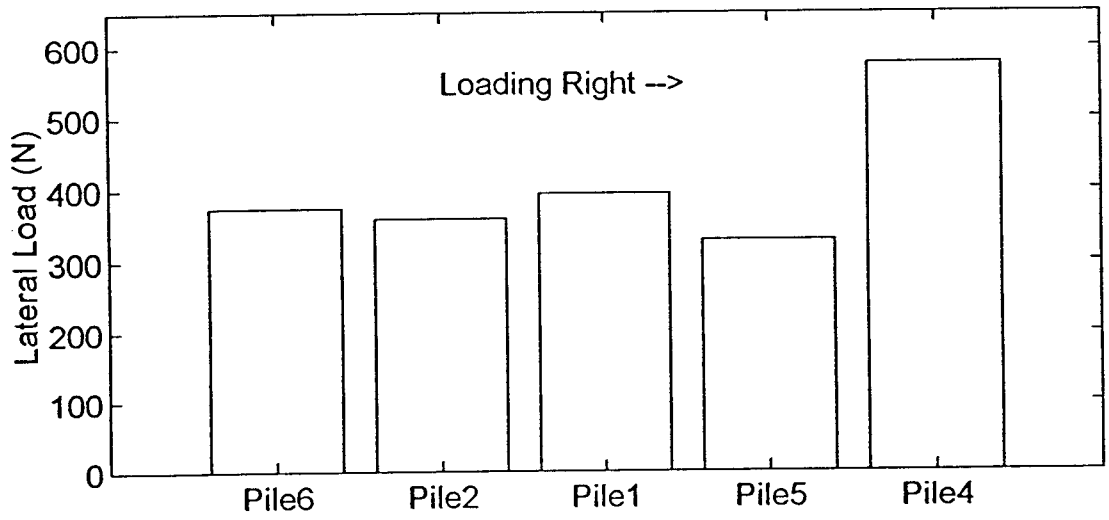
Loading Right -->
Lateral Load (N)
600
500
400
300
200
100
0
Pile6
Pile2
Pile1
Pile5
Pile4

Figure B15. Load distribution @ cycle 50 (next 14 plots).

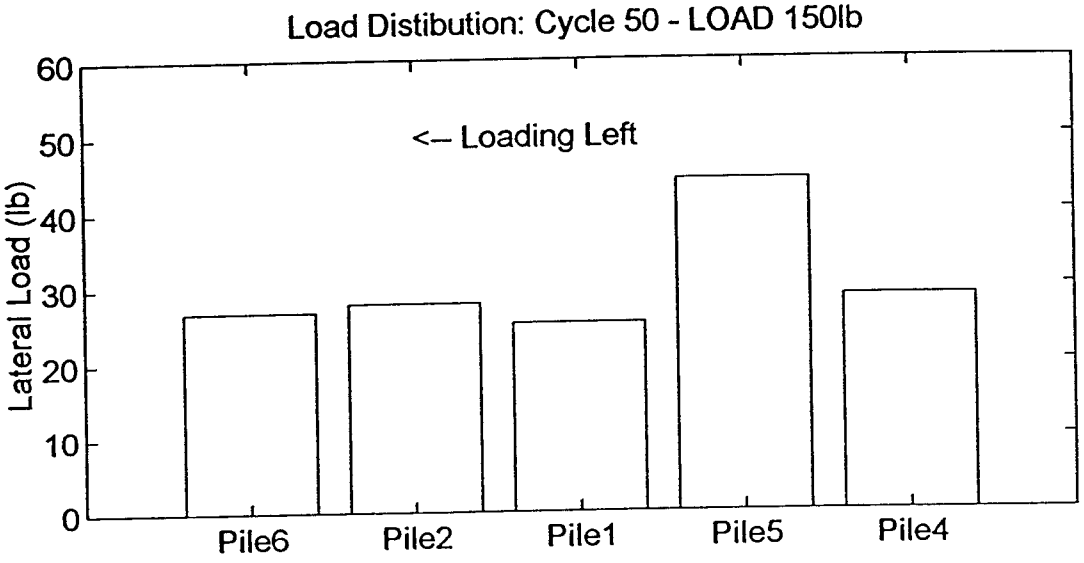
Load Distibution: Cycle 50 - LOAD 150lb
<-- Loading Left
Lateral Load (lb)
60
50
40
30
20
10
0
Pile6
Pile2
Pile1
Pile5
Pile4

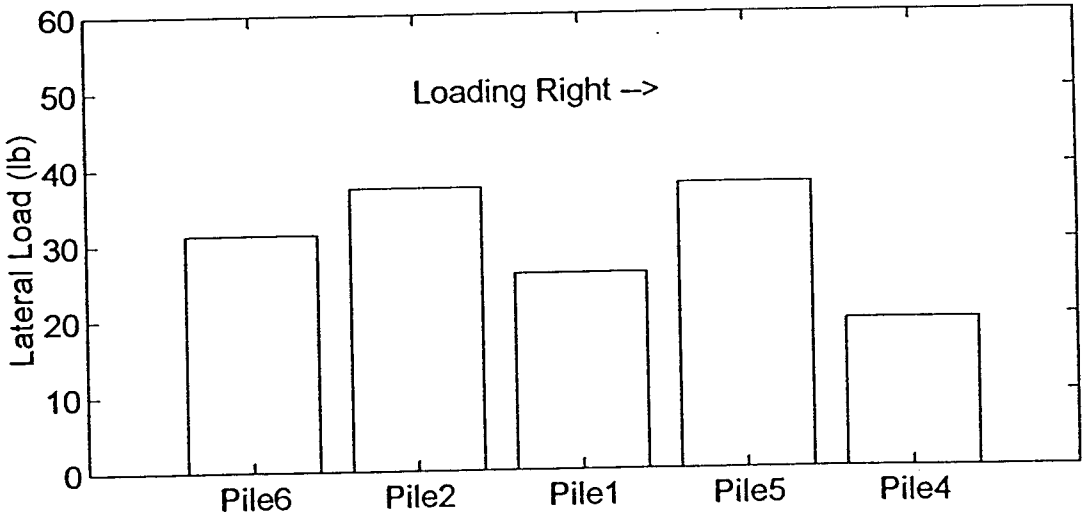
Loading Right -->
Lateral Load (lb)
60
50
40
30
20
10
0
Pile6
Pile2
Pile1
Pile5
Pile4

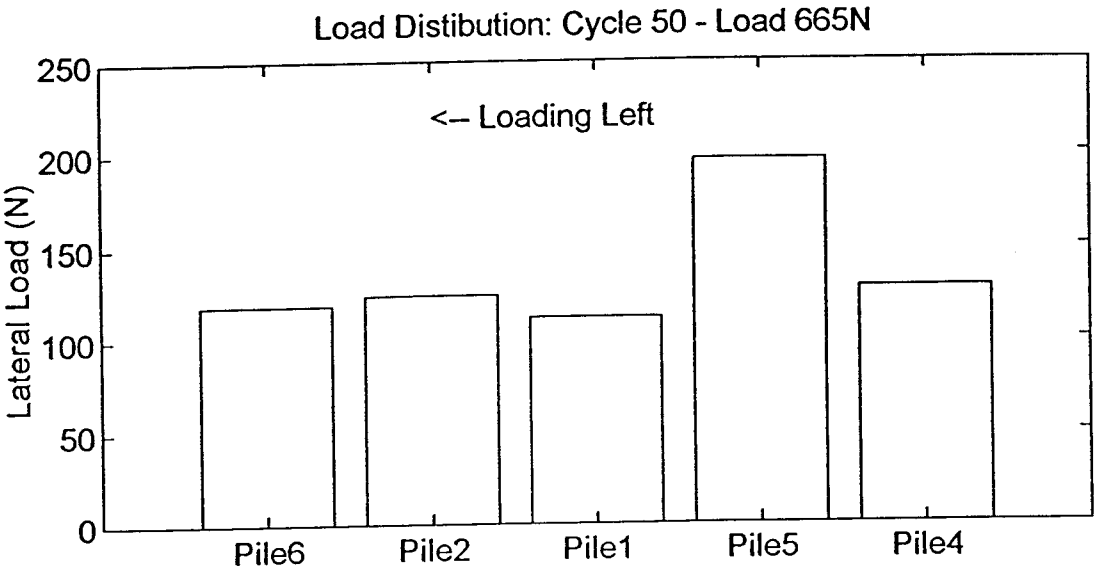
Load Distibution: Cycle 50 - Load 665N
<-- Loading Left
Lateral Load (N)
250
200
150
100
50
0
Pile6
Pile2
Pile1
Pile5
Pile4

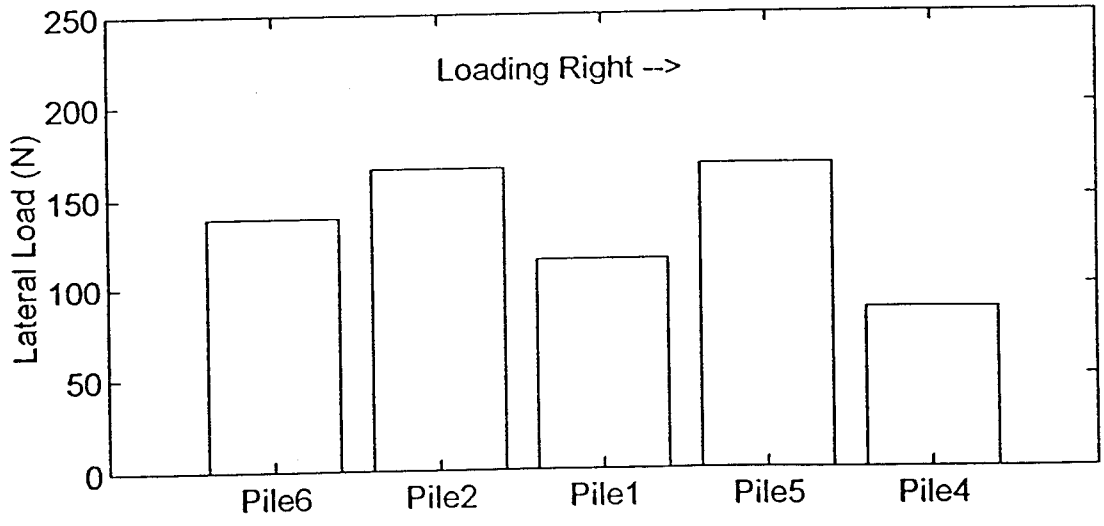
Loading Right -->
Lateral Load (N)
250
200
150
100
50
0
Pile6
Pile2
Pile1
Pile5
Pile4

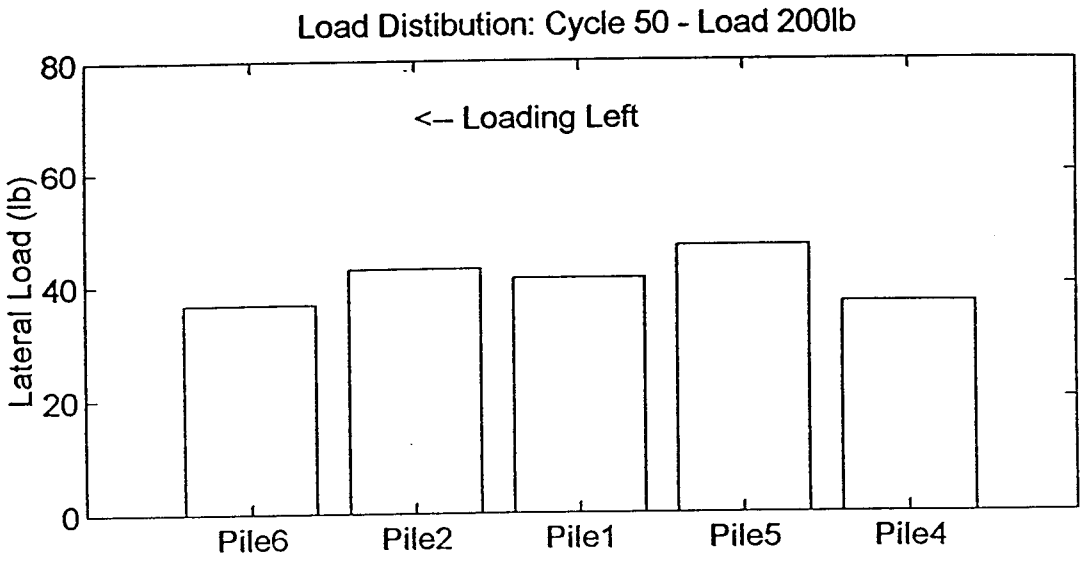
Load Distibution: Cycle 50 - Load 200lb
<-- Loading Left
Lateral Load (lb)
0
20
40
60
80
Pile6
Pile2
Pile1
Pile5
Pile4

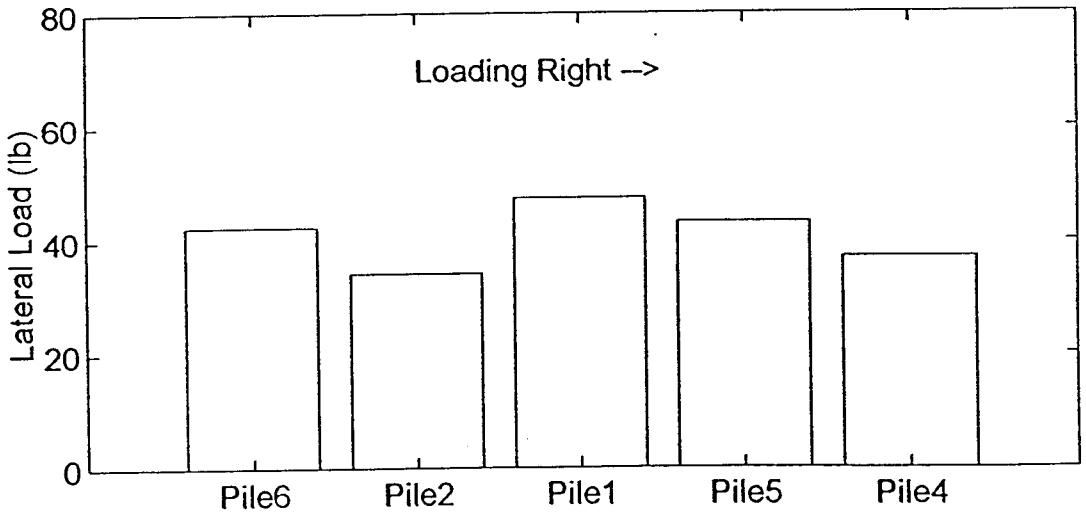
Loading Right -->
Lateral Load (lb)
0
20
40
60
80
Pile6
Pile2
Pile1
Pile5
Pile4

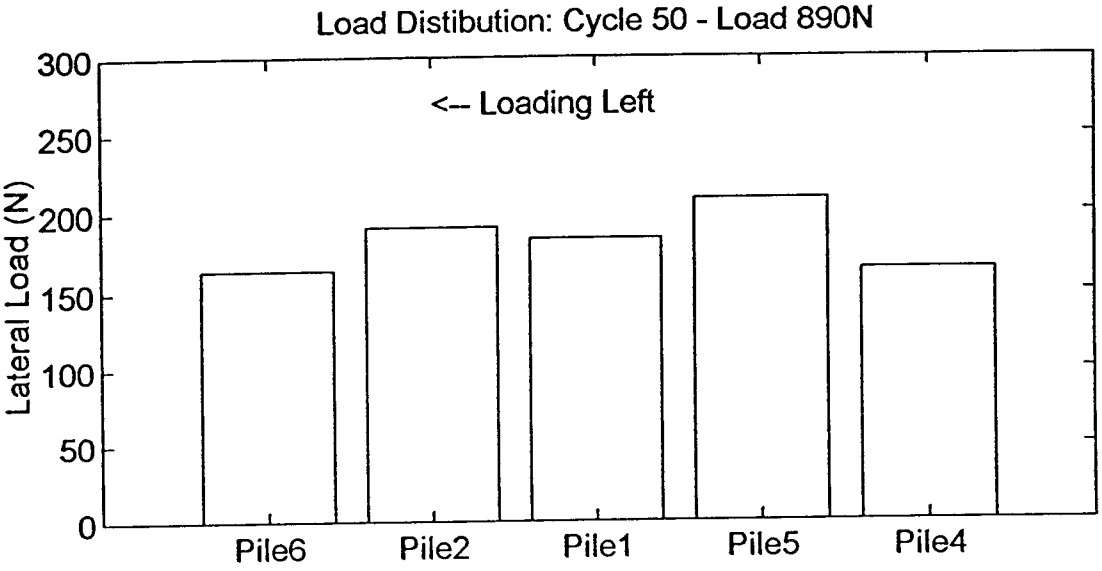
Load Distibution: Cycle 50 - Load 890N
<-- Loading Left
Lateral Load (N)
300
250
200
150
100
50
0
Pile6
Pile2
Pile1
Pile5
Pile4

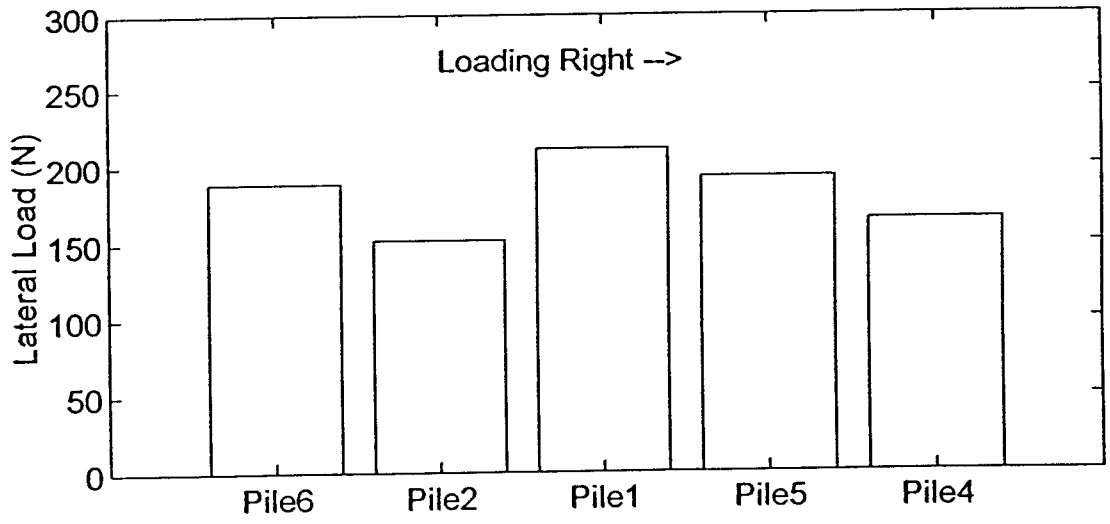
Loading Right -->
Lateral Load (N)
300
250
200
150
100
50
0
Pile6
Pile2
Pile1
Pile5
Pile4

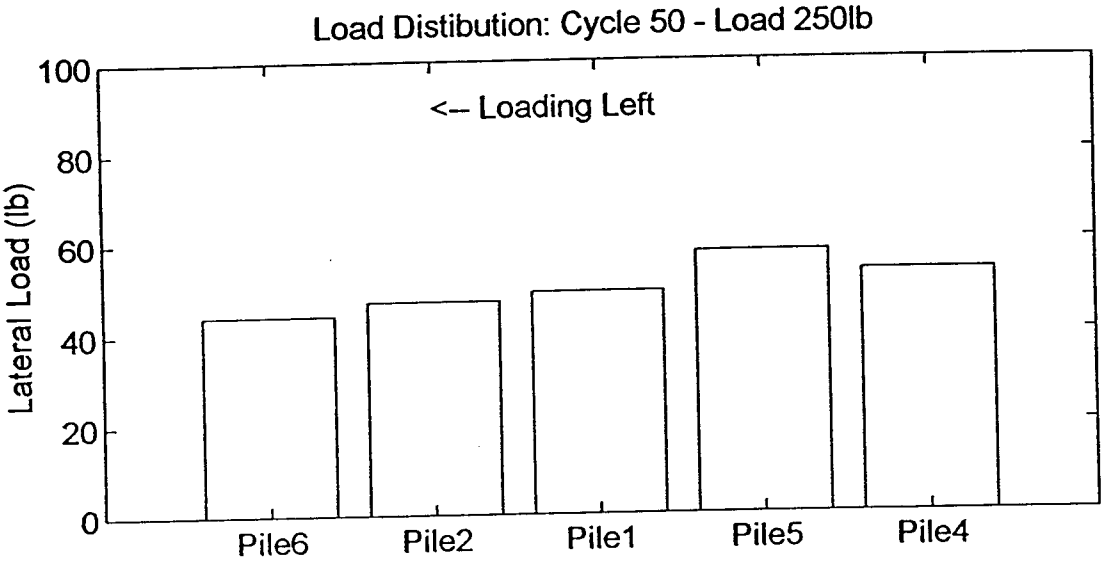
Load Distibution: Cycle 50 - Load 250lb
<-- Loading Left
Lateral Load (lb)
100
80
60
40
20
0
Pile6
Pile2
Pile1
Pile5
Pile4

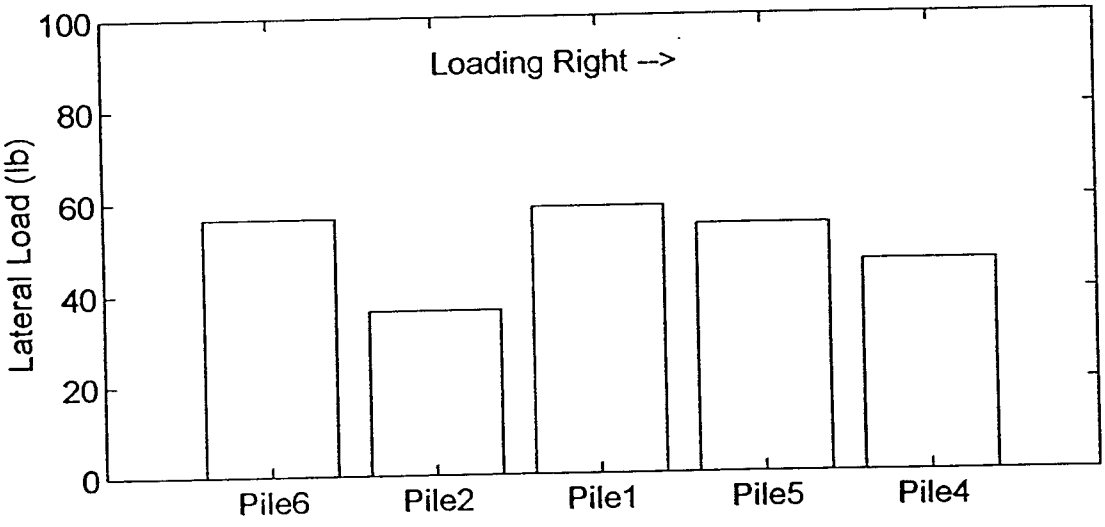
Loading Right -->
Lateral Load (lb)
100
80
60
40
20
0
Pile6
Pile2
Pile1
Pile5
Pile4

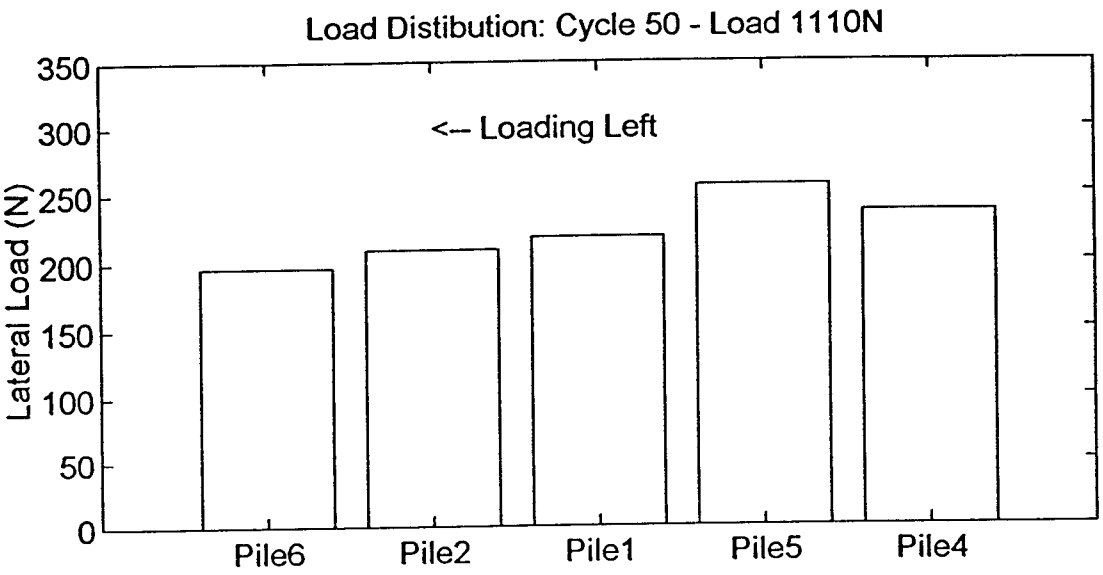
Load Distibution: Cycle 50 - Load 1110N
<-- Loading Left
Lateral Load (N)
350
300
250
200
150
100
50
0
Pile6
Pile2
Pile1
Pile5
Pile4

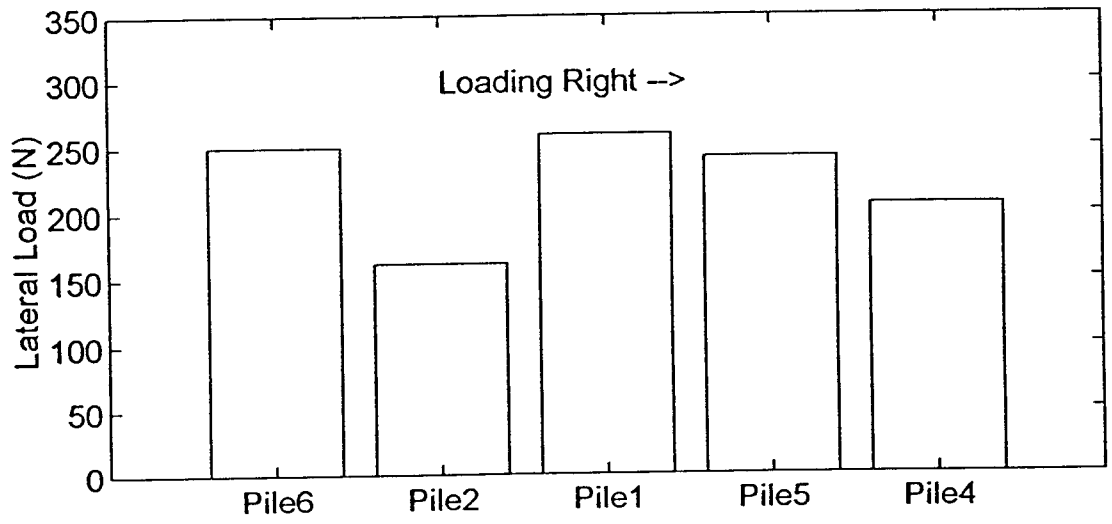
Loading Right -->
Lateral Load (N)
350
300
250
200
150
100
50
0
Pile6
Pile2
Pile1
Pile5
Pile4

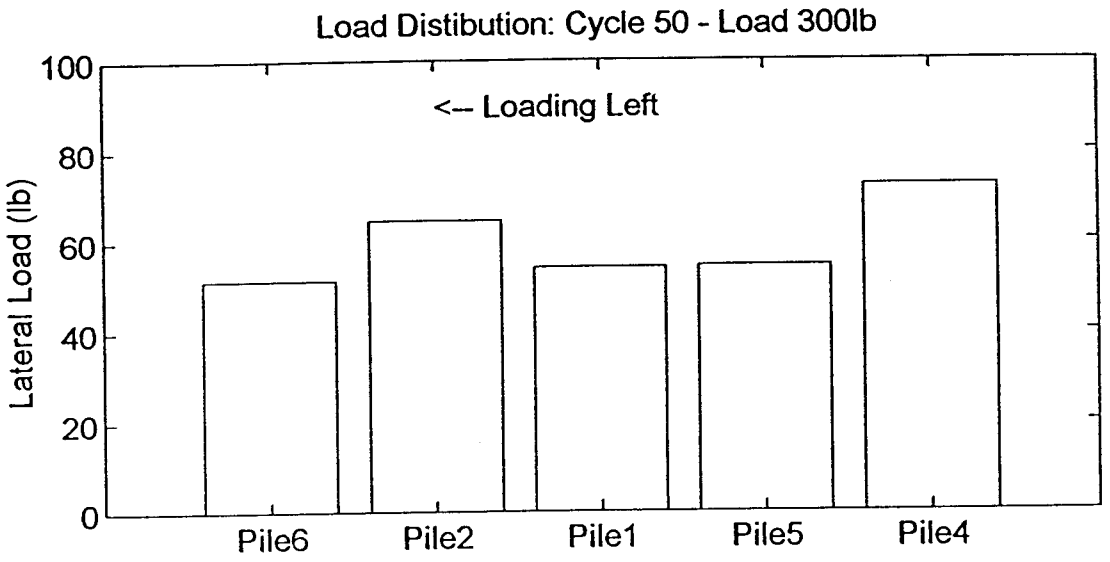
Load Distibution: Cycle 50 - Load 300lb
<-- Loading Left
Lateral Load (lb)
100
80
60
40
20
0
Pile6
Pile2
Pile1
Pile5
Pile4

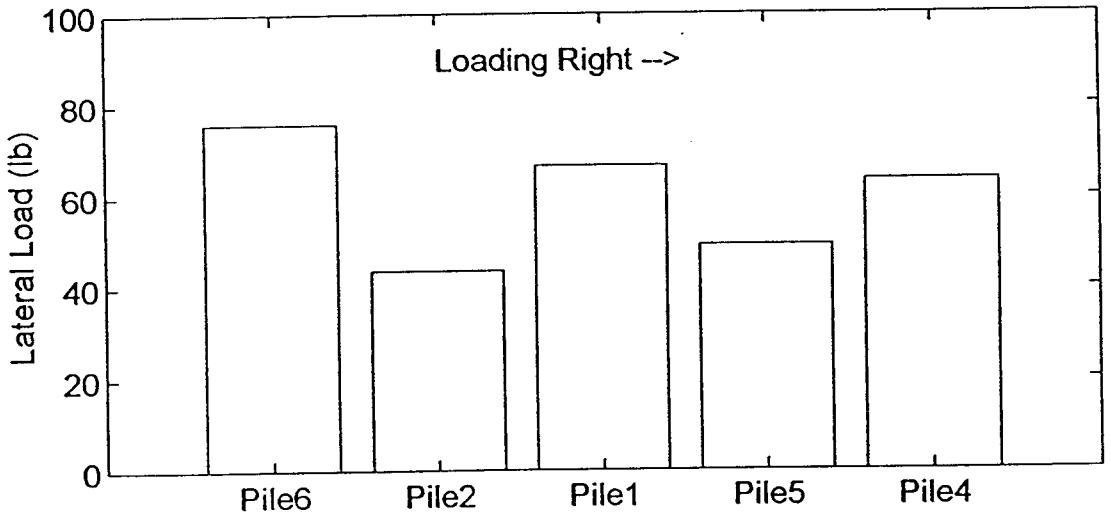
Loading Right -->
Lateral Load (lb)
100
80
60
40
20
0
Pile6
Pile2
Pile1
Pile5
Pile4

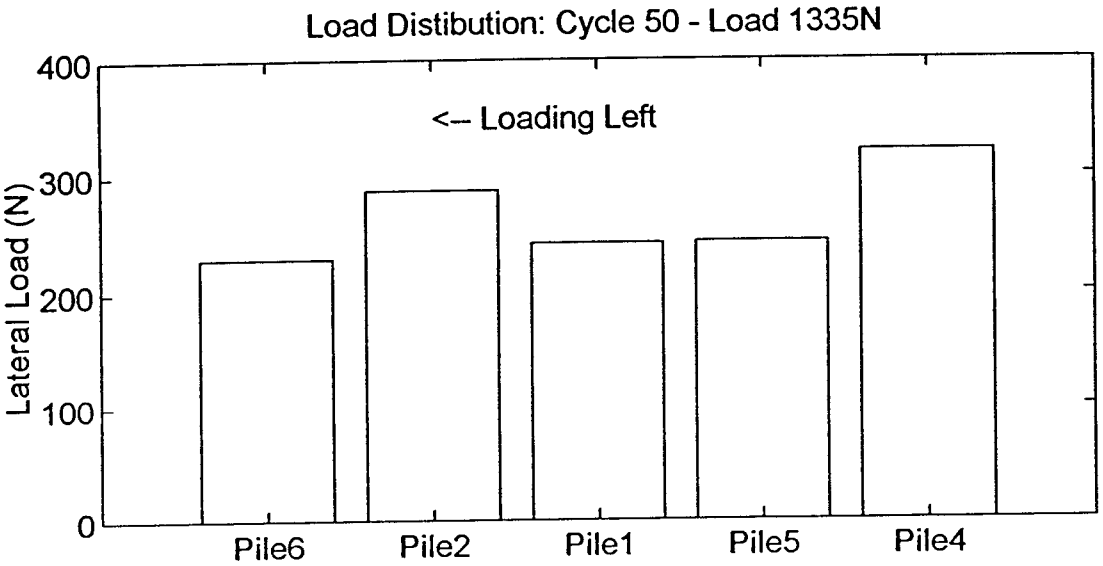
Load Distibution: Cycle 50 - Load 1335N
<-- Loading Left
Lateral Load (N)
400
300
200
100
0
Pile6
Pile2
Pile1
Pile5
Pile4

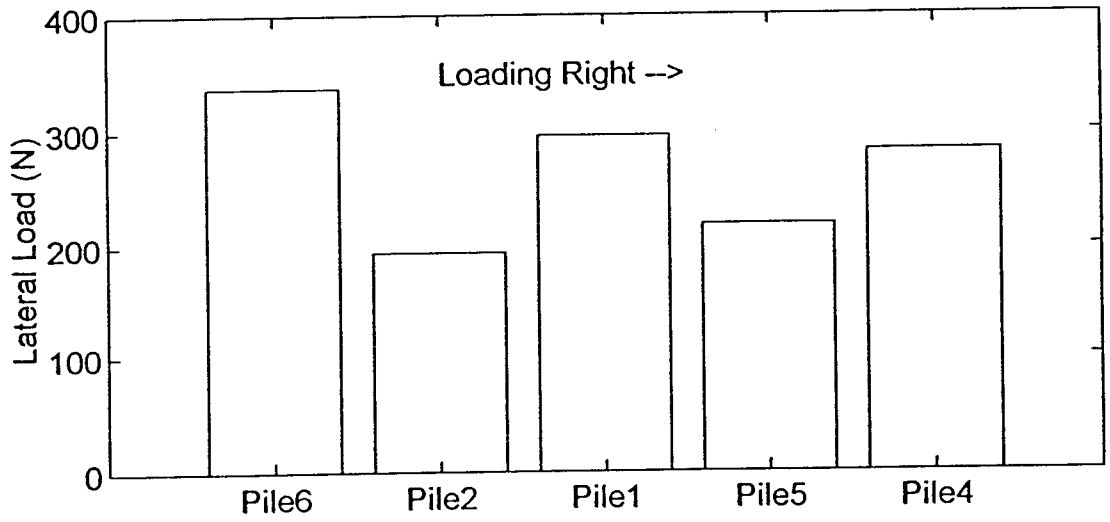
Loading Right -->
Lateral Load (N)
400
300
200
100
0
Pile6
Pile2
Pile1
Pile5
Pile4

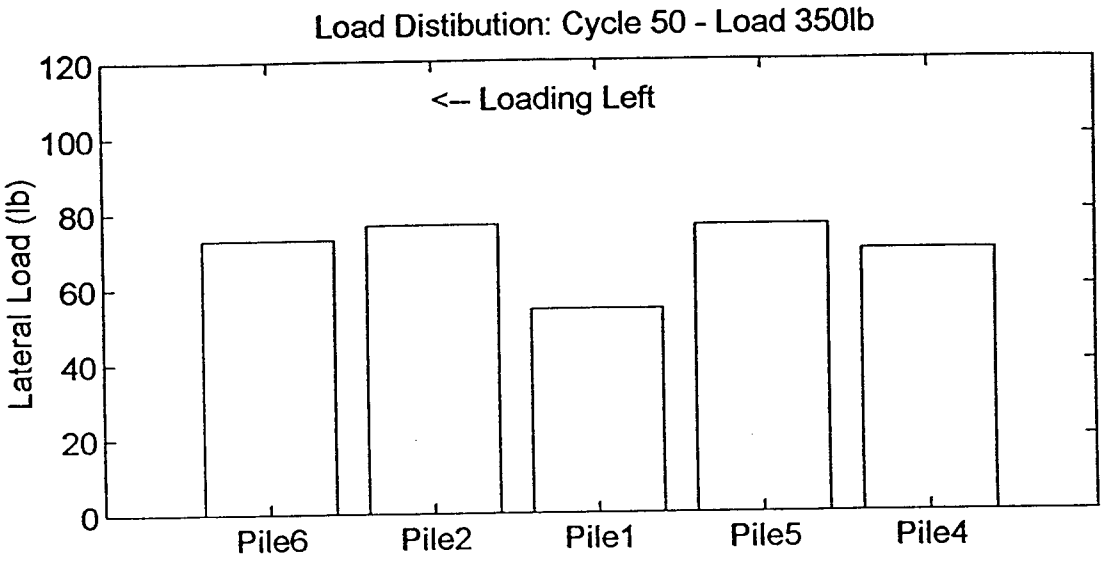
Load Distibution: Cycle 50 - Load 350lb
<-- Loading Left
Lateral Load (lb)
120
100
80
60
40
20
0
Pile6
Pile2
Pile1
Pile5
Pile4

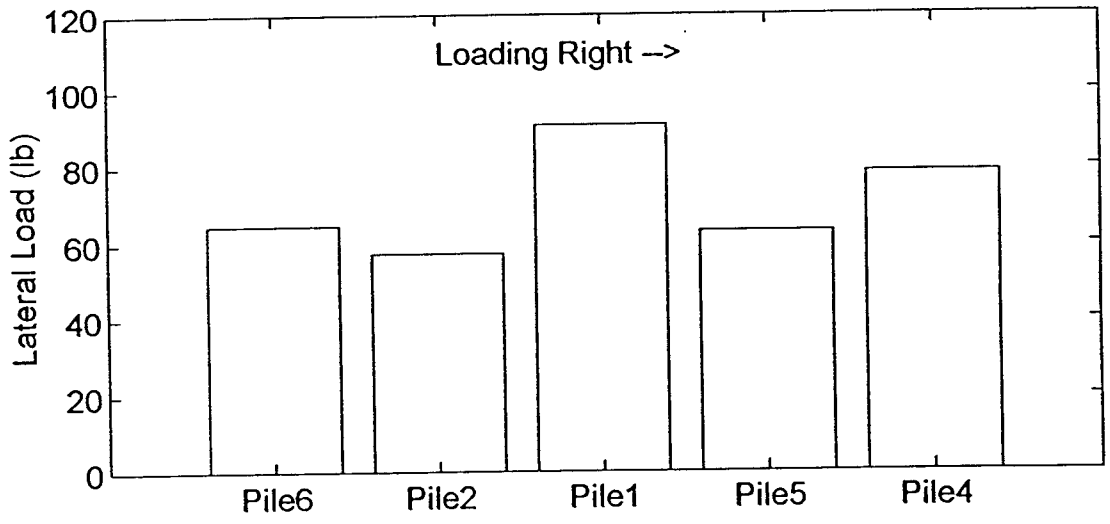
Loading Right -->
Lateral Load (lb)
120
100
80
60
40
20
0
Pile6
Pile2
Pile1
Pile5
Pile4

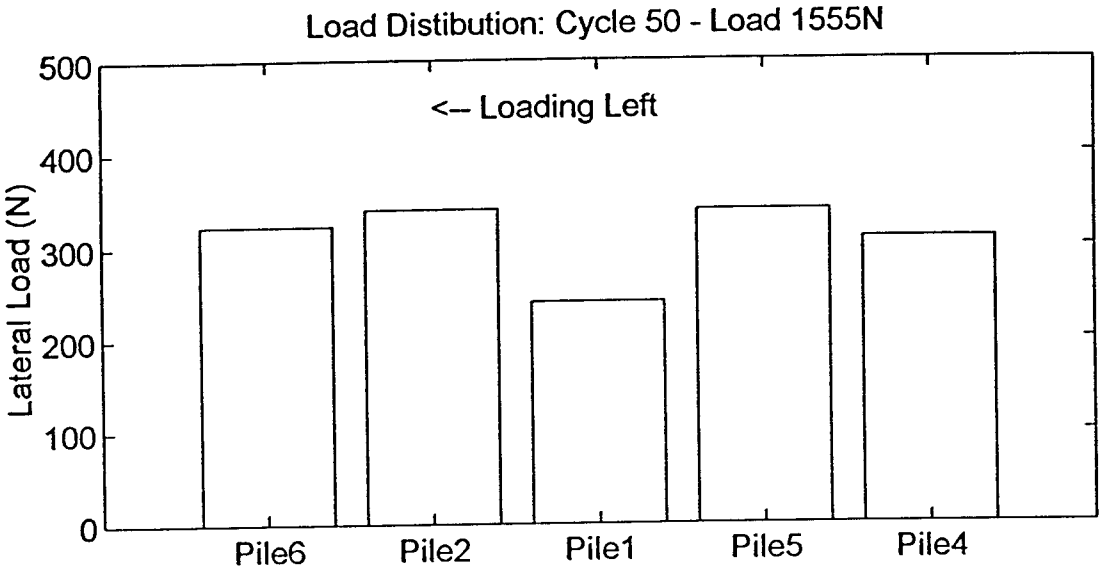
Load Distibution: Cycle 50 - Load 1555N
<-- Loading Left
Lateral Load (N)
500
400
300
200
100
0
Pile6
Pile2
Pile1
Pile5
Pile4

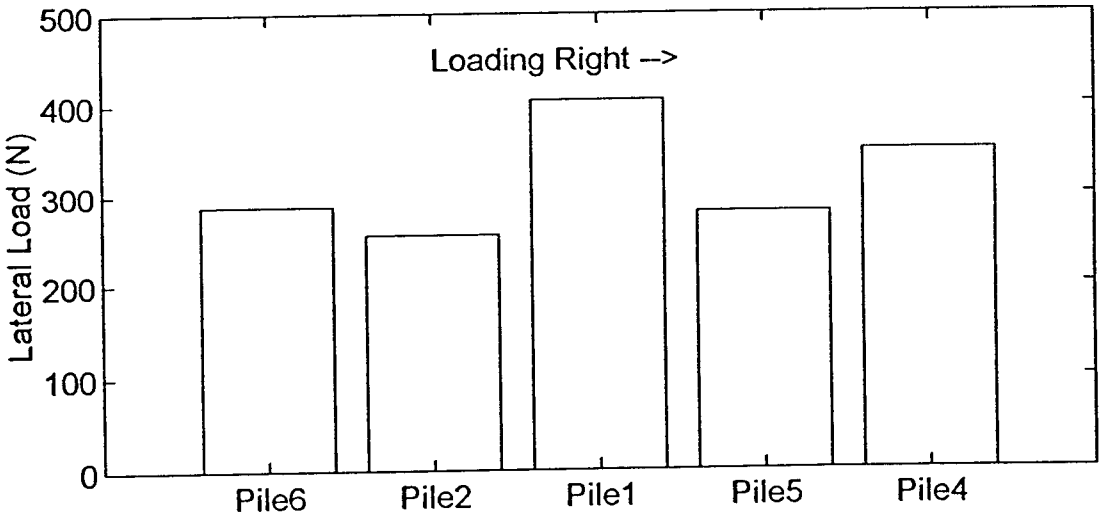
Loading Right -->
Lateral Load (N)
500
400
300
200
100
0
Pile6
Pile2
Pile1
Pile5
Pile4

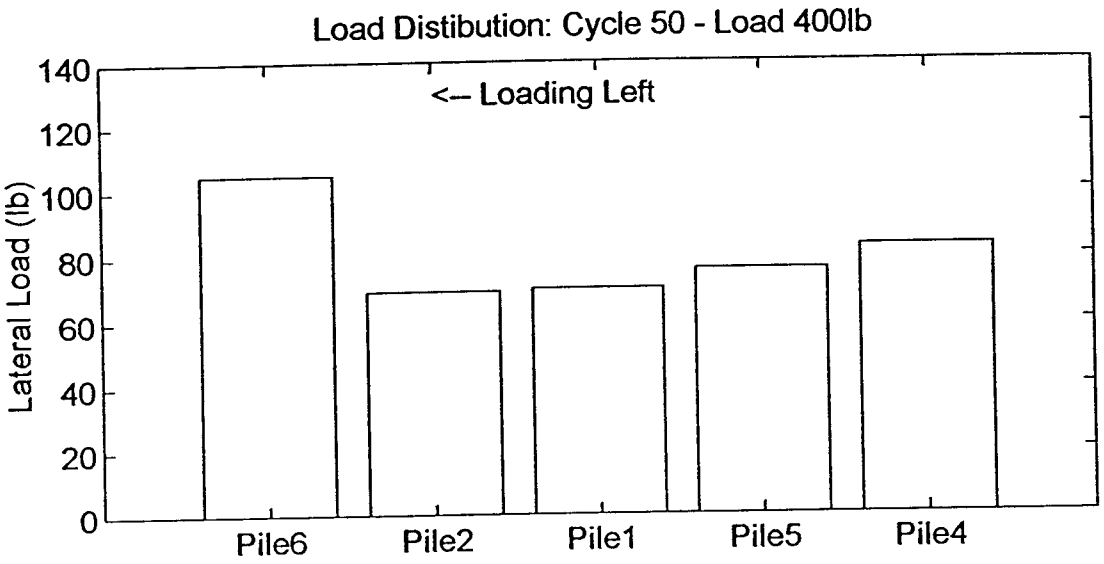
Load Distibution: Cycle 50 - Load 400lb
<-- Loading Left
Lateral Load (lb)
140
120
100
80
60
40
20
0
Pile6
Pile2
Pile1
Pile5
Pile4

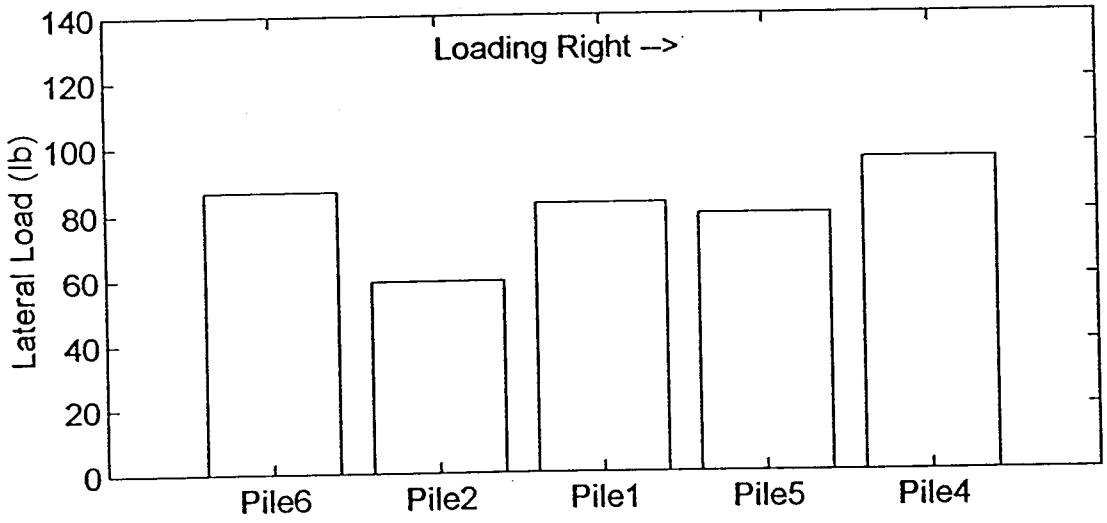
Loading Right -->
Lateral Load (lb)
140
120
100
80
60
40
20
0
Pile6
Pile2
Pile1
Pile5
Pile4

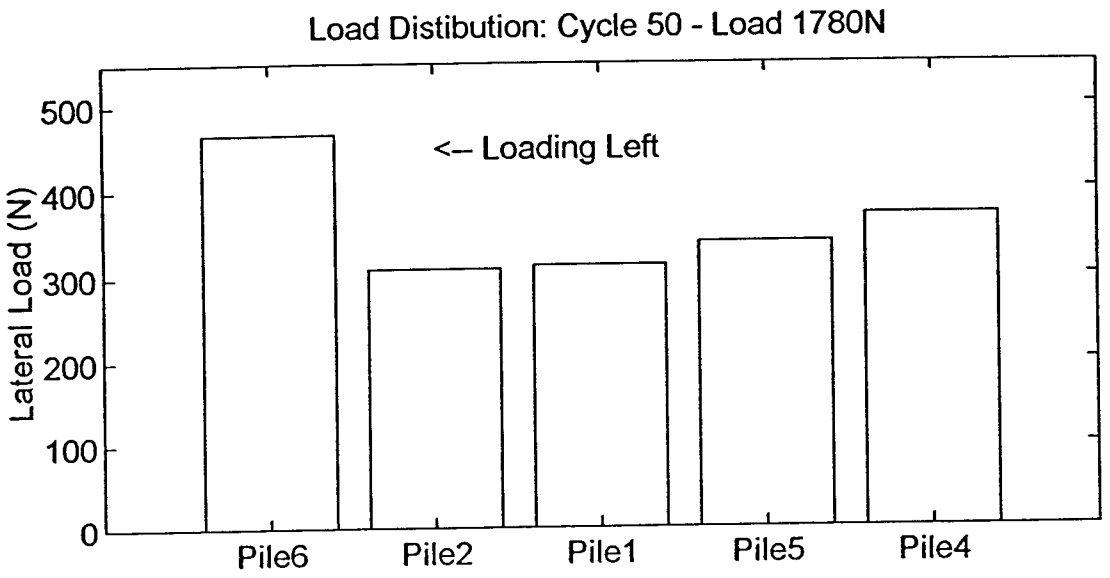
Load Distibution: Cycle 50 - Load 1780N
<-- Loading Left
Lateral Load (N)
500
400
300
200
100
0
Pile6
Pile2
Pile1
Pile5
Pile4

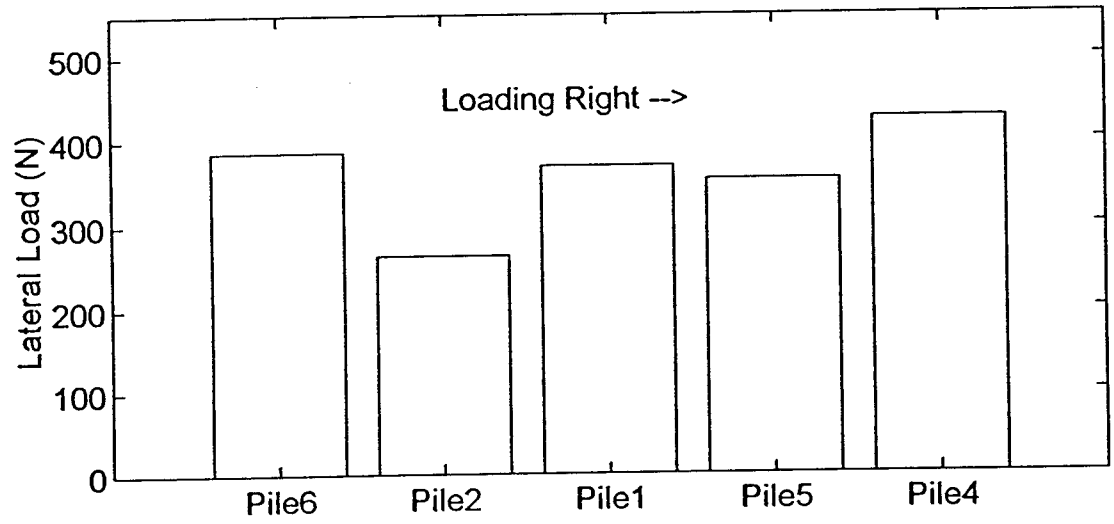
Loading Right -->
Lateral Load (N)
500
400
300
200
100
0
Pile6
Pile2
Pile1
Pile5
Pile4

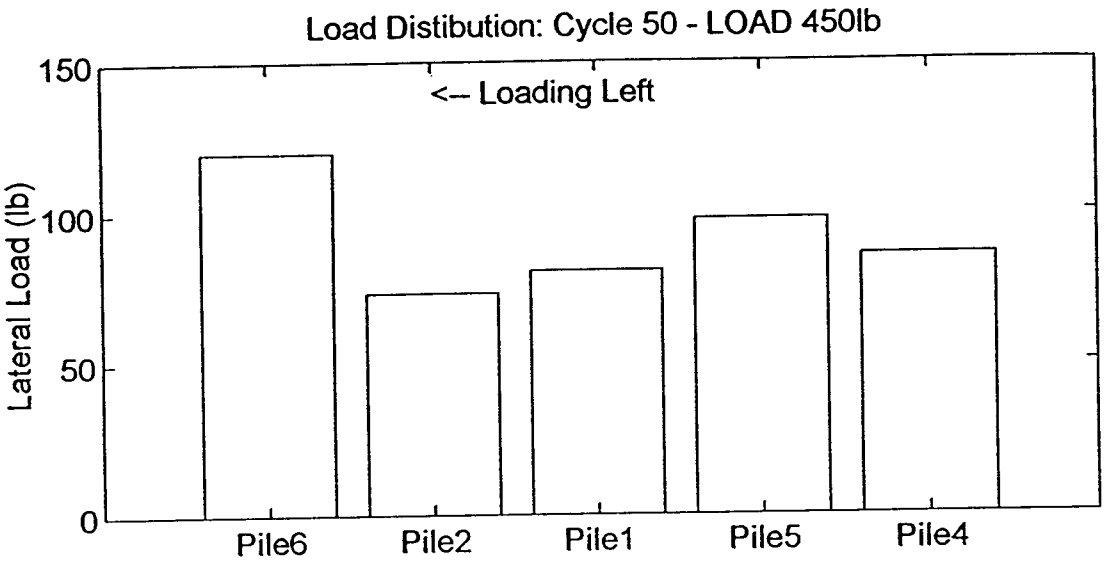
Load Distibution: Cycle 50 - LOAD 450lb
<-- Loading Left
Lateral Load (lb)
150
100
50
0
Pile6
Pile2
Pile1
Pile5
Pile4

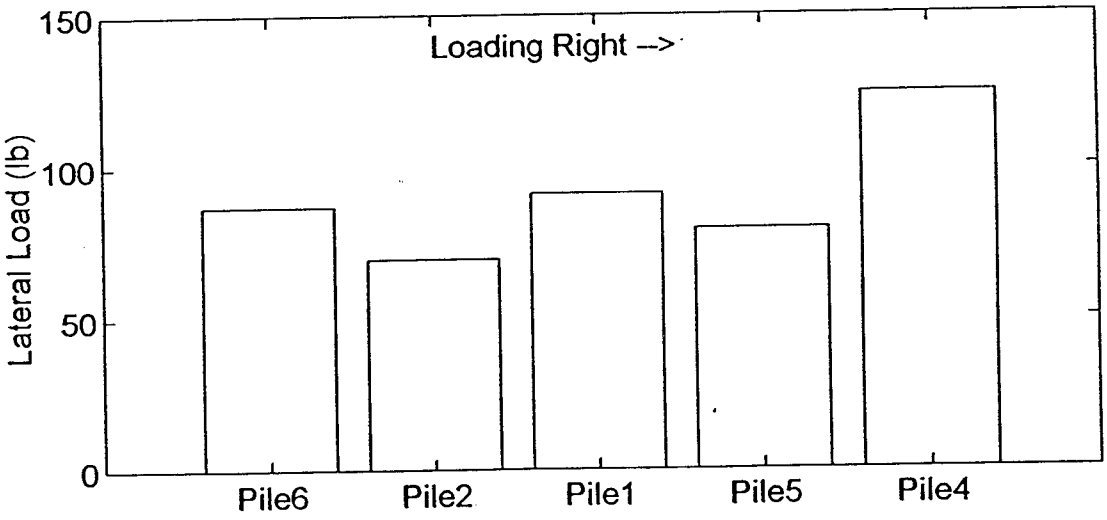
Loading Right -->
Lateral Load (lb)
150
100
50
0
Pile6
Pile2
Pile1
Pile5
Pile4

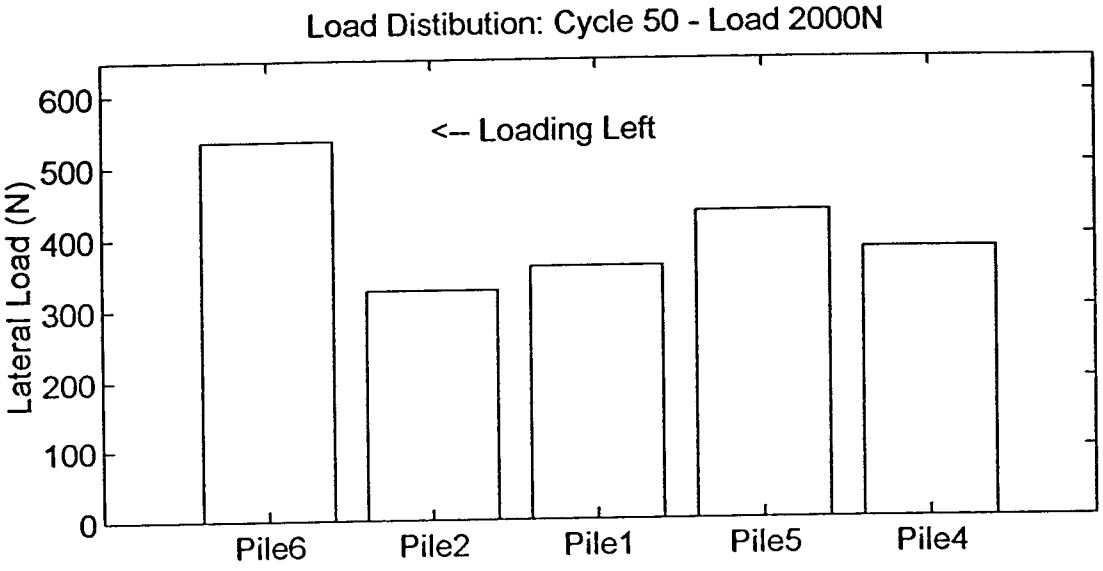
Load Distibution: Cycle 50 - Load 2000N
<-- Loading Left
Lateral Load (N)
600
500
400
300
200
100
0
Pile6
Pile2
Pile1
Pile5
Pile4

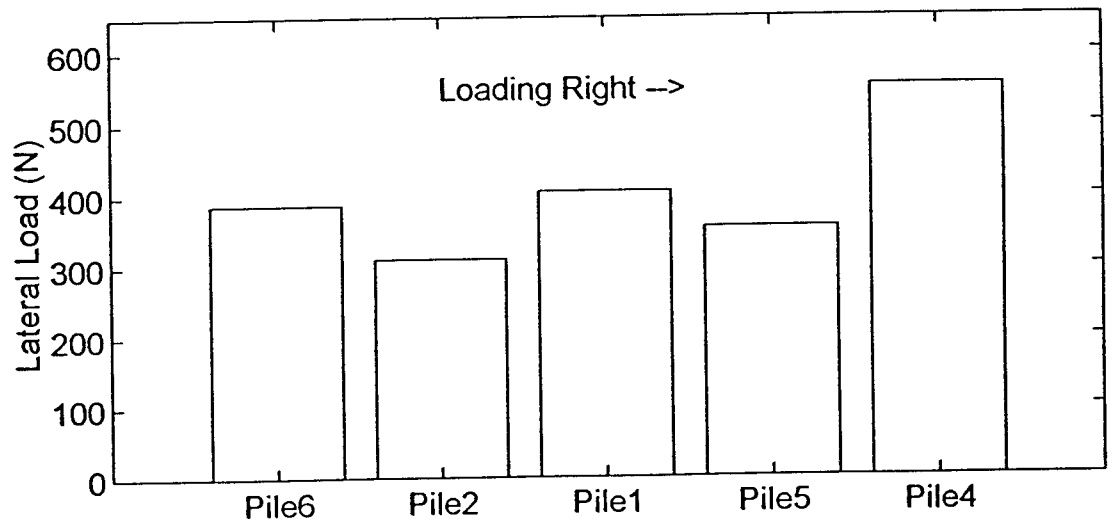
Loading Right -->
Lateral Load (N)
600
500
400
300
200
100
0
Pile6
Pile2
Pile1
Pile5
Pile4

Figure B16. Load vs. deflection for cycles 1, 5, 10, 25, & 50 (next 10 plots).

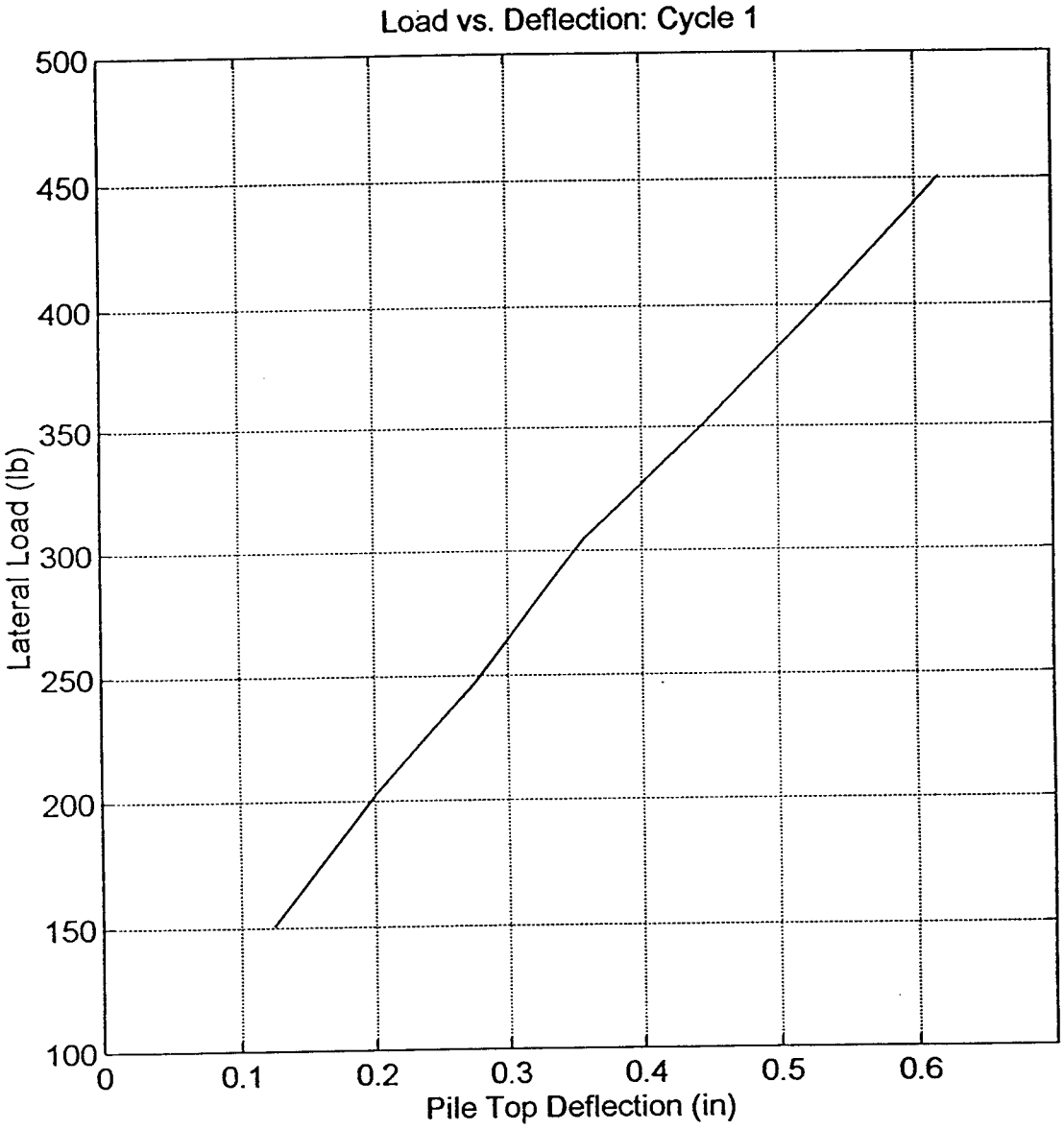
Load vs. Deflection: Cycle 1
Lateral Load (lb)
500
450
400
350
300
250
200
150
100
0
0.1
0.2
0.3
0.4
0.5
0.6
Pile Top Deflection (in)

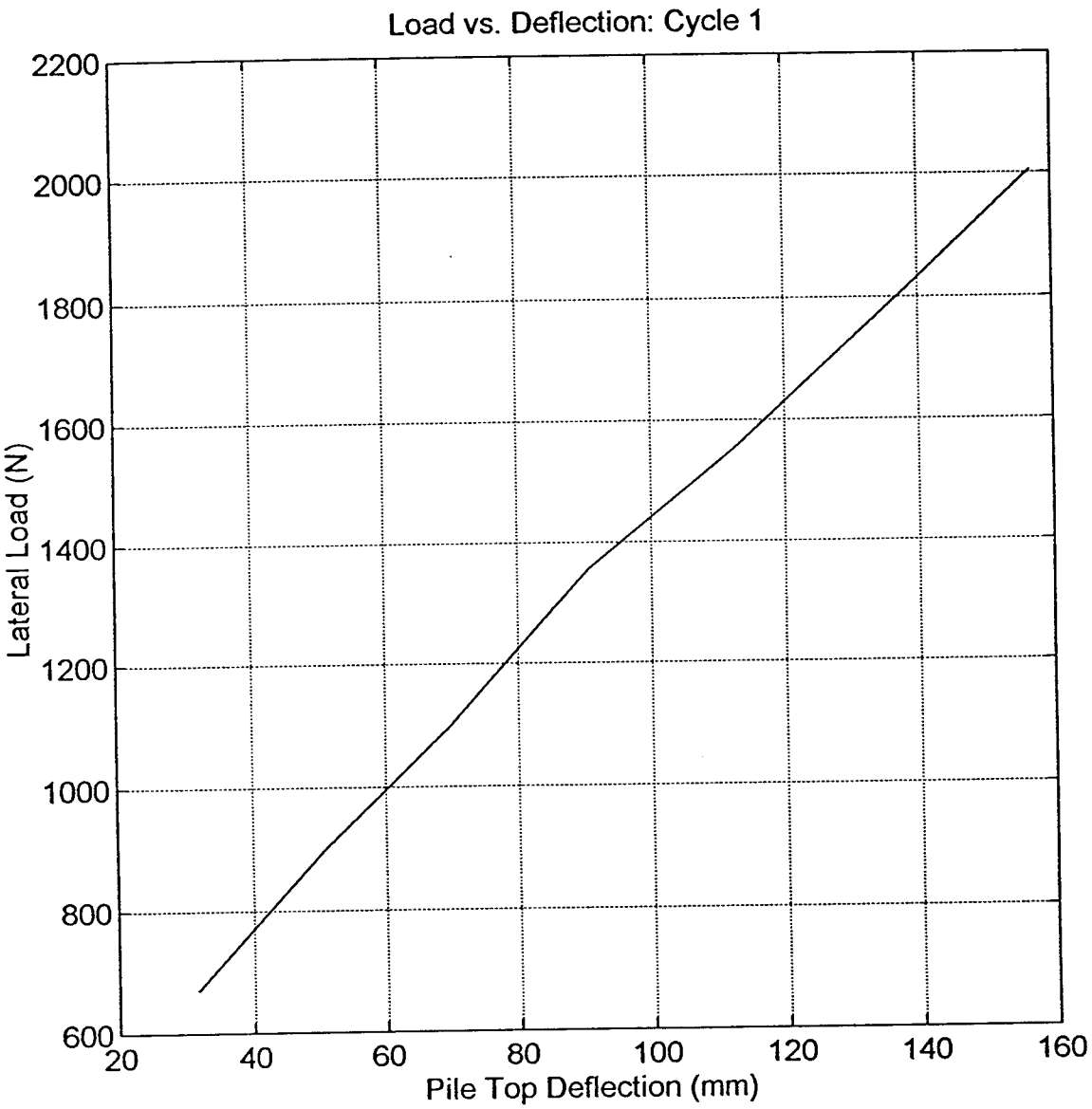
Load vs. Deflection: Cycle 1
Lateral Load (N)
2200
2000
1800
1600
1400
1200
1000
800
600
20
40
60
80
100
120
140
160
Pile Top Deflection (mm)

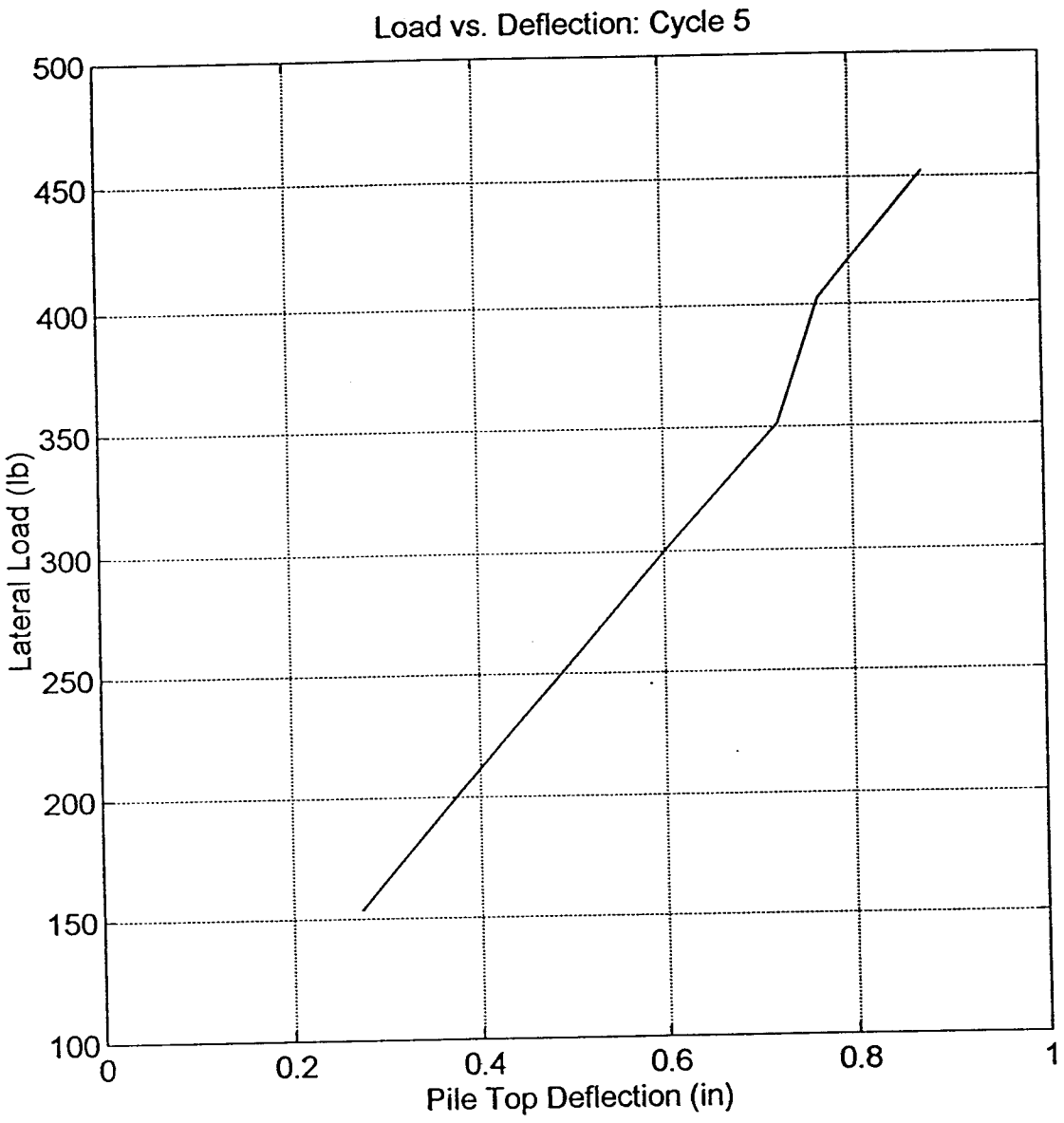
Load vs. Deflection: Cycle 5
Lateral Load (lb)
500
450
400
350
300
250
200
150
100
0
0.2
0.4
0.6
0.8
1
Pile Top Deflection (in)

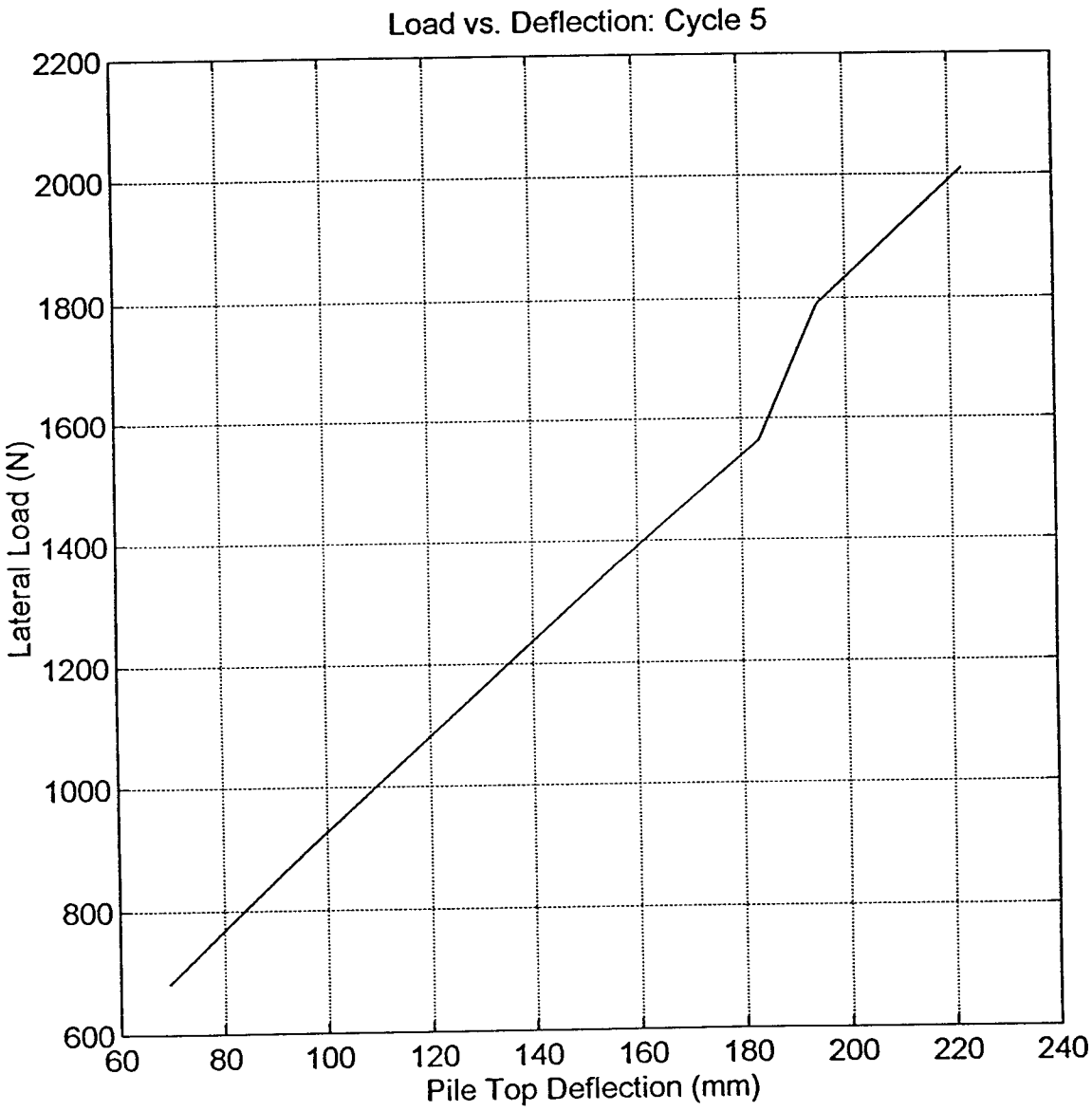
Load vs. Deflection: Cycle 5
Lateral Load (N)
2200
2000
1800
1600
1400
1200
1000
800
600
60
80
100
120
140
160
180
200
220
240
Pile Top Deflection (mm)

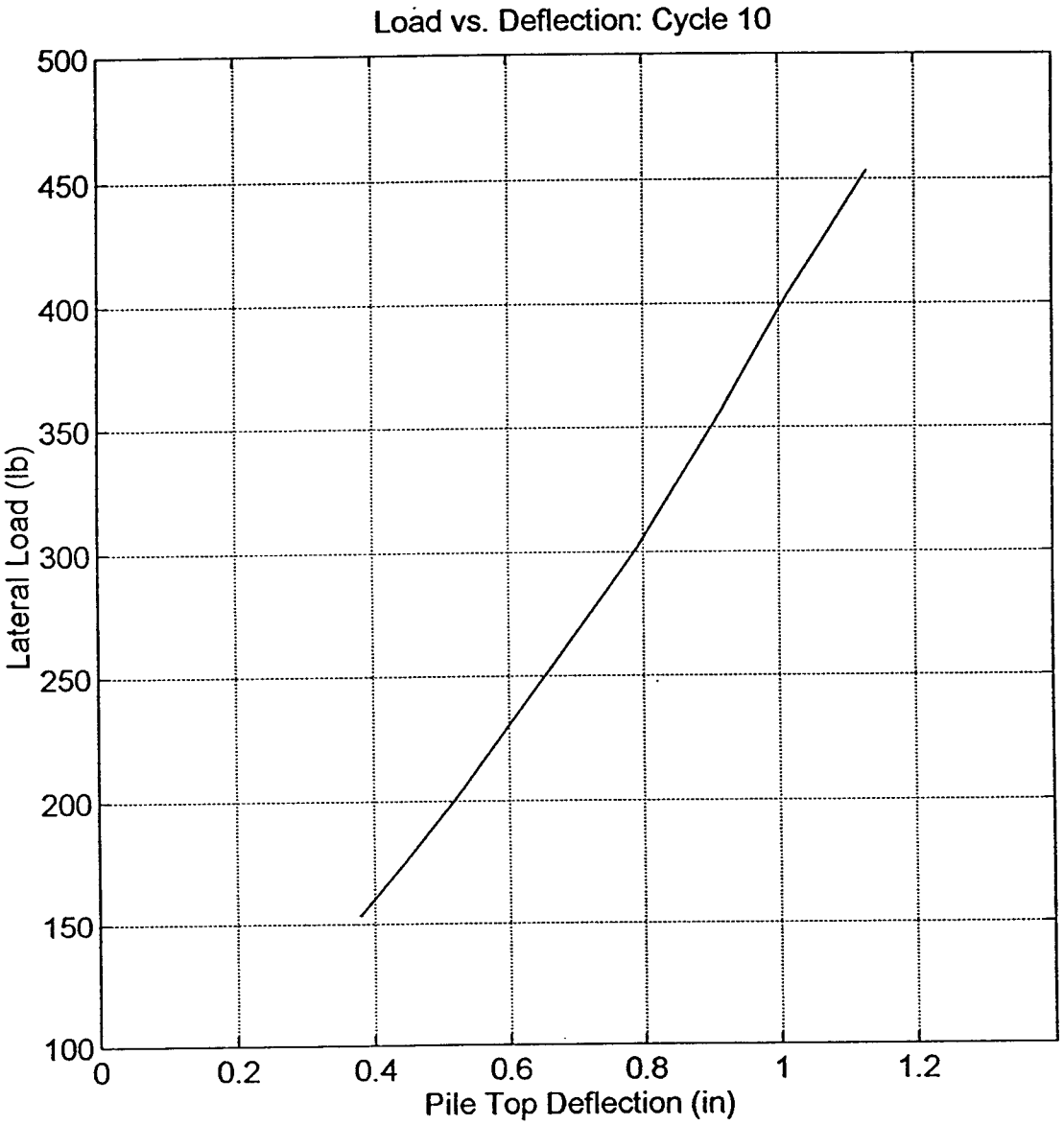
Load vs. Deflection: Cycle 10
Lateral Load (lb)
500
450
400
350
300
250
200
150
100
0
0.2
0.4
0.6
0.8
1
1.2
Pile Top Deflection (in)

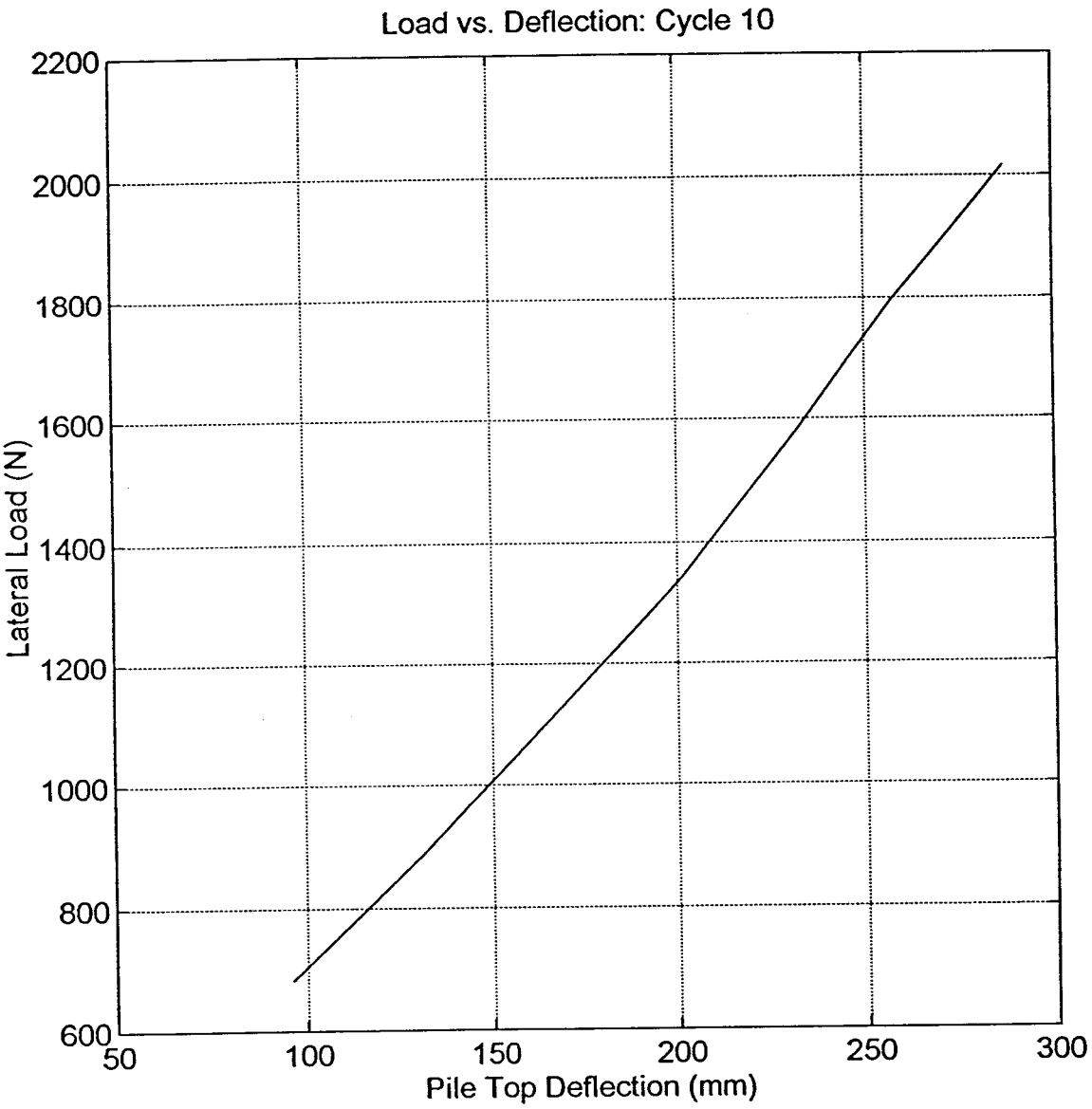
Load vs. Deflection: Cycle 10
Lateral Load (N)
2200
2000
1800
1600
1400
1200
1000
800
600
50
100
150
200
250
300
Pile Top Deflection (mm)

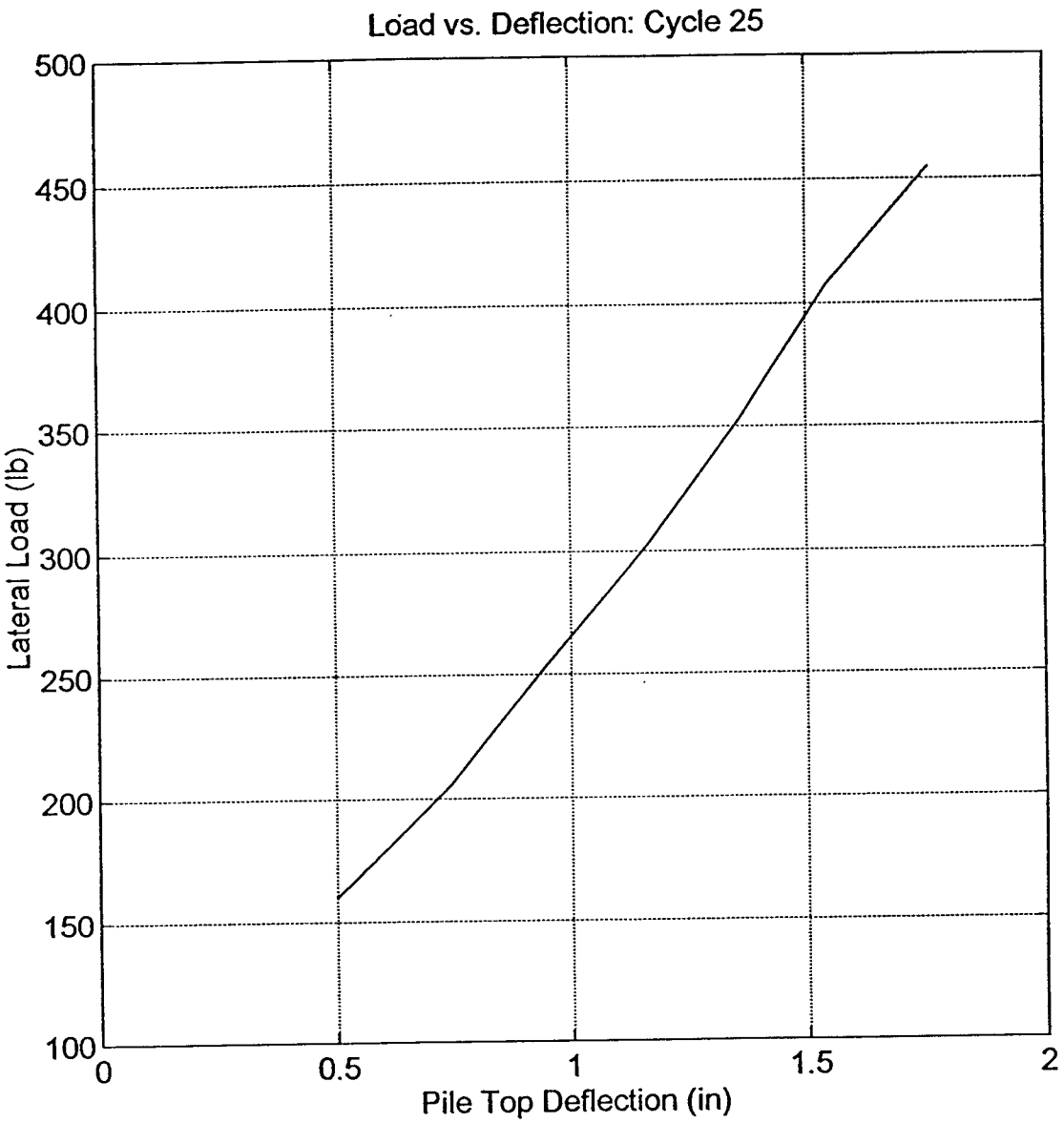
Load vs. Deflection: Cycle 25
Lateral Load (lb)
500
450
400
350
300
250
200
150
100
0
0.5
1
1.5
2
Pile Top Deflection (in)

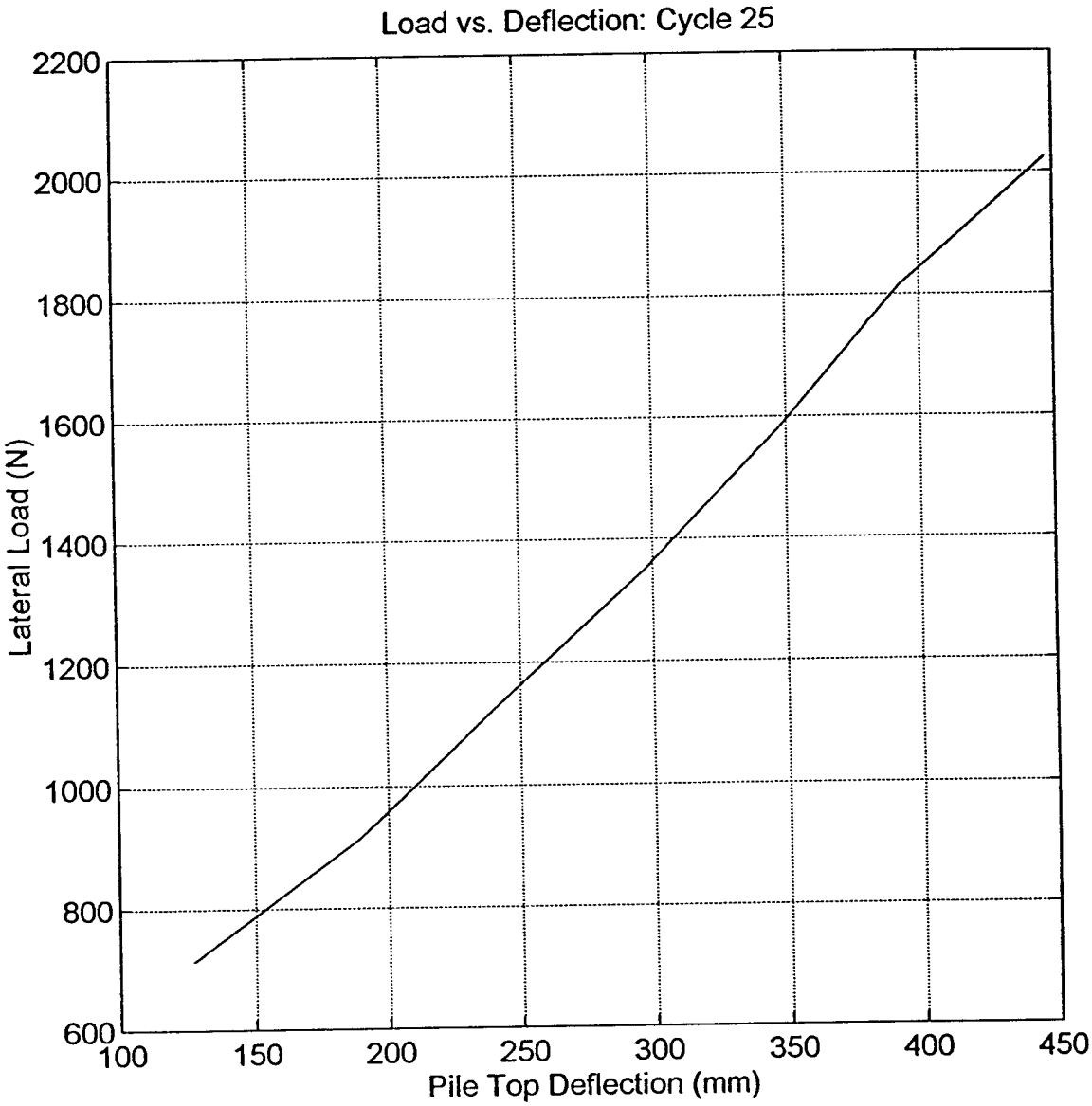
Load vs. Deflection: Cycle 25
Lateral Load (N)
2200
2000
1800
1600
1400
1200
1000
800
600
100
150
200
250
300
350
400
450
Pile Top Deflection (mm)

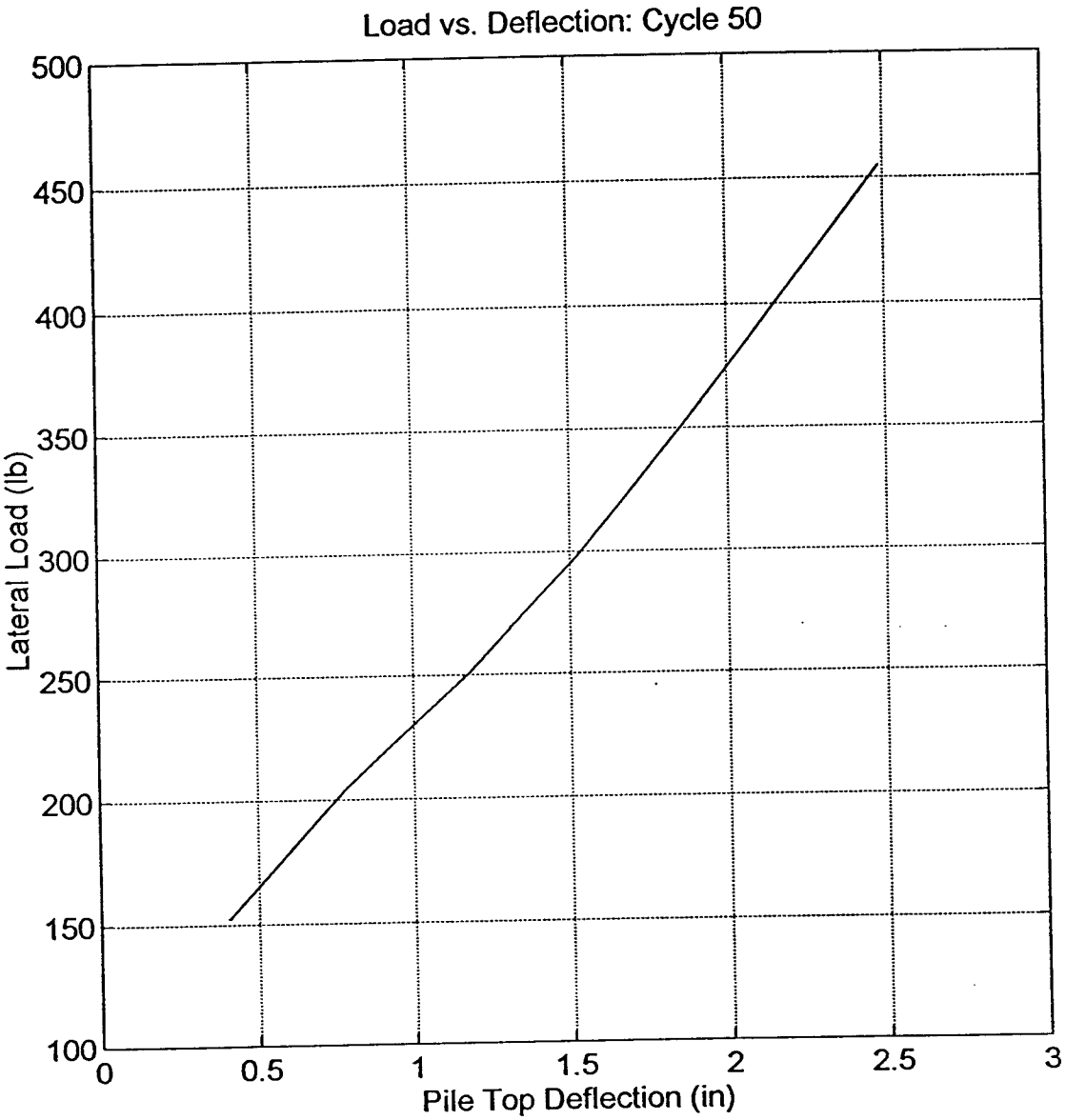
Load vs. Deflection: Cycle 50
Lateral Load (lb)
500
450
400
350
300
250
200
150
100
0
0.5
1
1.5
2
2.5
3
Pile Top Deflection (in)

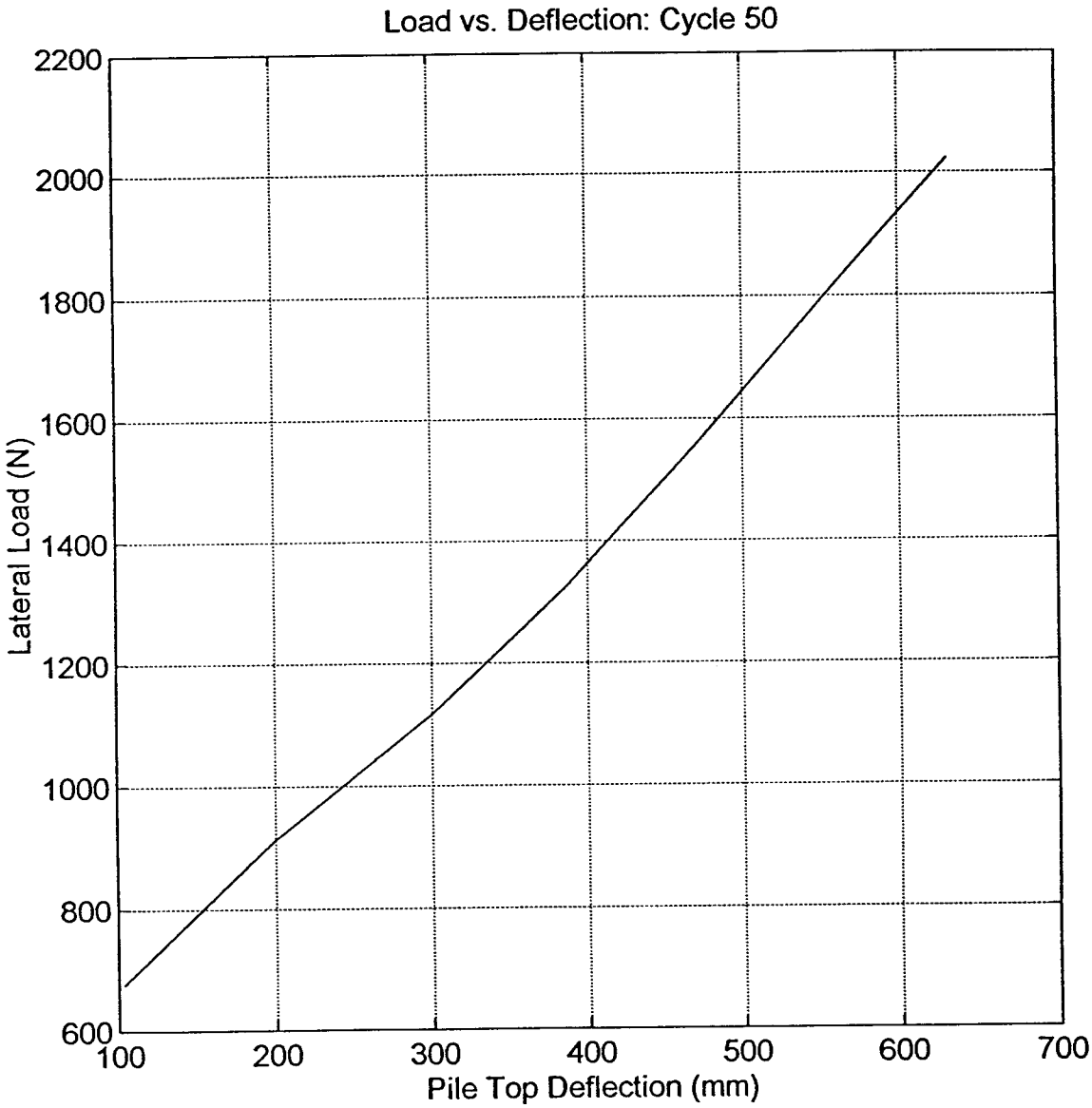
Load vs. Deflection: Cycle 50
Lateral Load (N)
2200
2000
1800
1600
1400
1200
1000
800
600
100
200
300
400
500
600
700
Pile Top Deflection (mm)

Figure B17. Load vs. deflection composite for all cycles (next 2 plots).

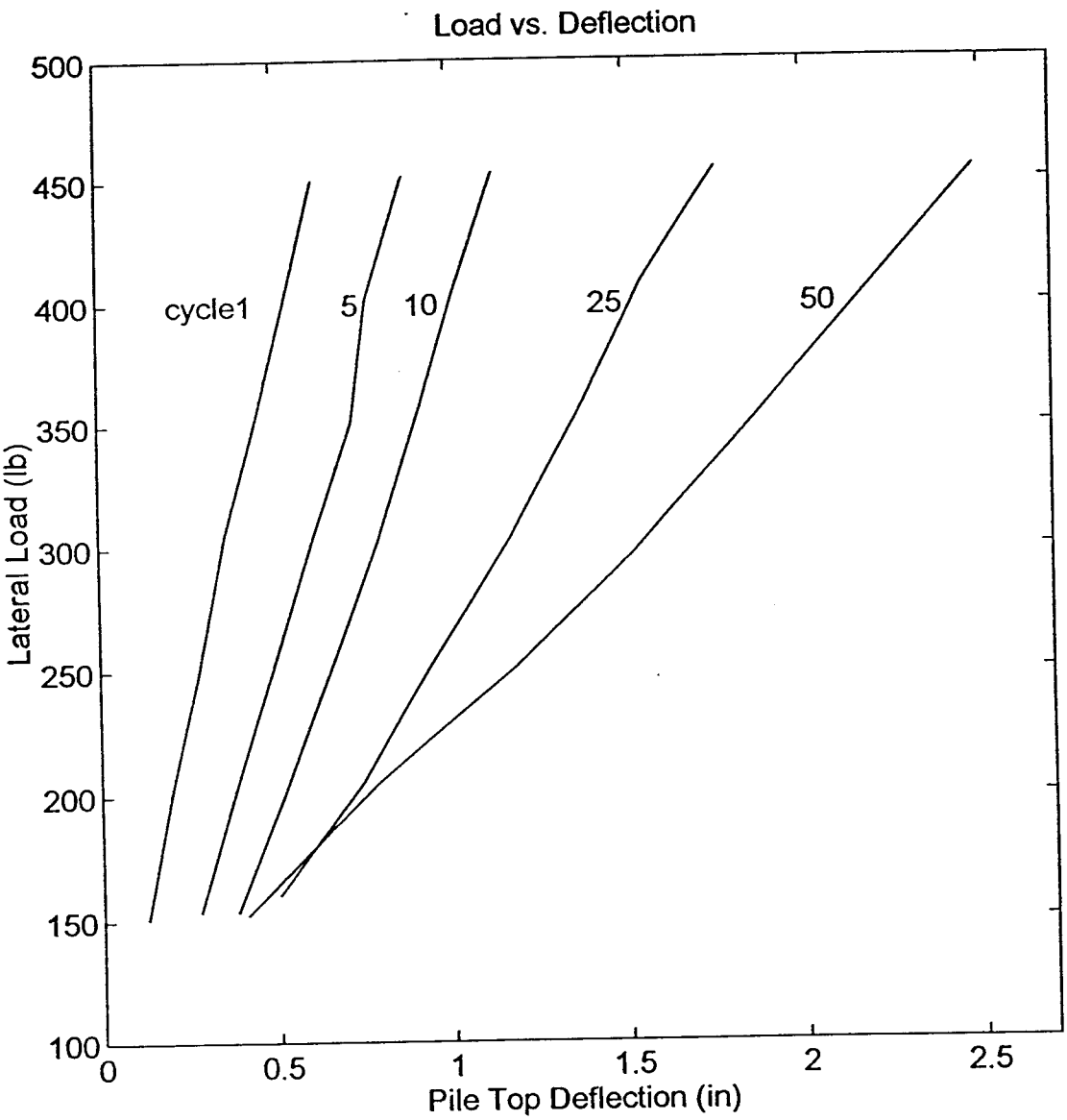
Load vs. Deflection
500
450
400
350
300
250
200
150
100
Lateral Load (lb)
cycle1
5
10
25
50
0
0.5
1
1.5
2
2.5
Pile Top Deflection (in)

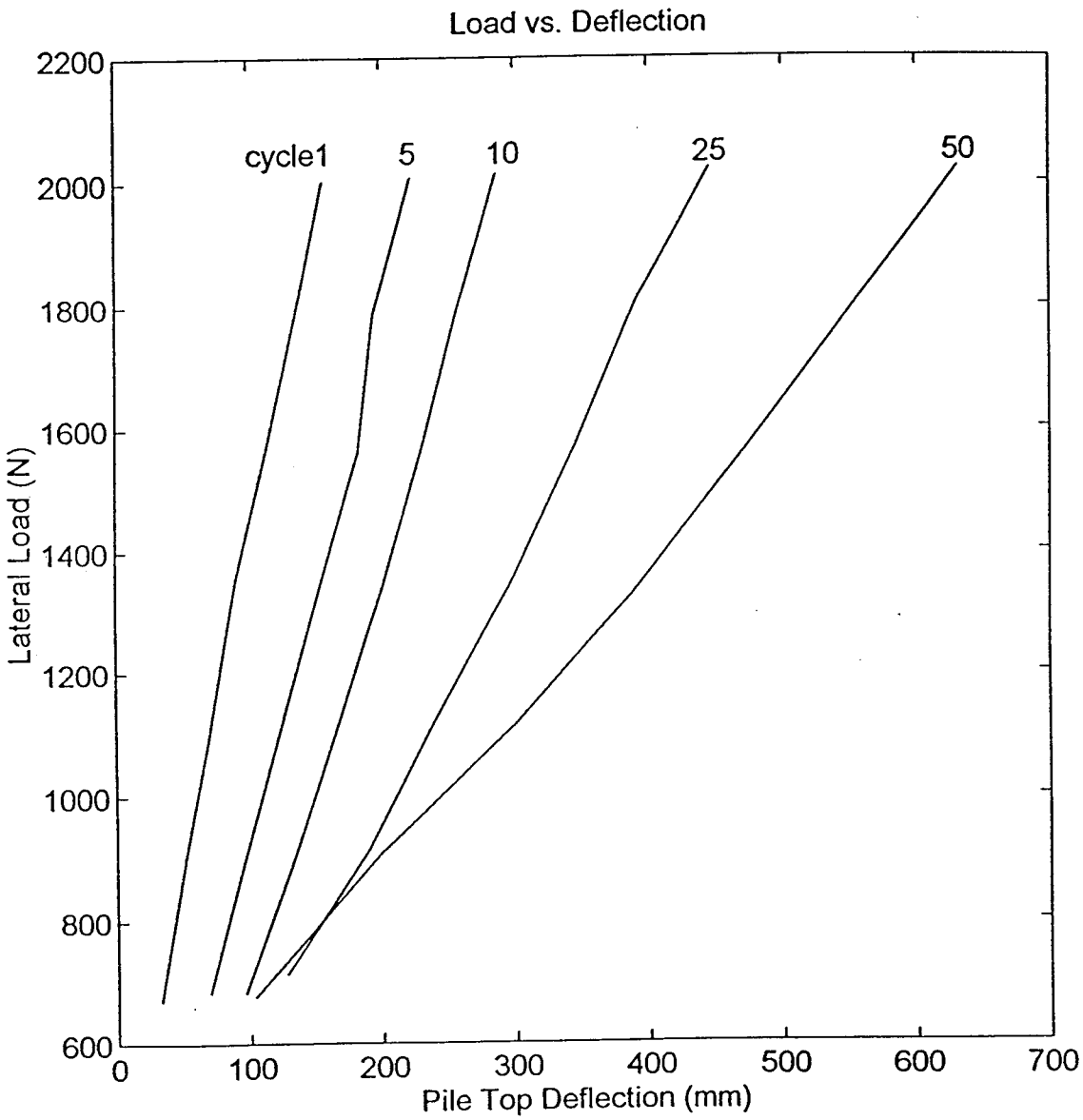
Load vs. Deflection
2200
2000
1800
1600
1400
1200
1000
800
600
Lateral Load (N)
cycle1
5
10
25
50
0
100
200
300
400
500
600
700
Pile Top Deflection (mm)